The biology of ELTD1/ADGRL4: a novel regulator of tumour angiogenesis



David Mordechai Favara

Balliol College

University of Oxford

A thesis submitted for the degree of

Doctor of Philosophy

Trinity 2017

Supervisors:

Professor Adrian L. Harris

Professor Alison H. Banham

Abstract

Background: Our laboratory identified ELTD1, an orphan GPCR belonging to the adhesion GPCR family (aGPCR), as a novel regulator of angiogenesis and a potential anti-cancer therapeutic target. ELTD1 is normally expressed in both endothelial cells and vascular smooth muscle cells and expression is significantly increased in the tumour vasculature. The aim of this project was to analyse ELTD1's function in endothelial cells and its role in breast cancer.

Method: 62 sequenced vertebrate genomes were interrogated for ELTD1 conservation and domain alterations. A phylogenetic timetree was assembled to establish time estimates for ELTD1's evolution. After *ELTD1* silencing, mRNA array profiling was performed on primary human umbilical vein endothelial cells (HUVECs) and validated with qPCR and confocal microscopy. ELTD1's signalling was investigated by applying the aGPCR 'Stinger/tethered-agonist Hypothesis'. For this, truncated forms of *ELTD1* and peptides analogous to the proposed tethered agonist region were designed. FRET-based 2nd messenger (Cisbio IP-1;cAMP) and luciferase-reporter assays (NFAT;NFκB;SRE;SRF-RE;CREB) were performed to establish canonical GPCR activation. To further investigate ELTD1's role in endothelial cells, *ELTD1 was* stably overexpressed in HUVECS. Functional angiogenesis assays and mRNA array profiling were then performed. To investigate ELTD1 in breast cancer, a panel of cell lines representative of all molecular subtypes were screened using qPCR. Furthermore, an exploratory pilot study was performed on matched primary and regional nodal secondary breast cancers (n=43) which were stained for ELTD1 expression. Staining intensity was then scored and compared with relapse free survival and overall survival.

Results: ELTD1 arose 435 million years ago (mya) in bony fish and is present in all subsequent vertebrates. ELTD1 has 3 evolutionary variants of which 2 are most common: one variant with 3 EGFs and a variant with 2 EGFs. Additionally, ELTD1 may be ancestral to members of aGPCR family 2. HUVEC mRNA expression profiling after ELTD1 silencing showed upregulation of the mitochondrial citrate transporter *SLC25A1*, and ACLY which converts cytoplasmic citrate to Acetyl CoA, feeding fatty acid and cholesterol synthesis, and acetylation. A review of lipid droplet (fatty acid and cholesterol) accumulation by confocal microscopy and flow cytometry

(FACS) revealed no changes with *ELTD1* silencing. Silencing was also shown to affect the Notch pathway (downregulating the Notch ligand *JAG1* and target gene *HES2*; upregulating the Notch ligand *DLL4*) and inducing *KIT*, a mediator of haematopoietic (HSC) and endothelial stem cell (ESC) maintenance. Signalling experiments revealed that unlike other aGPCRs, ELTD1 does not couple to any canonical GPCR pathways (Gαi, Gαs, Gαq, Gα12/13). *ELTD1* overexpression in HUVECS revealed that ELTD1 induces an endothelial tip cell phenotype by promoting sprouting and capillary formation, inhibiting lumen anastomoses in mature vessels and lowering proliferation rate. There was no effect on wound healing or adhesion to angiogenesis associated matrix components. Gene expression changes following ELTD1 overexpression included upregulation of angiogenesis associated *ANTRX1* as well as *JAG1* and downregulation of migration associated *CCL15* as well as *KIT* and *DLL4.* In breast cancer, none of the representative breast cancer cell lines screened expressed ELTD1. ELTD1 breast cancer immunohistochemistry revealed higher levels of vascular ELTD1 staining intensity within the tumour stroma contrasted to normal stroma and expression within tumour epithelial cells. Additionally, ELTD1 expression in tumour vessels was differentially expressed between the primary breast cancer microenvironment and that of the matched regional node. Due to the small size of the pilot study population, survival comparisons between the various subgroups did not yield significant results.

Conclusion: ELTD1 is a novel regulator of endothelial metabolism through its suppression of ACLY and the related citrate transporter *SLC25A1*. ELTD1 also represses KIT, which is known to mediate haematopoietic and endothelial progenitors stem cell maintenance, a possible mechanism through which endothelial cells maintain terminal endothelial differentiation. ELTD1 does not signal like other adhesion GPCRS with CTF and FL forms of ELTD1 not signalling canonically. Additionally, ELTD1 regulates various functions of endothelial cell behaviour and function, inducing an endothelial tip cell phenotype and is highly evolutionarily conserved. Lastly, ELTD1 is differentially expressed in tumour vessels between primary breast cancer and regional nodal metastases and is also expressed in a small subset of breast cancer cells *in vivo* despite no cancer cell lines expressing ELTD1. The pilot study investigating ELTD1 in the primary breast

cancer and regional involved nodes will be followed up with a larger study including the investigation of ELTD1 in distant metastases.

Dedication:

This thesis is dedicated to my parents and to the memory of my grandparents. Additionally, I dedicate this thesis to my teachers and patients.

Acknowledgements

First and foremost, I would like to pay tribute to my supervisors, Professor Adrian Harris (Department of Oncology, University of Oxford) and Professor Alison Banham (Nuffield Division of Clinical Laboratory Sciences, University of Oxford) for the opportunity and privilege of embarking on this project. I am indebted to them for their generous mentorship and guidance during my time in their laboratories. Under their watch, I have had the opportunity to immerse myself in cutting edge molecular and computational biology as well as to travel and collaborate with both industrial and academic laboratories. As a whole, my research experience has been a positively transformative experience and one for which I am very grateful for.

I would also like to pay tribute to the Rhodes Scholarship (Oxford University), The Clarendon Scholarship (Oxford University) and The Oppenheimer Memorial Trust (South Africa) for their generous funding of my studies. Without their generous support, none of this project would have been possible.

In addition to my supervisors, I would like to sincerely thank all the members of the Harris and Banham laboratories for their companionship and assistance. In the Harris Laboratory, I would like to sincerely thank my laboratory supervisor, Dr. Helen Sheldon (Senior Scientist, Department of Oncology) for all her advice and expert guidance. Additionally, I would also like to thank Dr Syed Haider (now at The Institute of Cancer Research, London) for his bioinformatics expertise and

enthusiasm for the subject as well as to Prof. Francesca Buffa (Group Leader, Department of Oncology) for her advice. I would also like to thank the members of the angiogenesis and notch group within the Harris Laboratory, including Dr. Esther Bridges and Mr. Koon Hwee Ang, who now continues the ELTD1 project. Additionally, I would also like to thank past and current members of the Harris laboratory who I have worked alongside and learnt from (in first name alphabetical order): Dr. Alan McIntyre, Dr. Alessandro Valli. Dr. Ana Miar Cuervo, Dr. Anand Sharma, Dr. Christos Zois, Dr. Dean Singleton, Dr. Dylan Jones, Dr. Eugene Teoh Dr. Hugh Wright, Dr. Ji-Liang Li, Dr. Karim Bensaad, Dr. Kate Feldinger, Dr. Massahiro Kawashima, Dr. Matteo Morotti, Dr. Shijie Cai, Dr. Simon Wigfield, Dr. Sofia Santos, Dr. Ulrike Harjes and Dr. Valentinos Kounnis. Special mention goes to Miss Sam Oats (PA to Prof. Harris) and Mrs. Penny Berry (PA to Prof. Peter McHugh and the Group Heads) for their generous administrative assistance as well as to Mrs. Linda Beattie and Mrs. Rose Earp for their support and help.

From the Banham Laboratory, I would like to sincerely thank Dr. Massimo Masiero for his generosity and advice in all aspects regarding the ELTD1 project. Additionally, I would like to thank Dr. Demin Li, Dr. Duncan Gascoyne and Dr. Simon Brooks for their combined support during the project.

I would also like to pay tribute to Dr. Ioannis Roxanis (Consultant histopathologist, Department of Cellular Pathology, John Radcliffe Hospital, Oxford University Hospitals NHS Foundation Trust,) for his significant help and his enthusiasm during the project. Thanks are also due to Dr. Russel Leek and Mr. Graham Steers (both

formerly of the Nuffield Division of Clinical Laboratory Sciences) for their significant assistance, and to Dr. Mario Buono, Dr. Christoffer Lagerholm and Dr. Esther Garcia (all of the Weatherall Institute of Molecular Medicine, University of Oxford) for their experimental assistance.

Special mention and thank you goes to our collaborators who have generously hosted me in their respective laboratories: to Dr. Ali Jazayeri, Dr Madhulika Nambiar and Dr. Fiona Marshall (Heptares Therapeutics Ltd, United Kingdom); to Dr. Ines Liebscher, Prof Torsten Schöneberg, Ms. Caroline Wilde and Mr. Kay-Uwe Simon (Rudolf Schönheimer Institute of Biochemistry, University of Leipzig, Germany); to Dr. Saskia Nijmeijer and Prof. Martine Smith (VU University Amsterdam, The Netherlands).

Thanks are also due to Prof. Jonathan Bard (Balliol College, University of Oxford), Prof. Raymond Dwek (Department of Biochemistry, University of Oxford), Prof. Siamon Gordon (Sir William Dunn School of Pathology, Universality of Oxford), Prof. Hsi-Hsien Lin (Department of Microbiology and Immunology, Chang Gung University, Taiwan) and Prof. Mashiko Setshedi (visiting scientist, Weatherall Institute of Molecular Medicine; Department of Medicine, University of Cape Town) for their combined support, guidance and inspiration.

Lastly, I would like to thank and pay tribute to my former teachers and mentors at the University of Cape Town who supported my application to the University of Oxford. Without their support, I would never have had this opportunity: Dr. Peter

Berman, Prof. Delawir Kahn, Prof. Marian Jacobs, Prof. Graham Louw, Prof. Marc Blockman and Prof. Tony Leiman (all of the University of Cape Town).

Table of contents

Chapter 1: Introduction **1**

1.1 Introduction **1**

1.2 ELTD1 and its domains **5**

1.3 Canonical GPCR signalling **11**

1.4 Adhesion GPCR signalling and the Stinger/Stachel Hypothesis **16**

1.5 ELTD1 and its role in angiogenesis and cancer **20**

1.6 Other roles for ELTD1 ..... **26**

1.7 Aims **28**

Chapter 2: Materials and methods **30**

2.1 Bioinformatics and statistical analyses **30**

2.1.1 Evolutionary biology 30

2.1.2 Codon optimisation 31

2.1.3 Construct design 31

2.1.4 Stinger/Stachel Peptide design 32

2.1.5 Microarray analysis 32

2.1.6 ELTD1 in cancer 33

2.1.7 Statistical analyses using Prism 34

2.2 Cell lines and maintenance **34**

2.2.1 Cell culture 34

2.2.2 Cell maintenance 34

2.2.3 Cell lines used 35

2.2.4 Cell counting 36

2.2.5 Freezing and thawing cells 37

2.3 Protein analysis **37**

2.3.1 Protein extraction and measurement 37

2.3.2 Western blotting: SDS-PAGE electrophoresis and transfer 38

2.3.3 Western blotting: probing 38
2.3.4 Western blotting: Detection 39
2.4 RNA analysis 40
2.4.1 RNA extraction 40
2.4.2 RNA quantification 40
2.4.3 Generation of cDNA 40
2.4.4 Real-time quantitative polymerase chain reaction (qPCR) 41
2.5 Flow cytometry 47
2.5.1 Flow cytometry for cell surface antigen detection 47
2.5.2 Flow cytometry for whole cell GFP expression detection 48
2.5.3 FACS sorting 48
2.6 Immunohistochemical (IHC) staining of patient samples 50
2.7 Confocal microscopy 51
2.8 RNA interference 52
2.9 Transient transfection 53
2.10 Cloning and lentiviral transduction 54
2.10.1 Cloning 54
2.10.2 Lentiviral assembly in HEK293T cells 56
2.10.3 HUVEC lentiviral transduction: 57
2.11 Cell based assays 58
2.11.1 Signalling assays: 58
2.11.1.1 HTRF FRET assays. 58
2.11.1.2 Luciferase reporter assays 59
2.11.1.3 AlphaScreen assay 60
2.11.1.4 Stinger/Stachel peptide dilution and application 61
2.11.2 Lipid droplet assays 61
2.11.2.1 Lipid droplet confocal microscopy 62
2.11.2.2 Lipid droplet FACS analysis 62

2.11.3 Angiogenesis assays 63
2.11.3.1 Hanging drop endothelial sprouting spheroid assay in matrigel 63
2.11.3.2 Fibrin gel bead assay 64
2.11.3.3 Tube formation assay on matrigel 65
2.11.3.4 Endothelial proliferation assay 65
2.11.3.5 Endothelial migration assay 66
2.11.3.6 MilliCoat extracellular matrix (ECM) adhesion assay: 67
2.11.3.7 Matrigel adhesion assay: 67

Chapter 3: ELTD1's evolution 69

3.1 Introduction 69

3.2 ELTD1 is encoded in the genomes of bony fish and all subsequent vertebrates suggesting that it became established in vertebrates approximately 435 million years ago at the same time as VEGFR2 70

3.3 ELTD1 is evolutionary highly conserved across multiple species suggesting an important biological role 73

3.4 ELTD1 domain amino acid conservation across 59 extant vertebrate orthologues reveals evolutionary ELTD1 variants and 3 areas of major conservation 76

3.5 Vertebrates with a deleted third EGF domain began appearing approximately 101 million years ago 89

3.6 ELTD1 is most similar to ADGRL3/LPHN3 and ADGRE3/EMR3 93

3.7 Conclusion 102

Chapter 4: Investigation of ELTD1's signalling capability 103

4.1 Introduction 103

4.2 Generation of codon optimised ELTD1 constructs: codon optimisation increases ELTD1 surface expression 104

4.3 Design, cloning and expression of ELTD1/ADGRL4 constructs for signalling assays 110

4.4 Overview of signalling assays and positive controls 116

4.5 ELTD1 signalling assays performed at Heptares, UK 120

4.5.1 HTRF FRET in HEK293T cells: ELTD1 does not activate Gαq or Gαs ... 120

4.5.2 Luciferase reporter assays in HEK23T cells: ELTD1 does not activate Gαq, G12/13 or Gαs 123

4.6 The Amsterdam CTF version of ELTD1 revealed no activity when experiments were independently reproduced in Oxford 128

4.7 Signalling assays performed at VU Amsterdam, The Netherlands..... 133

4.7.1 HA ELISA and GFP fluorescence expression assays 133

4.7.2 NFAT-luciferase reporter assay: neither the Amsterdam or Oxford CTF constructs activates NFAT..... 139

4.8 ELTD1 signalling assays performed at the University of Leipzig, Germany 143

4.8.1 HA ELISA surface expression experiments in two cell lines..... 143

4.8.2 Luciferase-reporter assays in HEK293T cells: ELTD1 does not activate Gαq, G12/13 or Gαs 146

4.8.3 AlphaScreen cAMP assay performed in Leipzig: ELTD1 does not signal through Gαs..... 149

4.9 Designing ELTD1 Stinger/Stachel peptides 151

4.10 ELTD1 Stinger/Stachel peptide experiments performed at Heptares, UK 153

4.10.1 Stinger/Stachel peptide HTRF FRET in HEK293T cells: ELTD1 peptides do not activate Gαs or Gαi..... 153

4.10.2 Stinger/Stachel peptide HTRF FRET in HUVECS: ELTD1 peptides do not activate Gαs or Gαi..... 156

4.11 Stinger/Stachel peptide experiments at the University of Leipzig, Germany 158

4.11.1 Stinger/Stachel peptide luciferase assays in HEK293T cells: peptides do not activate Gαq, Gαi or Gαs..... 159

4.11.2 Stinger/Stachel peptide AlphaScreen cAMP assay in HEK293T cells: peptides do not activate Gαs 166
4.12 Discussion 168
4.13 Conclusion 178
Chapter 5: The effect of ELTD1 silencing in endothelial cells 179
5.1 Introduction 179
5.2 ELTD1 Silencing in HUVEC cells 180
5.3 Microarray analysis of ELTD1 silenced HUVECS 182
5.4 ELTD1 silencing upregulates *ACLY* and *SLC25A1* 189
5.5 ELTD1 silencing does not affect lipid droplet accumulation 193
5.6 ELTD1 silencing does not affect fatty acid synthesis pathway genes 196
5.7 ELTD1 silencing downregulates Notch pathway genes *HES2* and *JAG1* and upregulates *DLL4* 200
5.8 ELTD1 silencing upregulates *KIT* 206
5.9 Discussion 210
5.9.1 ELTD1 and SLC25A1 and ACLY 210
5.9.2 ELTD1 and NOTCH GENES DLL4, JAG1 and HES2. 215
5.9.3 ELTD1 and KIT 220
5.10 Conclusion 222
Chapter 6: The effects of ELTD1 overexpression in primary human endothelial cells 223
6.1 Introduction 223
6.2 Microarray of transient ELTD1 ectopic expression in HEK293T cells 225
6.3 Stable codon optimised ELTD1 overexpression in HUVEC cells 236
6.4 Proof of stable coELTD1 overexpression in HUVECS 238
6.4.1 ELTD1 overexpression increases sprout size and number 241

6.4.2 ELTD1 overexpression affects vessel stalk formation by limiting anastomoses between vessels....246
6.4.3 ELTD1 overexpression increases capillary tube formation....249
6.4.4 ELTD1 overexpression decreases HUVEC proliferation....252
6.4.5 ELTD1 overexpression does not have an effect on endothelial cell migration....254
6.4.6 ELTD1 overexpression has no effect on HUVEC adhesion....256
6.5 Microarray of stable ELTD1 overexpression in HUVEC cells....259
6.6 Validation of significant differentially expressed genes in stable ELTD1 overexpressing HUVECS....266
6.7 Discussion....276
6.7.1 Review of genes affected by ELTD1 overexpression....279
6.7.2 Limitations....286
6.7.3 Future Experiments....286
6.8 Conclusion....287
Chapter 7: ELTD1 in the primary breast cancer and regional nodal microenvironment....288
7.1 Introduction....288
7.2 ELTD1 is randomly mutated in many cancer types with no domains specifically targeted....289
7.3 The majority of cancer cell lines (including breast cancer cell lines) do not express ELTD1....293
7.4 ELTD1 within primary breast cancer and regional lymph node metastases....297
7.4.1 Study methods....298
7.4.2 Patient characteristics....300

7.4.3 Vascular ELTD1 expression in primary breast cancer and regional lymph node metastasis 306
7.4.3.1 Vascular ELTD1 increases with increasing proximity to breast tumours. 306
7.4.3.2 Tumour vascular ELTD1 is differentially expressed between primary breast cancer and regional lymph node metastases 315
7.4.3.3 Vascular ELTD1 expression and survival 318
7.4.3.4 Tumour vascular ELTD1 expression combined with other characteristics and survival 321
7.4.4 Tumour cell ELTD1 expression in primary breast cancer and regional lymph node metastasis 327
7.4.4.1 A minority of breast cancer cells express ELTD1 within primary breast tumours and regional lymph node metastases 327
7.4.4.2 Tumour cell ELTD1 expression is not differentially expressed and is expressed at a lower intensity than vascular ELTD1 expression. 332
7.4.4.3 Tumour cell ELTD1 expression and survival 334
7.5 Discussion 336
7.6 Conclusion 341
Chapter 8: Final discussion and future plans 342
8.1 ELTD1's evolution 342
8.2 Investigation of ELTD1's signalling capability 345
8.3 The effect of ELTD1 silencing and overexpression in endothelial cells 347
8.3.1 ELTD1 and endothelial metabolism 347
8.3.2 ELTD1 and Notch signalling 349
8.3.3 ELTD1 and KIT 350
8.3.4 ELTD1 and angiogenesis 351
8.4 ELTD1 in the primary breast cancer and regional nodal microenvironment 353
8.5 Final remarks 355

9: Appendix 357

9.1 Investigation of ELTD1's signalling capability 357

9.1.1 wtFL ELTD1 in pCMV-Sport 6 vector (Geneservice; Ascension ID: BC025721.1) 357

9.1.1.1 Vector map 357

9.1.1.2 Nucleotide sequence 358

9.1.1.3 Amino acid sequence 360

9.1.2 coFL ELTD1: 360

9.1.2.1 Nucleotide sequence: 360

9.1.2.2 Amino acid sequence 362

9.1.3 wtFL ELTD1 with GFP C-terminal tag in pcDNA3.1 vector 363

9.1.3.1 Vector Map: 363

9.1.3.2 Nucleotide sequence 363

9.1.3.3 Amino acid sequence 366

9.1.4 coFL ELTD1 with GFP C-terminal tag in pcDNA3.1 vector 366

9.1.4.1 Nucleotide sequence 366

9.1.4.2 Amino acid sequence 368

9.1.5 coFL ELTD1 with HA N-terminal and FLAG C-terminal tags in pcDNA3.1 vector 369

9.1.5.1 Nucleotide sequence 369

9.1.5.2 Amino acid sequence 370

9.1.6 coCTF ELTD1 with N-terminal and FLAG C-terminal tags in pcDNA3.1 vector 371

9.1.6.1 Nucleotide sequence 371

9.1.6.2 Amino acid sequence 372

9.1.7 co7TMΔ ELTD1 with HA N-terminal and FLAG C-terminal tags in pcDNA3.1 vector 372

9.1.7.1 Nucleotide sequence 372

9.1.7.2 Amino acid sequence 373

9.1.8 coFL ELTD1 with GFP C-terminal tag in pcDNA3.1 vector 373
9.1.8.1 Nucleotide sequence 373
9.1.8.2 Amino acid sequence 376
9.1.9 coCTF ELTD1 with GFP C-terminal tag in pcDNA3.1 vector.....377
9.1.9.1 Nucleotide sequence 377
9.1.9.2 Amino acid sequence 377
9.1.10 co7TMΔ ELTD1 with GFP C-terminal tag in pcDNA3.1 vector 378
9.1.10.1 Nucleotide sequence 378
9.1.10.2 Amino acid sequence 378
9.2 R script: microarray performed on ELTD1 silenced HUVECS.....380
9.3 R script: microarray performed on transient ELTD1 overexpressing HEK293T cells. 388
9.4 R script: microarray performed on stable ELTD1 overexpressing HUVECS 396
9.5 FIJI: script to count cells within a field of view 403
10: Publications, talks, conference posters and collaborations related to thesis 404
11: Bibliography 407

List of Figures

Figure 1.1: The hallmarks of cancer. 4

Figure 1.2: Graphical overview of the five families making up the GPCR superfamily with focus on the adhesion family. 6

Figure 1.3: Schematic representation of ELTD1's putative structure. 10

Figure 1.4: Graphical representation of canonical GPCR signalling. 14

Figure 1.5: Graphical representation of the Stinger/Stachel tethered agonist hypothesis. 19

Figure 3.1: Cladogram depicting vertebrate evolution and the presence of genomic ELTD1 and the core angiogenetic genes VEGFR1 and VEGFR2. 72

Figure 3.2: Comparison of ELTD1 and VEGFR2 amino acid conservation across 61 vertebrate species with fully sequenced and annotated genomes. 74

Figure 3.3: Comparison of ELTD1 orthologues across extant vertebrate species. 80

Figure 3.4: ELTD1 amino acid residue diagram highlighting areas of high conservation across ELTD1 orthologues. 88

Figure 3.5: Timetree representing evolution in extant vertebrate species showing the emergence of ELTD1 variants. 92

Figure 3.6: Phylogenetic tree displaying the genetic difference between all adhesion GPCRS. 95

Figure 3.7: Phylogenetic sequence homology comparisons between adhesion GPCR domains belonging to members of adhesion GPCR Family 1 and Family 2. 97

Figure 4.1: ELTD1 cell surface expression at 24, 48, 72 hours following transient transfection in HEK293T cells. 106

Figure 4.2: Generation of codon optimised ELTD1 constructs. 109

Figure 4.3: The design of ELTD1's signal constructs. 111

Figure 4.4: FACS plots showing representative expression of the ELTD1 signalling constructs in transiently transfected HEK293T cells (48 hours). 114

Figure 4.5: Confocal microscopy of GFP (C-terminal) tagged coELTD1 constructs transiently expressed in HEK293T cells. 115

Figure 4.6: ELTD1 HTRF signalling experiments performed at Heptares: ELTD1 does not signal through Gαq or Gαs. 122

Figure 4.7: ELTD1 luciferase signalling experiments performed at Oxford: ELTD1 does not signal through Gαq, Gα12/13 or Gαs. 127

Figure 4.8: Comparison of the Oxford and Amsterdam CTF ELTD1 constructs. 130

Figure 4.9: Signalling assays comparing the Oxford and Amsterdam FL and CTF constructs. 132

Figure 4.10: Expression comparison between the Oxford and Amsterdam HA tagged ELTD1 constructs performed in Amsterdam. 137

Figure 4.11: NFAT luciferase assays with Amsterdam and Oxford ELTD1 constructs, performed in Amsterdam. 141

Figure 4.12: Surface expression comparison between ELTD1 constructs and signalling adhesion GPCRs published by the Laboratory of Dr. Ines Liebscher. 145

Figure 4.13: Luciferase reporter assays with ELTD1 constructs, performed in Leipzig. 148

Figure 4.14: AlphaScreen cAMP assay performed with ELTD1 constructs in Leipzig: none of the ELTD1 constructs activated any Gαs activity. 150

Figure 4.15: Design and sequences of the 21 ELTD1 Stinger/Stachel peptides. 152

Figure 4.16: ELTD1 Stinger/Stachel peptide Gαs and Gαi HTRF FRET assays in HEK293T cells. 155

Figure 4.17: ELTD1 Stinger/Stachel peptide Gαs Gαi HTRF FRET assays performed in HUVECS. 157

Figure 4.18: Radial cladogram showing similarities between all adhesion GPCR GPS domains. 160

Figure 4.19: CREB-luciferase reporter assay (n=2) showing increase in CREB associated luminescence downstream of Gαs signalling following addition of p133 (1mM in 1% DMSO) in HEK293T cells transfected with FL ADGRD1/GPR133 (unpaired Student's t-test $p < 0.0001$). 161

Figure 4.20: ELTD1 Stinger/Stachel peptide luciferase experiments performed in HEK239T cells transfected with codon optimised FL ELTD1. 164

Figure 4.21: ELTD1 Stinger/Stachel peptide AlphaScreen cAMP experiment (n=1) reveals that none of the peptides elicited an increase compared to the negative control in HEK293T cells expressing codon optimised FL ELTD1. 167

Figure 4.22: Possible explanation as to why the codon optimised 7TMΔ form of ELTD1 does not appear on the cell surface. 173

Figure 5.1: ELTD1 Silencing in HUVEC cells using two different siRNAs. 181

Figure 5.2: Outline of microarray analysis method used for analysing ELTD1 silenced HUVECS. 183

Figure 5.3: Volcano plots depicting differentially expressed genes for each siRNA following comparison between ELTD1 silenced HUVECS and control HUVECS. 185

Figure 5.4: Representation of statistically significant differentially expressed genes shared by both siRNA 1 and siRNA 2. 188

Figure 5.5: ELTD1 silencing upregulates ACLY and SLC25A1 expression. 192

Figure 5.6: ELTD1 silencing in HUVECS does not increase lipid droplet formation. 195

Figure 5.7: ELTD1 silencing in HUVECS does not significantly affect genes associated with the fatty acid synthesis pathway. 198

Figure 5.8: ELTD1 silencing affects the NOTCH ligands *DLL4* and *JAG1* and the NOTCH target gene *HES2*. 202

Figure 5.9: ELTD1 silencing increases surface expression of the Notch ligand DLL4 in HUVECs treated with each ELTD1 siRNA. 204

Figure 5.10: ELTD1 silencing in HUVECS decreases surface expression of the NOTCH ligand JAG1 only when using siRNA 1. 205

Figure 5.11: Endothelial cells co-express *ELTD1*, *KIT* and *KITLG* and are the only mature haematopoietic origin cells to do so. 208

Figure 5.12: ELTD1 silencing increases KIT expression both at mRNA and cell surface protein level. 209

Figure 5.13: ELTD1's documented relationship with VEGF and members of the Notch pathway in endothelial cells. 219

Figure 6.1: Overview of ELTD1 overexpression and FACS sorting in HEK293T cells. 227

Figure 6.2: Volcano plots depicting differentially expressed genes following FL and CTF coELTD overexpression in HEK293T cells. 230

Figure 6.3: Heatmap displaying significant expressed genes in FL and CTF coELTD1 overexpression in HEK293T cells. 232

Figure 6.4: Venn diagram showing that none of the genes differentially expressed in HEK293T cells expressing recombinant ELTD1 are shared with those differentially expressed in ELTD1 silenced HUVECS. 235

Figure 6.5: ELTD1 overexpression model in HUVECS. 238

Figure 6.6: Proof of successful stable overexpression of codon optimised FL ELTD1 in HUVECs. 240

Figure 6.7: Semi-manual but highly accurate method for quantifying the Hanging drop endothelial spheroid assay. 243

Figure 6.8: Hanging drop endothelial sprouting spheroid assay in matrigel: ELTD1 overexpression induces a tip cell phenotype. 245

Figure 6.9: Fibrin gel bead assay: ELTD1 overexpression lowers the number of vascular anastomoses/branches between adjacent vessels. 248

Figure 6.10: Tube formation assay: ELTD1 overexpression increases tube formation. 251

Figure 6.11: Proliferation assay: ELTD1 overexpression lowers HUVEC proliferation. 253

Figure 6.12: Endothelial migration assay: ELTD1 overexpression has no effect on endothelial migration. 255

Figure 6.13: MilliCoat extracellular matrix (ECM) adhesion assay: ELTD1 overexpression does not affect adherence to angiogenesis-associated ECM components. 258

Figure 6.14: Matrigel adhesion assay: ELTD1 overexpression does affect adhesion to matrigel. 259

Figure 6.15: Proof of FL coELTD1 overexpression from second FL coELTD1 lentiviral HUVEC transduction performed for microarray 263

Figure 6.16: FL coELTD1 stable overexpression in HUVECS: microarray results. 264

Figure 6.17: Venn diagram comparison between the microarray results from transient FL and CTF coELTD1 overexpression in HEK293T cells, ELTD1 silencing in HUVECS and FL coELTD1 stable overexpression in HUVECS. 265

Figure 6.18: qPCR validation of CHRNA1 in FL coELTD1 overexpressing HUVECS and ELTD1 silenced HUVECS. 266

Figure 6.19: qPCR validation of differentially expressed upregulated genes from the stable FL coELTD1 overexpression microarray, tested on HUVECS stably expressing FL coELTD1. 269

Figure 6.20: qPCR testing of significant differentially expressed genes from the FL and CTF ELTD1 overexpression HEK293T microarray, tested on FL coELTD1 overexpressing HUVECS. 271

Figure 6.21: qPCR testing of 6 differentially expressed genes affected by HUVEC ELTD1 silencing, tested on stable FL coELTD1 overexpressing HUVECS. 273

Figure 6.22: FL coELTD1 overexpression represses DLL4 at RNA level but has no effect on cell surface DLL4 protein expression. 274

Figure 6.23: FL coELTD1 overexpression represses JAG1 at RNA level but has no effect on cell surface JAG1 protein expression. 275

Figure 7.1: *ELTD1*'s mutational landscape in human cancer. 292

Figure 7.2: *ELTD1* is not expressed by the majority of cancer cell lines. 294

Figure 7.3: qPCR screen reveals that commonly used breast cancer cells do not express *ELTD1*. 296

Figure 7.4: Patient survival contrasted with patient characteristics. 305

Figure 7.5: Vascular ELTD1 expression is upregulated in breast cancer. 309

Figure 7.6: Representative vascular ELTD1 IHC in normal vessels at the margins of the primary breast tumour biopsy. 310

Figure 7.7: Representative images of tumour vascular ELTD1 IHC staining within the primary breast tumour, showing the range of staining (intensity expression score 0-3). 311

Figure 7.8: Representative images of tumour vascular ELTD1 IHC staining within regional lymph node metastases, showing the range of ELTD1 IHC intensity scores (intensity expression score 0-3). 312

Figure 7.9: Vascular ELTD1 expression increases with proximity to the tumour. 313

Figure 7.10: ELTD1 does not appear to be expressed by the lymphatic system used by primary breast tumours for metastatic spread. 314

Figure 7.11: Comparison of vascular ELTD1 IHC staining in primary breast cancer and regional lymph node metastases reveals that tumour vascular ELTD1 is differentially expressed between primary breast cancer and regional lymph node metastases. 316

Figure 7.12: Tumour vessel ELTD1 expression and survival. 320

Figure 7.13: A minority of breast tumour cells express ELTD1 within both primary breast cancer and regional node metastases. 329

Figure 7.14: Representative images of tumour cell ELTD1 IHC staining within the primary breast tumour, showing the range of tumour cell ELTD1 staining (IHC intensity scores 0-3). 330

Figure 7.15: Representative images of tumour cell ELTD1 IHC staining within regional lymph node metastases, showing the range of tumour cell ELTD1 staining (IHC intensity scores 0-3). 331

Figure 7.16: ELTD1 expression in tumour cells is not differentially expressed and is expressed at a lower level than vascular ELTD1 expression 333

Figure 9.1: pCMV-Sport 6 Vector Map. 357

Figure 9.2: pcDNA3.1 Vector Map. 363

List of Tables

Table 1.1: List of adhesion GPCRS whose signalling and activation mechanisms have been solved using the Stinger/Stachel hypothesis. 18

Table 2.1: Antibodies used for Western blotting. 39

Table 2.2: qPCR primer sequences. 46

Table 2.3: Antibodies used for cell surface FACS. 49

Table 2.4: siRNAs used for ELTD1 silencing. 53

Table 3.1: Predicted conserved domain sequence details for all ELTD1 orthologues used in the study. 87

Table 3.2: The number of species which do not contain any orthologues for adhesion GPCR family 1 and 2 members. 99

Table 3.3: List of species which do not encode orthologues of family 1 and 2 adhesion GPCRS. 101

Table 4.1: Table of signalling assays and their associated G proteins used in the ELTD1 signalling project. 117

Table 4.2: List of positive controls for use in ELTD1's signalling experiments. .. 119

Table 7.1: Patient characteristics. 303

Table 7.2: Patient characteristics and survival. 304

Table 7.3: Vascular ELTD1 expression and survival. 319

Table 7.4: Frequency table listing number of patients according to tumour vessel ELTD1 IHC score and breast tumour characteristics. 324

Table 7.5: Survival analyses performed on tumour vessel ELTD1 expression combined with multiple breast cancer characteristics. 325

Table 7.6: Tumour cell ELTD1 and survival. 335

List of abbreviations

°C	degrees Celsius
7TM	seven transmembrane domain
7TMΔ	7TM modified form
ACACA	Acetyl-CoA Carboxylase Alpha
ACACB	Acetyl-CoA Carboxylase Beta
ACLY	ATP-citrate lyase
ANOVA	Analysis of variance
APC	allophycocyanin
ATP	adenosine triphosphate
bFGF	basic fibroblast growth factor
bp	base pairs
BSA	bovine serum albumin
C-term	C terminal
Ca	calcium
CAI	codon adaptation index
cAMP	cyclic adenosine monophosphate
CCh	carbachol
CDS	coding-DNA-sequence

CI	confidence interval
CMV	cytomegalovirus
co	codon optimised
CO_2	carbon dioxide
co7TMΔ	codon optimised seven-transmembrane truncated ELTD1
coCTF	codon optimised C-terminal fragment ELTD1
coFL	codon optimised full length ELTD1
CSL	CBF1–Suppressor of Hairless–LAG1
CTF	C-terminal fragment
DAG	diacylglycerol
DAPI	4',6-Diamidino-2-Phenylindole, Dihydrochloride
DCIS	ductal carcinoma in situ
DEPC	diethyl pyrocarbonate
DLL4	delta-like ligand 4
DMEM	Dulbecco's modified Eagle's medium
DMSO	dimethyl sulfoxide
DNA	deoxyribonucleic acid
dNTP	deoxynucleotide triphosphates
E. coli	Escherichia coli

EBM-2	endothelial basal medium 2
EBV	Epstein-Barr virus
ECD	extracellular domain
ECL	enhanced chemiluminescence
EDTA	ethylenediaminetetraacetic acid
EGF	epidermal growth factor domain
EGF-Ca	calcium binding EGF domain
EGM-2	endothelial growth medium 2
ELTD1	EGF, latrophilin and seven transmembrane domain containing 1
EPC	Endothelial progenitor cell
ER	oestrogen receptor
FACS	fluorescence-activated cell sorting
FASN	Fatty acid synthase
FCS	fetal calf serum
FL	full length
FL-1	flow cytometry channel 1
FL-4	flow cytometry channel 4
FSC	forward scatter
FSK	forskolin

GAIN	GPCR autoproteolysis inducing domain
GDP	guanosine diphosphate
GMP	guanosine monophosphate
GPCR	G-protein coupled receptor
GPS	GPCR proteolytic site
GRK	GPCR kinases
GTP	guanine triphosphate
GWAS	genome-wide association studies
HEK293T	human embryonic kidney 293 cells expressing large T antigen
HER2	human epidermal growth factor receptor 2
HPC	haematopoietic progenitor cell
HRM	hormone receptor motif
HRP	horseradish peroxidase
HTRF FRET	Homogeneous Time-Resolved Fluorescence Resonance Energy Transfer
HUVEC	human umbilical vein endothelial cells
IBMX	3-isobutyl-1-methylxanthine
ICD	intracellular domain
IgG	immunoglobulin gamma

IHC	Immunohistochemistry
IP1	inositol monophosphate
IP3	inositol trisphosphate
IUPHAR	International Union of Basic and Clinical Pharmacology
L-broth	lysogeny broth
MAML1	mastermind
mg	milligram
ml	millilitre
mM	millimolar
N-term	N terminal
NCBI	National Center for Biotechnology Information
NDCLS	Nuffield Division of Clinical Laboratory Sciences
Neg CT	negative control
NICD	notch intracellular domain
nm	nanometre
NRR	negative regulatory region
ns	non-significant
NSCT	negative stain control comprising secondary only
NTF	N-terminal fragment

O_2	oxygen
OLF	olfactomedin
OS	overall survival
PBS	phosphate buffered saline
PBS-T	tween 20 in PBS
PCR	polymerase chain reaction
PEI	polyethylenimine
pg	picogram
PIP2	phosphatidylinositol 4,5-bisphosphate
PKA	protein kinase A
PKC	protein kinase C
PLCβ	β isotype of phospholipase C
PMA	phorbol myristate acetate
Pos CT	positive control
PVDF	polyvinylidene difluoride
RBL	rhamnose-binding lectin
RFS	relapse free survival
RGS	regulator of G protein signalling
RhoGEF	Rho guanine nucleotide exchange factors

RIPA	radioimmunoprecipitation assay buffer
RNA	ribonucleic acid
SCD	Stearoyl-CoA Desaturase
SCF	stem cell factor
siRNA	small interfering RNA
SOC	super optimal broth with catabolite repression
SSC	side scatter
TAG	triacylglycerols
TCGA	The Cancer Genome Atlas
TDLU	terminal ductal lobular unit
TMB	tetramethylbenzidine
TRIS	tris(hydroxymethyl)aminomethane
V	volt
VEGF	vascular endothelial growth factor
VEGFR1	vascular endothelial growth factor receptor 1
VEGFR2	vascular endothelial growth factor receptor 2
WHO	World Health Organization
wt	wild type
µg	microgram

µl	microlitre
µM	micromolar

Chapter 1: Introduction

*Note: portions of this text have been published in a modified form in Favara DM, Banham AH, Harris AL. A review of ELTD1, a pro-angiogenic adhesion GPCR. Biochem Soc Trans. 2014 Dec;42(6):1658-64.

1.1 Introduction

According to the World Health Organization (WHO), cancer is one of the leading causes of morbidity and mortality, accounting for nearly 1 in every 6 deaths worldwide, the overwhelming majority of them being in low and middle income countries (WHO, 2017). In 2012, there were approximately 14 million new cases of cancer diagnosed worldwide. This number is predicted to rise by over 70% over the next two decades (WHO, 2017). Understanding the complex processes which enable, initiate and drive cancer are thus of utmost importance if we are to find new strategies to curb this growing global health problem.

Cancers use a variety of mechanisms to further their own growth. These have been dubbed the “hallmarks of cancer” and comprise a variety of tumour enabling biological capabilities which are acquired during the multi-step process of cancer development (Hanahan and Weinberg, 2011). A summary of these hallmarks is presented in Figure 1.1. Amongst the hallmarks of cancer is the ability to induce angiogenesis. Angiogenesis is the process by which new blood vessels form from

pre-existing vessels (Carmeliet and Jain, 2011a). This tightly regulated process occurs physiologically throughout life during periods of controlled tissue growth, tissue repair and wound healing, as well as during the menstrual cycle and during placental implantation in the uterus (Daly et al., 2003). Pathological angiogenesis refers to inappropriate and excessive angiogenesis and is associated with a spectrum of diseases, most notably cancer (Jain, 2005).

Although angiogenesis is usually a tightly controlled process, it can be hijacked and manipulated by cancers (Carmeliet and Jain, 2011a). Such tumour-associated angiogenesis provides the neoplastic cells with oxygen and essential nutrients needed for tumour growth and expansion. It also provides the malignant cells with access to the vasculature, enabling metastasis (Hanahan and Weinberg, 2011). Understanding tumour-associated angiogenesis as well as seeking methods to limit it are thus important targets of current oncology research.

Since the first association between angiogenesis and tumour growth over 40 years ago (Folkman, 1971), much work has been invested into the search and development of anti-angiogenic therapies. The majority of anti-angiogenic approaches developed to date target components of either the vascular endothelial growth factor (VEGF) pathway or the NOTCH intercellular signalling pathway, which together make up the two most studied angiogenic pathways (Blanco and Gerhardt, 2013). However, despite the many positive results achieved in preclinical models, the translation of these therapies into clinical practice has yielded modest to poor results and has been marred by the development of tumour resistance to these

drugs when taken for prolonged periods, leading to the restoration of tumour growth and often, an increased rate of disease progression (Jayson et al., 2016, Bergers and Hanahan, 2008). An example of this occurs with the use of bevacizumab, a humanized anti-VEGF monoclonal antibody which initially limits tumour angiogenesis and thus decreases tumour bulk, but with chronic administration becomes ineffective as tumour resistance develops (Li et al., 2011). In addition, some tumours are already resistant even before exposure to therapy (Hanahan and Weinberg, 2011). It is presumed that tumours undergoing selective anti-angiogenic pressure (targeting a single pathway) are able over time to recruit alternative unknown parallel angiogenic pathways unaffected by the given therapy. The search for these novel parallel pathways as well as for predictive biomarkers for response to therapy is thus ongoing and vigorous.

In my supervisors' laboratories (referred to from here onwards as "our laboratories"), scientists turned to the use of bioinformatics in their search to identify novel regulators of tumour angiogenesis. To do this, they analysed the gene expression profile of 121 primary head and neck squamous cell carcinomas, 959 primary breast cancers and 170 primary clear cell renal cell carcinomas and then generated 3 tumour-specific gene signatures whose level of expression correlated with the expression of 15 well-established endothelial and angiogenesis associated "seed genes" (Masiero et al., 2013). Combining these three signatures generated a core signature composed of 43 genes whose correlation with angiogenesis appeared consistent in all tumour types tested. Expression of this core signature was then analysed in *in vivo* tumour xenografts treated with or without two anti-angiogenic therapies to indirectly confirm involvement in tumour angiogenesis (Masiero et al.,

2013). The highest ranked uncharacterised gene was *Epidermal growth factor, latrophilin and seven transmembrane domain containing 1 (ELTD1)* (Masiero et al., 2013). This introduction presents an overview of ELTD1 and highlights the many questions which remain unanswered regarding its role in both endothelial and cancer biology. These unknowns form the basis of this research project.

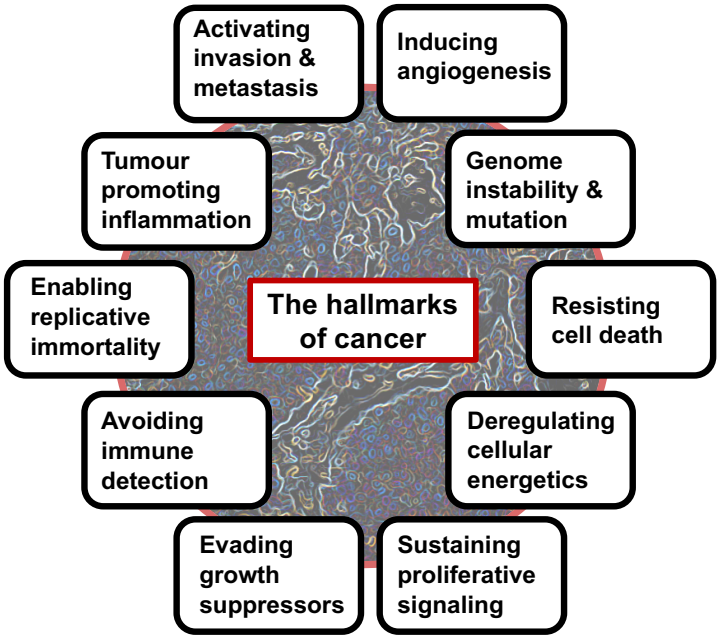


Figure 1.1: The hallmarks of cancer. These hallmarks refer to tumour enabling characteristic capabilities which the tumour cells acquire during the multistep development of cancer (Hanahan and Weinberg, 2011). These characteristics comprise the ability to induce angiogenesis, an inherently unstable genome and high levels of mutation, the ability to resist cell death by deregulation of apoptotic pathways, deregulating cellular energetics and altering cell metabolism, inducing sustained proliferative signalling, evading growth suppression, the ability to avoid immune detection by subverting surrounding immune cells, the enablement of

replicative immortality, the promotion of inflammation, and activation of invasion and metastasis. Figure adapted from (Hanahan and Weinberg, 2011)

1.2 ELTD1 and its domains

ELTD1 is an orphan member of the G protein-coupled receptors (GPCR) superfamily and was first discovered in 2001 (Nechiporuk et al., 2001). The GPCR superfamily comprises the largest receptor family in the human proteome with over 800 members and is divided into five groups according to the sequence homology of the seven-transmembrane domain (7TM), a domain present in all members (Schioth and Fredriksson, 2005). Within the GPCR superfamily, ELTD1 belongs to the 33 member 'adhesion GPCR family', so named as members all contain large extracellular domains containing adhesion motifs, a feature not found in other GPCR families (Bjarnadottir et al., 2004). In general, the adhesion GPCR family remains the most poorly studied and understood of the five GPCR families due to the large number of orphan receptors and a historical inability to activate canonical GPCR signalling in these receptors – something which has since changed (Promel et al., 2013, Hamann et al., 2015, Langenhan et al., 2015). Recently, the adhesion GPCR family underwent a nomenclature change with all receptors receiving new International Union of Basic and Clinical Pharmacology (IUPHAR) approved gene names (Hamann et al., 2015). This was introduced in order to simplify the previous naming system. ELTD1 was thus renamed ADGRL4 (adhesion GPCR L4) (Hamann et al., 2015). For the remainder of this thesis however, ELTD1/ADGRL4 will be referred to as ELTD1. All other adhesion GPCRS will be referred to by their new names followed by their old names (ie ADGRG6/GPR126). Within the 'adhesion family', ELTD1 is grouped into the 'family 1/latrophilin-like' subfamily. This grouping

is based solely on 7TM sequence homology (Bjarnadottir et al., 2004). ADGRL1, ADGRL2 and ADGRL3 form the other members of this group and are so named because of their ability to bind α-latrotoxin, a toxin produced by the black widow spider (*Latrodectus mactans*) (Matsushita et al., 1999). Figure 1.2 presents a graphical overview of the adhesion GPCR family.

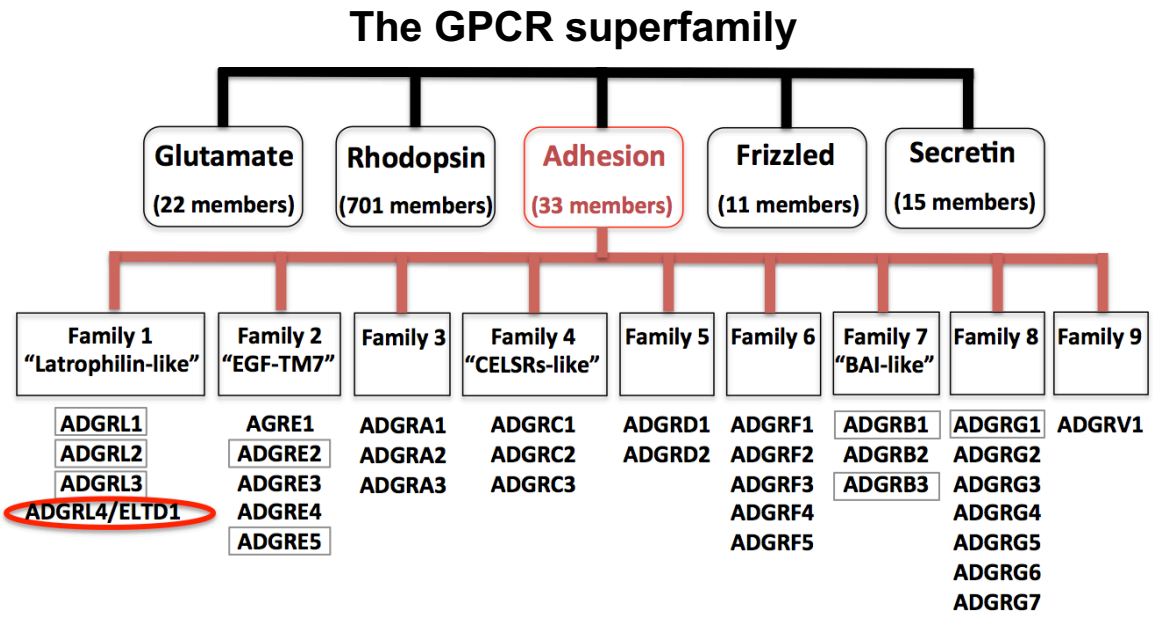


Figure 1.2: Graphical overview of the five families making up the GPCR superfamily with focus on the adhesion family. The adhesion family forms the second largest group and is the most poorly understood of the GPCRs. Adhesion GPCRS are listed by their recently new IUPHAR approved names and are grouped by family. Boxes surround members with a known ligand. ELTD1 is circled in red.

Located on chromosome 1p31.1, *ELTD1* encodes a 2673 nucleotide transcript translated as a 690 amino acid protein. *ELTD1* contains 15 exons, expressed as three splice variants: i) one full-length form of the receptor; ii) a149 amino acid

truncated C-terminal segment of the transmembrane domain; and iii) a 2223 base pair fragment which is degraded through the nonsense mediated decay pathway and is not translated. Like all adhesion GPCRs, ELTD1's predicted structure can be divided based on either topographical or cleavage-based compartmentation (Langenhan et al., 2013). Topographically, ELTD1 can be divided into 3 compartments: i) a large extra-cellular domain (ECD) containing receptor-specific ecto-domains as well as the 'GPCR autoproteolysis inducing domain' (GAIN) (which contains the GPCR proteolysis site (GPS)); ii) a 7-transmembrane domain (7TM); and iii) a short intracellular domain (ICD). Cleavage-based compartmentation centres on the GPS cleavage site and divides the adhesion GPCR into an i) N-terminal Fragment (NTF) and ii) C-terminal fragment (CTF) (Figure 1.3).

ELTD1's crystal structure remains unsolved. In humans, bioinformatic analysis predicts that the 430 amino acid ELTD1 ECD encodes an Epidermal Growth Factor (EGF) repeat and an EGF-Ca^{2+} binding repeat, and a GAIN domain (Figure 1.3). Interestingly, ELTD1's EGF adhesion motifs are not found in the other 'family 1/latrophilin-like' subfamily. Reciprocally, the rhamnose-binding lectin (RBL), olfactomedin (OLF) and hormone receptor motif (HRM) domains found in ADGRL1-3/LPHN1-3 are not found on ELTD1. Although the crystal structure of ADGRL3/LPHN3's interaction with its ligand FLRT has been solved (Jackson et al., 2015), this does not apply to ELTD1 as it does not share any of the involved domains. To date, ligands to any of ELTD1's extracellular domains have yet to be identified.

GAIN domains are found in all adhesion GPCRS bar one (ADGRA1/GPR123) and have been shown to be important for GPCR assembly and function (Arac et al., 2012a). Within ELTD1's GAIN domain is the GPS motif (Figure 1.3). During adhesion GPCR protein assembly in the endoplasmic reticulum, the GPS undergoes autoproteolytic cleavage before re-joining non-covalently through hydrophobic interactions at the site of cleavage and being exported to the Golgi complex and then to the cell membrane (Lin et al., 2004). This is understood to occur because of the inherent instability of the three-dimensional structure at the point of cleavage (Arac et al., 2012b). Although the GPS motif makes up a small area of the larger GAIN domain (53 out of 263 amino acids respectively in ELTD1), the entire GAIN domain itself is required for autoproteolysis to occur (Promel et al., 2013, Arac et al., 2012a).

The consensus amino acids involved in GPS autoproteolytic cleavage have been identified in all adhesion GPCRs which undergo autoproteolytic cleavage (Langenhan et al., 2013). ELTD1's GPS cleavage site comprises histidine (position 405), leucine (position 406) and threonine (position 407) with cleavage occurring between the leucine and threonine residue (Figure 1.3). More recently, the GPS site has been shown to be a critical component of adhesion GPCR activation and signalling, through the discovery that the amino acid sequence C-terminal to the cleavage site can act as a tethered agonist (described in the next section)(Liebscher et al., 2014, Hamann et al., 2015, Schoneberg et al., 2015). ELTD1's activation and signalling mechanism remains unknown.

It has also been hypothesized that autoproteolytic cleavage at the GPS may allow for swapping of extracellular domain fragments between receptors once at the cell surface (Langenhan et al., 2013). Although this has been noted with ADGRL1/LPHN1, ADGRE2/EMR2 and ADGRG1/GPR56, (Huang et al., 2012, Volynski et al., 2004, Silva et al., 2009) it remains unproven for the majority of adhesion GPCRs, including ELTD1. Interestingly, a mass spectrometry based study of the human plasma N-glycoproteome has identified a circulating NTF ELTD1 peptide fragment (Liu et al., 2005). Whether this was related to NTF shedding, swapping or cell death remains unknown. Lastly, ELTD1's 7TM comprises 237 amino acids and its short ICD contains 22 amino acids, the shortest ICD amongst members of the 'family 1/latrophilin-like' subfamily.

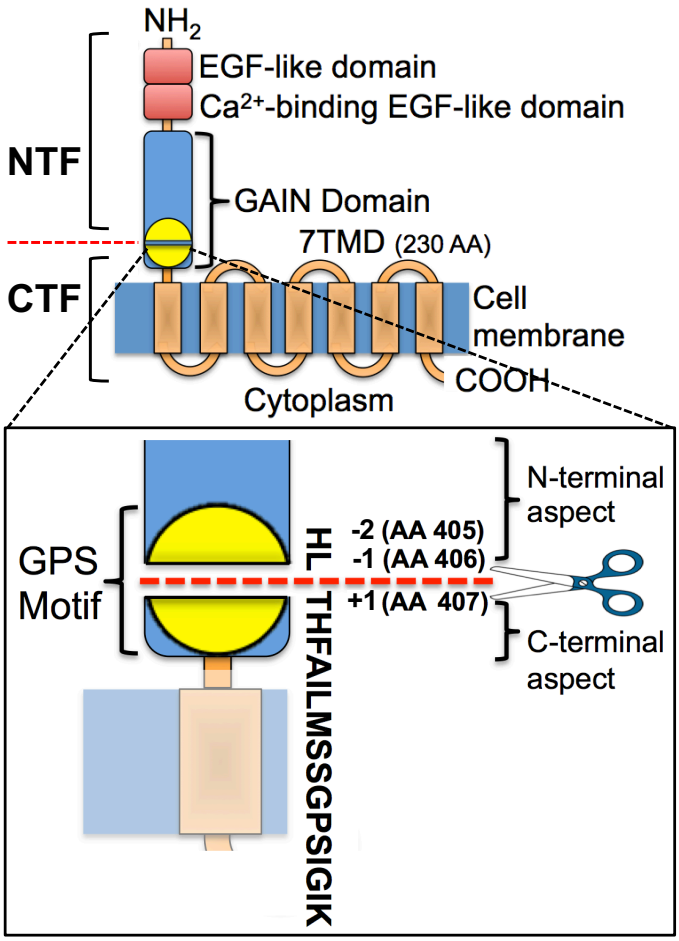


Figure 1.3: Schematic representation of ELTD1's putative structure. ELTD1's structure can be divided into an N-terminal fragment (NTF) and a C-terminal fragment (CTF) centred on the GPS cleavage site (ELTD1's consensus cleavage amino acid sequence: histidine, leucine, <cut>, threonine; cleavage position within ELTD1 sequence: 405, 406, <cut>, 407). The NTF comprises an EGF-like domain and a Ca^{2+} binding EGF-like domain as well as the majority of the GAIN domain and N-terminal portion of the GPS. The CTF comprises the C-terminal portion of the GPS as well as the 7TM domain and a short intracellular ICD. The autoproteolytic cleavage point is indicated by the dotted red line. (Abbreviations: AA=amino acid position; GAIN=GPCR autoproteolysis inducing domain; GPS=GPCR proteolysis site; H=histidine; L=leucine; T=threonine).

1.3 Canonical GPCR signalling

GPCR signalling occurs following the binding of an agonist ligand to the extracellular surface of the receptor's 7TM (Hanlon and Andrew, 2015). Binding triggers a conformational change in the GPCR which allows the intracellular portion of the 7TM to couple and activate a heterotrimeric G protein complex. The heterotrimeric G protein complex comprises of Gα, Gβ and Gγ subunits. In the non-active state, Gα is bound to guanosine diphosphate (GDP) in addition to the other members of the complex (Hanlon and Andrew, 2015). Following GPCR activation and conformational change, Gα exchanges GDP for guanosine triphosphate (GTP). Following this, the heterotrimeric G protein complex disassociates and canonical GPCR signalling is initiated through the activity of the guanosine triphosphate (GTP) bound Gα subunit (Ghosh et al., 2015). There are 4 main subtypes of Gα, with each activating a separate second messenger system and thus associated with a different canonical GPCR pathway (Wettschureck and Offermanns, 2005). Although the type of Gα determines the kind of canonical GPCR signalling, GPCRS are not restricted to one type of Gα and are able to bind several types with differencing intensity (Hanlon and Andrew, 2015).

Gαs binds and activates adenylyl cyclase in the cell membrane, which activates production of the second messenger cyclic adenosine monophosphate (cAMP) from adenosine triphosphate (ATP). cAMP activates protein kinase A (PKA) by binding to its regulatory subunits. This induces PKA's catalytic subunits to break away and travel to the nucleus where they affect gene transcription. Gαi binds and inactivates adenylate cyclase thereby inhibiting cAMP production and signalling (Hanlon and Andrew, 2015, McCudden et al., 2005). Activity of Gαs or Gαi can be

measured by measuring cAMP or a downstream transcription factor CRE which is modulated by cAMP activity (Cheng et al., 2010).

Gα12/13 binds and activates Rho guanine nucleotide exchange factors (RhoGEF) which in turn activates the RhoA second messenger pathway (Hanlon and Andrew, 2015). Although Gα12/13 is the least well characterised of the four Ga subtypes, it has been shown to be important for a number of physiological processes such as cell proliferation and changes in cell morphology (Suzuki et al., 2009). Activity of Gα12/13 can be measured by measuring the downstream transcription factor SRF-RE (Cheng et al., 2010).

Gαq binds and activates the β isotype of phospholipase C (PLCβ) which then cleaves phosphatidylinositol 4,5-bisphosphate (PIP2) into inositol trisphosphate (IP3) and diacylglycerol (DAG), activating the IP3 second messenger system (Hanlon and Andrew, 2015). Whilst DAG remains at the cell membrane (and activates protein kinase C (PKC)), IP3 diffuses into the endoplasmic reticulum (or the sarcoplasmic reticulum in muscle cells) and triggers the opening of Ca^{2+}channels thus increasing cytoplasmic Ca^{2+}. Gαq activity can be measured by measuring the by-products of IP3 signalling such as inositol monophosphate (IP1) or downstream transcription factors such as NFAT-RE (Hanlon and Andrew, 2015, Wettschureck and Offermanns, 2005, Cheng et al., 2010).

Canonical Gα driven signalling is deactivated when the GTP bound to Gα is hydrolysed back to GDP by the Gα, a process enhanced by Regulator of G protein

signalling (RGS) proteins. This inactivates Gα and leads to the re-association of the heterotrimeric G protein complex (McCudden et al., 2005). At the same time, GPCR kinases (GRKs) phosphorylate the C-terminal tail of activated GPCRs, which recruits β-arrestins (Luttrell and Lefkowitz, 2002). β-arrestin binding to the GPCR blocks further GPCR-heterotrimeric G protein coupling and induces receptor internalisation through clathrin-mediated endocytosis (Goodman et al., 1996, Lefkowitz, 2007). In addition to this role, β-arrestins can also regulate non-GPCR associated signal transduction by regulating mitogen-activated protein kinase such as ERK, JNK, and Akt (DeWire et al., 2007). Lastly, following receptor internalisation and endosomal processing, the receptor is recycled back to the cell surface without the bound ligand and becomes available for repeat activation. A graphical representation of canonical GPCR signalling is presented in Figure 1.4.

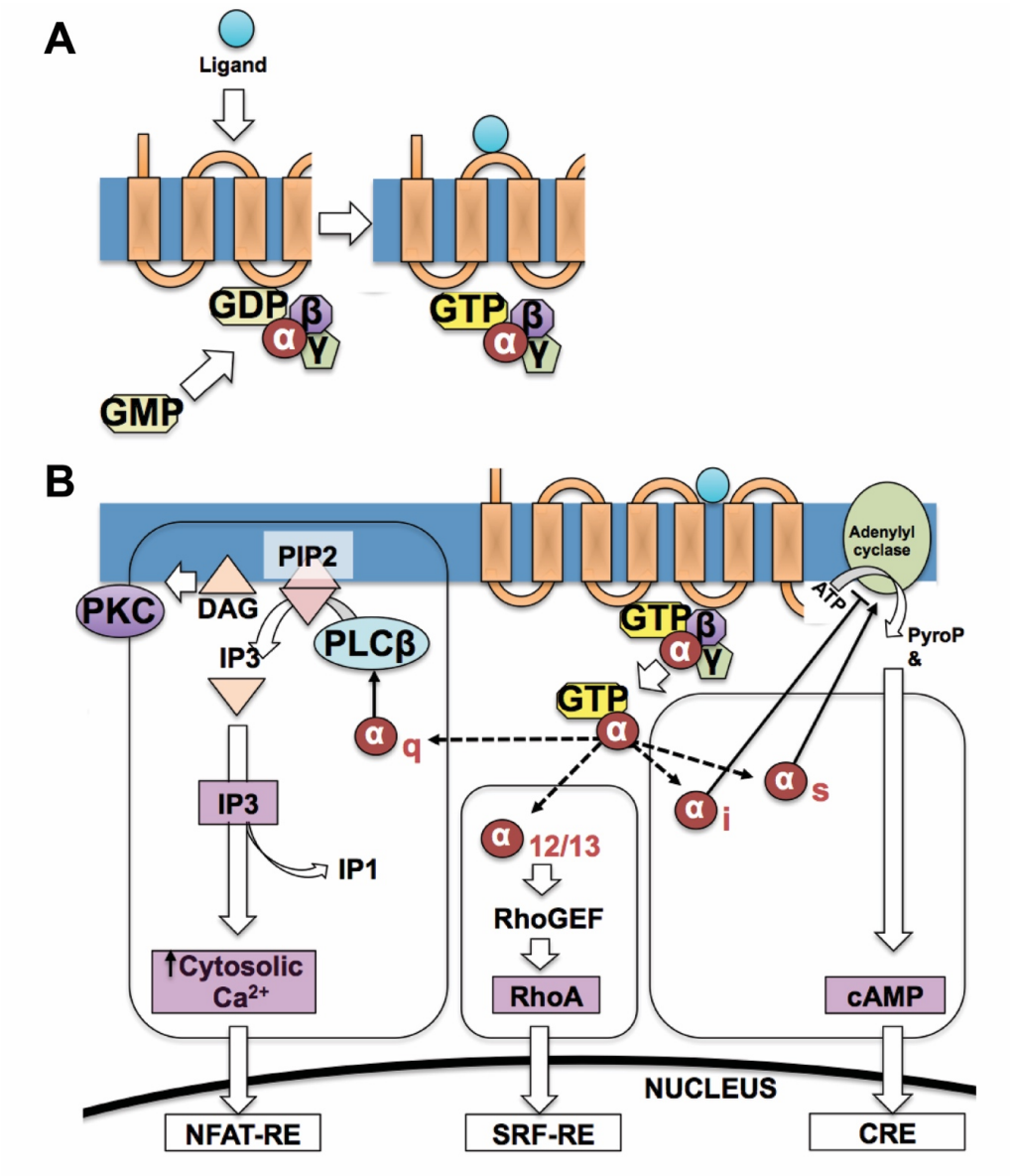


Figure 1.4: Graphical representation of canonical GPCR signalling. A) GPCR signalling is initiated by the binding of an agonist ligand to the extracellular surface of the receptor's 7TM, triggering a conformation change in the GPCR which allows the GPCR to bind a heterotrimeric G protein complex comprising of Gα, Gβ and Gγ subunits. In the non-active state, Gα is bound to guanosine diphosphate (GDP) but upon GPCR activation, Gα swaps the GDP for guanosine triphosphate (GTP) which forms guanine triphosphate (GTP). **B)** The heterotrimeric G protein complex disassociates and canonical GPCR signalling is initiated through the activated of the Gα subunit, dependent on the four main types of Gα. Gαs activates adenylyl

cyclase in the cell membrane which activates production of the second messenger cyclic adenosine monophosphate (cAMP) from adenosine triphosphate (ATP). Gαi inhibits this second messenger. CRE is a transcriptional factor downstream of both Gαs and Gαi. Gα12/13 activates Rho guanine nucleotide exchange factors (RhoGEF) which activates the RhoA second messenger pathway. SRF-RE is a transcriptional factor downstream of this pathway. Gαq activates the β isotype of phospholipase C (PLCβ) cleaving phosphatidylinositol 4,5-bisphosphate (PIP2) into inositol trisphosphate (IP3) and diacylglycerol (DAG). IP3 activates the IP second messenger system leading to an increase in intracellular Ca^{2+} (of which inositol monophosphate (IP1) is a by-product) whilst DAG activates protein kinase C (PKC). NFAT-RE is a transcriptional factor downstream of this pathway.

1.4 Adhesion GPCR signalling and the Stinger/Stachel Hypothesis

Until recently, adhesion GPCR signalling remained poorly characterised as the majority of receptors are orphans with no known agonist. Over the past few years, researchers have noted that a number of N-terminally truncated adhesion GPCRS are constitutively active when the truncation occurs at the consensus GPS cleavage domain. This was first shown with ADGRB2/BAI2 (Okajima et al., 2010) and later with ADGRG1/GPR56 (Paavola et al., 2011), ADGRL1/LPHN1 (Promel et al., 2012), ADGRB1/BAI1 (Stephenson et al., 2013), and ADGRG6/GPR126 (Paavola et al., 2014). However, despite these findings, the mechanism behind this auto-activation remained unknown and contested with the mechanism being hypothesised that the NTF suppressed the activity of the 7TM domain (termed the allosteric antagonist model) (Kishore and Hall, 2016). This changed when Liebscher and colleagues proposed a hypothesis detailing artificial adhesion GPCR activation which was validated in both ADGRG6/GPR126 and ADGRD1/GPR133 (Liebscher et al., 2014). This hypothesis, termed the Stinger/Stachel Hypothesis, has since revolutionised the adhesion GPCR signalling field.

The Stinger/Stachel Hypothesis proposed that all expressed adhesion GPCRs (except GPR123) contain a short 10-20 amino acid long tethered agonist C-terminally to the GPS cleavage site which is essential for adhesion GPCR activation through its action of striking the 7TM receptor loops and initiating signalling (the stinging action of a bee being the metaphor behind the name; “stachel” is German for sting). Liebscher furthermore hypothesised that to expose and activate this tethered agonist, the full length adhesion GPCR requires a form of N-terminal modification. This is proposed to occur either by the receptor’s NTF being pulled off

from the CTF or merely through changing conformation after binding of an interacting partner, resulting in the exposure of the tethered agonist at the NTF end of the CTF (Liebscher et al., 2014). The exposed tethered agonist (termed the Stinger/Stachel sequence) is then able to strike and interact with the extracellular loops of the 7TM domain initiating canonical GPCR signalling.

Additionally, the hypothesis proposes that no signalling will occur in either a mutated adhesion GPCR with no extracellular domain (no NTF; and CTF comprising only of the 7TM) or a mutated adhesion GPCR with mutated tethered agonist. If one applies soluble peptides (Stinger/Stachel peptides) analogous to the tethered agonist region to the cell culture medium, one may rescue the signalling ability of the adhesion GPCR via the ability of the peptide to bind the 7TM. Figure 1.5 presents a graphical overview of the Stinger/Stachel hypothesis.

Since its publication, the Stinger/Stachel hypothesis has been employed to solve the canonical GPCR signalling and activation of a number of adhesion GPCRs. These are presented in Table 1.1. Recently, results have revealed that at least one adhesion GPCR (ADGRG1/GPR56) is able to signal when only consisting of the 7TM (termed ‘stalk-less signalling’ by the authors) (Kishore et al., 2016). This remains to be proven for other adhesion GPCRs but suggests that there may be multiple ways of activating adhesion GPCRS through NTF modification. As ELTD1’s signalling remains unknown, the Stinger/Stachel Hypothesis provides a prime opportunity to investigate ELTD1’s signalling capability.

Adhesion GPCR	Signalling modality	Reference
ADGRG6/GPR126	Gαs	(Liebscher et al., 2014)
ADGRD1/GPR133	Gαs	(Liebscher et al., 2014)
ADGRG1/GPR56	Gα12/13; Gαi	(Stoveken et al., 2015)
ADGRF1/GPR110	Gαq	(Stoveken et al., 2015)
ADGRG5/GPR114	Gαs	(Wilde et al., 2016)
ADGRG2/GPR64	Gαs	(Demberg et al., 2015)
ADGRL1/LPHN1	Gαs	(Muller et al., 2015)
ADGRB1/BAI1	Gα12/13, Gαq	(Kishore et al., 2016)
ADGRG1/GPR56	Gα12/13, Gαq	(Kishore et al., 2016)
ADGRF5/GPR116	Gαq	(Brown et al., 2017)

Table 1.1: List of adhesion GPCRS whose signalling and activation mechanisms have been solved using the Stinger/Stachel hypothesis.

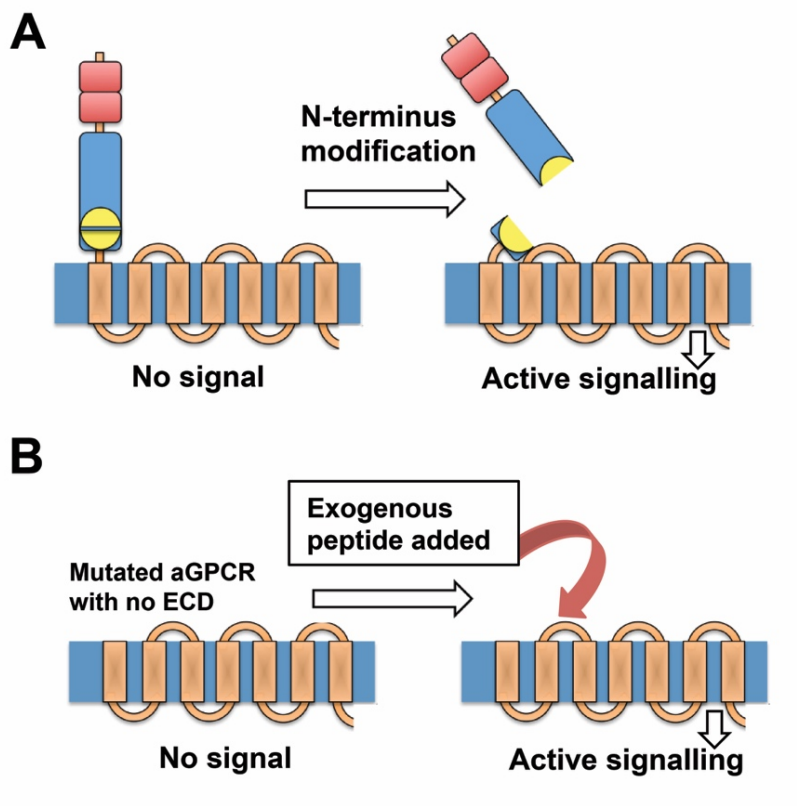


Figure 1.5: Graphical representation of the Stinger/Stachel tethered agonist hypothesis. A) The Stinger/Stachel hypothesis proposes that each adhesion GPCR contains a tethered agonist C-terminally to the GPS cleavage site (yellow semi-circle in the diagram). To activate this tethered agonist, the receptor requires a form of N-terminal modification such as ligand binding or binding to another cell. This exposed tethered agonist is then able to strike the extracellular loops of the 7TM domain initiating canonical GPCR signalling. **B)** The hypothesis further proposes that a receptor without a functional tethered agonist (i.e. a receptor without any extracellular domains or a receptor with a mutated tethered agonist) will not signal. The hypothesis proposes that signalling can be rescued if the receptor is exposed to soluble peptides analogous to the tethered agonist amino acid sequence. (Abbreviation: aGPCR=adhesion GPCR; ECD=extra-cellular domain)

1.5 ELTD1 and its role in angiogenesis and cancer

Strictly speaking, angiogenesis refers to the development of new blood vessels from a pre-existing source vessel or circulatory system (Jain, 2005). In the developing mammalian embryo, the formation of the circulatory system (vasculogenesis) occurs when progenitor endothelial cells called angioblasts differentiate into endothelial cells and form a primitive vascular network (Swift and Weinstein, 2009). This vascular network then differentiates into venous and arterial components through the activation of Notch signalling (Kangsamaksin et al., 2014). The Notch pathway is an ancient pathway which has been found to have a relationship with ELTD1 with both ELTD1 and the Notch ligand Delta-like protein 4 (DLL4) being shown to antagonise each other (Masiero et al., 2013). The growth of the developing vascular network occurs through new expansions (angiogenesis), which all originate from the existing network. The most studied mode of vessel expansion is termed sprouting angiogenesis whereby endothelial cells leave a pre-existing vessel under the guidance of growth factor and pro-angiogenic cues and form a new vessel which ultimately connects a new territory with the vessel they arose from. Intussusception is another mechanism of new vessel formation and occurs when a vessel splits into two producing two daughter vessels (Carmeliet and Jain, 2011a). Pathological angiogenesis within the tumour microenvironment is a hallmark of cancer with highly upregulated non-coordinated sprouting angiogenesis being highly upregulated (Hanahan and Weinberg, 2011). Additionally, tumour cells may co-opt new vessels (a process termed vessel co-option) or line new vessels themselves instead of endothelial cells (termed vascular mimicry) (Carmeliet and Jain, 2011a).

Sprouting angiogenesis is triggered and initiated by the release of angiogenic signals such VEGF-A or fibroblast growth factor (FGF) from hypoxic tissues. VEGF-A acts as a chemoattractant to endothelial cells, initiating endothelial cell migration towards the source of VEGF-A production (Benedito et al., 2009). Endothelial cells at the leading edge of this migration display a specific phenotype termed the 'tip cell' phenotype. This phenotype includes being migratory and invasive, having no lumen or any perfusion, not being highly proliferative (compared to the non-tip endothelial cells) and expressing long filopodia which allow the endothelial cell to follow the VEGF guidance gradient and microenvironment growth factor signals (Gerhardt et al., 2003, Benedito et al., 2009).

The leading edge of endothelial tip cells is followed by a train of proliferating endothelial cells, which will ultimately form the stalk of the new vessel. These endothelial cells exhibit their own unique phenotype which is induced by the leading edge tip cells and functions through activation of Notch signalling (Carmeliet and Jain, 2011b). These cells are termed stalk cells because their phenotype produces the process of tubulogenesis, which refers to the formation of patent, perfusable vessels (Benedito et al., 2009). In contrast to tip cells, stalk cells do not express long filopodia and they enclose a luminal space, and they are highly proliferative in order to elongate the growing vessel (Gerhardt et al., 2003, Benedito et al., 2009, Carmeliet and Jain, 2011a).

The tip cell phenotype is activated by VEGF signalling (Gerhardt et al., 2003), whilst the stalk phenotype is maintained through Notch signalling initiated by tip cells activating the Notch receptors in adjacent columns of stalk cells (Phng and

Gerhardt, 2009). Interestingly, these phenotypes are not permanent and are dependent on the VEGF gradient with endothelial cells continuously competing for tip cell position (Jakobsson et al., 2010). Inhibition of the Notch ligand DLL4 or deletion of the Notch receptor NOTCH1 inhibits Notch signalling in endothelial cells and induces a hypersprouting phenotype through an increase in the number of endothelial cells assuming the tip cell phenotype (Hellstrom et al., 2007, Thurston et al., 2007). These vessels however are poorly perfused as their stalk element fail to adequately develop leading to worsening hypoxia (Thurston et al., 2007). Overexpression of DLL4 and Notch signalling in endothelial cells induces failure of tip cell formation and with endothelial cells instead acquiring the stalk cell phenotype leading to a reduction in vasculature formation (Segarra et al., 2008). However, the induction of increased endothelial DLL4 expression is a strategy used by some tumour types (Patel et al., 2005). In such cases, downregulation of DLL4 expression induces a decrease in endothelial proliferation, migration and network formation (Patel et al., 2005). That said, the tumour benefits from high level of DLL4 expression are probably finely tuned within a specific range of expression and any expression over this limit negatively affects the cell. This is highlighted by the finding that retrovirus induced DLL4 overexpression in endothelial cells and tumour cells *in vivo* led to reduced tumour vascularisation and perfusion and increased hypoxia (Segarra et al., 2008).

ELTD1 expression was first noted to be expressed in rat bronchiolar and vascular smooth muscle cells and in both rat and human cardiomyocytes (Nechiporuk et al., 2001). In 2008, two separate studies found *ELTD1* to be part of the normal endothelial transcriptome in humans (Herbert et al., 2008) and mice (Wallgard et

al., 2008) respectively. In 2012, a study aiming to characterise the transcriptome of blood vessels associated with grade IV glioblastoma, found *ELTD1* to be one of 95 genes upregulated in these vessels (Dieterich et al., 2012). The same study found that VEGF-A and TGF-β2 upregulated *ELTD1* expression in these vessels but did not specifically associate ELTD1 as a regulator of angiogenesis (Dieterich et al., 2012). In early 2013, a gene array performed on human endothelial cells exposed to the anti-angiogenic compound Aeroplysinin-1 (an antibiotic produced by sea sponges) revealed a slight decrease in *ELTD1* expression, confirmed with Western blotting (Martinez-Poveda et al., 2013). Similarly, this study did not associate ELTD1 with angiogenesis. Independently of these studies, our laboratories identified *ELTD1* as a novel regulator of both physiological and tumour angiogenesis using a bioinformatics screen for previously uncharacterised genes associated with angiogenesis. This result was then functionally validated *in vitro* and *in vivo* (Masiero et al., 2013).

Results revealed that when compared to matched normal endothelial cells, ELTD1 expression was upregulated in tumour-associated endothelial cells in head and neck, renal, colorectal and ovarian cancer (Masiero et al., 2013). In addition to its expression in tumour associated endothelial cells, ELTD1 was also found to be highly expressed in vascular smooth muscle cells. ELTD1 was also regulated by two key angiogenic ligands, namely VEGF, upregulating ELTD1, and the Notch ligand DLL4, downregulating ELTD1 (Masiero et al., 2013). VEGF's effect on ELTD1 validated previous findings in glioblastoma-associated vessels where ELTD1 and DLL4 were also found to antagonise each other (Dieterich et al., 2012).

Additionally, ELTD1 silencing was shown to affect the likelihood of HUVECS taking up the tip cell phenotype (Masiero et al., 2013).

Furthermore, ELTD1 silencing using RNA interference in human umbilical vein endothelial cells (HUVECS) revealed greatly decreased levels of sprouting angiogenesis activity. This demonstrated ELTD1's important role in sprouting angiogenesis. Additionally, through use of the zebrafish (*Danio rerio*) embryo, eltd1 was shown to be important in vasculogenesis. In this model, eltd1 silencing using morpholinos prevented effective intersegmental vessel formation from the dorsal aorta leading to embryonic lethality (Masiero et al., 2013).

When human ovarian and colorectal tumour xenografts where implanted into mice, systemic *Eltd1* silencing in the murine stroma was found to substantially inhibit tumour growth. In addition to having smaller and fewer tumours, *Eltd1* silenced mice survived longer and had far fewer sites of metastasis when compared to controls. No significant toxicity was observed as body weight and heart to body weight ratios were unaffected.

Additionally, high tumour-associated endothelial cell ELTD1 expression was shown to correlate with improved overall survival (OS) in patients who subsequently went on to receive anti-cancer therapy in a number of cancer types, namely: head and neck squamous carcinoma, renal, colorectal and ovarian cancers. These findings

implicated ELTD1 as a putative prognostic marker of favourable outcome for these cancers types when treated with chemotherapy.

In terms of cancer cell expression, our laboratories noted that although ELTD1 was mostly expressed within the tumour vasculature, a minority of head and neck squamous carcinoma, renal, colorectal and ovarian cancers were found to express ELTD1 in the tumour cells, but at a lower intensity than seen in the vasculature. In contrast, ELTD1 has been shown to be highly upregulated in glioblastoma tumour cells and has been proposed as biomarker for this cancer type (Towner et al., 2013). Additionally, in glioblastoma cell lines, microRNA-139-5p was found to suppress ELTD1, inducing a decrease in cell proliferation and an increase in apoptosis (Dai et al., 2015a). In line with this result, ELTD1 was shown to be important for glioblastoma cell survival, with *ELTD1* mRNA silencing showing increasing glioblastoma cell death *in vitro* and *in vivo* (Serban et al., 2017, Ziegler et al., 2017).

In other tumours, *ELTD1* has been shown to be part of a group of nine genes upregulated in patients with ulcerative colitis harbouring an occult colorectal cancer (Pekow et al., 2013). More recently, *ELTD1* has been shown to be part of a group of 19 genes associated with colorectal cancer survival. In this series, higher *ELTD1* expression correlated with poorer survival (Abdul Aziz et al., 2016). This result goes against the original finding from our laboratories and will need to be further investigated.

Despite these advances in our understanding of ELTD1, many unanswered questions remain. These include how ELTD1 induces its effect on sprouting angiogenesis and whether it interacts or affects any other genes associated with angiogenesis. Additionally, the effect of ELTD1 overexpression remains unknown. Does it produce opposite changes to those seen with ELTD1 silencing? Furthermore, as Notch signalling is an important component of angiogenesis, it remains to be seen whether ELTD1 affects any other Notch genes in addition to DLL4. Within the tumour microenvironment, the question of whether ELTD1 has differing roles and expression profiles within the primary and secondary tumour microenvironments remains to be investigated. Additionally, the question as to why glioblastomas highly express ELTD1 whilst the majority of other cancer types do not remains unanswered.

1.6 Other roles for ELTD1

Other groups have shown Eltd1 expression to be important in rodent cardiomyocyte development (Nechiporuk et al., 2001), and in protecting against pathological hypertrophy in response to increased major vessel pressure loading in mice (Xiao et al., 2012). It should be noted that in this knockout model it is predicted that the Eltd1 NTF will still be present. This study also found that failed, hypertrophied human hearts in patients awaiting cardiac transplantation had significantly lower cardiac ELTD1 expression than healthy controls (Xiao et al., 2012). In this context, *ELTD1* polymorphisms have been found to be positively selected in a cohort of high-altitude living Andean people, possibly as a cardio-protective measure against lifelong low oxygen induced increased cardiac effort (Eichstaedt et al., 2014). This

cohort was also found to have an additional muscle layer in their pulmonary arteries (Eichstaedt et al., 2014).

Linkage analyses conducted to determine genes conferring vulnerability to cannabis use revealed that *ELTD1* (amongst other genes) may be associated with the genetic risk for cannabis use disorders (Agrawal et al., 2008). Additionally, a meta-analysis of nine genome-wide association studies (GWAS) revealed that an intergenic single nucleotide polymorphism (SNP) affecting *ELTD1* (rs11162963) was associated with an increase in event-free longevity (Walter et al., 2011). In contrast to this, a GWAS in African American patients revealed that an intergenic SNP affecting *ELTD1* (rs1937787) was one of 18 genetic variants implicated with greater risk of stroke (Carty et al., 2015). Additionally, an *ELTD1* SNP has been identified in cattle who are resistant to therapy against tick parasites (intergenic SNP rs29019303) (Porto Neto et al., 2011) and in patients at risk of developing graft versus host disease following haemopoietic stem cell transplants (Harkensee et al., 2013). *ELTD1* has also been described as one of eight genes responsible for subcutaneous fat thickness in both humans and pigs (Lee et al., 2011). Lastly, in the white perch fish (*Morone americana*), *Eltd1* was one of 4 genes found to be upregulated following exposure to the hormone 17β-estradiol (Schilling et al., 2015). In all these cases however, the mechanisms underlying ELTD1's association remain to be identified and suggest a wider role for ELTD1 within mammalian cell biology.

1.7 Aims

The aim of this thesis is to better understand ELTD1's functional role within its cellular context, with the long term goal of bringing ELTD1 targeted anti-cancer therapy into clinical use.

This thesis thus has the following aims centred around four themes:

1. ***ELTD1*'s evolution**
    - To investigate *ELTD1*'s evolution and conservation across extant species and conservation and contrast this to an established angiogenesis gene.
    - To investigate whether *ELTD1* has lost or gained any domains during its evolution (and if so, when?) and whether this informs on ELTD1's function.
    - To investigate and compare *ELTD1's* sequence to other adhesion GPCRS and to determine whether *ELTD1* is ancestral to other adhesion GPCRS.

2. **ELTD1's signalling**
    - To investigate ELTD1's signalling using the Stinger/Stachel Hypothesis and truncated forms of ELTD1
    - To investigate whether ELTD1's Stinger/Stachel amino acid sequence can be used as a functional soluble agonist for the receptor.

3. **ELTD1's roles within endothelial biology**

    - To investigate the transcriptional effect of ELTD1 silencing in HUVECS. Can this yield new roles for ELTD1 within endothelial biology?
    - To investigate the transcriptional and functional effect of ELTD1 overexpression in HUVECS. Similarly, can this yield new roles for ELTD1.

4. **ELTD1 within the primary breast tumour and regional lymph node metastasis microenvironment**

    - To investigate whether vascular ELTD1 is differentially expressed between primary breast cancer and regional lymph node metastases?
    - To investigate whether vascular ELTD1 expression in primary and regional nodal metastasis correlates with any biological variables
    - To investigate whether breast cancer cells express ELTD1 and if so, whether there is any differential ELTD1 expression between primary tumour and regional node metastases or any correlation between tumour cell ELTD1 expression and other biological variables?

Chapter 2: Materials and methods

2.1 Bioinformatics and statistical analyses

2.1.1 Evolutionary biology

ELTD1's evolutionary bioinformatics work was performed using the Ensembl database of publically available sequenced genomes (Ensembl version 88) (Flicek et al., 2014) and BioMart (Guberman et al., 2011). All nucleotide coding sequences and protein sequences as well as similarity comparisons between human ELTD1 and VEGFR2 and its orthologues were extracted from Ensembl and Biomart, as were exome-exome sequence comparisons. All sequence alignment was performed using Clustal Omega (McWilliam et al., 2013) using either nucleotide or amino acid sequences as stated. Amino acid conservation scores were performed using Jalview (Waterhouse et al., 2009) using a quantitative method taking into account the physico-chemical properties of each aligned column (Livingstone and Barton, 1993). Phylograms and cladograms were computed from the Clustal outputs and arranged using Dendroscope (Huson and Scornavacca, 2012). Conserved domain searches were performed using SMART (Letunic et al., 2015), Motif Finder (Kanehisa et al., 2017), and InterPro (Finn et al., 2017). Evolutionary timetree data was extracted from the Timetree.org database (Hedges et al., 2015) and edited using dendropscope. Orthologues and homologues of all interrogated

genes in extant organisms were extracted from the Ensembl and KEGG genome databases (Kanehisa et al., 2017).

2.1.2 Codon optimisation

GC content, codon usage analysis and codon optimisation were all performed using the JCat bioinformatics package (Grote et al., 2005). For GC content comparison between ELTD1 and all adhesion and secretin GPCRs the following was performed: each receptor's FASTA nucleotide sequence was accessed using the UNIPROT database (Magrane and Consortium, 2011). For this, UNIPROT's canonical sequences were used. JCat was then used to determine the GC% for each receptor. Receptor results were then ranked and graphed.

2.1.3 Construct design

Untagged codon optimised full length ELTD1 was exported from JCat and translated into amino acid acid form using Transeq (McWilliam et al., 2013). This sequence included the signal peptide sequence which was determined using the SignalP4.0 algorithm (Petersen et al., 2011). Conserved domains were mapped onto the amino acid sequence using the mean from two algorithms: SMART 2015 (Letunic et al., 2015) and NCBI Conserved Domain Search (Marchler-Bauer et al., 2015). This data was then mapped onto the codon optimised nucleotide sequence. ELTD1's signal peptide was determined using SignalP 4.0 (Petersen et al., 2011) and was used as the signal peptide for all subsequent ELTD1 constructs. Using the domain-mapped nucleotide sequence, the CTF construct was designed to contain ELTD1's sequence C-terminal to the GPS cleavage site (HL<cleave>THFAL…).

The 7TMΔ construct was designed to contain only the 7TM domain as predicted with SMART (Letunic et al., 2015) and the conserved domain database (Marchler-Bauer et al., 2015). As regards tagging, HA (N-terminal) and Flag (C-terminal) tags were added to one series of constructs and GFP (C-terminal) tag was added to the second series of constructs. All constructs were synthesised by Biomatik. Constructs were then cloned individually into pcDNA3.1 plasmid vectors. (The Appendix contains the full nucleotide and amino acid sequences for each construct).

2.1.4 Stinger/Stachel Peptide design

ELTD1's Stinger/Stachel Peptides were designed using the mapped ELTD1 nucleotide and protein sequence maps (described above in the construct design section). Peptides were designed to correspond to the amino acid sequence beginning at the consensus GPS cleavage site and extending C-terminally to the predicted start of the first 7TM membrane loop. The first ELTD1/Stinger peptide comprised the first four amino acids C-terminal to the GPS cleavage site with each subsequent peptide being extended by an additional amino acid. Peptides were synthesised and produced to a high purity (>90%) by Biomatik.

2.1.5 Microarray analysis

ELTD1 silencing and overexpression microarrays were analysed using the R environment (version 3.3.2). Microarrays were performed by reverse transcribing extracted mRNA into cDNA, and labelling the cDNA and then hybridising the labelled target to the microarray chip. Raw data outputted from the Illumina microarray scanner (Illumina iScan) using the HumanHT-12 v4 Expression

BeadChip Kit was analysed using “Limma” (Smyth, 2004) were it was pre-processed and normalised before undergoing linear modelling and contrast comparison. Differentially expressed genes were deemed statistically significant only if they fulfilled standard microarray criteria: i) an adjusted *p* value < 0.05; and ii) a fold change of > 2 < -2. For volcano plots, “GGplot2” was used (Wickham, 2009). For Heatmaps, “Morpheus” was used (https://github.com/cmap/morpheus.R). Other tools used for the analysis or visualisation of data include “dplyr” and “ggrepel”. Venn digrams were performed in R. The full R scripts for all microarray analyses are included in the Appendix. All microarray experiments are MIAME compliant (Brazma et al., 2001)

Pathway analysis was performed using “Enrichr” (Kuleshov et al., 2016) “KEGG” (Kanehisa et al., 2017), “Reactome” (Croft et al., 2014), “Wikipathways” (Kutmon et al., 2016) and “BioCarta” (Nishimura, 2001). The false discovery rate threshold was set to 0.05.

2.1.6 ELTD1 in cancer

ELTD1’s mutational profile as well as that of *KRAS* was extracted from the public database containing 4742 exome sequenced human tumours from 21 tumour types, available at tumorportal.org (Lawrence et al., 2014). *ELTD1’*s alteration frequency was interrogated across 48 curated cancer-genome datasets using the c-bioportal platform (Cerami et al., 2012). Lastly, *ELTD1*’s transcript expression within cancer cell lines was interrogated using the Broad Institute’s publically available “Cancer

Cell Line Encyclopedia" dataset (NCBI accession: GSE36133) (Barretina et al., 2012).

2.1.7 Statistical analyses using Prism

Prism 7 (Graphpad Software) was used to analyse results from all completed wet-lab experiments. For comparison of two groups, the Student's *t*-test was used. For unpaired data, an unpaired Student's *t*-test was performed whilst the paired Student's *t*-test was performed for paired or matched data. For comparison of two or more groups, a one-way ANOVA was computed. Lastly, Kaplan-Meier survival analyses were computed for all survival comparisons. Significance is denoted as: * $p \leq 0.05$, ** $p \leq 0.01$, *** $p \leq 0.001$, **** $p \leq 0.0001$.

2.2 Cell lines and maintenance

2.2.1 Cell culture

All cells were cultured in tissue culture incubators at a constant temperature of 37°C and with a humidified atmosphere of 5% CO_2 and 95% filtered atmospheric air. Cells were cultured on sterile, tissue culture grade, plastic cell culture ware (Corning). Culture medium used is presented in the cell line section.

2.2.2 Cell maintenance

Cells were passaged once 70-90% confluent. Passaging was performed by aspirating medium, washing the adherent cells with phosphate buffered saline (PBS, composed of 10mM sodium phosphate, 137mM sodium chloride and 2.7mM

potassium chloride) followed by scraping cells off with cell lifters when using tissue culture plates, or adding 1x trypsin-ethylenediaminetetraacetic acid (EDTA, Invitrogen) for 5 minutes until fully detached when using tissue culture flasks. Trypsin-EDTA was neutralised by adding 10% fetal calf serum (FCS). Cells were then centrifuged for 3 minutes at 1000g to yield a pellet which was then re-suspended in fresh medium, and then split 1:5 and reseeded. Medium was changed every 48 hours.

2.2.3 Cell lines used

Primary Human Umbilical Vein Endothelial Cells (HUVECs) pooled from multiple donors were purchased from Lonza. These were cultured in sterile flasks at 37°C in Endothelial Basal Medium 2 (EBM-2) (Lonza) supplemented with Endothelial Growth Medium 2 (EGM-2) (Lonza) as per the manufacturer's instructions. Medium was changed every 48 hours. Cells were used for experiments between passage 3 and 6 to retain their primary endothelial cell phenotype.

Human Embryonic Kidney 293 cells expressing the large T antigen (HEK293T) were purchased from Thermo Scientific and were cultured in Dulbecco's modified Eagle's medium (DMEM) supplemented with 10% FCS and 1% L-glutamine (Lonza). Medium was changed every 48 hours.

The GloResponse NFAT-RE-luc2P HEK293 Cell Line (Promega) (HEK293 cells stably expressing NFAT luciferase) was received as a gift from Heptares Therapeutics and was cultured in DMEM supplemented with 10% FCS and 1% L-glutamine (Lonza). Medium was changed every 48 hours.

COS-7 cells were purchased from ATCC and were cultured in DMEM supplemented with 10% FCS and 1% L-glutamine (Lonza). Medium was changed every 48 hours.

All cancer cell lines used (MDA-MB-468, MDA-MB-231, MCF7, BT-20, BT-549, T-47D, BT-474, PC-3, DU 145, HCT 116, SW48 and SU-DHL-10) were obtained from ATCC. SU-DHL-10, BT-549 and T-47D lines were cultured in RPMI supplemented with 10% FCS (Lonza). BT-474 was cultured in a 1:1 mix of DMEM and Ham's F12 Medium supplemented with 10% FCS (Lonza). MCF7, BT-20 and DU 145 lines were cultured in DMEM supplemented with 10% FCS and 1% L- glutamine (Lonza). HCT 116 was cultured in McCoys's 5a Medium Modified, supplemented with 10% FCS (Lonza). SW48, MDA-MB-231 and MDA-MB-468 lines were cultured using Leibovitz L-15 Medium, supplemented with 10% FCS (Lonza). PC-3 was cultured in Ham's F-12K (Kaighn's modification) Medium, supplemented with 10% FCS (Lonza). For all cell lines, medium was changed every 48 hours.

2.2.4 Cell counting

All cell counting was performed using a Cellometer Auto T4 cell counter (Nexcelcom Bioscience) as per the manufacturer's instructions. This entailed pipetting 20µL of cell suspension onto a Cellometer counter chamber (Nexcelom) and having the Cellometer machine analyse the chamber. The cell suspension was then diluted to the required concentration and seeded.

2.2.5 Freezing and thawing cells

For long term storage, cells were harvested, trypsinised, pelleted and then re-suspended in appropriate culture medium mixed with FCS (Invitrogen) and Dimethyl sulfoxide (DMSO, Sigma-Aldrich) at volume ratio of 6:3:1 before being transferred into a cryovial (Corning). To prevent initial freeze associated damage to cells, Cryovials were temporarily transferred into a Mr. Frosty^{TM} Freezing Container (Thermo Fisher Scientific) for 24 hours and placed in a -80°C freezer. Following 24 hours, all cryovials where removed from the freezing container and transferred to liquid nitrogen storage.

Thawing entailed removing cryovials from the liquid nitrogen storage tanks and incubating the cryovials in a 37 °C water bath for 2 minutes. Once thawed, the cell suspension was then immediately transferred into a 10mL of pre-warmed appropriate cell culture medium and centrifuged for 3 minutes at 1000g. The old medium was then aspirated out, and the cell pellet was then re-suspended in 30ml of appropriate new warmed medium and transferred into a T175 flask (Corning). Cells were used for experiments following one passage.

2.3 Protein analysis

2.3.1 Protein extraction and measurement

Cells were first washed with cool PBS (cooled in ice) and were scrapped off the plate in RIPA buffer (Sigma) containing a protease inhibitor (Roche). Samples were kept on ice for ten minutes and then centrifuged at 12 000 g for 10 minutes at 4°C. Supernatants were collected and protein was measured using the Bradford assay

(BioRad) with absorbance measured at 595nm using a μQuant microplate reader (Bio-Tek). Protein concentration was calculated based on a standard curve prepared for each assay using a serial dilution of 2mg/ml bovine serum albumin (Sigma). Protein was stored at -20°C.

2.3.2 Western blotting: SDS-PAGE electrophoresis and transfer

Protein samples were prepared for electrophoresis by adding appropriate amounts of sample buffer (NuPAGE LDS Sample Buffer (4x) (Invitrogen)), sample reducing agent (NuPAGE Sample Reducing Agent (10x) (Invitrogen)) and heated to 60°C for 10 minutes. Equal amounts of each protein sample were then loaded into a 4-12% Bis Tris polyacrylamide gel (Invitrogen) which then underwent electrophoretic separation at 130 V for 1.5 hours. Following this, proteins were transferred from the gel onto a polyvinylidene difluoride (PVDF) membrane (Millipore) using the Novex semi-dry blotter device (Invitrogen).

2.3.3 Western blotting: probing

Following semi-dry transfer, the PVDF membrane was incubated in a blocking solution comprising 5% milk in PBS / 0.1% tween 20 (PBS-T) for 1 hour at room temperature. Following this, primary antibodies were added for overnight incubation at 4°C. Following this, the membrane was washed three times with PBS-T and incubated with the appropriate secondary antibody for 1 hour at room temperature and followed by washing three times with PBS-T. Primary and secondary antibodies are listed in Table 2.1.

2.3.4 Western blotting: Detection

Membrane immunoreactivity was detected using the ECL Prime chemiluminescent reagent system (GE Healthcare), according to the manufacturer's instructions. Visualisation was performed using the ImageQuant LAS4000 digital imaging system (GE Healthcare).

Target	Dilution	Company (Product code)
Primary antibodies		
ELTD1 (produced in rabbit)	1:1000	Sigma (HPA025229)
β-actin conjugated to horseradish peroxidase (HRP)	1:10000	Sigma (3854)
Secondary antibodies:		
Anti-rabbit conjugated to HRP	1:2500	DAKO (P044801-2)

Table 2.1: Antibodies used for Western blotting.

2.4 RNA analysis

2.4.1 RNA extraction

RNA was extracted using the RNeasy Mini Kit (Qiagen) according to the manufacturer's guidelines. In brief, cells were harvested following two washes with ice-cooled PBS. Following this, cells were lysed with 350 µL of the kit's lysis buffer. Following this, 70% ethanol was added with the total volume applied to a RNA binding column. Columns were centrifuged, washed and the incubated with DNAse for 15 minutes at room temperature. Following this, the columns were further washed before DNA was eluted in RNAse free water. RNA samples were stored at -20°C.

2.4.2 RNA quantification

RNA quantification was performed using a NanoDrop 1000 spectrophotometer (NanoDrop Technologies) measuring absorbance at 260 nm.

2.4.3 Generation of cDNA

Reverse transcription was performed using the High Capacity cDNA Reverse Transcription kit (Applied Biosystems) according to the manufacturer's guidelines. In brief, reverse transcription buffer (1x), random primers (1x), 4 mM deoxynucleotide triphosphates (dNTP), 5 units of reverse transcriptase enzyme, diethyl pyrocarbonate (DEPC) treated water and 2000 ng of RNA were added to each reaction, totalling 10µL. For thermal cycling, a LabCycler (SensoQuest) was used. The cycle used was: 10 minutes at 25°C, followed by 2 hours at 37°C, followed by 5 minutes at 85°C.

2.4.4 Real-time quantitative polymerase chain reaction (qPCR)

qPCR was performed using the SensiFAST SYBR No-ROX kit (Bioline) according to the manufacturer's specifications. qPCR primers (comprising both forward and reverse primers) were prepared in RNAase-free water to a concentration of 10 µM. *GAPDH* or *Actin* were used as housekeeping genes. qPCR primers were designed using Primer-BLAST (Ye et al., 2012) and were synthesised by Invitrogen. qPCR primers used are listed in Table 2.2. In brief, 2µL of cDNA was missed with 1x the SYBR master-mix. Respective gene primers were then added to a final volume of 10 µL. The final concentration of primers was 0.3 nM. Samples were run using the 7900HT Fast Real-Time PCR System (ThermoFisher) in a 384 well format with the following reaction profile: 50°C for 2 minutes, 95°C for 10 minutes, followed by 40 cycling runs of 95°C for 15 seconds and 60°C for 1 minute. This was followed by a final 95°C for 15 seconds and 60°C for 15 seconds. Following this, the raw threshold cycle (C_t) values were analysed using the 2–[delta][delta]C_t method to obtain fold changes (Pfaffl, 2001). *GAPDH* or *ACTB* were used as control housekeeping genes.

Gene name	Forward primer (5'-3')	Reverse primer (5'-3')
ACACA	AACGTGAAGACGGATAAGCAG	CTTCTTCGGAGAATCTGACCA
ACACB	AGTTCGCCGACTTCCAT	TCTTCCACTCCAGGATGTCA
ACHE	CTGCCTGTACCTCAACGTGT	TCATTGGGATCCCCTGTGC
ACHE	GGTGTGGTGAAGGATGAGGG	TCATTGGGATCCCCTGTGC
ACHE	GTCTGGCACTGGAACGCC	CCTCTGATCCAGGAGACCCA
ACHE	GGTGTGGTGAAGGATGAGGG	TCATTGGGATCCCCTGTGC
ACLY	CCAGCAGGACAGCATCTTTT	GGATCTTGGACTTGGGACTG
ACTB	ATGCTCTCCCTCACGCCATC	CACGCACGATTTCCCTCTCA
AFP	GAGGGAGCGGCTGACATTAT	CATGGCCTCCTGTTGGCATA
ALB	CACGCCTTTGGCACAATGAA	CATCGAGCTTTGGCAACAGG
ANTXR1	GACAAGGGTACAGGACAGCC	CTCCCCAACGAACCTCCATT
ANTXR1	TTTGAAAGGGCCAGTGAGCA	TCCCCGTTTTCAGGAGTGTG
ANTXR1	CCACACACTGTTCTGACGGT	GCACGGGCTGTGTTAGGTTA
APOA2	AGCCTTGAAGGAGCTTTGGTT	GGTGTCAGCTGCTCCTTTGA
CCL14	TCCTCACGGGGACCTTACC	GACAATTCCGGGCTTGGAG
CCL14	GGGGGAAACCGAAGGTTGTT	GTGATGAAGACAATTCCGGGC
CCL15	GCCCAGTTCACAAATGATGCAG	AACTCACAGGAGGTGTTGGAG
CD36	GTGCCTATTCTTTGGCTTAATGA	TTACTTGACTTCTGAACATGTTTGC

CHRNA1	GGACCTACGACGGCTCTGT	GCTCTCCATGAAGTTGCTCAG
CRYAB	GGGTGTGGACAGAAAGCTAGT	GAAACCATGTTCATCCTGGCG
CRYAB	TCTTCTTCTCTGTCCCTATGCG	TCTATTTCTTGGGGGCTGCG
CRYAB	CCAAACGGCCTGGGTGGATA	CTCACTGAGCTGCTCTTTGCC
CRYAB	ACTGCAAGCACCAAGTGTGT	GGCGCATCTCTGAGAGTCCA
CYP26B1	GCCAACATGCTCTTTGAGGG	GAGAAGACCTTGCGCTTGTTG
CYP26B1	TGCTGCAGGTCTTCTCCAAG	GCAAAGATCAGCTCCAGGGT
DHRS9	AGCAGCTTATAGTCGTTCAGAG	GCTCATAAAAGCCAAGAAGTCCAG
DHRS9	GCTGCTGACAGGCAGTTACTA	ACCCCAGAGACCTTTCTCCC
DHRS9	TGAACTAGCAAGAGGACACCA	ATTAGGAGGCCTAGCACCCA
DHRS9	CTGCACACTGGAGACACCAT	CTGCCAAGTTTCCAAAGCCC
DLL4	CCCTGGCAATGTACTTGTGAT	TGGTGGGTGCAGTAGTTGAG
ELMOD1	ACTGTTCCAAAAGAAGACGTCAG	AGTGATATCCCTGCATTTCGGA
ELMOD1	GCACTTCCTGAGAATGTTGATCC	TCCATGGGGTCCTCTTCGAT
ELMOD1	CCAGGGAAGCCTCTGCAC	AGTGTCAACTGGACTCTGGC
ELTD1 (codon optimised)	GGCCTGCTGCACTACTTCTT	AGGTGGATGCCCTCGATAC
ELTD1 (wild type)	GCTCAAACCCACCCACATTAT	CACAGCCCTCTGAAGACCAG
FASN	CAGGCACACACAGGATGGAC	CGGAGTGAATCTGGGTTGAT
FILIP1L	TTCCTCTGGAACGTGCAGTC	GAAGAAGTGGTTCCACTGTAATTT

FILIP1L	GGATGAACAGCAAAGGTTGAAA	TCTCTTGAGAGGTGCCCTGA
FILIP1L	TTCCTCTGGAACGTGCAGTC	GAAGAAGTGGTTCCACTGTAATTT
FILIP1L	GAACTGCAGGCTCGAGATGA	GCTTTTGTTGAAGCTGGCGA
FILIP1L	ATTGTTCGGGCGACTCTCG	GCTTCTTTAATCTGAACTGCCTGC
FLRT3	TTCTCGTCTTCCTGGGTTCTG	AAATGAAACCCGCATCGCAG
FLRT3	TGGAGATGCTCAGTCCCAGT	TCCGTTACTTCAGAACCCTGC
FOXA1	ACTGTGAAGATGGAAGGGCA	AGTAGGCCTCCTGCGTGT
GAPDH	AGCCACATCGCTCAGACAC	GCCCAATACGACCAAATCC
HBB	ACTTCAGGCTCCTGGGCAAC	GGCCCTTCATAATATCCCCCAG
HBG1	GAGAAACCCTGGGAAGGCTC	TGTGCCTTGACTTTGGGGTT
HES2	CCAACTGCTCGAAGCTAGAGA	AGCGCACGGTCATTTCCAG
HEY1	CGAGCTGGACGAGCCCAT	GGAACCTAGAGCCGAACTCA
HEY2	GTACCATCCAGCAGTGCATC	AGAGAATTCAGGGCATTT
HNRNPF	GCGGTCCCTGTATTGGTCTC	AAATGTCCACGGAGGCGAG
HNRNPF	TCAACAAGCCTCAACTGCCT	TTTGTTCTCAACCTCGGCCT
HNRNPF	ACGCCGGACGCAGAAAC	TGGATGGTAATGAAATGTCCACG
HNRNPF	CTTCCTCAAGGTGGGGTTCG	ATGAAATGTCCACGGAGGCG
HNRNPF	CATTGGTGACATCTTGGCGG	TTTGTTCTCAACCACGCCAG
HNRNPF	CCCGCCAAAACACGTTTACC	ATGAAATGTCCACGGAGGCG
HSPA6	CGTGCCCGCCTATTTCAATG	AAAAATGAGCACGTTGCGCT

INPP5B	ATGAGGAGCTTGAGGAAGCAGG	GATCACATCATGGTTGCTGATGG
INPP5B	TTACCGGGGACGATGTCTCT	GTTAGAACCACCTCCGCCAA
JAG1	GAATGGCAACAAAACTTGCAT	AGCCTTGTCGGCAAATAGC
KIT	AATCCTCTCGTCAAAACTGAAGG	CCATCTCGCTTATCCAACAATGA
PAPPA	TGATCACAGGGCTGTATGACAA	GCCCCCTAACATGAGCACTT
RAET1G	ATCCAACTCCCCAATGGCAG	CAAAGAGAGTGAGGGTCGG
RASD1	CCCCTCTGCCCAATGAAACT	TGAAAACGTCTCCTGTGAGG
RASD1	CCCCTCTGCCCAATGAAACT	TCGAGGATCTGTGAGGATGGA
RYR1	TCAGCCGTGCTCTACTACCT	GACCTTCTCTCCGTTCTGGC
RYR1	TCAGCCGTGCTCTACTACCT	GACCTTCTCTCCGTTCTGGC
SCD	GACCTGCTTGCTGATCCTGT	CCATTCACGAAGCATCTCAC
SERPINB2	AATCCCAAACCTGCTACCCG	TCTCATGCGAGTTCACACGG
SERPINB2	AATCCCAAACCTGCTACCCG	TCTCATGCGAGTTCACACGG
SERPIND1	GATCGCCATCGACCTGTTCA	GGTGCGATGCTCGTAGATGA
SEZ6L2	GACAGGGCCTCTGACAACAG	CATCAGCCGGTCATTGTCCT
SEZ6L2	CAGAGCCTGGAAGTGAGACC	CATCAGCCGGTCATTGTCCT
SEZ6L2	TACCTGCCAGGGCCTCC	CTGTGACAGGTTCAGCGTCT
SEZ6L2	GACAGGGCCTCTGACAACAG	CATCAGCCGGTCATTGTCCT
SEZ6L2	CTAGCCCAATTCTGCCCCTC	GTCCCGATCAGATCCCTGG
SEZ6L2	CCAGAGCCTGGAAGTGAGAC	CGTCTGCACCTGGATCTCAA

SH2D3C	GCGTGGTCTACAGGTCAGTC	ATGGACACGGGTTACAGTGC
SH2D3C	CCGACAAGGCGATGAGGTAA	CTCCTTGGAGAACTGCACCTG
SH2D3C	AGACCAGCAAAAAGTTCAAGTTC	ACGTGGTCAAAGCTCTCCTG
SH2D3C	CGGTGCCTAGCCGGTTG	CTCCTTGGAGAACTGCACGA
SH2D3C	GCCTTCAGATATCCAAGGGGA	TTGGAGAACTTCACATAGTCGCT
SH2D3C	CATTTAAGGCCATGCGGTGG	ATGGACACGGGTTACAGTGC
SH2D3C	GCGTGGTCTACAGGTCAGTC	AGTCTCAAAACCCTCGGGAC
SLC25A1	TCAAGGTGCAGACAACTAAGC	GGGGTCATATAACGCTCTCCA
SLC39A6	CCAACCCAATGAAACCACCG	CATTGCGCCTTCGTCTCCG
SLC39A6	CCGCGGAGACTGTTTCAATG	GCTCTTGTGAGTCTGCTCGT
SPG7	GCAGGCGCTGGCAAAC	TGCGTGACTAGACCAGCAAG
SPG7	TATCTGAAGAGCCCAGAACGC	TTCAGTCAGCGGATTCCCAG
SPINK1	AAGAGACGTGGTAAGTGCGG	GAAGTCTGGCGTTTCCGATT
SPN	CATTCCTCAGCCAAGAGCCA	GCAAGAGCTGGGACCTGAG
SPN	CTTATCAGCCGAGCCGGTCC	GTGTCTGCACTGCTGTTGTG
TRIML2	GGATTTGAGGAGTCCAGAGC	AAGAGTATTTTGCATTCTTGAGCA
TRIML2	TCGTGGACTCTGAAGTTGCC	GGCCCAGTCTCTGTAGCATT

Table 2.2: qPCR primer sequences. Repeated genes indicate qPCR primers designed to probe all splice variants of a given gene.

2.5 Flow cytometry

2.5.1 Flow cytometry for cell surface antigen detection

Flow cytometry (FACS) was used to determine the expression of cell surface proteins. Although the acronym FACS historically refers to a specific form of flow cytometry, fluorescence-activated cell sorting, it is now accepted as an acronym for general flow cytometry.

In brief, cells were harvested using trypsin and then pelleted through centrifugation at 1000 *g* for 5 minutes and washed in 1ml PBS. Following this, cells were re-suspended in 200 µL of the appropriate primary antibody diluted in staining buffer comprising PBS and 3% FCS. FACS antibodies are listed in Table 2.3. A control sample was chosen as the negative stain control and was not exposed to the primary antibody. Cells were then incubated for 30 minutes in the dark on ice. Following this, cells were washed in 1mL of staining buffer (without antibody). Cells were then pelleted through centrifugation at 1000 *g* for 5 minutes and then re-suspended in 200 µL of the appropriate secondary antibody conjugated to allophycocyanin (APC) diluted in staining buffer. Incubation lasted for 30 minutes in the dark on ice. Following this, cells were washed with 1 mL of staining buffer (without antibody), centrifuged as above and re-suspended in 300 µL of staining buffer. Samples were then analysed using a BD FACSCalibur flow cytometer (BD Biosciences). Data was then analysed using FlowJo 10.0.7 (FlowJo LLC). In each experiment, unstained negative controls as well as stained positive controls were used to determine the correct voltage-settings.

2.5.2 Flow cytometry for whole cell GFP expression detection

This was performed similarly to the method above, except that no antibody staining was required as GFP fluorescence was the read out. In brief, cells were harvested and then analysed directly using a BD FACSCalibur flow cytometer (BD Biosciences). Data was then analysed as above.

2.5.3 FACS sorting

Before cell sorting for HA tag cell surface expression, cells were stained with primary and secondary antibodies as above. FACS sorting for either HA or GFP expression was performed using a FACSAria Fusion cell sorter (BD Bioscience). Gating is shown in the result section where cell sorting was performed. Cells were kept on ice prior to and after cell sorting. Thereafter cells were harvested for microarray analysis.

Target	Type	Dilution	Company
Primary antibodies			
ELTD1	Mouse IgG2 monoclonal	10 µg/mL	Professor Alison Banham, Oxford University (184.11)
HA tag	Mouse IgG1 monoclonal	1 in 50	Cell Signaling Technology (2367)
DLL4	Rat IgG2 monoclonal	10 µg/mL	R&D Systems (MAB1506)
JAG1	Mouse IgG2 monoclonal	1:200	Professor Alison Banham, Oxford University (J1-65D)
KIT	Mouse IgG1 monoclonal	1:200	Invitrogen (17-1178-41)
IgG1 isotype control	Mouse IgG1 monoclonal	10 µg/mL	Invitrogen (17-4714-41)
IgG2 isotype control	Mouse IgG2 monoclonal	10 µg/mL	Invitrogen (17-4724-41)
Secondary antibodies			
anti-mouse APC	Goat IgG	1 in 100	Invitrogen (A-865)
anti-rat APC	Goat IgG	1 in 100	Invitrogen (A10540)

Table 2.3: Antibodies used for cell surface FACS.

2.6 Immunohistochemical (IHC) staining of patient samples

In brief, breast cancer patients seen at the Medical Oncology Department's Breast Clinic, Churchill Hospital (Oxford University Hospitals NHS Foundation Trust, Oxford) between 1992 and 2000 were retrospectively reviewed. Patients were included in the study if they were biopsy positive for primary breast cancer as well as regional lymph node metastasis prior to the initiation of any anti-cancer therapy. Patients who had undergone previous anti-cancer therapy or who had relapsed were not included in the study.

Tissue sections comprising of matched primary breast cancer and regional nodal metastases, obtained from the John Radcliffe Hospital (Oxford) were prepared for immunohistochemistry. For positive controls, tonsil sections were used as they express ELTD1. Informed consent was obtained from all patients in accordance with the Declaration of Helsinki and local ethical approval was obtained from the Oxfordshire Research Ethics Committee. Patient samples were obtained from the Oxford Centre for Histopathology Research, under application number 17/A035. Staining was performed together with Mr. Graham Steers and Dr. Russell Leek (both former members of the Nuffield Division of Clinical Laboratory Sciences, Radcliffe Department of Medicine, University of Oxford). In brief, the formalin-fixed and paraffin embedded tissue sections were dewaxed, rehydrated and then heated for 10 minutes at 65 °C. Following this, dewaxing was performed using Citroclear (TCS Biosciences). This was performed twice, each for 5 minutes. Rehydration in industrial methylated spirits was then performed first using a concentration of 100% for 5 minutes followed by a concentration of 50% for 5 minutes. Slides were then placed in PBS. Sections were blocked using 10% normal horse serum (Vector

Laboratories) for 30 minutes. Thereafter, ELTD1 antibody (Sigma: HPA025229) was applied for 45 minutes at room temperature at a dilution of 1:500 in PBS with 10% FCS. Following this, the slides were washed in PBS for 5 minutes and the secondary antibody conjugated to HRP was applied for 45 minutes (Dako K4002). Visualisation was performed using the 3,3'-diaminobenzidine (DAB) peroxidase substrate kit (Vector Laboratories) for 5 minutes. Slides were then washed with tap water, counterstained with haematoxylin (Sigma: 1051740500) and then rinsed again in tap water. Following this, slides were mounted with Aquamount (Fisher Scientific: 14-390-5). Each histological section was then digitally scanned using a Hamamatsu NanoZoomer slide scanner (Hamamatsu). Following this, digital slides were manually scored by eye with Dr. Ioanis Roxanis (Consultant Histopathologist, John Radcliffe Hospital, Oxford University Hospitals NHS Foundation Trust).

For each histological section, ELTD1's expression (as measured by IHC) was assessed within 3 biological compartments using IHC intensity: 1) normal (non-tumour) vessels; 2) tumour-associated vessels; and 3) tumour cells. The IHC intensity score is a measure of overall staining intensity and is graded as follows: Score 0 = negative expression; Score 1 = weak expression; Score 2 = moderate expression; and Score 3 = strongest expression.

2.7 Confocal microscopy

Confocal microscopy was performed using the Zeiss LSM 780 Confocal Microscope (Zeiss) and was used during two experiments: i) to visualise lipid droplet accumulation in HUVECS; and ii) to visualise GFP expression in HEK293T cells transiently transfected with ELTD1 constructs C-terminally tagged with GFP. During

both experiments, cells were plated within confocal appropriate 24 well glass bottom plates with opaque walls (Greiner Bio-One International: 662892) and were imaged live. Nuclei were stained with 300 nM 4',6-Diamidino-2-Phenylindole, Dihydrochloride (DAPI) (Invitrogen D1306) for 10 minutes. Cells were then washed with PBS three times and imaged. During the lipid droplet experiment the LipidTOX Green dye was added following exposure to DAPI (this is expanded in the Lipid Droplet method section). A 60x oil lens was used for all confocal imaging. Laser strength was adjusted based on results on negative and positive controls. Every well imaged had a minimum of six images taken. Images were later analysed and edited using FIJI (Schindelin et al., 2012).

2.8 RNA interference

Transfection of small interfering RNA (siRNA) duplexes was performed using Lipofectamine RNAiMAX (Invitrogen) according to the manufacturer's instruction for a 6 well culture plate. Two days prior to the transfection, HUVEC cells were seeded into a 6 well culture plate (1x10^5 cells per well) and were prepared in appropriate medium free of antibiotics. All cells had a medium change prior to transfection. Cells were then assayed either at 24 hours or 48 hours post transfection. siRNAs were used at a final concentration of 20 nM. siRNAs used are listed in Table 2.4 and had been previously validated by (Masiero et al., 2013). Single siRNAs were purchased from Invitrogen. A medium GC negative control siRNA (Invitrogen) was used as a control as *ELTD1's* siRNAs were all medium GC in content. In brief, all medium was replaced from the well and 2 ml of fresh EGM2 (Lonza) was added to the well (6 well plate size). Thereafter, for each well, the intended siRNA with a final plating concentration of 20 nM was diluted into 250 µl of serum-reduced Opti-MEM medium

(Gibco 31985070). Simultaneously, 5 µl of Lipofectamine RNAiMAX was diluted into another 250 µl of serum-reduced Opti-MEM medium. After 20 minutes at room temperature, both were mixed yielding a 500 µl solution which was then added to the well (6 well plate size). This yielded a final 2.5 mL volume in the well resulting in a siRNAs concentration of 20 nM. Silencing was then checked using qPCR, Western blotting and FACS from 24 hours following silencing.

siRNA name	Target sequence (5'-3')	Manufacturer
ELTD1 siRNA 1	-GGGCUGUGAGCUGACAUACUCAAAU-	Invitrogen (HSS148831)
ELTD1 siRNA 2	-CAAUCAUUGCCGGACUGCUACACUA-	Invitrogen (HSS184653)
ELTD1 siRNA 3	-CGCAAUGGAAUUGAAGCCUGCUAUU-	Invitrogen (HSS148832)
Medium GC negative control		Invitrogen (12935300)

Table 2.4: siRNAs used for ELTD1 silencing.

2.9 Transient transfection

HEK293T and COS-7 cells were transiently transfected using Lipofectamine LTX (Invitrogen) according to manufacturer's guidelines (Thermo Scientific). Briefly, this involved mixing plasmid deoxyribonucleic acid (DNA) with the kit's transfection reagent (a cationic polymer) followed by droplet administration to previously seeded cells and incubation in an aseptic humidified incubator (5% carbon dioxide at 37°C)

for 48 hours. For a single well of a 6 well sized culture dish, 6.25 x 10^5 cells were seeded the day before transfection. On the day of transfection, the medium was changed and replaced with 2 ml of fresh DMEM. Transfection was performed by adding 2.5 µg of plasmid DNA to 500 µl of Opti-MEM medium. Following this, 6.5 µl of Lipofectamine LTX reagent was then added to this volume. Incubation was for 30 minutes at room temperature. Following this, the 500µL volume was added by droplet administration to the well. This yielded a final volume of 2.5 ml in the well. Transfection success was measured by qPCR, Western blotting and FACS from 24 hours after transfection.

2.10 Cloning and lentiviral transduction

2.10.1 Cloning

Cloning was performed using the Mammalian Expression System with Gateway Technology (Invitrogen) as per the manufacturer's protocol. This utilised the pENTR Directional TOPO Cloning Kit (Invitrogen) to produce the entry clone and the pLenti6.2/V5-DEST Gateway Vector Kit (Invitrogen) to produce the expression clone.

Initially, the coding-DNA-sequence (CDS) of the targeted gene was amplified by polymerase chain reaction (PCR) from plasmid containing the gene. For this PCR, primers were designed as per the pENTR Directional TOPO Cloning Kit protocol. This required that the 5' end of the forward primer start with CACC and forbade any complementarity to the sequence GTGG at the 5' end of the reverse primer. When cloning wild type FL ELTD1, forward (5' - CCTCCCGCTCCTAGTGGTT -3') and

reverse (5’ - GGGAGACAAGGTGTCTTGGT -3’) primers were purchased (Invitrogen).

PCR was performed on a Labcycler (SensoQuest) and used the Phusion High-Fidelity PCR Master Mix (Thermo Scientific) as per the Phusion 3-step cycling protocol. A range of annealing temperatures were tested. Products were then electrophoresed through a 1% agarose gel with 0.5 µg/ml ethidium bromide and visualised under ultra-violet light.

The blunt-ended PCR product was then cloned into the pENTR Directional TOPO entry vector (with kanamycin resistance) to create the entry clone (as per the kit’s protocol). The entry clone was then used to transform chemically competent *Escherichia coli* (*E. coli*) cells (Invitrogen). This entailed heat-shocking the bacteria for 30 seconds at 42°C (in the presence of the entry clone) and the addition of SOC medium (Super Optimal broth with catabolite repression) before eventually seeding the mixture onto a prewarmed agar plate mixed containing kanamycin and incubating overnight. Thereafter, *E. coli* colonies growing on the agar plate were selected, cultured overnight in lysogeny broth (L-broth) at 37°C and then processed to extract plasmid DNA using the Qiagen Mini-Prep Kit (Qiagen). DNA yield was measured using a Nanodrop ND-1000 spectrophotometer (NanoDrop Technologies). Extracted plasmid DNA was then sent for sequencing to verify ELTD1 insert presence. Primers used were the M13 forward and reverse primers supplied with the kit. Sequencing was performed by the DNA Sequencing Unit, Weatherall Institute of Molecular Medicine, University of Oxford. Alignment of

sequenced plasmid DNA to a reference sequence was done using BLAST (Altschul et al., 1997).

Following sequencing and alignment, an entry-clone with the correct full length CDS was selected. Recombination reaction was then performed using the Gateway LR Clonase II enzyme (Invitrogen), which swapped the gene's CDS from the entry clone into the pLenti6.2/V5-DEST expression vector (with ampicillin and blasticidin resistance). This expression clone was then used to transform chemically competent *E. coli* cells in an identical manner to that described above, except that the mixture was seeded onto an agar plate containing ampicillin. After being selected and then cultured in L-broth, *E. coli* cultures underwent plasmid DNA extraction. This was also sent for sequencing. Primer sequences were obtained from the kit.

Following successful sequencing, an expression clone containing a validated sequence was then used to again transform chemically competent *E. coli* cells. This time however a larger volume of *E. coli* was cultured in order to prepare a larger amount of plasmid DNA using the Qiagen Maxi-Prep Kit (Qiagen).

2.10.2 Lentiviral assembly in HEK293T cells

The ViraPower Lentiviral Expression System (Invitrogen) was used to transfect HEK293T and establish the shedding of lentiviruses containing the cloned gene into the supernatant. The purified expression clone was then transfected into HEK293T cells using Lipofectamine LTX (Invitrogen), alongside two packaging lentiviral

plasmids contained in the ViraPower Lentiviral Mix (Invitrogen). These plasmids comprised the psPAX2 packaging vector and the pMD2.G viral envelope vector. For a 10cm plate the amounts of DNA comprised: 5 µg plasmid containing gene of interest (i.e. *ELTD1*); 3.75 µg psPAX2 plasmid; and 1.25 µg pMD2.G plasmid. For a T175 sized flask, this comprised: 21.8µg plasmid containing gene of interest; 16.3 µg psPAX2 plasmid; and 5.4 µg pMD2.G plasmid.

2.10.3 HUVEC lentiviral transduction:

At 48 and 72 hours after lentiviral assembly in HEK293T, virus-rich supernatant from transfected cells was collected. Supernatant was filtered through a 0.45µm filter (Sartorius Biotech) and used to infect HUVECS. Supernatant collected at 48 hours was stored overnight at 4°C and then mixed with the 72 hour supernatant before being added to HUVECS which were approximately 50-70% confluent on the day of transfection. Hexadimethrine bromide (Polybrene) (6 µg/mL) (Gibco) was added to aid transduction. After 48 hours, media was replaced with EBM-2 supplemented with EGM-2 as well as blasticidin (4µg/mL) (Gibco) to select for transduced cells. Blasticidin was also given to a HUVEC control flask from the same batch, which had not been exposed to virus as a control. Medium containing blasticidin was replaced every two days for 1 week until all non-transduced cells in the control flask had died. The transduction was deemed a success if transduced HUVECS survived this. Proof of successful overexpression of the gene of interest was then determined using qPCR, Western blotting and FACS.

2.11 Cell based assays

2.11.1 Signalling assays:

2.11.1.1 HTRF FRET assays.

Homogeneous Time-Resolved Fluorescence Resonance Energy Transfer (HTRF FRET) assays were performed for Gαq, Gαs and Gαi signalling. For Gαq signalling, Cisbio's IP-1 assay (Cisbio) was performed. This assay detects the accumulation of inositol monophosphate (IP-1), a stable metabolite downstream of the second messenger inositol triphosphate (IP-3). For Gαs and Gαi signalling, Cisbio's cAMP assay (Cisbio) was performed. This measures accumulation of the second messenger cyclic adenosine monophosphate (cAMP). In both assays, ELTD1 signalling constructs were transiently transfected into HEK293T cells (6 well plate format) before being harvested at 24 hours. Thereafter, they were plated into an opaque-walled 96 well microplate (Corning) at 50 000 cells per well. At 48 hours post transfection the HTRF FRET assay was run. For the Cisbio IP-1 assay, this involved adding the IP-1 stimulation buffer for 30 minutes followed by 60 minutes of exposure to the IP1-d2 working solution and anti IP1-cryptate working solution for 60 minutes. This was followed by reading with a HTRF compatible BMG CLARIOstar microplate reader (BMG Labtech) at the 665 nm and 620 nm wavelengths. Following this, the fluorescent ratio (665 nm/ 620 nm) was calculated. This was then transformed in Prism using the formula: Y = (1/Y)*1000000. For the Cisbio cAMP assay (for both Gαs and Gαi), this involved adding the cAMP stimulation buffer for 30 minutes followed by 60 minutes of exposure to the cAMP-d2 working solution and cAMP-Cryptate working solution. This was followed by reading with a HTRF compatible BMG CLARIOstar microplate reader (BMG Labtech). For the cAMP assay (encompassing both Gαs and Gαi assays), the

phosphodiesterase inhibitor 3-isobutyl-1-methylxanthine (IMBX) was added to the medium at a final concentration of 0.5 mM in order to prevent cAMP degradation. Forskolin was also added at a final medium concentration of 10 μM to the Cisbio cAMP assay but only for the Gαi version of the assay (as Gαi activity decreases cAMP, adding forskolin allows the assay to begin with a high cAMP level).

2.11.1.2 Luciferase reporter assays

Luciferase reporter assays purchased from Promega were performed to assay the activity of transcription factors downstream of all the canonical G protein pathways: i) NFAT-luciferase and NFκB-luciferase for Gαq; ii) SRF-RE-luciferase for Gα12/13; iii) CRE-luciferase and CREB-luciferase for Gαs and Gαi; and iv) SRE-luciferase for Gαi, Gα12/13, Gαq and Gβγ. For the NFAT-luciferase assay, a HEK293 cell line stably expressing NFAT-luciferase (Promega) was obtained from Heptares, thus requiring only transfection with the GPCR plasmid. For the remainder of the luciferase reporters, dual transfection was performed (GPCR plasmid plus reporter plasmid). Constitutively active GPCRS as well as inducer compounds included in the protocols for each luciferase plasmid were used as positive controls. These are highlighted in the experimental results section. In brief, ELTD1 or control GPCR constructs as well as reporter plasmids were transiently transfected into HEK293T cells or COS-7 cells. For SRE-luciferase and SRF-RE-luciferase, DMEM with 5% FCS was removed and replaced with DMEM with 0.5% FCS (serum starved) 4 hours following transfection. On the day of induction, SRE-luciferase transfected cells were stimulated with either an induction (positive control) solution (40% FCS and 20ng/ml phorbol myristate acetate (PMA) in DMEM) or a DMEM control solution. For SRF-RE-luciferase transfected cells, an induction solution (40% FBS

in DMEM) or a control solution of DMEM was added. For CRE-luciferase transfected cells, an induction solution containing 1 mM forskolin or a control solution of DMEM solution was added. For the above assays, results were read after 5 hours. For the NFAT-luciferase assay, an induction solution (1 μM ionomycin and 10 ng/ml PMA) or a control solution (DMSO 1:1000 in DMEM with 5% FCS) was added with results being read 17 hours later.

Luminescence assays were either performed at 48 or 24 hours following transfection depending on what had historically been done in that particular laboratory. In Oxford, cells were harvested at 24 hours following transfection, counted and plated into an opaque-walled 96 well microplate (Corning) (50 000 cells per well) and into a 6 well plate for FACS. At 48 hours post transfection, cells were assayed and were read using a BMG FLUOstar optima luminescent plate reader (BMG Labtech). FACS was performed on these samples to determine the level of GPCR cell surface expression. In Amsterdam, constructs were directly transfected into an opaque-walled 96 well plate and then assayed at 48 hours without any intermediate steps. Luminescence was read using a SpectraMax L577 Microplate reader (Molecular Devices). Additionally, in Amsterdam, cells were transfected with polyethylenimine instead of Lipofectamine LTX. In Leipzig, cells were transfected into opaque-walled 96 well microplates (PerkinElmer) and at 24 hours were assayed for luminescence reading using a PerkinElmer EnVision plate reader (PerkinElmer).

2.11.1.3 AlphaScreen assay

PerkinElmer's AlphaScreen cAMP assay (PerkinElmer) was performed as an alternative assay for Gαs signalling. This was performed during the visits to Leipzig.

In brief, cells were transfected as above. At 48 hours, cells were incubated in medium containing IBMX (to prevent cAMP degradation) and then lysed in lithium buffer (PerkinElmer). Plates were then frozen for 24 hours at −20°C. The Alpha Screen cAMP assay kit was used to measure cAMP concentration as per the manufacturer's guidelines. Accumulation was measured in opaque-walled 96 well microplates (PerkinElmer) and read using the PerkinElmer EnVision plate reader (PerkinElmer).

2.11.1.4 Stinger/Stachel peptide dilution and application

ELTD1's Stinger/Stachel peptides were first diluted solely with DMSO yielding a final peptide concentration of 1mM in 2% DMSO. After visiting the Leipzig lab, an addition two steps were added following DMSO dilution to improve solubility. The additional steps consisted of diluting the peptides with 50mM tris(hydroxymethyl)aminomethane (TRIS) (pH 8) after the initial DMSO dilution followed by aspirating the sample many times using a 200 µL pipette tip cut half-way to enable better aspiration of the viscous peptide solution. This yielded a final peptide concentration of 1mM peptide in 1% DMSO. Peptides were applied to HUVECS and transiently transfected HEK293T cells for 30 minutes. A 1% DMSO solution was used an additional control. Thereafter cells were then assayed for canonical GPCR signalling activity using all the signalling assays described above.

2.11.2 Lipid droplet assays

Lipid droplets were stained with the LipidTOX Green neutral lipid stain (Invitrogen H34475). The LipidTOX Green stain is imaged with fluorescent filters appropriate

for Alexa Fluor 488 (absorbance: 495 nm; excitation 519 nm). It can thus be used for fluorescent microscopy and FACS.

2.11.2.1 Lipid droplet confocal microscopy

HUVECS plated were plated within confocal appropriate 24 well glass bottom plates with opaque walls (Greiner Bio-One International: 662892) and were ELTD1 silenced for 48 hours (as described in the RNA interference methods). 24 hours following silencing, oleic acid in bovine albumin (Sigma Aldrich: O3008) was added to the positive control well at a final concentration of 150 (150 μM). At 48 hours following silencing, cells were exposed to DAPI (300 nM) for 10 minutes at room temperature followed by washing 3 times with PBS. Thereafter, cells were exposed at room temperature to the LipidTOX Green stain (1:100) for 30 minutes in the dark. Thereafter, cells were imaged live. Confocal microscopy was performed using the the Zeiss LSM 780 Confocal Microscope (Zeiss), as described above in the confocal microscopy methods. The Alexa Fluor 488 filter set was used to capture fluorescence.

2.11.2.2 Lipid droplet FACS analysis

HUVECS plated were plated within 6 well plates and were ELTD1 silenced for 48 hours (as described in the RNA interference methods). 24 hours following silencing, oleic acid in bovine albumin (Sigma Aldrich: O3008) was added to the positive control well at a final concentration of 150 (150 μM). At 48 hours following silencing, cells were harvested and pelleted into 1.5 ml microtubes on ice. Thereafter, cells were exposed one ice to the LipidTOX Green stain (1:100) for 30 minutes in the

dark. DAPI staining was not performed. Thereafter, cells were imaged live using FACS using a BD FACSCalibur flow cytometer (BD Biosciences). The FL-1 laser was used to capture fluorescence in the Alexa Fluor 488 range.

2.11.3 Angiogenesis assays

2.11.3.1 Hanging drop endothelial sprouting spheroid assay in matrigel

ELTD1 overexpressing HUVEC spheroids were generated using the hanging-drop method (Kelm et al., 2003) and then embedded in matrigel (BD Biosciences). This involved harvesting HUVECs and re-suspending them at a cell density of $2.5x10^4$ cells/ml in EGM2 media (Lonza) supplemented with 2.5 µg/ml methylcellulose (Sigma). For each sample to be tested, one hundred 20 µL drops were then deposited onto a 15cm culture dish. These dishes were then inverted and incubated for 24 hours in an aseptic humidified incubator (5% carbon dioxide at 37°C), allowing for spheroid formation. Spheroids, each containing approximately 500 cells, were then harvested, centrifuged at 1000g for 1 minute and then embedded into matrigel. Spheroid photographs were taken using an AMG Evos XL Core digital microscope (Fisher Scientific) at 24 and 48 hours following embedding. Twenty photos were taken of each well. Following this, a self-made stylus (built using an empty pen, tinfoil and moist cotton wool) was used to accurately trace the outline of each spheroid. Traced images were then analysed using a script in FIJI (Schindelin et al., 2012) with total area and perimeter then being graphed and analysed using Prism 7 (GraphPad Software).

2.11.3.2 Fibrin gel bead assay

This assay was performed as originally described (Nakatsu et al., 2007) and consisted of ELTD1 overexpressing HUVECS coated onto cytodex beads which were then embedded in a fibrin gel overlaid with fibroblasts. Medium was changed every 2 days with EGM2 (Lonza) and images were taken every second day for 3 weeks. Cytodex beads (Amersham) were prepared as follows: 0.5 g of dry beads were hydrated using 50 ml PBS (pH 7.4) for 3 hours at room temperature on a rocker. Following this, supernatant was discharged and beads were washed 3 times in 50 ml of fresh PBS yielding 10 mg/ml of beads (approximately 30000 beads/ml). Bead suspension was then placed in a glass bottle, autoclaved and kept at 4°C. The day before the assay, the beads were coated with HUVECS. This was performed by adding 2500 beads to $1x10^6$ HUVECS in 1.5 ml of warm EGM2 within a FACS tube (Corning). These were incubated in an aseptic humidified incubator (5% carbon dioxide at 37°C) for 4 hours. During this period, each FACS tube was manually tapped/shaken every 20 minutes to prevent clumping. Following 4 hours, the coated beads were transferred to an upright T25 size flask in 5 ml of EGM2 with flasks left overnight in an upright position within an aseptic humidified incubator (5% carbon dioxide at 37°C). The following day, HUVEC coated beads were transferred to a 15 ml tube (Corning). Once the beads had settled, media was removed and beads were washed gently three times with 3 ml of EGM2. Thereafter, beads were counted by suspending beads on a slide (in triplicate) and counted using a haemocytometer. Following this, 1500 beads were added to a FACS tube (Corning) and all media was removed once beads had settled to bottom of tube. Following this, the beads were suspended in 3 ml of 2 mg/ml fibrinogen solution. 0.625 units/ml thrombin (Sigma-Aldrich) was then added to each well of the 24 well plate.

Thereafter, 0.5 ml of the fibrinogen-HUVEC bead solution was added to each well. This was followed by clotting and an incubation of 15 minutes in an aseptic humidified incubator (5% carbon dioxide at 37°C). Once clotting occurred, 1ml of EGM2 medium and 20 000 low passage fibroblasts (Lonza) were added to each well. Medium was changed every 2 days and photos were taken using an AMG Evos XL Core digital microscope (Fisher Scientific) over a 3 week period.

2.11.3.3 Tube formation assay on matrigel

Prior to the assay, 200 µL of matrigel (BD Biosciences) was plated per well into a 24 well plate followed by 30 minutes of solidification in an aseptic humidified incubator (5% carbon dioxide at 37°C). Control and ELTD1 overexpressing HUVECS were then plated at $5x10^4$ cells into each well on top of the matrigel. The plate was then placed within an Incucyte Imaging Incubator (5% carbon dioxide at 37°C) (Essen BioScience) and 10 photos were taken per well every hour for 24 hours. Photos were also taken manually of each well (10 photos per well) at 4 and 8 hours following HUVEC seeding. Tube formation was analysed by counting the number of complete polygons (comprising endothelial tubes) in each image field. Results were analysed and graphed using Prism 7 (GraphPad Software).

2.11.3.4 Endothelial proliferation assay

In this assay, control and ELTD1 overexpressing HUVECS were plated at $1x10^5$ cells per well (low confluence) into multiple 12 well sized plates. Every day, a plate was selected for photographing, harvesting and cell counting. This was repeated until both control and ELTD1 groups achieved confluence. Photographs were

performed using an Incucyte Imaging Incubator (5% carbon dioxide at 37°C) (Essen BioScience). Sixteen photographs were taken of each well. The plate was then removed from the Incucyte Imaging Incubator and cells were harvested and counted as described in the cell lines and maintenance methods section. Results were analysed and graphed using Prism 7 (GraphPad Software).

2.11.3.5 Endothelial migration assay

Control and ELTD1 overexpressing HUVECS were seeded at $5x10^5$ cells per well into a 24 well ImageLock plate (Essen BioScience) and grown to confluence. Once confluent, a scratch defect was introduced into each well using a 4 pin Essen Wound Maker (Essen BioScience). This manually operated device employs 4x sterile 20 µl pipette tips to scratch a strip of cells off each well in the 24 well plate. This ensures that each well receives the same scratch wound defect. Following this, wells were washed with PBS (to collect scratched cells) and replaced with 500µL of fresh EGM2 (Lonza). Cells at the border of the cell-free scratch were then imaged every 30 minutes until the scratch defect had been repaired by migrating and proliferating HUVECS. The cell-scratched areas of each well were then photographed every 30 minutes using an Incucyte Imaging Incubator (5% carbon dioxide at 37°C) (Essen BioScience). Images taken at the start of the assay contained both borders of the scratch wound. Photographs were taken at four different set positions for each well. This was repeated every 30 minutes using the same positions. The cell-free scratched areas of each group were then manually traced using the self-made stylus described above with the area quantified using FIJI. The size of the scratch wound for the control and ELTD1 overexpressing groups was compared at the start

of the assay and at the time point immediately before the first group closed the defect with new cells.

2.11.3.6 MilliCoat extracellular matrix (ECM) adhesion assay:

This assay was performed using the MilliCoat ECM Screening Kit (Merck: ECM105). Prior to the assay, each adhesion assay strip was rehydrated with 200 µl of PBS for 15 minutes. Thereafter, control and ELTD1 overexpressing HUVECS were seeded into wells coated individually with the various ECM adhesion components at $1x10^4$ wells per well (96 well format). Thereafter, 100 µL of EMG2 (Lonza) was added to each well and cells were incubated for 1 hour in an aseptic humidified incubator (5% carbon dioxide at 37°C). Thereafter cells wells were gently washed with PBS three times. 100 µl of 0.2% crystal violet in 10% ethanol was then added to each well for 5 minutes at room temperature before being washed 3 times with PBS. 100 µl of the kit's solubilisation buffer was then added to each well for 5 minutes. Thereafter, absorbance was read at 560 nm using a FLUOstar optima microplate reader (BMG Labtech). microplate reader. Results were then analysed using Prism 7 (GraphPad Software).

2.11.3.7 Matrigel adhesion assay:

For this assay, 100 µL of Matrigel (BD Biosciences) was plated per well into a 96 well plate. 12 technical replicates were performed for each experimental condition. Following matrigel solidification, control and ELTD1 overexpressing HUVECS were seeded at a density of $1x10^4$ into each well. Cells were incubated for 1 hour in an aseptic humidified incubator (5% carbon dioxide at 37°C) and then washed three

times with warmed PBS. Photographs were taken of each well (specifically at the centre point of each well) using an AMG Evos XL Core digital microscope (Fisher Scientific). A script was then written in FIJI to count adherent cells (included in the Appendix). Results were then analysed using Prism 7 (GraphPad Software).

Chapter 3: ELTD1's evolution

3.1 Introduction

Very little is known about the evolution of ELTD1. Previous work on the subject of adhesion GPCR evolution has revealed that the adhesion group is ancient and pre-dates members of the secretin GPCR family (Schioth et al., 2010, Nordstrom et al., 2009). To date, no work has specifically investigated ELTD1's evolution. The following questions underpin the rationale for our investigation:

1) Is *ELTD1* a highly conserved gene? How similar are its orthologues in extant species to human *ELTD1*? How does this similarity compare with the similarity across orthologues of an established angiogenesis gene? What is the oldest extant species whose genome contains an *ELTD1* orthologue?
2) Has ELTD1 lost or gained any domains during its evolution and could this inform us about its function? Is it possible to make time estimates for such an event?
3) How does *ELTD1*'s predicted structure compare to other adhesion GPCRS and could this inform about possible unknown ligands or additional functions? Can ELTD1's sequence suggest whether ELTD1 is ancestral to other adhesion GPCRS?

3.2 ELTD1 is encoded in the genomes of bony fish and all subsequent vertebrates suggesting that it became established in vertebrates approximately 435 million years ago at the same time as VEGFR2

The first question investigated was to determine which is the oldest extant species whose genome encodes an ELTD1 orthologue. As ELTD1 has been shown to be important in vessel sprouting, I hypothesised that the acquisition of ELTD1 would correlate with the development of i) endothelial cells and ii) a closed circulatory system. The very first endothelial cells as well as the first closed circulatory system arose approximately 550 million years ago with the first vertebrates: the jawless fish (Monahan-Earley et al., 2013). Today, members of this ancient group still exist namely the hagfish (Order: Myxiniformes) and the lamprey (Order: Petromyzontiformes). The lamprey has recently been fully genome sequenced (Smith et al., 2013).

The lamprey was chosen as a representative jawless fish and its annotated genome was then interrogated for the presence of *eltd1* and two important angiogenesis associated genes: *vegfr1* (vascular endothelial growth factor receptor 1) and *vegfr2* (vascular endothelial growth factor receptor 2). These two genes were chosen because of their core importance to the field of angiogenesis and because ELTD1 is known to be regulated by VEGF (Carmeliet and Jain, 2011a, Masiero et al., 2013). Methods are presented in the Methods chapter.

Results revealed that the lamprey encodes *vegfr1* but not *eltd1* nor *vegfr2*. Following this, the next evolutionary vertebrate group (bony fish; n=11 annotated

genomes) as well as all evolutionarily subsequent vertebrate groups (n=51 annotated genomes) were interrogated for the presence of orthologues to *ELTD1*, *VEGFR1* and *VEGR2*. Results revealed that *eltd1 and vegfr2* are encoded in the genomes of all bony fish and all subsequent vertebrates. Results are presented as an evolutionary cladogram in Figure 3.1.

The genomic presence of *VEGFR2* and *ELTD1* orthologues in bony fish and all subsequent vertebrates suggests that these genes were acquired during the development of a more complex circulatory system during the evolution of jawless fish to bony fish. Furthermore, these results suggest that ELTD1 is as evolutionary important as VEGFR2 as they appear to have arisen during the same evolutionary period. Thus, the acquisition of ELTD1 appears to correlate with the development of a complex closed circulatory system. Lastly, in terms of evolutionary time, as bony fish appeared approximately 435 million years ago (Luo et al., 2011, Hedges et al., 2015), these results suggest that ELTD1 and VEGFR2 became established in vertebrates during the same time period.

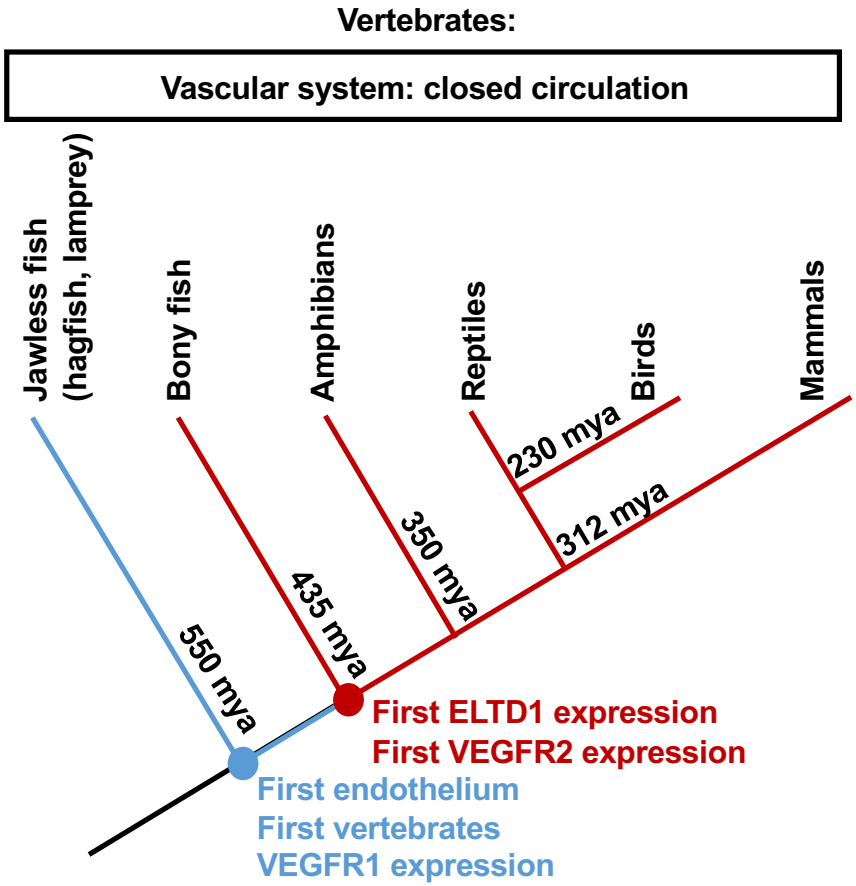


Figure 3.1: Cladogram depicting vertebrate evolution and the presence of genomic ELTD1 and the core angiogenetic genes VEGFR1 and VEGFR2. Blue represents the presence of genomic VEGFR1 without any VEGFR2 or ELTD1. Red indicates the presence of genomic VEGFR1, VEGFR2 and ELTD1. Jawless fish evolved approximately 550 million years ago; bony fish evolved approximately 435 million years ago; amphibians evolved approximately 350 million years ago; reptiles evolved approximately 230 million years ago; birds evolved approximately 150 million years ago; and mammals evolved approximately 160 million years ago. Evolutionary time estimates from (Luo et al., 2011, Hedges et al., 2015). Cladogram not drawn to scale.

3.3 ELTD1 is evolutionary highly conserved across multiple species suggesting an important biological role

Next, ELTD1's conservation across vertebrate genomes was investigated. This was performed by comparing *ELTD1's* amino acid sequence to the amino acid sequences of ELTD1 orthologues in extant members of all the major vertebrate groups (n=61 annotated genomes). As a comparison, this was also done for VEGFR2. Preferential conservation similar to that of the important angiogenesis gene VEGFR2 would suggest an important evolutionary role. As a control, the percentage similarity between each species' exome contrasted to the human exome was reviewed. Methods are presented in the Methods chapter.

Results revealed that ELTD1's amino acid sequence is highly conserved across all 61 sequenced vertebrate genomes with even the least similar orthologues (bony fish) having a similarity > 50% to human *ELTD1* (Figure 3.2 A). ELTD1's conservation across all 61 species is no different to that of the highly conserved and evolutionarily important angiogenesis gene *VEGFR2* (unpaired Student's *t*-test $p = 0.1$) (Figure 3.2 B). Such similar high level conservation suggests an important biological role for ELTD1.

For the majority of species, exome similarity to the human exome follows a trend similar to ELTD1 and VEGFR2. However, in all bony fish reviewed (n=11 anotated genomes), *eltd1* is conserved to a far greater extent than the conservation of the fish exome (unpaired Student's *t*-test $p < 0.0001$) (Figure 3.2 A and C). This

suggests that *eltd1* plays an important biological role in fish. This assumption is further supported by the finding that *eltd1* silencing in zebrafish embryos is lethal, causing major disruption to the developing vasculature (Masiero et al., 2013). Higher vertebrates are more likely to have evolved additional redundancy to protect against such events which is possibly why *Eltd1* knockout in murine embryos is not lethal (Xiao et al., 2012). Taken together, these findings further support ELTD1 as an evolutionarily important gene playing an important biological role in vertebrate biology.

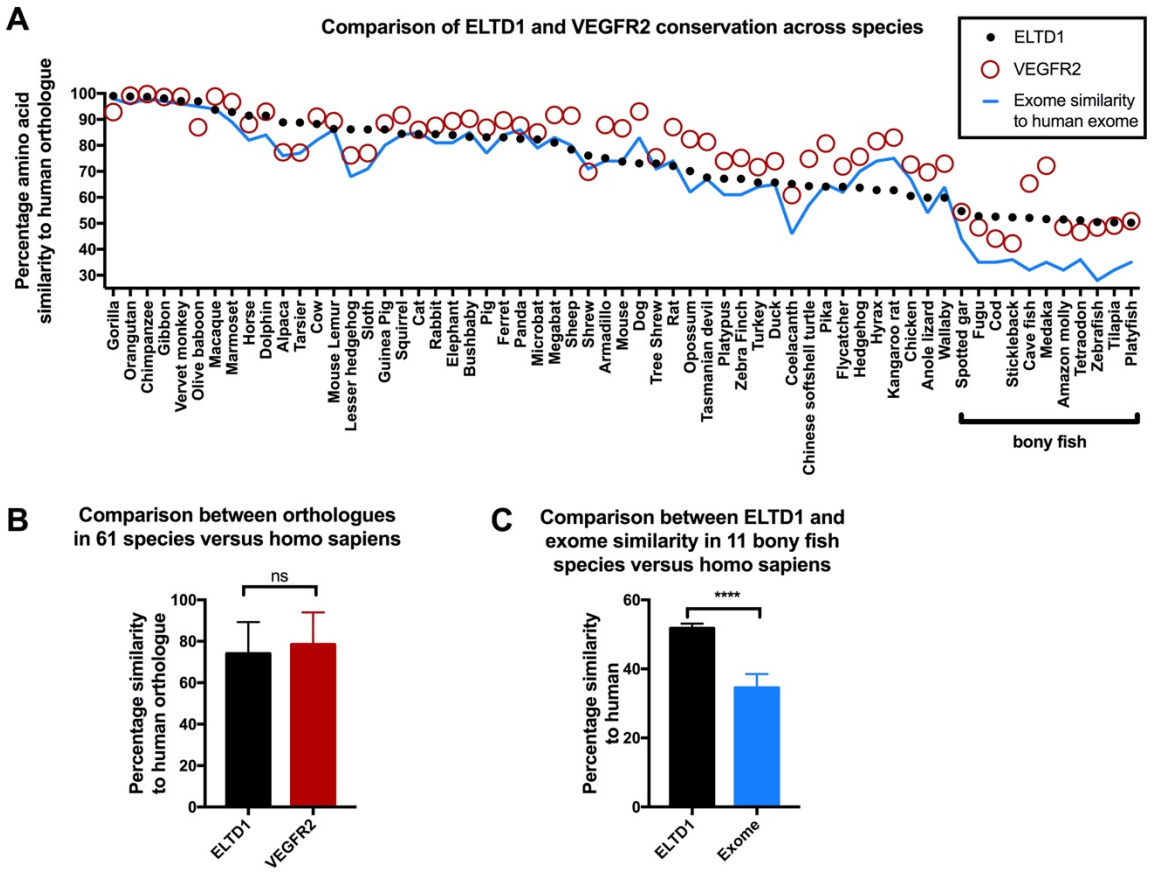


Figure 3.2: Comparison of ELTD1 and VEGFR2 amino acid conservation across 61 vertebrate species with fully sequenced and annotated genomes. **A)** ELTD1 is evolutionary highly conserved across all vertebrates**.** Each data point represents the percentage similarity of orthologue to human *ELTD1* (black dot) or

VEGFR2 (red circle). Both ELTD1 and VEGFR2 follow a similar trend, revealing high conservation across species. The blue line (representing the percentage similarity of each species' exome contrasted to the human exome) reveals that in bony fish, ELTD1's conservation is significantly higher than the exome similarity. This suggests that ELTD1 is highly important for these vertebrates and confirms previous *in vivo* experiments. **B)** Comparison across orthologues reveals no statistical difference in evolutionary conservation between ELTD1 and VEGFR2 (unpaired Student's *t*-test $p = 0.1$). This suggests that ELTD1 is as highly conserved as VEGFR2. **C)** Percentage similarity comparison of bony fish ELTD1 and bony fish exomes to human reveals that ELTD1 in bony fish is conserved to a far greater extent than the conservation of the fish exome (unpaired Student's *t*-test $p < 0.0001$).

3.4 ELTD1 domain amino acid conservation across 59 extant vertebrate orthologues reveals evolutionary ELTD1 variants and 3 areas of major conservation

Next, the evolution of ELTD1's sequence during vertebrate evolution was investigated. The question behind this experiment was whether ELTD1 had lost or gained any predicted domains during its evolution and whether specific domains were more highly conserved than others. As the current understanding of how ELTD1 functions is limited, this information could give good insight about which domains are critical for ELTD1's functions.

This analysis was performed by aligning ELTD1's amino acid sequences in 59 extant vertebrate species, representative of all major vertebrate groups from bony fish to primates. An amino acid conservation score was then calculated for each aligned amino acid using a quantitative method which takes into account the physico-chemical properties of each aligned column (Livingstone and Barton, 1993). Additionally, each sequence was scanned for conserved domains using a variety of amino acid sequence conservation databases (KEGG motif, SMART and CDD) and then annotated with domain information. Finally, results from the amino acid alignment were used to create a phylogenetic tree showing evolutionary distance between ELTD1 orthologues. Methods are presented in the Methods chapter.

Results, presented as a colour coded sequence alignment, reveal high level conservation across all 59 ELTD1 orthologues (Figure 3.3 A). In this sequence

alignment, ELTD1 orthologues are stacked in evolutionary order, with primates at the top and bony fish at the bottom. Strikingly, the most heavily conserved areas were i) the first EGF Ca^{2+} binding domain, ii) the N-terminal half of the GAIN domain, iii) GPS domain and iv) the majority of the 7TM domain (Figure 3.3 A).

Results further reveal that ELTD1 appears to have three evolutionary variants. The oldest as well as the majority of vertebrate ELTD1 orthologues encode 3 EGF domains (termed ELTD1 variant 1) comprising: i) EGF domain (most N-terminal EGF domain); ii) EGF Ca^{2+} binding domain 1; and iii) EGF Ca^{2+} binding domain 2 (Figure 3.3 A). Interestingly, the majority of primates (including human ELTD1) and other more recent vertebrates only encode 2 EGF domains (termed ELTD1 variant 2) comprising: i) EGF domain; and ii) EGF C^{a2+} binding domain 1. Two vertebrates (zebra finch and platypus) exhibited changes suggestive of a third ELTD1 variant (termed ELTD1 variant 3) which did not contain the first EGF domain, whilst containing both EGF Ca^{2+} binding domain 1 and 2. (Figure 3.3 A). Lastly, 2 bony fish (spotted gar and fugu) appeared to have replaced an EGF Ca^{2+} binding domain with an EGF domain, maintaining their three EGF's. This may represent a subdivision of ELTD1 variant 1 however the sample size is too small to make this inference. Figure 3.3 B illustrates the structure of ELTD1's evolutionary variants.

The high level conservation of the EGF Ca binding domain 1, GAIN, GPS and 7TM domains all point to their importance in ELTD1's biology (Figure 3.3 A).

Although ELTD1's ligand is unknown, we hypothesise that it interacts with the EGF domains. The finding that more recent vertebrates only have two EGF domains

suggests that this probable ligand is able to sufficiently activate the receptor through its interaction with the first two EGF domains. The finding that the second EGF domain is most conserved of the two EGF domains common to all ELTD1 orthologues suggests that this is the most important EGF domain as regards ELTD1's core biological function.

According to the Stinger/Stachel Hypothesis (presented in chapter 1), the GAIN and GPS domains are important for the activation of all adhesion GPCRs. Although ELTD1's activation and signalling mechanism is unknown, a growing number of adhesion GPCRS have been shown to function through the stinger mechanism (Liebscher et al., 2014, Stoveken et al., 2015, Wilde et al., 2016, Demberg et al., 2015, Muller et al., 2015, Brown et al., 2017). As adhesion GPCR signalling is initiated when a tethered agonist or ligand binds to a specific extracellular portion of the 7TM, one can use ELTD1's conservation mapping across orthologues to predict which are the most important 7TM loops involved in ELTD1's activation. This reveals that ELTD1's conserved 7TM extracellular amino acid loops numbered 2-3, and 4-5 are most likely to be involved in ELTD1's signal transduction (

Figure 3.4). Once ELTD1's signalling activation is solved, future mutational experiments targeting these 7TM regions will reveal exactly which residues are important for agonist binding.

A phylogenetic tree showing evolutionary distance between ELTD1 orthologues (calculated by amino acid similarity) is presented in Figure 3.3 C. Results show that each ELTD1 orthologue localises to a grouping representing their respective

evolutionary vertebrate group. Additionally, results revealed how evolutionary similar mammalian ELTD1 sequences are to each other, despite differences in EGF domain number in ELTD1 variant 1 and 2 forms of the receptor. The amino acid details of ELTD1's predicted domains across orthologues analysed in the above conservation analysis are presented in Table 3.1.

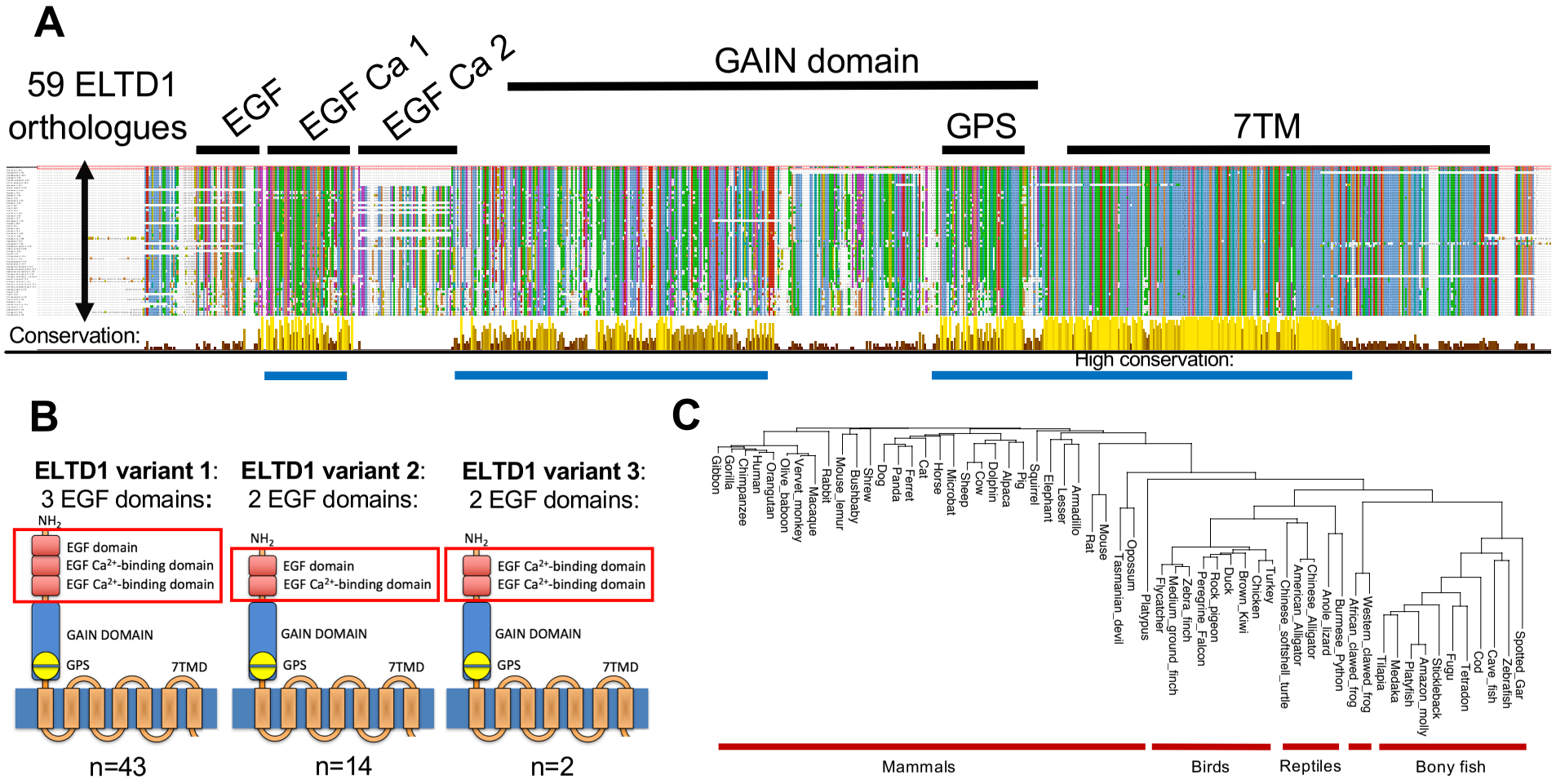


Figure 3.3: Comparison of ELTD1 orthologues across extant vertebrate species. A) ELTD1 amino acid sequence alignment across 59 extant vertebrate genomes reveals that the majority of orthologues belong to 2 evolutionary ELTD1 variants with 3 areas

of major conservation: i) the first EGF Ca^{2+} binding domain; ii) GAIN domain and GPS domain; iv) 7TM domain. Conservation scores are presented in the conservation track below the alignments; the highest scores being presented as yellow tall bars and the lowest with no bars. These results highlight ELTD1's 2 main evolutionary variants: the oldest (and majority) of ELTD1 sequences comprise 3 EGF domains, whilst the more evolutionary recent species encode only 2 EGF domains. ELTD1's domains are annotated with black bars. Highly conserved areas are annotated with blue bars. Aligned genomes are listed starting with human (primate) continuing down the evolutionary ladder until platyfish (bony fish). **B)** Graphical summary of ELTD1's three evolutionary variants showing the frequency of each variant in the sample of orthologues examined. **C)** Phylogenetic tree depicting amino acid similarity and thus evolutionary distance between ELTD1 orthologues in 59 vertebrate species; schematic drawn to scale.

			Amino acid positions:				
Scientific name	**Common name**	**Total EGFs**	**EGF**	**Ca binding EGF 1**	**Ca binding EGF 2**	**GPS**	**Sequence length**
Primates							
Homo sapiens	Human	2	21-57	58-108	None	366-418	690
Gorilla gorilla gorilla	Gorilla	2	21-57	58-108	None	297-349	621
Pongo abelii	Orangutan	2	21-57	58-108	None	297-349	513
Pan troglodytes	Chimpanzee	2	21-57	58-108	None	366-418	690
Nomascus leucogenys	Gibbon	2	21-57	58-108	None	366-418	690
Chlorocebus pygerythrus	Vervet monkey	2	21-57	58-108	None	366-418	690
Papio anubis	Olive baboon	2	21-57	58-108	None	366-418	690
Macaca mulatta	Macaque	2	21-57	58-108	None	355-407	623
Tarsius syrichta	Tarsier	2	21-57	58-108	None	366-418	652
Microcebus murinus	Mouse Lemur	3	21-57	58-108	109-158	416-468	740
Otolemur garnettii	Bushbaby	2	1-51	55-101	None	359-411	683

Tupaia glis	Tree shrew	3	21-57	58-108	109-158	416-468	740
Rodentia / Rodents							
Mus musculus	Mouse	3	21-57	58-107	108-157	414-467	739
Oryctolagus cuniculus	Rabbit	3	21-57	58-108	109-158	416-468	740
Rattus norvegicus	Rat	3	21-56	57-106	107-156	413-466	738
Ictidomys tridecemlineatus	Squirrel	3	21-57	58-108	109-158	416-468	740
Laurasiatheria / Originating from Europe & Asia							
Vicugna pacos	Alpaca	2	21-57	58-108	none	366-418	690
Felis catus	Cat	2	97-133	134-184	185-234	492-544	816
Bos taurus	Cow	2	21-57	58-108	none	365-417	689
Canis lupus familiaris	Dog	3	21-57	58-108	109-158	416-468	740
Tursiops truncatus	Dolphin	2	21-57	58-108	none	366-418	690
Mustela putorius furo	Ferret	3	21-57	58-108	109-158	416-468	740
Equus caballus	Horse	3	21-57	58-108	109-158	415-467	739

Myotis lucifugus	Microbat	3	21-56	57-107	108-157	376-428	700
Ailuropoda melanoleuca	Panda	3	21-57	58-108	109-158	416-468	740
Sus scrofa	Pig	3	21-57	58-108	109-158	417-469	741
Ovis aries	Sheep	2	21-57	58-108	none	363-415	687
Afrotheria / Originating from Africa							
Loxodonta africana	Elephant	2	21-57	58-108	none	365-417	689
Echinops telfairi	Lesser hedgehog	2	21-57	58-108	none	365-416	668
Procavia capensis	Hyrax	2	13-49	50-89	none	357-409	675
Xenarthra / Originating from the Americas							
Choloepus hoffmanni	Sloth	2	21-57	58-108	none	365-416	687
Dasypus novemcinctus	Armadillo	3	55-91	92-131	144-190	448-500	800
Originating from Australia							
Monodelphis domestica	Opossum	3	21-57	58-108	109-160	422-474	746
Ornithorhynchus anatinus	Platypus	2	none	32-82	83-134	392-444	782

Sarcophilus harrisii	Tasmanian devil	3	21-57	58-108	109-160	418-470	742
Aves / Birds							
Taeniopygia guttata	Zebrafinch	2	24-54	58-94	none	365-408	735
Meleagris gallopavo	Turkey	2	none	6-42	57-94	366-418	683
Anas platyrhynchos	Duck	3	3-30	34-70	85-122	390-434	712
Ficedula albicollis	Flycatcher	3	22-57	58-108	109-160	411-462	734
Gallus gallus domesticus	Chicken	3	77-107	111-147	162-199	466-510	788
Columba livia	Rock pigeon	3	22-57	58-108	109-160	411-463	735
Apteryx australis mantelli	Brown Kiwi	3	24-53	58-95	109-146	413-457	735
Falco peregrinus	Pergrine falcon	3	22-57	58-108	109-160	411-463	735
Geospiza fortis	Medium ground finch	3	24-54	58-94	109-146	413-456	734
Reptilia / Reptiles							
Alligator mississippiensis	American Alligator	3	22-57	58-108	111-162	415-467	739
Alligator sinensis	Chinese alligator	3	22-57	58-108	111-162	415-467	739
Pelodiscus sinensis	Chinese soft-shelled turtle	3	24-54	58-94	109-114	413-457	735

Anolis carolinensis	Anole lizard	3	58-86	96-131	147-184	456-500	778
Python bivittatus	Burmese Python	3	55-95	96-146	147-198	450-502	774
Amphibia / Amphibians							
Xenopus laevis	African clawed frog	3	20-55	56-105	106-154	408-460	733
Xenopus tropicalis	Western clawed frog	3	20-55	56-97	107-152	406-458	743
Osteichthyes / Bony fish							
Lepisosteus oculatus	Spotted gar	3	27-67	71-117	118-167*	429-481	753
Takifugu rubripes	Fugu	3	16-57	61-107*	108-157	514-467	739
Gadus morhua	Cod	3	3-33	38-72	82-117	387-430	708
Gasterosteus aculeatus	Stickleback	3	16-57	58-107	108-157	414-466	738
Astyanax mexicanus	Cave fish	3	26-67	71-117	121-167	421-473	745
Oryzias latipes	Medaka	3	19-59	60-109	110-159	416-468	740
Poecilia formosa	Amazon molly	3	9-44	45-94	95-144	400-452	724
Tetraodon nigroviridis	Tetraodon	3	21-58	61-110	111-161	413-465	737
Danio rerio	Zebrafish	3	31-66	70-116*	117-165	419-470	766

Oreochromis niloticus	Tilapia	3	56-84	88-123	138-170	444-496	768
Xiphophorus maculatus	Platyfish	3	34-69	70-119	120-169	425-477	749

Table 3.1: Predicted conserved domain sequence details for all ELTD1 orthologues used in the study. Amino acid positions are presented for each predicted domain. Prediction of conserved domain was performed using SMART, KEGG motif and INTERPRO. * indicates bony fish which have replaced a Ca^{2+} binding EGF domain with an EGF domain.

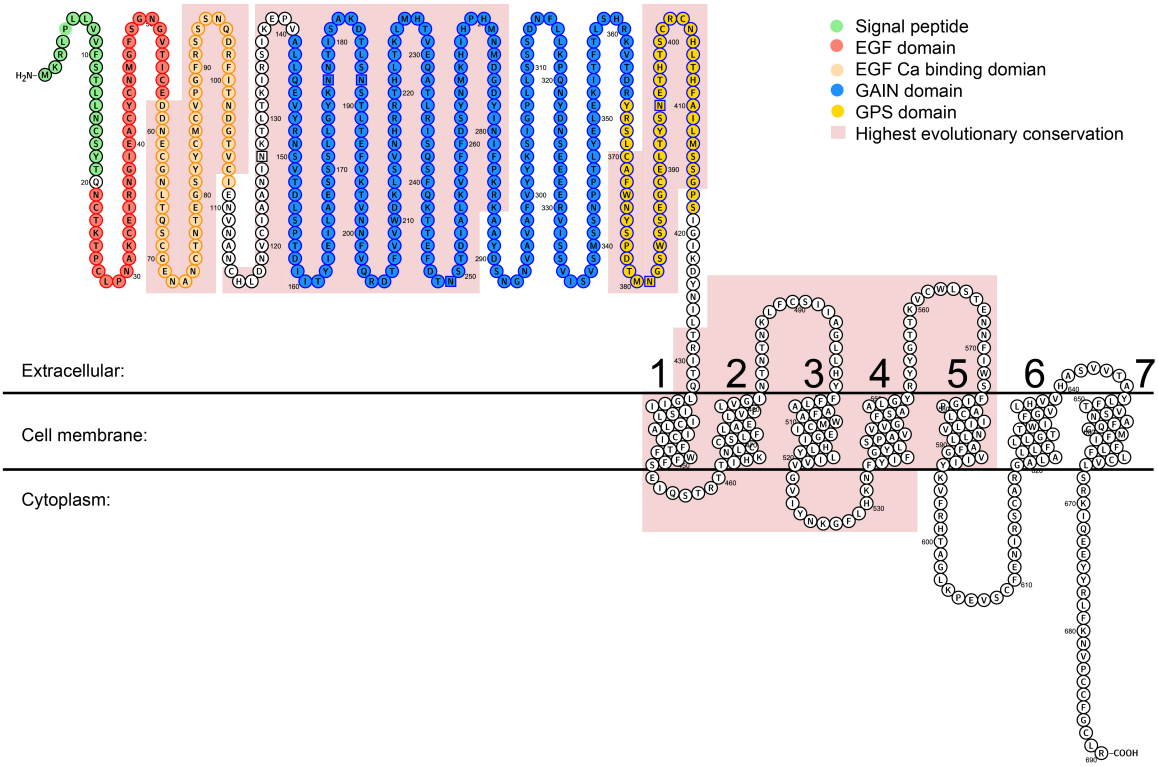


Figure 3.4: ELTD1 amino acid residue diagram highlighting areas of high conservation across ELTD1 orthologues. Domains with the highest conservation comprise the EGF Ca^{2+} domain, the N-terminal half of the GAIN domain, the majority of the GPS domain, and the first 5 transmembrane loops of the 7TM. As GPCR signalling occurs when ligand binds to the extracellular portion of the 7TM, it can be hypothesised that the conserved 7TM extracellular amino acid loops numbered 2-3, and 4-5 are most likely to be involved in ELTD1's signal transduction. ELTD1's signal peptide sequence as well as all domains are colour coded and are detailed in the legend.

3.5 Vertebrates with a deleted third EGF domain began appearing approximately 101 million years ago

Following on from the discovery of ELTD1's evolutionary variants, I next investigated which possible periods in vertebrate development prompted the development of the second ELTD1 variant.

To answer this, an evolutionary phylogenetic timetree (a phylogenetic tree with superimposed robust estimates of evolutionary time) detailing 59 extant vertebrate species who have been fully genome sequenced. Approximate phylogenetic difference between species and evolutionary time estimates were derived from the curated "Timetree: timescales of life" database (Hedges et al., 2015). Details regarding expression ELTD1's variants were then added.

The model for determining the approximate initial time period for the emergence of ELTD1 variants 2 and 3 relied on the assumption that ELTD1 variant 1 was the first form of ELTD1. Evolutionary time was then measured from the earliest point of divergence from an ancestor common to an ELTD1 variant 1 and variant 2 or 3 expressing vertebrate (in other words, from the point of emergence of an ancestor unique to an ELTD1 variant 2 or 3 encoding vertebrate). Methods are presented in the Methods chapter.

The resulting timetree is presented Figure 3.5. As has been already shown earlier, the very earliest extant vertebrates (bony fish) all express ELTD1 variant 1 only. The same is also true for the amphibian group although our sample size is smaller.

Results reveal that the very earliest vertebrates to encode ELTD1 variant 2 were the three included mammals from the Afrotheria group (hyrax, elephant and lesser hedgehog) who diverged from their common ELTD1 variant 1 encoding ancestor approximately 101 million years ago during the Cretaceous Period (145-65 million year ago). ELTD1 variant 2 encoding primates (10 out of the 12 primates investigated in this study) diverged from their ELTD1 variant 1 encoding common ancestor approximately 74 million years ago. Approximately 66 million years ago, the ELTD1 variant 2 encoding sloth diverged from its ELTD1 variant 1 encoding common ancestor.

Next, ELTD1 variant 2 expressing members of the Laurasiatheria group diverged from their common ELTD1 variant 1 encoding ancestor approximately 62 million years ago during the Paleogene Period (65-23 million years ago). Within birds, ELTD1 variant 2 has only more recently started to be expressed by 1 member: zebra finches, whose ancestor diverged from ELTD1 variant 1 encoding descendants approximately 38 million years ago (Paleogene Period).

ELTD1 variant 3 is encoded in the platypus, which evolved from its common ELTD1 variant 1 encoding ancestor approximately 177 million years ago during the Jurassic Period (199-145 million years ago) and in the turkey, which evolved from its common ELTD1 variant 1 encoding ancestor approximately 38 million years ago (Paleogene Period). Whether these represent a true third ELTD1 variant remains unclear because of their low evolutionary frequency amongst sampled vertebrates.

Furthermore, it is interesting to note that ELTD1 variant 2 is always evolutionarily forward of ELTD1 variant 1 with no examples in the studied cohort of return to variant 1 expression following variant 2 expression by an ancestor. This suggests that deletion of the third EGF domain (EGF Ca binding domain 2) has been evolutionarily beneficial for newer species. Additionally, as EGF Ca binding domain 1 is present in every ELTD1 variant, it is probably the most functionally important of the EGF domains in ELTD1. Lastly, it is also plausible to consider that ELTD1's EGF domain deletions may have occurred in response to a simultaneous evolutionary modification to ELTD1's as yet unsolved ligand.

In summary, these results establish the evolutionary importance of EGF Ca binding domain 1 as well as the first temporal reference for the emergence of ELTD1 variants during vertebrate evolution.

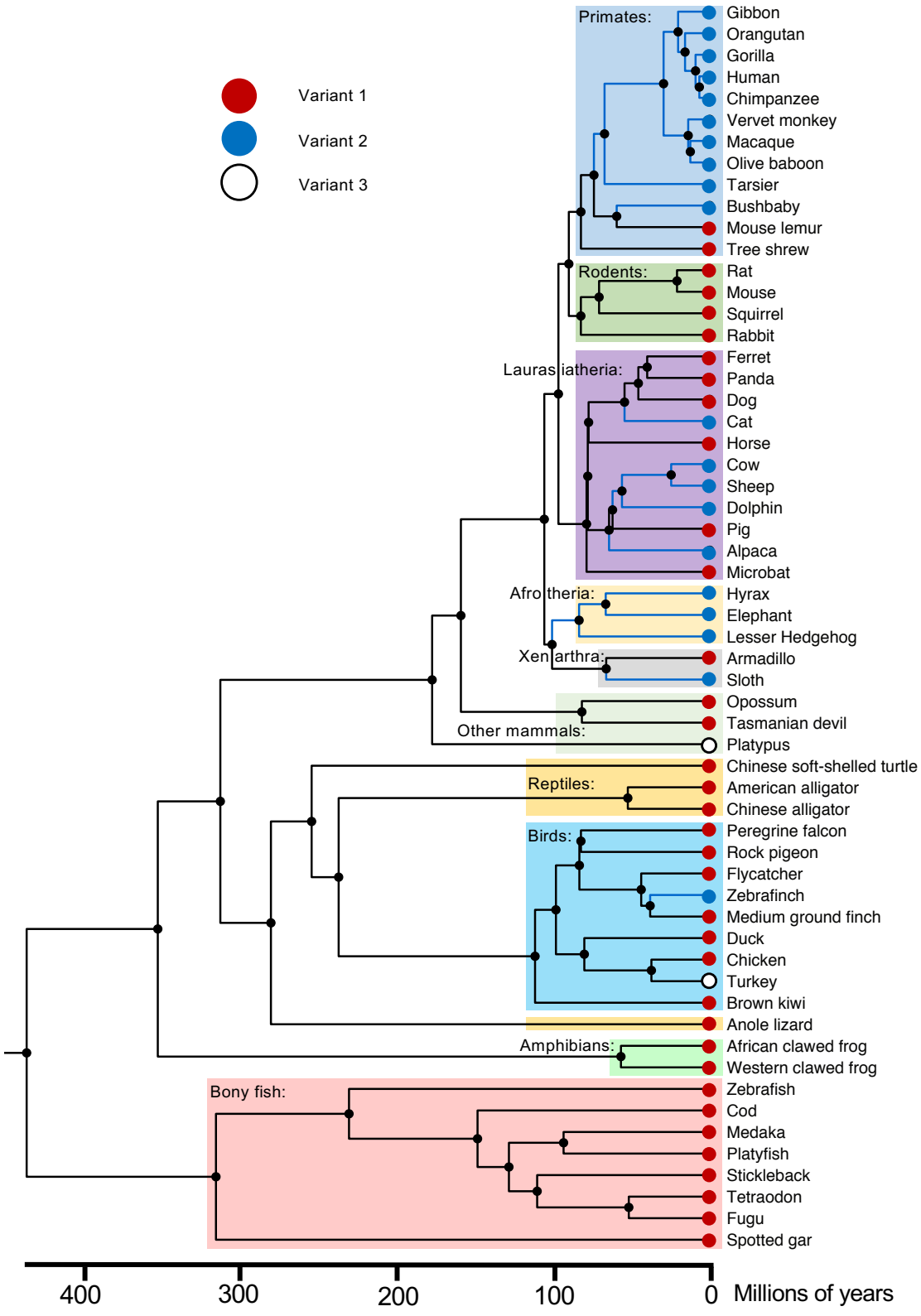


Figure 3.5: Timetree representing evolution in extant vertebrate species showing the emergence of ELTD1 variants. Red terminal nodes indicate ELTD1

variant 1; blue terminal nodes indicate ELTD1 variant 2; and the white circles indicate the low frequency ELTD1 variant 3. Blue phylogenetic lines indicate the emergence of ELTD1 variant 2 expression according to the model. The earliest vertebrates to encode ELTD1 variant 2 were the three included mammals from the Afrotheria group (hyrax, elephant and lesser hedgehog) diverging from their common ELTD1 variant 1 encoding ancestor approximately 101 million years ago.

3.6 ELTD1 is most similar to ADGRL3/LPHN3 and ADGRE3/EMR3

Lastly, ELTD1 was compared to other members of the human adhesion GPCR family. As ELTD1's ligand and signalling mechanism is unknown, this was performed with the aim of finding close sequence similarity with other adhesion GPCRS which have already had their ligands or signalling mechanism elucidated and thus possibly share a ligand or activation mechanism with ELTD1.

This was performed by contrasting the amino acid sequences of all adhesion GPCRS and plotting phylograms. Thereafter, phylogenetic comparisons were made of each of ELTD1's domains. Methods are presented in the Methods chapter.

The outcome of our initial amino acid sequence comparisons of all adhesion GPCRS is presented in Figure 3.6. This neatly separates all adhesion GPCRS into their respective families, and is the very basis for their original categorisation into distinct families (Schioth and Fredriksson, 2005). Note that adhesion GPCR family 1 (of which ELTD1 is a member) shares its common ancestor with adhesion GPCR family 2 (Figure 3.6). This is because all members of family 2 contain EGF domains

on their N-terminal fragment (NTF), as does ELTD1. Interestingly, ELTD1 is the only member of family 1 to express EGF domains.

We then investigated the similarity of ELTD1's EGF domains to those expressed on the members of GPCR family 2. This was performed through domain specific phylogenetic comparisons between ELTD1's various domains (EGFs, GAIN, GPS and 7TM) with the domains of all members of family 1 and 2 members. Domains in each adhesion GPCR were predicted and averaged using a number of conserved domain databases.

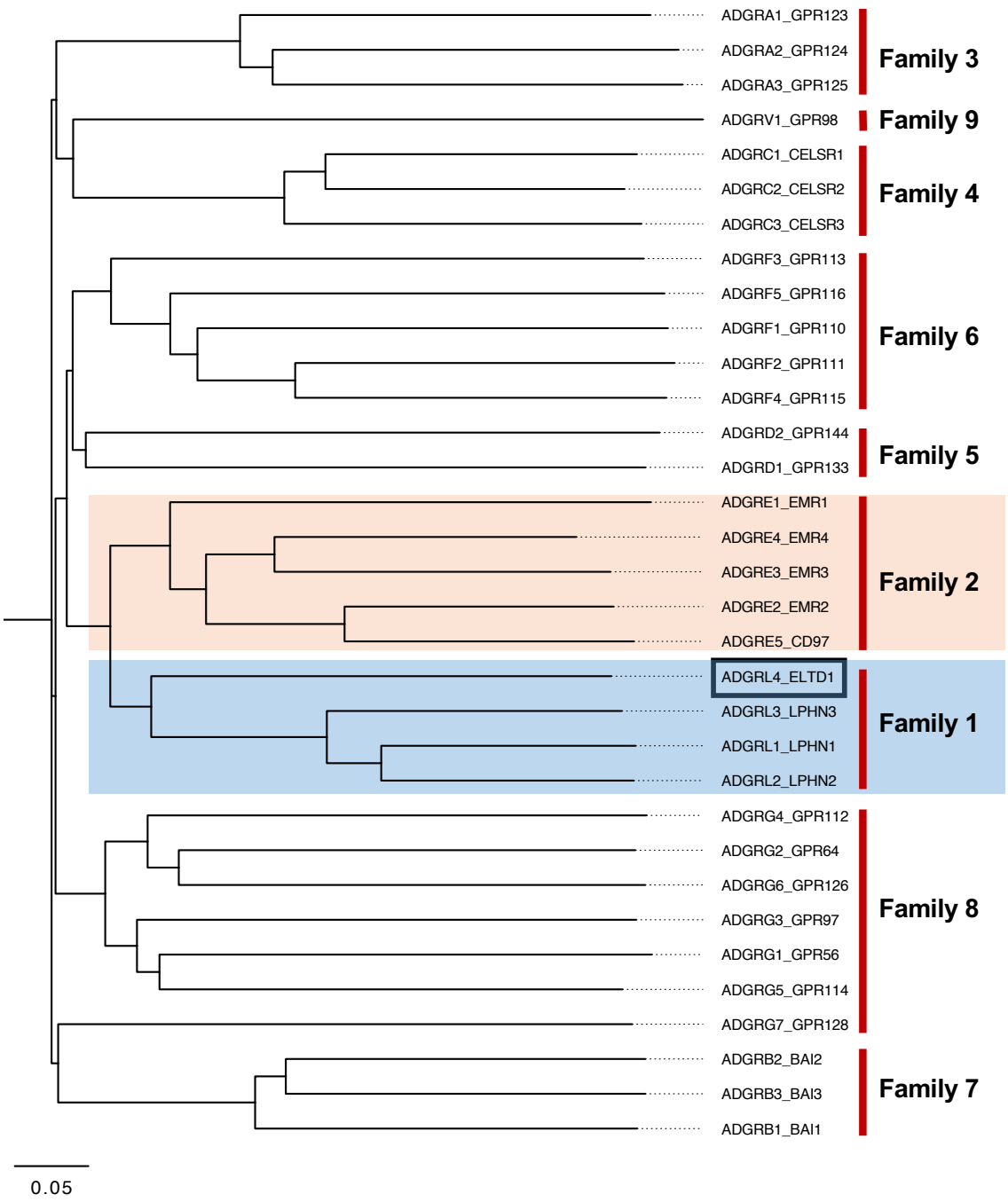


Figure 3.6: Phylogenetic tree displaying the genetic difference between all adhesion GPCRS. Amino acid sequence alignment and phylogeny separates all adhesion GPCRs into their respective families. Adhesion GPCR family 1 (which contains ELTD1) shares its common ancestor with family 2.

Results, presented in Figure 3.7, revealed that ELTD1's EGF domains are most similar to family 2's ADGRE3/EMR3 (Figure 3.7 A) and that ELTD1's GAIN domain (including the GPS domain) and 7TM domains are most similar to family 1's ADGRL3/LPHN3 (Figure 3.7 B and C). This is summarised in Figure 3.7 D. These results, combined with the knowledge that the majority of adhesion GPCR families contain extracellular domains unique to that family, suggest that ELTD1 is possibly a hybrid comprising of elements from both adhesion GPCR family 1 and 2. With regards to possible shared ligands, although ligands to ADGRE3/EMR3 remain unknown unknown, the EGF motif ligands of other family 2 members are known, namely: dermatan sulfate (Stacey et al., 2003) for both ADGRE2/EMR2 and ADGRE5/CD97; and CD55 (Hamann et al., 1996), CD90 (Wandel et al., 2012), and integrins α5β1, avβ3 (Wang et al., 2005) for ADGRE5/CD97. These are not known to associate with ELTD1.

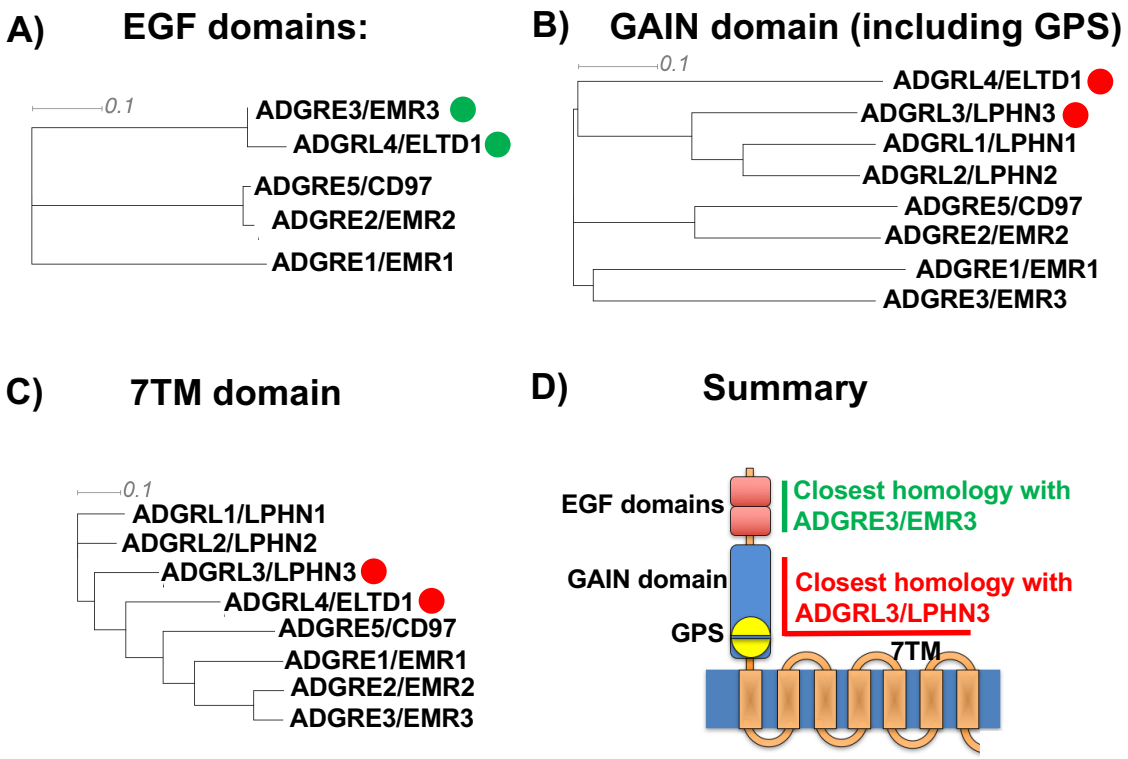


Figure 3.7: Phylogenetic sequence homology comparisons between adhesion GPCR domains belonging to members of adhesion GPCR Family 1 and Family 2. Scale bar represents the amount genetic change, represented as the number of nucleotide substitutions per nucleotide site. A) ELTD1's EGF domains are most closely related to ADGRE3/EMR3's EGF domains. B-C) ELTD1's GAIN domain (including the GPS domain) as well as its 7TM domain are most similar to the respective domains in ADGRL3/LPHN3. D) Graphical summary of ELTD1's phylogenetic relationships.

ELTD1's domain homology results beg the question: which developed first, the members of adhesion GPCR family 1 or those of GPCR family 2 and could ELTD1 be ancestral to members of family 2? This question was approached by reviewing known and predicted orthologues of all the adhesion GPCR family 1 and 2 members using the Ensembl gene browser. Each adhesion GPCR was then reviewed for orthologues in bony fish (n=11), bird and reptile (n=7) and mammalian (n=38) genomes. This revealed that in general, more vertebrate species do not express members of family 2 than family 1 (Table 3.2). In addition, when reviewing the earliest vertebrate group expressing adhesion GPCRS (bony fish), all reviewed fish expressed orthologues of family 1 adhesion GPCRS, whilst the same was not true for family 2 adhesion GPCRS (Table 3.2). Table 3.3 lists the species which do not express orthologues of family 1 and 2 adhesion GPCRS. That family 1 members are more widely expressed than the closely related family 2 members suggests that they may be evolutionarily older. Thus, it is possible that very early on in vertebrate evolution, ELTD1 was ancestral to members of adhesion GPCR family 2.

	Family 1				Family 2			
Vertebrate genomes	**ADGRL1 /LPHN1**	**ADGR2 /LPHN2**	**ADGRL3 /LPHN3**	**ADGRL4 /ELTD1**	**ADGRE1 /EMR1**	**ADGRE2 /EMR2**	**ADGRE3 /EMR3**	**ADGRE5 /CD97**
Mammals (n=38)	6	0	1	0	5	10	10	6
Birds & Reptiles (n=7)	4	0	1	0	6	4	4	5
Bony fish (n=11)	0	0	0	0	3	3	3	0

Table 3.2: The number of species which do not contain any orthologues for adhesion GPCR family 1 and 2 members. 0 = all listed species contain an orthologue for that adhesion GPCR. Whilst all reviewed bony fish species encode all family 1 members, a few fish species do not encode all family 2 adhesion GPCRS. Additionally, in higher vertebrates, family 1 adhesion GPCRS are not encoded in far fewer species than family 2.

ADGRL1/LPHN1	**ADGR2/LPHN2**	**ADGRL3/LPHN3**	**ADGRL4/ELTD1**
Alpaca *(Vicugna pacos)*	N/A	Panda *(Ailuropoda melanoleuca)*	N/A
Chicken *(Gallus gallus)*		Xenopus *(Xenopus tropicalis)*	
Duck *(Anas platyrhynchos)*		Zebra Finch *(Taeniopygia guttata)*	
Gibbon *(Nomascus leucogenys)*			
Hedgehog *(Erinaceus europaeus)*			
Shrew *(Sorex araneus)*			
Sloth *(Choloepus hoffmanni)*			
Tarsier (Tarsius syrichta)			
Turkey (*Meleagris gallopavo)*			
Zebra Finch *(Taeniopygia guttata)*			
ADGRE1/EMR1	**ADGRE2/EMR2**	**ADGRE3/EMR3**	**ADGRE5/CD97**
Amazon molly *(Poecilia formosa)*	Amazon molly *(Poecilia formosa)*	Amazon molly *(Poecilia formosa)*	Alpaca *(Vicugna pacos)*
Anole lizard *(Anolis carolinensis)*	Chicken *(Gallus gallus)*	Chicken *(Gallus gallus)*	Chicken *(Gallus gallus)*
Chicken *(Gallus gallus)*	Dolphin *(Tursiops truncatus)*	Flycatcher *(Ficedula albicollis)*	Duck *(Anas platyrhynchos)*
Duck *(Anas platyrhynchos)*	Flycatcher *(Ficedula albicollis)*	Guinea Pig *(Cavia porcellus)*	Flycatcher *(Ficedula albicollis)*

Flycatcher *(Ficedula albicollis)*	Guinea Pig *(Cavia porcellus)*	Hedgehog *(Erinaceus europaeus)*	Hedgehog *(Erinaceus europaeus)*
Hedgehog *(Erinaceus europaeus)*	Lesser hedgehog *(Echinops telfairi)*	Kangaroo rat *(Dipodomys ordii)*	Horse *(Equus caballus)*
Hyrax *(Procavia capensis)*	Marmoset *(Callithrix jacchus)*	Medaka *(Oryzias latipes)*	Sloth (*Choloepus hoffmanni)*
Medaka *(Oryzias latipes)*	Medaka *(Oryzias latipes)*	Mouse *(Mus musculus)*	Tarsier *(Tarsius syrichta)*
Microbat *(Myotis lucifugus)*	Mouse *(Mus musculus)*	Mouse Lemur *(Microcebus murinus)*	Tree Shrew *(Tupaia belangeri)*
Platyfish *(Xiphophorus maculatus)*	Pika *(Ochotona princeps)*	Pig *(Sus scrofa)*	Turkey (*Meleagris gallopavo)*
Rabbit *(Oryctolagus cuniculus)*	Platyfish *(Xiphophorus maculatus)*	Pika *(Ochotona princeps)*	Zebra Finch (*Taeniopygia guttata*
Shrew *(Sorex araneus)*	Rat *(Rattus norvegicus)*	Platyfish *(Xiphophorus maculatus)*	
Turkey *(Meleagris gallopavo)*	Shrew *(Sorex araneus)*	Rabbit *(Oryctolagus cuniculus)*	
Zebra Finch *(Taeniopygia guttata)*	Sloth *(Choloepus hoffmanni)*	Rat *(Rattus norvegicus)*	
	Tree Shrew *(Tupaia belangeri)*	Shrew *(Sorex araneus)*	
	Turkey *(Meleagris gallopavo)*	Turkey *(Meleagris gallopavo)*	
	Wallaby *(Macropus eugenii)*	Wallaby *(Macropus eugenii)*	
	Xenopus *(Xenopus tropicalis)*	Xenopus *(Xenopus tropicalis)*	
	Zebra Finch *(Taeniopygia guttata)*	Zebra Finch *(Taeniopygia guttata)*	

Table 3.3: List of species which do not encode orthologues of family 1 and 2 adhesion GPCRS. The majority of missing orthologues belongs to adhesion GPCR family 2.

3.7 Conclusion

This work shows that the orphan receptor ELTD1 is a highly conserved gene which emerged in the vertebrate genome during the evolution of bony fish approximately 435 million years. ELTD1's high conservation across all subsequent vertebrate species is similar to that of the core angiogenic gene VEGFR2. This work also shows that ELTD1 has three evolutionary variants, comprising variations in EGF domain number and reveals the evolutionary time estimates for the emergence of each. In terms of inferring insight into ELTD1's function, the first EGF-Ca^{2+} is likely to be the most important of the EGFs in terms of ELTD1's activation and cellular function as it is present in all variants. Additionally, results from conservation analysis across orthologues suggests that ELTD1's extracellular 7TM loops 2-3 and 4-5 are most likely sites for tethered agonist binding during signalling. Lastly, results show that ELTD1 contains structural elements common to both adhesion GPCR family 1 and 2 as well as ELTD1 being possibly ancestral to members of family 2

Chapter 4: Investigation of ELTD1's signalling capability

4.1 Introduction

Like the majority of adhesion GPCRs, ELTD1's activation and signalling remains unknown (Hamann et al., 2015). In addition, ELTD1 remains an orphan receptor, with no known ligands or interacting partners. As previously stated, our project aimed to better understand ELTD1's functional role within its cellular context, with the long term goal of bringing ELTD1 targeted anti-cancer therapy into clinical use. Important questions regarding ELTD1's functionality remained unanswered. These included: i) how does ELTD1 signal?; ii) what are the downstream effects of ELTD1 activation?; and iii) what are ELTD1's ligands? Unfortunately, without a reliable downstream readout system for receptor activation or a known ligand, exploring these unanswered challenges becomes very challenging, if not impossible.

Attempts at removing these obstacles (common to the functional characterisation of the majority of adhesion GPCRs) have been fraught with difficulty until recently when Liebscher and colleagues proposed the Stinger/Stachel Hypothesis (discussed in detail in Chapter 1). In brief, this proposes that the majority of adhesion GPCRS contain a tethered agonist C-terminal to the GPS cleavage point which when exposed following NTF modification (such as ligand binding to the NTF) is able to strike the receptor's extracellular 7TM loops and initiate canonical GPCR

signalling. Since its publication, the Stinger/Stachel hypothesis has been employed to solve the canonical GPCR signalling and activation of growing a number of adhesion GPCRs (These are listed in Table 1.1, Chapter 1).

As ELTD1's signalling remains unknown, I employed the Stinger/Stachel hypothesis to explore the following two scientific questions, which are explored in this chapter:

i) Does ELTD1 signal like a canonical GPCR and if so, which canonical GPCR signalling pathway does it signal through and what are the downstream effects of ELTD1's activation?

ii) Could ELTD1's Stinger/Stachel sequence be used as a functional soluble agonist for the receptor? (This would have important consequences for future *in vivo* experiments)

4.2 Generation of codon optimised ELTD1 constructs: codon optimisation increases ELTD1 surface expression

Studying ELTD1's signalling activity requires the production of a variety of recombinant ELTD1 proteins in suitable cell types for downstream analysis. Wild type (wt) full length (FL) *ELTD1* (accession ID:BC025721.1) in a pCMV-SPORT6 backbone was obtained from GeneService (Cambridge, UK; its ELTD1 sequence was independently verified and this data is presented in the signalling chapter Appendix) and cloned using standard cloning techniques into a pcDNA3.1 backbone for eukaryotic expression.

For *in vitro* culture, primary human umbilical vein endothelial cells (HUVECs) are the most commonly used model system to study endothelial cell biology (Goodwin,

2007, Staton et al., 2009) and are known to highly express ELTD1 (Masiero et al., 2013). Being primary cells, HUVECS are difficult to transiently transfect, especially with plasmids carrying genes as large as *ELTD1* (protein product of 690 amino acids). Attempts to transiently transfect various plasmids (including those carrying variants of ELTD1) into HUVECs using multiple methods (lipofection, $CaPO_4$ transfection, and electroporation) were unsuccessful for these large plasmids. In contrast, I was able to successfully transiently transfect wt FL ELTD1 into HEK293T cells using lipofection and with total cell and cell surface ELTD1 protein expression being highest between 24 and 48 hours following transfection (Figure 4.1). Due to the abovementioned transfection issues with HUVECS, the decision was made to use HEK293T cells for my signalling experiments. Importantly, HEK293T cells had been successfully used in the first GPCR Stinger/Stachel hypothesis papers (Liebscher et al., 2014, Stoveken et al., 2015), even though they did not normally express the adhesion GPCR under investigation.

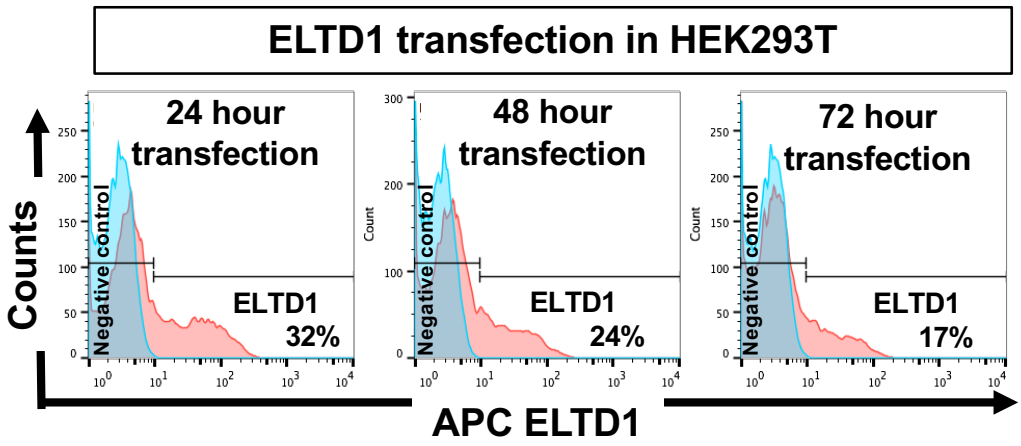


Figure 4.1: ELTD1 cell surface expression at 24, 48, 72 hours following transient transfection in HEK293T cells. ELTD1 cell surface expression assayed using FACS was highest between 24 and 48 hours following transfection. Data representative of multiple (n > 3) FACS experiments. (Primary FACS anti-ELTD1 surface antibody generated by Professor Alison Banham's laboratory, University of Oxford).

Our collaborators, Heptares Therapeutics, noted that wt FL ELTD1's nucleotide sequence had a low GC nucleotide content of 34% (Codon Adaptation Index [CAI] 0.18) (Figure 4.2 A). When compared to other adhesion and secretin GPCRS (the secretin family being an evolutionary descendant of the adhesion family (Nordstrom et al., 2009, Krishnan et al., 2012)), it was noticed that ELTD1 had the lowest GC concentration in these two families (Figure 4.2 A). As a reference, the average GC content for coding sequences in *Homo sapiens* is 52% (Milo et al., 2010).

As low GC content has been linked to regulated low gene expression (Quax et al., 2015, Frenkel-Morgenstern et al., 2012), bioinformatic codon optimisation was

performed on wt FL ELTD1's nucleotide sequence to boost the GC content of the coding sequence without affecting the final amino acid sequence (the translated amino acid sequences of both wt and co ELTD1 were checked for exactness). Through this process, ELTD1's GC content increased from 34% to 58% (CAI 0.76) (Figure 4.2 B) . When compared, codon optimised (co) FL ELTD1 had a GC content higher than the majority of adhesion GPCR receptors (Figure 4.2 B)

As low receptor expression levels have plagued adhesion GPCR signalling research previously (especially as regards mutant forms) (Liebscher et al., 2014), I investigated whether codon optimisation would increase total cellular expression of ELTD1. This was performed by transiently transfecting both co and wt forms of FL ELTD1 (both in pcDNA 3.1 plasmid vectors) into HEK293T cells and analysing total cell ELTD1 protein expression at 48 hours using Western blotting and detection with an anti-ELTD1 polyclonal antibody produced in rabbit (Sigma HPA025229, now discontinued). Results revealed a signifcantly increased total amount of ELTD1 protein produced in cells transfected with co FL ELTD1 (Figure 4.2 C). This was repeated three times.

Similar experiments were also performed by transiently transfecting co and wt FL ELTD1 constructs into HEK293T cells followed by flow cytometry (FACS). As both co and wt ELTD1 expression contructs used had a C-terminal GFP tag, GFP-mediated fluorescence was assessed by FACS. Results revealed that co FL ELTD1 expression was consistently higher than wt FL ELTD1 expression (Figure 4.2 D).Additionally, a mouse monoclonal antibody ("184.4") developed in-house by

Professor Alison Banham's laboratory (University of Oxford), was used to target surface ELTD1 expression revealing a similar percentage positive signal to that of total cell flourescene (Figure 4.2 D). All experiments were performed three times.

In summary, codon optimisation greatly increases ELTD1's total cell and cell surface expression. Due to this significant increase, co ELTD1 was used for all subsequent signalling experiments.

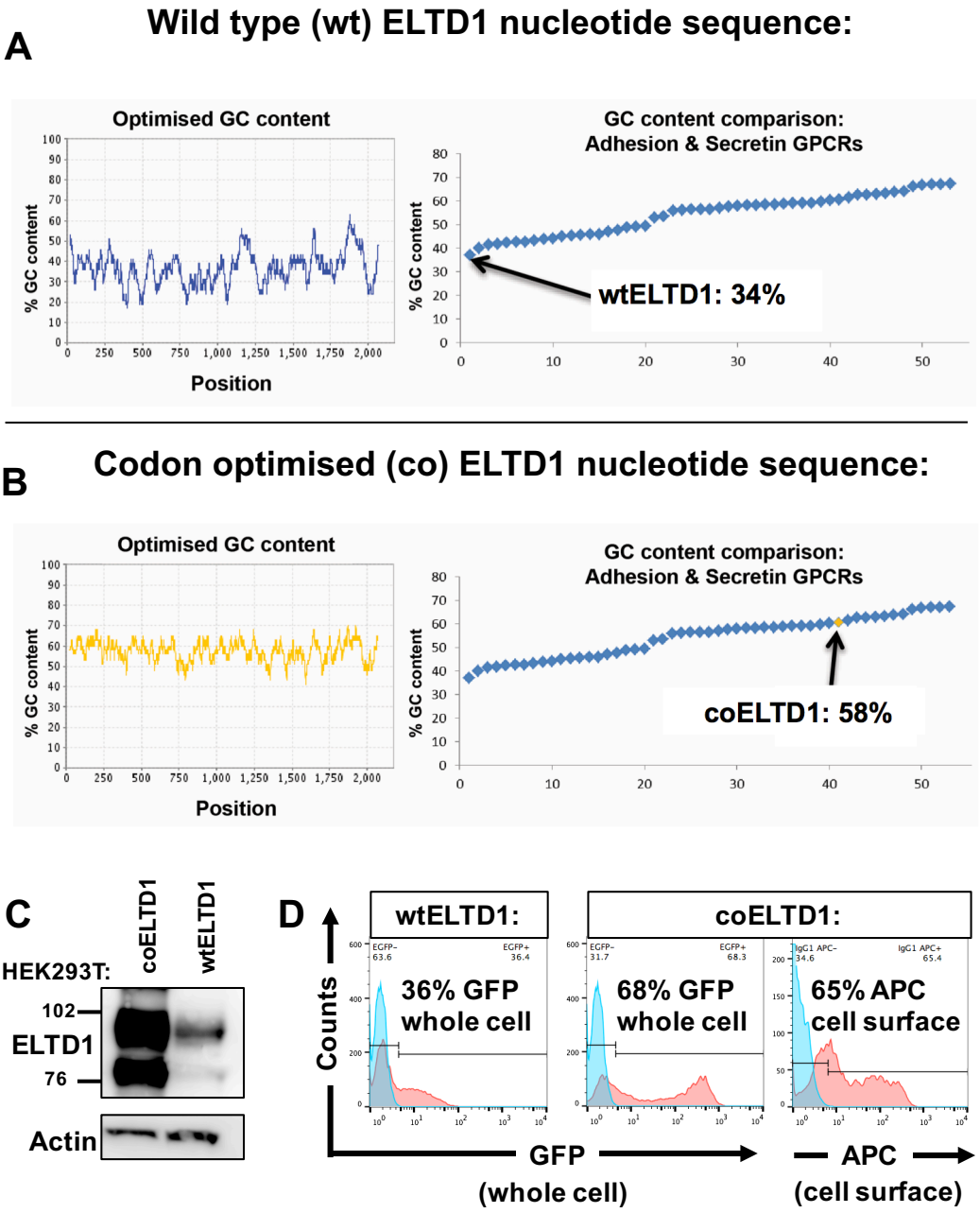


Figure 4.2: Generation of codon optimised ELTD1 constructs. A) Wild type (wt), full length (FL), ELTD1 GC content (34%) and comparison to members of the adhesion and secretin GPCR families: ELTD1 has the lowest GC content in these two families. **B)** Codon optimised (co), FL ELTD1's GC content (58%) and its comparison with members of the GC content of the adhesion and GPCR families. **C)** Western blot of co FL ELTD1 and wt ELTD1 in transiently transfected HEK293T cells: codon optimisation increases total ELTD1 expression (Primary anti-ELTD1

antibody used: Sigma HPA025229, now discontinued). **D)** Representative FACS plots showing that co FL ELTD1 expression was consistently higher than wt FL ELTD1 expression. Additionally, the frequency of total cell fluorescence (GFP) approximates to the ELTD1 cell surface receptor signal (Primary FACS anti-ELTD1 surface antibody used generated by Professor Alison Banham's laboratory, University of Oxford).

4.3 Design, cloning and expression of ELTD1/ADGRL4 constructs for signalling assays

Next, a range of recombinant ELTD1/ADGRL4 constructs were designed, to test the Stinger/Stachel Hypothesis (Liebscher et al., 2014). Three recombinant forms of ELTD1 were selected (Figure 4.3):

i) a FL form of the receptor (hypothesised not to signal constitutively according to the Stinger/Stachel model);

ii) ii) a C-terminal fragment (CTF) form of the receptor where everything N-terminal to the GPS consensus cleavage site (amino acids HL//T) (Langenhan et al., 2013) was removed (hypothesised to signal constitutively as tethered agonist peptide is free to contact 7TM loops); and

iii) iii) a seven-trans-membrane modified form (7TMΔ) lacking the N-terminus from the 7TM loops and containing no tethered agonist (hypothesised not to signal without the exogenous addition of Stinger/Stachel peptides).

Each construct was then tagged, to aid monitoring recombinant ELTD1 expression with the same detection reagents because ELTD1 proteins lacking the ECD will not be detectable using the existing anti-ELTD1 ECD targeting monoclonal antibodies. In order to minimise the risk of a specific tag interfering with signalling, two series of constructs were designed with different tagging strategies. One set of constructs contained both N-terminal HA and C-terminal FLAG tags (Figure 4.3 A), whilst a second set contained only a C-terminal GFP tag (Figure 4.3 B).

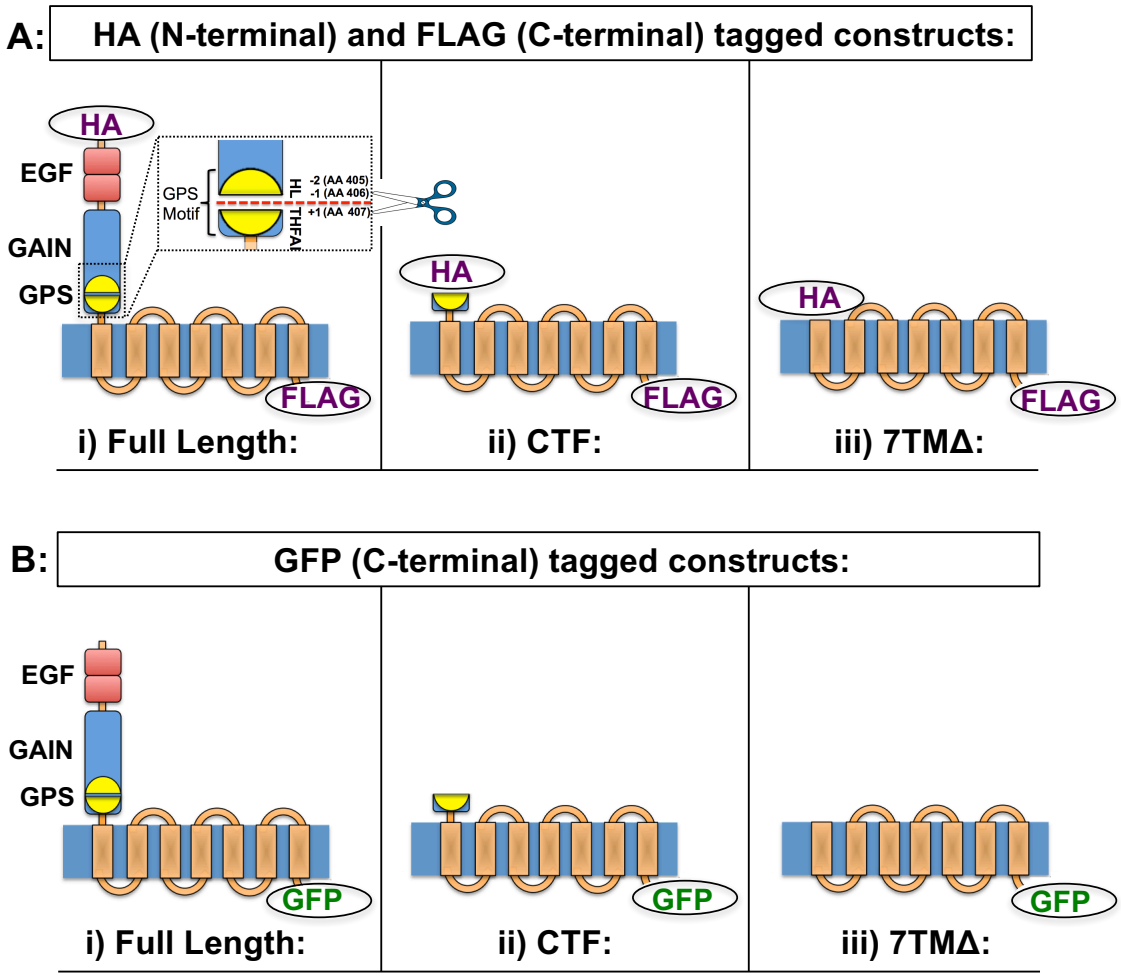


Figure 4.3: The design of ELTD1's signal constructs. Three codon optimised forms of ELTD1were designed: i) a full length (FL) form; ii) a C-terminal fragment (CTF) form; and iii) a seven-transmembrane truncated (7TMΔ) form. In order to

minimise the risk that an added tag would interfere with signalling, two differing construct sets were designed: a set with a N-terminal HA and C-terminal FLAG tag **(A)**; and a set with only a C-terminal GFP tag **(B)**.

Construct design was performed using various bioinformatics tools. In brief, the FL ELTD1 amino acid sequence was scanned for conserved domains using multiple conserved domain databases. Conserved domains were then mapped onto the codon optimised nucleotide sequence. ELTD1 constructs where then designed from this mapped template and tags added as described above. Additionally, the signal peptide from FL ELTD1 was mapped and used as the signal peptide for all designed constructs. Construct synthesis was performed by Biomatik. Constructs were then cloned individually into pcDNA3.1 plasmid vectors. (The Appendix contains the full nucleotide and amino acid sequences for each construct).

Each construct was then individually transiently transfected into HEK293T cells with ELTD1 protein expression assessed using FACS detection of the tags. N-terminally HA tagged constructs were assessed for surface ELTD1 expression using an α-HA primary with an APC secondary whilst C-terminally GFP tagged constructs were assessed for total cell fluorescence.

FACS results (n=10) from the N-terminally HA tagged constructs revealed consistent cell surface expression for the FL and CTF constructs with CTF surface

expression being consistently half the intensity of FL surface expression. Interestingly, the 7TMΔ construct failed to present the HA tag on the cell surface (further explored in the discussion at the end of this chapter). Representative FACS plots of the N-terminally tagged constructs are presented in Figure 4.4 A.

FACS results (n=10) from the C-terminally GFP tagged constructs revealed equal overall fluorescence for each construct, signifying intracellular ELTD1 construct expression. As GFP fluorescence does not indicate cell surface expression, the in-house mouse monoclonal antibody ("184.4") was used with the FL GFP expressing construct. This revealed similar levels of expression between whole cell GFP fluorescence and cell surface ELTD1 expression. Cell surface expression of the GFP C-terminally tagged CTF or 7TMΔ constructs could not be tested as at present no commercial antibodies exist for any of ELTD1's external 7TM membrane loops. Representative FACS plots of GFP expression in the C-terminally GFP tagged constructs are presented in Figure 4.4 B. In order to determine the localisation of the GFP C-terminally tagged constructs, confocal microscopy was performed on HEK29T cells transiently expressing these constructs. Results revealed surface and cytoplasmic expression for FL and CTF constructs whilst in contrast, 7TMΔ expression was only cytoplasmic (Figure 4.5).

Despite the lack of surface expression for both HA tagged and GFP tagged 7TMΔ constructs, it was nonetheless decided to include them both in subsequent signalling experiments as it was unclear at the time whether the receptors could be functioning within the cytoplasm. The rationale for this was the finding that 7TMΔ

forms of ADGRG1/GPR56 and ADGRB1/BAI1 were found to signal constitutively (Kishore et al., 2016))

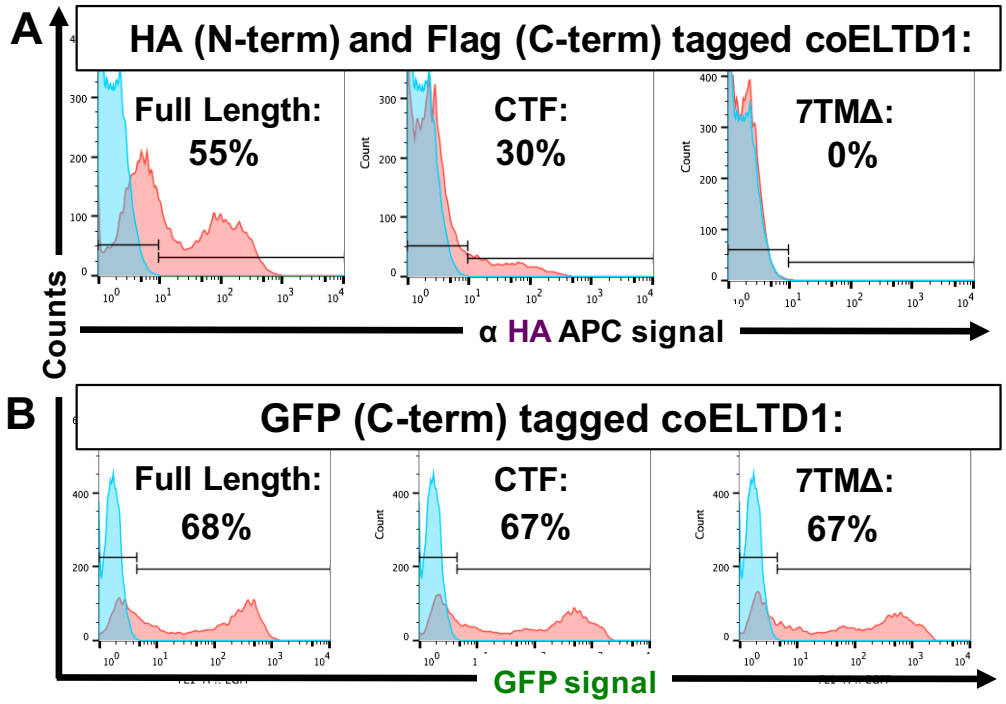


Figure 4.4: FACS plots showing representative expression of the ELTD1 signalling constructs in transiently transfected HEK293T cells (48 hours). A) Representative HA tag expression of the N-terminally HA tagged constructs revealed the following surface expression: 55% positivity in full length (FL) ELTD1 expressing cells; 30% positivity in C-terminal fragment (CTF) expressing cells and no surface expression (0%) in seven-transmembrane truncated (7TMΔ) form expressing cells. **B)** Representative total GFP expression in the C-terminally tagged GFP constructs, each giving similar levels of total fluorescence. Unlike the N-terminally tagged HA-tagged constructs, we were unable to determine surface expression of GFP tagged receptors as there are no commercially available FACS antibodies (at time of writing) to the external portion of ELTD1 seven transmembrane loops.

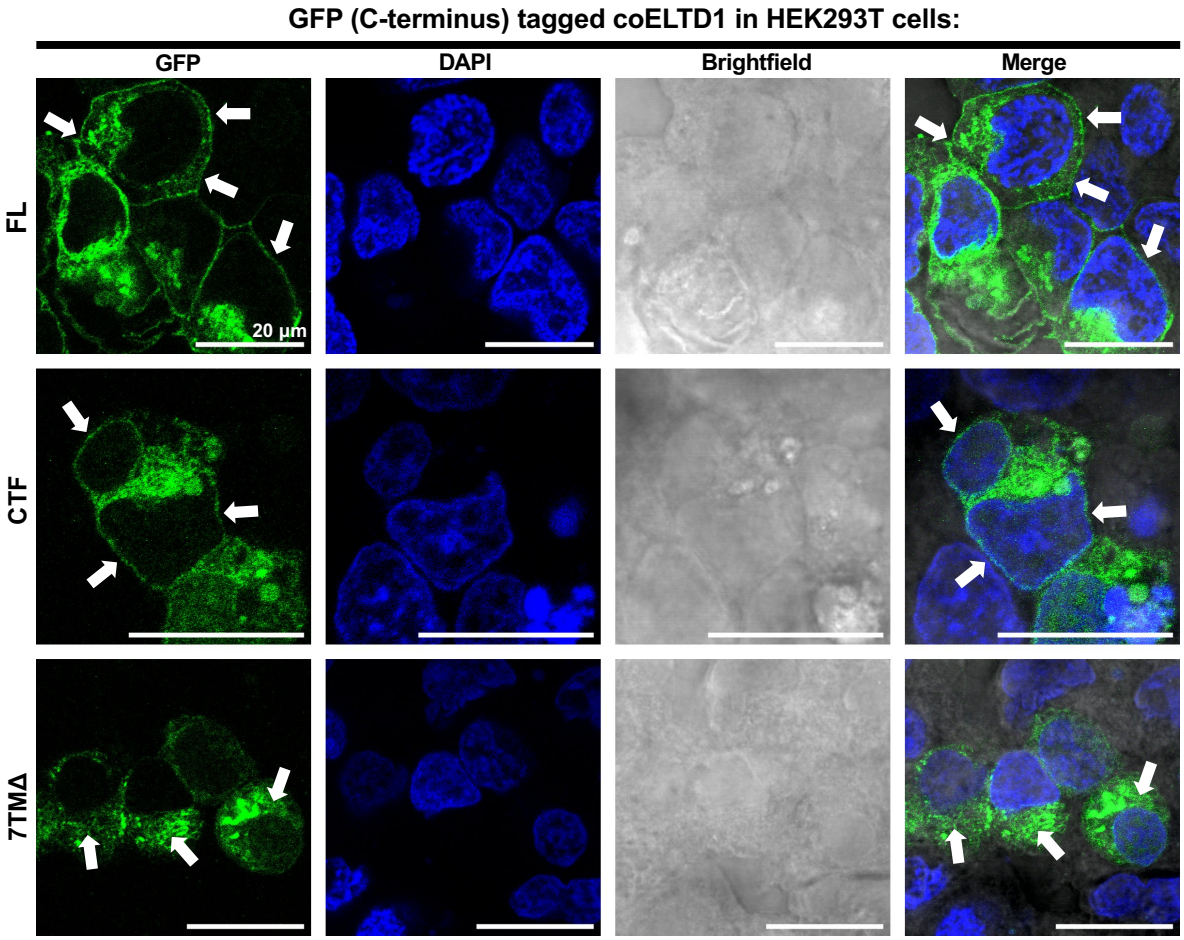


Figure 4.5: Confocal microscopy of GFP (C-terminal) tagged coELTD1 constructs transiently expressed in HEK293T cells. Representative confocal microscopy for GFP fluorescence reveals both surface and cytoplasmic expression for FL and CTF constructs with cell surface expression highlighted with arrows. With the 7TMΔ construct, expression appeared to be cytoplasmic only (arrows) with no cell surface expression in contrast to the FL and CTF constructs.

4.4 Overview of signalling assays and positive controls

GPCR signalling assays were performed using three experimental approaches. The first approach utilised Cisbio's Homogeneous Time-Resolved Fluorescence Resonance Energy Transfer (HTRF FRET) system, which assessed upstream products of specific G protein pathway coupling. The second approach utilised Promega's luciferase reporter based assay system which assessed downstream transcription factor changes related to specific G protein pathway coupling. The third approach utilised Perkin Elmer's AlphaScreen system, which also assessed upstream products of G protein pathway coupling. As all of these assays are accumulation assays, the decision was taken to perform all assays at 48 hours following transfection to allow ELTD1 to be expressed and the cell surface for the strongest signals to have accumulated. Table 4.1 lists all the signalling assays used in all subsequent signalling experiments.

HTRF FRET assays:	Associated G protein
i) IP-1 HTRF	Gαq
ii) cAMP HTRF	Gαs; Gαi

Luciferase reporter assays:	Associated G protein
i) NFAT-luciferase	Gαq
ii) NFκB-luciferase	Gαq
iii) SRF-RE-luciferase	Gα12/13
iv) SRE-luciferase	Gαi; Gα12/13; Gαq; Gβγ
v) CRE-luciferase	Gαs; Gαi
vi) CREB-luciferase	Gαs; Gαi

AlphaScreen assays:	Associated G protein
i) cAMP Alphascreen	Gαs; Gαi

Table 4.1: Table of signalling assays and their associated G proteins used in the ELTD1 signalling project. (HTRF FRET - Homogeneous Time-Resolved Fluorescence Resonance Energy Transfer; IP-1 - inositol phosphate 1; cAMP - Cyclic adenosine monophosphate)

In order to adequately control our signalling experiments, a range of positive controls were used, listed in Table 4.2. Expression constructs for the viral GPCRs US28 and BILF1 were both gifted to us by Dr. Saskia Nijmeijer (VU University, Amsterdam). US28, a constitutively active human cytomegalovirus-encoded GPCR signals through Gαq and Gα12/13 (Melnychuk et al., 2004). BILF1, constitutively active Epstein-Barr Virus GPCR, signals through Gαi (Paulsen et al., 2005). In addition, constitutively active CTF forms of the adhesion GPCRs ADGRG6/GPR126 and ADGRF5/GPR116 were both generously gifted to us by Dr. Ines Liebscher (University of Leipzig, Amsterdam), signalling through Gαs (Liebscher et al., 2014) and Gαq (Brown et al., 2017) respectively. These, and those from Dr. Nijmeijer, were all N-terminally HA tagged. The muscarinic acetylcholine receptor M3 (CHRM3/M3) receptor was also generously gifted by Dr. Liebscher. M3 signals promiscuously through all canonical GPCR pathways in the presence of its ligand, carbachol (CCh). Lastly, Ionomycin and phorbol 12-myristate 13-acetate (PMA) were used as a positive control in luciferase NFAT assays. Ionomycin and PMA directly activate NFAT, a transcription factor downstream of Gαq.

	Positive control	Activity	G protein
1	US28 (CMV GPCR)	Constitutive	Gαq; Gα12/13
2	BILF1 (EBV GPCR)	Constitutive	Gαi
3	ADGRG6/GPR126 CTF	Constitutive	Gαs
4	ADGRF5/GPR116 CTF	Constitutive	Gαq
5	CHRM3/M3 Receptor	Needs ligand	Binds all
6	Ionomycin & PMA	Needs NFAT expression	Directly activates transcription factor downstream of Gαq

Table 4.2: List of positive controls for use in ELTD1's signalling experiments.

Note: the muscarinic acetylcholine receptor M3 requires its ligand, carbachol to signal and does so by promiscuously engaging all canonical GPCR pathways. (CMV – human cytomegalovirus; EBV – Epstein-Barr Virus; PMA - phorbol 12-myristate 13-acetate)

4.5 ELTD1 signalling assays performed at Heptares, UK

The first ELTD1 signalling assays were performed in collaboration with Heptares UK, who are experts in studying GPCR-mediated signalling. In total, I spent approximately 6 months at Heptares, learning the required technical and scientific skills and ultimately performing the assays.

4.5.1 HTRF FRET in HEK293T cells: ELTD1 does not activate Gαq or Gαs

At Heptares, I used CISBIO's HTRF FRET assays to assess the more upstream products of specific G protein pathway coupling. This assay system allows interrogation of the Gαq (IP-1 assay) and the Gαs/Gαi (cAMP assay) G protein signalling systems (Table 4.1). This method does not yet have the ability to assess Gα12/13.

In order to limit the risk of a specific tag interfering with signalling, both sets of ELTD1 constructs (set 1: HA N-tagged and FLAG C-tagged; set 2: GFP C-tagged) were tested using these assays. In brief, constructs were transiently transfected into HEK293T cells (6-well plate format) followed by harvesting at 24 hours and plating into a 96 well plate at 50 000 cells per well. At 48 hours, the HTRF FRET assay was performed and read using a HTRF compatible plate reader.

As Heptares did not have a FACS facility, I was unable to assay each construct's surface expression level at the time of performing the HTRF FRET assays. However, as mentioned earlier, n>10 experiments assayed through FACS at our Oxford laboratory had produced confidence in reproducible FL and CTF surface

expression and signalling experiments used plasmid preparations that had been demonstrated to enable ELTD1 expression. Although there was no surface expression with the 7TMΔ construct, it was included in all subsequent assays due to the finding that 7TMΔ forms of GPR56 and GPR116 were constitutively active independent of the tethered agonist (Kishore et al., 2016). Lastly at the time of running these assays, FACS expression measurement following signalling assays was not being routinely used by groups active in the field (personal communication with both Dr. Ali Jazayeri (Heptares) and Dr. Ines Liebscher, (University of Leipzig)).

The first assay performed was the Cisbio IP-1 HTRF assay for Gαq coupling. For both HA and GFP tagged groups, results from n=3 experiments revealed no signal activation or difference between the FL, CTF and 7TMΔ forms of the receptor and the empty vector negative control (Figure 4.6 A) . Only the positive control (US28) induced signalling via Gαq, showing that the assay worked (one-way ANOVA $p < 0.0001$).

Next, Cisbio cAMP HTRF assays for Gαs coupling were performed. Here too, for both HA and GFP tagged groups, results from n=3 experiments revealed no signal activation and difference between the FL, CTF and 7TMΔ forms of the receptor and the empty vector negative control (Figure 4.6 B). Only the positive control (CTF form of GPR126), induced signalling via Gαs, showing that the assay worked (one-way ANOVA $p < 0.0001$).

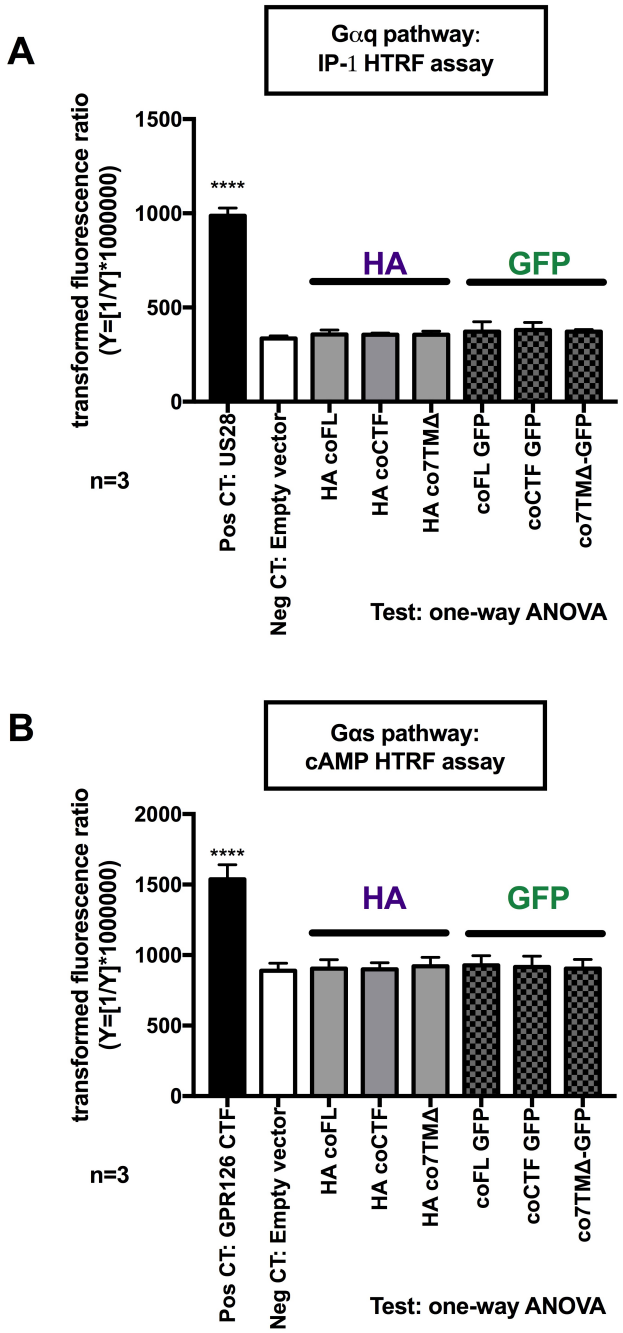


Figure 4.6: ELTD1 HTRF signalling experiments performed at Heptares: ELTD1 does not signal through Gαq or Gαs. A) Representative graph of n=3 Cisbio IP-1 HTRF assays for Gαq coupling reveals no signal activity in any ELTD1 signalling construct. US28 was used as the positive control (one-way ANOVA $p < 0.0001$). **B)** Representative graph of n=3 Cisbio IP-1 HTRF assays for Gαs coupling reveals no signal activity in any ELTD1 signalling construct. The CTF form of

ADGRLG6/GPR126 was used as the positive control and was the only statistically different sample (one-way ANOVA $p < 0.0001$) (Abbreviations: Pos CT=positive control; Neg CT=negative control; coFL=codon optimised full length ELTD1; coCTF=codon optimised C-terminal fragment ELTD1; co7TMΔ=codon optimised seven-transmembrane truncated ELTD1)

4.5.2 Luciferase reporter assays in HEK23T cells: ELTD1 does not activate Gαq, G12/13 or Gαs

Following the lack of ELTD1 activity in the HTRF FRET assays, I returned to Oxford to perform luciferase-reporter assays, each assaying luciferase expression under the control of an element regulated by a transcription factor specific to a canonical G protein pathway. For these assays, a range of luciferase-reporters were used which covered the activity of transcription factors downstream of all the canonical G protein pathways: i) NFAT-luciferase for Gαq; ii) SRF-RE-luciferase for Gα12/13 and iii) CRE-luciferase for Gαs. For the NFAT-luciferase assay, a HEK293 cell line stably expressing NFAT-luciferase (Promega, UK) was obtained from Heptares. This has the benefit of producing more reproducible results due to transient transfection giving variable copy number of the reporter between experiments. For the remainder of luciferase reporters, we utilised transient dual transfection in HEK293T cells as we had no stable lines for these reporters.

In brief, all constructs were first transiently transfected into their target cells (6 well plate format). For the HEK293 cell line stably expressing NFAT-luciferase, this

involved only transfecting the various ELTD1 constructs. For the remaining luciferase reporter assays, dual transfection was employed, transfecting both the relevant ELTD1 construct as well as the relevant luciferase reporter into the HEK293T cells. A series of optimisation experiments were previously performed to obtain the optimal total DNA/lipofectamine mixture (data not shown). At 24 hours, all cells were harvested, counted and plated into 96 well plates at 50 000 cells per well. The remaining cells were plated back into 6 well plates for FACS analysis at 48 hours. Finally, at 48 hours post initial transfection, the assay was read using a luminescent capable plate reader and FACS was performed to determine ELTD1 construct expression via detection of the HA tag or GFP fluorescence.

The first assay performed was the stable NFAT-luciferase assay for Gαq signalling. For both sets of constructs (set 1: HA N-tagged, FLAG C-tagged; set 2: GFP C-tagged) results from n=3 experiments revealed no signal activation or difference between the FL, CTF and 7TMΔ forms of the receptor and the negative empty vector control (Figure 4.7 A and B). Only the assay positive control (PMA) induced signalling and was statistically different showing activation of NFAT activity (one-way ANOVA $p < 0.0001$). FACS analysis revealed positive surface expression for the HA N-tagged FL and CTF constructs but not of 7TMΔ, and positive GFP expression across all GFP C-tagged constructs (Figure 4.7 A and B).

Next, Gα12/13 signalling was assayed using the transient SRF-RE-luciferase assay. Results from n=3 experiments revealed no signal activation with the FL, CTF and 7TMΔ forms of the receptor (Figure 4.7 C). Additionally, all ELTD1 constructs

consistently had lower luciferase signal than the negative control (Figure 4.7 C). This phenomena, which does not represent signal deactivation, has also been noted anecdotally by other groups working on other adhesion GPCRS and is thought to be related to plasmid competition during transfection and protein assembly (the empty vector plasmid is smaller and allowing more of the reporter plasmid to be transfected) (Personal communication: Dr. Ines Liebscher (University of Leipzig)). US28 was successfully used as a positive control demonstrating that the assay was working (one-way ANOVA $p < 0.0001$). FACS revealed positive surface expression for HA N-tagged FL and CTF constructs but not of 7TMΔ, and positive GFP expression across all GFP C-tagged constructs (Figure 4.7 C). In contrast to the single transfection ELTD1 expression experiments presented earlier (Figure 4.4 A and B), the current dual transfection experiments all exhibited lower HA surface expression and lower GFP fluorescence. This decrease is expected due to plasmid competition during dual transfection.

Lastly, Gαs was assayed using the transient CRE-luciferase assay. Results from n=3 experiments revealed no signal activation or difference between the FL, CTF and 7TMΔ forms of the receptor (figure 2.5D). Only the positive control (CTF form of GPR126), induced signalling and was statistically different (one-way ANOVA $p < 0.0001$). Similarly to the previous two experiments, FACS analysis revealed positive surface expression for HA N-tagged FL and CTF constructs but not of 7TMΔ, and positive GFP expression across all GFP C-tagged constructs (Figure 4.7D).

In summary, our first round of upstream (HTRF FRET) and downstream (luciferase-reporter) ELTD1 experiments revealed that the CTF form of ELTD1 does not constitutively activate any canonical GPCR pathways as was initially hypothesised it would according to the Stinger/Stachel model.

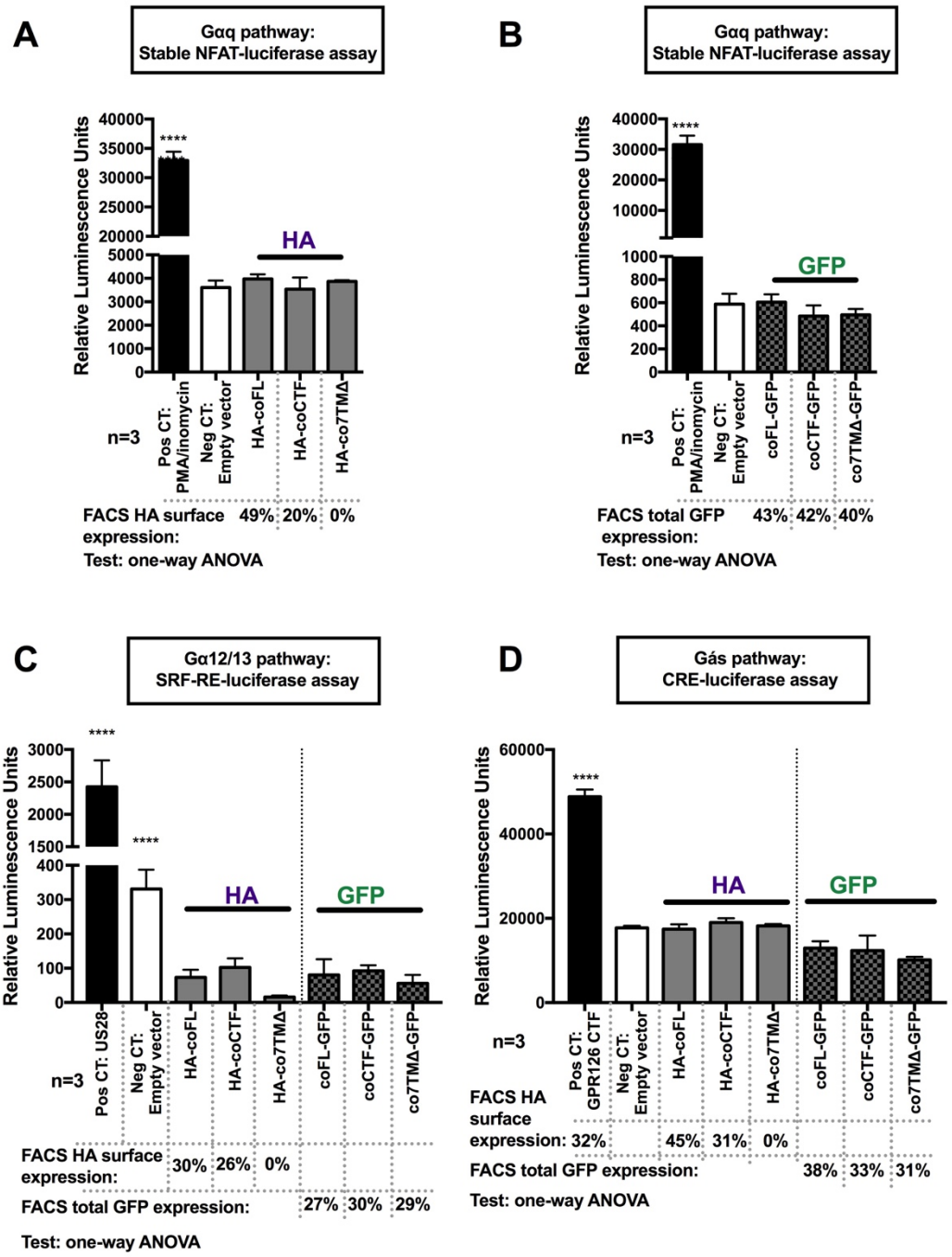


Figure 4.7: ELTD1 luciferase signalling experiments performed at Oxford: ELTD1 does not signal through Gαq, Gα12/13 or Gαs. A-B) Representative of n=3 stable NFAT-luciferase assays for Gαq coupling reveals no NFAT signalling activity in any ELTD1 signalling construct. Ionomycin and PMA were used as the positive control and was statistically different (one-way ANOVA $p < 0.0001$). FACS measurements of HA surface expression and total GFP expression are listed below

the graph. **C)** Representative of n=3 stable SRF-RE-luciferase assays for Gα12/13 coupling reveals no signal activity in any ELTD1 signalling construct. US28 was used as the positive control (one-way ANOVA $p < 0.0001$). FACS measurements of HA surface expression and total GFP expression are listed below the graph. **D)** Representative of n=3 stable CRE-luciferase assays for Gαs coupling reveals no signal activity in any ELTD1 signalling construct. The CTF form of GPR126 was used as the positive control and was statistically different (one-way ANOVA $p < 0.0001$). FACS measurements of HA surface expression are listed below the graph. (Abbreviations: Pos CT=positive control; Neg CT=negative control; coFL=codon optimised full length ELTD1; coCTF=codon optimised C-terminal fragment ELTD1; co7TMΔ=codon optimised seven-transmembrane truncated ELTD1)

4.6 The Amsterdam CTF version of ELTD1 revealed no activity when experiments were independently reproduced in Oxford

During late 2015, a group in Amsterdam working on ELTD1 presented an abstract which stated that their CTF version of ELTD1 signalled and activated NFAT-luciferase (Nijmeijer et al., 2015). These results were further presented in 2016 at the Biennial Adhesion GPCR Conference in Leipzig with activation effects being >10 fold. (Nijmeijer, 2016). As this data was contrary to my findings, our groups made contact and a collaboration was established in order to better understand the differences in our results.

With this in mind, the Amsterdam group kindly shared their wild type (wt) FL and CTF versions of ELTD1 with us (henceforth termed the Amsterdam ELTD1

constructs). A comparison of the Amsterdam and Oxford CTF was performed, as well as signalling experiments using both upstream (IP-1 HTRF) and downstream (NFAT-luciferase) assays for Gαq activation.

Amino acid sequence comparisons of the Amsterdam CTF construct to the Oxford CTF construct revealed that both included an identical GPS cleavage site and an identical 7TM sequence C-terminal to the GPS cleavage site. Additionally, both constructs contained N-terminal HA tags with a preceding signal peptide (Figure 4.8 A). In terms of differences, the Amsterdam CTF contained i) a non-codon optimised ELTD1 sequence; ii) an inserted two amino acid restriction site between the N-terminal HA tag and the start of the GPS cleavage site; and iii) an inserted C-terminal extension comprising of a 24 amino acid flexible linker joined to a mVenus fluorescent tag, effectively doubling the length of ELTD1's intracytoplasmic tail (FL ELTD1/ADGRL4's predicted cytoplasmic tail is approximately 20 amino acids in length) (Figure 4.8 A). Lastly, the Amsterdam CTF's plasmid backbone was pcDEF3 which is identical to the Oxford CTF's pcDNA3.1 apart from the substitution of pcDNA's CMV promoter for the more efficient EF-1α promoter (Gopalkrishnan et al., 1999).

FACS analysis performed on HEK293T cells transiently transfected with the Oxford and Amsterdam ELTD1 CTF constructs at 48 hours consistently revealed greater surface HA signal with the Oxford CTF when compared to the Amsterdam CTF (Figure 4.8 B).This difference was most likely due to the effect of codon optimisation as only the Oxford ELTD1 CTF was codon optimised and mVenus detection

demonstrated that nearly 90% of the HEK293T cells has been transfected with the Amsterdam ELTD1 CTF construct.

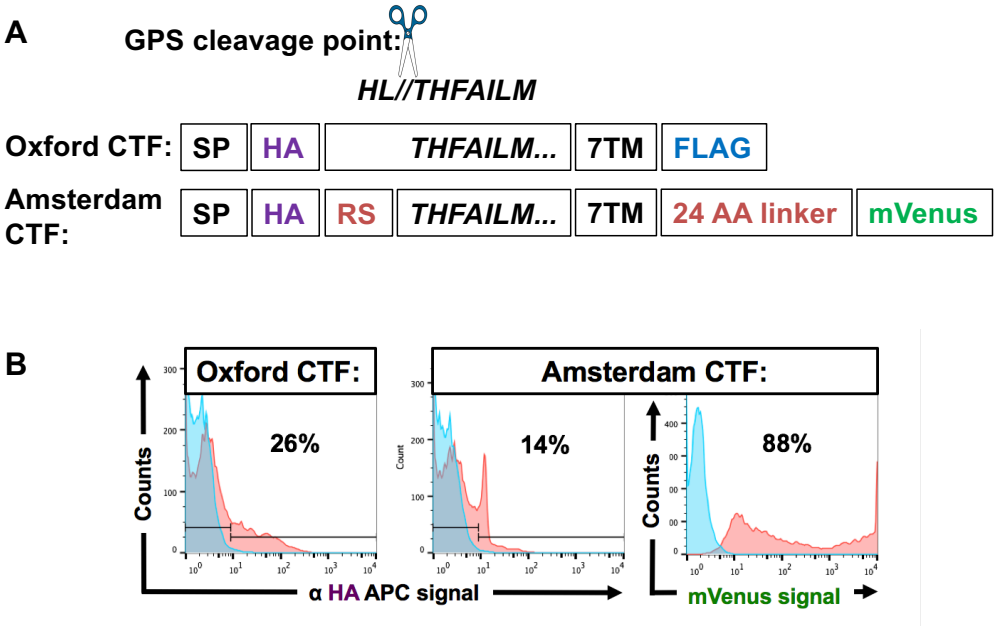


Figure 4.8: Comparison of the Oxford and Amsterdam CTF ELTD1 constructs. **A)** Graphical summary of CTF constructs. All modifications are presented in colour. Both share the addition of an N-terminal HA tag (purple) and have identically included ELTD1's amino acid sequence C-terminal to the GPS cleavage point (HL//T). The Amsterdam CTF differs through the addition of a 2 amino acid restriction site (RS) N-terminal to the GPS cleavage point, and a C-terminal 24 amino acid linker and mVenus tag. The Oxford CTF has a C-terminal FLAG tag. **B)** Representative HA tag FACS plot revealing that the codon optimised Oxford CTF had consistently better surface expression than the non-codon optimised Amsterdam CTF. FACS for mVenus fluorescence is also presented. (Abbreviations: 7TM=seven transmembrane domain; CTF= C-terminal fragment; GPS=G protein proteolytic site; RS=restriction site; SP=signal peptide)

The FL and CTF forms of the Oxford and Amsterdam constructs were then assayed for Gαq activation (the G protein upstream of NFAT) using the upstream IP-1 HTRF assay in transiently transfected HEK293T cells at 48 hours with appropriate controls. Results from n=3 experiments revealed no activation or any difference in signal between the FL and CTF Amsterdam constructs or Oxford constructs with only the assay's positive control (US28) being statistically significantly able to activate Gαq (one-way ANOVA $p < 0.0001$) (Figure 4.9 A).

Following this, I performed the stable NFAT-luciferase assay for Gαq signalling comparing the Oxford and Amsterdam constructs at 48 hours with appropriate controls. Results from n=3 experiments further revealed that there was no activation or any difference in signal between the FL and CTF Amsterdam constructs or Oxford constructs. Only the assay positive controls (Ionomycin, PMA; US28), were both significantly able to activate the NFAT-luciferase reporter (one-way ANOVA $p < 0.0001$) (Figure 4.9 B).

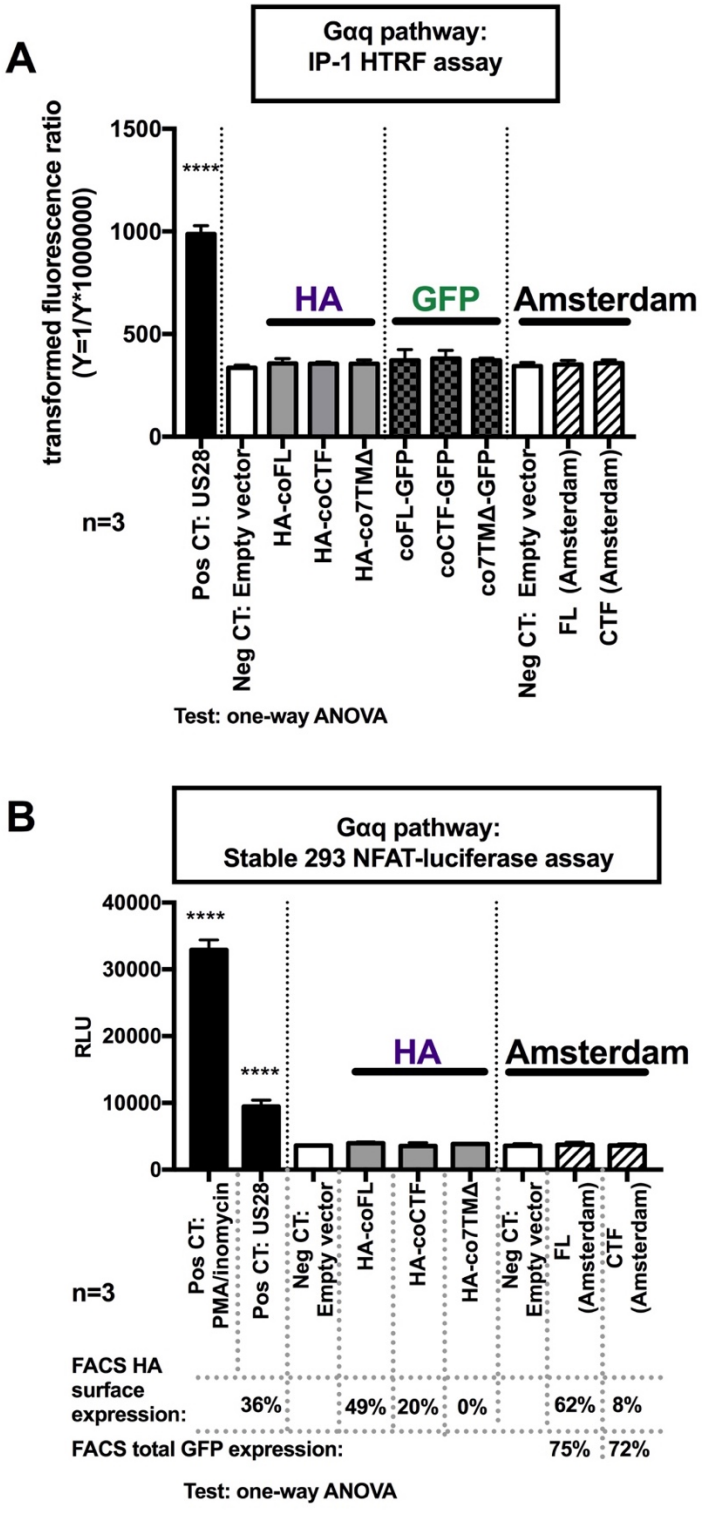


Figure 4.9: Signalling assays comparing the Oxford and Amsterdam FL and CTF constructs. A) Representative results from the Cisbio IP-1 HTRF assay for Gαq activation revealed no activation in either of the Amsterdam FL or CTF constructs, with similar results obtained to the Oxford constructs. Only the positive

control (US28) was statistically significant (one-way ANOVA $p < 0.0001$). **B)** Similarly, representative results from the stable NFAT luciferase assay for Gαq activation revealed no activation in either of the Amsterdam constructs. Ionomycin\PMA and US28 were used as positive controls (one-way ANOVA $p < 0.0001$). FACS measurements of HA surface expression are listed below the graph. (Abbreviations: Pos CT=positive control; Neg CT=negative control; coFL=codon optimised full length ELTD1; coCTF=codon optimised C-terminal fragment ELTD1; co7TMΔ=codon optimised seven-transmembrane truncated ELTD1)

4.7 Signalling assays performed at VU Amsterdam, The Netherlands.

As I was unable to replicate the Amsterdam group's findings independently using their FL and CTF constructs in Oxford I was invited to Amsterdam to perform the comparative assays alongside Dr. Nijmeijer. For these experiments, all the codon optimised Oxford constructs (FL, CTF and 7TMΔ ELTD1; in both HA N-tag and GFP-C-tag form) were brought to Amsterdam with assays performed at the VU Amsterdam University under the guidance of Dr Nijmeijer.

4.7.1 HA ELISA and GFP fluorescence expression assays

The first experiment I performed at the Amsterdam lab was to contrast the expression of both the Oxford and Amsterdam ELTD1 constructs using the methods historically used in the Nijmeijer lab for checking expression, namely: HA surface ELISA for HA tagged receptors; and GFP fluorescence for GFP and mVenus tagged receptors. At the Amsterdam lab, FACS was historically not performed alongside

GPCR signaling assays as it was deemed easier to perform the ELISA and fluorescent assays

In brief, all assays were performed using transient transfection with polyethylenimine (PEI). This differed from our transfection which were performed using Lipofectamine. In contrast to our prior experiments, constructs were directly transiently transfected into a 96 well plate and then assayed at 48 hours (without any intermediary steps). On the advice of my host, construct DNA was titrated from 25ng to 500ng per well for each experiment performed. This was to make sure that differences in expression where not related or affected by DNA amount. In order to mimic the conditions of the subsequent transient NFAT reporter assay during our expression assay, the NFAT-luciferase reporter was also transiently transfected. Lastly, pcDEF empty vector was added to the DNA mixture to ensure that each well received a total of 1000ng total DNA (construct, reporter and empty vector). As was the practise in the Amsterdam laboratory, none of the assays incorporated a control luciferase plasmid. Despite the benefits of using a control plasmid (less variation and more reproducible results) many adhesion GPCR groups do not use them due to the added complexity they often bring to the experiment. Results were read 48 hours after transfection.

Results from the HA surface ELISA assay (n=4) revealed positive surface expression for both the Amsterdam CTF and the FL and CTF Oxford HA N-tagged constructs (as before, there was no expression for the Oxford 7TMΔ; the Amsterdam group had not designed a 7TMΔ construct)(Figure 4.10 A).

Interestingly, despite the codon optimised Oxford FL and CTF constructs having higher HA surface expression than the non-codon optimised Amsterdam construct, the difference in expression was not as great as the expression difference between wild type and codon optimised Oxford constructs. This is most likely related to the stronger and more efficient EF-1α promoter present in the Amsterdam construct plasmids which is able to compensate for the construct's low GC content.

Results from the GFP expression assay (n=4) revealed that all fluorescently tagged Oxford and Amsterdam ELTD1 constructs had positive GFP expression compared to the negative control (Figure 4.10 B). Surprisingly, there was a consistently high background fluorescence in the negative control sample. This was most likely due to the culture medium interfering with the detection capabilities of the plate reader, a problem not present when using the more sensitive modality of FACS.

Both the Amsterdam and Oxford GFP tagged samples exhibited a dose responsive expression pattern, with expression correlating to the amount of DNA transfected. A similar dose response was also noted for HA surface expression in the Amsterdam HA tagged construct. In contrast, the FL and CTF HA tagged Oxford constructs which did not display any dose responsive expression patterns. In summary, for the Oxford codon optimised constructs: surface expression is not dose responsive (possibly due to the effect of codon optimisation boosting surface expression to the maximal level tolerated by the cell) whilst overall cell expression is. The other possibility is that the HA and GFP tagged Oxford constructs function

differently within the cell. Whilst this may be possible, the signalling results from both groups are all similar.

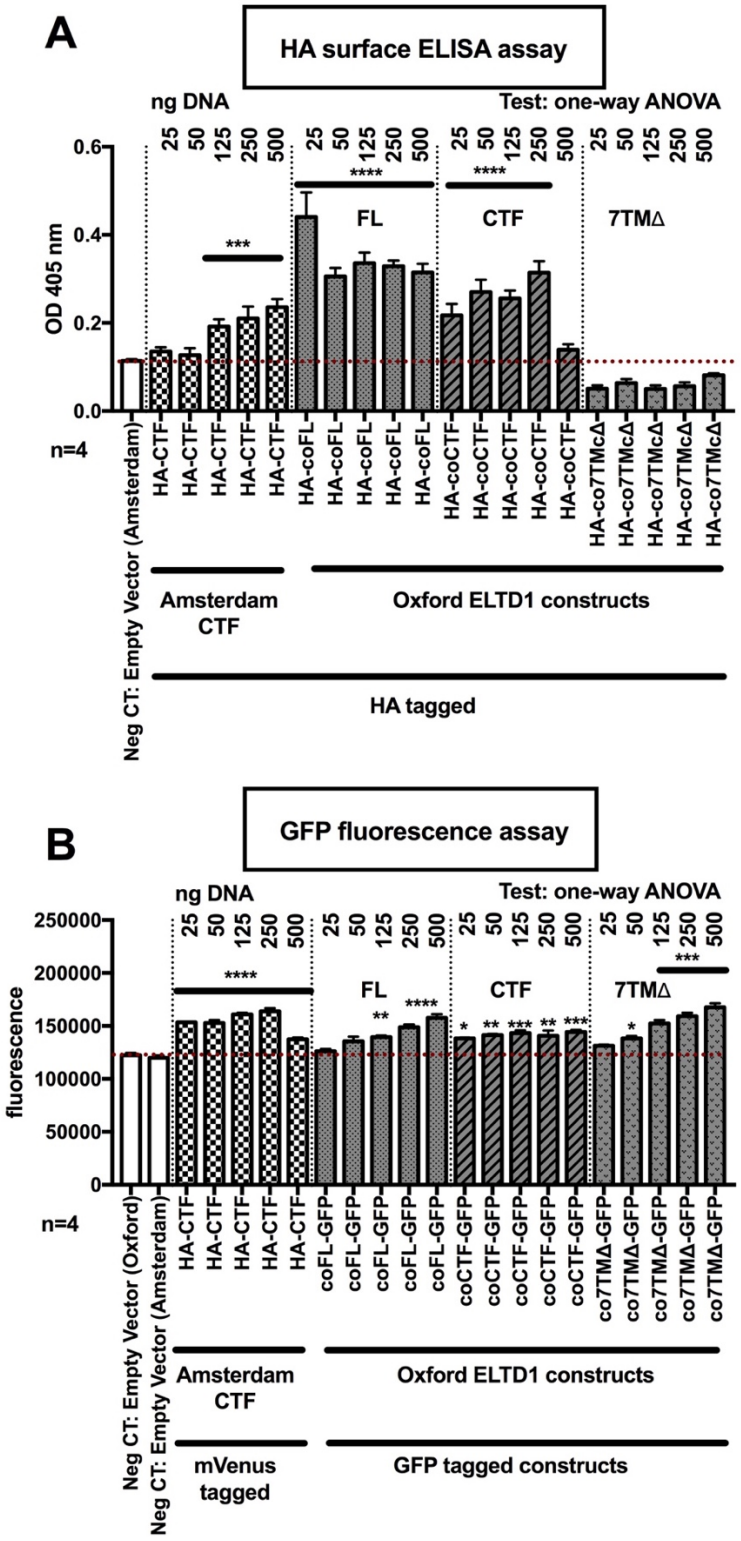


Figure 4.10: Expression comparison between the Oxford and Amsterdam HA tagged ELTD1 constructs performed in Amsterdam. A) HA surface ELISA assay results showed that all titrated DNA amounts used of the Oxford FL and CTF ELTD1

constructs resulted in surface expression compared to a negative control (one-way ANOVA compared to negative control: $p = 0.0001$). With the Amsterdam CTF, only the 125ng/well DNA titration and above resulted in surface expression compared to a negative control (one-way ANOVA compared to negative control: $p = 0.0004$). Additionally, both the Oxford FL and CTF had higher levels of surface expression than the Amsterdam CTF. There was no surface expression with the Oxford 7TMΔ construct. **B)** GFP expression reveals that all fluorescently tagged Oxford and Amsterdam ELTD1 constructs had GFP expression compared to a negative control. For the Amsterdam CTF, all DNA titration concentrations resulted in statistically significant GFP expression (one-way ANOVA compared to negative control: $p = 0.0001$). The Oxford GFP tagged FL contract: 125ng/well DNA titration and above resulted in statistically significant expression (one way Anova ** $p = 0.006$; **** $p = 0.0001$). For the Oxford GFP tagged CTF, all DNA titration amounts used resulted in statistically significant expression compared to control (one way Anova * $p = 0.01$; ** $p = 0.002$; *** $p = 0.0002$). For the Oxford 7TMΔ, only 50ng/well DNA titration and above resulted in statistically significant expression compared to control (one-way ANOVA * $p = 0.02$; *** $p = 0.0001$). (Abbreviations: co=codon optimised; Neg CT=negative control; FL=full length ELTD1; CTF=C-terminal fragment ELTD1; 7TMΔ=seven-transmembrane truncated ELTD1)

4.7.2 NFAT-luciferase reporter assay: neither the Amsterdam or Oxford CTF constructs activates NFAT.

The NFAT-luciferase assays were then performed according to the instructions of the Amsterdam lab. This work was performed in conjunction with Dr Nijmeijer, who performed half of the experiments in parallel with me.

As with the expression assays above, all NFAT-luciferase reporter assays were performed transiently and read at 48 hours using the conditions and DNA concentrations described above. A full and detailed description of these experiments is available in the Methods chapter.

Results from the (n=4) HA tagged Amsterdam CTF ELTD1 construct revealed a single statistically significant 2 fold increase in NFAT luminescence signal in only one of the titration group samples (125ng/well) compared to control (one way Anova p = 0.04) (Figure 4.11 A). When compared to the highly induced positive control, the single 2 fold increase in signal appears to be physiologically irrelevant. Furthermore, this was not the DNA concentration which yielded the highest HA surface expression in the HA ELISA assay (Figure 4.10 A), making it even less likely that this was biologically relevant. Lastly, one would also expect more than one of the titration amounts to yield significant changes for this to be considered physiologically relevant.

In the same assay, none of the HA-tagged Oxford constructs had any increase in signal greater than 1 fold change compared to the control (Figure 4.11 A). This

supports our previous findings. Interestingly, all HA-tagged Oxford constructs exhibited a dose-dependent decrease in NFAT signal, most likely due to plasmid competition during transfection. Lastly, the positive control US28 gave consistently higher signal than had been previously recorded at Oxford (Figure 4.11 A). This could be due to the Amsterdam lab's luminescence plate reader being more sensitive that the device in Oxford or may be related to improved dual transfection efficiency when using the Amsterdam group's transfection agent (PEI). Both reason explain why I could not replicate their data whilst in Oxford.

Luminescence results (n=4) for the Amsterdam CTF contrasted with Oxford GFP-tagged samples revealed no statistically significant increase in fold change compared to control for either the Amsterdam CTF or the Oxford constructs (Figure 4.11 B). Similarly to the HA-tagged Oxford constructs, the Oxford GFP-tagged constructs exhibited a dose-dependent decrease in NFAT signal.

In summary, the results in Amsterdam validated my previous findings that the Oxford ELTD1 constructs do not signal through Gaq pathway or activate NFAT. Additionally, the report that the Amsterdam CTF consistently activates NFAT signalling was not found to be reproducible, even within the original laboratory reporting this finding.

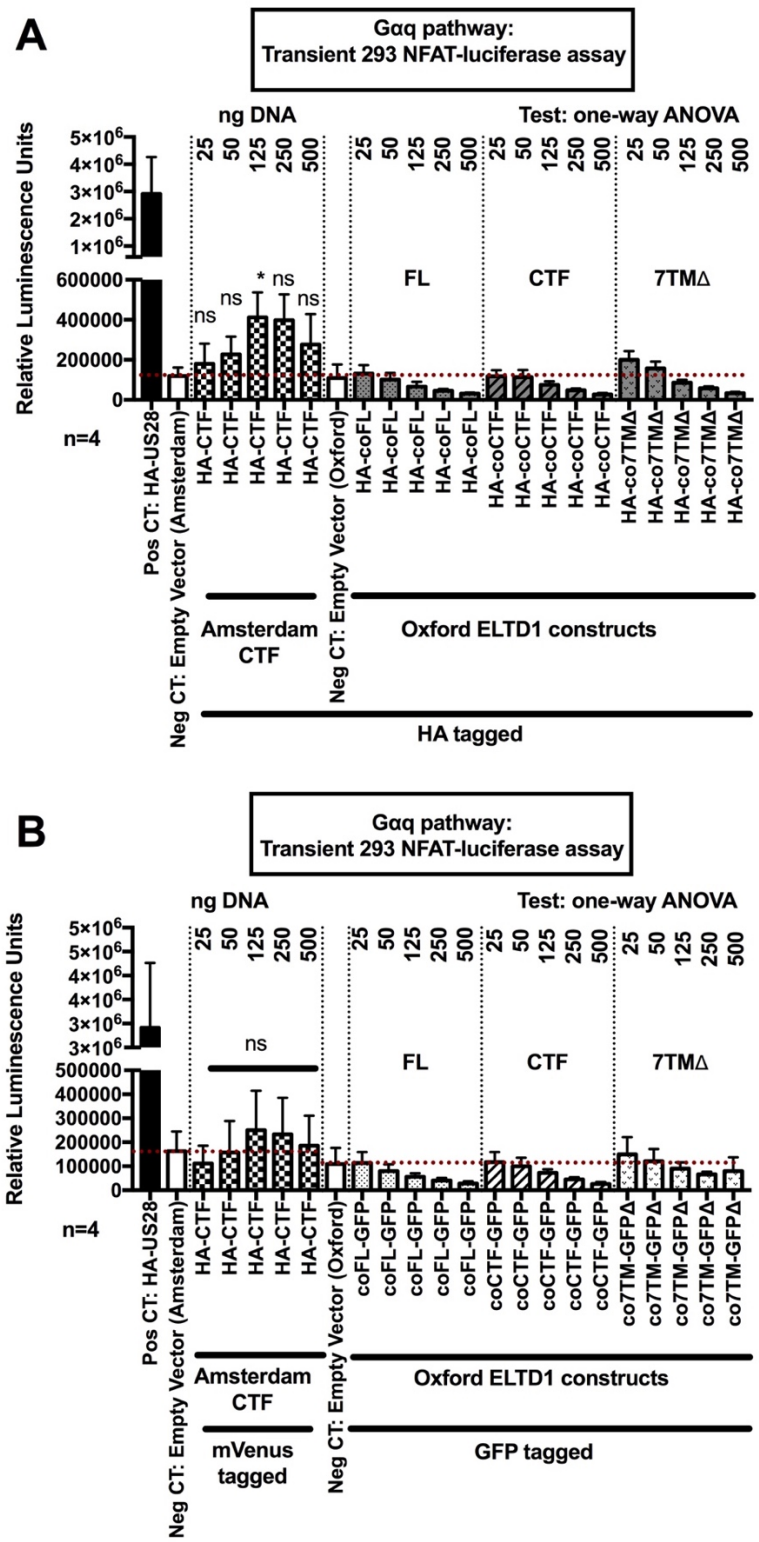


Figure 4.11: NFAT luciferase assays with Amsterdam and Oxford ELTD1 constructs, performed in Amsterdam. A) Comparison with HA-tagged Oxford constructs: results from n=4 experiments show that only 1 DNA titration amount

(125ng/well) of the Amsterdam CTF produced a statistically significant (2 fold) increase in NFAT signal (one way Anova $p = 0.04$). This went contrary to previous claims of a much larger fold change. Additionally, it can be argued that this is physiologically irrelevant as the positive control (US28) results in a much fold change. For the Oxford HA-tagged constructs, there was no increase in NFAT activity greater than 1 fold (compared to negative control). Lastly, all Oxford constructs exhibited a dose-dependent decrease in baseline NFAT signal, likely due to competition with the NFAT reporter during transfection. **B)** Comparison with GFP-tagged Oxford constructs: results from n=4 experiments show that none of the Amsterdam CTF constructs in these experiments induced a statistically significant upward change in NFAT. Similarly to the HA-tagged Oxford constructs, the GFP-tagged Oxford constructs did not elicit any significant increase in NFAT signal. (Abbreviations: Pos CT=positive control; Neg CT=negative control; coFL=codon optimised full length ELTD1; coCTF=codon optimised C-terminal fragment ELTD1; co7TMΔ=codon optimised seven-transmembrane truncated ELTD1)

4.8 ELTD1 signalling assays performed at the University of Leipzig, Germany.

To further address my concerns regarding the disparate reports of ELTD1's signalling activity, I visited the laboratory of the originator of the Stinger/Stachel Hypothesis, Dr. Ines Liebscher, at the University of Leipzig. It must be noted that our collaboration with Dr. Liebscher began at the start of the ELTD1 signalling project, when she generously shared expertise and advice with us about ELTD1 construct design.

The experimental plan in Leipzig was straightforward and comprised performing all the canonical luciferase reporter experiments using their protocols and published positive controls (Liebscher et al., 2014).

In addition to the above luciferase assays, it was decided to also use the Leipzig group's sensitive AlphaScreen cAMP assay for Gαs activation, as another family 1 member ADGRL1/LPHN1 had recently had its signalling solved to Gαs (Muller et al., 2015).

4.8.1 HA ELISA surface expression experiments in two cell lines

In Leipzig, the first experiment was to compare surface expression levels between all the Oxford ELTD1 constructs and the adhesion GPCR constructs published by the Leipzig group that were used to establish the Stinger/Stachel model. It was decided to do this using two cell types: HEK293T and COS-7 cells, both of which are easy to transfect at high efficiency and had been used successfully for such

assays in the past. The positive controls chosen for these surface expression assays were i) P2y12 receptor (a Rhodopsin-like GPCR with very high surface expression) (Bohnekamp and Schoneberg, 2011); ii) FL ADGRG6/GPR126; and iii) CTF ADGRG6/GPR126 (Liebscher et al., 2014). All positive controls were N-terminally HA tagged, using the same strategy we adopted for ELTD1, and were chosen because of their high surface expression as detected with ELISA.

In brief, both HEK293T and COS-7 cells in 48 well plates were transiently transfected using Lipofectamine with all constructs and controls before being analysed at 48 hours using surface ELISA against the N-terminal HA tags.

Results (n=2) revealed that the HA-tagged Oxford ELTD1 constructs were expressed at the same and greater levels than the published ADGRG6/GPR126 FL and CTF adhesion GPCR constructs in both cell lines (Figure 4.12 A and B). In all experiments, the highest cell surface expression signal came from the P2y12 receptor.

In summary, our HA tagged ELTD1/ADGRL4 constructs had a cell surface expression level comparable to those adhesion GPCRs with demonstrable tethered agonist signalling activity. At the 2016 Adhesion GPCR Conference in Leipzig, it had been questioned whether our negative findings were a consequence of low or insufficient surface ELTD1 protein expression. The similar surface expression to the Leipzig laboratories adhesion GPCRS put this question to rest and gave considerable confidence to the validity of our previously negative signalling findings.

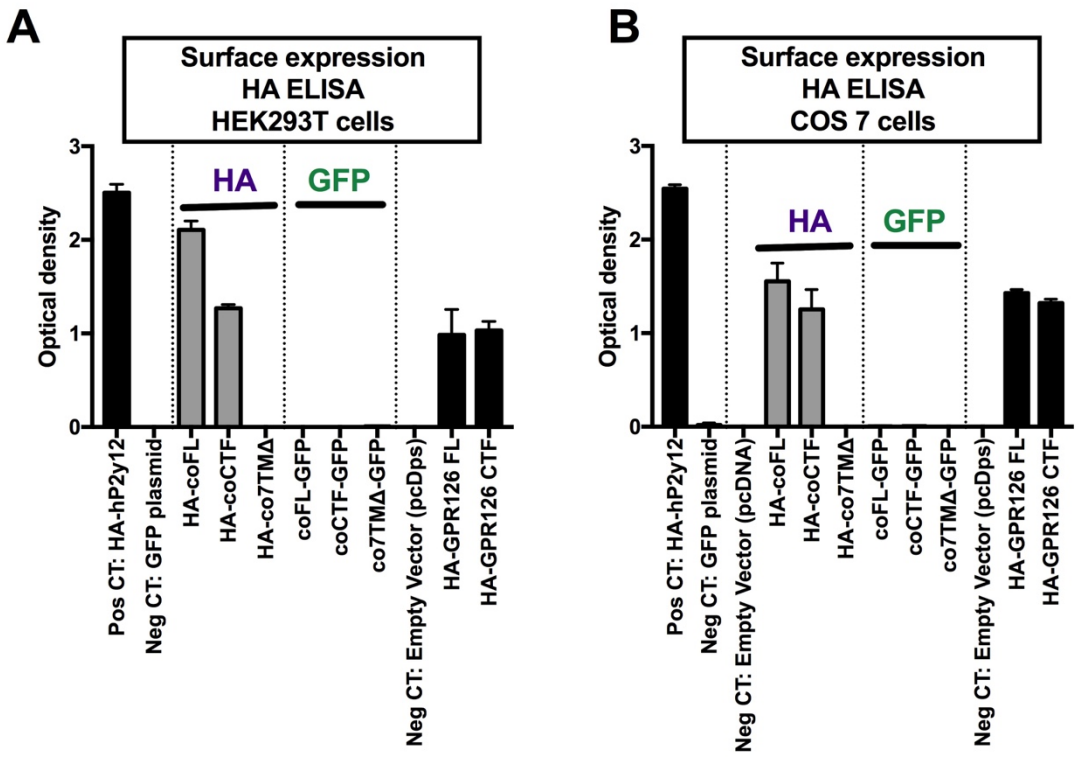


Figure 4.12: Surface expression comparison between ELTD1 constructs and signalling adhesion GPCRs published by the Laboratory of Dr. Ines Liebscher. A) Results from transient transfection in HEK293T cells (n=2) reveal that the Oxford HA-tagged ELTD1 constructs have a higher surface expression than published FL and CTF forms of ADGRG6/GPR126. The GFP-tagged Oxford constructs elicit no signal as they are not HA tagged. **B)** Similarly in COS 7 cells, the Oxford HA-tagged ELTD1 constructs express equally to the FL and CTF forms of ADGRG6/GPR126. (Abbreviations: Pos CT=positive control; Neg CT=negative control; FL=full length; coFL=codon optimised full length ELTD1; CTF=C-terminal fragment; coCTF=codon optimised C-terminal fragment ELTD1; co7TMΔ=codon optimised seven-transmembrane truncated ELTD1)

4.8.2 Luciferase-reporter assays in HEK293T cells: ELTD1 does not activate Gαq, G12/13 or Gαs

A range of luciferase-reporter assays covering all the canonical G protein pathways were then performed using transient transfection in HEK293T cells. As the Leipzig lab performed all their luciferase-reporter assays at 24 hours following transfection (rather than the 48 hours employed in earlier assays), this method was followed during my time there.

In brief, all the Oxford ELTD constructs and respective luciferase-reporter were transiently transfected using Lipofectamine into HEK293T cells and read at 24 hours. As was the historical practise in the Leipzig laboratory and similarly to the Amsterdam laboratory, none of the luciferase reporter assays incorporated a control plasmid. As these results were consistent with our previous experimental findings and as it was only possible to undertake a short visit to Leipzig, all luciferase experiments were performed only once (n=1).

Results for the NF-κB-luciferase reporter assay (downstream of Gαq activation) revealed that ELTD1 does not activate this reporter as all ELTD1 constructs had a signal lower or equal to the negative control (Figure 4.13 A). As alluded to earlier, this lower signal is understood to be related to a problem inherent to dual transfection without a control plasmid, namely transfection competition between plasmids of differing sizes. The counter argument to this effect (and reason why it is largely ignored) is that when a GPCR activates signalling, the fold change difference related to signalling will be substantial enough to overcome any plasmid

competition related issues (Personal communication: Dr. Ines Liebscher, University of Leipzig). For this assay, the CHRM3/M3 receptor with 10uM of carbachol (CCh) was successfully used as the positive control. Results from the SRF-RE-luciferase reporter assay (downstream of Gα12/13 activation) revealed no activation for any of the ELTD1 constructs, with all constructs having lower signal than the negative control (Figure 4.13 B). The CHRM3/M3 receptor exposed to 10uM of CCh was used as the positive control. Lastly, the CREB-luciferase reporter assay (downstream of Gαs) showed no activation in cells transfected any of the ELTD1 constructs (Figure 4.13 C). Here the CTF form of ADGRG6/GPR126 was used as the positive control.

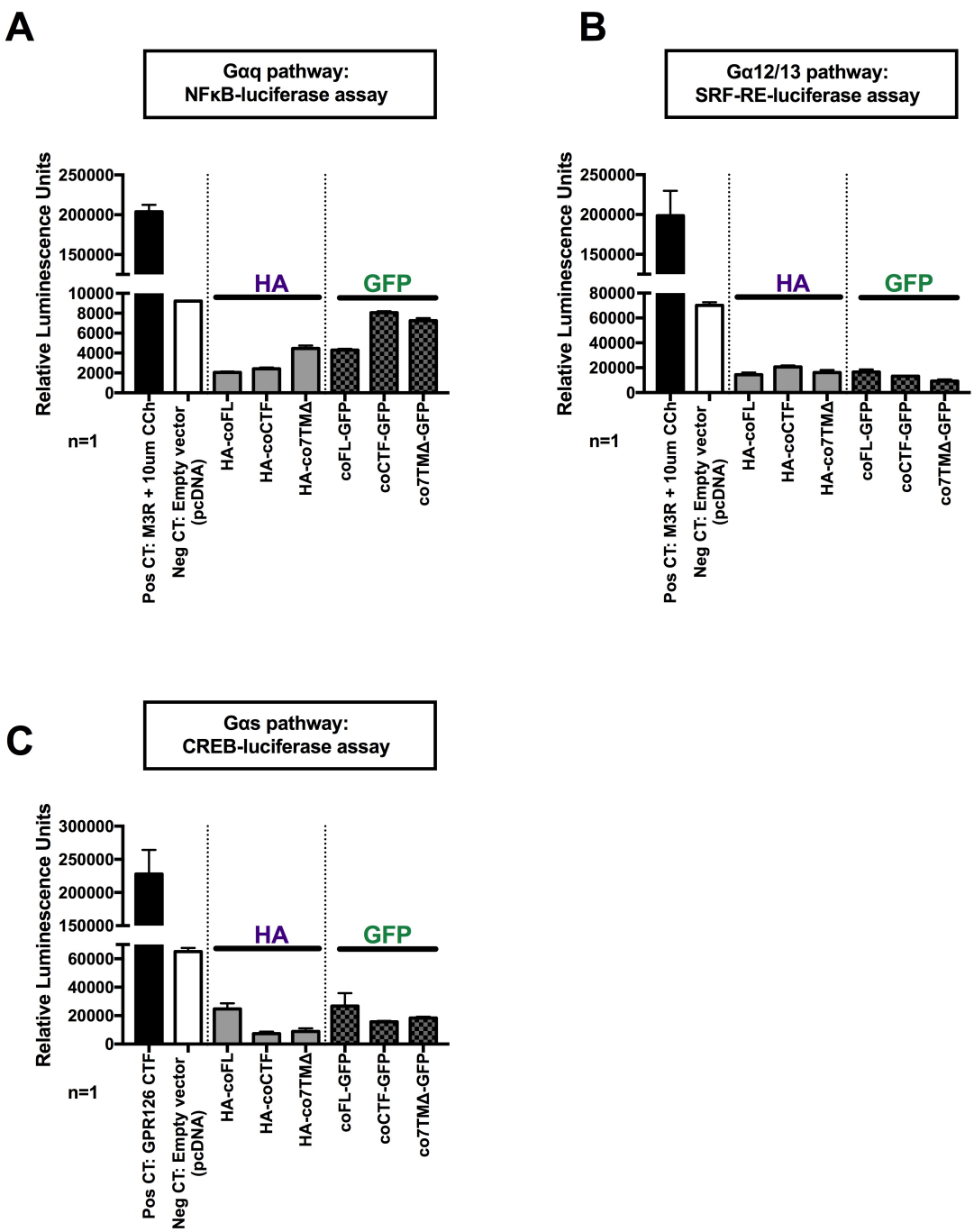


Figure 4.13: Luciferase reporter assays with ELTD1 constructs, performed in Leipzig. A) ELTD1 constructs do not signal through NFκB (downstream of Gαq), as all had an NFκB signal below or equal to the negative control (n=1). CHRM3/M3 receptor with 10uM of carbachol (CCh) was used as the positive control. **B)** ELTD1 constructs do not signal through SRF-RE (downstream of Gα12/13), as all constructs had a signal below that of the negative control (n=1). The CHRM3/M3

receptor exposed to 10uM of CCh was used as the positive control. **C)** ELTD1 constructs do not signal through CREB (downstream of Gαs), as all constructs had a signal below that of the negative control (n=1). The CTF form of ADGRG6/GPR126 was used as the positive control. (Abbreviations: Pos CT=positive control; Neg CT=negative control; coFL=codon optimised full length ELTD1; CTF=C-terminal fragment; coCTF=codon optimised C-terminal fragment ELTD1; co7TMΔ=codon optimised seven-transmembrane truncated ELTD1)

4.8.3 AlphaScreen cAMP assay performed in Leipzig: ELTD1 does not signal through Gαs

Lastly, an AlphScreen cAMP (Gαs) assay (PerkinElmer, UK) was performed on all ELTD1 constructs with appropriate controls. The CTF form of ADGRG6/GPR126 was used as a positive control, as was forskolin.

Results revealed that none of the Oxford ELTD1 constructs affected cAMP and Gαa signalling (Figure 4.14) despite the CTF form of ADGRG6/GPR126 inducing signalling. As this validated my previous Gαs findings from experiments performed in Oxford, it was only performed once.

In summary, none of the Oxford ELTD1 constructs showed any significant activation in any of the luciferase-reporter assays or the AlphaScreen cAMP assay performed

at the Leipzig lab. These results further reinforced and validated our previous findings that ELTD1 did not appear to activate any canonical GPCR pathways.

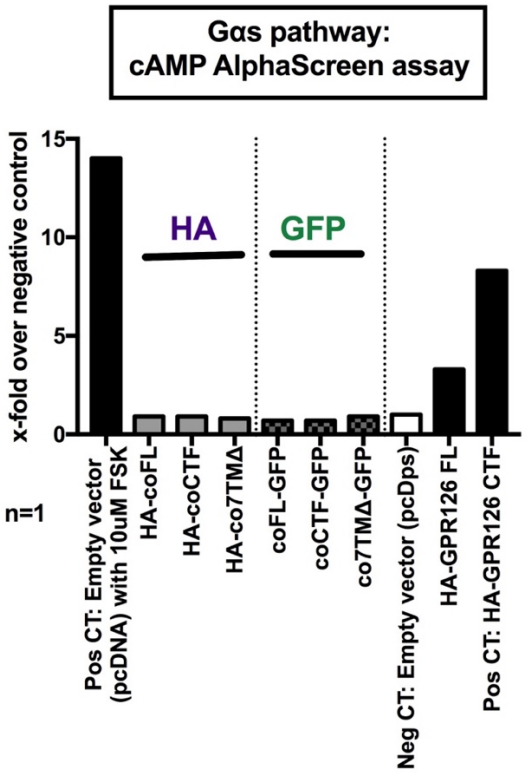


Figure 4.14: AlphaScreen cAMP assay performed with ELTD1 constructs in Leipzig: none of the ELTD1 constructs activated any Gαs activity. 10uM forskolin (FSK), and the FL and CTF forms of ADGRG6/GPR126 were used as positive controls. (Abbreviations: Pos CT=positive control; Neg CT=negative control; FL=full length; coFL=codon optimised full length ELTD1; CTF=C-terminal fragment; coCTF=codon optimised C-terminal fragment ELTD1; co7TMΔ=codon optimised seven-transmembrane truncated ELTD1)

4.9 Designing ELTD1 Stinger/Stachel peptides

Thus far, I had shown through work in multiple laboratories that ELTD1 did not appear to activate canonical G protein signalling, either in the CTF form (which should be constitutive) or in the FL form. However, on reflection, it could be argued that despite CTF ELTD1's tethered agonist being exposed, its ability to bind to the external 7TM loops and generate a signal was too transient to generate a signal strong enough to be detected using our conventional assays. To investigate this possibility, one would need to dramatically increase the concentration of the tethered agonist in close proximity to the receptor. Designing and producing peptides corresponding to predictions of ELTD1's tethered agonist (Stinger/Stachel peptides) and exposing ELTD1 to high concentrations of these peptides was thus an obvious experiment.

Twenty one Stinger/Stachel peptides were thus designed for ELTD1 with each being of varying length corresponding to the amino acid sequence beginning at the consensus GPS cleavage site and extending C-terminally to the predicted start of the first 7TM membrane loop (Figure 4.15). 7TM domain prediction was performed using two separate conserved domain databases. Peptides were then synthesised and produced to a high purity (>90%) by Biomatik.

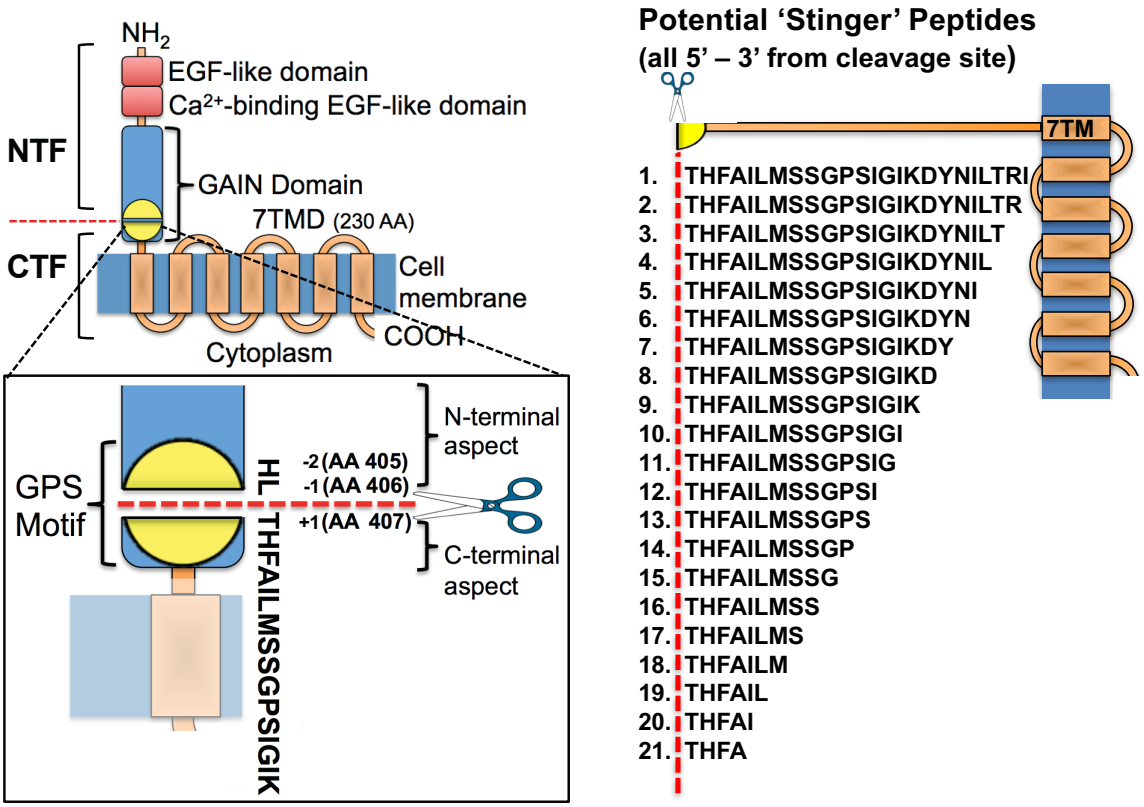


Figure 4.15: Design and sequences of the 21 ELTD1 Stinger/Stachel peptides. All ELTD1 Stinger/Stachel peptides are analogous to the amino acid sequence beginning at the consensus GPS cleavage site and continuing C-terminally until the start of the first predicted 7TM membrane loop. (Abbreviations: CTF=C-terminal fragment; NTF=N-terminal fragment; GAIN=GPCR autoproteolysis inducing domain; GPS=GPCR proteolytic site)

4.10 ELTD1 Stinger/Stachel peptide experiments performed at Heptares, UK

I returned to Heptares to perform HTRF FRET experiments on cells expressing ELTD1 which had been exposed to the ELTD1 Stinger/Stachel peptides. The cell types chosen were HEK293T transiently transfected with ELTD1 and HUVECS, which constitutively express ELTD1.

The first hurdle was titrating a range of peptide concentrations as the majority of peptides were very insoluble and would instantly precipitate at dimethyl sulfoxide (DMSO) concentrations lower than 1%. We thus decided to instead use only high peptide and DMSO concentrations (1mM peptide; DMSO concentration of 2%). This limited precipitation (however not entirely) and was the same peptide concentration as used in the original Stinger/Stachel Hypothesis paper (Liebscher et al., 2014).

4.10.1 Stinger/Stachel peptide HTRF FRET in HEK293T cells: ELTD1 peptides do not activate Gαs or Gαi

The first ELTD1 Stinger/Stachel peptide experiments were performed using HEK293T cells transiently transfected with FL codon optimised ELTD1. The FL form was chosen because for ADGRG6/GPR126 and ADGRD1/GPR133, adding Stinger/Stachel peptides initiated canonical GPCR signalling (Liebscher et al., 2014). In brief, forty-eight hours following transfection, cells were exposed to the 21 ELTD1 Stinger/Stachel peptides (1mM in 2% DMSO) for 30 minutes before commencing with the HTRF FRET assay.

With the Gαs HTRF FRET assay, results (n=2) revealed that in HEK293T cells expressing FL codon optimised ELTD1, adding ELTD1 Stinger/Stachel peptides did not induce any increase in Gαs signalling when compared to empty vector (Figure 4.16 A). Similar results were found with Gαi HTRF FRET with results (n=2) revealing that ELTD1's Stinger/Stachel peptides did not activate Gαi signalling compared to empty vector in HEK293T cells expressing codon optimised FL (Figure 4.16 B). Experiments were performed only twice due to the peptides not inducing signalling and peptide supplies running low.

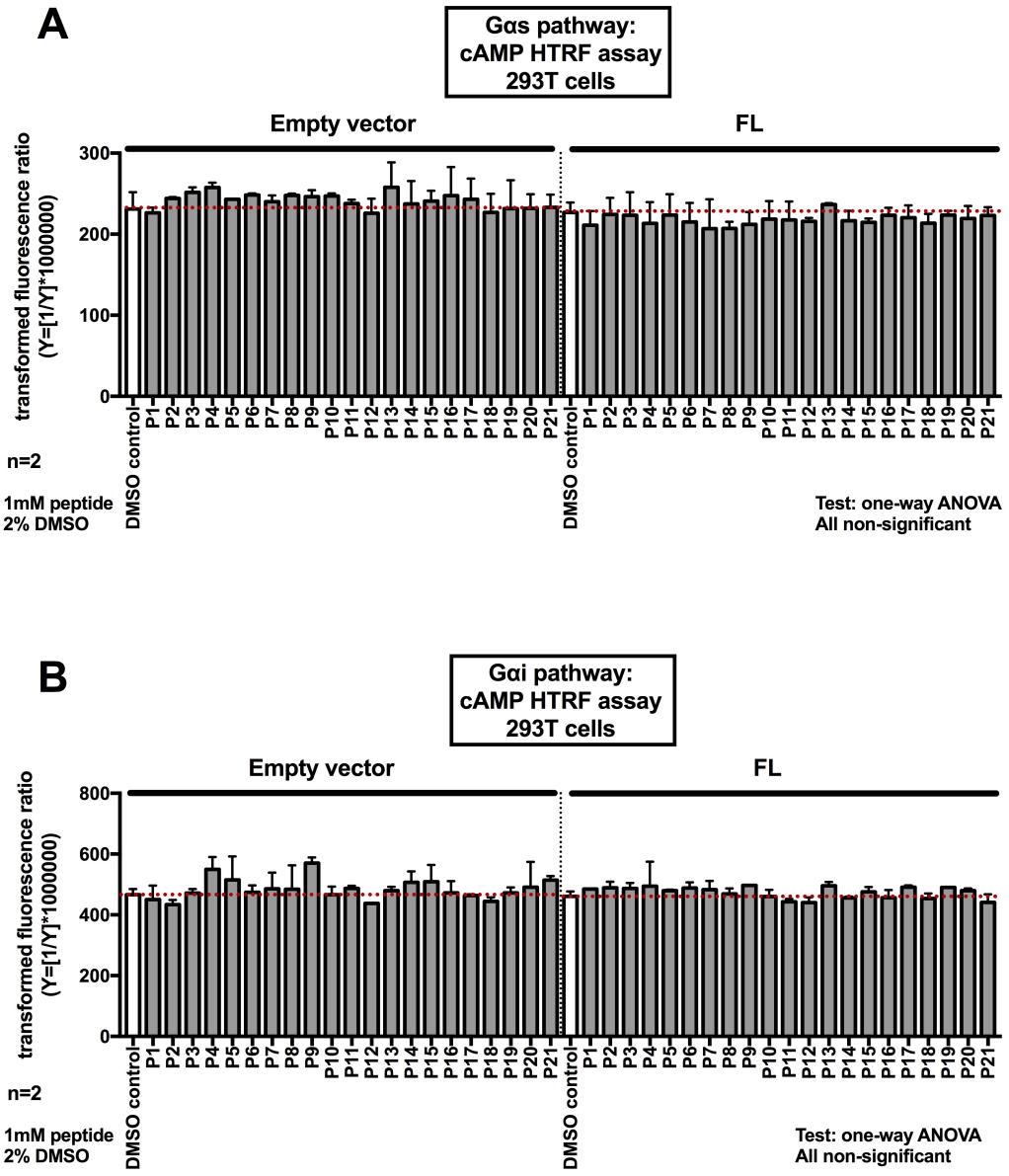


Figure 4.16: ELTD1 Stinger/Stachel peptide Gαs and Gαi HTRF FRET assays in HEK293T cells. A) ELTD1 Stinger/Stachel peptides do not induce any increase in Gαs signalling when added to FL ELTD1 and contrasted to an empty vector (n=2) (one-way ANOVA p = 0.9). **B)** ELTD1 Stinger/Stachel peptides do not induce any increase in Gαi signalling when added to FL ELTD1 and contrasted to an empty vector (n=2) (one-way ANOVA p = 0.2)**.** Peptides were added at a concentration of 1mM in 2% DMSO. (Abbreviations: FL=full length; DMSO=dimethyl sulfoxide; mM=millimolar)

4.10.2 Stinger/Stachel peptide HTRF FRET in HUVECS: ELTD1 peptides do not activate Gαs or Gαi

Next, ELTD1's Stinger/Stachel peptides (1mM in 2% DMSO) were applied to HUVECS and analysed using HTRF FRET under similar conditions. Results (n=2) revealed that the addition of the ELTD1 Stinger/Stachel peptides neither activated Gαs signalling (Figure 4.17 A) or Gαi signalling. Similarly, to the previous experiments, these assays were performed only twice due to a lack of signal induction by any of the peptides and due to a low supply of peptides. In summary, our preliminary ELTD1 Stinger/Stachel peptide results revealed that none activated signalling through Gαs or Gαi in HEK293T cells transfected with codon optimised FL ELTD1 or in HUVECS which constitutively express wild type FL ELTD1.

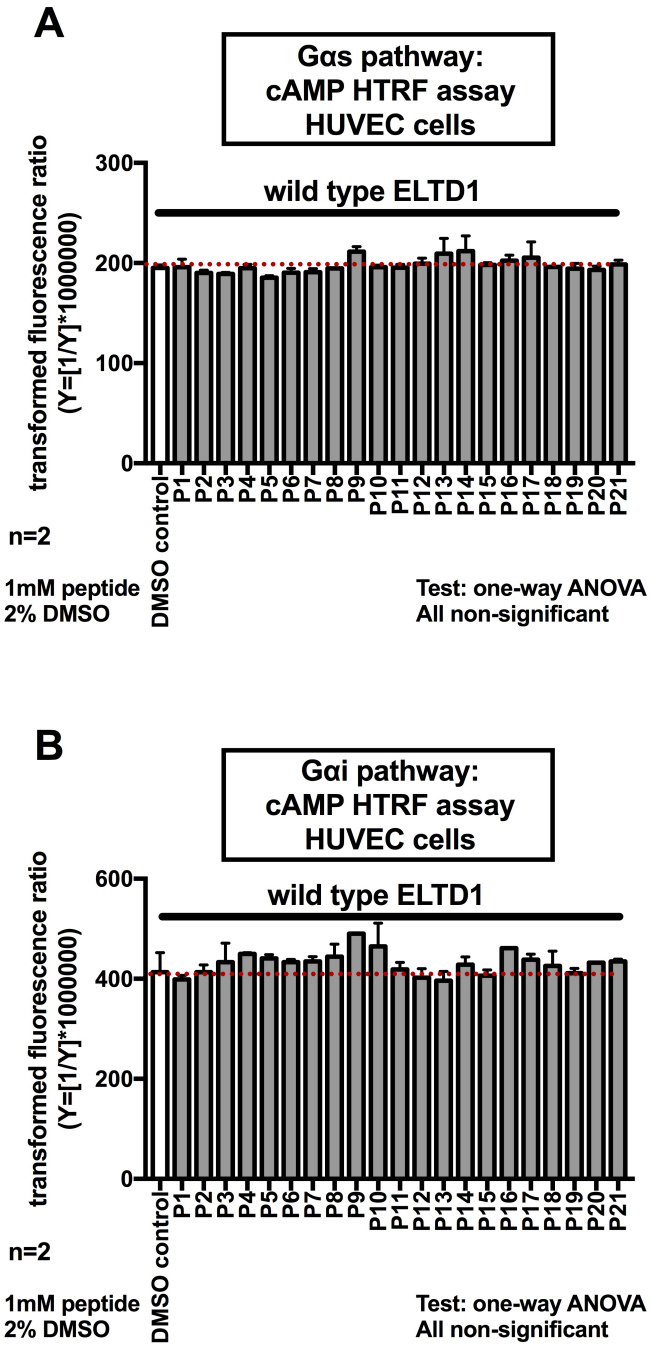


Figure 4.17: ELTD1 Stinger/Stachel peptide Gαs Gαi HTRF FRET assays performed in HUVECS. A) The addition of ELTD1 Stinger/Stachel peptides does not induce any increase in Gαs signalling when added to HUVECS (n=2) (All one-way ANOVA results were non-statistically significant). **B)** The addition of ELTD1 Stinger/Stachel peptides does not induce any increase in Gαi signalling when added

to HUVECS (n=2) (All one-way ANOVA results were non-statistically significant). Peptides were added at a concentration of 1mM in 2% DMSO. (Abbreviations: DMSO=dimethyl sulfoxide; mM=milli molar)

4.11 Stinger/Stachel peptide experiments at the University of Leipzig, Germany

Whilst at Heptares, there was only enough peptide to complete Gαs and Gαi experiments, leaving Gαq untested. After more peptide was synthesised, I returned to Leipzig to complete a panel of peptide experiments in a range of luciferase-reporter assays corresponding to the canonical G protein pathways. In light of costs, it was decided to only synthesise 11 potential stinger/stachel peptides for these experiments, choosing peptides 10-20 (see Figure 4.15 for peptide details). These were chosen because the majority of published Stinger/Stachel peptides have been of a length within that range.

Back in Leipzig, I was advised that peptide solubilisation could be improved by changing the solubilisation protocol. In brief, instead of diluting solely with DMSO, the Leipzig lab was also adding a second diluent: 50mM of tris(hydroxymethyl)aminomethane (TRIS) (pH 8). This had the benefit of dropping the DMSO concentration to 1% whilst maintaining peptide concentration at 1mM. Additionally, a 200µL pipette with its tip cut half-way was used to better aspirate the viscous peptide solution. These adaptions all significantly helped in improving ELTD1's Stinger/Stachel peptide solubilisation.

Returning to Leipzig additionally allowed the opportunity to compare the solubility of Dr. Liebscher's published Stinger/Stachel peptides with ELTD1's potential peptides. The result revealed that ELTD1's potential peptides are in general less soluble than other adhesion GPCR Stinger/Stachel peptides, with only ADGRG1/GPR56 having similar solubility to ELTD1 derived peptides.

4.11.1 Stinger/Stachel peptide luciferase assays in HEK293T cells: peptides do not activate Gαq, Gαi or Gαs

For these experiments, it was decided to test ELTD1's Stinger/Stachel peptides using all the canonical GPCR luciferase-reporter assays available in the Leipzig laboratory. Being back in Leipzig also allowed me to investigate a further question, namely, whether there was any cross reactivity between other adhesion GPCR Stinger/Stachel peptides and ELTD1.

Before experiments began, bioinformatics phylogeny comparisons were conducted on all the GPS domains in the GPCR family to determine the relative with the most similar GPS domain to ELTD1. Results are presented in Figure 4.18 and reveal that ADGRG1/GPR133 has the most similar GPS domain (and thus potential stinger/stachel peptide) to ELTD1. This was a surprising result as when one compared homology of the entire GAIN domain (which includes the GPS), ELTD1 is most similar to ADGRL3/LPHN3 (as presented in the previous results chapter). Fortunately, ADGRD1/GPR133 was one of the original Stinger/Stachel peptides solved and its Stachel/Stinger peptide (p133) was thus chosen (p133 amino acid sequence: THFGVLMDLPRSA) (Liebscher et al., 2014). Due its good solubility,

ADGRG5/GPR114's peptide (p114) was also chosen as a control sequence (p114 amino acid sequence: TYFAVLMQLSGDPVPAEL) (Wilde et al., 2016).

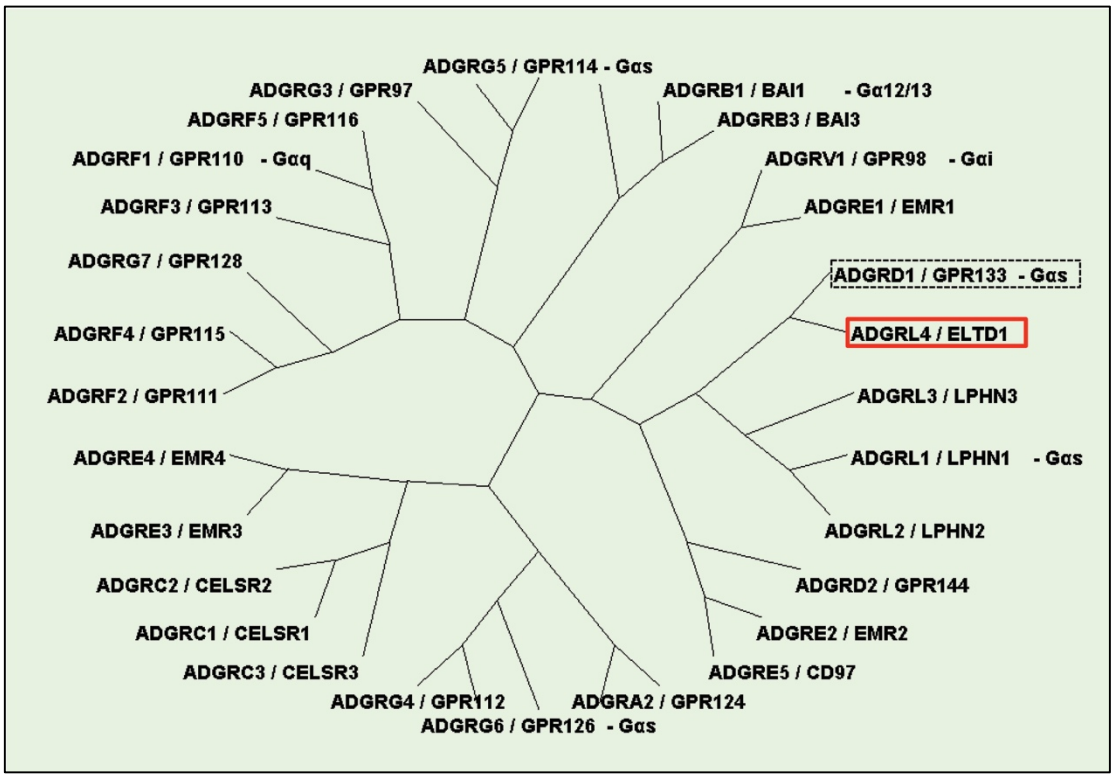


Figure 4.18: Radial cladogram showing similarities between all adhesion GPCR GPS domains. ELTD1's GPS site (red box) is most similar to ADGRD1/GPR133's GPS site (black box) which signals through Gαs. Adhesion GPCRS with solved canonical GPCR signalling pathways have this information listed after their name. Note: ADGRA1/GPR123 was not included as it does not contain a GPS domain or a cleavage site.

The first experiment was undertaken to demonstrate whether I was able to reproduce p133's activation of ADGRD1/GPR133, as had been published (Liebscher et al., 2014). In brief, non-codon optimised FL ADGRD1/GPR133 was transiently transfected into HEK293T cells along with the CREB-luciferase reporter plasmid. After 24 hours, the p133 peptide (1mM peptide; 1% DMSO) was added and incubated with the cells for 30 minutes with plain medium with 1% DMSO as a control before being read. Results from n=2 experiments revealed a significant increase (unpaired Student's t-test $p<0.0001$) in luminescence (indicating increased Gαs signalling) following the addition of the p133 to cells expressing ADGRD1/GPR133, thus reproducing the published results (Figure 4.19).

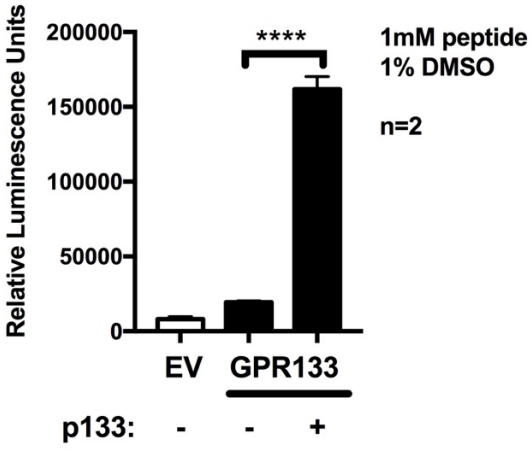
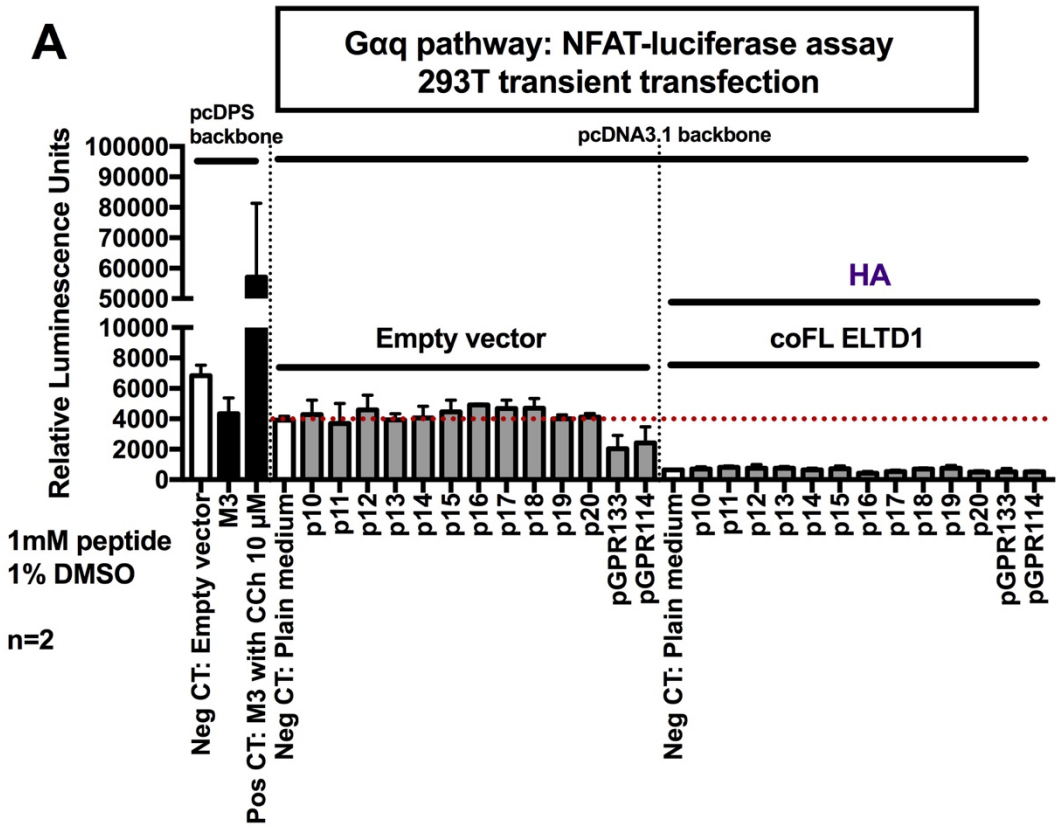
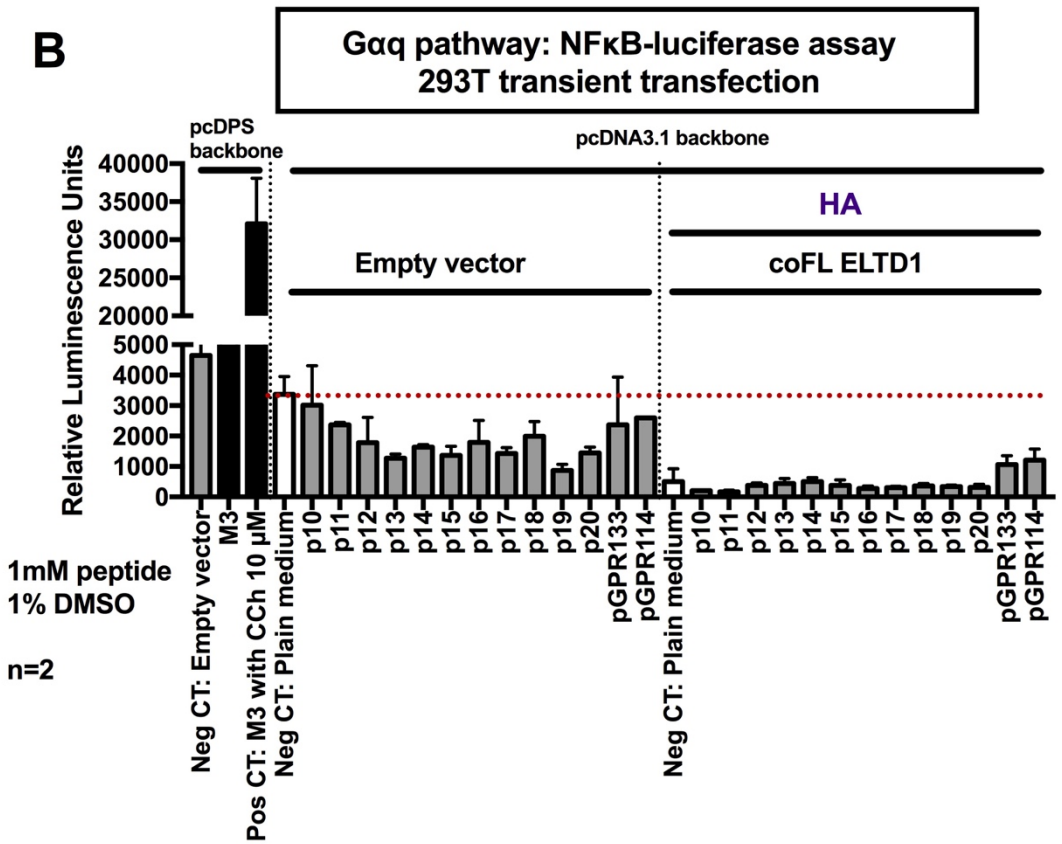


Figure 4.19: CREB-luciferase reporter assay (n=2) showing increase in CREB associated luminescence downstream of Gαs signalling following addition of p133 (1mM in 1% DMSO) in HEK293T cells transfected with FL ADGRD1/GPR133 (unpaired Student's t-test $p < 0.0001$). (Abbreviations: DMSO=dimethyl sulfoxide; EV = empty vector; mM=millimolar; p133 = ADGRD1/GPR133's Stinger/Stachel peptide with amino acid sequence: THFGVLMDLPRSA).

The 11 selected ELTD1 Stinger/Stachel peptides (1mM peptide; 1% DMSO) were then screened for activation using the NFAT-, NFκB-, SRE-; and CREB-luciferase assays, alongside p133 and p114. CHRM3/M3 Receptor exposed to 10uM carbachol was used as a positive control for all assays (through its promiscuous activation of all canonical GPCR pathways).

Results reveal that ELTD1's Stinger/Stachel peptides did not elicit any NFAT activation (Gαq) (Figure 4.20 A), NFκB activation (Gαq) (Figure 4.20 B), SRE activation (Gαi; Gαq; Gα12/13; Gβγ) (Figure 4.20 C), or CREB activation (Gαs) (Figure 4.20 D) in HEK293T cells transfected with codon optimised FL ELTD1. The CREB result is particularly interesting because despite ELTD1 having a GPS most similar to ADGRD1/GPR133 (which signals through Gαs), it does not signal in a similar manner. In addition, the addition of p133 or p114 did not induce signalling in any of the above assays. Similarly to previous dual transfection luciferase assays without a control plasmid, these assays also revealed evidence of transfection related plasmid competition. This is evident by the low luciferase baseline in the FL ELTD1 samples (a large plasmid which would compete with the smaller luciferase plasmid during transfection) with the consistently higher baseline in the empty vector samples (a smaller plasmid). In summary, none of the ELTD1 potential Stinger/Stachel peptides appeared to activate canonical GPCR pathways in FL ELTD1.


A
Gαq pathway: NFAT-luciferase assay
293T transient transfection
pcDPS backbone
pcDNA3.1 backbone
HA
Empty vector
coFL ELTD1
Relative Luminescence Units
100000
90000
80000
70000
60000
50000
10000
8000
6000
4000
2000
0
1mM peptide
1% DMSO
n=2
Neg CT: Empty vector
M3
Pos CT: M3 with CCh 10 µM
Neg CT: Plain medium
p10
p11
p12
p13
p14
p15
p16
p17
p18
p19
p20
pGPR133
pGPR114
Neg CT: Plain medium
p10
p11
p12
p13
p14
p15
p16
p17
p18
p19
p20
pGPR133
pGPR114


B
Gαq pathway: NFκB-luciferase assay
293T transient transfection
pcDPS backbone
pcDNA3.1 backbone
HA
Empty vector
coFL ELTD1
Relative Luminescence Units
40000
35000
30000
25000
20000
5000
4000
3000
2000
1000
0
1mM peptide
1% DMSO
n=2
Neg CT: Empty vector
M3
Pos CT: M3 with CCh 10 µM
Neg CT: Plain medium
p10
p11
p12
p13
p14
p15
p16
p17
p18
p19
p20
pGPR133
pGPR114
Neg CT: Plain medium
p10
p11
p12
p13
p14
p15
p16
p17
p18
p19
p20
pGPR133
pGPR114

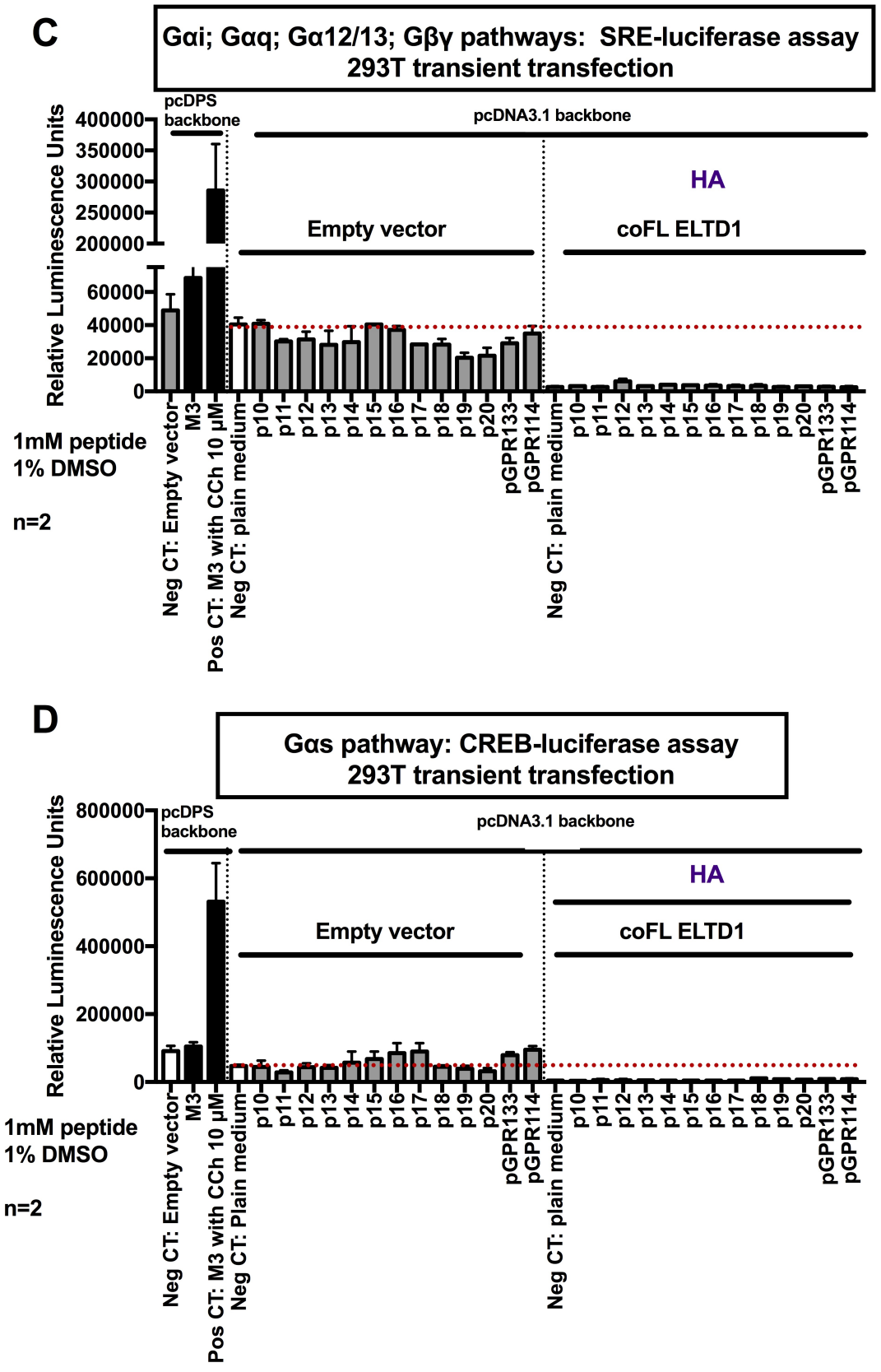


Figure 4.20: ELTD1 Stinger/Stachel peptide luciferase experiments performed in HEK239T cells transfected with codon optimised FL ELTD1. For all assays,

the CHRM3/M3 GPCR receptor was used as a positive control, exposed to 10uM carbachol. **A)** Representative (n=2) NFAT-luciferase assay (Gαq) reveals no increase in NFAT signal with any of the ELTD1 peptides compared to control when applied to FL ELTD1 expressing HEK293T cells. Additionally, the addition of p133 and p114 has no effect on NFAT signal. **B)** Representative (n=2) NFκB-luciferase assay (Gαq) reveals no increase in NFAT signal with any of the ELTD1 peptides compared to control when applied to FL ELTD1 expressing HEK293T cells. The addition of p133 and p114 has a small positive effect NFAT signal in FL ELTD1 expressing cells, however both are lower than the empty vector negative control. **C)** Representative (n=2) SRE-luciferase assay (Gαi; Gαq; Gα12/13; Gβγ) reveals no increase in SRE signal with any of the ELTD1 peptides compared to control when applied to FL ELTD1 expressing HEK293T cells. The addition of p133 and p114 has no effect. **D)** Representative (n=2) CREB-luciferase assay (Gαs) reveals no increase in CREB signal with any of the ELTD1 peptides compared to control when applied to FL ELTD1 expressing HEK293T cells. The addition of p133 and p114 has no effect. (Abbreviations: Pos CT=positive control; Neg CT=negative control; coFL=codon optimised full length ELTD1; DMSO=dimethyl sulfoxide; mM=millimolar; μM=micromolar)

4.11.2 Stinger/Stachel peptide AlphaScreen cAMP assay in HEK293T cells: peptides do not activate Gαs

The final assay performed in Leipzig was using the AlphaScreen cAMP assay using ELTD1's Stinger/Stachel peptides. This assay was performed to further scrutinise whether ELTD1 signalled through (Gαs) as another family 1 member had recently had their Gαs signalling solved using this assay (Muller et al., 2015). Transfection in HEK293T cells and application of peptides was performed as per the luciferase assays reported above.

Results (n=1) revealed no significant activation of cAMP signalling (Gαs) with any of the ELTD1 peptides used on FL ELTD1 expressing HEK293T cells, compared to a negative control (Figure 4.21). Forskolin (FSK) was used a positive control. This result further validated similar previous findings. The addition of p133 and p114 similarly had no effect.

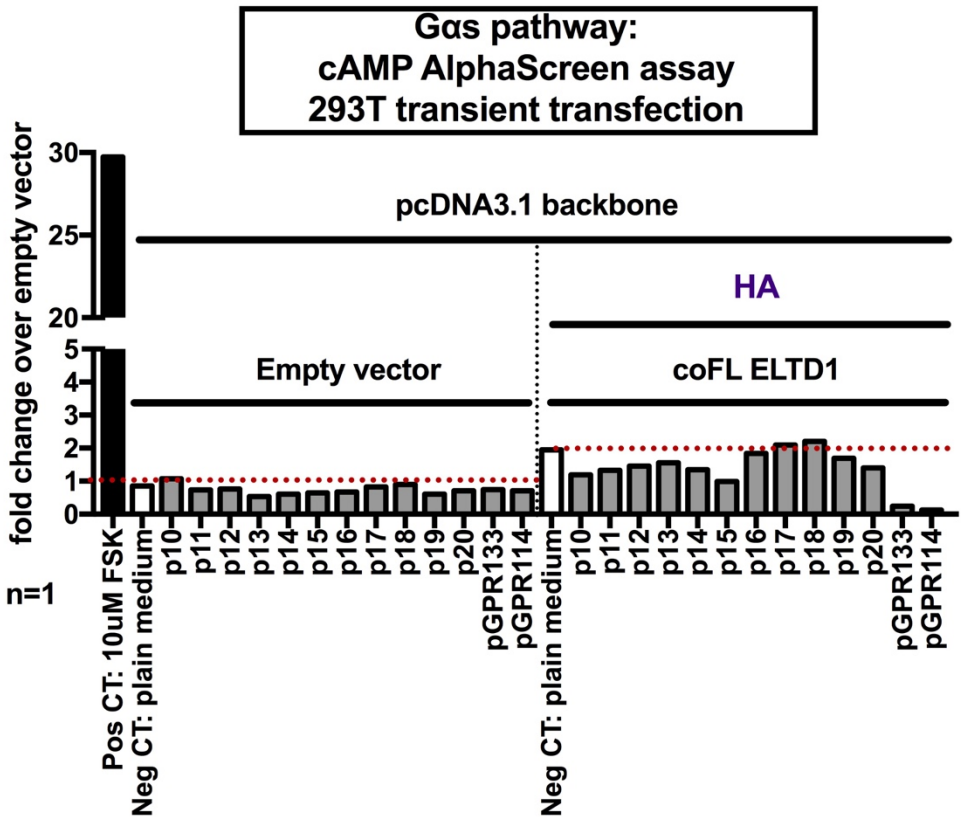


Figure 4.21: ELTD1 Stinger/Stachel peptide AlphaScreen cAMP experiment (n=1) reveals that none of the peptides elicited an increase compared to the negative control in HEK293T cells expressing codon optimised FL ELTD1. The CHRM3/M3 GPCR receptor exposed to 10uM carbachol was used as a positive control. (Abbreviations: Pos CT=positive control; Neg CT=negative control; coFL=codon optimised full length ELTD1; coCTF=codon optimised C-terminal fragment ELTD1; co7TMΔ=codon optimised seven-transmembrane truncated ELTD1)

4.12 Discussion

This work shows that ELTD1 does not signal like a conventional canonical GPCR with the Stinger/Stachel hypothesis being unable to activate Gαq, Gα12/13, Gαi or Gαs in ELTD1. At present, there are no published reports of other adhesion GPCR exhibiting such behaviour. A critical assessment of the work reveals multiple strengths as well as limitations. Each will be reviewed as will be various issues raised by the experiments performed.

The strength in this work lies in the thoroughness of its investigation. Despite repeated negative results, there was a concerted effort to show that these results were genuine and not due to methodological or technical ineptitude. This entailed using multiple methodologies to test ELTD1's signalling in multiple leading GPCR laboratories. Another positive aspect of this work was the effort that went into attempting to replicate the seemingly disparate results from the Amsterdam laboratory. This and the difficulty and challenges of replicating results outside of the reporting laboratory which will be commented on later.

This study also has its limitations. The first is the cell types used. The majority of experiments were performed using transiently transfected HEK293T which do not express ELTD1. It can be argued that such cells may not contain the cellular machinery necessary for ELTD1 activation and signalling. Despite this, the majority of published adhesion GPCR Stinger/Stachel papers all utilise HEK293T cells for their signalling assays. On the other hand, HUVECS, the ideal experimental host cell because of their constitutive ELTD1 expression, where unable to be used due

to their resistance to large plasmid transient transfection, a biological problem common to most primary cell types. In order to have used HUVECS, a lentivirus containing the recombinant codon optimised ELTD1 would need to have been created, followed by HUVEC transduction. This would have worked for the HTRF experiments but not for the luciferase reporter assays as they would require transfection of luciferase reporters. For these experiments, the ideal situation would have been to create stable HUVEC cell lines for each luciferase reporter followed by viral transduction with a recombinant ELTD1 containing lentivirus. None of this was possible due to time constraints.

Another limitation was the use of tags. Experiments were performed using recombinant ELTD1 tagged either on both N and C termini (HA and FLAG respectively) or only on the C-terminus (FLAG). Some in the adhesion GPCR field have questioned whether tags may interfere with activation and signal transduction (personal communication: Prof. His-Hsien Lin, University of Taiwan; and Prof Torsten Schöneberg, University of Leipzig). An example of such interference in the adhesion GPCR field was the finding that adding GFP to the c-terminus of the orthologue of ADGRL1/LPHN1 in the worm *Caenorhabditis elegans* inactivated the receptor, whilst inserting the GFP within the third intracellular loop did not affect the receptor's function (Promel et al., 2012). Despite this, N and C-terminus tags have been incorporated in all the published Stinger/Stachel signalling adhesion GPCRS. Additionally, the addition of C-terminal GFP is common in the wider GPCR field as the α-subunit of the heterotrimeric G protein has been shown to critically interact with residues on the GPCR's third intracellular loop (rather than the C-terminal end of the receptor) in a growing number of GPCRs (Oldham and Hamm, 2008). In our case, we were forced to use tags as there were no commercially available

antibodies for the various CTF and NTF ends of our recombinant ELTD1 constructs. HA (9 amino acids) and FLAG (8 amino acids) tags were chosen as they have been previously engineered onto CTF constructs which have had their Stinger/Stachel signalling solved. This list comprises ADGRG6/GPR126 and ADGRD1/GPR133 (Liebscher et al., 2014), ADGRG5/GPR114 (Wilde et al., 2016), ADGRG2/GPR64 (Demberg et al., 2015) and ADGRL1/LPHN1 (Muller et al., 2015). GFP (238 amino acid) was used as an C-terminal tag to control any effects brought on solely by the presence of the HA and FLAG tag. As our results have shown, both tagging strategies revealed similar signalling results.

The issue of tagging returned when we were faced with contrasting the Oxford constructs with the Amsterdam FL and CTF construct. The tagging strategy of the Amsterdam group entailed adding a C-terminal extension to ELTD1's 21 amino acid long cytoplasmic tail which comprised a flexible linker (24 amino acids) joined to a mVenus fluorescent tag (240 amino acids). Needless to say, although neither Amsterdam nor Oxford constructs exhibit any biologically relevant NFAT signalling, both construct groups appear to function differently within the cell in terms of dose response and expression levels: i) Amsterdam CTF expresses in a dose dependent manner; whilst ii) Oxford HA tagged constructs do not express on the cell surface in a dose dependant manner; and iii) Oxford GFP tagged constructs do express (total cell expression) in a dose dependent manner. Lastly, although some of the constructs had an C-terminal FLAG tag, this was never assayed in our assays. In retrospect, this should have been assayed following the finding that HA/FLAG tagged 7TMΔ ELTD1 was not appearing on the cell surface. This tag will be of use

in future experiments when one explores the various intracellular compartments ELTD1 is trafficked through during its life cycle and following activation.

Another potential limitation of this work is the assumption that ELTD1 may signal using the tethered agonist Stinger/Stachel peptide hypothesis. It may be the case that ELTD1 is not activated through this mechanism and is thus an outlier to the growing list of adhesion GPCRS who signal in this manner. In favour of ELTD1's tethered agonist activation however is the finding that ELTD1's GPS is highly conserved and contains a sequence very similar to the described tethered agonist region of ADGRG1/GPR133's GPS site. It is of interest to note that two adhesion GPCRS do not need the Stinger/Stachel peptide sequence present to signal: ADGRB1/BAI1 and ADGRG1/GPR56 (Kishore et al., 2016). For both of these adhesion GPCRS, the 7TMΔ form are able to constitutively signal by themselves. Interestingly however, CTF forms of these receptors are also able to signal constitutively themselves. In the case of ADGRG1/GPR56 it appears the CTF form (with an exposed tethered agonist) increases Gα12/13 and Gαq signalling compared to the 7TMΔ. For ADGRB1/BAI1, the CTF form induces greater constitutive signalling only for Gα12/13; whilst the 7TMΔ form generates greater constitutive Gαq signalling (Kishore et al., 2016).

Another limitation relates to this work focussing solely on canonical GPCR signalling. The basis for this assumption was that all the published Stinger/Stachel activated adhesion GPCRS activate canonical GPCR pathways. Due to time and experimental constraints, this study did not explore the possibility of beta arrestin signalling, which forms another component of GPCR signalling. This work, alongside an exploration of non-canonical GPCR signalling will be completed in the future.

During the experimental process, various interesting and challenging issues arose which will now be discussed. The first to arise was why the HA tagged 7TMΔ form of ELTD1 was never found to be expressed on the cell surface of transfected cells. Our 7TMΔ form of ELTD1 was designed to contain only the predicted 7TM component of ELTD1, with N-terminal HA and C-terminally FLAG tags (Figure 4.22 A). Additionally, like the codon optimised FL and CTF ELTD1 constructs, the 7TMΔ form of ELTD1 contained ELTD1's original signal peptide sequence. Yet, despite this, it consistently did not express on the cell surface of transfected cells (Figure 4.22 B).

The Swiss Model bioinformatics tool allows one to align an amino acid sequence and compare it to the most similar solved crystal structure (Biasini et al., 2014). Using this tool following the completion of all signalling experiments, ELTD1's amino acid sequence was contrasted to CRHR1 (a secretin GPCR which is evolutionarily downstream of the adhesion GPCR family and which has had its crystal structure previously solved). Results revealed that our 7TMΔ form of ELTD1 appeared to contain a truncated first α-helix, suggesting that ELTD1's true 7TM actually starts more N-terminally than was originally predicted (Figure 4.22 C). In the future, it is planned that a new 7TMΔ form of ELTD1 reflecting the full inclusion of the previously truncated α-helix will be synthesised and used in subsequent signalling experiments.

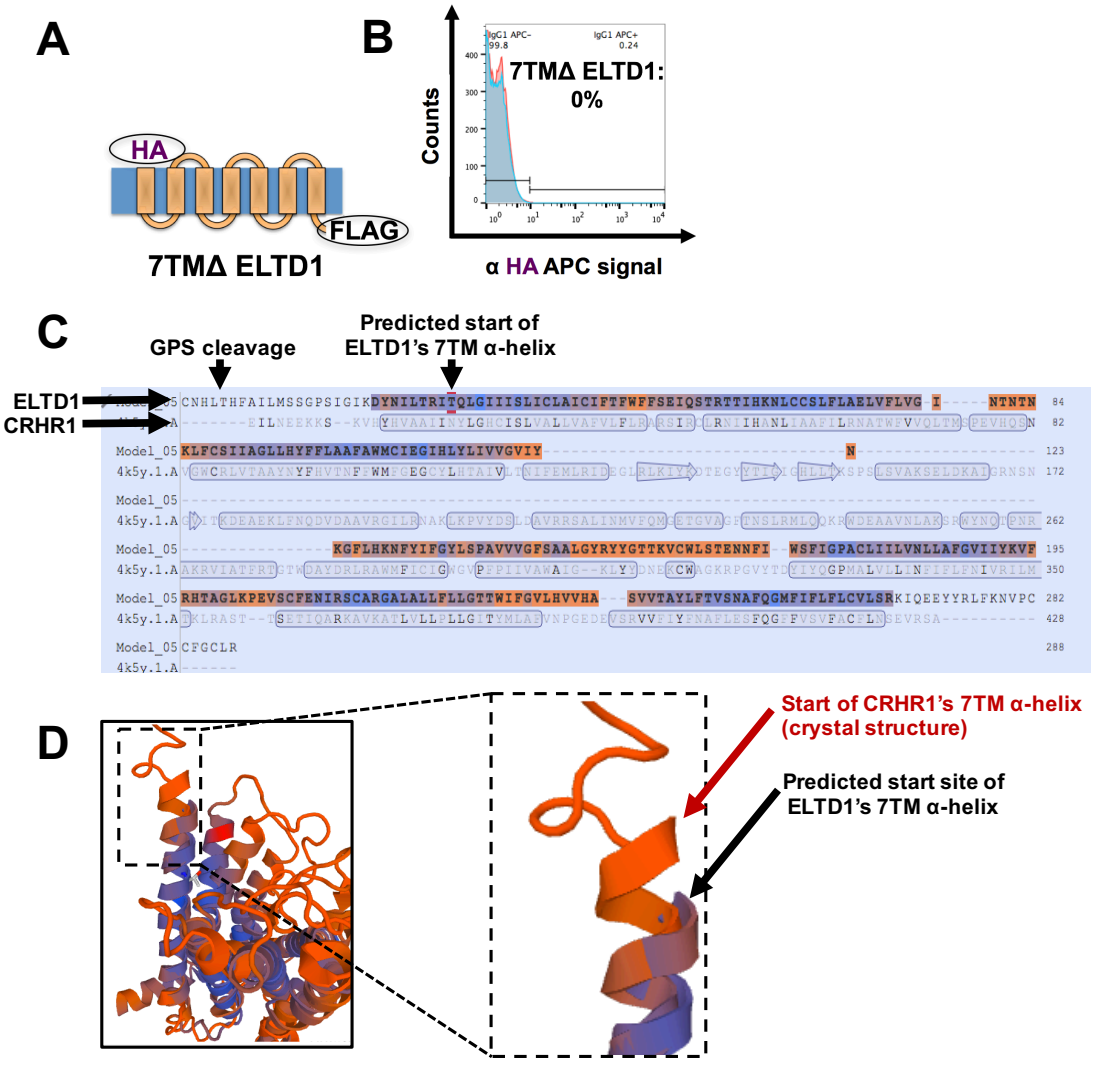


Figure 4.22: Possible explanation as to why the codon optimised 7TMΔ form of ELTD1 does not appear on the cell surface. A) Graphical representation of the 7TMΔ form ELTD1, N-terminal HA tagged and C-terminally FLAG tagged. The location of the start of the 7TM domain was predicted using multiple conserved domain database. ELTD1's original signal peptide is included in this sequence. **B)** Representative FACS plot showing zero surface expression for the 7TMΔ form of ELTD1. **C)** Alignment of the crystal structure of secretin GPCR CRHR1 with the amino acid sequence of ELTD1 (blue=good fit; red=poor fit). This reveals that the predicted start of ELTD1's first 7TM membrane loop (start of the α-helix indicated with arrow) is C-terminal to the start of the CRHR's first 7TM α-helix. This suggests

that the 7TMΔ form of ELTD1 contains a truncated first α-helix, which explains why the receptor is unable to be anchored and expressed on the cell surface. **D)** Graphical representation of CRHR1's 7TM domain crystal structure with ELTD1's predicted 7TM sequence modelled over it. The red arrow points to the start of CRHR1's α-helix, whilst the black arrow points to the start of the 7TMΔ form ELTD1, suggesting that ELTD1's real 7TM actually starts more N-terminally than was originally predicted.

Another issue that arose during experimentation was the issue including a control plasmid when using luciferase-reporter assays. Despite the benefits of using a control plasmid (less variation and increased reproducibility), all three GPCR laboratories I visited did not use them. As a result, many of my luciferase assays suffered from irregular luciferase baselines due to plasmid competition between the transfected luciferase reporter and GPCR. Only in the stable NFAT assay which was generously donated by Heptares was this pitfall avoided due to the luciferase reporter being stably expressed for all cells. Whilst adhesion GPCR biologists are mindful of this issue, the general consensus in the field is that if a GPCR activates genuine GPCR signalling, the fold change difference will be substantial enough to overcome any plasmid competition related issues. To date, the only Stinger/Stachel hypothesis papers to use a control plasmid with the luciferase reporter assays are those from the Tall (Stoveken et al., 2015) and Hall (Kishore et al., 2016) laboratories.

This study also highlighted the challenge of replicating results from other laboratories as was the case when I tried to replicate the Amsterdam groups results. Surprisingly, it turned out the group had a very sensitive luminescence reader which explained why I was not able to detect the changes when using their plasmids and controls outside of their laboratory. Having contrasted the Amsterdam and Oxford constructs at both the Oxford and Amsterdam laboratories, we feel confident to state that neither group's CTF construct activates NFAT or Gαq signalling.

An issue related to replication was the problem of trying to standardise methodologies between the various laboratories visited. For example, the detection of expression was checked with FACS in Oxford, with ELISA and fluorescence plate reader in Amsterdam and with ELISA alone in Leipzig. Of the lot, I found that FACS was the most sensitive and fastest quantitative method. Interestingly, both in Amsterdam and Leipzig, surface expression experiments were not concurrently done in the same experiment as the signalling experiment. The downside to this being false negatives if transfection was inadequate.

Another interesting finding from the study was the realisation of how important the plasmid's promoter is. As has been documented at the start of this chapter, we overcame low protein expression in transient ELTD1 expression by codon optimising ELTD1, which produced a large increase in total and cell surface expression. When comparing the FACS expression of our codon optimised receptor (pcDNA 3.1 plasmid) to the Amsterdam group's wild type ELTD1 (pcDEF3 plamsmid), it was surprising to note that this difference was less marked. It is

hypothesised that this effect is due to the stronger promoter (EF-1α) present in pcDEF3 which is able to compensate for wild type ELTD1's low GC content. In the future, further signalling work will be performed using our constructs cloned into the pcDEF3 plasmid.

ELTD1's Stinger/Stachel peptides were unfortunately all very water insoluble and very difficult to dissolve, instantly precipitating at DMSO concentrations lower than 1%. This proved to be very challenging as such DMSO concentrations are toxic for cells. In order to use the peptides at the published Stinger/Stachel peptide concentration (1mM), we were initially forced to use a 2% DMSO concentration. This prevented us from attempting any assays with a peptide application time of more than 30 minutes due to cell toxicity. Following the assistance of the team in Leipzig, ELTD1's peptides were made slightly more soluble by adding TRIS (pH 8) to the DMSO solubilisation protocol and adding a more vigorous shaking routine. This enabled us to drop the DMSO content to 1% whilst maintaining a peptide concentration of 1mM. Additionally, during the course of experiments, various modifications were added to the N- and C- peptide termini to try and improve solubility. These included the addition of biotin PEG2 molecules, betaine and the water soluble amino acids KKRR. Unfortunately, none helped improve solubility any further. In contrast, some adhesion GPCRS have very water soluble Stinger/Stachel peptides, for example GPR116's p116 (Brown et al., 2017). Why this is the case remains unsolved but may relate to the receptor's function.

A recent development in the adhesion GPCR field has been the discovery of Stinger/Stachel peptide promiscuity between members within and between adhesion GPCR families (Demberg et al., 2017). This work, from the Liebscher laboratory, found that the Stinger/Stachel peptide of ADGRF1/GPR110 was able to activate signalling in ADGRG2/GPR64 and ADGRG6/GPR126 (Demberg et al., 2017). During the final experiments in Leipzig, I attempted to see whether this would also apply to ELTD1. GPR133 was chosen due to its GPS similarity to ELTD1's GPS as was the peptide of GPR114 due to its ease of solubility: neither activated any canonical GPCR signalling in ELTD1. It remains to be seen whether other more water soluble Stinger/Stachel peptides may have an effect on ELTD1.

Lastly, future work is discussed. First, a new 7TMΔ form of ELTD1 will be designed which will contain the full non-truncated first 7TM loop α-helix. It will be of interest to determine whether this form of ELTD1 has any signalling activity of its own. Following this, an HUVEC ELTD1 overexpression cell line will be created using lentiviral transduction. This cell line will be assayed for canonical GPCR signalling using the HTRF FRET assays which do not require any transfection. Next, β-arrestin signalling will be investigated using all constructs. Should neither experiment show any positive association, ELTD1 stably overexpressing HUVECS will undergo proteomic evaluation and analysis. This last approach would have the benefit of allowing us to interrogate and discover ELTD1's signalling pathway as well as its binding partners.

4.13 Conclusion

In summary, this work shows that ELTD1 does not signal like a conventional canonical GPCR with the Stinger/Stachel Hypothesis not activating Gαq, Gα12/13, Gαi or Gαs in CTF or FL ELTD1. Additionally, this work refutes the claim that CTF ELTD1 signals through NFAT. These results thus suggest that ELTD1 activation is unlike most adhesion GPCRs and is likely non-canonical in nature.

Chapter 5: The effect of ELTD1 silencing in endothelial cells

5.1 Introduction

Although my supervisors' laboratories have previously noted that silencing *ELTD1* with siRNA in endothelial cells inhibits sprouting angiogenesis (Masiero et al., 2013), the gene expression changes and mechanisms that underpin these changes remain unknown. In addition, our understanding of ELTD1's role and function in endothelial biology remains very limited. Unresolved questions include:

i. What are the gene expression changes that underpin ELTD1's relationship with sprouting angiogenesis?
ii. Does ELTD1 have any other roles in endothelial biology apart from angiogenesis and could global transcriptional profiling help us explore this?
iii. Could global transcriptional profiling aid in deciphering how ELTD1 signals?
iv. Can ELTD1's role(s) within endothelial cells allow us to better understand ELTD1's role in tumour biology?

In order to explore these unanswered questions, I utilised the approach of global transcriptional profiling to identify the effects of modulating ELTD1 expression. To do this I performed transient *ELTD1* silencing in primary HUVEC cells, using siRNA,

followed by global transcriptional profiling using the Illumina microarray platform. The aim of this work was to further our understanding of ELTD1's endothelial function and biology with the longer term goal of using this knowledge to better understand how we could target ELTD1 for therapeutic benefit within the cancer microenvironment. This chapter presents this work.

5.2 ELTD1 Silencing in HUVEC cells

In HUVEC cells, wild type ELTD1 expression was silenced using two different siRNAs (siRNA 1 and siRNA 2; sequence in Methods chapter). As described in the previous chapter, HUVECS are primary endothelial cells which constitutively express ELTD1. In brief, 3 separate pools of HUVECS (each pool comprising differing donors) were transiently transfected with each siRNA using Lipofectamine RNAiMAX, and the cells were harvested two days later. A medium GC content Invitrogen Stealth siRNA was used as a negative control (details in Methods chapter). ELTD1 transcript and protein expression was then quantified using qPCR (primer sequences in Methods chapter), Western blotting (antibody: Sigma HPA025229, now discontinued), and FACS (anti-ELTD1 (184.11) surface antibody generated by Professor Alison Banham's laboratory, University of Oxford). Results from n=3 experiments revealed that following 48 hours of silencing, both siRNAs significantly suppressed *ELTD1* mRNA expression (Figure 5.1 A) as well as ELTD1 total protein expression (Figure 5.1 B) and ELTD1 cell-surface protein expression (Figure 5.1 C and D). Importantly for subsequent functional analyses, the level of ELTD1 protein expression was barely detectable after silencing.

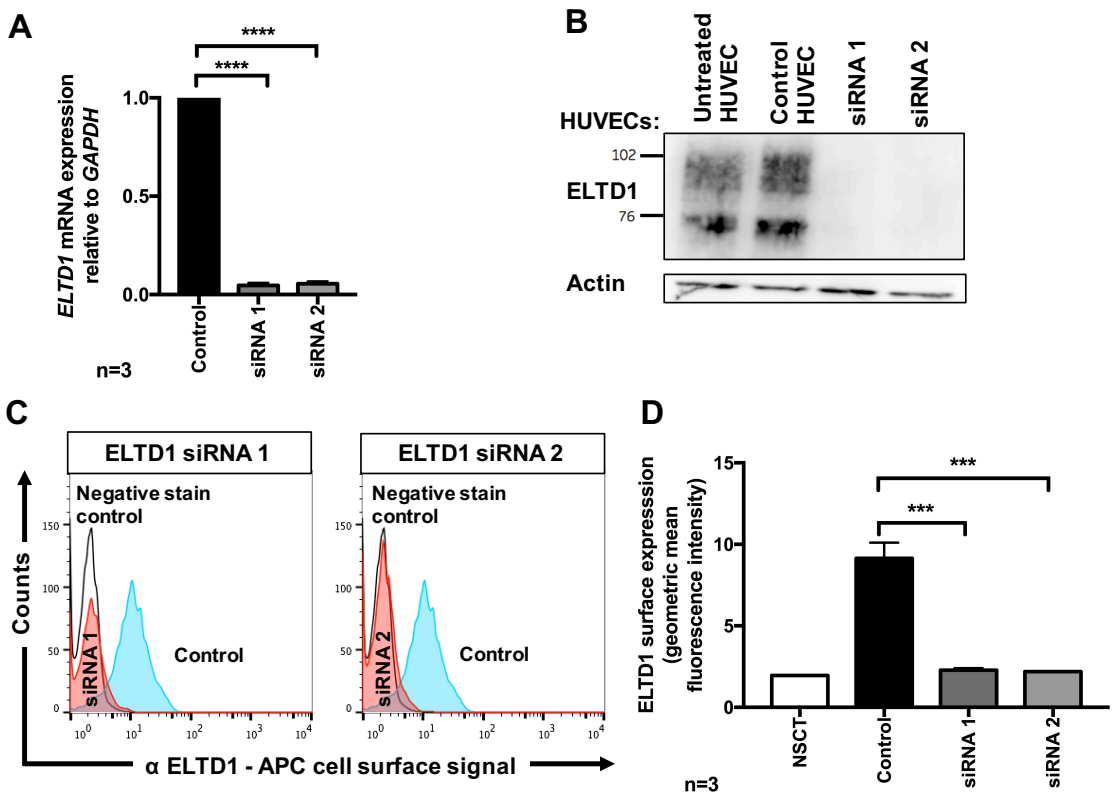


Figure 5.1: ELTD1 Silencing in HUVEC cells using two different siRNAs. A) qPCR reveals adequate *ELTD1* mRNA silencing (unpaired Student's t-test $p<0.0001$ for both comparisons). **B)** Representative Western blot reveals complete loss of ELTD1 protein in *ELTD1* silenced HUVECS for both siRNAs. The first lane contains untreated HUVECS, which have the same expression as the control HUVECs treated with a non-targeting siRNA. **C)** FACS reveals complete loss of ELTD1 cell surface expression after treatment with each siRNA. HUVECS treated with both siRNAs had an ELTD1 surface expression equal to the negative control. **D)** Quantification of FACS ELTD1 surface expression showed that there was no surface expression for HUVECS treated with both siRNAs: Control versus siRNA 1 (unpaired Student's t-test $p<0.0003$); Control versus siRNA 2 (unpaired Student's t-test $p<0.0002$). (Abbreviations: NSCT=negative stain control comprising secondary only).

5.3 Microarray analysis of ELTD1 silenced HUVECS

An Illumina microarray was then performed on 3 biological replicates of *ELTD1* silenced HUVECS, each from the same donor pool (to remove variability caused by heterogeneity between individuals), using both siRNA 1 and siRNA 2. Each biological replicate was generated sequentially from a different cell passage (passages used: 2, 3 and 4). In brief, following the confirmation of successful ELTD1 silencing after 48 hours, via qPCR and Western blotting, HUVECS were harvested and RNA was extracted for microarray analysis using an Illumina microarray scanner (Illumina iScan). Thereafter, I performed microarray data analysis and linear modelling within the R scripting environment with the help of a bioinformatician, Dr Syed Haider. The steps of this process are outlined in detail in Figure 5.2. All my microarray analysis and visualisation coding scripts written in R are included in the Appendix; methods are outlined in the Methods chapter.

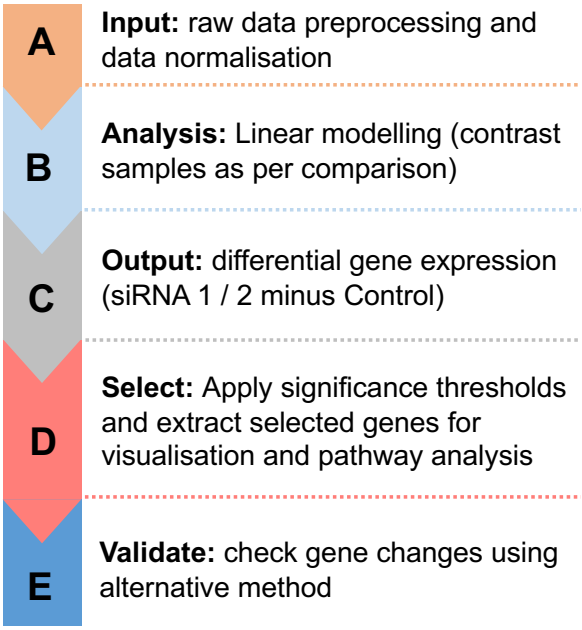


Figure 5.2: Outline of microarray analysis method used for analysing ELTD1 silenced HUVECS. All subsequent microarray experiments performed during this project followed a similar algorithm. **A)** Raw data output from the microarray reader (Illumina iScan) was first pre-processed and normalised using the Limma R package. **B)** A linear model was then applied onto the normalised data, contrasting each silenced ELTD1 sample against the control HUVEC samples. This was done for each biological replicate and then averaged. This model calculated two comparisons: i) siRNA 1 minus control; and ii) siRNA 2 minus control. **C)** These comparisons yielded two datasets of differential gene expression, one corresponding to each siRNA. **D)** Standardised thresholds (adjusted *p* value <0.05 and $\log_2$ fold change > 1) were then applied to extract significant differentially expressed genes. These were then visualised using volcano plots and heatmaps and inputted into established pathway analysis databases. **E)** Finally, significant differentially expressed genes were validated using qPCR.

For differential gene expression following *ELTD1* silencing, two comparisons (one for each siRNA) were calculated: i) ELTD1 siRNA 1 treated HUVECS compared to control HUVECS (siRNA 1 minus control); and ii) ELTD1 siRNA 2 treated HUVECS compared to control HUVECS (siRNA 2 minus control). For both comparisons, differentially expressed genes were deemed statistically significant only if they fulfilled two criteria: i) an adjusted *p* value < 0.05; and ii) a fold change of > or < 2. Volcano plots depicting differential gene expression are presented for siRNA 1 (Figure 5.3 A) and for siRNA 2 (Figure 5.3 B). In each volcano plot, *ELTD1* had the lowest adjusted *p* value of the downregulated significant genes (and was the most downregulated) whilst *ATP Citrate Lyase* (*ACLY*) had the lowest adjusted *p* value in the upregulated significant genes.

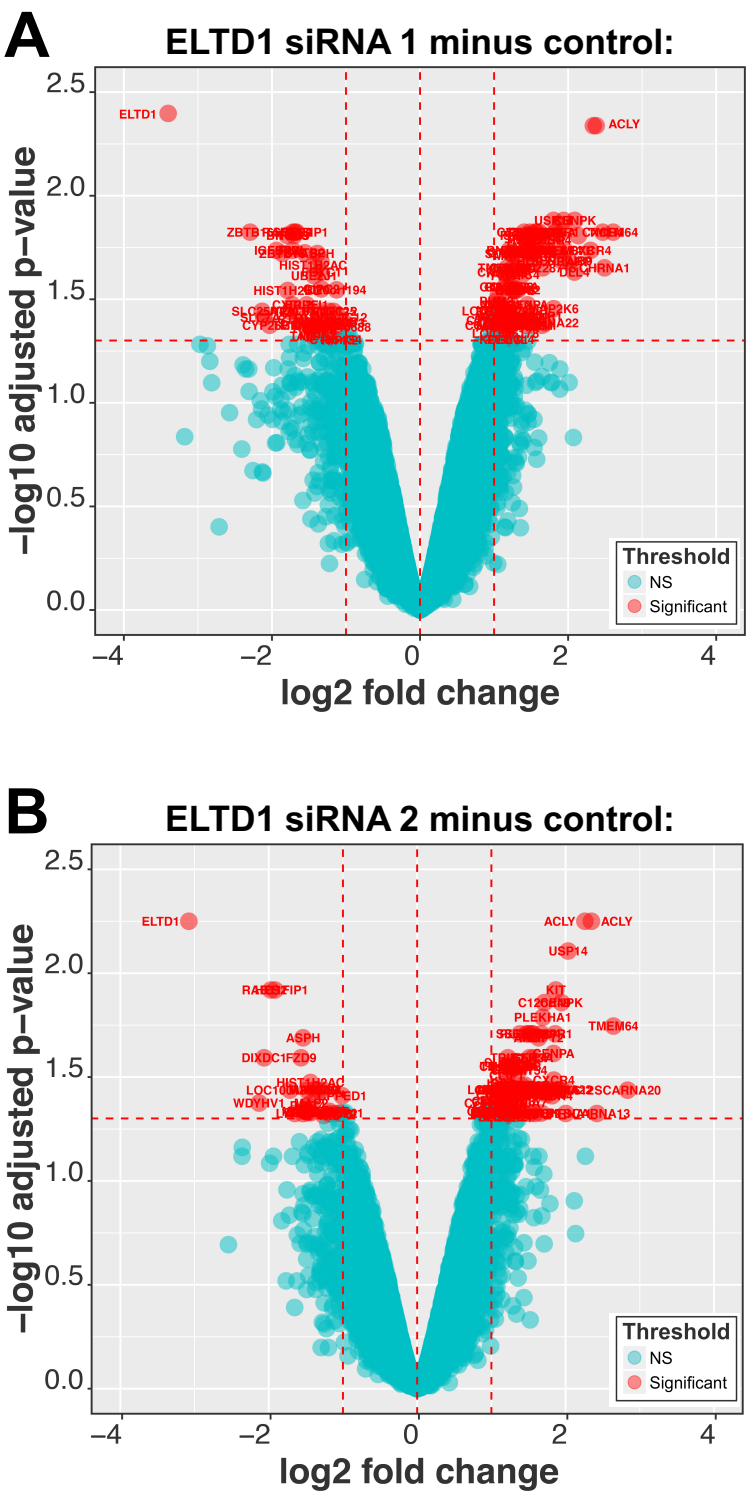


Figure 5.3: Volcano plots depicting differentially expressed genes for each siRNA following comparison between ELTD1 silenced HUVECS and control HUVECS. Significant differentially expressed genes (indicated in red) are filtered based on an adjusted *p* value <0.05 and fold change > < 2. **A)** Differential gene

expression for siRNA 1 treated HUVECS compared to control HUVECS. Of the downregulated genes, *ELTD1* has the lowest adjusted *p* value and greatest negative fold change. Of the upregulated genes, *ACLY* has the lowest adjusted *p* value. **B)** Differential gene expression for siRNA 2 treated HUVECS compared to control HUVECS. Results are similar to A. (Abbreviations: NS=non-significant).

A Venn diagram comparison was then performed to determine how many significant differentially expressed genes were common to both siRNA 1 and siRNA 2 treated HUVECS. Results revealed that 68 differentially expressed genes were common to both groups, with 70 genes being unique to siRNA 1 HUVECS and 57 genes being unique to siRNA 2 HUVECS (Figure 5.4 A). A heatmap displaying the expression level z-score of the 68 common genes in all microarrayed samples was created showing that the majority of common genes were upregulated following ELTD1 silencing (Figure 5.4 B).

Pathway analysis was then performed, however none of the curated pathway databases (KEGG, Reactome, Wikipathways and BioCarta) yielded any associations with significant adjusted *p* values. This was likely to be related to the low number of significantly differentially expressed genes extracted from the microarray.

A number of statistically significantly ELTD1 regulated genes were selected for validation of the array data using an independent technique and for further investigation. Selected genes reflected our laboratory's expertise and interest. Upregulated genes comprised the metabolic gene *ACLY* (which had the lowest adjusted *p* value of all upregulated genes) and the haematopoietic lineage market KIT. The NOTCH associated gene *HES2* was chosen from the short list of downregulated genes. Future work is planned to analyse and explore the remainder of the significantly differentially expressed genes.

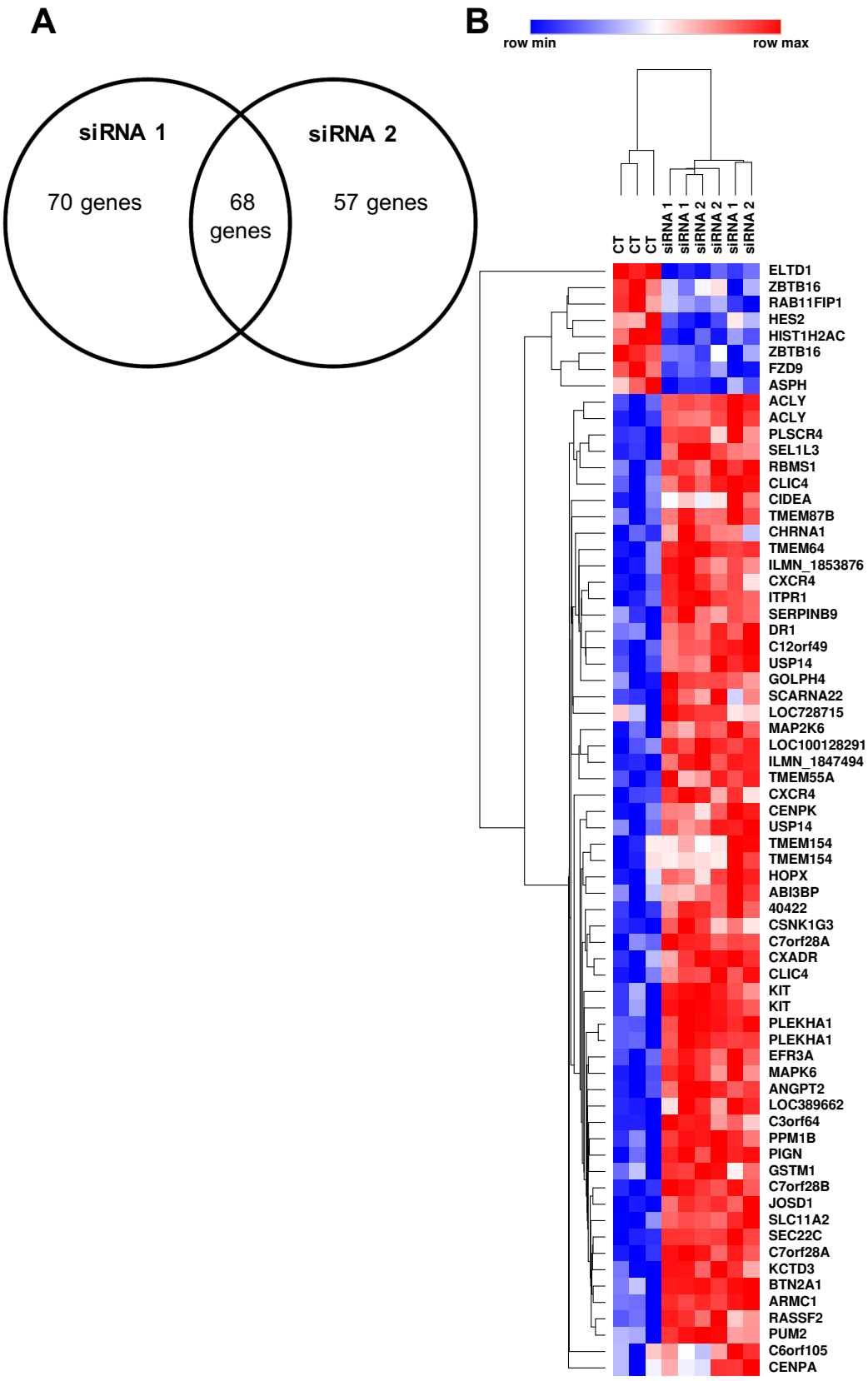


Figure 5.4: Representation of statistically significant differentially expressed genes shared by both siRNA 1 and siRNA 2. A) Venn diagram showing that 68

significant differentially expressed genes were shared by both siRNA 1 and siRNA 2 treated HUVECS. **B)** Heatmap displaying 68 significant differentially expressed genes shared by both siRNA 1 and siRNA treated HUVECS. Row and column clustering was performing using Euclidean distance hierarchical clustering. The intensity colouring (low=blue; high=red) represents the z-score for each gene (the number of standard deviations by which a gene's expression in an individual sample (as determined by microarray) differs from the mean expression for that gene across all samples). In the above heatmap, 2 microarray gene probes (LMN_1853876, LMN_1847494) had no associated HGNC gene names and have thus been labelled with their Illumina probe identifier numbers. The inclusion of duplicate gene entries arises from there being multiple probes for some genes within the microarray. (Abbreviations: CT=control; HGNC=HUGO Gene Nomenclature Committee).

5.4 ELTD1 silencing upregulates *ACLY* and *SLC25A1*

The first gene studied in detail was *ATP-citrate lyase* (*ACLY*), located on chromosome 17q21.2. *ACLY* encodes a cytoplasmic enzyme which converts glycolysis-derived cytoplasmic citrate into Acetyl CoA through the reaction: citrate + ATP -> acetyl-CoA + oxaloacetate + ADP + P_i (Chypre et al., 2012). The produced acetyl-CoA then feeds into 2 important biosynthetic metabolic pathways: i) the fatty acid synthesis pathway; and ii) cholesterol synthesis (Zaidi et al., 2012). ACLY thus links glucose metabolism with both fatty acid and cholesterol synthesis pathways. Furthermore, ACLY is also regulates histone acetylation, controlling the acetylation of genes associated with glucose metabolism and uptake. This list consists of the glucose transporter *GLUT4* and three glycolysis regulators, *HK2*, *PFK-1* and *LSH1* (Wellen et al., 2009).

To validate the differential expression of ACLY detected using microarrays, ELTD1 silenced HUVECS were tested for *ACLY* transcript expression using qPCR (qPCR primers in Methods chapter) and ACLY protein expression using Western blotting (Abcam ab61762). Results revealed that both *ACLY* mRNA (Figure 5.5 A) and ACLY protein (Figure 5.5 B) were increased following ELTD1 silencing with each independent siRNA, confirming the microarray result.

As mentioned already, pathway analysis performed on the 68 differentially expressed genes did not yield any significant pathway associations. In order to search for other metabolism genes affected by ELTD1 silencing, differential gene expression was reanalysed using a lowered fold change threshold. This granted significance to genes with a fold change greater or less than 1.5, whilst maintaining an adjusted *p* value of < 0.05. Pathway analysis was then performed on this extended dataset using the KEGG pathway database (Kanehisa et al., 2017). This revealed that the gene *SLC25A1*, encoding the mitochondrial citrate transporter SLC25A1, was also upregulated following ELTD1 silencing. *SLC25A1* is located on chromosome 22q11.21 and transports citrate out of the mitochondria into the cytoplasm, which is then catalysed by ACLY (Jiang et al., 2016). This result was then validated using qPCR (primers in Methods chapter) with results confirming that *SLC25A1* mRNA was significantly increased following ELTD1 silencing with each siRNA (although less than the change seen in *ACLY* expression) (Figure 5.5 C).

A model was thus proposed hypothesising that by inhibiting *SLC25A1* and *ACLY*, ELTD1 limits the flow of citrate from the mitochrondria into the cytoplasm and its conversion into acetyl-CoA, ultimately regulating endothelial cell lipid metabolism and glycolytic acetylation. This hypothesis is represented by the diagram in Figure 5.5 D.

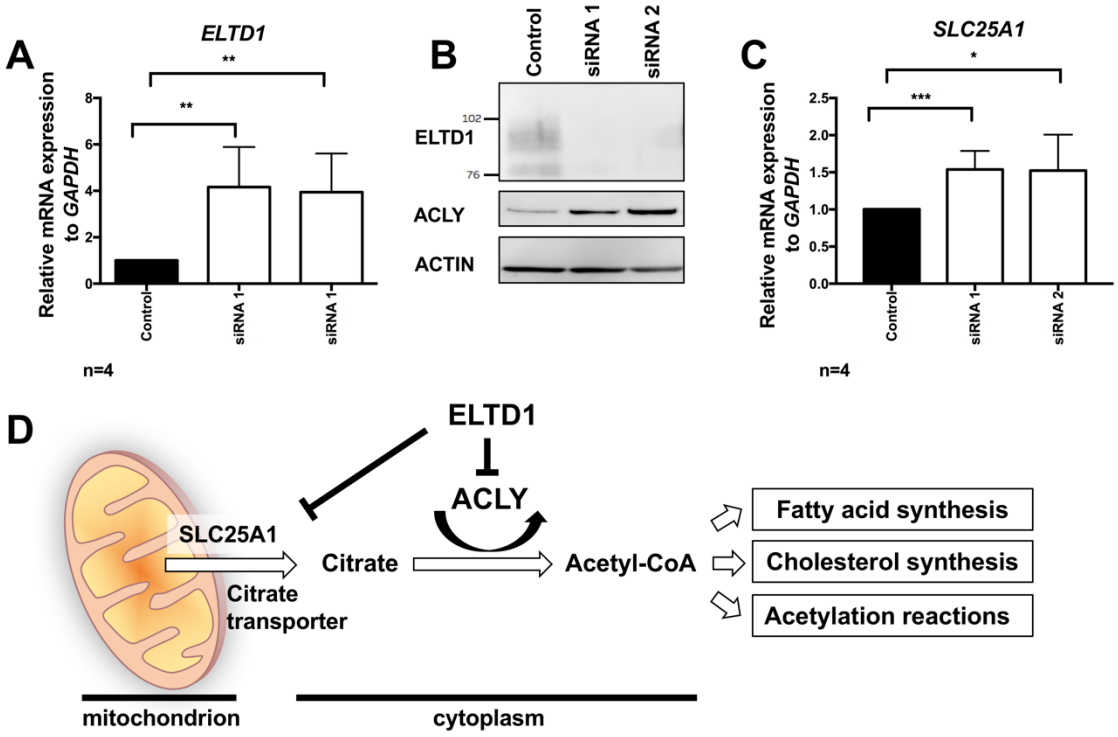


Figure 5.5: ELTD1 silencing upregulates ACLY and SLC25A1 expression. A) qPCR result showing that *ACLY* mRNA increases by nearly 3 fold following ELTD1 silencing in both siRNA 1 and siRNA 2 treated HUVECS (siRNA 1 vs control unpaired Student's *t* test = 0.001; siRNA 2 vs control unpaired Student's *t* test = 0.004). **B)** Western blot data showing that ACLY protein expression increases following ELTD1 silencing with both siRNAs. **C)** qPCR data showing that *SLC25A1* mRNA expression increases following ELTD1 silencing in both siRNA 1 and siRNA 2 treated HUVECS. (siRNA 1 vs control unpaired Student's *t* test = 0.0001; siRNA 2 vs control unpaired Student's *t* test = 0.01). **D)** Proposed model showing ELTD1 inhibiting the expression of SLC25A1 and ACLY. SLC25A1 transports citrate out of the mitochondria into the cytoplasm which is then converted into Acetyl-CoA by ACLY. This Acetyl-CoA then enters either fatty acid synthesis, cholesterol synthesis or regulates the acetylation of glycolytic genes. By inhibiting SLC25A1 and ACLY,

ELTD1's limits both citrate transport out of the mitochondria and its conversion to acetyl-CoA, thereby regulating lipid synthesis and glycolytic gene acetylation.

5.5 ELTD1 silencing does not affect lipid droplet accumulation

In order to investigate whether ELTD1 regulates endothelial lipid metabolism, it was decided to examine whether ELTD1 silencing affects total lipid storage. Storage was chosen as a surrogate marker for lipid synthesis activity with the rationale that if lipid synthesis was significantly increased, the produced lipids would overload the cell's lipid requirements and be stored within lipid droplets. Lipid droplets are cytoplasmic organelles which store excess fatty acids and cholesterols (Bensaad and Harris, 2014). They are found in all eukaryotic cells (with highest expression in adipocytes (Beller et al., 2010)) and comprise a neutral hydrophobic lipid core of triacylglycerols (TAGs) and cholesterol esters surrounded by a phospholipid monolayer – the only organelle not to have a bilayer (Martin and Parton, 2006, Melo et al., 2011). In addition to lipid storage, lipid droplets also function to scavenge reactive lipid species (thus protecting the cell from damage) and are involved in membrane synthesis, cell signalling and inflammation (Bickel et al., 2009, Kusminski et al., 2009).

In brief, the lipid droplet assay was performed using ELTD1 silenced HUVECS (48 hour silencing as described previously) stained for lipid droplets using fluorescent HCS LipidTOX Green neutral lipid staining (Thermo Fisher: H34475). This was followed by visualisation with confocal microscopy and quantification using FACS for total fluorescence. Oleic acid (a long-chain unsaturated fatty acid) (150 μM) in

bovine albumin induces an increase in lipid droplet formation and was used a positive control (Sigma Aldrich: O3008).

Results from n=9 biological replicate experiments revealed that ELTD1 silencing did not affect lipid droplet quantity or size, despite the positive control (oleic acid) demonstrating that the assay was working. Confocal microscopy revealed no visual difference between non-silenced control HUVECs and ELTD1 silenced HUVECS, whilst the oleic acid positive control samples revealed a significant increase in lipid droplet number and size (Figure 5.6 A). FACS analysis performed to quantify any differences in fluorescence generated the same result, with both siRNA samples having similar fluorescent readings to the non-silenced control HUVECS (Figure 5.6 B and C).

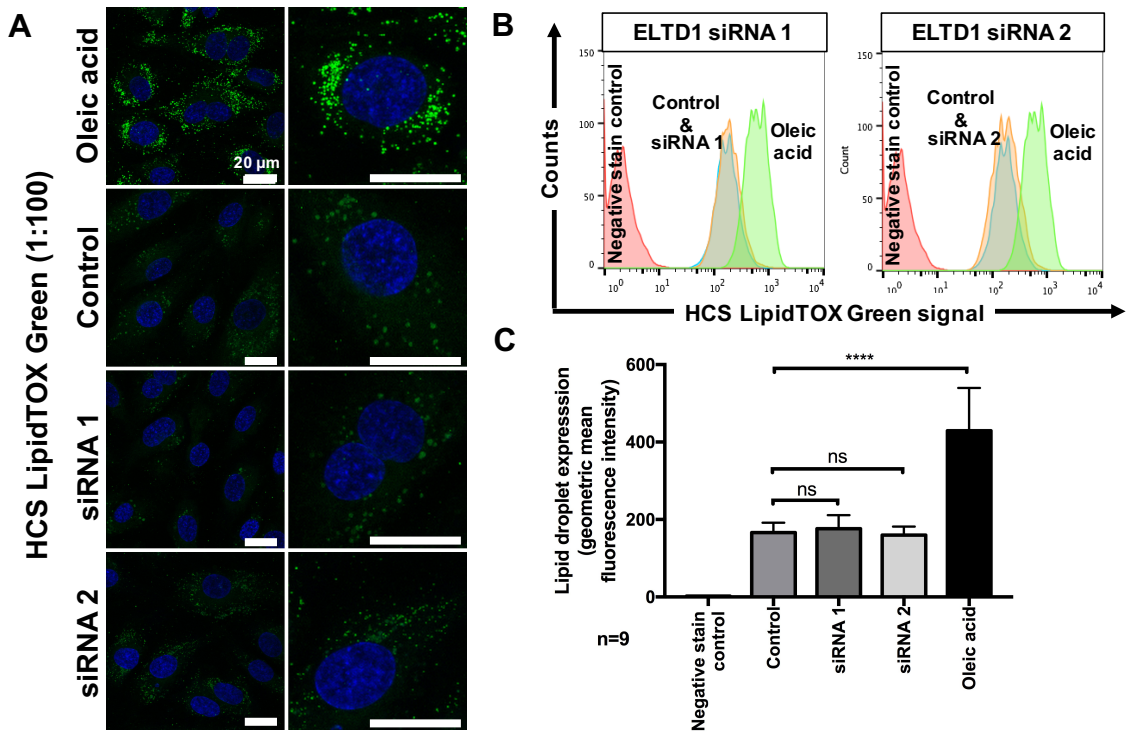


Figure 5.6: ELTD1 silencing in HUVECS does not increase lipid droplet formation. A) Representative confocal microscopy results showing that ELTD1 silencing does not lead to an increase in lipid droplet formation when compared to control. HCS LipidTox Green (1:100) was used to stain lipid droplets and oleic acid (150 µM) was used a positive control. **B)** FACS histograms showing that HCS LipidTOX Green signal for both siRNA 1 and 2 was equal to that of the control. The negative stain control refers to HUVECS treated without any HCS LipidTOX dye. C) Quantification of FACS data showing that silencing does not induce an increase in lipid droplet formation (siRNA 1 vs control, unpaired Student's *t* test = 0.5; siRNA 2 vs control, unpaired Student's *t* test = 0.5; oleic acid positive control vs control, unpaired Student's *t* test < 0.0001).

5.6 ELTD1 silencing does not affect fatty acid synthesis pathway genes

Having observed that ELTD1 silencing did not affect total lipid storage, it was then decided to investigate whether ELTD1 silencing affected expression of the genes encoding the fatty acid synthesis pathway. The rationale for this was the finding that in cancer cells, aberrant metabolic reprogramming upregulates ACLY as well fatty acid synthesis (Zaidi et al., 2012, Baenke et al., 2013).

In brief, following ELTD1 silencing in HUVECS, qPCR was performed on all the key fatty acid synthesis pathway genes (primers in Methods chapter). The key fatty acid genes comprise i) Acetyl-CoA Carboxylase Alpha (ACACA) which converts acetyl-CoA into malonyl-CoA; ii) Acetyl-CoA Carboxylase Beta (ACACB) which also converts acetyl-CoA into malonyl-CoA; iii) Fatty acid synthase (FASN) that converts malonyl-CoA into saturated fatty acids such as palmitate; iv) Stearoyl-CoA Desaturase (SCD) which converts saturated fatty acids into monounsaturated fatty acids; and v) CD36, which transports exogenous fatty acids (amongst other ligands) from the extracellular space into the cytoplasm (Bensaad and Harris, 2014).

Results from n=4 biological replicate experiments reveal effective ELTD1 silencing (Figure 5.7 A) with no associated statistically significant mRNA changes shared by both siRNAs for any of the fatty acid synthesis pathway genes (Figure 5.7 B-F). Interestingly, both *FASN* and *SCD* displayed statistically significant upregulation in only in one siRNA (siRNA 1) (Figure 5.7 D and E). These changes were however small. Furthermore, CD36 was significantly downregulated in the same siRNA (siRNA 1) whilst being not significantly affected by siRNA 2 (Figure 5.7 F). If ELTD1

silencing did increase fatty acid synthesis, the suppression of CD36 transporting exogenous fatty acids into the cell would be a logical response to this increase. This result did not occur for siRNA 2, so we cannot rule out that this might be an off target effect, but it might also be genuine if siRNA 1 is able to suppress ELTD1 more quickly. Thus this data suggests that ELTD1 silencing may be affecting fatty acid synthesis at a functional (phosphorylation) level and thus require a different and more sensitive form of investigation or a wider panel of siRNAs. Figure 5.7 G presents a diagrammatic representation of ELTD1's relationship with ACLY in relation to the fatty acid synthesis pathway. ELTD1 silencing thus does not induce fatty acid synthesis gene expression or induce an increase in lipid droplet formation, despite upregulating SLC25A1 mRNA and ACLY protein expression.

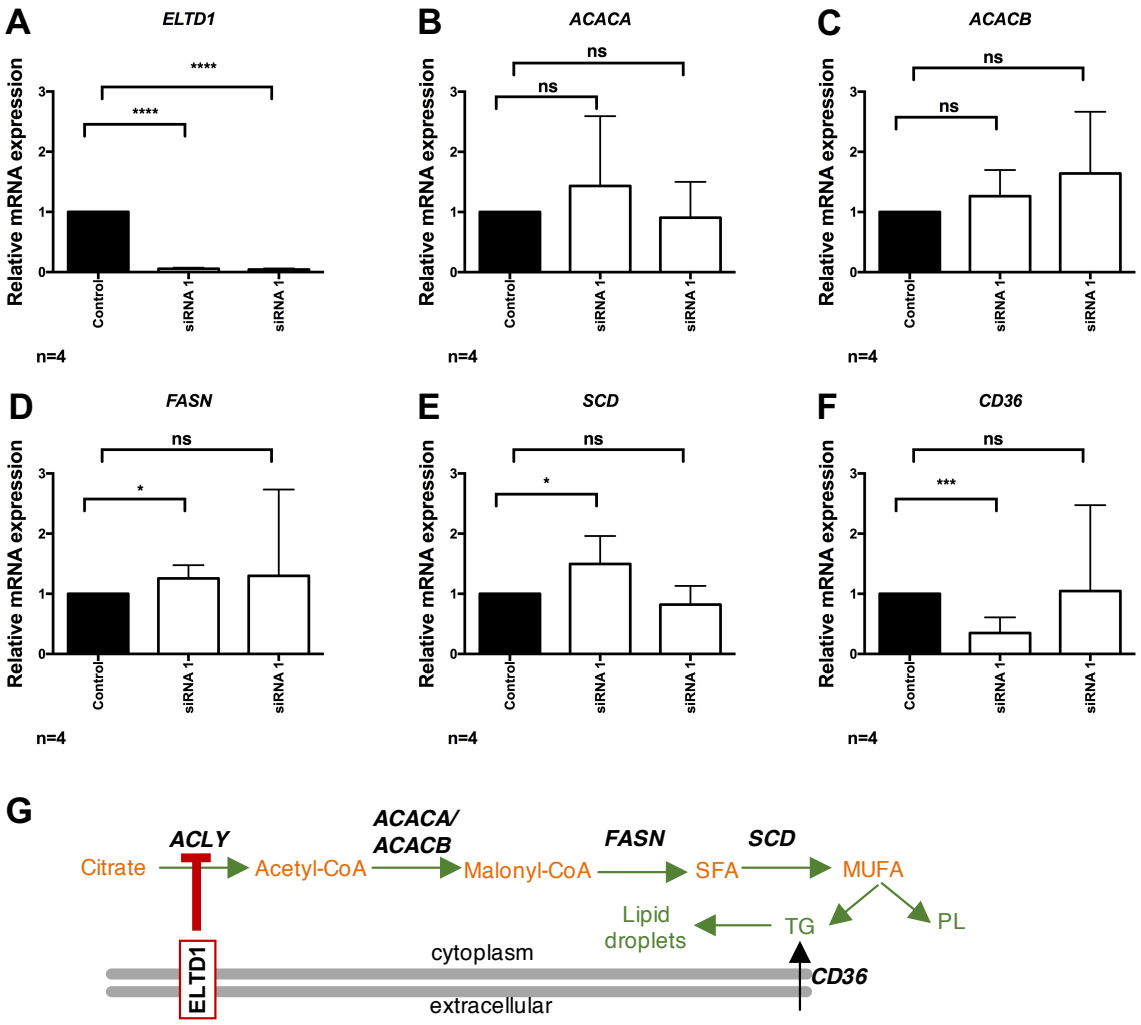


Figure 5.7: ELTD1 silencing in HUVECS does not significantly affect genes associated with the fatty acid synthesis pathway. A) qPCR result showing effective *ELTD1* suppression with both siRNAs (siRNA 1 vs control, unpaired Student's *t* test*:* $p < 0.0001$; siRNA 2 vs control, unpaired Student's *t* test: $p < 0.0001$). **B)** qPCR result showing that *ACACA* expression is not significantly changed following ELTD1 silencing (siRNA 1 vs control, unpaired Student's *t* test*:* $p = 0.3$; siRNA 2 vs control, unpaired Student's *t* test: $p = 0.7$). **C)** qPCR result showing that *ACACB* expression is not significantly changed following ELTD1 silencing (siRNA 1 vs control, unpaired Student's *t* test*:* $p = 0.1$; siRNA 2 vs control, unpaired Student's *t* test: $p = 0.2$). **D)** qPCR result showing that although *FASN*

expression is significantly upregulated in siRNA 1 treated HUVECS, it is not so for siRNA 2 treated HUVECS. Additionally, the significant upregulation is very small, rendering this change unlikely to physiologically relevant. (siRNA 1 vs control, unpaired Student's *t* test*: p* = 0.01; siRNA 2 vs control, unpaired Student's *t* test: *p* = 0.6). **E)** qPCR result showing that *SCD* expression is significantly upregulated in siRNA 1 treated HUVECS whilst not significantly changed for for siRNA 2 treated HUVECS. (siRNA 1 vs control, unpaired Student's *t* test*: p* = 0.02; siRNA 2 vs control, unpaired Student's *t* test: *p* = 0.2). **F)** qPCR result showing that *CD36* expression is significantly downregulated in siRNA 1 treated HUVECS whilst not being significantly altered in siRNA 2 treated HUVECS. If *de*-novo fatty acid synthesis was increased following ELTD1 silencing, it would make biological sense that the cell membrane fatty acid transporter *CD36* be downregulated (siRNA 1 vs control, unpaired Student's *t* test*: p* = 0.0002; siRNA 2 vs control, unpaired Student's *t* test: *p* = 0.9). **G)** Graphical representation of ELTD1's relationship with *ACLY* and the fatty acid synthesis pathway. Key fatty acid synthesis enzymes are in black and substrates are in orange. ELTD1 is labelled in red and supresses the expression of ACLY. (Abbreviations: FFA=free fatty acids; MUFA= monounsaturated fatty acid; ns=non-significant; PL=phospholipid; SFA=saturated fatty acid; TG=triglyceride;

5.7 ELTD1 silencing downregulates Notch pathway genes *HES2* and *JAG1* and upregulates *DLL4*

The next gene selected for further study from the ELTD1 silencing microarray was the Notch target gene *HES2* which was downregulated in both ELTD1 siRNA treated HUVECs. This was of interest as the Notch system is an evolutionarily ancient signalling pathway that is also a major regulator of angiogenesis (Carmeliet and Jain, 2011a). Interestingly, the list of significantly altered genes shared between both siRNAs did not contain the Notch ligand *DLL4*, which has been previously been shown to antagonise and be antagonised by ELTD1 (Masiero et al., 2013). On further analysis of the microarray data, *DLL4* was significantly differentially expressed only in siRNA 1 treated HUVECS (using the standard significance threshold of adjusted *p* value < 0.05; and a fold change of > 2 <). Only after lowering the fold change threshold to > 1.5 < (whilst maintain an adjusted *p* value < 0.05) did DLL4 qualify as a significant differentially expressed gene in siRNA2 treated HUVECS. This suggests that potentially, siRNA 1 may silence ELTD1 more efficiently than siRNA 2, although both appear to be effectively silenced after 48 hours by qPCR.

Because of the known linkage of ELTD1 and DLL4, it was decided that in addition to validating ELTD1's regulation of *HES2* expression, a wider panel of Notch genes would be assayed using qPCR in ELTD1 silenced HUVECS. The panel comprised the Notch ligands *DLL4* (located 15q15.1) and *JAG1* (located 20p12.2) and the NOTCH target genes *HES2* (located 1p36.31), *HEY1* (located 8q21.13), and *HEY2* (located 6q22.31). DLL4 is an established regulator of angiogenesis, with JAG1 being antagonistic to DLL4's angiogenic activity (Benedito et al., 2009). Similarly,

HEY1 and *HEY2* were chosen due to their importance in angiogenesis, being required for successful embryonic angiogenesis (Fischer et al., 2004).

In brief, HUVECS underwent ELTD1 silencing with each of siRNA 1 or siRNA 2 for 48 hours using methods previously described. Thereafter, qPCR was performed and statistical testing applied (primers listed in Methods chapter).

Results from n=4 experiments revealed effective ELTD1 silencing (Figure 5.8 A) as well as significant gene changes mirroring the microarray results in the Notch ligands *DLL4* (mRNA upregulated approximately 3 fold following ELTD1 silencing) (Figure 5.8 B) and *JAG1* (mRNA down regulated approximately 0.25 fold following ELTD1 silencing) (Figure 5.8 C). Of the Notch target genes, *HES2* was significantly downregulated (approximately 0.5 fold) Figure 5.8 D) whilst *HEY1* and *HEY2* remaining unchanged (Figure 5.8 E and F). These results suggest new relationships between ELTD1 and the Notch pathway.

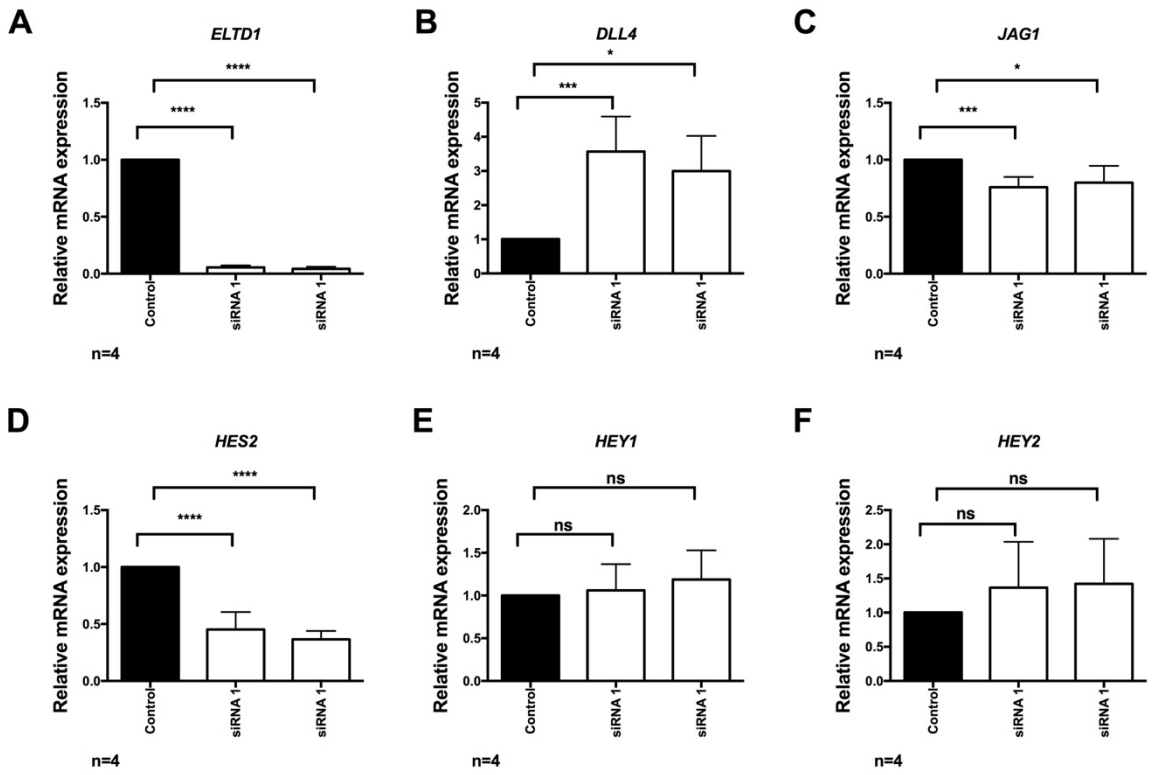


Figure 5.8: ELTD1 silencing affects the NOTCH ligands *DLL4* and *JAG1* and the NOTCH target gene *HES2*. A) qPCR result showing effective *ELTD1* mRNA suppression with both siRNAs (siRNA 1 vs control, unpaired Student's *t* test*: p* < 0.0001; siRNA 2 vs control, unpaired Student's *t* test: *p* < 0.0001). **B)** qPCR result showing significant *DLL4* mRNA upregulation in both siRNAs (siRNA 1 vs control, unpaired Student's *t* test*: p* = 0.0006; siRNA 2 vs control, unpaired Student's *t* test: *p* = 0.03). **C)** qPCR result showing significant *JAG1* mRNA downregulation in both siRNAs (siRNA 1 vs control, unpaired Student's *t* test*: p* = 0.0004; siRNA 2 vs control, unpaired Student's *t* test: *p* = 0.03). **D)** qPCR result showing significant *HES2* mRNA downregulation in both siRNAs (siRNA 1 vs control, unpaired Student's *t* test*: p* < 0.0001; siRNA 2 vs control, unpaired Student's *t* test: *p* < 0.0001). **E)** qPCR result showing no significant changes to *HEY1* mRNA in both siRNAs (siRNA 1 vs control, unpaired Student's *t* test*: p* = 0.6; siRNA 2 vs control, unpaired Student's *t* test: *p* = 0.3). **F)** qPCR result showing no significant changes

to *HEY2* mRNA in both siRNAs (siRNA 1 vs control, unpaired Student's *t* test*: p* = 0.2; siRNA 2 vs control, unpaired Student's *t* test: *p* = 0.2). (abbreviations: ns=non-significant)

In order to test whether ELTD1's effect on the Notch genes translated to a change in their protein expression, it was decided to investigate whether ELTD1 silencing affected the cell surface expression of the Notch ligands DLL4 and JAG1. In brief, HUVECS underwent ELTD1 silencing over 48 hours and were then assayed for either DLL4 or JAG1 surface protein expression using FACS (DLL4 antibody: R&D Systems MAB1506; JAG1 antibody: anti-JAG1 surface (J1-65D) antibody generated by Professor Alison Banham's laboratory, University of Oxford).

For DLL4, results from n=3 experiments showed that ELTD1 silencing resulted in a statistically significant increase in surface DLL4 protein expression in HUVECs treated with each ELTD1 targeting siRNA (Figure 5.9 A and B). This result was in keeping with the qPCR results. For JAG1, results from n=3 experiments showed that silencing resulted in a statistically significant decrease in surface JAG1 expression only in samples treated with siRNA 1 (Figure 5.10 A and B). This equivocal result fitted with the very small change both siRNAs induced in *JAG1* mRNA expression.

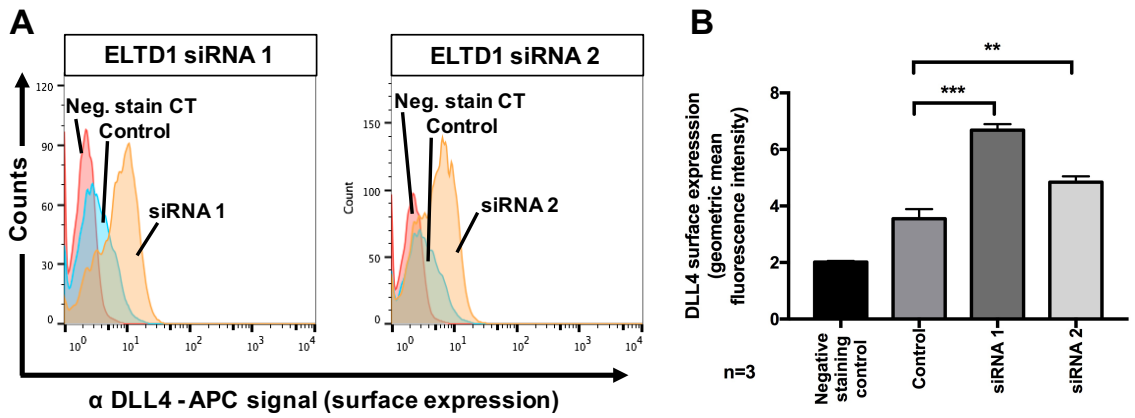


Figure 5.9: ELTD1 silencing increases surface expression of the Notch ligand DLL4 in HUVECs treated with each ELTD1 siRNA. A) Representative FACS histogram showing that DLL4 surface expression signal increases when ELTD1 is silenced using each siRNA. **B)** Quantification of DLL4 surface expression showing that silencing ELTD1 with either siRNA 1 or siRNA 2 induces upregulation in surface DLL4 expression (siRNA 1 vs control: unpaired Student's t-test p = 0.0002; siRNA 2 vs control: unpaired Student's t-test p = 0.005). (Abbreviations: Neg. stain CT=negative stain control).

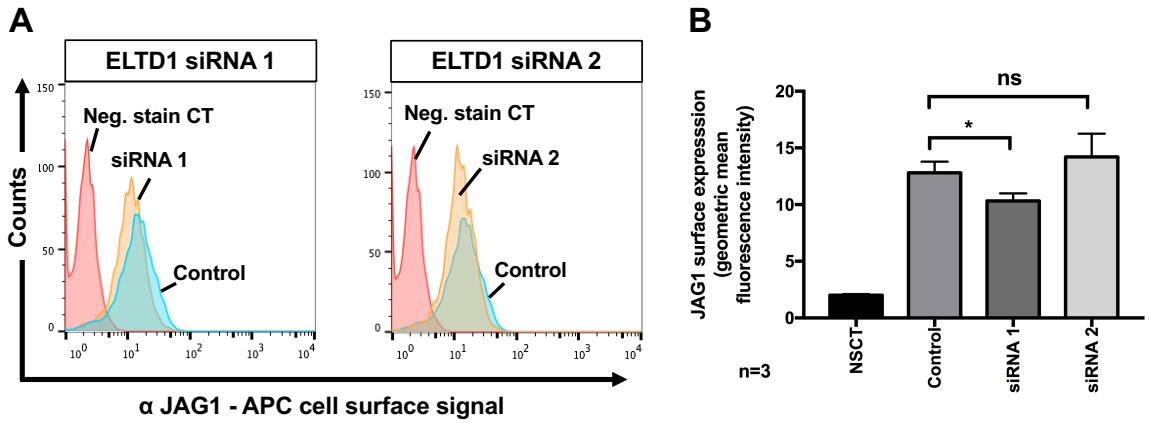


Figure 5.10: ELTD1 silencing in HUVECS decreases surface expression of the NOTCH ligand JAG1 only when using siRNA 1. A) Representative FACS histogram showing that JAG1 surface expression signal decreases slightly in both siRNAs following ELTD1 silencing. **B)** Quantification of the FACS JAG1 surface expression reveals that only the shift seen in siRNA 1 is statistically significant (siRNA 1 vs control: unpaired Student's t-test $p = 0.04$; siRNA 2 vs control: unpaired Student's t-test $p = 0.05$). (Abbreviations: Neg. stain CT and NSCT=negative stain control; ns=non-significant).

5.8 ELTD1 silencing upregulates *KIT*

The last gene selected from the ELTD1 silencing microarray was *KIT*, which was also upregulated in the ELTD1 silenced HUVECs. The *KIT* gene (located 4q12) encodes a transmembrane receptor tyrosine kinase known to regulate haematopoietic and endothelial stem cell and progenitor cell maintenance and survival, cell proliferation and cell migration (Lennartsson and Ronnstrand, 2012). *KIT* is also a proto-oncogene with gain of function mutations driving gastrointestinal stromal tumours, germ cell tumours and leukaemia (Ashman and Griffith, 2013). KIT's ligand is KITLG, also known as stem cell factor (SCF). Endothelial cells express KIT and can also express KITLG (Lennartsson and Ronnstrand, 2012). In relation to angiogenesis, the addition of KITLG to endothelial cells has been shown to promote survival, migration and capillary formation in endothelial cells (Matsui et al., 2004).

Silenced ELTD1's upregulation of KIT was validated in ELTD1 silenced HUVECS (as performed previously over 48 hours) that were assayed for *KIT* transcript expression using qPCR (primers in Methods chapter) and KIT cell surface protein expression using FACS. The KIT FACS antibody was generously shared with us by Dr. Mario Buono of the MRC WIMM Molecular Haematology Unit (KIT-APC conjugate: Biolegend 104D2).

Results from 3 biological replicates revealed that ELTD1 silencing induces significant increases in *KIT* mRNA expression (Figure 5.12 A) and KIT protein expression at the cell surface in HUVECs (Figure 5.12B and C). Interestingly, in the

ELTD1 silenced cells, there are appear to be two populations of cells: one population with KIT expression similar to control and one with increased KIT expression (Figure 5.12 B). This was not seen with any of the other cell surface FACS stains performed on ELTD1 silenced HUVECS. These two separate populations require further investigation.

As KIT and KITLG have important roles in haematopoiesis and endothelial development, the expression of ELTD1, KIT and KITLG was computationally analysed in data derived from cells of the haematopoietic and endothelial systems. In brief, RNA-Seq expression data from the Blueprint Epigenome Project was analysed (Stunnenberg and Hirst, 2016). This contained RNA-Seq expression data from the haematopoietic and endothelial lineages from healthy subjects.

Results reveal that, ELTD1, KIT and KITLG expression are co-expressed together only by endothelial cells, with proliferating endothelial cells having higher mRNA levels of all three genes (Figure 5.11). These results also reveal the known widespread KIT expression (low level expression compared to endothelial cells) across haematopoietic cells as well as the near absence of KITLG and ELTD1 in these cells.

These results are novel and interesting as they introduce ELTD1 as a regulator of KIT-KITLG signalling through suppressing KIT expression. As KIT-KITLG signalling is known to promote angiogenesis (Yamaguchi et al., 1996), it is plausible that

ELTD1's suppressive role is nuanced to provide fine-tuned regulation to endothelial angiogenic activity.

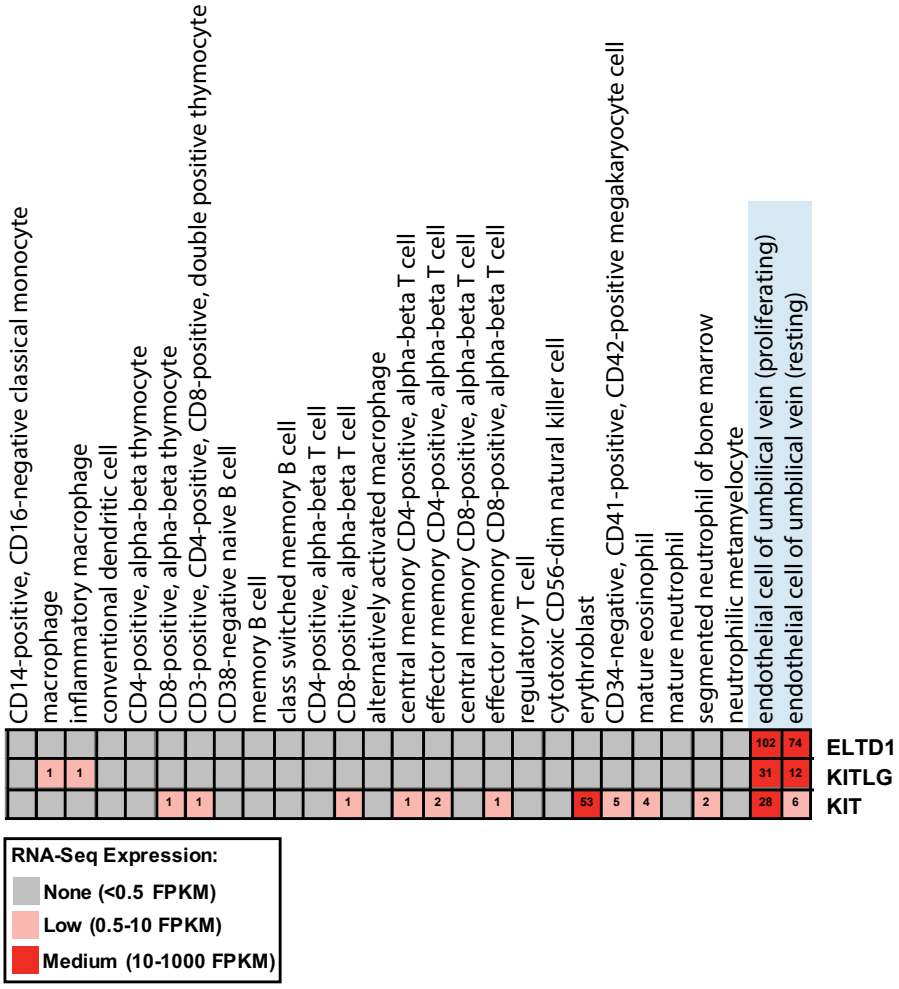


Figure 5.11: Endothelial cells co-express *ELTD1*, *KIT* and *KITLG* and are the only mature haematopoietic origin cells to do so. This figure represents RNA-Seq mRNA expression levels in common mature haematopoietic origin cells using the publically available datasets from the Blueprint Epigenome Project. Expression levels are measured as Fragments Per Kilobase of transcript per Million mapped reads (FPKM). The FPKM scale is listed in the figure. Endothelial cells are highlighted in blue. KIT was found to be expressed across a majority of tested cell

types at a low concentration with only endothelial cells expressing it at medium level expression. In contrast, KITLG was only expressed by macrophages and endothelial cells.

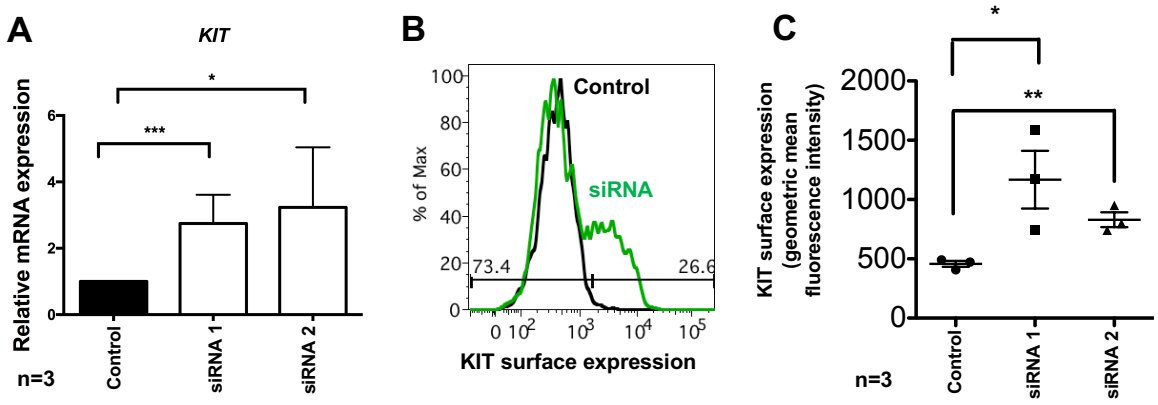


Figure 5.12: ELTD1 silencing increases KIT expression both at mRNA and cell surface protein level. A) qPCR results showing that *KIT* mRNA expression is significantly induced by ELTD1 silencing using each siRNA (siRNA 1 vs control: unpaired Student's t-test p = 0.0007; siRNA 2 vs control: unpaired Student's t-test p = 0.02). **B)** Representative FACS histogram showing increase in KIT surface expression upon ELTD1 silencing (ELTD1 siRNA 1 is shown as representative for both siRNAs). Interestingly, it appears that there are two populations of KIT expressing cells in the ELTD1 silenced group. **C)** Quantification of FACS surface KIT expression (using the geometric mean fluorescent intensity) showing an increase in KIT expression in siRNA treated HUVECS (siRNA 1 vs control: unpaired Student's t-test p = 0.04; siRNA 2 vs control: unpaired Student's t-test p = 0.005).

5.9 Discussion

5.9.1 ELTD1 and SLC25A1 and ACLY

In the first part of this chapter, ELTD1 silencing in HUVECS was found to induce upregulation of *SLC25A1* mRNA and ACLY mRNA and protein, suggesting that ELTD1 inhibits the expression of both of these genes. Both SLC25A1 and ACLY are important players within cellular metabolism (Jiang et al., 2016, Zaidi et al., 2012) and will be discussed further, with a focus on their relationship with ELTD1 and how this relates to endothelial cell and cancer cell metabolism.

As was introduced earlier, SLC25A1 (also known as citrate transport protein CTP), is a mitochondrial membrane transporter which traffics citrate produced during the citric acid cycle out of the mitochondria to the cytoplasm, whilst transporting malate from the cytoplasm to the mitochondria. (Geer et al., 2010, Sun et al., 2010). This citrate provides the acetyl units for lipogenesis and is catalysed by ACLY producing acetyl-CoA which feeds fatty acid synthesis, cholesterol synthesis or regulates glycolytic histone medication (Chypre et al., 2012, Wellen et al., 2009). The first question is how does ELTD1's downregulation of SLC25A1 and ACLY benefit endothelial cells? For this, one needs to review the relevant literature regarding the role of this pathway in endothelial and cancer cell biology.

Endothelial cells depend on glycolysis for the generation of their ATP (De Bock et al., 2013). In addition, both glycolysis and fatty acid metabolism control specific aspects of endothelial cell behaviour. Glycolysis has been shown to regulate endothelial vessel branching *in vivo* (inhibiting the glycolytic enzyme 6-

Phosphofructo-2-Kinase/Fructose-2,6-Biphosphatase 3 (PFKFB3) results in a decrease in vessel branching) (Schoors et al., 2014). Furthermore, VEGFA, the initiating ligand for endothelial cell sprouting increases endothelial glycolysis (De Bock et al., 2013). Fatty acid synthesis has been shown to regulate endothelial migration, for example inhibiting FASN leads to a reduction in endothelial migration (Wei et al., 2011). Additionally, instead of using fatty acid oxidation as an alternative source of energy, endothelial cells use beta oxidation to generate carbon for endothelial DNA synthesis (Schoors et al., 2015).

In contrast to endothelial cells, cancer cells rely heavily on upregulated *de novo* lipid synthesis, a shift which occurs by metabolic pathway reprogramming during oncogenesis favouring an increase in the activity of the fatty acid and cholesterol synthesis pathways (Hanahan and Weinberg, 2011). These synthesised lipids are essential for rapid cancer cell growth and are used to build cancer cell membranes, as sources of additional energy, and for signalling (Currie et al., 2013). As means of comparison, the majority of fatty acids utilised by normal cells (such as endothelial cells) are dietary in origin and are not synthesised *de-novo* (Harjes et al., 2016, Zaidi et al., 2012).

Due to its importance in linking glycolysis to lipid synthesis, ACLY is often upregulated in various cancers and is recognised as a key player in cancer metabolism. Cancer types which upregulate *ACLY* include bladder (Turyn et al., 2003), lung (Hatzivassiliou et al., 2005), liver (Yahagi et al., 2005), breast (Wang et al., 2017) and gastric cancers (Varis et al., 2002). Furthermore, ACLY silencing has

been shown to reduce cancer proliferation both *in vitro* and *in vivo* (Wang et al., 2017, Hatzivassiliou et al., 2005, Migita et al., 2013). Similarly, SLC25A1 has also been shown to be targeted by metabolic reprogramming in cancer cells, being upregulated in lung cancer, oestrogen receptor negative breast cancer and ovarian cancer (Kolukula et al., 2014).

Our results, reveal a previously unknown function of ELTD1: the regulation of SLC25A1 and ACLY. However, as our results show, this regulation does not induce an increase in the accumulation of lipid droplets, nor upregulate the genes involved in fatty acid synthesis. Hints that fatty acid synthesis may be affected by ELTD1 exist in the qPCR results in HUVECS treated with siRNA 1: in these samples, both *FASN* and *SCD* mRNA are statistically upregulated, whilst the fatty acid transporter *CD36*'s mRNA is significantly downregulated. Although not occurring with siRNA 2, these findings support the need for an alternative and more-sensitive method of investigation such as radiolabelled carbon fatty acid analysis.

ELTD1's suppression of SLC25A1 and ACLY is also contrary to the metabolic reprogramming induced *de-novo* lipid synthesis strategy employed by many cancers (facilitated through SLC25A1 and ACLY upregulation). This may be one reason as to why the majority of cancer cell lines used in laboratory research do not express ELTD1 (this result is presented in the last chapter), as it would be metabolically costly to do so. This then begs the question: how does ELTD1's downregulation of SLC25A1 and ACLY benefit endothelial cells? The answer lies within the character of endothelial metabolism. As has been already mentioned,

endothelial metabolism utilises glycolysis for energy production and tightly regulates fatty acid synthesis for specific angiogenesis related tasks such as endothelial cell migration. By tightly downregulating SLC25A1 and ACLY, ELTD1 contributes to maintaining this endothelial metabolic phenotype. It must be noted however that ELTD1's inhibition of these genes is not complete. As can be seen from ACLY's Western blot (Figure 5.5 B), unsilenced HUVECS contain a baseline level of ACLY protein which is likely to function within the confines of endothelial cell metabolism.

Possibilities as to how ELTD1 suppresses SLC25A1 and ACLY remain unclear. Could this be direct inhibition? this seems unlikely as their expression is de-regulated at the transcript level, or is this as an indirect result mediated by other molecules affected directly by ELTD1? Additionally, who is downstream to who? To interrogate this further, a possible future experiment may entail silencing SLC25A1 and ACLY individually and together in HUVECS and performing qPCR for these genes as well as ELTD1. If silencing SLC25A1 and ACLY has no effect on ELTD1, one can presume that ELTD1 is upstream to them.

A possible reason as to why the performed ELTD1 silencing lipid droplet experiments failed to yield any significant changes may be due to endothelial cells tightly controlling ACLY's activity in order to maintain the endothelial metabolic phenotype. As ACLY requires phosphorylation for its activation (Potapova et al., 2000), the cell may respond in a compensatory manner to a non-physiological increase in ACLY mRNA and protein expression by dephosphorylating ACLY to reduce its activity. In order to investigate this, a future experiment needs to be

performed looking at ACLY's catalytic activity (rate of citrate to acetyl-CoA conversion) with and without ELTD1 silencing in HUVECS.

Another possibility is that under physiological conditions, endothelial cells tightly control the levels of mitochondrial citrate available to be exported to the cytoplasm, resulting in no downstream lipid changes irrespective of the level of SLC25A1 or ACLY. If this was the case, one could attempt to override this control by stimulating endothelial mitochondrial citrate production with ELTD1 silencing to determine whether there is any downstream lipid effect.

Lastly, the effect of ELTD1's suppression of SLC25A1 and ACLY on histone acetylation remains unexplored, requiring testing for global acetylation changes following ELTD1 silencing and contrasting this to the effect seen with and without the use of histone deacetylase inhibitors. Previously, the glucose transporter GLUT4 and three glycolysis regulators, HK2, PFK-1 and LSH1 have been shown to be regulated by ACLY through histone modification (Wellen et al., 2009). Specifically, ACLY silencing lead to a decrease in transcription in these glycolytic genes. ELTD1's partial suppression of ACLY in HUVECS thus suggests that one of ELTD1's roles is to indirectly regulate glycolysis. This further suggests that ELTD1 is important for maintaining the endothelial metabolism phenotype and is an exciting hypothesis requiring future metabolic flux experiments in HUVECS with and without ELTD1 silencing.

5.9.2 ELTD1 and NOTCH GENES DLL4, JAG1 and HES2.

Results from the ELTD1 silencing microarray and subsequent experiments present new relationships between ELTD1 and members of the Notch pathway HES2 and JAG1, as well confirming the previously documented relationship between ELTD1 and DLL4 (Masiero et al., 2013). The Notch signalling pathway is an evolutionarily ancient and conserved signalling system which regulates angiogenesis, cellular lineage commitment, stem cell renewal and maintenance, cellular differentiation and cell cycle regulation (Nowell and Radtke, 2017, Carmeliet and Jain, 2011a). Notch signalling will be further discussed with ELTD1 in mind.

Canonical Notch signalling is dependent on cell-cell contact with signalling initiated when a Notch ligand, expressed by a signal initiating cell, binds to a Notch receptor expressed by the signal receiving cell (Kitagawa, 2016). This directionality of activation is termed trans-activation (Andersson et al., 2011). Additionally, ligands inhibit receptors expressed on the same surface, a feature termed cis-inhibition (del Alamo et al., 2011). There are four Notch receptors (NOTCH1-4) of which only NOTCH1 and 4 are expressed in human endothelial cells (Kuhnert et al., 2011). Similarly, to ELTD1, these receptors have multiple EGF-like repeats. In the case of the Notch receptors, these EGFs are essential for ligand binding. Although ELTD1 remains an orphan receptor, is probable that ELTD1 EGFs function in a similar manner to bind ligand.

The Notch system comprises 5 notch ligands, all belonging to the Delta-Serrate-Lag (DSL) family. They comprise delta-like 1 (DLL1), DLL3, DLL4, and jagged 1 (JAG1) and JAG2 (Bray, 2016). Interestingly, DLL3 is unable to activate canonical notch signalling in trans and possibly functions solely as a cis-inhibition ligand (Ladi

et al., 2005). In terms of angiogenesis, DLL4-notch signalling is a major regulator of physiological and tumour angiogenesis, guiding the specification of sprouting endothelial cells into stalk cells (the phalanx of cells making up the trunk of the sprouting vessel) from VEGF initiated tip cells (those at the leading edge of the growing vascular sprout) (Carmeliet and Jain, 2011b, Lobov et al., 2007). Whilst the tip cell phenotype induces Notch signalling as well as the stalk phenotype in surrounding cells, cells expressing the stalk phenotype actively repress neighbouring cells from expressing the tip phenotype, instead promoting a pro stalk cell phenotype in these cells. In relation to this, DLL4-signalling has been described as the most potent pro stalk-cell signal known (Harjes et al., 2016). Additionally, JAG1 has been shown to antagonise DLL4-Notch signalling (Benedito et al., 2009). As ELTD1 has previously been shown to be important for tip cell function and sprouting angiogenesis (Li et al., 2014) questions arise the regarding the degree of ELTD1 expression within stalk cell phenotype endothelial cells. A potential method to perform this experiment would be to perform a HUVEC spheroid experiment and trigger vessel sprouting following by staining of the sprouting vessels with ELTD1, DLL4 and VEGFR2.

Each Notch receptors contains a negative regulatory region (NRR) which inhibits the receptor until it is bound by its cognate ligand, and an intracellular portion, termed the Notch intracellular domain (NICD) which is essential for Notch signal transduction (Nowell and Radtke, 2017). On Notch ligand binding, the Notch receptor's NRR undergoes confirmatory change to expose a hidden cleavage site which is then cleaved by the cell surface metalloproteinase ADAM10. This is then

followed by γ-secretase cleavage of the cytoplasmic NICD liberating it from the rest of the receptor (Nowell and Radtke, 2017). Once released, the NICD translocates to the cell's nucleus where it forms a complex with the DNA binding protein CBF1–Suppressor of Hairless–LAG1 (CSL) and the co-activator Mastermind (MAML1) (Hori et al., 2013). This complex then stimulates the transcription of notch target genes with most characterised being members of the *HES* and *HEY* gene families (Andersson et al., 2011). Both families are important for angiogenesis (Fischer et al., 2004, Lobov et al., 2007). Ultimately, the Notch target genes encode proteins which bind to and repress their target loci ultimately leading to changes in cell behaviour and fate (Nowell and Radtke, 2017). Interestingly, the initiation of Notch signalling appears to share similar aspects to adhesion GPCR activation and the initiation of signal transduction. Firstly, there are the similar extracellular EGF domains which both the Notch receptors and ELTD1 contain. Then there is the repressive function of the NRR which is very similar to the hypothesised repressive effect of the adhesion GPCR's NTF. Additionally, a change in the conformation of the receptor initiates signalling in both, however using different mechanisms.

Returning to metabolism, it is now known that DLL4-Notch signalling decreases endothelial glycolysis and mitochondrial respiration as well as increases endothelial exogenous fatty acid uptake (Harjes et al., 2014). In contrast, VEGFA increases glycolysis (De Bock et al., 2013). It has also been found that inhibition of endothelial fatty acid oxidation interferes with characteristics of the endothelial stalk cell phenotype, suggesting that DLL4-Notch signalling utilises fatty acid oxidation to maintain this phenotype. Related to this, it was found that DLL4-Notch signalling

increased FABP4, a protein which mediates fatty acid flux (Harjes et al., 2014). ELTD1's suppression of DLL4-Notch therefore may prevent a decrease in endothelial glycolysis, thus maintaining the endothelial metabolic phenotype described in the previous sections.

Although it is known that the vascular endothelial growth factor (VEGF) pathway activates both ELTD1 as well as DLL4-Notch signalling (Masiero et al., 2013), it remains unclear at which level and how ELTD1 interacts with the Notch pathway and *vice versa*. Additionally, it remains unclear whether ELTD1's effect on the Notch ligands DLL4 and JAG1 is downstream to ELTD1's effect on *HES2* – or could it be the other way around? To begin answering these questions, additional experiments in HUVECS where each Notch ligand or target gene is silenced before undergoing qPCR for ELTD1 need to be performed. Additional experiments include exposing HUVECS to the ligands DLL4 or JAG1 with and without ELTD1 silencing followed by qPCR for ELTD1 and a wider panel of Notch-associated genes. It also remains unclear whether ELTD1's effect on Notch is inverse to that of ELTD1 silencing when ELTD1 is overexpressed in HUVEC cells. Lastly, proteomic studies in HUVECS will likely be of great benefit in determining ELTD1's binding partners. In closing, ELTD1's new relationships with HES2 and JAG1 as well as ELTD1's previously documented relationships with DLL4 and VEGF are presented in Figure 5.13.

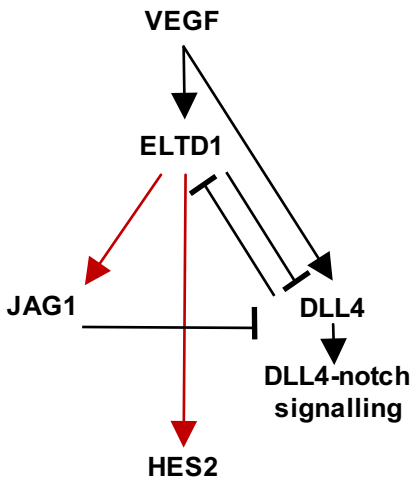


Figure 5.13: ELTD1's documented relationship with VEGF and members of the Notch pathway in endothelial cells. The two new relationships with HES2 and JAG1 are illustrated in red. VEGF induces expression of ELTD1 (Li et al., 2014) and induces DLL4 expression leading to DLL4-Notch signalling in adjacent cells (Lobov et al., 2007). DLL4 is known to antagonise ELTD1 and be antagonised by JAG1 (Masiero et al., 2013, Li et al., 2014) . It remains unknown whether ELTD1's effect on JAG1 and DLL4 are upstream or downstream of HES2 or vice versa.

5.9.3 ELTD1 and KIT

The finding that ELTD1 silencing in HUVECS upregulates *KIT* mRNA and surface protein is novel and establishes ELTD1 as a new regulator of endothelial KIT-KITLG signalling.

KIT and KITLG are both known to have an important role in haematopoiesis as well as endothelial development. In haematopoiesis, KIT is expressed by early haematopoietic progenitor cells (HPC) (including stem cells) which regulate stem cell renewal as well lineage differentiation (Lennartsson and Ronnstrand, 2012). Endothelial progenitor cells (EPC) also express KIT and derive from these early HPCs (Heissig et al., 2002). These EPCs play an important in role maintaining vascular integrity (Heissig et al., 2002). Additionally, mature endothelial cells also have an important role in maintaining HPCs and EPCs via the expression and interaction of KIT and KITLG (Yamaguchi et al., 1996). As HPC and EPC progenitors strongly express KIT, it may be possible that ELTD1's incomplete repression of KIT in endothelial cells (endothelial cells express KIT despite being repressed by ELTD1) is a possible mechanism through which endothelial cells maintain terminal endothelial differentiation. This hypothesis however requires further investigation.

To date, the only known relationship between ELTD1 and HPCs is limited to the perivascular niche in breast cancer where *ELTD1* was found to be part of a gene signature regulating breast cancer progression (Ghajar et al., 2013). Interestingly, KIT and KITLG were not included in this signature. Whether or how ELTD1 is

involved in contact-related regulation of progenitor endothelial populations remains known. Another unanswered question is what is ELTD1's effect on KITLG. This forms the basis of another future experiment to investigate ELTD1's effect on KITLG as well as the effect of silencing of both KIT and KITLG on ELTD1 within endothelial cells.

Interestingly, in the ELTD1 silenced cells, there appear to be two populations of cells: one population with KIT expression similar to control and one with increased KIT expression. This was not seen with any of the other cell surface FACS stains performed on ELTD1 silenced HUVECS. These two separate populations require further investigation. Do they represent a subpopulation of primary endothelial cells with separate cellular responses to ELTD1 signalling? A possible future experiment would be to FACS sort these two populations and perform qPCR experiments on them looking for differences in a panel of Notch, metabolic and core angiogenic genes.

Lastly, KIT has also been linked to metabolism. In adipocytes, KIT-KITLG signalling has been found to upregulate the transcriptional coactivator PPARGC1A (which induces expression of the fatty acid transporter *CD36* amongst other effects) as well as inducing mitochondrial biogenesis (Huang et al., 2014). This may explain the possible regulation of *CD36* seen with one ELTD1 siRNA. Thus, ELTD1's regulation of KIT in endothelial cells further adds weight to ELTD1's importance in regulating endothelial homeostasis and biology.

5.10 Conclusion

Using global transcriptional profiling, this chapter reveals new data regarding ELTD1's role within endothelial biology. ELTD1's suppression of the key metabolic genes *ACLY* and *SLC25A1* establish ELTD1 as a potentially important regulator of endothelial metabolism. Furthermore, ELTD1's relationship with the Notch signalling pathway is extended to include upregulation of HES2 and JAG1 whilst confirming previous ELTD1's suppression of DLL4. Lastly, ELTD1's suppression of KIT establishes a new relationship with endothelial KIT/KITLG signalling. These findings present us with many additional questions (covered in the chapter's discussion) and will be the subject of future investigations.

Chapter 6: The effects of ELTD1 overexpression in primary human endothelial cells

6.1 Introduction

In the previous chapter, global transcriptional profiling was successfully employed in ELTD1 silenced HUVECS to uncover previously unknown relationships between ELTD1 and endothelial metabolism, Notch signalling and KIT-KITLG signalling. Importantly ELTD1 is upregulated in tumour endothelial cells and it is possible that there may be associated with distinct functional effects associated with ELTD1 overexpression. To investigate this possibility, it was decided to further study ELTD1's role in endothelial cell biology by applying both global transcriptional profiling and functional angiogenic assays to an ELTD1 overexpression cell model. Questions underpinning this approach included:

1. What is the effect of ELTD1 overexpression on transcription? Can this reveal further new relationships with ELTD1 or shed light on ELTD1's signalling? Additionally, does overexpression just induce gene changes opposite to those seen with ELTD1 silencing or might it generate additional changes?

2. What is the functional effect of ELTD1 overexpression in endothelial cells? And can one explain the functional effect through changes in gene expression? Can ELTD1 overexpression allow us to better understand ELTD1's role in tumour biology?

This chapter presents this work.

6.2 Microarray of transient ELTD1 ectopic expression in HEK293T cells

The initial model for assessing gene expression changes as a consequence of ELTD1 ectopic expression consisted of using FL and CTF codon optimised ELTD1 constructs transiently overexpressed in HEK293T cells. Cells would then be sorted for highest expressing using FACS and then microarrayed. HEK293T cells were chosen as the host cell type because of their ease of transient transfection and their historical use in adhesion GPCR research. As for the ELTD1 constructs, FL and CTF codon optimised ELTD1 constructs (with two different tagging strategies) were chosen following their use in the ELTD1 signalling experiments. Due to the possibility that my 7TMΔ form of ELTD1 contained a truncated first α-helix (discussed in results chapter 2), this construct was not used. Two differing sets of tagged ELTD1 constructs were used in order to minimise any potential tag-related interference: one set contained HA (N-term) and FLAG (C-term) tags, whilst the other contained only GFP (C-term) tags. Both sets of included ELTD1 constructs are graphically represented in Figure 6.1 A and B.

In brief, all selected ELTD1 constructs were transiently transfected using Lipofectamine LTX into HEK293T cells for 24 hours before the cells were harvested and FACS sorted. Three biological replicates were performed with ELTD1 expression being assessed using FACS (surface HA expression for HA tagged constructs and total cellular GFP fluorescence for GFP tagged constructs). As each ELTD1 construct was packaged within a pcDNA 3.1 plasmid, empty pcDNA 3.1 plasmids were used as empty vector controls. Twenty-four hours were chosen as a transfection time as this time point was found to produce the highest levels of ELTD1 expression (see Figure 1 in signalling chapter). FACS sorting was performed using

anti-HA antibodies (Cell Signalling Technology, 2367) for HA tagged samples and GFP fluorescence for GFP tagged samples. In ELTD1 transfected cells, only live cells with the highest signal were selected from FL and CTF groups (Figure 6.1 C and D). For controls, a similar number of live cells with a negative FACS signal were selected.

Following sorting, RNA was then extracted and prepared for microarray scanning. This entailed reverse transcribing and labelling the mRNA and then hybridising the labelled target to the microarray chip (HumanHT-12 v4 Expression BeadChip) following by microarray scanning using an Illumina microarray scanner (Illumina iScan). Thereafter, microarray data analysis and linear modelling was performed within the R scripting environment. The analysis method and algorithm used were the same as those outlined in Chapter 5 (Figure 5.2) and consisted of pre-processing with the Limma R package, linear modelling to create differentiate gene expression, and visualisation of differentially expressed genes using volcano plots and heatmaps. All of my microarray analysis and visualisation coding scripts written in R are included in the Appendix. Lastly, it was anticipated that the microarray would be unable to detect the presence of codon optimised FL and CTF ELTD1 overexpression as the microarray would only contain probes against wild type FL ELTD1.

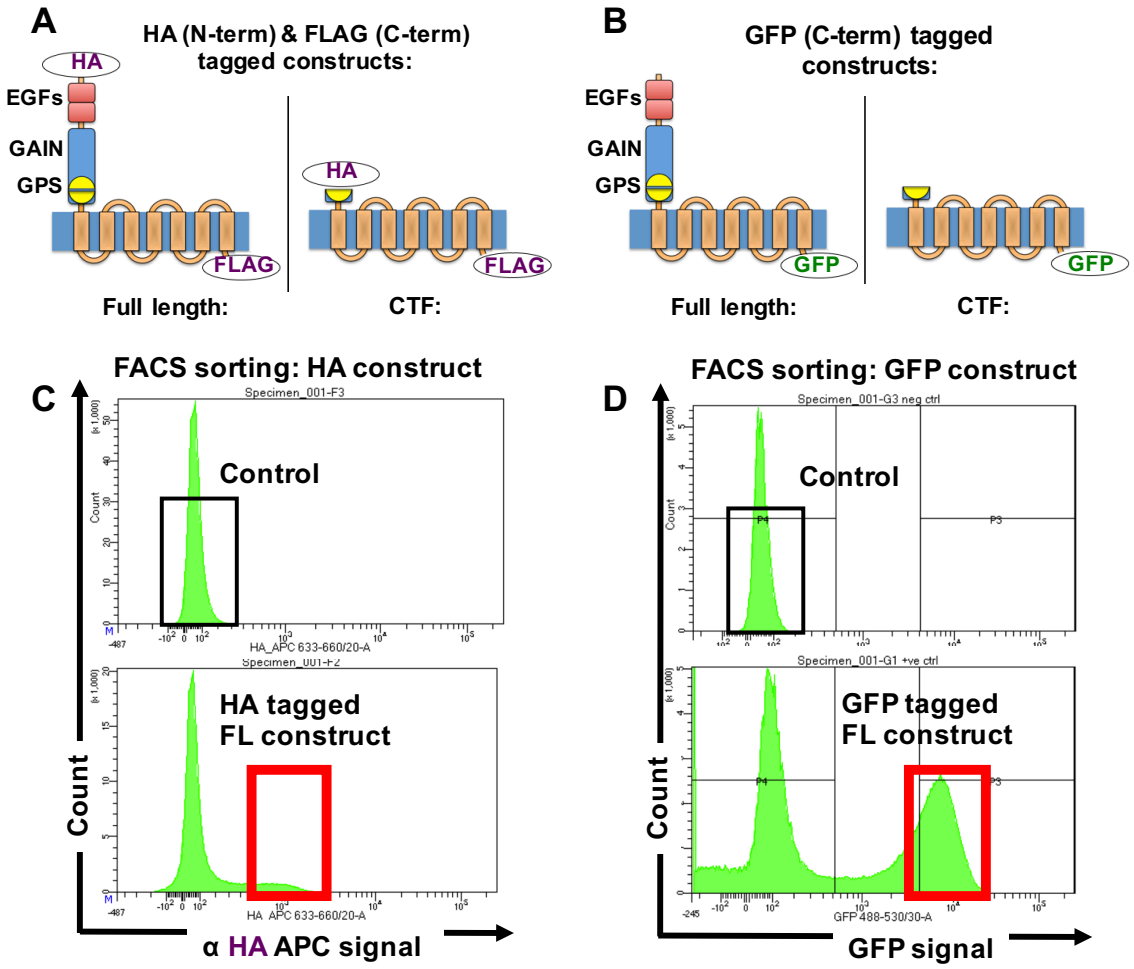


Figure 6.1: Overview of ELTD1 overexpression and FACS sorting in HEK293T cells. Two sets of tagged constructs were used. **A)** Graphical representation of HA (N-term) and FLAG (C-term) tagged codon optimised FL and CTF coELTD1 constructs. **B)** Graphical representation of GFP (C-term) tagged codon optimised FL and CTF coELTD1 constructs. **C)** Representative FACS plot showing sorting strategy for HA tagged constructs: for ELTD1 transfected samples, only live cells with the highest surface HA expression were selected (red box). For control cells (empty vector), an equivalent number of live cells with negative fluorescence were selected (black box). **D)** Representative FACS plot showing sorting strategy for GFP tagged constructs: for ELTD1 transfected samples, only live cells the highest surface GFP fluorescence expression were selected (red box). For control cells

(empty vector), an equivalent number of live cells with negative fluorescence were selected (black box).

For differential gene expression, two comparisons were calculated: i) FL coELTD1 expression compared to control (empty vector); and ii) CTF coELTD1 expression compared to control (empty vector). For both comparisons, HA and GFP tagged samples were analysed together (ie. FL comparison: HA + GFP; CTF comparison: HA + GFP). Analysing the HA and GFP constructs together yielded the same results as analysing them individually, suggesting that both tagging strategies had a similar effect. Differentially expressed genes were deemed statistically significant only if they fulfilled standard microarray criteria: i) an adjusted *p* value < 0.05; and ii) a fold change of > 2 < -2. Volcano plots depicting differential gene expression are presented for FL coELTD1 (Figure 6.2 A) and for CTF coELTD1 (Figure 6.2 B). For FL coELTD1 overexpressing cells, the most upregulated gene was the heat shock protein HSPA6 whilst the most downregulated was the phosphatase INPP5B (Figure 6.2 A). For CTF coELTD1 overexpressing cells, the most upregulated gene was also HSPA6 whilst the most downregulated gene was the ribonucleoprotein HNRNPF (Figure 6.2 B). Neither microarray detected overexpressed FL or CTF coELTD1 due to microarray probes for ELTD1 being against wild type FL ELTD1 only.

Heatmaps were then generated displaying the expression level z-score of all significant differentially expressed genes for both FL (Figure 6.3 A) and CTF

(Figure 6.3 B) coELTD1 overexpression. The majority of significant gene changes for FL overexpression were upregulated in nature whilst the majority for CTF overexpression were downregulated. A Venn diagram comparison was then performed to determine how many significant differentially expressed genes were common to both FL and CTF coELTD1 overexpressing HEK293T cells. Results revealed that only 10 differentially expressed genes were common to both groups, with 12 genes being unique to FL overexpression and 33 genes being unique to CTF overexpression (Figure 6.3 C). Shared genes are listed in the both heatmaps.

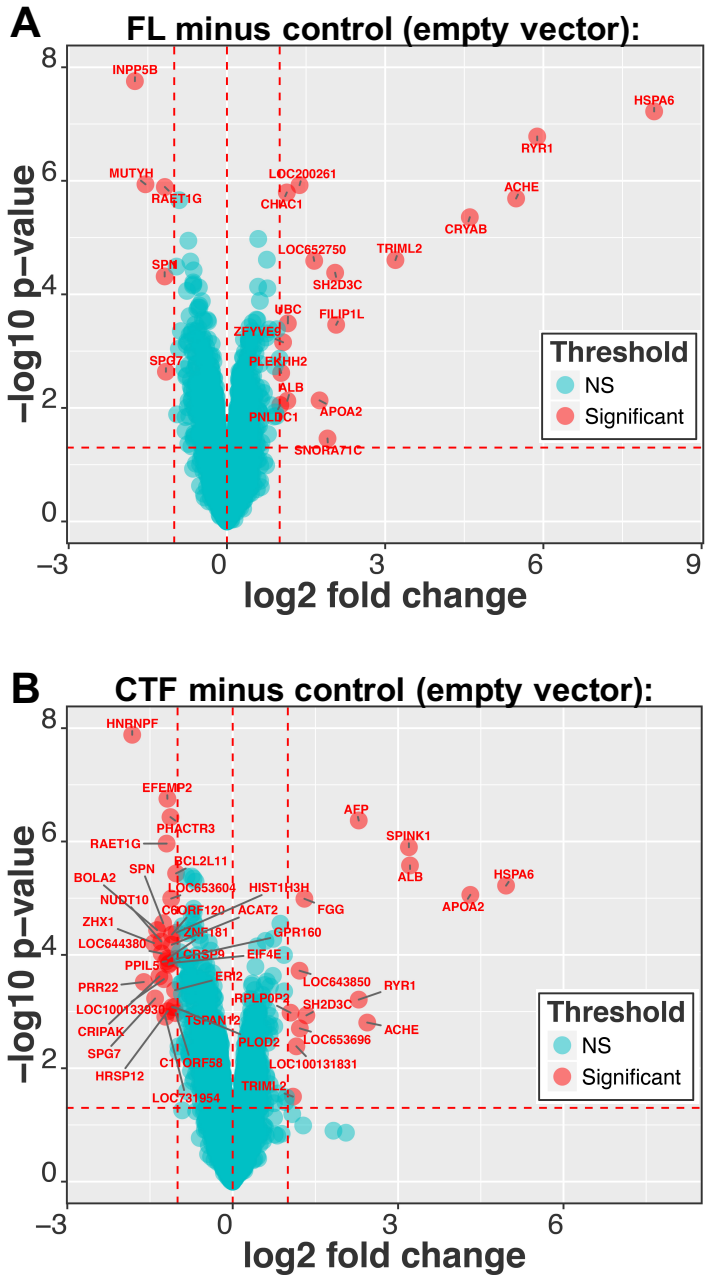


Figure 6.2: Volcano plots depicting differentially expressed genes following FL and CTF coELTD overexpression in HEK293T cells. The threshold for statistical significance was set as a *p* value of < 0.05 and log2 fold change > 1 and < -1. Neither microarray detected overexpressed FL or CTF coELTD1 due to microarray probes for ELTD1 being against wild type FL ELTD1 only. **A)** Volcano plot depicting significant differentially expressed genes (in red) following FL coELTD1 overexpression in HEK293T cells. The heading “FL minus control” refers

to the direction of the linear model comparison. In FL overexpressing HEK293T cells, HSPA6 was the most upregulated gene whilst INPP5B was the most supressed gene. **B)** Volcano plot depicting significant differentially expressed genes (in red) following CTF coELTD1 overexpression in HEK293T cells. In CTF overexpressing HEK293T cells, HSPA6 was the most upregulated gene whilst HNRNPF was the most downregulated gene. (Abbreviation: NS=non-significant)

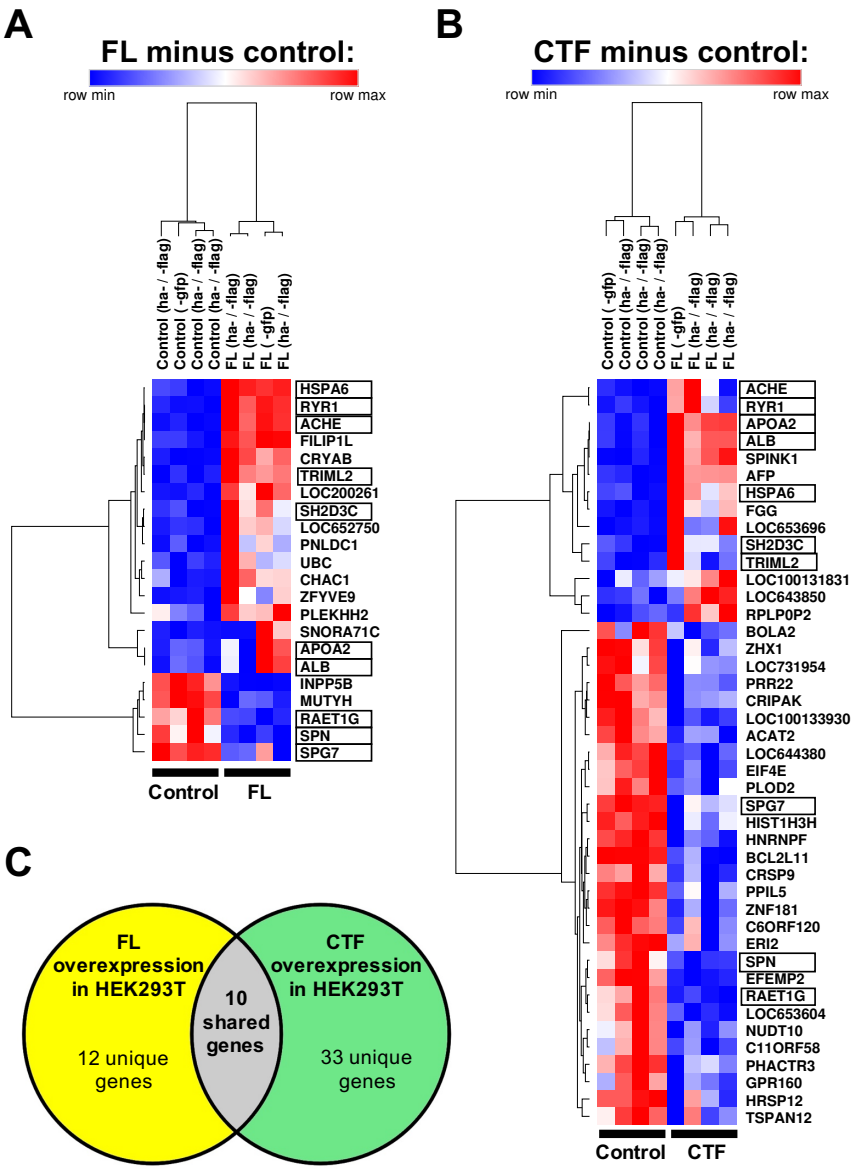


Figure 6.3: Heatmap displaying significant expressed genes in FL and CTF coELTD1 overexpression in HEK293T cells. In each heatmap, the row and column clustering was performing using Euclidean distance hierarchical clustering. The intensity colouring (low=blue; high=red) represents the z-score for each gene (the number of standard deviations by which a gene's expression in an individual sample (as determined by microarray) differs from the mean expression for that gene across all samples). Neither microarray detected expressed FL or CTF coELTD1 due to microarray probes for ELTD1 being against wild type FL ELTD1

only. In each microarray, boxed genes indicate genes shared between both experiments. **A)** Heatmap of significant differentially expressed genes following FL coELTD1 expression in HEK293T cells. The majority of gene changes are upregulated in nature. **B)** Heatmap of significant differentially expressed genes following CTF coELTD1 expression in HEK293T cells. In contrast to FL overexpression, the majority of gene changes are downregulated in nature. **C)** Venn diagram showing that only 10 differentially expressed genes are shared between FL and CTF overexpression in HEK293T cells. Shared genes are highlighted with boxes in each heatmap.

All significant differentially expressed genes for both FL and CTF expression experiments were then inputted into multiple curated pathway analysis databases. Results yielded no significant association with any pathway. Pathway databases interrogated consisted of KEGG (Kanehisa et al., 2017), Reactome (Croft et al., 2014), Wikipathways (Kutmon et al., 2016) and BioCarta (Nishimura, 2001).

Before initiating qPCR and Western blotting validation experiments for the above microarray results, all differentially expressed genes from both FL and CTF expressing HEK293T cells were compared with the 59 genes affected by ELTD1 silencing in HUVECS. The expectation here was the detection of genes shared between the ectopic expression and silencing experiments, with opposing expression (i.e. if up on ectopic expression, then down in silencing). A Venn

diagram comparison was performed revealing no overlap between the HEK293T and HUVEC gene sets (Figure 6.4).

This lack of overlap posed problems as it was expected that there be some shared genes between ectopic expression and silenced cells if even some of ELTD1's activity was conserved across cell types. Firstly, it was unclear whether the codon optimised FL and CTF coELTD1 constructs were functionally active. This was further complicated by neither having a positive read out system for activity and that our previous findings had shown that neither activate canonical GPCR activity. Additionally, a hypothesis was raised that HEK293T cells do not have the appropriate cellular machinery for ELTD1 function as they do not express ELTD1 or that the tags added to ELTD1 interfered with function. The argument about cellular machinery is unlikely to be completely valid as this cell is commonly used by the adhesion GPCR community for functional work (i.e. signalling) despite a lack of adhesion GPCR expression (indeed, this lack of expression and ease of transfection make this cell line a very attractive adhesion GPCR cellular model system). As for the tagging strategy used, this has been successfully employed in the majority of published Stinger/Stachel adhesion GPCR signalling papers (Wilde et al., 2016, Schoneberg et al., 2015, Demberg et al., 2015, Liebscher et al., 2014, Liebscher et al., 2013).

Because of the lack of overlap between the expression in HEK293T cells and silencing in HUVECS it was decided to change the ELTD1 ectopic expression

model in HEK293T to overexpression in HUVEC, which is more biologically relevant to the ELTD1 upregulation observed in tumour endothelium.

This required an alternative approach to facilitate ELTD1 overexpression as HUVECS, being a primary cell type, are notoriously difficult to transiently transfect, even with small plasmids. To counter this, a lentiviral system needed to be employed to transduce HUVECS with codon optimised ELTD1. It was thus decided to postpone qPCR validation of the genes identified from the HEK293T ectopic expression microarray and only validate those genes common to HUVECS overexpressing coELTD1 that might contribute to tumour endothelial cell biology.

.

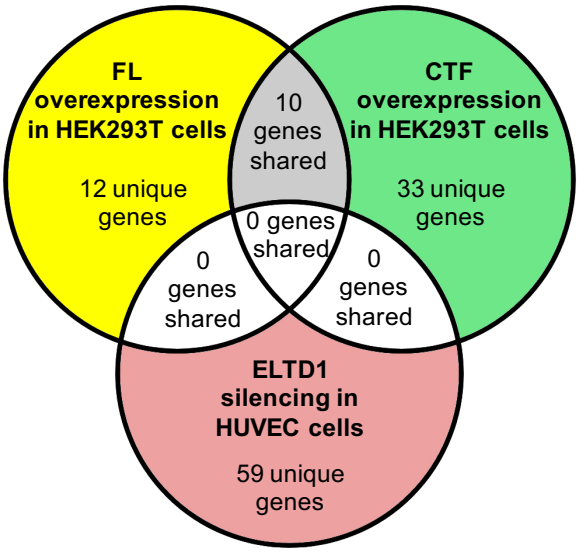


Figure 6.4: Venn diagram showing that none of the genes differentially expressed in HEK293T cells expressing recombinant ELTD1 are shared with those differentially expressed in ELTD1 silenced HUVECS. Results detailing ELTD1 silencing in HUVEC cells are presented in the previous chapter.

6.3 Stable codon optimised ELTD1 overexpression in HUVEC cells

The model used for ELTD1 overexpression in HUVECS comprised using a lentiviral vector containing codon optimised FL ELTD1 to transduce low passage HUVEC cells from multiple donors. As developing such a lentiviral system is very time consuming, it was decided to first begin with creating a FL coELTD1 containing lentivirus before starting to create a CTF coELTD1 lentivirus. Using wild type ELTD1 was ruled out in favour of coELTD1 because of the benefits in expression. In order to minimise the potential risk of tag-related interference with function, tags were removed from the original FL coELTD1 construct. This resulted in the codon optimised FL construct having the same translated amino acid sequence as wild type ELTD1. As HUVECS constitutively express wild type ELTD1, the use of transduced coELTD1 allowed for simultaneous wild type and codon optimised ELTD1 expression monitoring at the mRNA level using qPCR as both had different nucleotide sequences. This had the added benefit of allowing us to investigate whether ELTD1 protein expression negatively regulates mRNA expression. A graphical representation of the FL coELTD1 construct cloned into the lentiviral system is presented in Figure 6.5 A.

In brief, the FL coELTD1 construct (labelled as coELTD1 in subsequent figures) was cloned into a pLenti6/V5-DEST lentiviral expression vector using the pLenti6/V5-DEST Gateway Vector system (Invitrogen). The FL coELTD1 containing lentivirus was the then assembled in HEK293T cells. This was performed by triple transfecting these cells with the lentiviral expression vector, the psPAX2 packaging vector and the pMD2.G viral envelope vector. A pLenti6/V5-DEST lentiviral expression vector without any insert was used as the empty vector control. During

the lentiviral assembly process in HEK293T cells, low triple transfection efficiency became the biggest bottleneck. Initially, the inexpensive calcium phosphate transfection method was used, however this resulted in low virus titres which did not adequately transduce HUVECS. It was only after changing the transfection reagent to Lipofectamine LTX that the transfection reached a high enough efficiency and adequately transduced HUVECS.

Following lentiviral assembly in HEK293Ts, the virus rich supernatant was harvested and applied onto 3 batches of early passage HUVECS, each from a unique donor pool (HUVEC batch 1 – 3) (Figure 6.5 B). As HUVECS are a primary line and can only maintain their endothelial and angiogenic phenotype for 6-7 passages, we transduced all our HUVECS at passage 2 and discarded cells at passage 5. Transduced HUVECS were then selected for 1 week with the blasticidin selection antibiotic, resistance to which the lentivirus was carrying. Selection was considered complete once a batch of non-transduced HUVEC representative of all HUVEC batches had died following antibiotic exposure. Transduced HUVECS then underwent testing to confirm FL coELTD1 expression using qPCR, western blotting and FACS. Following this, a panel of functional angiogenesis experiments were performed to demonstrate that the recombinant ELTD1 was biologically active. These consisted of the hanging drop endothelial spheroid assay, the fibrin gel bead assay, the endothelial tube formation assay proliferation, cell migration assay and adhesion assays.

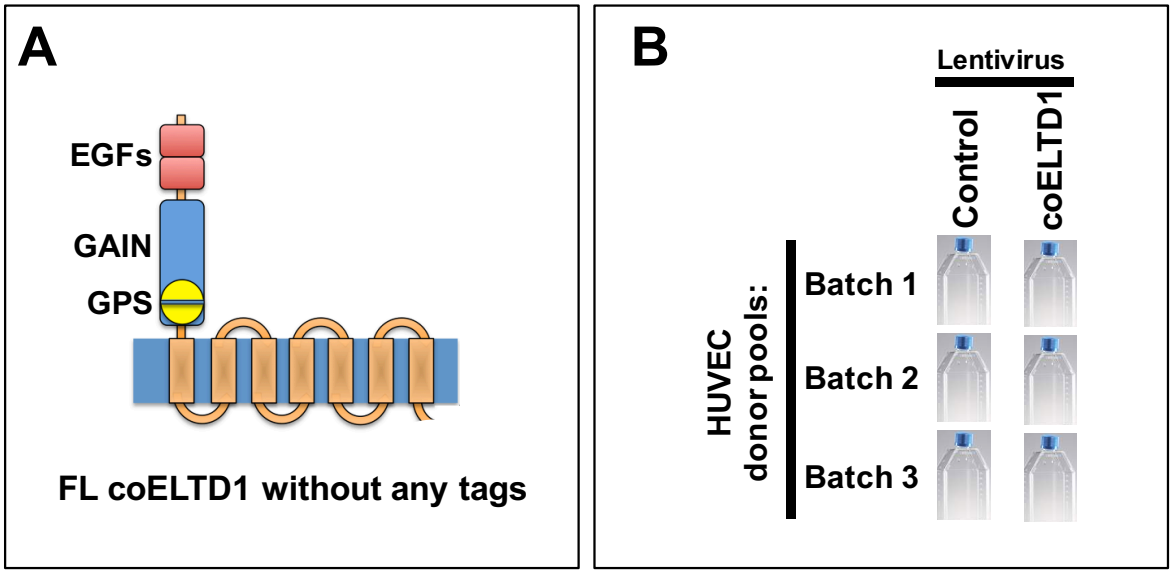


Figure 6.5: ELTD1 overexpression model in HUVECS. A) Graphical representation of FL codon optimised ELTD1 (without tags) used in the overexpression experiments. **B)** Lentivirus transduction strategy for HUVECS: 3 different batches of HUVECS (each from a different pool of donors) were transduced with either control or FL coELTD1 (labelled as coELTD1 in the figure).

6.4 Proof of stable coELTD1 overexpression in HUVECS

Following successful lentiviral transduction, each HUVEC batch was firstly harvested and tested for proof of FL coELTD1 overexpression. In brief, mRNA expression was tested using qPCR (primers in Methods Chapter), total protein expression with Western blotting (Sigma Aldrich HPA025229; now discontinued) and surface protein expression with FACS (N-terminal targeting anti-ELTD1 monoclonal antibody 'clone 184.11'; generated by the laboratory of Professor Alison Banham, University of Oxford).

Results revealed successful FL coELTD1 overexpression. RNA expression analysis using qPCR revealed the presence of *coELTD1* mRNA in the coELTD1 transduced HUVECS (Figure 6.6 A). Interestingly, wild type *ELTD1* mRNA expression was similar for both control and coELTD1 transduced samples (Figure 6.6 A). This suggested that ELTD1 protein overexpression does not exert negative feedback onto wild type *ELTD1* expression. Western blot analysis revealed massive ELTD1 protein overexpression in the FL coELTD1 overexpression samples as well as normal levels of ELTD1 expression in the control samples (Figure 6.6 B). ELTD1's surface expression was also profiled with FACS revealing that FL coELTD1 overexpression samples all had much higher surface ELTD1 expression compared to the control samples (Figure 6.6 C). This surface overexpression remained constant and unchanged throughout all subsequent HUVEC passages used in the subsequent functional experiments (cell passage level 2-5, data not shown). Following successful overexpression validation, a panel of functional angiogenesis experiments were then performed.

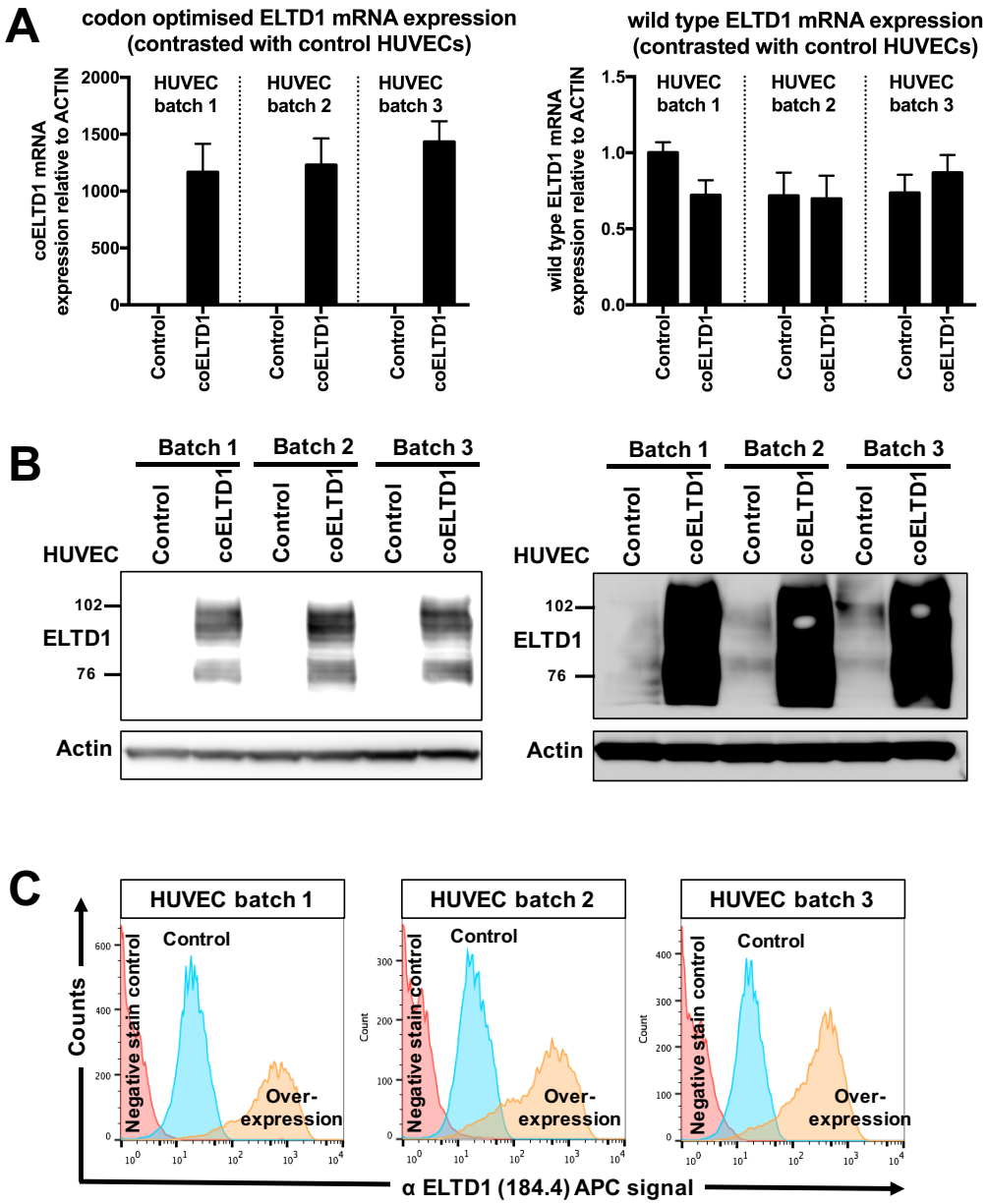


Figure 6.6: Proof of successful stable overexpression of codon optimised FL ELTD1 in HUVECs. A) qPCR results showing FL coELTD1 mRNA expression in HUVEC batches transduced with FL coELTD1 lentivirus (coELTD1 group). No FL *coELTD1* mRNA was detected in control transduced HUVECS. Both control and FL coELTD1 transduced HUVECs were found to have similar levels of wild type *ELTD1* mRNA, suggesting that ELTD1 does not negatively regulate its expression. **B)** Western blot results reveal massive ELTD1 protein overexpression in the FL

coELTD1 overexpression group (coELTD1 group). The overexposed blot is presented to show the presence of ELTD1 expression in the control group. **C)** FACS results show that FL coELTD1 expressing samples all have a much higher cell surface level of ELTD1 compared to control HUVEC batches. Control HUVECS exposed only to the secondary APC antibody were used as a negative stain control (anti-ELTD1 monoclonal antibody 'clone 184.11' used, generated by the laboratory of Professor Alison Banham, University of Oxford).

6.4.1 ELTD1 overexpression increases sprout size and number

The first functional angiogenesis related assay performed was the hanging-drop sprouting spheroid assay. This assay reproduces sprouting angiogenic activity in endothelial cells and runs over 48 hours. Sprouting angiogenesis refers to the formation of new blood vessel developing from an existing vessel through the development of an outgrowth or sprout of endothelial cells (Carmeliet and Jain, 2011a). The hanging-drop sprouting spheroid assay measures sprouting activity with endothelial cells forming sprouts from a central three-dimensional endothelial spheroid. During sprouting angiogenesis, the leading edge of endothelial cells assume a characteristic phenotype termed the tip cell phenotype whilst the trailing column of endothelial cells (which eventually form the vessel lumen) assume a different phenotype termed the stalk cell phenotype (Goel et al., 2011). The tip cell phenotype is induced through VEGF signalling and is highly competitive as each sprout can only have one leading edge endothelial cell expressing the tip cell phenotype. Tip cells actively induce Notch signalling in the column of endothelial cells behind them thus inducing the stalk cell phenotype (Carmeliet and Jain, 2011b). This is discussed in further detail in the chapter's discussion.

In brief, the hanging-drop sprouting spheroid assay entails embedding HUVEC spheroids generated by the hanging drop method (Kelm et al., 2003) into matrigel (a basement membrane secreted by Engelbreth-Holm-Swarm mouse sarcoma cells), with regular imaging over 48 hours (see Method Chapter for further details). As images had differing background intensities, scripting an accurate computational method to extract spheroid perimeter information from each image proved very challenging. To counter this, a semi-manual but highly accurate method was devised to accurately trace and analyse all images. This comprised a self-made stylus (built using an empty pen, tinfoil and moist cotton wool), which enabled highly accurate tracing of spheroid outlines using a laptop's trackpad (Figure 6.7). Traced images were then analysed using a script in FIJI with total area and perimeter then being graphed and analysed.

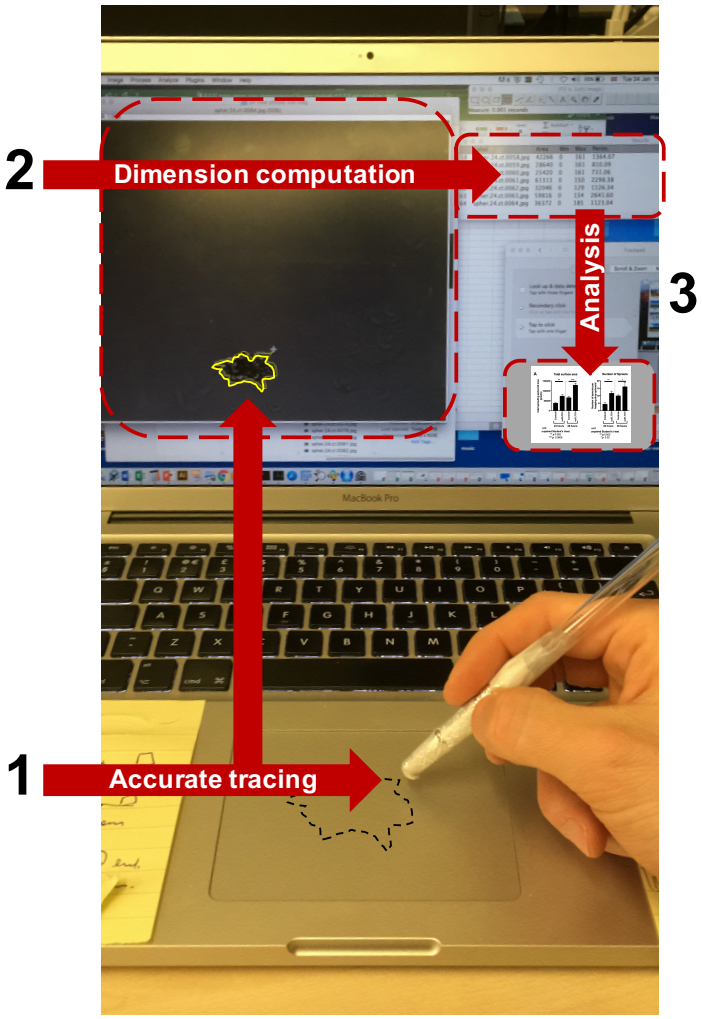


Figure 6.7: Semi-manual but highly accurate method for quantifying the Hanging drop endothelial spheroid assay. 1) A self-made stylus was assembled which enabled highly accurate individual tracing of each spheroid and its sprouts. **2)** The traced outline was recorded onto of the original image using the FIJI image analysis software. **3)** Outline dimensions were then extracted for analysis.

Results from n=3 biological replicate experiments revealed that coELTD1 overexpression significantly increased both the total surface area of the sprouting spheroids (Figure 6.8 A) and increased the number of sprouts per endothelial spheroid at both 24 and 48 hours (Figure 6.8 B). The observed increase in size of coELTD1 overexpressing sprouting spheroids appeared to be due to the increased number of sprouts, rather than an increase in the size of central spheroid ball. Representative images showing these findings are presented in (Figure 6.8 C).

These results suggest that ELTD1 overexpression induces a sprouting tip cell phenotype in the hanging-drop sprouting spheroid assay. This complements the previous findings that ELTD1 silencing inhibits sprout formation (Masiero et al., 2013). Taken together, these findings reveal that ELTD1 is an important player in the initiation of sprouting angiogenesis.

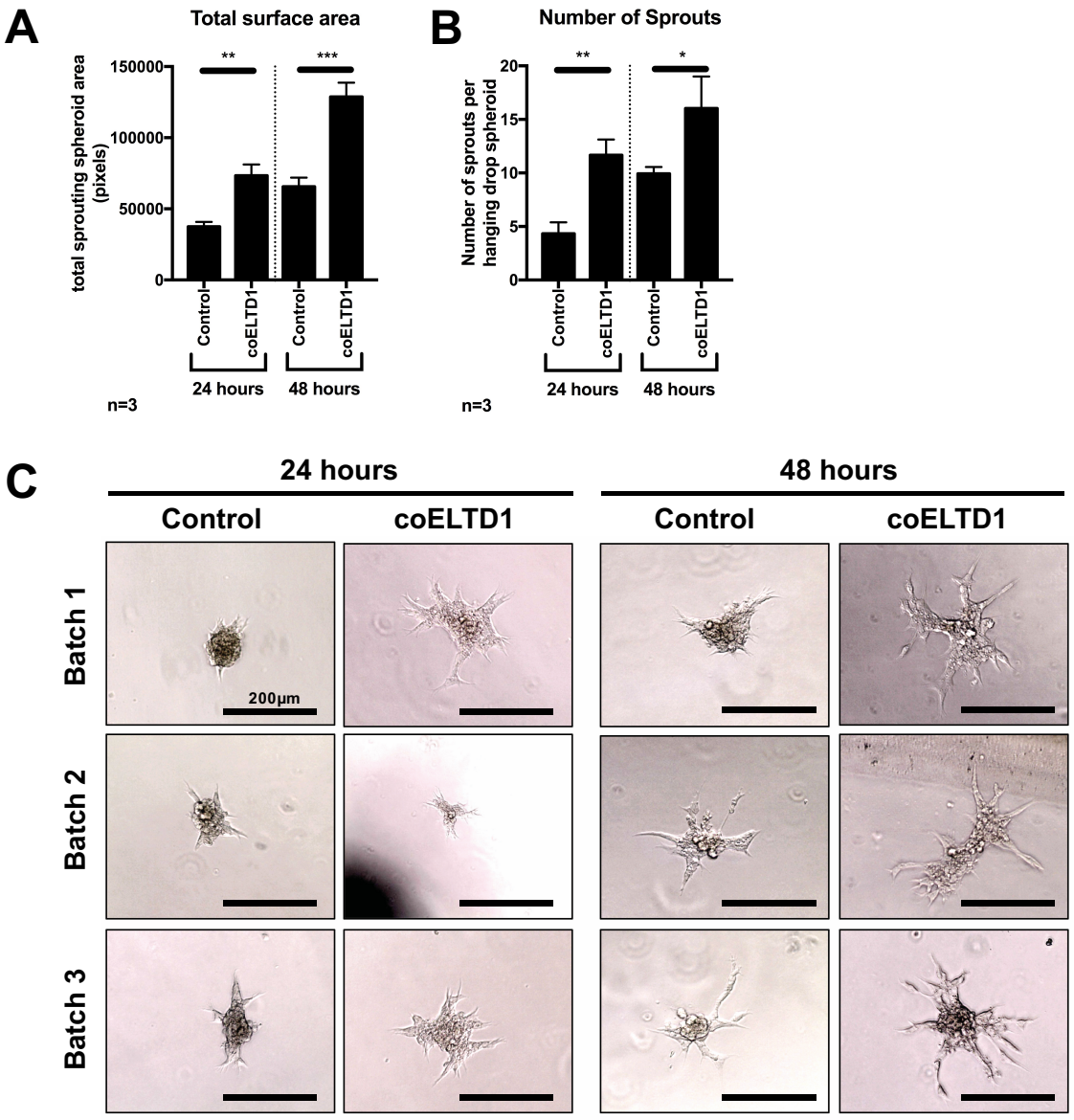


Figure 6.8: Hanging drop endothelial sprouting spheroid assay in matrigel: ELTD1 overexpression induces a tip cell phenotype. A) coELTD1 overexpression increases total spheroid surface area at 24 hours (unpaired Students *t* test $p = 0.002$;) and 48 hours (unpaired Student's *t* test $p = 0.0008$). **B)** coELTD1 overexpression also increases the number of sprouts at 24 (unpaired Students *t* test; $p = 0.002$) and 48 hours (unpaired Students *t* test $p = 0.03$). **C)** Representative images from each HUVEC batch showing the increase in total surface area and total number of sprouts in coELTD1 overexpressing HUVECS.

6.4.2 ELTD1 overexpression affects vessel stalk formation by limiting anastomoses between vessels

The next functional assay performed was the fibrin gel bead assay. This longer assay lasts for up to three weeks and reproduces the key stages of sprouting angiogenesis (Nakatsu et al., 2007). Within the context of the fibrin gel bead assay, this consists of VEGF driven sprouting which is then followed by Notch signalling driven tubulogenesis (the formation of vessels with patent lumens) and anastomoses between nearby vessels (Benedito et al., 2009, Nakatsu and Hughes, 2008).

In brief, the fibrin gel bead assay entails coating HUVECS onto cytodex beads followed by embedding the HUVEC-bead complexes in a fibrin gel. Fibroblasts are then plated on top of the gel, providing nourishment to the HUVECS and photographs are taken at set intervals (see Methods Chapter for further details) (Nakatsu et al., 2007).

Results from n=3 biological replicate experiments revealed that at 3 weeks (the conclusion of the assay), coELTD1 overexpressing HUVECS had significantly fewer anastomotic branch points between neighbouring vessels (Figure 6.9A). Interestingly, both control and overexpression groups appeared to have similar-looking patent vessel lumens. Representative images from the experiment are displayed in Figure 6.9B.

These results suggested that coELTD1 overexpression incompletely inhibited inter-vessel branching/anastomoses, a process which is part of tubulogenesis and is regulated by Notch signalling. Referring back to the previous chapter's findings that ELTD1 silencing induces DLL4 protein expression whilst repressing *JAG1* and *HES2* mRNA expression, the current results hint that coELTD1 overexpression interacts with Notch signalling in a manner which still allows for partial tubulogenesis and stalk formation with an associated decrease in vessel branching. Taken together with the previous sprouting results, ELTD1 overexpression induces a tip cell phenotype whilst negatively affecting the stalk phenotype. These results suggest the possibility that levels of constitutive ELTD1 expression in endothelial cells may be modulated during different stages of sprouting angiogenesis (i.e. highest in tip cells during sprouting angiogenesis and lowered but still expressed in stalk cells during tubulogenesis). This forms the basis of future experiments.

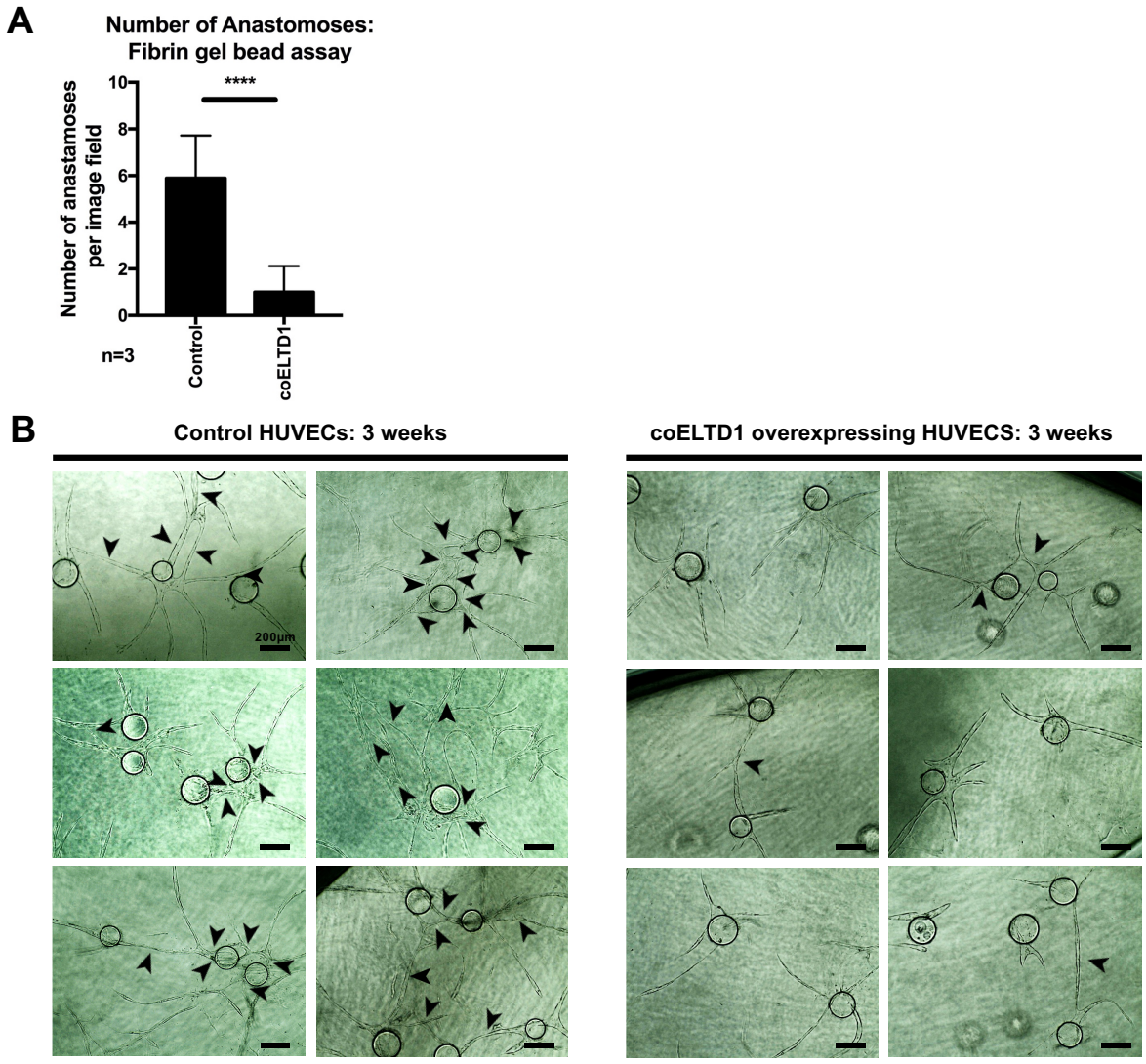


Figure 6.9: Fibrin gel bead assay: ELTD1 overexpression lowers the number of vascular anastomoses/branches between adjacent vessels. A) Results from the fibrin gel bead assay reveal that at 3 weeks (the conclusion of the assay), coELTD1 overexpression decreases the number of anastomoses between vessels (unpaired Student's *t* test; $p < 0.00001$). **B)** Representative images from the control HUVEC group show adequate lumen formation and anastomoses with neighbouring lumens (arrowheads point to anastomotic branches). In the coELTD1 overexpressing group, lumen formation appears to be similar to the control group,

however there are fewer anastomoses with neighbouring lumens. This suggests that coELTD1 overexpression inhibits vessel branching, a process regulated by Notch signalling.

6.4.3 ELTD1 overexpression increases capillary tube formation

The next assay performed was the endothelial tube formation assay. This assay, lasting 24 hours, reproduces sprouting angiogenesis and the formation of capillary-like structures (Ponce, 2009). In brief, HUVECS were plated onto matrigel and then imaged every hour for 24 hours. Tube formation was analysed by counting the number of complete polygons in each image field. Polygons consisted of endothelial tubes (see Methods chapter for further details).

Results from n=3 biological replicate experiments reveal that when compared to the control, coELTD1 overexpression increased early tube formation and significantly increased the overall number of endothelial tube polygons present (Figure 6.10A). This effect was visible from 4 hours onwards and lasted until the end of assay 24 hours later. Figure 6.10 B displays representative images from each tested HUVEC batch showing the increase in tube formation in the coELTD1 group.

Following the completion of the assay, HUVECS were harvested from the matrigel and analysed for ELTD1 surface expression using FACS. This was performed to test whether coELTD1 transduced HUVECS change the level of ELTD1 surface expression following angiogenic activity. Unlike the sprouting spheroid or fibrin gel assays, the tube formation assay allowed for post-assay harvesting and FACS

analysis because cells were plated onto matrigel rather than embedded within it. Results revealed no change in the level and pattern of ELTD1 expression in the overexpression and control groups following interaction with matrigel and capillary sprouting (Figure 6.10 C).

These results reveal that coELTD1 overexpression induces increase capillary-like tube formation. As the tube formation assay is another method of assessing sprouting angiogenesis, these results further complement the finding that ELTD1 overexpression induces a sprouting tip cell phenotype.

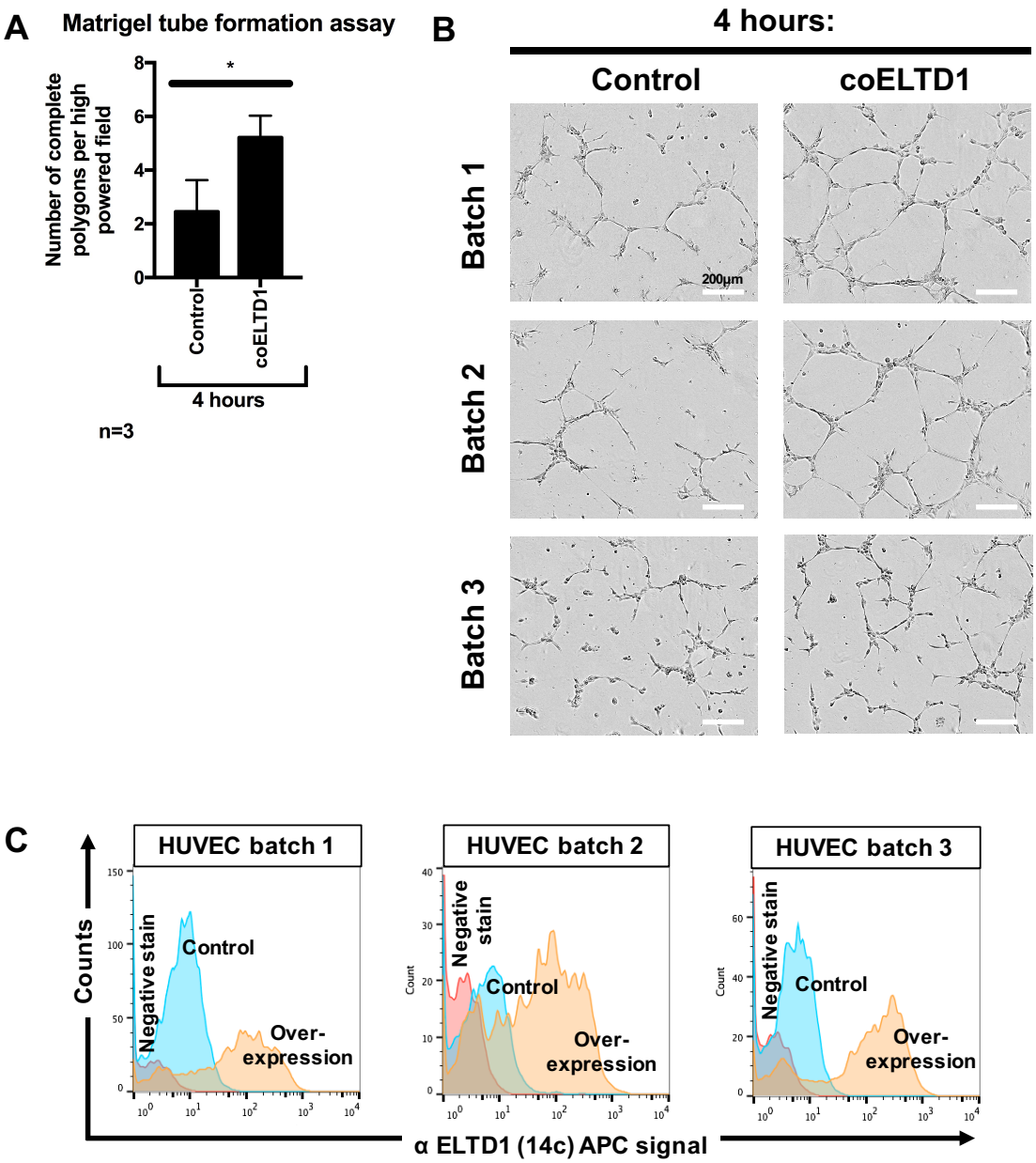


Figure 6.10: Tube formation assay: ELTD1 overexpression increases tube formation. A) ELTD1 overexpression (coELTD1) increases the number of capillary-like tubes by 4 hours in the tube formation assay (unpaired Student's *t* test; p = 0.03). This effect lasts until the assay ends. **B)** Representative tube formation images from each of HUVEC batch assayed. **C)** To test whether surface expression of ELTD1 was affected by the assay, all cells were harvested and analysed by FACS

after the tube formation assay was completed. This revealed no change in the high level surface expression of ELTD1 in the overexpression samples.

6.4.4 ELTD1 overexpression decreases HUVEC proliferation

The next assay performed was the proliferation assay. In brief, this was performed by plating HUVECS at low confluence into multiple multi-well plates. Every day, a plate was photographed and its HUVECS harvested and counted. This continued until confluence was achieved (see Methods chapter for further details).

Data from n=4 biological replicate experiments revealed that coELTD1 overexpression significantly reduced HUVEC proliferation with control HUVECS reaching confluence within 48 hours and coELTD1 overexpressing HUVECS reaching confluence within 72 hours (Figure 6.11 A). Furthermore, at 24 hours, there were 40% fewer coELTD1 overexpressing HUVECS than control HUVECS (unpaired Student's *t* test; $p = 0.01$). Similarly, at 48 hours, there were 28% fewer HUVECS in the ELTD1 overexpression wells (unpaired Student's *t* test; $p = 0.0003$). This difference was unlikely to be due to an increase in cell death as the number of floating dead cells in control and overexpression cells was noted to be similar. Additionally, these dead cells were removed prior to harvesting. Representative images showing the reduction in cell number following coELTD1 overexpression are presented in Figure 6.11 B.

One of the characteristics of the endothelial tip cell phenotype is a decreased level of proliferation when compared to endothelial cells expressing the stalk cell

phenotype (Gerhardt et al., 2003). Thus, the result that coELTD1 overexpression lowers endothelial cell proliferation further complements the finding that coELTD1 overexpression induces a tip cell phenotype.

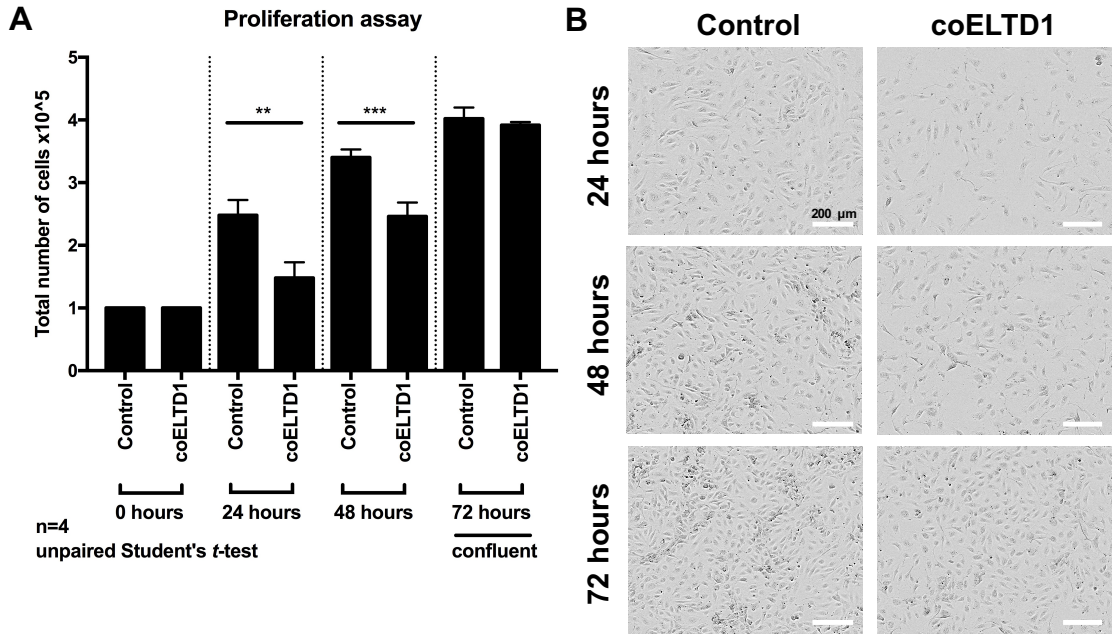


Figure 6.11: Proliferation assay: ELTD1 overexpression lowers HUVEC proliferation. A) ELTD1 overexpression lowered the rate of cell proliferation in coELTD1 overexpressing HUVECS. At 24 hours there were 40% fewer cells in the ELTD1 overexpression wells (unpaired Student's *t* test; $p = 0.01$); at 48 hours, there were 28% fewer cells (unpaired Student's *t* test; $p = 0.0003$). In this experiment, confluence occurred in the coELTD1 group by 72 hours. **B)** Representative images from a single HUVEC batch revealing that coELTD1 overexpression decreases cell proliferation (images where taken prior to harvesting and counting).

6.4.5 ELTD1 overexpression does not have an effect on endothelial cell migration

The next assay performed was the endothelial scratch assay. This assay, run over 16 hours, can be used to measure the migratory capabilities of endothelial cells. In brief, HUVECS were grown to confluence in 24 well plates and then were scratched using a mechanical device ensuring that each well received a similar sized scratch. Cells at the border of the cell-free scratch were then imaged every 30 minutes until the scratch defect had been repaired by migrating and proliferating HUVECS. The cell-free scratched areas of each group were then traced using the self-made stylus described earlier and quantified using FIJI (see Methods chapter for further details).

Results from n=9 biological replicate experiments revealed that coELTD1 overexpression did not significantly affect endothelial migration with both control and coELTD1 overexpressing HUVECS having a similar rate of scratch defect closure. Twelve hours was chosen as the final time point as following this, both groups closed the cell-free scratch gap. Representative images from each HUVEC batch revealing similar HUVEC migration for control and coELTD1 HUVECS are presented in Figure 6.12 B.

The finding that coELTD1 overexpression does not influence endothelial migration is puzzling as one would assume that the tip cell phenotype induced by coELTD1 overexpression would increase HUVEC invasiveness and migration. However, as the scratch assay measures scratch wound closure and relies on both HUVEC migration and proliferation for closure, it can be argued that this assay was not

wholly appropriate following the finding that coELTD1 decreases HUVEC proliferation. In this case, an increase in coELTD1 HUVEC migration would be countered by faster cell proliferation in the control group. A more accurate endothelial migration assay measuring migration between chambers of a Boyden Chamber is planned for the future (Merck: ECM210).

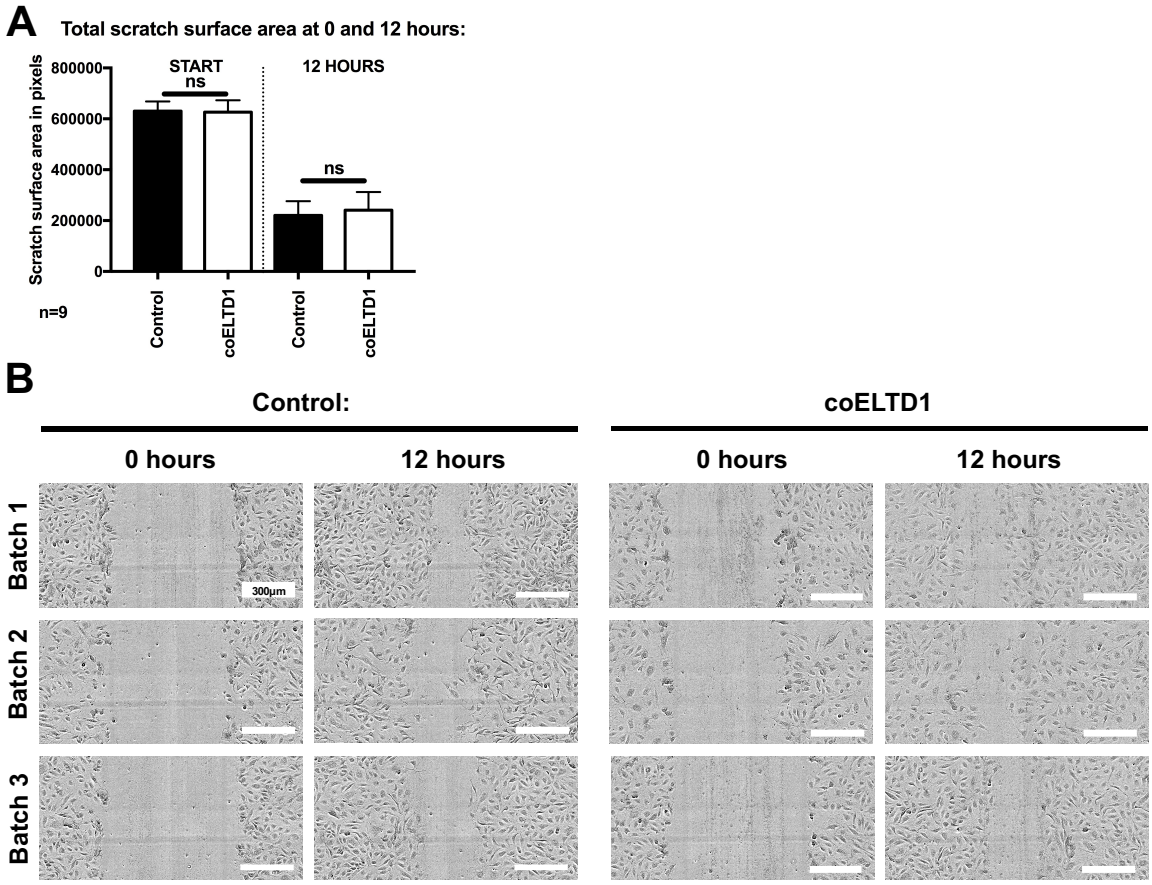


Figure 6.12: Endothelial migration assay: ELTD1 overexpression has no effect on endothelial migration. A) coELTD1 overexpression in HUVECs had no effect on wound healing (Comparison of the cell-free scratched area at start of assay: unpaired Student's *t* test $p = 0.8$; Comparison of the cell-free scratched area at 12 hours: unpaired Students *t* test at end: $p = 0.4$). 12 hours was chosen as the final

time point in the assay as after this both control and coELTD1 overexpression HUVECS closed the scratch gap. **B)** Representative images from all HUVEC batches reveal no difference in wound healing.

6.4.6 ELTD1 overexpression has no effect on HUVEC adhesion

The final functional assays performed were two different adhesion assays: one comprising ECM components and the other matrigel. Adhesion GPCRS are so named because they contain extracellular domains which are associated with cell-cell or cell-ECM adhesion (Langenhan et al., 2013). Although ELTD1 remains an orphan receptor without any known ligand, ELTD1 silencing was shown to decrease adhesion to matrigel (Masiero et al., 2013). These assays tested whether ELTD1 overexpression had the opposite effect.

The first assay performed was the MilliCoat assay (Merck: ECM205). This was used to investigate whether coELTD1 overexpression affected endothelial adhesion to a number of angiogenesis-associated extracellular components. In brief, control and coELTD1 overexpressing HUVECS were seeded into wells coated with an angiogenesis-associated matrix component. After 1 hour, all wells were washed and cells were fixed and stained with crystal violet. Adhesion was measured by measuring the absorbance (560nm) of remaining adherent cells (see Methods chapter for further details).

Results from n=3 biological replicate experiments revealed that coELTD1 overexpression had no significant effect on the adhesion of endothelial cells to any

of the five main angiogenesis-associated matrix components tested: Collagen I (Figure 6.14 A), collagen IV (Figure 6.14 B), laminin (Figure 6.14 C), vitronectin (Figure 6.14 D) and fibronectin (Figure 6.14 E).

For completeness, an alternative adhesion was also performed as this assay had previously been performed on ELTD1 silenced HUVECS and demonstrated a functional effect (Masiero et al., 2013). In brief, the matrigel adhesion assay entailed seeding HUVECS onto matrigel in 96 well plates for 1 hour followed by multiple washes. Photographs were taken of each well and cells were counted. In order to do this more efficiently, I wrote an FIJI script to count and quantify the number of cells in each image field (script is included in the Appendix; further details available in the Methods chapter).

Results from n=3 biological replicate experiments revealed that ELTD1 overexpression did not significantly affect HUVEC adherence to matrigel (Figure 6.14 A). Representative images revealing from the experiment are presented in (Figure 6.14 B).

In summary, ELTD1 overexpression does not affect adhesion to angiogenesis associated collagen I, collagen IV, laminin, vitronectin, fibronectin or to matrigel. This is not so unsurprising when one considers that coELTD1 overexpression induces a tip cell phenotype.

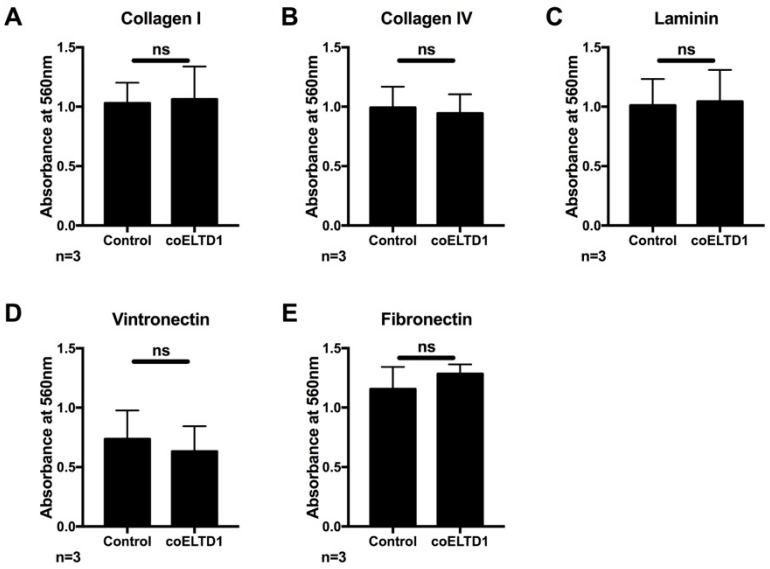


Figure 6.13: MilliCoat extracellular matrix (ECM) adhesion assay: ELTD1 overexpression does not affect adherence to angiogenesis-associated ECM components. A) coELTD1 overexpression does not affect adhesion to Collagen I (unpaired Student's *t* test; $p = 0.9$). **B)** coELTD1 overexpression does not affect adhesion to Collagen IV (unpaired Student's *t* test; $p = 0.7$). **C)** coELTD1 overexpression does not affect adhesion to Laminin (unpaired Student's *t* test; $p = 0.9$). **D)** coELTD1 overexpression does not affect adhesion to Vitronectin (unpaired Student's *t* test; $p = 0.6$). **E)** coELTD1 overexpression does not affect adhesion to Fibronectin (unpaired Student's *t* test; $p = 0.3$). (Abbreviation: ns=non-significant)

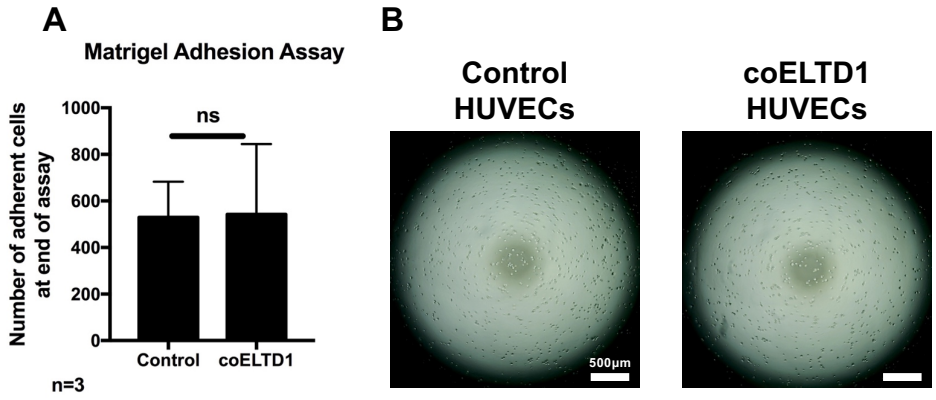


Figure 6.14: Matrigel adhesion assay: ELTD1 overexpression does affect adhesion to matrigel. A) Bar graph showing that coELTD1 overexpression does not affect HUVEC adhesion to matrigel when compared to control (unpaired Student's *t* test; $p = 1$). **B)** Representative image of the experiment showing no difference in adhesion. (Abbreviation: ns=non-significant)

6.5 Microarray of stable ELTD1 overexpression in HUVEC cells

During the design of the HUVEC ELTD1 overexpression experiments, it was intended that transcriptional profiling would be performed to determine the genetic basis for observed functional changes. Unfortunately, the initiation of my overexpression experiments coincided with the discontinuation of Illumina microarray chips worldwide in favour of their RNA-Seq products. Due to timing and financial constraints, it was decided not to pursue RNA-Seq. Additionally, it was decided not to use the Affymetrix microarray platform as my previous ELTD1 microarrays had all been performed using the Illumina platform and there was the risk that results would not be comparable.

I had previously shared my cloned FL coELTD1 containing lentiviral vector with Dr. Helen Sheldon (the senior post-doctoral scientist in our laboratory) who had used the vector to make her own limited supply of ELTD1 overexpressing HUVECS for exosome experiments. At the time of the announcement of final orders for Illumina microarray chips, I still had not successfully transduced HUVECS on the large scale required for the functional angiogenesis experiments. Therefore, Dr. Sheldon kindly agreed that we would send her coFL overexpressing HUVEC mRNA for microarray analysis instead of waiting for my overexpressing HUVECS to be ready and risk missing the final submission deadline.

In brief, Dr. Sheldon had transduced my FL coELTD1 lentiviral vector as well as the packaging vector psPAX2 and the envelope vector pMD2.G into HEK293T cells using Lipofectamine 2000. A pLenti6/V5-DEST vector with no insert was used as the empty vector control. The virus rich supernatant from these cells was then used to transduce two batches of HUVECS from separate donors with virus infected HUVECS selected with blasticidin for 1 week prior to harvesting for the microarray. ELTD1 overexpression was confirmed using qPCR and Western blot and then sent off for microarray reading. A complicating factor here was the lack of three biological replicates as only two different HUVEC batches had been transduced by Dr. Sheldon (HUVEC batch 4 and batch 5). This limited the statistical strength of any differential gene comparisons. Following a discussion with the microarray facility regarding this concern, we were advised to submit two technical replicates for each of the two biological replicates to be tested (this remains a limitation of this work). I then analysed the raw microarray output, following a similar algorithm as has been previously presented earlier in this chapter and in the previous chapter (all my

microarray analysis programming scripts in “R” are included in the Appendix). Finally, in order to link back results to the functional assays, it was decided that all microarray results would be tested and validated using qPCR on mRNA harvested from my ELTD1 overexpressing HUVECS which had undergone functional angiogenesis experiments.

qPCR and Western blotting were performed by Dr. Sheldon on her HUVECS transduced by my FL coELTD1 lentivirus. These revealed that coELTD1 lentiviral transduction was successful at both the mRNA (Figure 6.15 A) and protein (Figure 6.15 B) levels. When compared to the protein expression of my FL coELTD1 HUVEC transduction experiment (Figure 6.6 B), Dr. Sheldon’s FL coELTD1 overexpressing HUVECS appeared to have higher coELTD1 mRNA levels but slightly lower ELTD1 protein levels.

For differential gene expression, the following comparison was calculated: FL coELTD1 overexpression compared to control (empty vector). Differentially expressed genes were deemed statistically significant if they fulfilled the standard microarray significance criteria: i) an adjusted p value < 0.05; and ii) a fold change of > 2 < -2. Volcano plots depicting differential gene expression are presented for FL coELTD1 (Figure 6.16 A). Because of the issue of there being only 2 biological replicates, only a few statistically significant differential gene expression changes were found. Additionally, the microarray was unable to detect overexpressed coELTD1 due to it only containing probes for wild type ELTD1. The most upregulated gene was *D4S234E* which has been associated with neuronal vesicle

trafficking (Muthusamy et al., 2015), whilst the most downregulated gene was *DHRS9* which has been associated with the conversion of retinol to retinal (Hu et al., 2016). A heatmap was then generated displaying the expression level z-score of all significant differentially expressed genes (Figure 6.16 B).

Significant differentially expressed genes were then inputted in multiple curated pathway analysis databases (KEGG, Reactome, Wikipathways and BioCarta). Due to the small number of significant differentially expressed genes, results revealed no significant association with any pathway.

A Venn diagram comparison was then performed to determine how many significant differentially expressed genes were common to all ELTD1 microarray experiments performed: i) transient FL and CTF coELTD1 overexpression in HEK293T cells; ii) ELTD1 silencing in HUVEC cells; iii) stable FL coELTD1 overexpression in HUVEC cells (Figure 6.17). Results revealed that no genes were common to all microarrays. Only 1 gene, *CHRNA1* was shared between ELTD1 silenced and FL coELTD1 overexpressing HUVECS. *CHRNA1* encodes the alpha subunit of the acetylcholine receptor and was upregulated in both ELTD1 silencing and FL coELTD1 overexpression arrays.

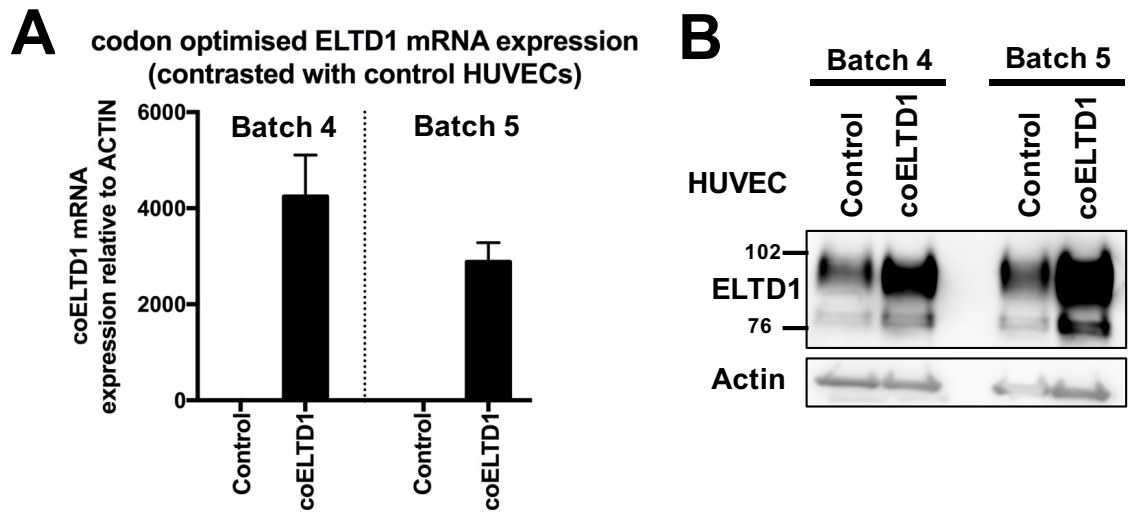


Figure 6.15: Proof of FL coELTD1 overexpression from second FL coELTD1 lentiviral HUVEC transduction performed for microarray. **A)** qPCR results showing FL coELTD1 mRNA expression in HUVEC batches transduced with FL coELTD1 lentivirus (coELTD1 group). **B)** Western blot revealing increased ELTD1 protein expression in the FL coELTD1 overexpression group (coELTD1 group). The qPCR and Western blot for ELTD1 expression were performed by Dr. Helen Sheldon.

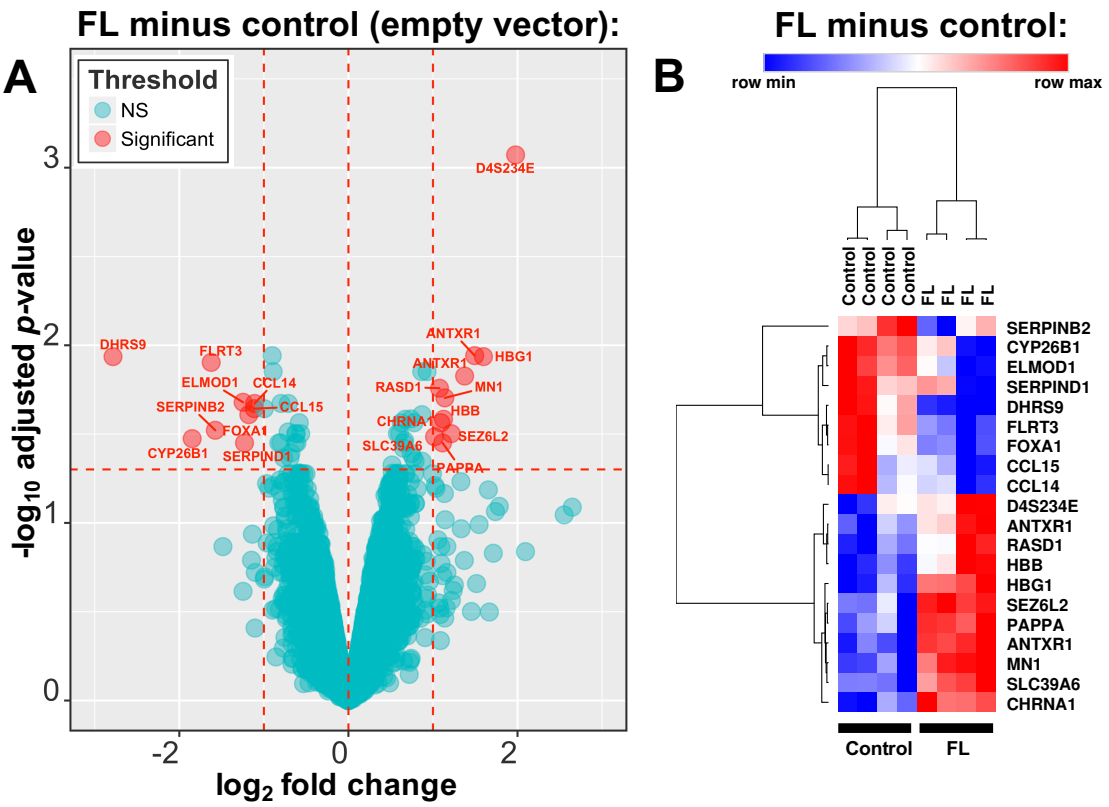


Figure 6.16: FL coELTD1 stable overexpression in HUVECS: microarray results. A) Volcano plot depicting differentially expressed genes following FL coELTD stable overexpression in HUVEC cells. Significant differentially expressed genes are presented in red. The threshold for statistical significance was set as a *p* value of < 0.05 and log2 fold change > 1 and < -1. The heading "FL minus control" refers to the direction of the linear model comparison. **B)** Heatmap depicting significant differentially expressed genes following FL coELTD stable overexpression in HUVEC cells. The row and column clustering was performing using Euclidean distance hierarchical clustering. The intensity colouring (low=blue; high=red) represents the z-score for each gene (the number of standard deviations by which a gene's expression in an individual sample (as determined by microarray) differs from the mean expression for that gene across all samples). The microarray

did not detect overexpressed FL *coELTD1* due to microarray probes for *ELTD1* being against wild type *ELTD1* only. (Abbreviation: NS=non-significant)

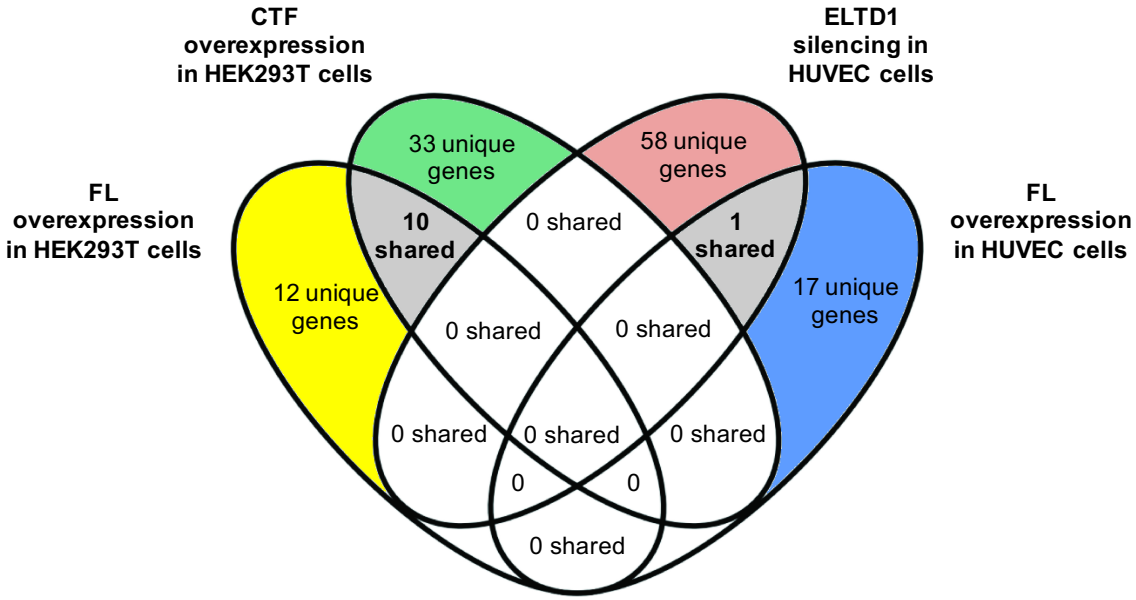


Figure 6.17: Venn diagram comparison between the microarray results from transient FL and CTF coELTD1 overexpression in HEK293T cells, ELTD1 silencing in HUVECS and FL coELTD1 stable overexpression in HUVECS. In the figure, grey shading indicates shared genes. Although 10 genes were shared between FL and CTF coELTD1 overexpression in HEK293T cells, none where shared between FL coELTD1 overexpression in HEK293T and HUVEC cells. Additionally, only one gene (CHRNA1) was shared between ELTD1 silenced HUVECS and FL coELTD1 overexpressing HUVECS, and was upregulated in both.

6.6 Validation of significant differentially expressed genes in stable ELTD1 overexpressing HUVECS

First, *CHRNA1,* the only gene shared between the HUVEC ELTD1 silencing and overexpression microarrays was tested. In both microarrays, CHRNA1 was upregulated. In brief, qPCR was used to test for CHRNA mRNA in both ELTD1 silenced and overexpressing HUVECS. Results revealed significant CHRNA1 up-regulation in FL coELTD1 overexpressing HUVECS (Figure 6.18 A) but no significant change in ELTD1 silenced HUVECS (Figure 6.18 B). This result will be discussed further in discussion

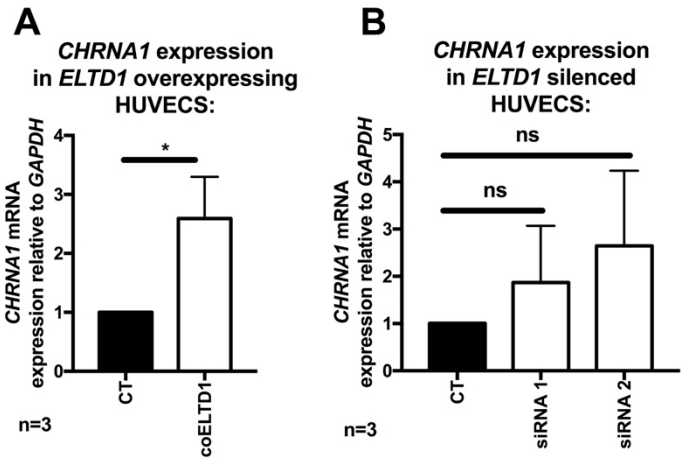


Figure 6.18: qPCR validation of CHRNA1 in FL coELTD1 overexpressing HUVECS and ELTD1 silenced HUVECS. A) *CHRNA* mRNA expression was significantly upregulated following ELTD1 overexpression in HUVECS (unpaired Student's *t* test; $p = 0.02$). **B)** *CHRNA* mRNA expression was not significantly affected by ELTD1 silencing in HUVECS (unpaired Student's *t* test: siRNA 1 compared to control $p = 0.1$; siRNA 1 compared to control $p = 0.3$). (Abbreviations: CT=control)

Following this, multiple sets of genes were tested using qPCR on the FL coELTD1 overexpressing HUVECS which had undergone functional angiogenesis experiments. The first set comprised differentially expressed genes from the ELTD1 overexpression HUVEC microarray. The aim of this experiment was to validate the results of the microarray. The second set of genes comprised significant differentially expressed genes from the FL and CTF ELTD1 overexpression microarray performed in HEK293Ts. This was performed ot determine whether there was any overlap between ELTD1 overexpression in HEK293T and HUVECS. The final set consisted of significant differentially expressed genes from the ELTD1 silencing microarray performed in HUVECS. Here, the aim was to determine whether ELTD1 overexpression induced opposite effects in these genes.

Seventeen significant differentially expressed genes from the microarray performed on Dr. Sheldon's FL coELTD1 overexpressing HUVECS were then tested on mRNA harvested (HUVEC passage level 3) from the FL coELTD1 overexpressing HUVECS, which had undergone functional angiogenesis experiments.

qPCR results reveal that of the 8 tested genes which had been upregulated in the FL coELTD1 HUVEC overexpression microarray, only *ANTXR1* (Figure 6.19 A), *SLC39A6* and *HBB* were significantly upregulated when tested using qPCR on FL coELTD1 overexpressing HUVECS (Figure 6.19 A). The remainder of upregulated microarray genes where found to be non-significantly altered (Figure 6.19 A). Of the 9 tested genes which had been downregulated in the microarray, only *CCL15,*

ELMOD1, and *CYP26B1* were significantly altered with the remainder having non-significant changes (Figure 6.19 B). Interestingly, although *ELMOD1* was significantly downregulated in the microarray, it was significantly upregulated when tested with qPCR. In summary, these results validate some of the microarray results obtained from expression profiling of Dr. Sheldon's FL coELTD1 overexpressing HUVECS, and will be discussed alongside all other significant validated genes in more detail in the discussion.

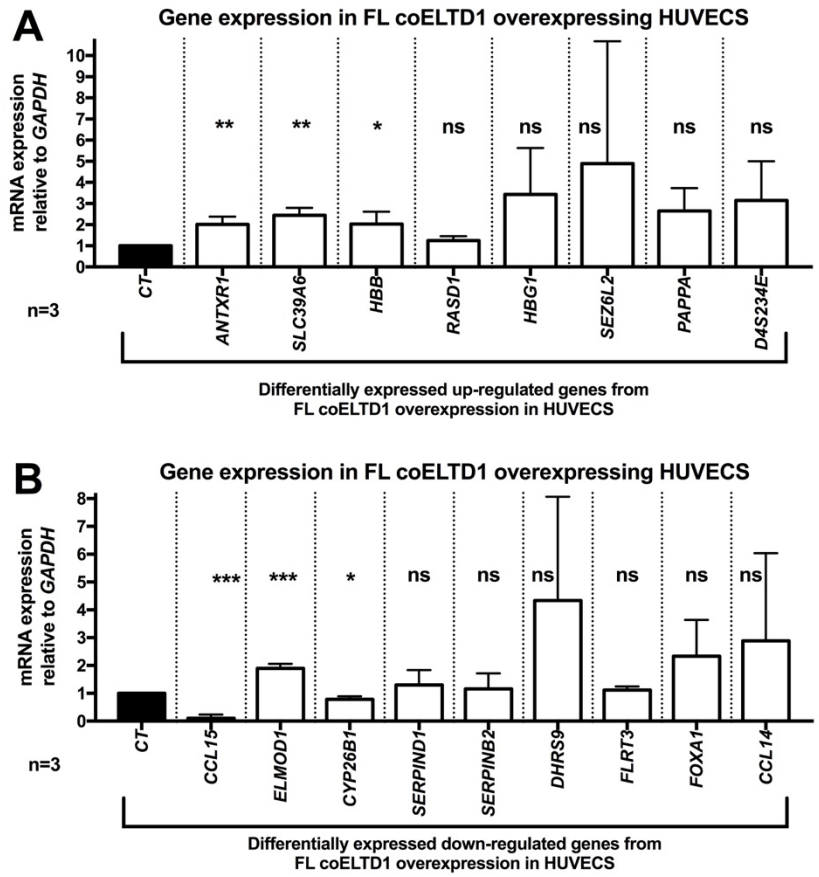


Figure 6.19: qPCR validation of differentially expressed upregulated genes from the stable FL coELTD1 overexpression microarray, tested on HUVECS stably expressing FL coELTD1. A) FL coELTD1 overexpression significantly induced *ANTXR1* (p = 0.009), *SLC39A6* (p = 0.002), and *HBB* (p = 0.04) mRNA expression. FL coELTD1 overexpression did not significantly affect *RASD1* (p = 0.01), *HBG1* (p = 0.1), *SEZ6L2* (p = 0.3), *PAPPA* (p = 0.06), or *D4S234E* mRNA (p = 0.1) mRNA expression. **B)** FL coELTD1 overexpression significantly altered *CCL15* (p = 0.0003), *ELMOD1* (p = 0.0006) and CYP26B1 (p = 0.03) mRNA expression. FL coELTD1 overexpression did not significantly affect *SERPIND1* (p= 0.4), *SERPINB2* (p = 0.6), *CCL14* (p = 0.4), *DHRS9* (p = 0.2), *FLRT3* (p = 0.2) and *FOXA1* (p = 0.2) mRNA expression. Statistical analyses performed with unpaired Student's t test (Abbreviation: ns=non-significant).

Next, genes from the FL and CTF ELTD1 overexpression microarray in HEK293T cells were then tested on mRNA from the FL coELTD1 overexpressing HUVECS. First, 6 differentially expressed genes common to both FL or CTF ELTD1 constructs were tested with qPCR. Results revealed that only *HSPA6* and *RYR1* were significantly upregulated in FL coELTD1 overexpressing HUVECS, with the remaining 4 genes not being significantly affected (Figure 6.20 A). Next, 4 genes unique to the HEK293T FL coELTD1 overexpression group were tested. Of these, only *SH2D3C* and *INPP5B* were significantly upregulated (Figure 6.20 B). Although *INPP5B* produced a significant change, the change (less than 0.2-fold change) was too small to be deemed physiologically relevant. The remaining genes were not significantly affected. Next, 4 genes unique to the HEK293T CTF coELTD1 overexpression group were tested. Although *HNRNPF* was significantly affected, the change was less than 0.2-fold and was deemed to be physiologically irrelevant (Figure 6.20 B). The remaining 3 genes were not significantly affected. The finding that some of the differentially expressed genes form the HEK293T ELTD1 overexpression array were significantly altered in HUVECS overexpressing ELTD1 suggests that the initial HEK293T approach was appropriate as it did identify some genes relevant to endothelial biology.

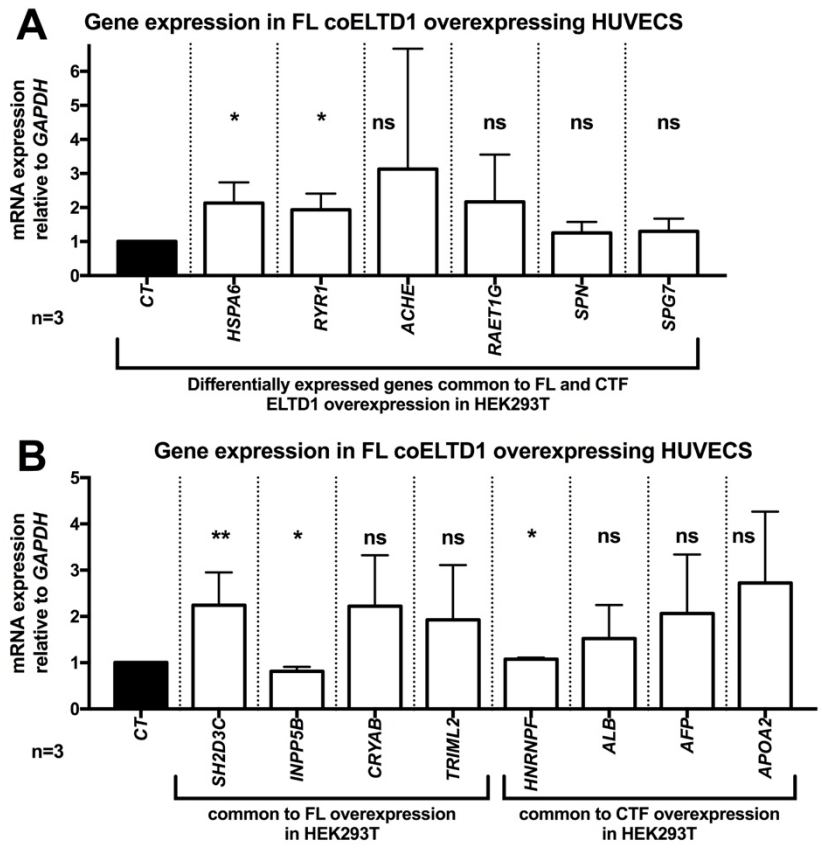


Figure 6.20: qPCR testing of significant differentially expressed genes from the FL and CTF ELTD1 overexpression HEK293T microarray, tested on FL coELTD1 overexpressing HUVECS. A) FL coELTD1 overexpression significantly induced *HSPA16* (p = 0.03) and *RYR1* (p = 0.03) mRNA expression. FL coELTD1 overexpression did not significantly affect *ACHE* (p = 0.4), *RAET1G* (p = 0.2), *SPN* (p = 0.2) or *SPG7* (p = 0.2) mRNA expression. **B)** FL coELTD1 overexpression significantly induced *SH2D3C* (p = 0.002), *INPP5B* (p = 0.03) and *HNRNPF* (p = 0.01) mRNA expression. The effect on both *INPP5B* and *HNRNPF* was deemed biologically irrelevant as the fold change was < 0.1 fold. FL coELTD1 overexpression did not significantly affect *CRYAB* (p = 0.1), *TRIML2* (p = 0.2), *ALB* (p = 0.3), *AFP* (p = 0.2) and *APOA2* (p = 0.2) mRNA expression. Statistical analyses performed with unpaired Student's t test (Abbreviation: ns=non-significant).

Lastly, 6 validated differentially expressed genes from the HUVEC ELTD1 silencing experiment (detailed in the previous chapter) were tested on mRNA from the FL coELTD1 overexpressing HUVECs, which had undergone functional angiogenesis experiments. The rationale of performing this was to determine whether these genes were inversely affected by ELTD1 overexpression.

Results revealed that the metabolic genes *SLC25A1* and the *ACLY* were not significantly affected by ELTD1 overexpression in HUVECS although both had been induced by ELTD1 silencing (Figure 6.21). Of the Notch pathway genes tested, *DLL4* and *JAG1* were significantly affected by ELTD1 overexpression with *DLL4* being repressed and *JAG1* being induced (Figure 6.21). These results are inverse to the results following ELTD1 silencing. *HES2* was not significantly altered by ELTD1 overexpression despite being suppressed by ELTD1 silencing (Figure 6.21). Lastly, *KIT* was significantly repressed following ELTD1 overexpression which was opposite to the effect of ELTD1 silencing (Figure 6.21). These results thus reveal genes shared between ELTD1 silencing and overexpression in HUVECS, despite the microarray expression profiling failing to detect any shared genes between the two experiments.

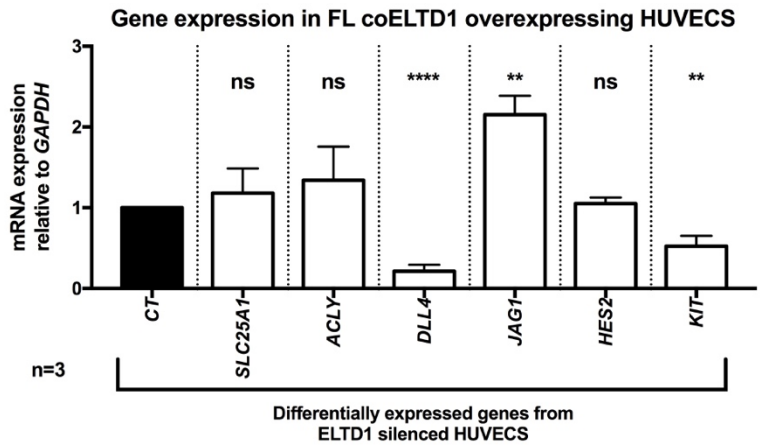


Figure 6.21: qPCR testing of 6 differentially expressed genes affected by HUVEC ELTD1 silencing, tested on stable FL coELTD1 overexpressing HUVECS. FL coELTD1 overexpression significantly affected *DLL4* ($p < 0.0001$), *JAG1* ($p = 0.001$) and *KIT* ($p = 0.003$) mRNA expression. FL coELTD1 overexpression did not alter *SLC25A1* ($p = 0.4$), *ACLY* ($p = 0.3$) and *HES2* ($p = 0.3$) mRNA expression. Statistical analyses performed with unpaired Student's t test (Abbreviation: ns=non-significant).

To investigate whether the above effect on the Notch ligands DLL4 and JAG1 translated to a change in protein expression, control and FL coELTD1 overexpressing HUVECS were assayed for cell surface DLL4 and JAG1 protein expression. In brief, HUVECS overexpressing ELTD1 were assayed with FACS for both DLL4 (DLL4 antibody: R&D Systems MAB1506) and JAG1 (JAG1 antibody: mouse monoclonal antibody (J1-65D), generated by Professor Alison Banham's laboratory, University of Oxford). Results reveal that both DLL4 (Figure 6.22) and JAG1(Figure 6.23) cell surface expression are unaffected by ELTD1

overexpression in HUVECS. Interestingly, in ELTD1 silenced HUVECS, the change noted in *DLL4* mRNA was translated into a change in surface protein expression whilst the change in *JAG1* mRNA was not (Chapter 5**:** Figure 5.9 and Figure 5.10**)**. Returning to the ELTD1 overexpressing HUVECS, it would be of interest to determine whether ELTD1 overexpression induces any changes in DLL4 or JAG1 surface expressing during any of the functional angiogenesis assays which were affected by overexpression. In summary, ELTD1 overexpression suppresses *DLL4* mRNA and induces *JAG1 mRNA* but has no effect on protein expression.

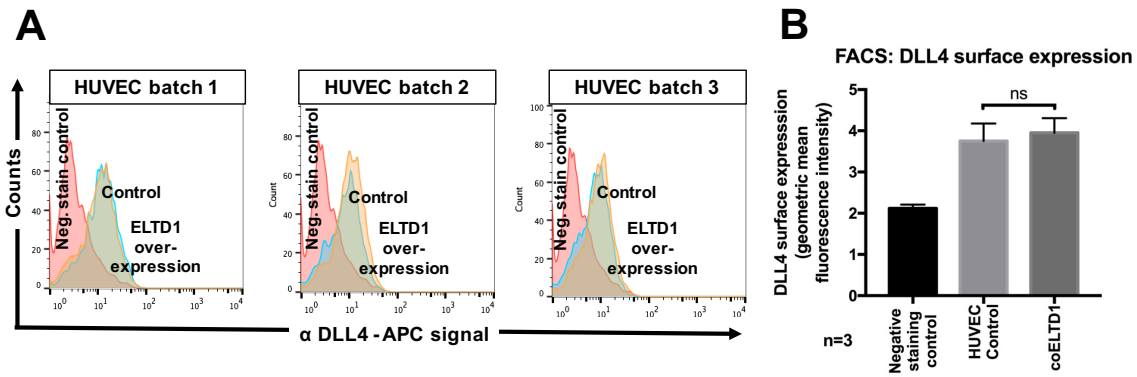


Figure 6.22: FL coELTD1 overexpression represses DLL4 at RNA level but has no effect on cell surface DLL4 protein expression. A) FACS histograms reveal that surface DLL4 expression is not affected by ELTD1 overexpression. **B)** Quantification of FACS surface DLL4 expression reveals no significant change in DLL4 protein expression between control and overexpression HUVECS (unpaired Student's *t* test; $p = 0.6$).

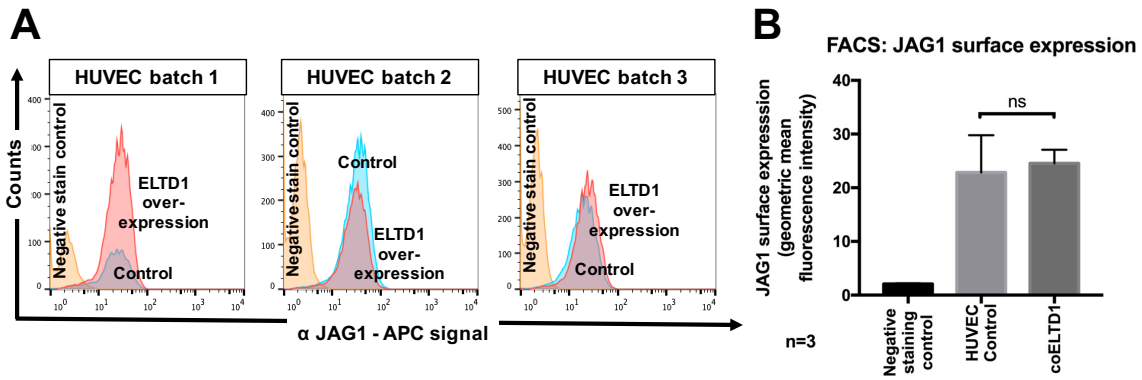


Figure 6.23: FL coELTD1 overexpression represses JAG1 at RNA level but has no effect on cell surface JAG1 protein expression. A) FACS histograms reveal that surface JAG1 expression is not affected by ELTD1 overexpression. **B)** Quantification of FACS surface JAG1 expression reveals no change in JAG1 protein expression between control and overexpression HUVECS (unpaired Student's *t* test; $p = 0.7$).

6.7 Discussion

This chapter details the transcriptional and functional effect of ELTD1 overexpression. First, tagged FL and CTF forms of coELTD1 were transiently ectopically expressed in HEK293T cells that normally lack ELTD1 expression. The gene expression profile of these cells was then analysed using Illumina microarrays to determine the effect of ELTD1 overexpression on the HEK293T transcriptome. When the significant differentially expressed genes did not overlap with any of the genes affected by ELTD1 silencing in primary HUVECS, it was decided to include an additional model and perform stable overexpression of untagged FL coELTD1 in HUVECS, which constitutively express ELTD1. The rationale for overexpression in endothelial cells is that ELTD1 upregulation has been commonly observed in the tumour vasculature. Functional angiogenic assays, as well as microarray analysis of gene expression changes, were then performed which confirmed earlier findings from silencing experiments (Masiero et al., 2013) and demonstrated that ELTD1 overexpression further promotes an endothelial tip cell phenotype, controlling various functions of endothelial biology. This discussion reviews the ELTD1 overexpression findings in the context of both angiogenesis and endothelial biology.

Angiogenesis as well as the interplay between VEGF and Notch signalling governing the tip and stalk cell endothelial phenotypes has been reviewed in Chapter 1. Our laboratories previously established ELTD1 as a regulator of physiological and pathological angiogenesis, showing its upregulation within tumour vessels and revealing that silencing suppressed sprouting angiogenesis and induced *DLL4* mRNA expression and affected the likelihood of endothelial cells

taking up the tip cell position (Masiero et al., 2013). In the previous chapter, results from the ELTD1 silencing microarray in HUVECS confirmed that ELTD1 silencing induced expression of the Notch ligand DLL4, and revealed additional suppression of the Notch ligand *JAG1* and target gene *HES2*. The antagonistic relationship between ELTD1 and DLL4 as well as silenced ELTD1's effect on sprouting provide a clue that ELTD1 plays a role in the tip cell phenotype. ELTD1 overexpression however provides more definitive evidence.

The functional experiments presented in the current chapter reveal that FL coELTD1 overexpression was able to further enhance an endothelial tip cell phenotype, thus explaining the benefit of ELTD1's upregulation in the tumour vasculature. This was revealed by ELTD1 overexpression in primary HUVECs inducing various tip cell phenotype characteristics: increased sprouting activity (hanging-drop endothelial spheroid assay and tube formation assays), a decreased proliferation rate (proliferation assay) and inhibition of inter-vessel anastomoses (fibrin gel bead assay). Surprisingly, ELTD1 overexpression did not affect migration (as would have been expected for a tip cell phenotype). This is discussed below. Lastly, overexpression had no effect on adhesion to any of the core ECM angiogenesis-associated components or to matrigel.

The induction of sprouting following ELTD1 overexpression suggests that ELTD1 is an important component of the endothelial tip cell phenotype. Furthermore, the inhibition of vessel anastomosis suggests that during sprouting angiogenesis, ELTD1's level of expression in the endothelial tip cell is modulated. Anastomoses

occur when two sprouts lead by endothelial tip cells meet and merge, with resultant loss of the tip cell phenotype and induction of the stalk phenotype. The finding that ELTD1 overexpression decreases anastomoses suggests failure in “switching off” the tip cell phenotype. This suggests that ELTD1’s expression may be regulated at different periods during sprouting angiogenesis, for example, high levels may be expressed during early sprout formation with later downregulation when anastomosis is required. However, this remains unknown and presents a good basis for a future experiment.

Regarding ELTD1 overexpression’s lack of effect on cell migration, it can be argued that the assay used (scratch wound assay) was not the most appropriate assay for migration and may have confounded the results. This is because this assay measures a combination of migration and cell proliferation and thus any putative increase in FL coELTD1 migration would have been balanced out by lowered proliferation rate associated with ELTD1 overexpression. Additionally, the experiment showing that ELTD1 silencing had no effect on migration used the same methodology (Masiero et al., 2013). A future experiment using a two chambered Boyden Chamber is planned to determine the effect of overexpression on migration.

6.7.1 Review of genes affected by ELTD1 overexpression

For the transcriptional effects of ELTD1 overexpression, differentially expressed genes identified from the HUVEC overexpression and silencing microarrays as well as the HEK293T overexpression microarrays were pooled and tested on FL coELTD1 overexpression HUVECS. These results revealed that there were multiple differentially expressed genes common to both HUVEC and HEK293T overexpression experiments despite the microarray data comparisons yielding no commonalities. This points to the insensitivities of microarray technology, and its dependency on very short probes which may not detect all isoforms, which have now been addressed by the more sensitive RNA-Seq technology. Results showed that ELTD1 overexpression in HUVECs upregulated *CHRNA1*, *ANTXR1*, *SLC39A6*, *HBB*, *ELMOD1*, *HSPA6*, *RYR1*, *JAG1* and *SH2D3C*. In terms of downregulation, ELTD1 overexpression downregulated *CCL15*, *CYP26B1*, *INPP5B*, *DLL4* and *KIT*. These findings where are now discussed in relation to angiogenesis and tumour biology.

CHRNA1 encodes the α1 subunit of nicotinic acetylcholine receptors. These pentameric receptors comprise of 2 α-subunits, 1 β-subunit, 1 γ-subunit, and 1 δ-subunits and are primarily found in neurons and at the neuro-muscular junction (Cooke and Ghebremariam, 2008). None of the other subunits were differentially expressed in any of the microarray experiments performed. Mutations in *CHRNA1* are associated with increased susceptibility to myasthenia gravis (Heckmann et al., 1996, Garchon et al., 1994). Although *CHRNA1* has no associations with angiogenesis or endothelial cell biology, the Alpha-7 acetylcholine nicotinic receptor (an α7 subunit homomer encoded by *CHRNA7*) has been associated with

angiogenesis with increased endothelial expression corresponding with increased angiogenesis *in vitro* and *in vivo* (Heeschen et al., 2001, Heeschen et al., 2002). Within endothelial biology, ELTD1's induction of *CHRNA1* is interesting result as it suggests that ELTD1 induce affects a nicotinic acetylcholine receptor which has not been associated with angiogenesis before.

ANTXR1 is a transmembrane receptor which is upregulated in tumour endothelial cells (St Croix et al., 2000) with expression upregulating tumour angiogenesis and endothelial proliferation (Reeves et al., 2010) and silencing in xenografts (of diverse tumour origin) reducing tumour size (Chaudhary et al., 2012). Furthermore, ANTXR1 has been identified as a biomarker for breast cancer stem cells (Chen et al., 2013). ANTXR1 has been shown to induce keratinocyte migration (Wang et al., 2016a) , although the same effect does not apply to endothelial cells (Reeves et al., 2010). Thus overexpressed ELTD1's upregulation of ANTXR1 fits with the increase in sprouting angiogenesis. However, this leads to additional questions: is ELTD1 upstream or downstream of ANTXR1 and what happens to ELTD1 when ANTXR1 is silenced or overexpressed? These could form the basis of future experiments.

SLC39A6 is a transmembrane zinc-influx transporter which has been shown to be involved in cancer progression. It is expressed and upregulated in the cancer cells of Chinese oesophageal squamous cell carcinoma patients, with upregulation inducing invasion and associated with a poor prognosis (Cui et al., 2015). In breast cancer, SLC39A6 has been associated with oestrogen receptor status and metastasis to regional lymph nodes (Manning et al., 1994). It's link to angiogenesis

is its association with a gene signature predicting benefit to the anti-angiogenic agent Bevacizumab plus paclitaxel in treating HER2-negative metastatic breast cancer (Mendiola et al., 2016). ELTD1's induction of *SLC39A6* expression suggests that ELTD1 may be an important target in both oesophageal cancer and breast cancer (in both the tumour vasculature and in tumour cells that express ELTD1) although in both of these cancer types, expression of SLC39A6 may be driven by another interaction. A confounding factor is that increased ELTD1 expression has been associated with improved survival in patients who subsequently receive anti-cancer therapy (Masiero et al., 2013), suggesting the need for further investigation.

HBB is the beta subunit of haemoglobin expressed by red blood cells. Although HBB is not associated with angiogenesis, endothelial cells are linked to haematopoiesis. During embryological development, a portion of progenitor endothelial cells transition into haemogenic endothelial cells that give rise to haematopoietic stem cells (HSC), which then produce the different blood cells (Swiers et al., 2013). The growth signals controlling this have recently been identified allowing for endothelial cells to be reprogrammed into HSCs *in vitro* (Lis et al., 2017). In this context, ELTD1's upregulation of HBB in endothelial cells is interesting and suggests that ELTD1 is possibly involved in HSC biology. This is further strengthening by ELTD1's relationship with KIT (upregulated by ELTD1 silencing and downregulated by ELTD1 overexpression), a stem cell marker expressed on HSCs. The role of ELTD1 in the haemogenic endothelium and in HSC biology presents an exciting new direction for ELTD1 research.

ELMOD1 is a GTPase-activating protein belonging to the ELMO protein family (Xu and Jin, 2017). In chemotaxis and cell migration, ELMO protein family members as such as ELMO1 (not ELMOD1) have been shown to be involved in GPCR signal transduction, functioning as GTPase activators of Rac proteins downstream of Gα and Gβγ GPCR subunits (Wang et al., 2016b, Xu and Jin, 2017). The literature has no reports however of ELMOD1 functioning in this manner or being expressed in endothelial cells. Nonetheless, this result is interesting as it suggests that ELTD1 upregulates a protein whose family members regulate GPCR signalling.

HSPA6 is a member of the cytoprotective and anti-apoptotic heat shock protein family (HSP), so named due to their induction following heat shock, heavy metal exposure and proteasome inhibition (Wang et al., 2013). HSPA6 is stress inducible and functions in stressed cells as a molecular chaperone alongside other HSP members to counter newly synthesised protein misfolding and aggregation. (Noonan et al., 2008, Deane and Brown, 2017). Additionally, HSPA6 has been shown to be linked to angiogenesis, being induced in endothelial cells exposed to the anti-angiogenic interferon antigen Sp100 which represses the pro-angiogenic transcription factor ETS-1 (Yordy et al., 2005). This experiment was performed using Sp100 viral transduction. In both this experiment and the HUVEC ELTD1 overexpression experiments, HSPA6 was induced following viral vector transduction (with each virus carrying a gens with opposing angiogenic effect). Thus, induction of HSPA6 is likely to be related to cell stress caused by massive protein overexpression.

SH2D3C is a signalling adaptor protein member of the NSP family of adaptor proteins (Al-Shami et al., 2010) and is expressed in endothelial cells (Vervoort et al., 2007). SH2D3C binds members of the Ras family of GTPases and also forms a complex with Crk-associated substrate regulating the actin cytoskeleton during cell migration (Dail et al., 2004). There are no studies which have robustly linked SH2D3C to GPCR signalling or to angiogenesis. ELTD1's upregulation of SH2D3C suggests that endothelial ELTD1 overexpression has an effect on the actin cytoskeleton of the cell. SH2D3C's relationship with cell migration further emphasises that the question of migration in ELTD1 overexpression HUVECS needs to be relooked at.

RYR1 is a calcium release channel belonging to the ryanodine receptor family and is expressed in the sarcoplasmic reticulum of striated muscle. It is activated by nitric oxide (Kakizawa, 2013) and releases calcium from the sarcoplasmic into the cytoplasm initiating calcium signalling and muscle contraction (Lanner et al., 2010). No published information details the expression of RYR1 in endothelial cells, however reviewing the raw HUVEC RNA-Seq data from the publically available Blueprint Epigenome Project (Stunnenberg and Hirst, 2016) reveals that HUVECS do not physiologically express *RYR1*. Furthermore, the qPCR C_t value for RYR1 for control and ELTD1 overexpression HUVECS was > 34 confirming that this is not expressed and that the changes are very small and are likely to be biologically irrelevant. In cardiac muscle another member of the ryanodine family, RYR2 has been shown to be a downstream target of, Gαs signalling through cAMP (Salazar et al., 2007). No similar associations have been made for RYR1. Additionally, in a RYR2 gene knockin mouse model, RYR2 was shown to accelerate cardiac

pressure-overload hypertrophy (van Oort et al., 2010), a result similar to that seen in a mouse *ELTD1* knockout model (Xiao et al., 2012). ELTD1's small induction of *RYR1* expression may suggest that one of ELTD1's downstream effects is to increase cytoplasmic calcium. A future experiment would be to test for changes in intracellular calcium in control and ELTD1 overexpressing cells. If calcium does appear to be regulated by ELTD1, this may prove to be the direction of future work into ELTD1's non-canonical GPCR signalling.

The final upregulated gene in response to ELTD1 overexpression was the Notch ligand JAG1. Already introduced in the previous chapter, both JAG1 and DLL4 are established regulators of angiogenesis with JAG1 being antagonistic to DLL4's activation of Notch signalling (Benedito et al., 2009). In the previous chapter, ELTD1 silencing repressed both *JAG1* and *HES2* mRNAs whilst inducing *DLL4* mRNA and protein. ELTD1 overexpression has the opposite effect, inducing *JAG1* mRNA and repressing *DLL4* mRNA whilst having no effect on *HES2* mRNA or JAG1 and DLL4 protein expression. It is thus possible that *HES2* changes following ELTD1 silencing were probably related to DLL4 induction. Additionally, although the surface levels of JAG1 and DLL4 were unchanged following ELTD1 overexpression, it remains unclear whether there is a change in the total cell protein expression for these proteins. ELTD1's induction of a tip cell phenotype is likely to be aided by the induction of *JAG1* mRNA and repression of *DLL4* mRNA although interactions with other pro-angiogenic genes such as *ANTXR1* are also important and require further study.

CCL15 is a secreted chemokine which binds to CCR1, CCR3 and CC5 on T cells and monocytes. CCR1 and CCR3 are also expressed by endothelial cells, while CCL15 has been shown to induce endothelial cell migration, cell proliferation and sprouting angiogenesis (Hwang et al., 2004). The suppression of *CCL15* mRNA in ELTD1 overexpressing HUVECS suggests that *CCL15* is negatively regulated as part of a compensatory response to the sustained pro-angiogenic effect of ELTD1 overexpression. Potentially, CCL15's suppression may be associated with the lack of migration noted with ELTD1 overexpression.

CYP26B1 is a member of the cytochrome P450 family and is involved in the metabolism of retinoic acid (Ross and Zolfaghari, 2011). In endothelial cells, CYP26B1 has been shown to regulate sprouting angiogenesis with CYP26B1 silencing inducing a reduction in sprouting (Messner et al., 2013). The suppression of *CYP26B* is probably similar to that of *CCL15*, occurring as a compensatory response to the sustained pro-angiogenic effect of ELTD1 overexpression.

INPP5B is a cytoplasmic and mitochondrial enzyme which belongs to a family of proteins which modulates calcium signalling through the inactivation of inositol phosphates (Williams et al., 2007). INPP5B is plays a role in the formation of phagosomes (Bohdanowicz et al., 2012) and in the secretory pathway through its binding to RAB proteins (Shin et al., 2005). There are no reports of INPP5B affecting angiogenesis or endothelial cell function. ELTD1's suppression of *INPP5B* is interesting as it gives further weight to the call for investigating whether ELTD1 overexpression affects calcium signalling or accumulation.

6.7.2 Limitations

A main limitation of the work performed in this chapter is the use of overexpression to better understand how a protein functions. Overexpression is non-physiological and thus there is a high risk that results may not representative of what occurs during normal physiology. Additionally, this study utilised microarrays which have recently been superseded by the more sensitive RNA-Seq technology. Within the HEK293T overexpression experiments, a limiting factor was the use of FACS sorting to select cells for microarray analysis, a procedure which is known to stress cells, as well as the use of tags. Additionally, HEK293T cells do not normally express ELTD1. Lastly in the FL coELTD1 overexpression microarray performed in HUVECS, only two biological replicates were used for reasons already described.

6.7.3 Future Experiments

These results provide fertile ground for many future studies. Within the functional assays performed on FL coELTD1 overexpressing HUVECS, a key experiment will be to perform migration assays using a Boyden Chamber to adequately assess whether overexpression affects migration. Additionally, FL coELTD1 overexpressing HUVECS in the hanging drop spheroid assay and fibrin gel bead assay could be stained for ELTD1, DLL4, JAG1, VEGFR2. This will provide invaluable information about whether ELTD1's expression is modulated in the developing vessel. Regarding signalling, the FL coELTD1 overexpression HUVECS will all be tested for canonical GPCR signalling. These will also be used for future work on the presumed non-canonical activity of ELTD1. Additionally, the many gene

changes induced by FL coELTD1 overexpression all provide additional avenues for new experiments, which are discussed in the discussion. Finally, CTF coELTD1 will be cloned into a lentiviral vector and transduced into HUVECS to determine whether it has the same effect as FL coELTD1. This will yield invaluable information regarding determining how ELTD1 is activated.

6.8 Conclusion

This chapter investigates and reveals the transcriptional and functional effect of ELTD1 overexpression on endothelial cells. ELTD1 overexpression induced a more active endothelial tip cell phenotype through further increased sprouting activity, decreasing proliferation and inhibiting inter-vessel anastomoses. Overexpression had no effect on adhesion to various angiogenesis-associated ECM components or to cell migration. Transcriptionally, ELTD1 upregulated *CHRNA1, ANTXR1, SLC39A6, HBB, ELMOD1, HSPA6, RYR1, JAG1* and downregulated *CCL15, CYP26B1, INPP5B, DLL4* and *KIT*. Future experiments are planned to further explore these relationships.

Chapter 7: ELTD1 in the primary breast cancer and regional nodal microenvironment

7.1 Introduction

The previous four results chapters have explored ELTD1's evolution, its signalling, and new functional roles and relationships within endothelial biology. This last result chapter explores ELTD1's role within the tumour microenvironment. As has already been introduced in the Introduction chapter, ELTD1 was first shown to be upregulated in the tumour microenvironment of glioblastomas, being expressed in both endothelial cells and tumour cells (Dieterich et al., 2012, Towner et al., 2013). Following on from this, work completed in our laboratories showed that when comparing tumour and normal matched tissue samples, tumour-associated endothelial cells expressed higher levels of ELTD1 than the matched normal tissue endothelial cells. This was shown for multiple tumour types: head and neck squamous carcinoma, renal, colorectal and ovarian cancer (Masiero et al., 2013). Although ELTD1 was mostly expressed within the vasculature of these tumour samples, a minority of tumours were also found to express ELTD1, however at a lower intensity. Furthermore, this work revealed that higher tumour-associated

endothelial cell ELTD1 protein expression was shown to correlate with improved overall survival (OS) in patients who subsequently received anti-cancer therapy. This relationship was shown for head and neck squamous carcinoma, renal, colorectal and ovarian cancers (Masiero et al., 2013). This effect has been hypothesised to be related to improved micro-vessel density and resultant improved drug delivery.

Despite these advances in knowledge, many unanswered questions remain. Primary amongst them is the role of ELTD1 within primary and secondary tumour microenvironments as well as the role of ELTD1 within endothelial versus tumour cells. To investigate this further, a study was initiated to investigate the effects of ELTD1 within primary breast cancer and regional lymph node metastases. This involved staining and reviewing primary tumour and positive regional lymph node biopsies taken over a ten year period from patients seen prior to treatment at the Department of Medical Oncology's Breast Clinic at the Churchill Hospital, Oxford (Oxford University Hospitals NHS Foundation Trust). ELTD1 expression results were then analysed alongside patient survival patient survival.

7.2 ELTD1 is randomly mutated in many cancer types with no domains specifically targeted

Before beginning the clinicopathological study, I investigated whether any of ELTD1's domains were preferentially mutated in cancer. The rationale for this work stemmed from the work performed on oncogenes which revealed that oncogenes often share the same targeted point mutations across many tumour types

(examples include mutations in members of the *TP53*, *RAS* and *PIK3CA* pathways) (Vogelstein et al., 2013). Additionally, understanding these mutations has led to a better understanding of how these genes function (Vogelstein and Kinzler, 2015). Although ELTD1 has never been associated as a cancer driver, mutations targeting or excluding specific ELTD1 domains which are shared across many tumour types would suggest that this domain is important for ELTD1's activation and function within the tumour microenvironment.

This work was performed bioinformatically by interrogating the Broad Institute's exome sequencing dataset comprising of 4742 human tumours from 21 cancer types assembled from The Cancer Genome Atlas (TCGA) and non-TCGA exome sequenced projects, alongside matched normal tissue samples (Lawrence et al., 2014). Specifically, ELTD1's mutational profile was compared across multiple tumour types.

Results reveal that across multiple tumour types, ELTD1 did not have any domains which were preferentially mutated, with mutations being spread evenly across ELTD1's amino acid sequence (Figure 7.1 A). Additionally, none of ELTD1's extracellular domains (EGFs, GAIN or GPS) or 7TM loops were preferentially spared or targeted. The even spread and lack of specific domain targeting suggests that these are random and functionally meaningless mutations.

Following on from this, *ELTD1*'s alteration frequency in cancer was reviewed. To do this, mutation frequency data was obtained from 48 curated cancer-genome

datasets available from the cBioPortal cancer genomics data repository (Cerami et al., 2012). This revealed that *ELTD1*'s mutational frequency within tumours is low with the majority of cancer types having a mutational frequency of <10% (Figure 7.1 B). Only the melanoma and lung squamous carcinoma datasets were found to have a mutation frequency ≥10 %. Additionally, bladder carcinoma, sarcoma and uterine carcinosarcoma datasets all exhibited *ELTD1* amplification without any other alterations, however the frequency of these events was low (Figure 7.1 B).

As ELTD1 is mostly expressed by tumour endothelial cells (and not tumour cells) (Masiero et al., 2013), a criticism of the above bioinformatics approaches is that both only analysed tumour genomes and did include any tumour microenvironment cells such as tumour endothelial cells. Nonetheless these results are important as they show that in the cancer cell, *ELTD1* appears to be randomly mutated across all its domains in multiple cancer types and that for the majority of cancer types reviewed, the frequency of these alterations was very low. Taken together, this suggests that in the cancer cell, *ELTD1 is* not a gene which is targeted for specific alterations.

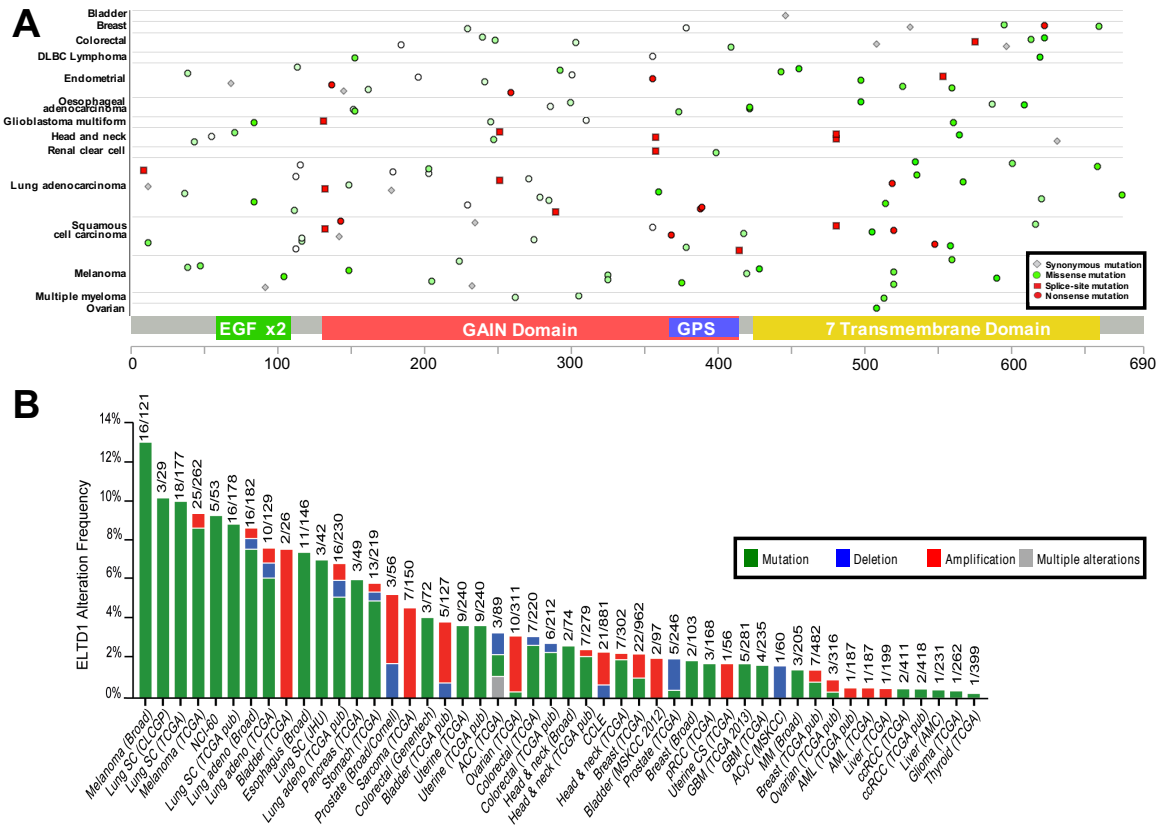


Figure 7.1: *ELTD1*'s mutational landscape in human cancer. A) An analysis of *ELTD1* mutations present in 4742 exome sequenced human tumours reveals that *ELTD1* mutations are random with no ELTD1 domain being preferentially mutated or protected across multiple cancer types. Mutations listed comprise synonymous, missense, splice-site and nonsense mutations. Data obtained from the Broad Institute's publicly available collection of 21 exome sequenced cancer types assembled from both The Cancer Genome Atlas (TCGA) and non-TCGA exome sequenced projects (Lawrence et al., 2014). Tumour types are listed on the y axis. The x axis represents ELTD1's amino acid sequence. ELTD1's domains listed are listed above this. **B)** *ELTD1*'s alteration frequency in cancer is low. ELTD1's alteration frequency in 48 curated cancer-genome datasets reveals that the majority of cancers have an ELTD1 mutational frequency of <10%. Only melanoma and lung squamous carcinoma have a mutational frequency > 10%. Amplification without

other ELTD1 alterations occurs in bladder carcinoma, sarcoma and uterine carcinosarcoma datasets. The number of altered cases and total cases per dataset is listed above each column. Data obtained from 48 curated cancer-genome datasets obtained from the cBioPortal cancer genomics data repository (Cerami et al., 2012). (Abbreviations: ACyC=adenoid cystic carcinoma; adeno=adenocarcinoma; AML=acute myeloid leukaemia; ccRCC=kidney renal clear cell carcinoma; CCLE=Cancer Cell Line Encyclopedia; CML=chronic myeloid leukaemia; DLBC lymphoma=diffuse large B-cell lymphoma; GBM=glioblastoma multiforme; MM=multiple myeloma; NCI60=National Cancer Institute 60 human tumour cell line screen; pRCC=renal papillary cell carcinoma; SC=squamous carcinoma).

7.3 The majority of cancer cell lines (including breast cancer cell lines) do not express ELTD1

Next, *ELTD1*'s expression within cancer cell lines was investigated. This was performed bioinformatically by interrogating *ELTD1*'s expression across 1036 cancer cells from the Broad Institute's publically available "Cancer Cell Line Encyclopedia" dataset (Barretina et al., 2012). This dataset comprises microarray gene expression data from 1036 established cancer cell lines.

Results revealed that *ELTD1* is poorly expressed in the majority of cancer cell lines (Figure 7.2) with only 7% of the 1036 microarrayed cell lines expressing *ELTD1* and with no expression in the breast cancer cell lines. Of the cell lines which did express *ELTD1*, expression was highest in meningioma, osteosarcoma, chondrosarcoma,

Hodgkin's lymphoma and thyroid tumour cell lines. Of these, only the meningioma cell lines had a median expression of above 7 (Log_2 Robust Multi-Array Average). As a comparison, the median expression of the proto-oncogene *KRAS* was >10 for all cancer types in the same dataset. The expression of *ELTD1* in the high-grade neurological cancer lines correlates with the finding that *ELTD1* is expressed by high grade gliomas (Towner et al., 2013).

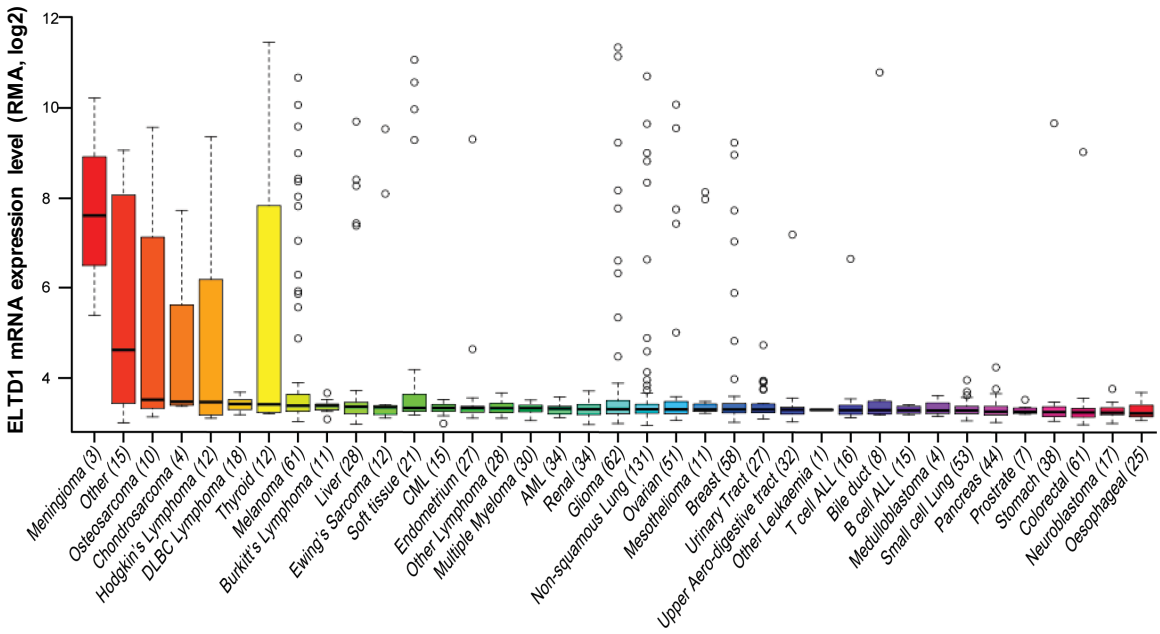


Figure 7.2: *ELTD1* is not expressed by the majority of cancer cell lines. Microarray gene expression data for *ELTD1* expression in the 1036 cancer cell lines microarrayed as part of the Broad Institute's publically available "Cancer Cell Line Encyclopedia" (Barretina et al., 2012) reveals that *ELTD1* is poorly expressed by 93% of microarrayed cell lines with expression limited to meningioma, osteosarcoma, chondrosarcoma, Hodgkin's lymphoma and thyroid tumour cell lines. The numbers on the x axis refer to the number of cancer cell line per tumour type. (Abbreviations: RMA=Robust Multi-Array Average).

The results from the above cancer cell line bioinformatics study were then validated using qPCR. As the clinicopathological project aimed to investigate *ELTD1*'s expression in primary breast cancer and regional node metastases, a panel of commonly used breast cancer cell lines representative of the major molecular subtypes of breast cancer (Luminal A, Luminal B, Basal, Claudin-low, HER2) (Perou et al., 2000, Holliday and Speirs, 2011) were grown and harvested for ELTD1 expression profiling using qPCR. The cell lines all express variations of the commonly used classical immunohistochemistry (IHC) markers ER, PR and HER2, which are used alongside tumour size, grade and nodal involvement to assess patient prognosis and guide management (Dai et al., 2015b). Additionally, HUVEC cells, which constitutively express ELTD1, were silenced for ELTD1 over 48 hours and harvested for qPCR analysis to provide positive and negative controls for ELTD1 expression. HEK293T cells, which do not constitutively express ELTD1 were grown and harvested as an additional negative control for ELTD1 expression. Finally, a panel of additional cell lines available in our laboratory were grown and harvested for ELTD1 expression profiling. These comprised melanoma prostate cancer, colorectal cancer and lymphoma cell lines.

Results revealed that all tested breast cancer cell lines (representative of all molecular breast cancer subtypes) did not express ELTD1 as levels of *ELTD1* mRNA expression were lower than both *ELTD1* silenced HUVECS (Western blot included in Figure) and the HEK293T negative control (Figure 7.3). Additionally, the panel of additional cell lines tested also revealed negative *ELTD1* expression when

compared to the *ELTD1* silenced HUVEC and HEK293T negative controls (Figure 7.3). These results suggested that *ELTD1* did not play a role in breast cancer cell lines, however it remained to be seen whether the same results held for human breast cancer cells biopsied from patients.

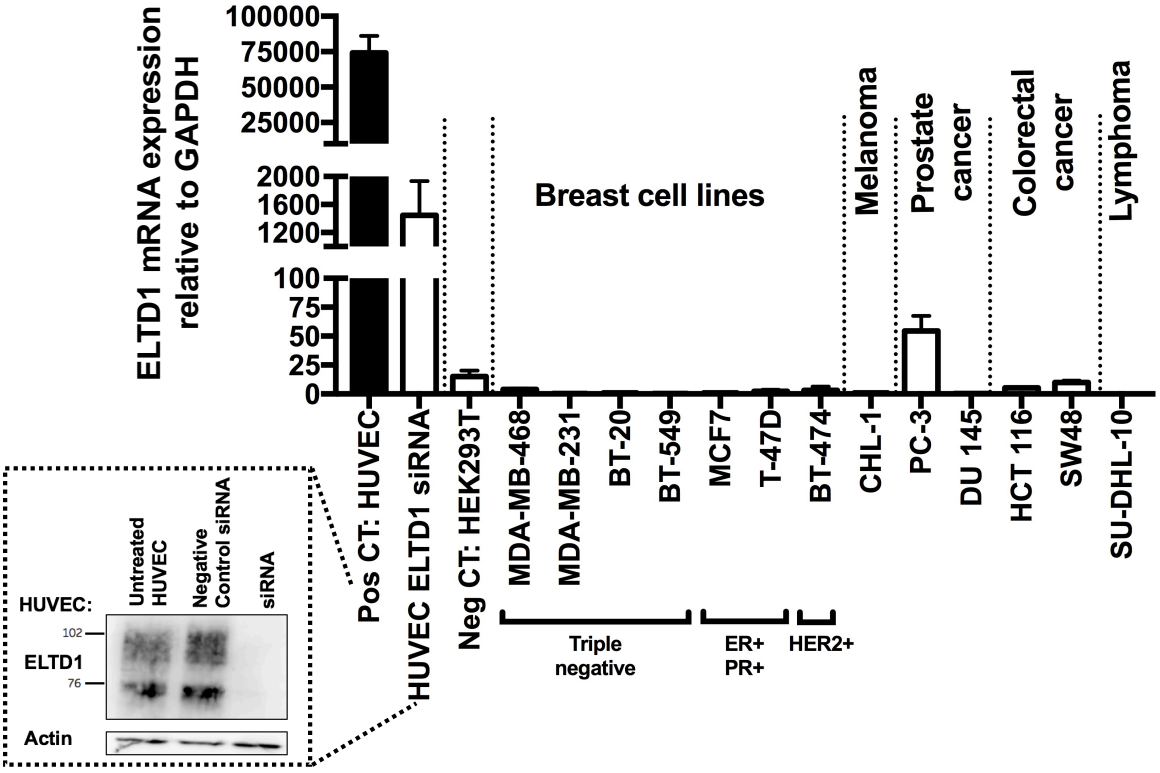


Figure 7.3: qPCR screen reveals that commonly used breast cancer cells do not express *ELTD1*. In the figure, the breast cancer cell lines (representative of the major molecular subtypes of breast cancer) are grouped according to the expression of classical breast cancer IHC markers ER, PR and HER2. HUVECS which constitutively express *ELTD1* were used a positive control and *ELTD1* silenced HUVECS were used a negative control. A western blot of ELTD1 silenced HUVECS is shown to validate ELTD1 silencing at the protein level. HEK293T cells which do not express *ELTD1* were used as an additional negative control. Breast

cancer *ELTD1* expression was lower than both HUVEC and HEK239T negative controls. In addition to the tested breast cancer cell lines, a panel of cell lines representing other tumour types were also screened for *ELTD1*, revealing similar negative results when compared to both HUVEC and HEK293T negative controls.

7.4 ELTD1 within primary breast cancer and regional lymph node metastases

Next, the clinicopathological ELTD1 breast cancer study was performed. The aim of this study was to investigate the role and effect of ELTD1 within the tumour microenvironment in both primary breast cancer and regional lymph node metastases and aimed to answer the following questions:

1. Is there any differential vascular ELTD1 expression between primary breast cancer tumours and regional lymph node metastasis?

1) Does vascular ELTD1 expression in primary and regional nodal metastasis correlate with Relapse Free Survival (RFS)? Does vascular ELTD1 expression correlate with any additional patient characteristic?

2) Do any breast cancers contain ELTD1 positive tumour cells and if so, is there any differential ELTD1 expression in these cells between primary breast cancers and regional node metastases?

3) Does tumour cell ELTD1 expression in primary and regional nodal metastasis correlate with Relapse Free Survival (RFS)?

7.4.1 Study methods

In brief, breast cancer patients seen at the Medical Oncology Department's Breast Clinic, Churchill Hospital (Oxford University Hospitals NHS Foundation Trust, Oxford) between 1992 and 2000 were retrospectively reviewed and accepted into the study if they were biopsy positive for primary breast cancer as well as regional lymph node metastasis prior to the initiation of any anti-cancer therapy. Patients who had undergone previous anti-cancer therapy or who had relapsed were not included in the study. Informed consent was obtained from all patients in accordance with the Declaration of Helsinki and local ethical approval was obtained from the Oxfordshire Research Ethics Committee.

Once recruited, each patient's tumour biopsies (comprising matched primary tumour and regional lymph node metastasis biopsies) were cut into histological sections and immunohistochemically stained for ELTD1 expression (anti-ELTD1 antibody: Sigma HPA025229; 1:500 dilution). In order to allow for as large a field of examination as possible, whole tumour sections were used instead of smaller tissue microarrays. This allowed for a thorough investigation of the tumour and its microenvironment, as well as the surrounding normal tissue. Following ELTD1 staining, each histological section was then digitally scanned using a Hammatsu NanoZoomer slide scanner. Details are presented in the Methods chapter. Staining was performed together with Mr. Graham Steers and Dr. Russel Leek (both formerly members of the Nuffield Division of Clinical Laboratory Sciences, Radcliffe Department of Medicine, University of Oxford).

For each histological section, ELTD1's expression (as measured by IHC) was assessed within 3 biological compartments: 1) normal (non-tumour) vessels; 2) tumour-associated vessels; and 3) tumour cells. Assessment of ELTD1's expression was performed using the commonly used IHC intensity scoring system which has been used for previous ELTD1 IHC studies (Masiero et al., 2013). In brief, the IHC intensity score is a measure of overall staining intensity and is graded as follows: Score 0 = negative expression; Score 1 = weak expression; Score 2 = moderate expression; and Score 3 = strongest expression. For each histological section, the recorded ELTD1 intensity score for each biological compartment (normal vessels; tumour-associated vessels; tumour cells) corresponded with the average ELTD1 expression within the biological compartment being assessed. ELTD1 IHC expression scoring was performed in conjunction with Dr. Ioanis Roxanis (Consultant histopathologist, John Radcliffe Hospital, Oxford University Hospitals NHS Foundation Trust).

Patient characteristics as well as survival data following treatment (as of 2010) were then received from the University of Oxford Department of Oncology for each patient. This data was then contrasted with the histological ELTD1 intensity scores for Kaplan Meier survival analyses (Kaplan and Meier, 1958). Recorded patient characteristics comprised: oestrogen receptor (ER) status, human epidermal growth factor receptor 2 (HER2) status, tumour subtype, primary tumour size, primary tumour grade, number of positive nodes, age at diagnosis, relapse-free survival (RFS), relapse and relapse site, overall survival (OS) and whether the patient had died from breast cancer.

7.4.2 Patient characteristics

43 patients were recruited to the study and had their matched primary and regional node histological sections stained for ELTD1. The study's patient characteristics are presented in Table 7.1. The majority of patients were above 50 years of age, had a tumour size of T2 (> 2 cm but < 5 cm), a nodal status of pN1 (1-3 involved nodes), and had Luminal A subtype breast cancer. Additionally, the majority of patents ended up relapsing during follow-up, with metastatic spread being the commonest relapse site. The mean RFS was 6.4 years (95% confidence interval (CI) 27.91 ±1.6 years) and the mean OS was 7.2 years (95% CI ±1.6 years).

Kaplan-Meier survival analyses were then performed on each of the above patient characteristics to determine whether they influenced survival (RFS and OS) in this patient population. This was performed to determine whether our patient population behaved in a similar way to established trends in breast cancer survival. These trends include improved survival in younger patients, patients with smaller initial tumours and fewer positive nodes, ER positive, HER2 negative tumours and the Luminal A molecular subtype. Due to the small size of our patient population, only one characteristic (the number positive of lymph nodes) yielded a significant difference for both RFS and OS: patients with >10 positive nodes having a significantly worse survival than those with fewer nodes (RFS log-rank p = 0.005; OS log-rank p = 0.006) (Table 7.2 and Figure 7.4 A and B). For the other patient characteristics, survival analyses yielded no significant associations with survival (Table 7.2). Nonetheless, despite the lack of survival significance, the survival

trends for ER status (Figure 7.4 C), HER2 status (Figure 7.4 C) and molecular subtype (Figure 7.4 D) all correlated with established breast cancer survival outcomes. This suggested that the lack of statistical significance was due to the small size of the study.

Cases included in study	Number
Total cases included in study	43
Age at diagnosis	
Age < 50 years	9 (21%)
Age > 50 years	34 (79%)
Primary tumour Size:	
T1 (<2 cm)	9 (21%)
T2 (>2 cm <5 cm)	27 (63%)
T3 (>5 cm)	8 (19%)
Tumour grade:	
Grade 1	1 (2%)
Grade 2	18 (42%)
Grade 3	24 (56%)
Number of positive lymph nodes:	
pN1 (1-3 nodes)	23 (53%)
pN2 (4-9 nodes)	13 (30%)
pN3 (>10 nodes)	7 (16%)
Relapse status during follow-up period	
Relapse negative	19 (44%)
Relapse positive	24 (56%)

Relapse site in relapse positive cases: (n=24)	
Ipsilateral breast	5 (20%)
Contralateral breast	3 (13%)
Metastatic disease	16 (67%)
ER status	
ER negative	23 (53%)
ER positive	20 (47%)
HER2 status	
HER2 negative	33 (77%)
HER2 positive	10 (23%)
Molecular subtype	
Luminal A	20 (47%)
Luminal B	3 (7%)
Triple negative	12 (28%)
HER2	8 (18%)

Table 7.1: Patient characteristics. Percentages have been calculated from a total of n=43 cases included in the study. The relapse site percentage is based on the total number of relapses (n=24).

Patient characteristics and survival:	**Log-rank p value**	
Log-rank *p* value:	**RFS**	**OS**
Age at diagnosis	0.7	0.8
Primary tumour size	0.7	0.3
Primary tumour grade	0.7	0.6
Number of positive lymph nodes	**0.005**	**0.006**
ER status	0.5	0.5
HER2 status	0.7	0.7
Molecular subtype	0.8	0.8

Table 7.2: Patient characteristics and survival. Those with statistical significance are shown in bold. (Abbreviations: RFS= relapse free survival; OS=overall survival).

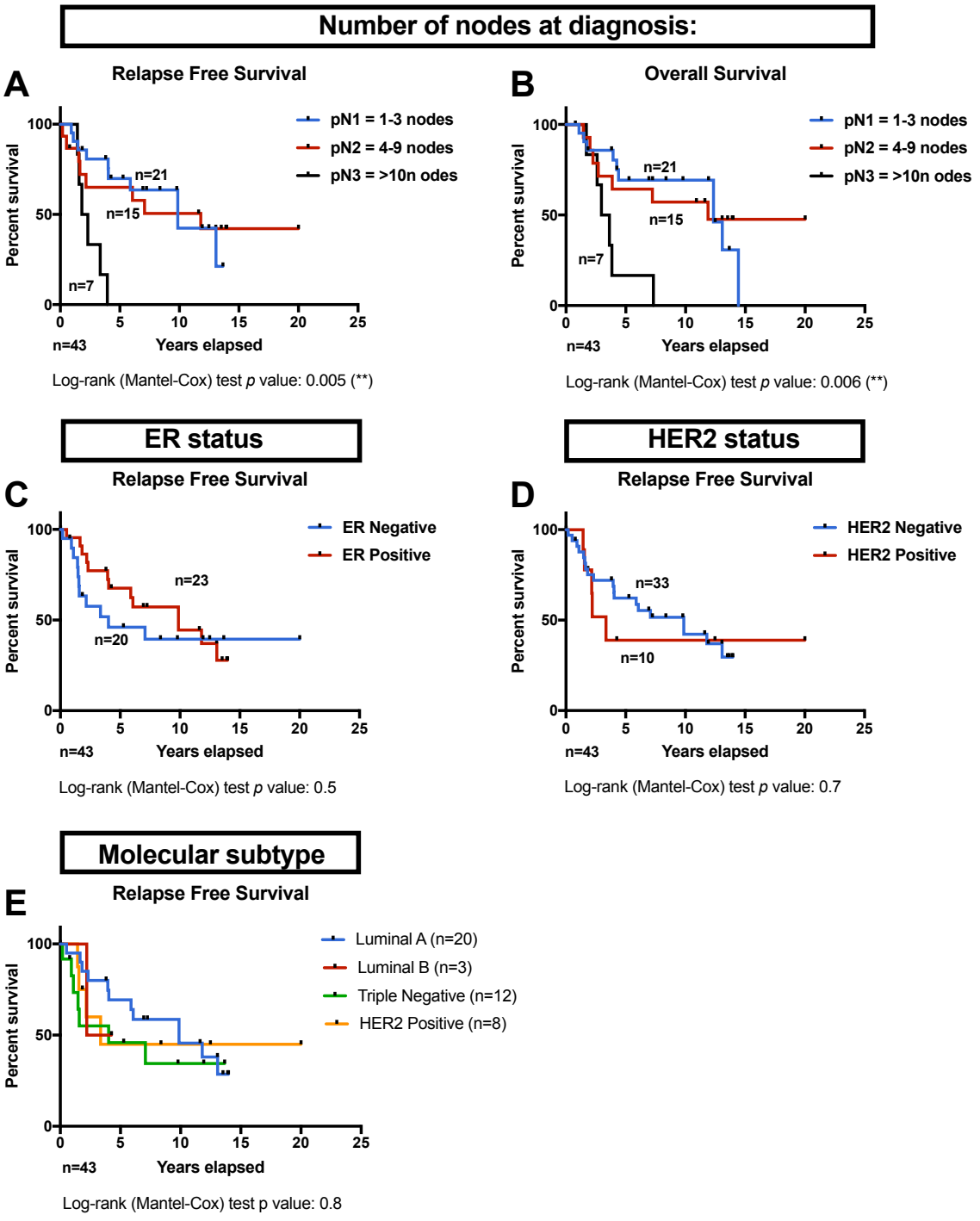


Figure 7.4: Patient survival contrasted with patient characteristics. A-B) The number of positive nodes at diagnosis corresponds significantly with RFS and OS: patients with >10 nodes did significantly worse than patients with fewer nodes (RFS Log-rank (Mantel-Cox) test: *p* value = 0.005; OS Log-rank (Mantel-Cox) test: *p* value = 0.006). **C)** Although ER status did not have a significant effect on survival (Log-

rank (Mantel-Cox) test: *p* value = 0.5), ER positive patients appeared to do better than ER negative patients, which correlates with established breast cancer survival outcomes. **D)** Similarly, although HER2 status did not have a significant effect on survival (Log-rank (Mantel-Cox) test: *p* value = 0.7), HER2 negative patients appeared to do better than HER2 positive patients, which correlates with established breast cancer survival outcomes. **E)** Finally, although not being significant (Log-rank (Mantel-Cox) test: *p* value = 0.8), Luminal A breast cancers appeared to do the best of all other subtypes in the study's patient population, which correlates with established breast cancer survival outcomes.

7.4.3 Vascular ELTD1 expression in primary breast cancer and regional lymph node metastasis

Following ELTD1 staining, all histological sections were scored for ELTD1 IHC staining intensity (Score 0 = negative expression; Score 1 = weak expression; Score 2 = moderate expression; and Score 3 = strongest expression).

7.4.3.1 Vascular ELTD1 increases with increasing proximity to breast tumours.

Before initiating statistical comparisons, a histogram was created to determine the distribution of vascular ELTD1 IHC scores for both normal vessels and tumour associated vessels in both primary breast tumour and regional node metastasis samples. Normal vessels were defined as non-tumour associated vessels located at the peripheral margin of normal tissue surrounding each tumour biopsy. Results revealed that the majority of normal vessels expressed ELTD1 at an intensity of 0

(negative) or 1 (weak expression) (Figure 7.5 A). This was the case for both primary breast tumours and regional lymph node metastases.

In contrast, the majority of tumour vessels in both primary breast cancer and regional lymph node metastases showed increased ELTD1 IHC staining, with the majority of samples being scored 2 (moderate expression) or 3 (strongest expression) (Figure 7.5 A). This distribution pattern clearly thus separated normal vascular ELTD1 expression (score 0-1) from tumour vascular ELTD1 expression (score 2-3). Statistical testing further confirmed this, showing a statistically significant increase in ELTD1 expression within tumour vessel ELTD1 expression (Figure 7.5 B). This finding is similar to that previously shown by our laboratories for ELTD1 expression in head and neck, renal, colorectal and ovarian cancer (Masiero et al., 2013).

Representative images of normal vessel ELTD1 IHC staining are presented in Figure 7.6. Representative images showing the full range of ELTD1 IHC staining for primary breast tumours and regional lymph node metastases are shown in Figure 7.7 and Figure 7.8 respectively. Representative images of tumour vessels showing increasing ELTD1 IHC staining with increasing proximity to the breast tumour are presented in Figure 7.9. The reasons for the increase in vascular ELTD1 expression surrounding the tumour remains unknown and untested. Tumours are known to overexpress VEGF for secretion into the microenvironment which results in increased angiogenesis which is essential for tumour growth (Carmeliet and Jain, 2011b). As ELTD1 is induced by VEGF stimulation, it can be hypothesised that the

increase in ELTD1 IHC staining is due to the effect of increased VEGF expression. Staining these sections with VEGF and other growth factors such as fibroblast growth factor will help answer this question. A future experiment investigating this is planned.

Lastly, it was noted that ELTD1 did not appear to be expressed by the lymphatic vessels used by primary breast tumours for metastatic spread. Although not specifically stained for with a lymphatic marker, lymphatic vessels were identified by consultant histopathologist Dr. Roxanis whenever tumour cells were noted within a vessel-like structure in the primary breast sections. The first clue that these were lymphatic vessels came from the lymphatic system being the commonest route through which breast cancer metastases leave the primary breast tumour (Rahman and Mohammed, 2015). Additional evidence included these tumour-filled vessels being one cell layer thick, in contrast to nearby, similar sized blood vessels which contained a thicker vessel wall and were always ELTD1 IHC positive (IHC score of 1-3). Furthermore, blood vessels often contained red blood cell debris, which was never present in any of the lymphatics identified in this manner. Lastly, none of the afferent lymphatic vessels and subcapsular sinuses of the lymph nodes housing the regional nodal metastases were IHC positive for ELTD1. Representative images of negative ELTD1 IHC staining in primary breast tumour lymphatics are presented in Figure 7.10. It is planned that the lymphatic marker LYVE1 (Jackson, 2004) will be stained in these sections in the future.

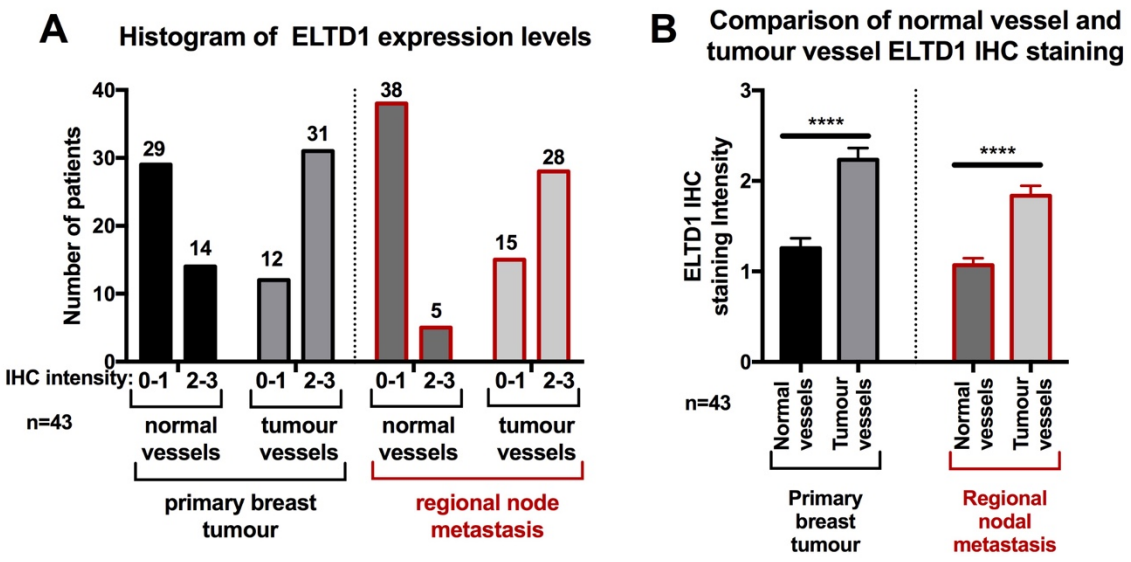


Figure 7.5: Vascular ELTD1 expression is upregulated in breast cancer. A) Histogram showing range of vascular ELTD1 IHC staining intensities for normal stroma vessels and tumour stroma vessels in both primary breast cancer and regional lymph node metastases. The majority of normal stroma vessels express ELTD1 at an IHC intensity of 0-1 whereas the majority of tumour stroma vessels express ELTD1 at an IHC intensity of 2-3. **B)** Vascular ELTD1 expression increases within the tumour vasculature of both primary tumour and regional lymph node metastases, when compared to normal vessels in the same biopsy (paired Student's *t* test; $p < 0.0001$ for both primary tumour and regional node comparisons).

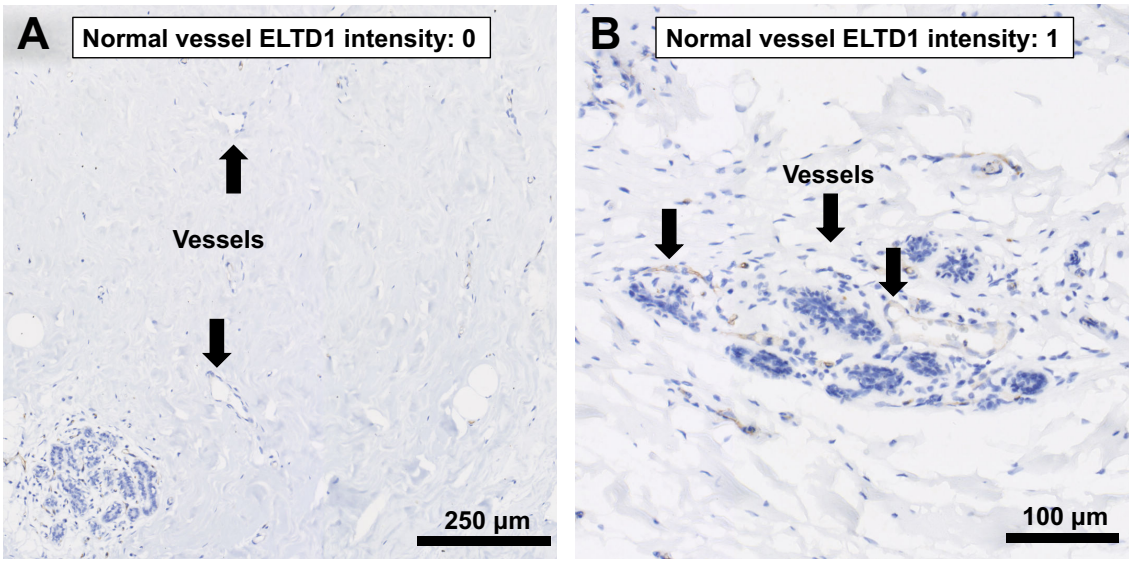


Figure 7.6: Representative vascular ELTD1 IHC in normal vessels at the margins of the primary breast tumour biopsy. Black arrows indicate vessels. **A)** Normal vessel ELTD1 IHC intensity score of 0 (negative expression). **B)** Normal vessel ELTD1 IHC intensity score of 1 (weak expression).

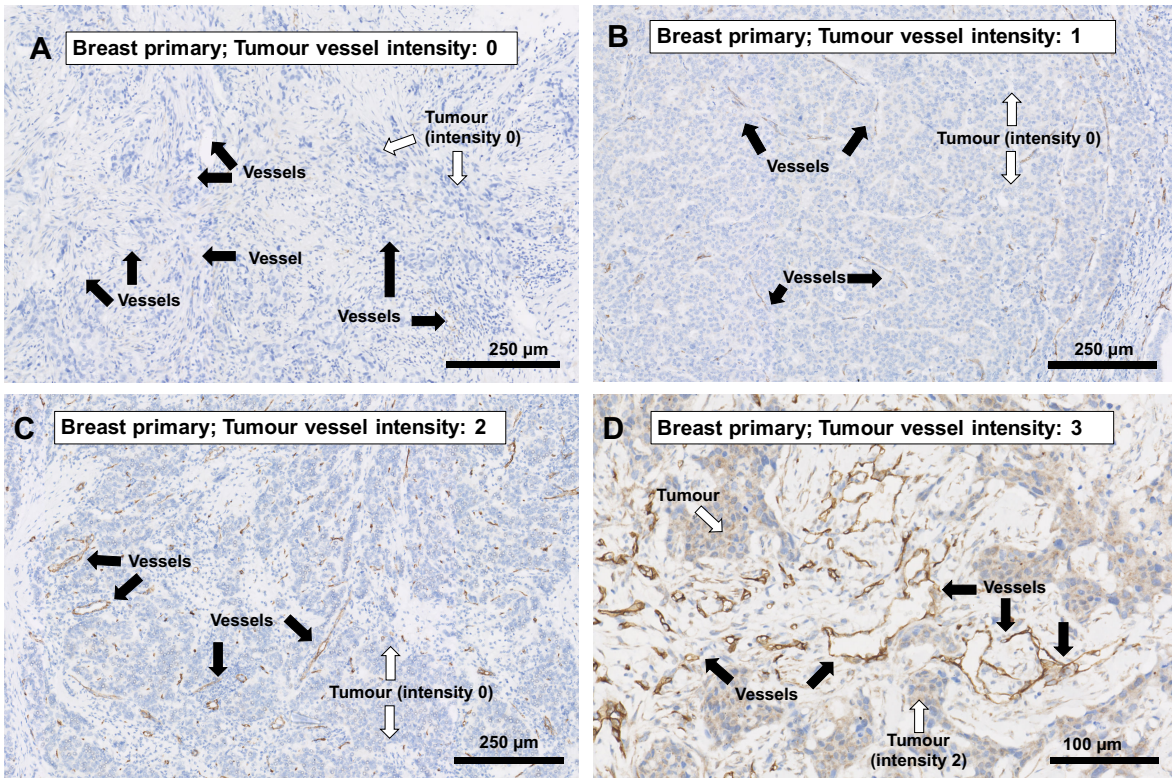


Figure 7.7: Representative images of tumour vascular ELTD1 IHC staining within the primary breast tumour, showing the range of staining (intensity expression score 0-3). Black arrows point to tumour vessels. White arrows point to tumour cells. **A)** Representative image showing tumour vascular ELTD1 IHC intensity score 0 (negative expression). Tumour cell ELTD1 IHC intensity is 0 (negative). **B)** Representative image showing tumour vascular ELTD1 IHC intensity 1 (weak expression). Tumour cell ELTD1 IHC intensity is 0 (negative expression). **C)** Representative image showing tumour vascular ELTD1 IHC intensity 2 (moderate expression). Tumour cell ELTD1 IHC intensity is 0 (negative). **D)** Representative image showing tumour vascular ELTD1 IHC intensity 3 (strongest expression). Tumour cell ELTD1 expression intensity is 2 (moderate).

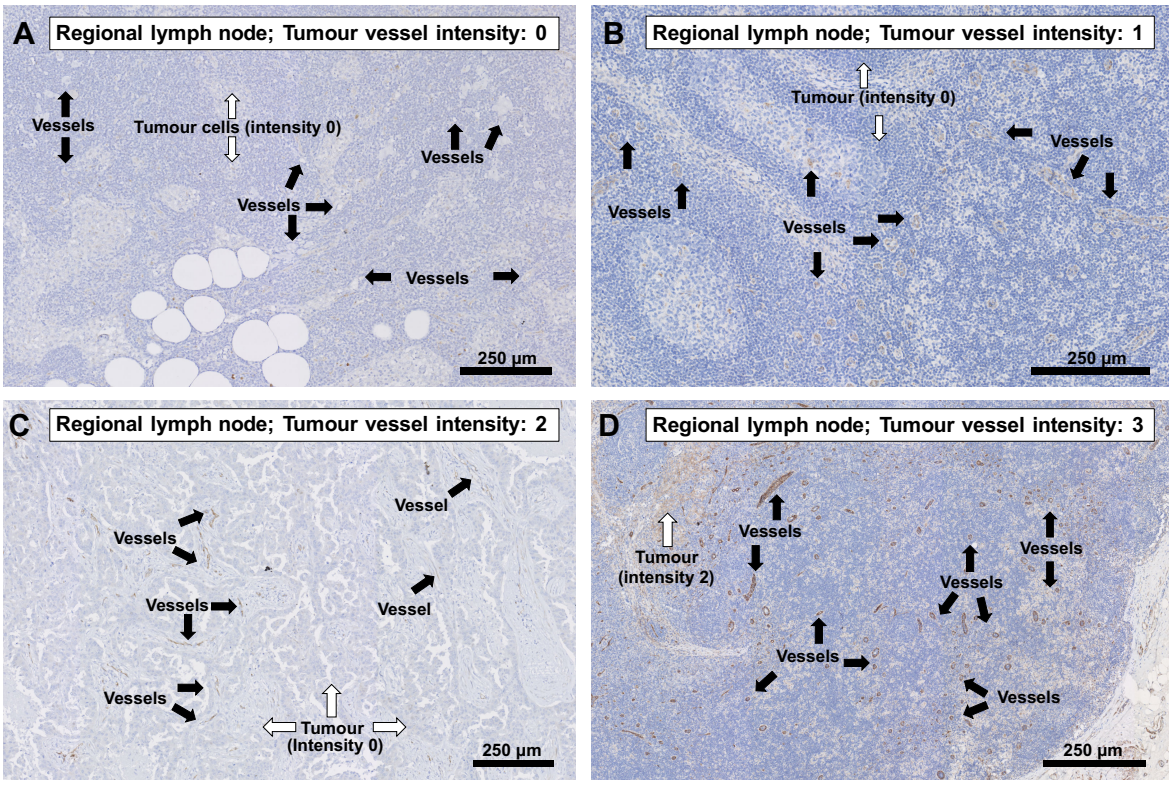


Figure 7.8: Representative images of tumour vascular ELTD1 IHC staining within regional lymph node metastases, showing the range of ELTD1 IHC intensity scores (intensity expression score 0-3). Black arrows point to tumour vessels. White arrows point to tumour cells. **A)** Representative image showing tumour vascular ELTD1 IHC intensity 0 (negative expression). Tumour cell ELTD1 IHC intensity is 0 (negative expression). **B)** Representative image showing tumour vascular ELTD1 IHC intensity 1 (weak expression). Tumour cell ELTD1 IHC intensity is 0 (negative expression). **C)** Representative image showing tumour vascular ELTD1 IHC intensity 2 (moderate expression). Tumour cell ELTD1 IHC intensity is 0 (negative expression). **D)** Representative image showing tumour vascular ELTD1 IHC intensity 3 (strongest expression). Tumour cell ELTD1 IHC intensity is 2 (moderate expression).

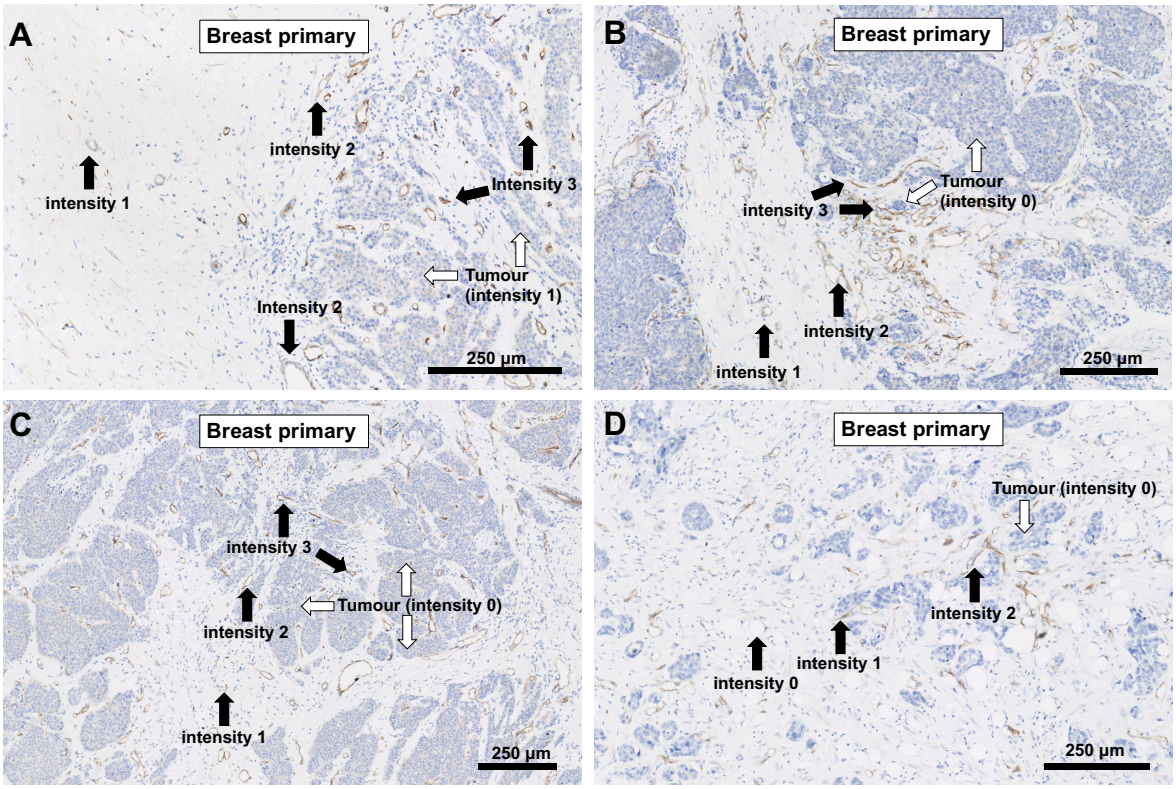


Figure 7.9: Vascular ELTD1 expression increases with proximity to the tumour. A-D) Representative breast tumour sections showing an increase in tumour vessel ELTD1 IHC staining intensity with increasing proximity to the tumour. Black arrows indicate tumour vessels; white arrows indicate tumour. ELTD1 IHC intensity scale: 0 = negative expression; 1 = weak expression; 2 = moderate expression; 3 = strongest expression.

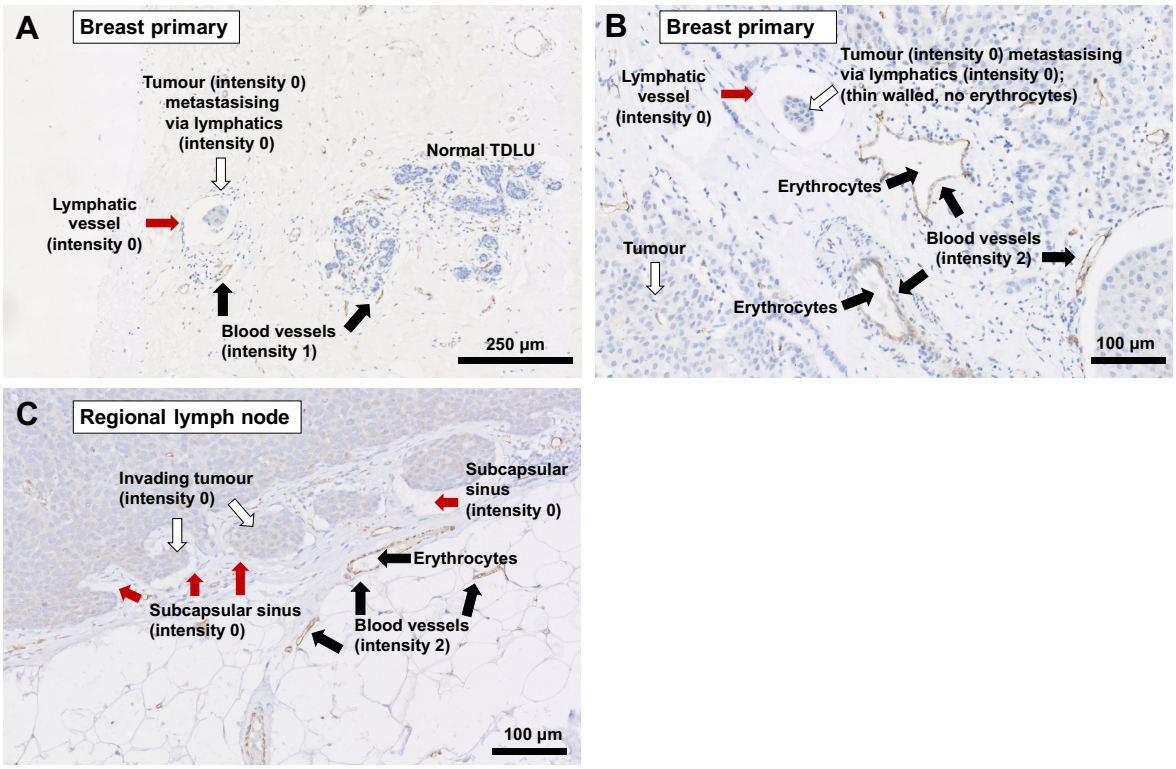


Figure 7.10: ELTD1 does not appear to be expressed by the lymphatic system used by primary breast tumours for metastatic spread. Red arrows indicate lymphatics, black arrows indicate blood vessels or erythrocytes within blood vessels, and black arrows indicate tumour. **A)** Representative image of a primary breast tumour lymphatic vessel containing metastasising breast tumour. Both tumour and lymphatic endothelium are IHC negative for ELTD1 (score 0). Adjacent to normal TDLU, ELTD1 IHC positive (score 1) blood vessels are visible**. B)** In this image, erythrocytes are visible within the ELTD1 IHC positive (score 2) blood vessels near to the ELTD1 IHC negative (score 0) lymphatic vessel containing metastasising breast tumour. **C)** Representative image showing that the lymph node subcapsular sinus (in regional nodal metastases) is ELTD1 IHC negative (score 0) as tumour metastases enter the lymph node from the breast. ELTD1 IHC positive (score 2) blood vessels with erythrocytes are visible nearby. (Abbreviations: TDLU=terminal duct lobular unit)

7.4.3.2 Tumour vascular ELTD1 is differentially expressed between primary breast cancer and regional lymph node metastases

Next, the question of whether vascular ELTD1 is differentially expressed between the primary breast tumour and regional node metastases was explored. This was performed by comparing the average ELTD1 IHC intensity scores for the primary and metastasis sites. This was performed for both normal vessels (located at the periphery of the biopsies) and for tumour vessels.

Results reveal that although normal vessel ELTD1 expression was not differentially expressed, tumour vascular ELTD1 expression was significantly differentially expressed between primary breast cancer and regional nodal metastases, with ELTD1 expression levels decreasing in the regional nodal metastases (Figure 7.11 A). Graphical representations showing the primary and metastasis vascular ELTD1 expression trend for each patient are presented for normal vessels (showing no change) (Figure 7.11 B) and tumour vessels (showing differential downward expression) (Figure 7.11 C). It can be argued that the differential change is small and thus potentially irrelevant. What goes against this is that a significant difference was observable despite the small sample size. This may suggest that once the breast tumour metastasises to the regional lymph node, it alters its VEGF secretion patterns, leading to a decrease in ELTD1 expression. Additionally, there is more tumour bulk in the primary tumour site, which may further may explain why there is greater ELTD1 expression in the primary breast tumour vessels. To explore this further, staining VEGF in the tumour and regional lymph node metastatic sites and comparing this to ELTD1 staining in the same sites is planned for the future.

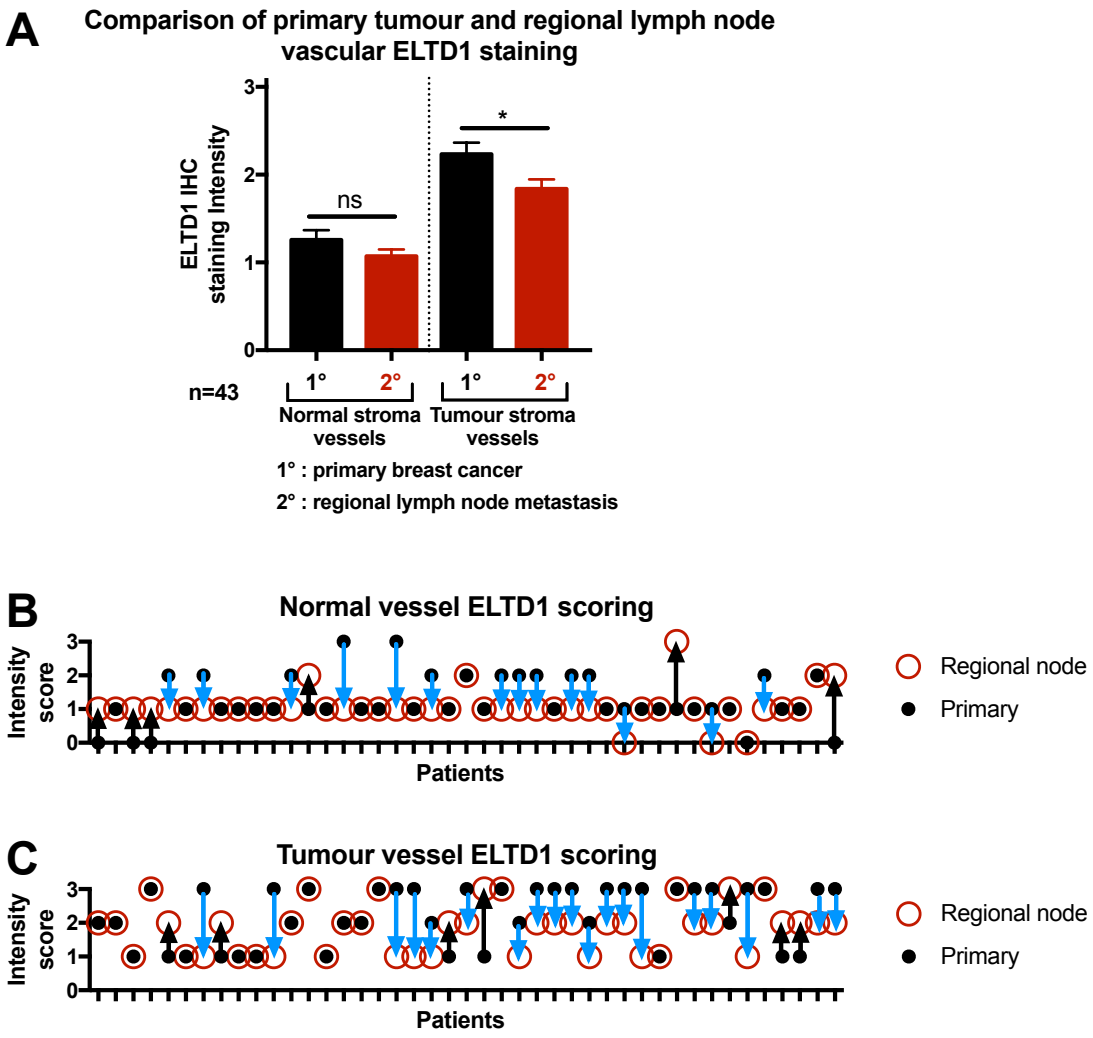


Figure 7.11: Comparison of vascular ELTD1 IHC staining in primary breast cancer and regional lymph node metastases reveals that tumour vascular ELTD1 is differentially expressed between primary breast cancer and regional lymph node metastases. A) Graph showing mean ELTD1 IHC intensity (0-3) for both primary breast cancer (labelled as 1° in graph; black bars) and regional lymph node metastases (labelled as 2° in graph; red bars). Tumour vessel ELTD1 expression is differentially expressed between primary breast cancer and regional nodal metastases, with ELTD1 expression levels decreasing in the regional nodal metastases (paired Student's *t* test; $p = 0.01$). There is no significant differential expression for normal stroma vascular ELTD1 expression between primary breast

cancer and regional nodal metastases (paired Student's *t* test; $p = 0.2$). **B)** Graphical representation of normal stroma vascular ELTD1 IHC intensity scores for each patient. For the majority of patients, there is no difference in normal vessel ELTD1 expression between the primary tumour and the regional metastatic node. Black circles indicate expression in the primary tumour and red circles indicate expression in the regional nodal metastasis. Black arrows indicate upward expression from primary tumour to metastatic node in the same patient; blue arrows indicate downwards expression in the same patient. **C)** Graphical representation (using the colour scheme described above) of tumour vessel ELTD1 IHC intensity scores for each patient. This shows that for the majority of patients, tumour vessel ELTD1 expression decreases (blue arrow) in the regional nodal metastasis and is thus differentially expressed.

7.4.3.3 Vascular ELTD1 expression and survival

Next, survival analyses were performed to determine whether vascular ELTD1 correlated with either RFS or OS. For each analysis, patients were divided into two groups: one with low ELTD1 expression (IHC score 0-1) and one with high ELTD1 expression (IHC score 2-3).

Results revealed that tumour vessel ELTD1 expression in primary breast cancer correlated significantly with survival, revealing that patients with low tumour vessel ELTD1 expression had an improved RFS (Log-rank (Mantel-Cox) test *p* value = 0.04) (Table 7.3 and Figure 7.12 A). There was no significant survival correlation with any of the other vascular ELTD1 expression comparisons performed (Table 7.3). This was a surprising result as this was opposite to what our laboratories had found in other tumour types (Masiero et al., 2013). In addition to having a significantly larger study population than ours, these studies used TMAs and not whole tumour biopsy sections and were not performed on breast cancer. Interestingly, the relationship between low tumour vessel ELTD1 and improved survival did not appear to be an isolated finding in our comparisons. Despite the lack of significance in the other tumour vessel ELTD1 comparisons, each comparison appeared to follow the same trend: patients with low levels of tumour vessel ELTD1 expression all appeared to have a slower deterioration and better survival than patients with high ELTD1 levels (Figure 7.12 B-D).

In summary however, although the relationship between low tumour vessel ELTD1 and improved RFS in primary breast cancer is statistically significant, it is important

to bear in mind that the study's sample size is too small to make any definite inferences on this finding, especially when it goes against previous results from a much larger study. As this is an exploratory pilot study, a study with a larger patient population will be needed before calling judgment on this question.

	Primary breast cancer		Regional node metastasis	
Log-rank *p* value:	**RFS**	**OS**	**RFS**	**OS**
Normal (non-tumour) vessel ELTD1	0.9	0.9	0.3	0.4
Tumour vessel ELTD1	0.04*	0.07	0.2	0.3

Table 7.3: Vascular ELTD1 expression and survival. Only tumour vessel ELTD1 expression in primary breast cancer correlated with a significant effect on survival (Log-rank (Mantel-Cox) test *p* value = 0.04). Comparisons performed with ELTD1 expressing patients divided into low (IHC score 0-1) versus high (IHC score 2-3) vascular ELTD1 expressing groups. * indicates the degree of significance. (Abbreviations: OS=overall survival; RFS=relapse-free survival).

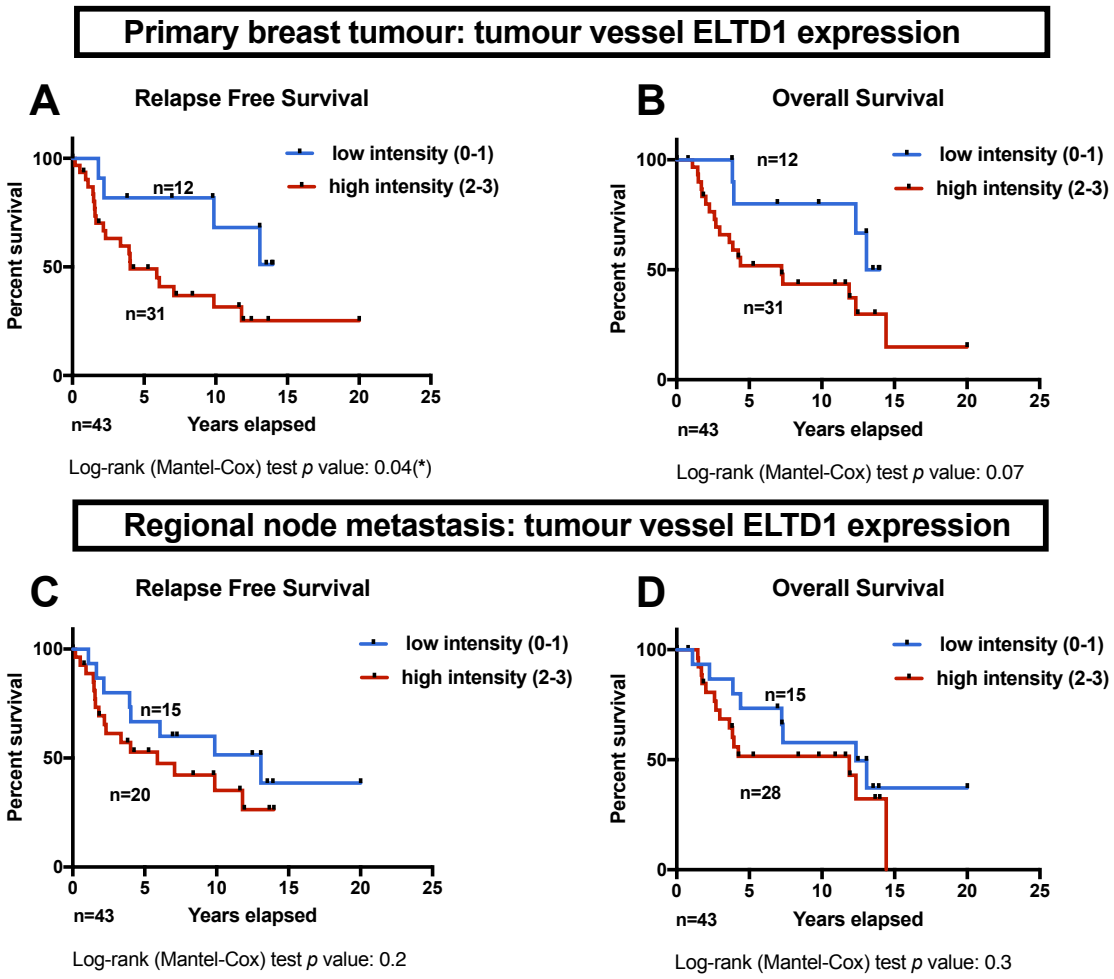


Figure 7.12: Tumour vessel ELTD1 expression and survival. Comparisons were performed by dividing patents into 2 groups: those with low ELTD1 expression (IHC score 0-1) and those with high ELTD1 expression (IHC score 2-3). **A)** Tumour vessel ELTD1 expression in primary breast cancer correlates significantly with RFS: patients with low ELTD1 expression have an improved RFS (Log-rank (Mantel-Cox) test *p* value = 0.04). **B)** Tumour vessel ELTD1 expression in primary breast cancer does not correlate significantly with OS, however it follows a similar trend with low ELTD1 expression patients appearing to do better (Log-rank (Mantel-Cox) test *p* value = 0.07). **C)** Tumour vessel ELTD1 expression in primary breast cancer in regional node metastases does not correlate significantly with RFS (Log-rank (Mantel-Cox) test *p* value = 0.2). Despite this, the survival curve suggests that

patients with low ELTD1 expression appear to do better. **D)** Tumour vessel ELTD1 expression in primary breast cancer in regional node metastases does not correlate significantly with OS (Log-rank (Mantel-Cox) test *p* value = 0.3). (Abbreviations: OS=overall survival; RFS=relapse-free survival).

7.4.3.4 Tumour vascular ELTD1 expression combined with other characteristics and survival

Next, survival analyses were performed on patients divided by vascular ELTD1 expression and sub-divided by other breast cancer characteristics. Similar to the previous survival analyses, tumour vessel ELTD1 expression was divided into two groups: low expression (IHC score 0-1) and high expression (IHC score 2-3). Table 7.4 lists the number of patients divided by tumour vessel ELTD1 expression and subdivided by an additional characteristic.

Following this, survival analyses were performed on the various subgroups. This revealed that in patients with 4-9 tumour positive lymph nodes, low ELTD1 expression significantly correlated with improved RFS and OS (RFS: Log-rank (Mantel-Cox) test *p* value = 0.02; OS: Log-rank (Mantel-Cox) test *p* value = 0.03) (Table 7.5). Additionally, in patients with ER positive primary breast tumours, low ELTD1 significantly correlated with improved OS (Log-rank (Mantel-Cox) test *p* value = 0.03; 3) (Table 7.5). Lastly, patients with HER2 negative primary breast tumours, low ELTD1 significantly correlated with improved RFS and OS (RFS: Log-rank (Mantel-Cox) test *p* value = 0.03; OS: Log-rank (Mantel-Cox) test *p* value = 0.01) (Table 7.5). The remainder of the survival analyses yielded non-significant

results (Table 7.5). These results need to be treated with caution as they are all limited by the small size of each subgroup due to small size of the study's patient population. Nonetheless, is interesting to note that these results are similar to the previous section's vascular ELTD1 expression and survival result, namely, low ELTD1 expression appears to correlate with improved survival. However, before these findings can be accepted, these analyses will need to be repeated on a larger number of patients.

	Primary breast tumours		Regional lymph node metastases	
Tumour vessel ELTD1 IHC score:	**0-1:**	**2-3:**	**0-1:**	**2-3:**
Age at diagnosis				
Age < 50 years	1	8	3	6
Age > 50 years	11	23	11	22
Primary tumour Size:				
T1 (<2 cm)	3	6	4	5
T2 (>2 cm <5 cm)	7	19	8	18
T3 (>5 cm)	2	6	3	5
Tumour grade:				
Grade 1	1	0	1	0
Grade 2	8	10	16	2
Grade 3	3	21	21	3
Number of positive lymph nodes:				
pN1 (1-3 nodes)	7	16	10	13
pN2 (4-9 nodes)	3	10	5	8
pN3 (>10 nodes)	2	5	1	6
Relapse status during follow-up				
Relapse negative	8	11	12	7
Relapse positive	4	20	16	8
Relapse site (relapse cases n=24)				

Ipsilateral breast	1	4	2	3
Contralateral breast	0	3	0	3
Metastatic disease	3	13	6	10
ER status				
ER negative	1	19	4	16
ER positive	11	12	11	12
HER2 status				
HER2 negative	10	23	13	20
HER2 positive	2	8	3	7
Molecular subtype				
Luminal A	9	11	11	9
Luminal B	2	1	0	3
Triple negative	1	11	1	11
HER2	0	8	3	5

Table 7.4: Frequency table listing number of patients according to tumour vessel ELTD1 IHC score and breast tumour characteristics. As per previous analyses, tumour vessel ELTD1 expression was divided into two groups: low ELTD1 expression (IHC score 0-1) and high ELTD1 expression (IHC score 2-3).

	Primary breast tumours		Regional node metastases	
Log-rank *p* value:	**RFS**	**OS**	**RFS**	**OS**
Number of positive lymph nodes:				
pN1 (1-3 nodes)	0.7	0.8	0.7	0.4
pN2 (4-9 nodes)	0.02*	0.03*	0.7	0.9
pN3 (>10 nodes)	0.6	0.6	0.1	0.1
ER status				
ER negative	0.4	0.3	0.5	0.7
ER positive	0.09	0.03*	0.9	0.3
HER2 status				
HER2 negative	0.03*	0.01*	0.6	0.4
HER2 positive	0.9	0.6	0.4	0.3
Age at diagnosis	0.3	0.3	0.7	0.7
Primary tumour Size:	0.5	0.4	0.8	0.6
Primary Tumour grade:	0.3	0.5	0.7	0.6
Molecular subtype	0.3	0.4	0.8	0.1

Table 7.5: Survival analyses performed on tumour vessel ELTD1 expression combined with multiple breast cancer characteristics. Patients were divided by tumour vessel ELTD1 expression (low versus high) and were then further divided into according to the various breast cancer characteristics listed. In patients with 4-9 positive lymph nodes or HER2 negative primary breast tumours, low ELTD1 significantly correlated with improved RFS and OS. In patients with ER negative

primary tumours, low ELTD1 significantly correlated with improved OS. None of the other combinations yielded positive results. Because of the small subgroup sizes, these results need to be retested in a larger patient population.

7.4.4 Tumour cell ELTD1 expression in primary breast cancer and regional lymph node metastasis

Experiments performed at the start of this results chapter showed that breast cancer cell lines do not express ELTD1 (Figure 7.2 and Figure 7.3). Despite this, a number of histological sections examined during the breast cancer study revealed positive ELTD1 IHC staining within tumour cells. This section explores these findings.

7.4.4.1 A minority of breast cancer cells express ELTD1 within primary breast tumours and regional lymph node metastases

A histogram was created to determine the distribution of tumour cell ELTD1 IHC staining scores for primary breast tumour and regional node metastasis samples. Results revealed that 16% (n=7) of primary breast cancer cases and 12% (n=5) of regional lymph node metastases expressed ELTD1 at a high level (IHC score 2-3) (Figure 7.13). In the majority of samples however, tumour cells either did not express ELTD1 (IHC score 0) or only did so weakly (IHC score 1) (Figure 7.13). Figure 7.14 shows the representative IHC range of tumour cell ELTD1 expression for primary breast tumours. A representative IHC range of tumour cell ELTD1 expression in regional node metastases is presented in Figure 7.15.

Regarding the molecular subtype of the 7 primary breast tumours which expressed high tumour cell ELTD1, 3 were Luminal A, 2 were Triple Negative and 2 were HER2 positive. Of these 7 cases, only 2 (1 Luminal A and 1 Triple Negative) shared a similar result within their regional node metastasis, with the remainder of cases exhibiting negative (IHC score 0) or weak (IHC score 1) tumour cell ELTD1

expression in their respective metastatic regional nodes. Of the 5 regional node metastasis cases with high tumour cell ELTD1 expression, 3 were Luminal A, 1 was Luminal B, and 1 was Triple Negative. Three of these cases exhibiting negative (IHC score 0) or weak (IHC score 1) tumour cell ELTD1 expression in their respective primary breast tumours. These results show that high tumour cell ELTD1 expression may alternate between the primary and metastatic site, suggesting the possibility that tumour cell ELTD1 expression is regulated by microenvironment cues. However, this needs to be tested in a much larger patient population.

Lastly, for all the above cases with high tumour cell ELTD1 expression, tumour vessel ELTD1 expression was also high (IHC score 2-3). Although this is an interesting observation, the relationship between vessel and tumour cell ELTD1 expression remains unclear as the majority of slides with high vascular ELTD1 expression contained tumour cells with no ELTD1 expression.

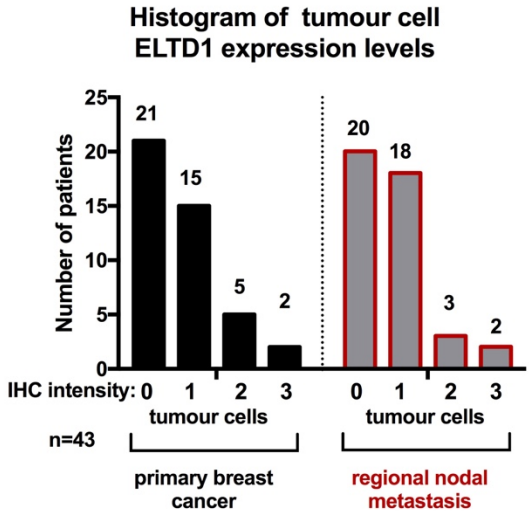


Figure 7.13: A minority of breast tumour cells express ELTD1 within both primary breast cancer and regional node metastases. Histogram showing the range of tumour ELTD1 IHC staining for both primary breast cancer and regional lymph node metastases. The majority of cases do not express ELTD1 (IHC score 0), or do so weakly (IHC score 1). Only 16% (n=7) of primary breast cancer cases and 12% (n=5) of regional lymph node metastases expressed high level ELTD1 expression (IHC score 2-3).

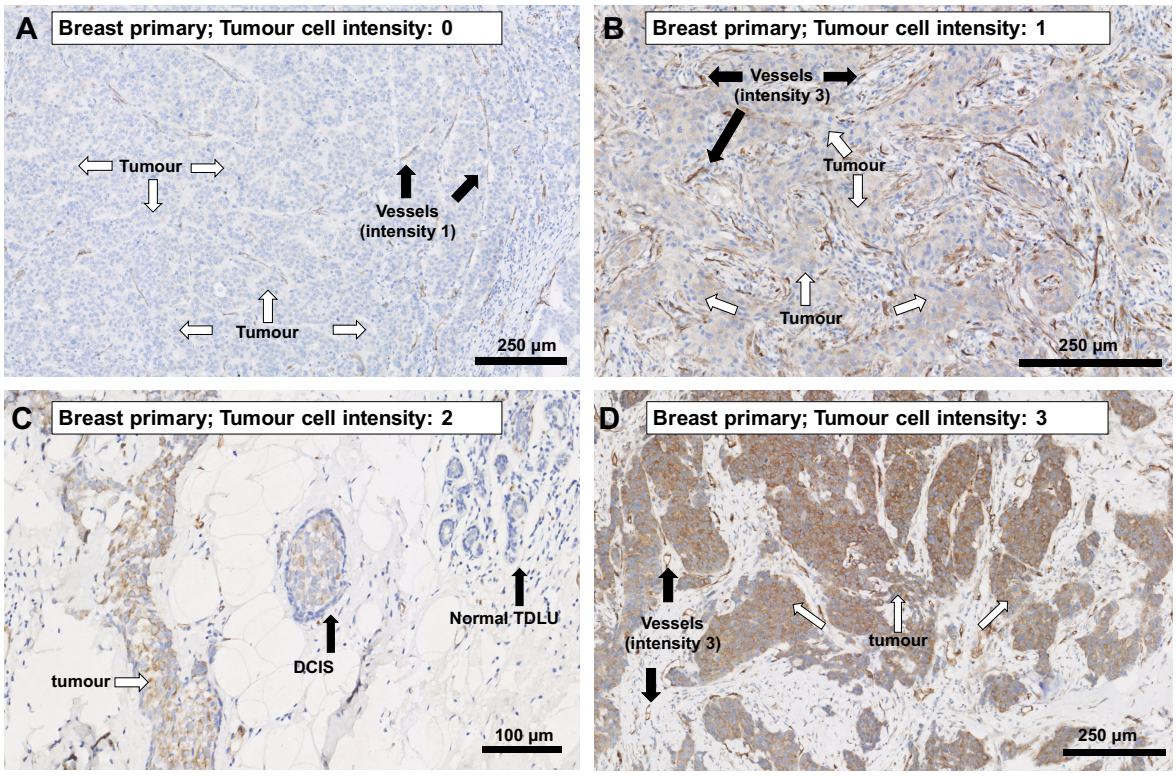


Figure 7.14: Representative images of tumour cell ELTD1 IHC staining within the primary breast tumour, showing the range of tumour cell ELTD1 staining (IHC intensity scores 0-3). White arrows point to tumour cells; black arrows point to tumour vessels. **A)** Representative image showing tumour cell ELTD1 IHC intensity score 0 (negative ELTD1 expression). Vascular ELTD1 IHC intensity is 0 (negative). **B)** Representative image showing tumour cell ELTD1 IHC intensity score 1 (weak expression). Vascular ELTD1 IHC intensity is 3 (strongest expression). **C)** Representative image showing tumour cell ELTD1 IHC intensity score 2 (moderate expression) within the infiltrating tumour. ELTD1 expressing ductal carcinoma in situ (DCIS) cells are also visible as are ELTD1 negative cells within adjacent normal breast tissue terminal ductal lobular units (TDLU). **D)** Representative image showing tumour cell ELTD1 IHC intensity score 3 (strongest expression). Vascular ELTD1 IHC intensity is 3 (strongest expression). (Abbreviations: DCIS=ductal carcinoma in situ; TDLU=terminal ductal lobular unit)

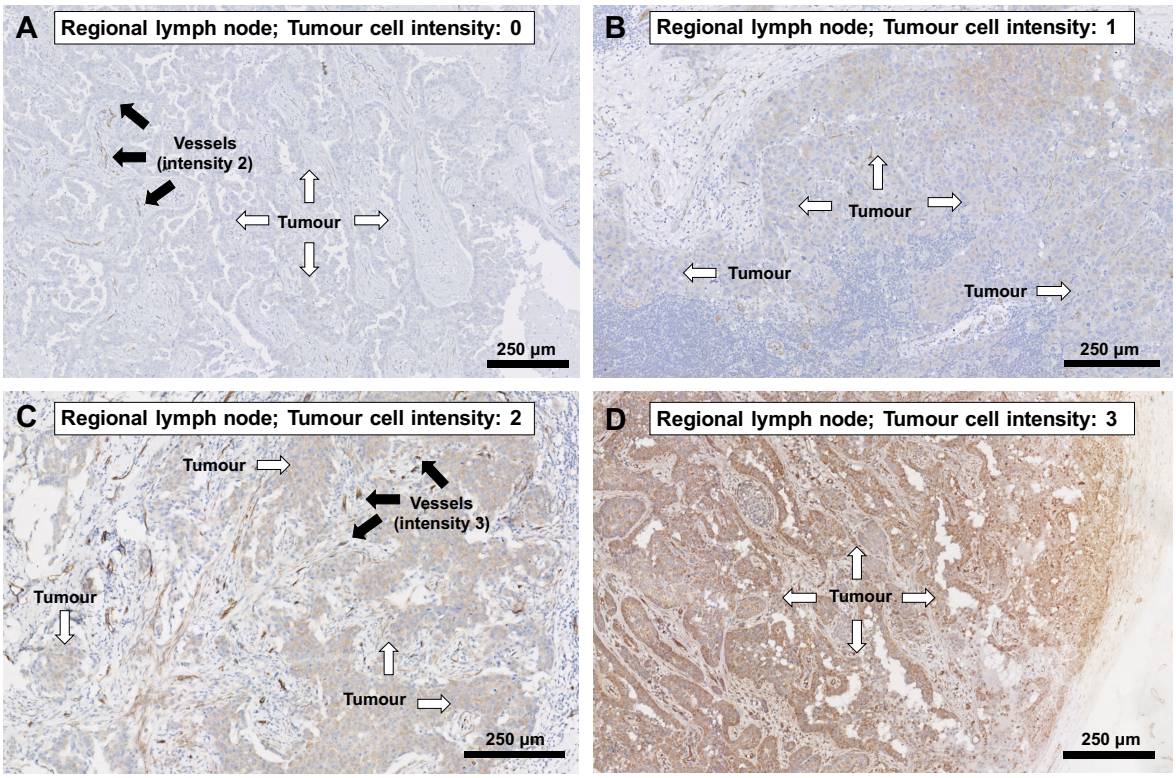


Figure 7.15: Representative images of tumour cell ELTD1 IHC staining within regional lymph node metastases, showing the range of tumour cell ELTD1 staining (IHC intensity scores 0-3). White arrows point to tumour cells; black arrows point to tumour vessels. **A)** Representative image showing tumour cell ELTD1 IHC intensity score 0 (negative ELTD1 expression). Vascular ELTD1 IHC intensity is 2 (moderate). **B)** Representative image showing tumour cell ELTD1 IHC intensity score 1 (weak expression). In the right corner of the image, a small area of the tumour expresses higher levels of ELTD1 with an IHC score of 2 (moderate expression). **C)** Representative image showing tumour cell ELTD1 IHC intensity score 2 (moderate expression) within the infiltrating tumour. Vascular ELTD1 IHC intensity is 3 (strongest expression). **D)** Representative image showing tumour cell ELTD1 IHC intensity score 3 (strongest expression). Vascular ELTD1 IHC intensity is 3 (strongest expression).

7.4.4.2 Tumour cell ELTD1 expression is not differentially expressed and is expressed at a lower intensity than vascular ELTD1 expression.

Tumour cell ELTD1 expression was then tested for differential expression between the primary breast tumour and regional node metastases. This was performed by comparing the average tumour cell ELTD1 IHC intensity scores for the primary and metastasis sites.

Results reveal that tumour cell ELTD1 expression was not significantly differentially expressed between primary and regional node metastases (Figure 7.16 A). Additionally, results show that the mean tumour cell ELTD1 expression was significantly less than the mean normal and tumour vessel ELTD1 expression (Figure 7.16 A). A graphical representation of each patient's tumour cell IHC ELTD1 expression score is presented in Figure 7.16 B. This visualisation highlights the finding that majority of patients which did express high levels of tumour cell ELTD1 (IHC score 2-3) did so only in one tumour site (and not both). As this is a small pilot study, these analyses will need to be performed on a larger population.

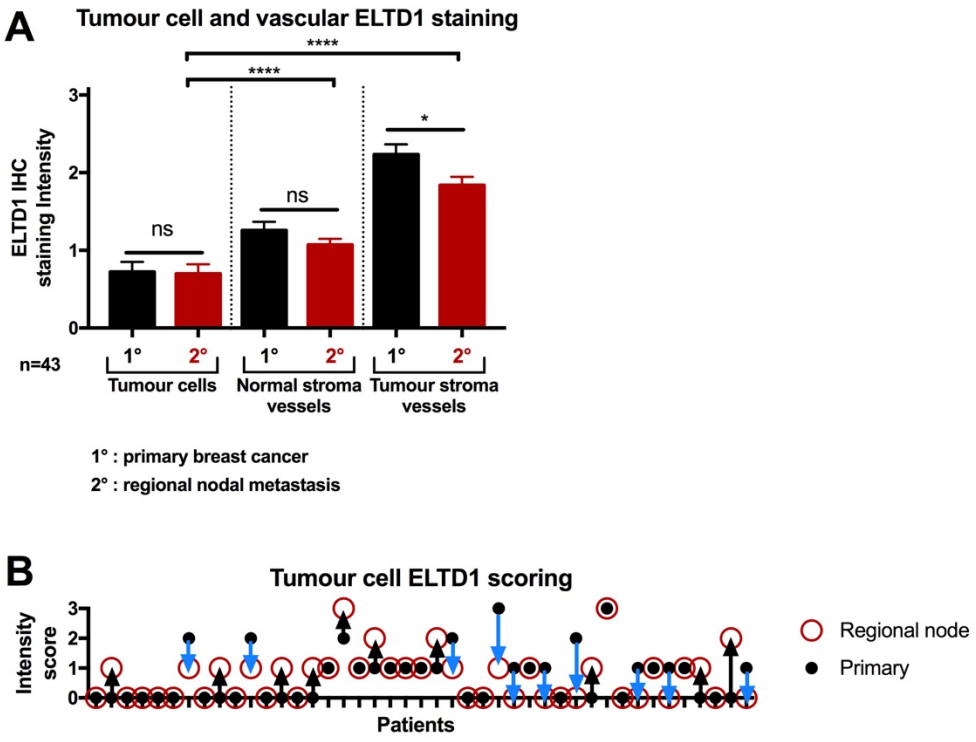


Figure 7.16: ELTD1 expression in tumour cells is not differentially expressed and is expressed at a lower level than vascular ELTD1 expression. **A)** Comparison of ELTD1 IHC staining in primary breast cancer and regional lymph node metastases reveals that tumour cell ELTD1 expression is not differentially expressed between primary breast tumours and regional node metastases (unpaired Student's t test; p = 0.9). Graph displays mean ELTD1 IHC intensity (0-3) for both primary breast cancer (labelled as 1° in graph; black bars) and regional lymph node metastases (labelled as 2° in graph; red bars). Additionally, tumour cell ELTD1 expression is lower than vascular ELTD1 expression when compared to normal and tumour vessels (paired Student's t test; p <0.0001 for both comparisons). As has been previously shown earlier in this chapter, normal vessel ELTD1 expression is not differentially expressed (paired Student's t test; p = 0.2), whilst tumour vessel ELTD1 is (paired Student's t test; p = 0.01). **B)** Graphical representation of tumour cell ELTD1 IHC intensity scores for each patient. For the

majority of patients, there was no difference in tumour cell ELTD1 expression between the primary tumour and the regional metastatic node. Black circles indicate expression in the primary tumour and red circles indicate expression in the regional nodal metastasis. Black arrows indicate upward expression from primary tumour to metastatic node in the same patient; blue arrows indicate downwards expression in the same patient.

7.4.4.3 Tumour cell ELTD1 expression and survival

Next, the relationship between tumour cell ELTD1 expression and RFS and OS was examined. For this, patients were divided into two groups according to tumour cell IHC scores: one with low tumour cell ELTD1 expression (IHC score 0-1) and one with high tumour cell ELTD1 expression (IHC score 2-3). Following this, survival analyses were performed. This was performed for both primary breast tumours and for regional node metastases.

Results revealed that tumour ELTD1 expression had no effect on survival in either primary breast tumours or in regional node metastases (Table 7.6). These results however need to be treated with caution as the ELTD1 expressing tumour cell group was very small in an already small patient population. Thus, these analyses will need to be performed on a larger patient population before they can be accepted.

Lastly, because of the small number of ELTD1 expressing tumour cell cases, it was not possible to perform statistically meaningful survival analyses on cases subdivided by tumour cell ELTD1 expression as well as various breast cancer

characteristics (as had been done earlier with the tumour vascular ELTD1 expression analyses). As this is a small pilot study, these analyses will need to be performed on a larger patient population in the future.

	Primary breast tumours		Regional node metastases	
Log-rank *p* value:	**RFS**	**OS**	**RFS**	**OS**
Tumour cell ELTD1 expression	0.5	0.3	0.9	0.6

Table 7.6: Tumour cell ELTD1 and survival. Tumour cell ELTD1 expression did not correlate with survival in either the primary breast tumour or regional node metastases. Comparisons were performed with patients divided into tumour cell ELTD1 low (IHC score 0-1) versus high (IHC score 2-3) groups. As the ELTD1 expressing tumour cell population was very small within an already small study population, these survival analyses will need to be performed on a larger population before results the results can be accepted. (Abbreviations: OS=overall survival; RFS=relapse-free survival).

7.5 Discussion

This chapter investigates ELTD1's role within the tumour microenvironment of breast cancer. Specifically, it investigates ELTD1's role within the primary breast tumour and regional node metastasis environments. What makes this study unique is that this is the first study to look at ELTD1 within the primary and secondary tumour microenvironment in any tumour type. This discussion reviews the chapter's results and its limitations. Additionally, plans for future experiments are explored.

ELTD1 was first associated with cancer when it was found to be upregulated in the glioblastoma tumour microenvironment, in both vascular endothelial cells and within tumour cells (Dieterich et al., 2012, Towner et al., 2013). In glioblastomas, ELTD1 has been shown to be important for tumour cell survival. First, in glioblastoma cell lines, microRNA-139-5p was found to suppress ELTD1, inducing a decrease in cell proliferation and an increase in apoptosis (Dai et al., 2015). More recently, *ELTD1* mRNA silencing increasing glioblastoma cell death *in vitro* and *in vivo* (Serban et al., 2017, Ziegler et al., 2017). In the ELTD1 overexpression chapter, I show that ELTD1 is important for inducing the angiogenic tip cell phenotype in endothelial cells, leading to the expansion of the vascular network. It is possible that ELTD1 overexpression in glioblastomas aids the tumour in an analogous manner thus helping it grow. It is also possible that ELTD1 expressing glioblastoma cells are involved in angiogenesis through the process of vascular mimicry, which entails tumour cells lining new vessels instead of endothelial cells. Although these are untested hypothesis, this would explain why silencing ELTD1 is as good as anti-VEGF therapy for glioblastomas (Ziegler et al., 2017). ADGRD1/GPR133 is another adhesion GPCR that has been shown to be upregulated within Glioblastoma tumour

cells, specifically being upregulated in CD133 expressing glioblastoma stem cells (Bayin et al., 2016). In these cells, high ADGRD1/GPR133 expression was noted to be induced by hypoxia through a Hif1α binding site on ADGRD1/GPR133's promoter sequence. To determine whether this also applies to ELTD1, a review of the genomic regions upstream and downstream of ELTD1's coding sequence were reviewed for HIF binding motifs, revealing no binding sites. Additionally, HUVECs cultured under hypoxic conditions failed to show any changes in ELTD1 protein expression compared to normoxic HUVECS (unpublished data; not included in thesis).

Our laboratories showed that ELTD1 was upregulated in the tumour vascular endothelium of a range of tumours: head and neck, renal, colorectal and ovarian cancer (Masiero et al., 2013). For the majority of these tumour types, ELTD1 was shown to be negatively expressed by tumour cells with only a minority of tumour cells weakly expressing ELTD1. This was in direct contrast to the high levels of ELTD1 expressed by glioblastomas. Our laboratories found that by silencing endothelial ELTD1 expression in mice (by means of siRNA incorporated into chitosan nanoparticles), both an ovarian and a colorectal human tumour xenograft model shrunk. As these tumour cells did not express ELTD1, the effect was understood to be related to the vascular response to ELTD1 silencing. In contrast, with glioblastomas, ELTD1 silencing is likely to directly affect both vessels and tumour cells. Additionally, our laboratories found that high levels of tumour vessel ELTD1 expression (biopsied prior to the initiation of anti-cancer therapy) correlated significantly with improved RFS in patients in with head and neck, renal, colorectal and ovarian cancers (Masiero et al., 2013). This effect being hypothesised to be

related to improved micro-vessel density and resultant drug delivery. More recently, ELTD1 has been shown to be part of a gene expression signature (comprising 19 genes) associated with colorectal cancer survival (Abdul Aziz et al., 2016). In this series, *ELTD1* mRNA was expressed at higher levels in patients whose OS was under 5 years compared to patients who survived over 5 years. This result goes against our teams' earlier findings and will need to be explored further.

In this chapter, I show that across many human tumour types, ELTD1 is not specifically targeted for alteration. Additionally, the majority of cancer cells lines are shown not to express ELTD1 with the exceptions being the primary brain tumour cell lines. The role of ELTD1 within the primary breast tumour and regional lymph node metastasis was then explored. This study was performed as a pilot study for a larger future study. The pilot study is limited by its small study population (n=43) and will need to be followed up by a study on a larger population (n=>100) to verify results and solve unanswered questions. In terms of strengths, this study is the first to investigate ELTD1 within a matched primary and secondary tumour environment. Additionally, the follow up period for the cases reviewed was very long (up to 18 years).

This study found that tumour vessel ELTD1 is differentially expressed between primary breast cancer (higher expression) and regional nodal metastases (lower expression). As this change was small, it remains unclear if this is biologically significant. However, the difference was significant despite the small sample size. As ELTD1 is induced by VEGF expression (Masiero et al., 2013) and breast cancers

overexpress VEGF (Weidner et al., 1991), this may suggest that breast tumours alter their VEGF secretion patterns once they metastasise, leading to a decrease in ELTD1 expression. Alternatively, the decrease may be related to the fact that there is more tumour bulk in the primary tumour and thus more VEGF secreted. To explore this further, staining VEGF in the tumour and regional lymph node metastatic sites and comparing this to ELTD1 staining in the same sites is planned for the future.

Additionally, the study found that tumour vascular ELTD1 increased with increasing proximity to breast tumours and that ELTD1 expression increased in tumour vessels when contrasted to normal vessels in both primary breast cancer and involved nodes. This is similar to previous findings in head and neck, renal, colorectal and ovarian cancer (Masiero et al., 2013). Interestingly, ELTD1 did not appear to be expressed by the lymphatic vessels used by the primary breast tumours for metastatic spread. Although the lymphatic marker LYVE1 was not stained for, lymphatics containing metastasising tumour were identified visually by our collaborating histopathologist, Dr. Roxanis. This suggests that ELTD1 plays a role in preventing or regulating breast cancer metastasis. These samples will be stained with LYVE1 and this will be further examined in the larger future study.

The ELTD1 survival analyses are all limited by the small sample size of the pilot study and will require being repeated as the planned larger future study before being properly accepted. The study found that patients with low tumour vessel ELTD1 expression had a statistically significant increase in RFS. A similar survival trend

was noted on the survival curves in regional node metastases although these were not statistically significant. When ELTD1 expression combined with other breast cancer characteristics was analysed for survival, similar results were noted, showing that low ELTD1 expression coupled with either ER positive status, HER2 negative status and 4-9 positive lymph node were associated with a statistically significant improvement in RFS and or OS. These results go against our previous findings in head and neck, renal, colorectal and ovarian cancers where low ELTD1 (in pre-treatment biopsies) correlated with improved RFS (Masiero et al., 2013). That said, the pilot study's sample size is too small to make any definite inferences on these findings, especially when it goes against previous results from a much larger previous study in other tumour types. These results will need to be repeated and re-examined in the planned larger future study.

Lastly, despite breast cancer cell lines being negative for ELTD1, this study revealed that ELTD1 is strongly expressed a minority of breast cancer cells within the primary breast tumour (7/43 cases) and regional lymph node metastases (5/43 cases). Of the 7 primary breast tumour cases with high tumour cell ELTD1 expression, only 2 cases had a similar result in their matched regional node metastasis. This suggests that tumour cell ELTD1 expression may alternate between the primary and metastatic site, suggesting the possibility that tumour cell ELTD1 expression is regulated by microenvironment cues. This will need to be tested in a future experiment. Additionally, the cases with high cancer cell ELTD1 expression did not belong to a specific molecular subtype of breast cancer. As the role of high tumour cell ELTD1 in breast cancer remains unclear, a future experiment is planned where ELTD1 will be overexpressed in a panel of breast

cancer cell lines to determine its effect. Lastly, unlike tumour vessel ELTD1 expression, there was no associated differential expression and tumour cell ELTD1 expression did not correlate with survival benefit. These results will need to be verified in a larger future study.

7.6 Conclusion

This chapter reveals that ELTD1 is not targeted for alteration in a wide range of cancers, is not expressed in the majority of cancer cell lines and plays an important role in the breast cancer primary and regional node metastasis sites. ELTD1 expression within tumour vessels was noted to be increased with increasing proximity to breast tumour cells and was found to be differentially expressed between primary and metastatic sites. Additionally, ELTD1 did not appear to be expressed by lymphatic vessels used for metastasis. A minority of breast tumours cells were also noted to strongly express ELTD1. Survival analyses were also performed but will require verification in a larger study to be performed in the future before their results are accepted.

Chapter 8: Final discussion and future plans

In this final discussion, the key results from each chapter are discussed and plans for future experiments are presented.

8.1 ELTD1's evolution

The aims of the ELTD1 evolution work was to investigate ELTD1's conservation and evolution in extant species, to gain insight into how ELTD1 functions by investigating whether *ELTD1* has lost or gained any domains during its evolution, and to contrast and compare ELTD1 to other adhesion GPCRS to determine whether *ELTD1* is ancestral to other adhesion GPCRS. During the course of the investigation, all of these questions were answered.

The presence of a closed circulatory system containing endothelial cells is a characteristic of all vertebrates (Monahan-Earley et al., 2013). Results from this project show that *eltd1* is not expressed in the very first vertebrate group (jawless fish) and arose approximately 435 million years ago alongside the core angiogenic gene *vegfr2* within members of the next vertebrate group, bony fish. In all subsequent vertebrates, *ELTD1*'s orthologues are highly conserved, to a similar degree as *VEGFR2*. The suggests that ELTD1's incorporation into the vertebrate

genome coincided with increasing complexity of the closed circulatory system, suggesting that ELTD1 is an evolutionarily important vascular gene. Although vertebrate cell biology contains many instances of redundancy, it is very likely that during *eltd1's* incorporation into the bony fish genome it was one of only a few vascular genes and thus critical for life. This is emphasised by this study's finding that *eltd1's* conservation in bony fish (compared to *ELTD1)* being greater than the conservation for the fish exome compared to human. This further potentially provides one possible explanation as to why *eltd1* silencing in zebrafish embryos is lethal whilst causing no lethality in mice (Masiero et al., 2013, Xiao et al., 2012).

Work on ELTD1's orthologues also revealed three evolutionary ELTD1 variants based on deletions to ELTD1's EGF domains. The majority of orthologues express either variant 1 (1x EGF and 2x EGF Ca^{2+} domains) or variant 2 (1x EGF and 1x EGF Ca^{2+}) with a small minority expressing variant 3 (no EGF, 2x EGF Ca^{2+} domains). Variant 1 appears to be the oldest version of ELTD1, first expressed in bony fish with variant 2 arising in mammals from the Afrotheria group approximately 101 million years ago. Primates for example, nearly all express variant 2. Additionally, it was noted that once a vertebrate acquires variant 2 (by deleting an EGF), its descendants do not reacquire variant 1. Whilst this is interesting from an evolutionary perspective, it also provides functional insight into how ELTD1 may function as the first EGF Ca domain appears to be the most conserved and thus probably the most likely to be involved in ELTD1's cellular function in all examined vertebrate genomes.

Additionally, ELTD1's orthologues display high level of conservation at specific sites across the receptor: parts of the GAIN domain, the GPS domain and first 4 loops of the 7TM. Although the Stinger/Stachel Hypothesis applied to ELTD1 has revealed that ELTD1 does not signal like a canonical GPCR, the high level conservation of these adhesion GPCR structures suggests that these sites are highly likely to be important in ELTD1's activation and probable non-canonical signalling. Based on this high level orthologue conservation, it is also likely that ELTD1's agonist binds to ELTD1's 2^{nd}-3^{rd} or 4^{th}-5^{th} extracellular 7TM loops. Once ELTD1's signalling has been solved, experiments mutating individual amino acids within these loops should be performed to determine exactly which amino acids are important for ELTD1's activation. This will have important effect, especially when considering the development of activating or blocking ELTD1 antibodies for therapeutic use.

Lastly this work shows that *ELTD1*'s domains are closely shared between adhesion GPCR subfamily 1 and 2 with ELTD1's EGFs being most similar to ADGRE3/EMR3's EGF domains whilst ELTD1's GAIN, GPS and 7TM are most similar to ADGRL3/LPHN3. This is explained by the finding that ELTD1 is more widely present in evolutionarily early and subsequent vertebral genomes than any member of subfamily 1 or 2, suggesting that ELTD1 is possibly ancestral to members of family 2.

In summary, all of these results support the hypothesis that ELTD1 is an evolutionarily important vascular regulator, warranting further biological investigation.

8.2 Investigation of ELTD1's signalling capability

The aim of this work was to investigate ELTD1's signalling using the Stinger/Stachel Hypothesis and to investigate whether a peptide analogous to ELTD1's putative Stinger/Stachel amino acid sequence could be used as a soluble agonist.

Results revealed that ELTD1 does not signal like a conventional canonical GPCR with the Stinger/Stachel hypothesis being unable to activate Gαq, Gα12/13, Gαi or Gαs in ELTD1. The strengths of this work lie in the thoroughness of its investigation and the use of multiple methodologies to verify repeated negative results. Additionally, ELTD1's putative Stinger/Stachel peptides were found to be highly insoluble (regardless of N and C-terminal modifications to improve solubility) and did not activate canonical GPCR signalling. Limitations of the work included the use of receptor tagging and HEK293T cells (which do not constitutively express ELTD1). That said, both tagging and the use of transient expression in HEK293T cells have been successfully used in other Stinger/Stachel activation projects (Demberg et al., 2017, Wilde et al., 2016, Demberg et al., 2015, Liebscher et al., 2014). Additionally, canonical GPCR signal was not activated in ELTD1 through promiscuous binding of other adhesion GPCR peptides. Despite ELTD1's GPS being more similar to GPR133/ADGRD1, neither GPR133/ ADGRD1's or GPR114/ADGRG5's published Stinger/Stachel peptides activated canonical GPCR signalling in ELTD1.

The positive endothelial phenotype found in ELTD1 stable overexpression in HUVECS (Chapter 6) suggests that ELTD1 must signal once it is expressed on the

cell surface. These ELTD1 stable overexpressing cells are thus key for future ELTD1 signalling experiments. Using these cells, a future experiment is planned to assay canonical GPCR signalling using the HTRF FRET assays which do not require any transfection. A similar experiment will be performed in HUVECS acutely transduced with an ELTD1 lentivirus (within 48 hours of transduction). This will remove the possibility that ELTD1 overexpressing HUVECS may downregulate high level ELTD1 signalling over time as a form of compensation. Furthermore, another future experiment may include the CTF form of ELTD1 being cloned into a lentiviral vector and similar experiments performed on CTF transduced HUVECS. Additionally, the correctly truncated 7TMΔ ELTD1 should be synthesised and tested. It will be of interest to determine whether this behaves in a similar manner to the stalk-less signalling found in ADGRG1/GPR56 and ADGRB1/BAI1 (Kishore et al., 2016). Furthermore, experiments to assay β-arrestin signalling in the above lentivirus transduced HUVECS should be performed.

If the above experiments fail to reveal canonical signalling, ELTD1's non-canonical signalling must be explored. For this, proteomic evaluation of ELTD1 overexpressing HUVECS will need to be performed both in cells acutely transduced with an ELTD1 lentivirus as well as those with long term overexpression. This approach will provide a number of benefits, the principal being the discovery of ELTD1's binding partners as well as elucidating ELTD1's signalling pathway. Once ELTD1's non-canonical signalling is solved, focus should return to ELTD1's Stinger/Stachel peptides to determine if they are able to activate ELTD1's non-canonical signalling. If so, this will be a significant milestone in the ELTD1 project as it will allow us to activate ELTD1 within the tumour microenvironment of *in vivo*

cancer models. Additionally, such a result would make ELTD1 the first adhesion GPCR to activate non-canonical GPCR signalling using the Stinger/Stachel Hypothesis. Beyond this, additional questions still remain unanswered. These include how ELTD1 is recycled from the cell surface and whether ELTD1 plays an active signalling role within endosomal structures in the cell. Additionally, ELTD1's ligand(s) remain unsolved. It is probable that ELTD1's ligand is present on the cells that endothelial and vascular smooth muscle cells make contact with. Additionally, ELTD1's ligand may be present on blood cells. There is also the possibility that ELTD1 may also signal remotely if ELTD1's NTF is shed into the circulation. These questions will be examined in future experiments following elucidation of ELTD1's non-canonical signalling.

8.3 The effect of ELTD1 silencing and overexpression in endothelial cells

8.3.1 ELTD1 and endothelial metabolism

The aim of the ELTD1 silencing and overexpression chapters was to investigate ELTD1's transcriptional effect in HUVECS in order to determine new roles for ELTD1. Results from the silencing experiment revealed that ELTD1 has a novel role within endothelial metabolism, with silencing upregulating *SLC25A1,* which transports citrate out of the mitochondria, and ACLY, (which catalyses citrate into Acetyl-CoA. Acetyl-CoA then either enters the fatty acid synthesis pathway, the cholesterol synthesis pathway or is used for histone acetylation. ELTD1's suppression of SLC25A1 and ACLY is contrary to the metabolic reprogramming induced *de-novo* lipid synthesis strategy employed by many cancers (facilitated through SLC25A1 and ACLY upregulation). This may be one reason as to why the majority of cancer cell lines used in laboratory research do not express ELTD1.

Under physiological conditions, endothelial metabolism utilises glycolysis for energy production and tightly regulates fatty acid synthesis for specific angiogenesis related tasks such as endothelial cell migration (Wei et al., 2011, De Bock et al., 2013). By tightly regulating and downregulating *SLC25A1* and ACLY, ELTD1 contributes to maintaining this endothelial metabolic phenotype. Possibilities as to how ELTD1 suppresses *SLC25A1* and ACLY remain unclear. Additionally, is unknown whether the effect on SLC25A1 and ACLY is up or downstream to ELTD1. A possible future experiment may entail silencing *SLC25A1* and *ACLY* individually and together in HUVECS and performing qPCR for these genes as well as *ELTD1*.

ELTD1 silencing was found not to affect endothelial lipid synthesis as measured by the accumulation of lipid droplets or affect any of the genes involved in fatty acid synthesis. The effect of silencing on histone acetylation remains unexplored however. A possible future experiment would include testing for global and specific acetylation changes following ELTD1 silencing. As ACLY has been shown to repress key glycolytic genes through histone acetylation (*GLUT4, HK2, PFK-1* and *LSH1*)(Wellen et al., 2009), ELTD1's partial suppression of ACLY in HUVECS suggests that ELTD1 indirectly regulates glycolysis. To explore this further, a possible future metabolic flux experiment in HUVECS with and with ELTD1 silencing is warranted.

Lastly, ELTD1 overexpression in HUVECS did not appear to affect *ACLY* or *SLC25A1* expression. At a protein level, results from the silencing experiment

suggested that ELTD1's suppression of ACLY was partial rather than complete. The results that show that ELTD1's suppressive effect on both of these targets appears to have its maximum effect at physiological ELTD1 expression levels.

8.3.2 ELTD1 and Notch signalling

Results from both the ELTD1 silencing and overexpression experiments performed in HUVECS confirmed ELTD1's known relationship with the Notch signalling system by showing that ELTD1 represses DLL4. These experiments additionally revealed new relationships with Notch, with ELTD1 silencing downregulating the Notch target gene *HES2* and the Notch ligand *JAG1*, whilst ELTD1 overexpression induced *JAG1* but had no effect on *HES2.* These results correlate with the findings that ELTD1 overexpression in HUVECS induces a tip cell phenotype as DLL4 antagonises the tip cell phenotype and JAG1 is known to compete with DLL4 and induce a weaker notch signal than DLL4 (Benedito et al., 2009). The effect of ELTD1 overexpression on angiogenesis is discussed below in the ELTD1 and angiogenesis section.

Lastly, it remains unclear how ELTD1 interacts with the Notch pathway and vice versa. Are ELTD1's effects on the Notch ligands DLL4 and JAG1 downstream to ELTD1's effect on *HES2* – or could it be the other way around? To begin answering these questions, experiments could be performed where each Notch ligand or target gene is silenced before undergoing qPCR for *ELTD1*. Additional potential experiments include exposing HUVECS to DLL4 or JAG1 with and without ELTD1

silencing followed by qPCR for ELTD1 and a wider panel of Notch-associated genes.

8.3.3 ELTD1 and KIT

ELTD1 was found to negatively regulate KIT expression with ELTD1 silencing inducing KIT expression and ELTD1 overexpression repressing *KIT*. This establishes ELTD1 as a new regulator of endothelial KIT-KITLG signalling.

KIT is known to have an important role in in haematopoiesis through its expression on haematopoietic stem cells (Lennartsson and Ronnstrand, 2012). Additionally, Kit expressed on mature endothelial cells plays a role in maintaining HPC and endothelial progenitors (Yamaguchi et al., 1996). As HPC and EPC progenitors strongly express KIT, it may be possible that ELTD1's incomplete repression of KIT in endothelial cells (endothelial cells express KIT despite being repressed by ELTD1) is a possible mechanism through which endothelial cells maintain terminal endothelial. This hypothesis however requires further investigation. To date, the only known relationship between ELTD1 and HPCs is limited to the perivascular niche in breast cancer where *ELTD1* was found to be part of a gene signature regulating breast cancer progression (Ghajar et al., 2013). ELTD1's suppression of KIT thus opens up possible links with the regulation of haematopoiesis.

Lastly, during FACS performed on ELTD1 silencing there appeared to be two populations of KIT expressing HUVECS: one population with high KIT and one with low KIT expression. This was not seen with any of the other cell surface receptors

affected by ELTD1 expression and thus these separate populations require further investigation. A possible approach would be to FACS sort these two populations and perform transcriptional analysis on them both. Additional experiments include investigating whether KITLG expression is affected by ELTD1 silencing and expression as well as performing determining whether ELTD1 silencing and overexpression affects HSC interaction with endothelial cells.

8.3.4 ELTD1 and angiogenesis

Functional angiogenesis experiments performed on ELTD1 overexpressing HUVECS revealed that ELTD1 is important in enhancing an endothelial tip cell phenotype. Results showed that HUVEC ELTD1 induced various tip cell phenotype characteristics such as increased sprouting activity, decreased proliferation rate and inhibition of inter-vessel anastomoses. Overexpression did not affect migration but this may be due to the confounding effect of decreased proliferation affecting the scratch assay used. To rectify this potential issue, migration will be assayed again in the future using a two chambered Boyden Chamber. ELTD1 overexpression did not affect adhesion to angiogenesis-associated ECM components or matrigel. In contrast, ELTD1 silencing only affected sprouting and adhesion to matrigel – both negatively. The finding that ELTD1 is an important component of the endothelial tip cell phenotype is also probably why tumours induce ELTD1 expression within the tumour vasculature. Additionally, as ADGRL1/LPHN1 has been shown to function as a mechanoreceptor in the fruit fly (*Drosophila melanogaster*) (Scholz et al., 2015), could the same also apply to ELTD1 with ELTD1 sending blood flow and vascular pressure? This area remains unexplored. Additionally, what happens to ELTD1 expression when vascular pressure changes?

To investigate these questions, a useful approach could include using a flow chamber seeded with ELTD1 silenced and overexpressing HUVECS and measuring ELTD1's response to changes in flow and pressure.

Lastly, when sprouting vessels anastomose, tip cells acquire the stalk cell phenotype. Thus, the inhibition of anastomosis in ELTD1 overexpression suggests that ELTD1 expression may be modulated during the different stages of sprouting angiogenesis, with this regulation being overcome by artificial overexpression. This however remains unknown and presents a good basis for a future experiment exploring this.

Transcriptionally, ELTD1 overexpression upregulated the following related genes: *CHRNA1, ANTXR1, SLC39A6, HBB, ELMOD1, HSPA6, RYR1, JAG1* and downregulated *CCL15, CYP26B1, INPP5B, DLL4* and *KIT*. Of these genes, 5 (*ANTXR1, DLL4, JAG1, CCL15* and *CYP26B1*) have direct associations with angiogenesis. *ANTXR1* induction is associated with increased *in vivo* tumour angiogenesis (Chaudhary et al., 2012). This suggests that ELTD1's pro-angiogenesis role is mediated together with ANTXR1. It remains to be explored how and at what level ELTD1 interacts with ANTXR1. Although *CCL15* and *CYP26B1* induce angiogenesis (Hwang et al., 2004, Messner et al., 2013), ELTD1 overexpression repressed both genes. This may be explained as a compensatory response to the sustained pro-angiogenic effect of ELTD1 overexpression. The fact that this does not occur with *ANTXR1* suggests that ANTXR1 is potentially more directly affected by ELTD1. Additionally, CCL15's suppression may be associated

with the lack of migration noted with ELTD1 overexpression. *DLL4* and *JAG1* are Notch pathway ligands with DLL4 expression promoting the stalk phenotype (Hellstrom et al., 2007) and JAG1 competing with DLL4 and inducing a weaker Notch signal (Benedito et al., 2009). At the mRNA level, the effect of ELTD1 overexpression on both *DLL4* and *JAG1* is opposite to that of ELTD1 silencing. The other genes affected by ELTD1 overexpression are all reviewed in Chapter 6's discussion.

Taken together, these results provide fertile ground for many future experiments. These include migration assays using a Boyden Chamber to adequately assess whether overexpression affects migration and staining FL coELTD1 overexpressing HUVECS in both the hanging drop spheroid assay and fibrin gel bead assay for ELTD1, DLL4, JAG1, VEGFR2. This will provide invaluable information about whether ELTD1's expression is modulated in the developing vessel. Lastly, it would be useful and interesting to determine the effect of CTF coELTD1 overexpression in HUVECS and whether this produces differing results to FL coELTD1 overexpression.

8.4 ELTD1 in the primary breast cancer and regional nodal microenvironment

The focus of the final results chapter was to explore ELTD1's role within the breast cancer primary tumour and regional lymph node metastasis microenvironments. This was performed as a small exploratory pilot (n=43) for a larger future study. The aim of this work was to determine whether vascular ELTD1 is differentially

expressed between primary breast cancer and regional lymph node metastasis and whether this correlates with any biological variables. Additional questions include whether breast cancer cells differentially express ELTD1 between the primary and metastatic breast cancer sites and whether this correlates with survival. This represents the first study investigating ELTD1's role in the primary and metastatic tumour site.

Results from the clinical study revealed that tumour vascular ELTD1 is differentially expressed between primary breast cancer and regional lymph node metastases, with a decrease in ELTD1 IHC expression occurring in the regional lymph node metastases. This is interesting as it suggests that ELTD1 may play differing roles at either site. Additionally, it was found that vascular ELTD1 increased with increasing proximity to breast tumours which confirmed previous work performed by our laboratory in other tumour types (Masiero et al., 2013). It is likely that this increase is related to the tumours secreting VEGF and fibroblast growth factor, which have both been shown to induce ELTD1 expression (Masiero et al., 2013). This provides ground for a future experimenting co-staining these sections for VEGF, fibroblast growth factor as well as other growth factors and comparing their expression gradient with ELTD1.

In terms of survival, the study found that patients with low tumour vessel ELTD1 expression had a statistically significant increase in RFS. A similar survival trend was noted on the survival curves in regional node metastases although these were not statistically significant. This was surprising as these results go against previous

findings in head and neck, renal, colorectal and ovarian cancers where low ELTD1 (in pre-treatment biopsies) correlated with improved RFS (Masiero et al., 2013). As this study was a small, exploratory pilot study, all the survival analyses were limited by the small sample size and will require being repeated in a larger future study before being accepted.

Lastly, despite breast cancer cell lines being negative for ELTD1, ELTD1 was found to be strongly expressed by a minority of breast cancer cells within the primary breast tumour (7/43 cases) and regional lymph node metastases (5/43 cases). Interestingly, only 2 of the 7 cases with high tumour cell ELTD1 expression in their primary tumours had a similar result in their involved regional lymph node. This suggests that tumour cell ELTD1 expression may be regulated by microenvironment cues. A future study is planned where ELTD1 will be overexpressed in a panel of breast cancer cell lines to determine its effect on proliferation and invasion. Lastly, results revealed that tumour cell ELTD1 expression did not correlate RFS or OS. Before these survival results can be accepted, the pilot study will need to be repeated in a larger study.

8.5 Final remarks

This study provides evidence of new roles for ELTD1 within endothelial biology as well as advancing understanding of ELTD1's established role as a regulator of angiogenesis. New discoveries include ELTD1's evolutionary variants, regulation of endothelial metabolism, new relationships with the Notch pathway, interaction with KIT-KITLG signalling and a lack of canonical GPCR signalling. ELTD1's role in

angiogenesis is expanded revealing the extent of its role in inducing the tip cell phenotype as well as revealing genes which are affected by ELTD1 overexpression. Additionally, this thesis contains the first study comparing ELTD1 expression in a primary and metastatic tumour site, revealing differential ELTD1 expression in breast cancer primary and regional nodal metastatic sites. Lastly, this thesis raises many further questions about ELTD1's role in both endothelial and tumour biology which will require examination. It is an exciting time to be an ELTD1 researcher!

Chapter 9: Appendix

9.1 Investigation of ELTD1's signalling capability

9.1.1 wtFL ELTD1 in pCMV-Sport 6 vector (Geneservice; Ascension ID: BC025721.1)

9.1.1.1 Vector map

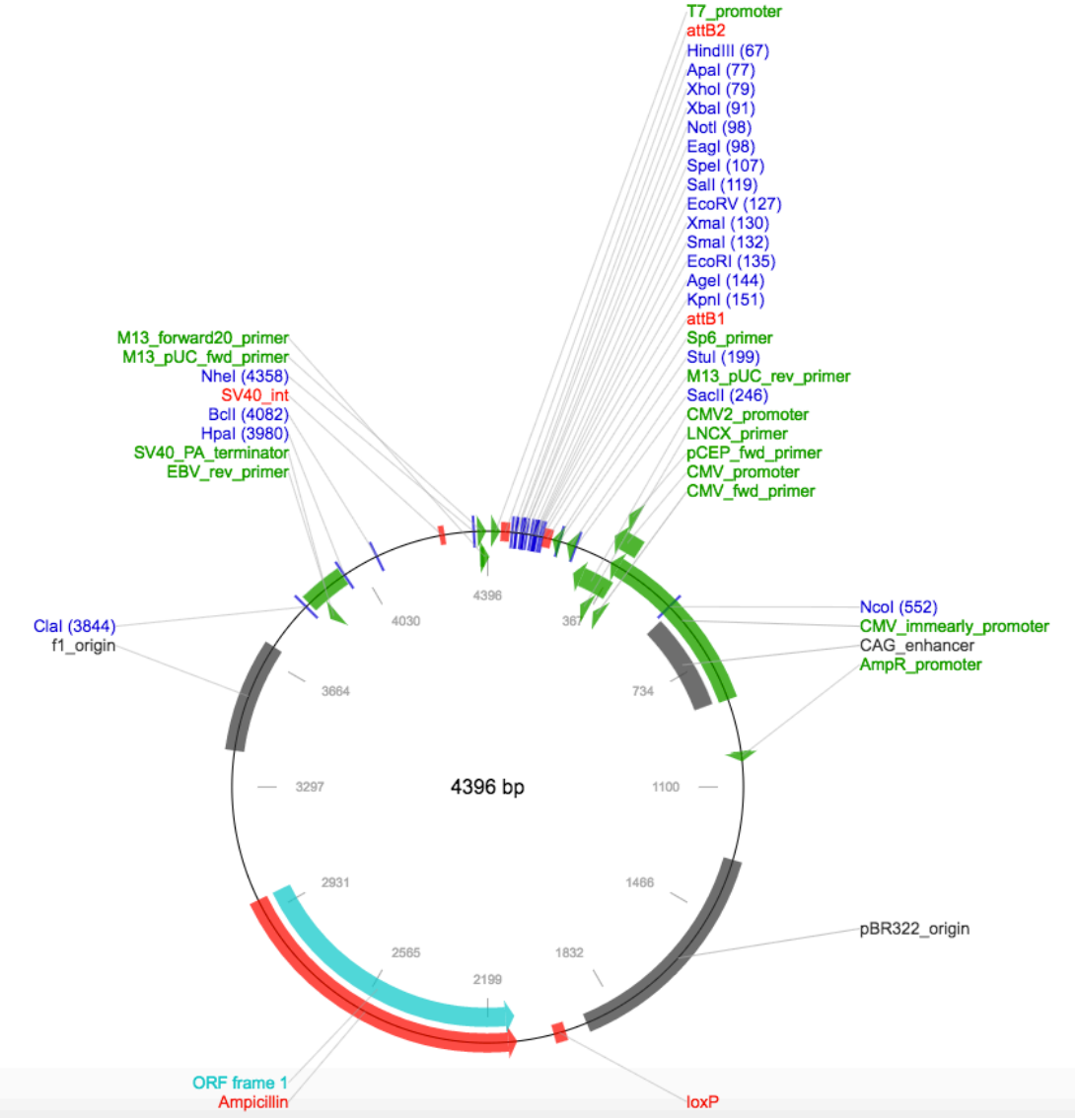


Figure 9.1: pCMV-Sport 6 Vector Map. Image adapted from the Addgene Repository (Kamens, 2015)

9.1.1.2 Nucleotide sequence

GCCACCACTGCGGCCACCGCCAATGAAACGCCTCCCGCTCCTAGTGGTTTTT

TCCACTTTGTTGAATTGTTCCTATACTCAAAATTGCACCAAGACACCTTGTCTC

CCAAATGCAAAATGTGAAATACGCAATGGAATTGAAGCCTGCTATTGCAACAT

GGGATTTTCAGGAAATGGTGTCACAATTTGTGAAGATGATAATGAATGTGGAA

ATTTAACTCAGTCCTGTGGCGAAAATGCTAATTGCACTAACACAGAAGGAAGT

TATTATTGTATGTGTGTACCTGGCTTCAGATCCAGCAGTAACCAAGACAGGTT

TATCACTAATGATGGAACCGTCTGTATAGAAAATGTGAATGCAAACTGCCATT

TAGATAATGTCTGTATAGCTGCAAATATTAATAAAACTTTAACAAAAATCAGAT

CCATAAAAGAACCTGTGGCTTTGCTACAAGAAGTCTATAGAAATTCTGTGACA

GATCTTTCACCAACAGATATAATTACATATATAGAAATATTAGCTGAATCATCT

TCATTACTAGGTTACAAGAACAACACTATCTCAGCCAAGGACACCCTTTCTAA

CTCAACTCTTACTGAATTTGTAAAAACCGTGAATAATTTTGTTCAAAGGGATAC

ATTTGTAGTTTGGGACAAGTTATCTGTGAATCATAGGAGAACACATCTTACAA

AACTCATGCACACTGTTGAACAAGCTACTTTAAGGATATCCCAGAGCTTCCAA

AAGACCACAGAGTTTGATACAAATTCAACGGATATAGCTCTCAAAGTTTTCTT

TTTTGATTCATATAACATGAAACATATTCATCCTCATATGAATATGGATGGAGA

CTACATAAATATATTTCCAAAGAGAAAAGCTGCATATGATTCAAATGGCAATG

TTGCAGTTGCATTTTTATATTATAAGAGTATTGGTCCTTTGCTTTCATCATCTG

ACAACTTCTTATTGAAACCTCAAAATTATGATAATTCTGAAGAGGAGGAAAGA

GTCATATCTTCAGTAATTTCAGTCTCAATGAGCTCAAACCCACCCACATTATAT

GAACTTGAAAAAATAACATTTACATTAAGTCATCGAAAGGTCACAGATAGGTA

TAGGAGTCTATGTGCATTTTGGAATTACTCACCTGATACCATGAATGGCAGCT

GGTCTTCAGAGGGCTGTGAGCTGACATACTCAAATGAGACCCACACCTCATG

CCGCTGTAATCACCTGACACATTTTGCAATTTTGATGTCCTCTGGTCCTTCCA

TTGGTATTAAAGATTATAATATTCTTACAAGGATCACTCAACTAGGAATAATTA

TTTCACTGATTTGTCTTGCCATATGCATTTTTACCTTCTGGTTCTTCAGTGAAA

TTCAAAGCACCAGGACAACAATTCACAAAAATCTTTGCTGTAGCCTATTTCTT

GCTGAACTTGTTTTTCTTGTTGGGATCAATACAAATACTAATAAGCTCTTCTGT

TCAATCATTGCTGGACTGCTACACTACTTCTTTTTAGCTGCTTTTGCATGGAT

GTGCATTGAAGGCATACATCTCTATCTCATTGTTGTGGGTGTCATCTACAACA

AGGGATTTTTGCACAAGAATTTTTATATCTTTGGCTATCTAAGCCCAGCCGTG

GTAGTTGGATTTTCGGCAGCACTAGGATACAGATATTATGGCACAACCAAAG

TATGTTGGCTTAGCACCGAAAACAACTTTATTTGGAGTTTTATAGGACCAGCA

TGCCTAATCATTCTTGTTAATCTCTTGGCTTTTGGAGTCATCATATACAAAGTT

TTTCGTCACACTGCAGGGTTGAAACCAGAAGTTAGTTGCTTTGAGAACATAAG

GTCTTGTGCAAGAGGAGCCCTCGCTCTTCTGTTCCTTCTCGGCACCACCTGG

ATCTTTGGGGTTCTCCATGTTGTGCACGCATCAGTGGTTACAGCTTACCTCTT

CACAGTCAGCAATGCTTTCCAGGGGATGTTCATTTTTTTATTCCTGTGTGTTTT

ATCTAGAAAGATTCAAGAAGAATATTACAGATTGTTCAAAAATGTCCCCTGTT

GTTTTGGATGTTTAAGGTAAACATAGAGAATGGTGGATAATTACAACTGCACA

AAAATAAAAATTCCAAGCTGTGGATGACCAATGTATAAAAATGACTCATCAAA

TTATCCAATTATTAACTACTAGACAAAAAGTATTTTAAATCAGTTTTTCTGTTTA

TGCTATAGGAACTGTAGATAATAAGGTAAAATTATGTATCATATAGATATACTA

TGTTTTTCTATGTGAAATAGTTCTGTCAAAAATAGTATTGCAGATATTTGGAAA

GTAATTGGTTTCTCAGGAGTGATATCACTGCACCCAAGGAAAGATTTTCTTTC

TAACACGAGAAGTATATGAATGTCCTGAAGGAAACCACTGGCTTGATATTTCT

GTGACTCGTGTTGCCTTTGAAACTAGTCCCCTACCACCTCGGTAATGAGCTC

CATTACAGAAAGTGGAACATAAGAGAATGAAGGGGCAGAATATCAAACAGTG

AAAAGGGAATGATAAGATGTATTTTGAATGAACTGTTTTTTCTGTAGACTAGCT

GAGAAATTGTTGACATAAAATAAAGAATTGAAGAAACACAAAAAAAAAAAAAA

AAAAAAAAAAAAAA

9.1.1.3 Amino acid sequence

MCVPGFRSSSNQDRFITNDGTVCIENVNANCHLDNVCIAANINKTLTKIRSIKEPV

ALLQEVYRNSVTDLSPTDIITYIEILAESSSLLGYKNNTISAKDTLSNSTLTEFVKTV

NNFVQRDTFVVWDKLSVNHRRTHLTKLMHTVEQATLRISQSFQKTTEFDTNSTDI

ALKVFFFDSYNMKHIHPHMNMDGDYINIFPKRKAAYDSNGNVAVAFLYYKSIGPL

LSSSDNFLLKPQNYDNSEEEERVISSVISVSMSSNPPTLYELEKITFTLSHRKVTD

RYRSLCAFWNYSPDTMNGSWSSEGCELTYSNETHTSCRCNHLTHFAILMSSGP

SIGIKDYNILTRITQLGIIISLICLAICIFTFWFFSEIQSTRTTIHKNLCCSLFLAELVFLV

GINTNTNKLFCSIIAGLLHYFFLAAFAWMCIEGIHLYLIVVGVIYNKGFLHKNFYIFG

YLSPAVVVGFSAALGYRYYGTTKVCWLSTENNFIWSFIGPACLIILVNLLAFGVIIY

KVFRHTAGLKPEVSCFENIRSCARGALALLFLLGTTWIFGVLHVVHASVVTAYLFT

VSNAFQGMFIFLFLCVLSRKIQEEYYRLFKNVPCCFGCLR

9.1.2 coFL ELTD1:

9.1.2.1 Nucleotide sequence:

ATGAAGAGACTGCCCCTGCTGGTGGTGTTCAGCACCCTGCTGAACTGCAGC

TACACCCAGAACTGCACCAAGACCCCCTGCCTGCCCAACGCCAAGTGCGAG

ATCAGAAACGGCATCGAGGCCTGCTACTGCAACATGGGCTTCAGCGGCAAC

GGCGTGACCATCTGCGAGGACGACAACGAGTGCGGCAACCTGACCCAGAG

CTGCGGCGAGAACGCCAATTGCACCAACACCGAGGGCAGCTACTACTGTAT

GTGCGTGCCCGGCTTCAGAAGCAGCAGCAACCAGGACCGGTTCATCACCAA

CGACGGCACCGTGTGCATCGAGAACGTGAACGCCAACTGCCACCTGGACAA

CGTGTGTATCGCCGCCAACATCAACAAGACCCTGACCAAGATCCGGTCCATC

AAAGAACCCGTGGCCCTGCTGCAGGAAGTGTACCGGAACAGCGTGACCGAC

CTGAGCCCCACCGACATCATCACCTACATCGAGATCCTGGCCGAGAGCAGC

AGCCTGCTGGGCTACAAGAACAACACCATCAGCGCCAAGGACACCCTGAGC

AACTCCACCCTGACCGAGTTCGTGAAAACCGTGAACAACTTCGTGCAGCGG

GACACCTTCGTCGTGTGGGACAAGCTGAGCGTGAACCACAGACGGACCCAC

CTGACAAAGCTGATGCACACCGTGGAACAGGCCACCCTGCGGATCAGCCAG

AGCTTCCAGAAAACCACCGAGTTTGACACCAACAGCACCGATATCGCCCTGA

AGGTGTTCTTCTTCGACTCCTACAACATGAAGCACATCCACCCCCACATGAA

CATGGACGGCGACTACATCAACATCTTCCCCAAGCGGAAGGCCGCCTACGA

CAGCAACGGAAATGTGGCCGTGGCCTTCCTGTACTACAAGAGCATCGGCCC

CCTGCTGAGCAGCTCCGACAACTTCCTGCTGAAGCCTCAGAACTACGACAAC

AGCGAGGAAGAGGAACGCGTGATCAGCAGCGTGATCTCCGTGTCCATGTCC

AGCAACCCCCCCCACCCTGTACGAGCTGGAAAAGATCACCTTCACCCTGTCCC

ACCGGAAAGTGACCGACAGATACCGGTCCCTGTGCGCCTTCTGGAACTACA

GCCCCGACACCATGAACGGCAGCTGGTCTAGCGAGGGCTGCGAGCTGACCT

ACAGCAACGAGACACACACCAGCTGCAGATGCAACCATCTGACCCACTTCGC

CATCCTGATGAGCAGCGGCCCCAGCATCGGCATCAAGGACTACAACATCCT

GACCCGGATCACACAGCTGGGCATCATCATCAGCCTGATCTGCCTGGCTATC

TGCATCTTCACCTTTTGGTTCTTCAGCGAGATCCAGAGCACCCGGACCACCA

TCCACAAGAACCTGTGCTGCAGCCTGTTTCTGGCCGAGCTGGTGTTCCTCGT

GGGCATCAACACCAATACCAACAAGCTGTTCTGCAGCATCATTGCCGGCCTG

CTGCACTACTTCTTTCTGGCTGCCTTCGCCTGGATGTGTATCGAGGGCATCC

ACCTGTACCTGATCGTCGTGGGCGTGATCTACAACAAGGGCTTCCTGCACAA

GAACTTCTACATCTTCGGCTACCTGTCCCCAGCCGTGGTCGTGGGATTTTCT

GCCGCCCTGGGCTACCGGTACTACGGCACCACAAAAGTGTGCTGGCTGAGC

ACCGAGAACAATTTCATCTGGTCCTTCATCGGCCCAGCCTGCCTGATCATCC

TCGTGAACCTGCTGGCCTTCGGAGTGATCATCTACAAGGTGTTCCGGCACAC

AGCCGGCCTGAAGCCTGAGGTGTCCTGCTTCGAGAACATCAGAAGCTGCGC

CAGAGGGGCCCTGGCTCTGCTGTTTCTGCTGGGCACCACCTGGATCTTCGG

CGTGCTGCATGTGGTGCACGCCAGCGTCGTGACCGCCTACCTGTTCACCGT

GTCCAACGCCTTCCAGGGGATGTTCATCTTTCTGTTTCTGTGCGTGCTGAGC

CGGAAGATTCAGGAAGAGTACTACCGGCTGTTCAAGAACGTGCCCTGTTGCT

TCGGCTGCCTGAGA

9.1.2.2 Amino acid sequence

MKRLPLLVVFSTLLNCSYTQNCTKTPCLPNAKCEIRNGIEACYCNMGFSGNGVTI

CEDDNECGNLTQSCGENANCTNTEGSYYCMCVPGFRSSSNQDRFITNDGTVCI

ENVNANCHLDNVCIAANINKTLTKIRSIKEPVALLQEVYRNSVTDLSPTDIITYIEILA

ESSSLLGYKNNTISAKDTLSNSTLTEFVKTVNNFVQRDTFVVWDKLSVNHRRTHL

TKLMHTVEQATLRISQSFQKTTEFDTNSTDIALKVFFFDSYNMKHIHPHMNMDGD

YINIFPKRKAAYDSNGNVAVAFLYYKSIGPLLSSSDNFLLKPQNYDNSEEEERVIS

SVISVSMSSNPPTLYELEKITFTLSHRKVTDRYRSLCAFWNYSPDTMNGSWSSE

GCELTYSNETHTSCRCNHLTHFAILMSSGPSIGIKDYNILTRITQLGIIISLICLAICIF

TFWFFSEIQSTRTTIHKNLCCSLFLAELVFLVGINTNTNKLFCSIIAGLLHYFFLAAF

AWMCIEGIHLYLIVVGVIYNKGFLHKNFYIFGYLSPAVVVGFSAALGYRYYGTTKV

CWLSTENNFIWSFIGPACLIILVNLLAFGVIIYKVFRHTAGLKPEVSCFENIRSCAR

GALALLFLLGTTWIFGVLHVVHASVVTAYLFTVSNAFQGMFIFLFLCVLSRKIQEE

YYRLFKNVPCCFGCLR

9.1.3 wtFL ELTD1 with GFP C-terminal tag in pcDNA3.1 vector

9.1.3.1 Vector Map:

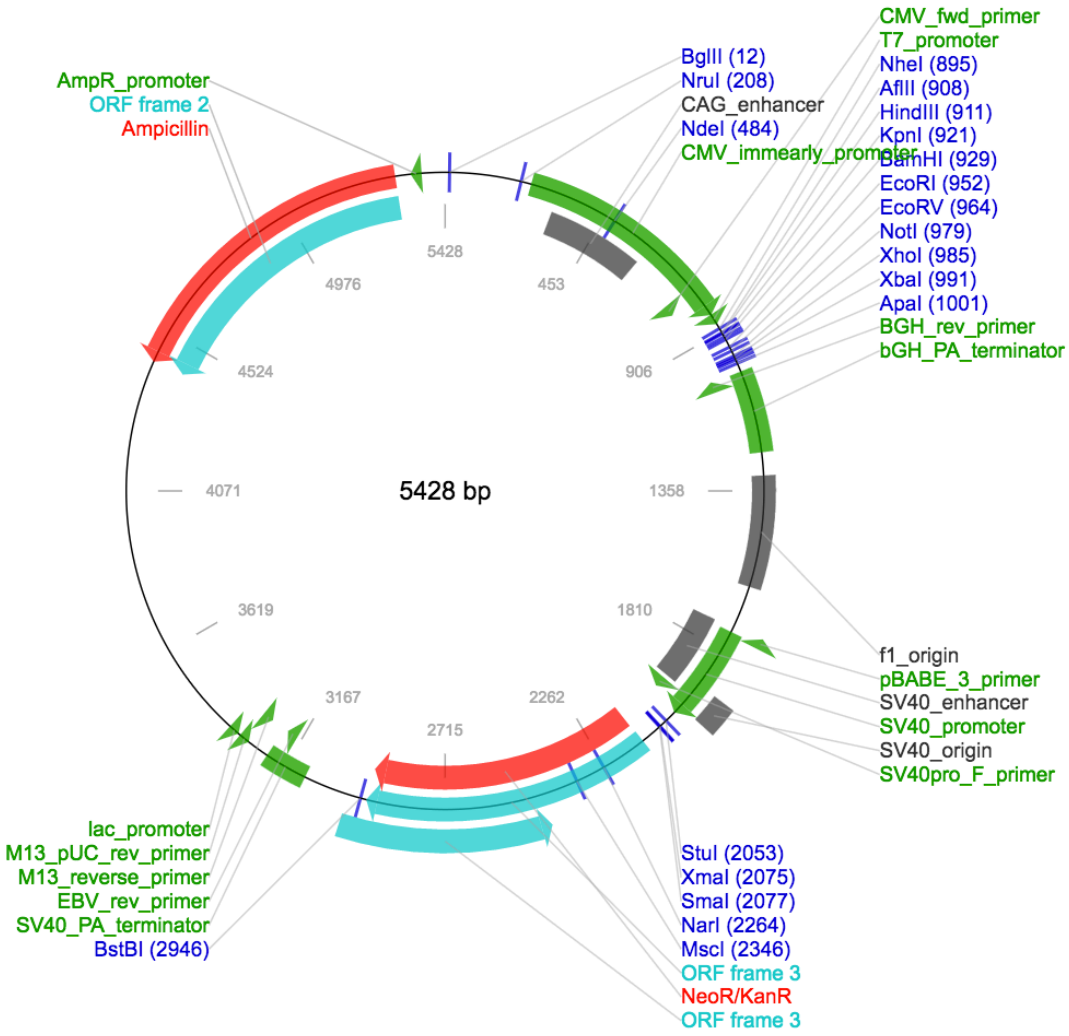


Figure 9.2: pcDNA3.1 Vector Map. Image adapted from the Addgene Repository (Kamens, 2015)

9.1.3.2 Nucleotide sequence

ATGAAGAGACTGCCCCTGCTGGTGGTGTTCAGCACCCTGCTGAACTGCAGC

TACACCCAGAACTGCACCAAGACCCCCTGCCTGCCCAACGCCAAGTGCGAG

ATCAGAAACGGCATCGAGGCCTGCTACTGCAACATGGGCTTCAGCGGCAAC

GGCGTGACCATCTGCGAGGACGACAACGAGTGCGGCAACCTGACCCAGAG

CTGCGGCGAGAACGCCAATTGCACCAACACCGAGGGCAGCTACTACTGTAT

GTGCGTGCCCGGCTTCAGAAGCAGCAGCAACCAGGACCGGTTCATCACCAA

CGACGGCACCGTGTGCATCGAGAACGTGAACGCCAACTGCCACCTGGACAA

CGTGTGTATCGCCGCCAACATCAACAAGACCCTGACCAAGATCCGGTCCATC

AAAGAACCCGTGGCCCTGCTGCAGGAAGTGTACCGGAACAGCGTGACCGAC

CTGAGCCCCACCGACATCATCACCTACATCGAGATCCTGGCCGAGAGCAGC

AGCCTGCTGGGCTACAAGAACAACACCATCAGCGCCAAGGACACCCTGAGC

AACTCCACCCTGACCGAGTTCGTGAAAACCGTGAACAACTTCGTGCAGCGG

GACACCTTCGTCGTGTGGGACAAGCTGAGCGTGAACCACAGACGGACCCAC

CTGACAAAGCTGATGCACACCGTGGAACAGGCCACCCTGCGGATCAGCCAG

AGCTTCCAGAAAACCACCGAGTTTGACACCAACAGCACCGATATCGCCCTGA

AGGTGTTCTTCTTCGACTCCTACAACATGAAGCACATCCACCCCCACATGAA

CATGGACGGCGACTACATCAACATCTTCCCCAAGCGGAAGGCCGCCTACGA

CAGCAACGGAAATGTGGCCGTGGCCTTCCTGTACTACAAGAGCATCGGCCC

CCTGCTGAGCAGCTCCGACAACTTCCTGCTGAAGCCTCAGAACTACGACAAC

AGCGAGGAAGAGGAACGCGTGATCAGCAGCGTGATCTCCGTGTCCATGTCC

AGCAACCCCCCCACCCTGTACGAGCTGGAAAAGATCACCTTCACCCTGTCCC

ACCGGAAAGTGACCGACAGATACCGGTCCCTGTGCGCCTTCTGGAACTACA

GCCCCGACACCATGAACGGCAGCTGGTCTAGCGAGGGCTGCGAGCTGACCT

ACAGCAACGAGACACACACCAGCTGCAGATGCAACCATCTGACCCACTTCGC

CATCCTGATGAGCAGCGGCCCCAGCATCGGCATCAAGGACTACAACATCCT

GACCCGGATCACACAGCTGGGCATCATCATCAGCCTGATCTGCCTGGCTATC

TGCATCTTCACCTTTTGGTTCTTCAGCGAGATCCAGAGCACCCGGACCACCA

TCCACAAGAACCTGTGCTGCAGCCTGTTTCTGGCCGAGCTGGTGTTCCTCGT

GGGCATCAACACCAATACCAACAAGCTGTTCTGCAGCATCATTGCCGGCCTG

CTGCACTACTTCTTTCTGGCTGCCTTCGCCTGGATGTGTATCGAGGGCATCC

ACCTGTACCTGATCGTCGTGGGCGTGATCTACAACAAGGGCTTCCTGCACAA

GAACTTCTACATCTTCGGCTACCTGTCCCCAGCCGTGGTCGTGGGATTTTCT

GCCGCCCTGGGCTACCGGTACTACGGCACCACAAAAGTGTGCTGGCTGAGC

ACCGAGAACAATTTCATCTGGTCCTTCATCGGCCCAGCCTGCCTGATCATCC

TCGTGAACCTGCTGGCCTTCGGAGTGATCATCTACAAGGTGTTCCGGCACAC

AGCCGGCCTGAAGCCTGAGGTGTCCTGCTTCGAGAACATCAGAAGCTGCGC

CAGAGGGGCCCTGGCTCTGCTGTTTCTGCTGGGCACCACCTGGATCTTCGG

CGTGCTGCATGTGGTGCACGCCAGCGTCGTGACCGCCTACCTGTTCACCGT

GTCCAACGCCTTCCAGGGGATGTTCATCTTTCTGTTTCTGTGCGTGCTGAGC

CGGAAGATTCAGGAAGAGTACTACCGGCTGTTCAAGAACGTGCCCTGTTGCT

TCGGCTGCCTGAGAATGGTGAGCAAGGGCGAGGAGCTGTTCACCGGGGTG

GTGCCCATCCTGGTCGAGCTGGACGGCGACGTAAACGGCCACAAGTTCAGC

GTGTCCGGCGAGGGCGAGGGCGATGCCACCTACGGCAAGCTGACCCTGAA

GTTCATCTGCACCACCGGCAAGCTGCCCGTGCCCTGGCCCACCCTCGTGAC

CACCCTGACCTACGGCGTGCAGTGCTTCAGCCGCTACCCCGACCACATGAA

GCAGCACGACTTCTTCAAGTCCGCCATGCCCGAAGGCTACGTCCAGGAGCG

CACCATCTTCTTCAAGGACGACGGCAACTACAAGACCCGCGCCGAGGTGAA

GTTCGAGGGCGACACCCTGGTGAACCGCATCGAGCTGAAGGGCATCGACTT

CAAGGAGGACGGCAACATCCTGGGGCACAAGCTGGAGTACAACTACAACAG

CCACAACGTCTATATCATGGCCGACAAGCAGAAGAACGGCATCAAGGTGAAC

TTCAAGATCCGCCACAACATCGAGGACGGCAGCGTGCAGCTCGCCGACCAC

TACCAGCAGAACACCCCCATCGGCGACGGCCCCGTGCTGCTGCCCGACAAC

CACTACCTGAGCACCCAGTCCAAGCTGAGCAAAGACCCCAACGAGAAGCGC

GATCACATGGTCCTGCTGGAGTTCGTGACCGCCGCCGGGATCACTCTCGGC

ATGGACGAGCTGTACAAGTAA

9.1.3.3 Amino acid sequence

MKRLPLLVVFSTLLNCSYTQNCTKTPCLPNAKCEIRNGIEACYCNMGFSGNGVTI
CEDDNECGNLTQSCGENANCTNTEGSYYCMCVPGFRSSSNQDRFITNDGTVCI
ENVNANCHLDNVCIAANINKTLTKIRSIKEPVALLQEVYRNSVTDLSPTDIITYIEILA
ESSSLLGYKNNTISAKDTLSNSTLTEFVKTVNNFVQRDTFVVWDKLSVNHRRTHL
TKLMHTVEQATLRISQSFQKTTEFDTNSTDIALKVFFFDSYNMKHIHPHMNMDGD
YINIFPKRKAAYDSNGNVAVAFLYYKSIGPLLSSSDNFLLKPQNYDNSEEEERVIS
SVISVSMSSNPPTLYELEKITFTLSHRKVTDRYRSLCAFWNYSPDTMNGSWSSE
GCELTYSNETHTSCRCNHLTHFAILMSSGPSIGIKDYNILTRITQLGIIISLICLAICIF
TFWFFSEIQSTRTTIHKNLCCSLFLAELVFLVGINTNTNKLFCSIIAGLLHYFFLAAF
AWMCIEGIHLYLIVVGVIYNKGFLHKNFYIFGYLSPAVVVGFSAALGYRYYGTTKV
CWLSTENNFIWSFIGPACLIILVNLLAFGVIIYKVFRHTAGLKPEVSCFENIRSCAR
GALALLFLLGTTWIFGVLHVVHASVVTAYLFTVSNAFQGMFIFLFLCVLSRKIQEE
YYRLFKNVPCCFGCLRMVSKGEELFTGVVPILVELDGDVNGHKFSVSGEGEGDA
TYGKLTLKFICTTGKLPVPWPTLVTTLTYGVQCFSRYPDHMKQHDFFKSAMPEG
YVQERTIFFKDDGNYKTRAEVKFEGDTLVNRIELKGIDFKEDGNILGHKLEYNYNS
HNVYIMADKQKNGIKVNFKIRHNIEDGSVQLADHYQQNTPIGDGPVLLPDNHYLS
TQSKLSKDPNEKRDHMVLLEFVTAAGITLGMDELYK*

9.1.4 coFL ELTD1 with GFP C-terminal tag in pcDNA3.1 vector

9.1.4.1 Nucleotide sequence

ATGAAGAGACTGCCCCTGCTGGTGGTGTTCAGCACCCTGCTGAACTGCAGC
TACACCCAGTACCCCTACGACGTCCCCGACTACGCCAACTGCACCAAGACC
CCCTGCCTGCCCAACGCCAAGTGCGAGATCAGAAACGGCATCGAGGCCTGC
TACTGCAACATGGGCTTCAGCGGCAACGGCGTGACCATCTGCGAGGACGAC

AACGAGTGCGGCAACCTGACCCAGAGCTGCGGCGAGAACGCCAATTGCACC

AACACCGAGGGCAGCTACTACTGTATGTGCGTGCCCGGCTTCAGAAGCAGC

AGCAACCAGGACCGGTTCATCACCAACGACGGCACCGTGTGCATCGAGAAC

GTGAACGCCAACTGCCACCTGGACAACGTGTGTATCGCCGCCAACATCAACA

AGACCCTGACCAAGATCCGGTCCATCAAAGAACCCGTGGCCCTGCTGCAGG

AAGTGTACCGGAACAGCGTGACCGACCTGAGCCCCACCGACATCATCACCT

ACATCGAGATCCTGGCCGAGAGCAGCAGCCTGCTGGGCTACAAGAACAACA

CCATCAGCGCCAAGGACACCCTGAGCAACTCCACCCTGACCGAGTTCGTGA

AAACCGTGAACAACTTCGTGCAGCGGGACACCTTCGTCGTGTGGGACAAGC

TGAGCGTGAACCACAGACGGACCCACCTGACAAAGCTGATGCACACCGTGG

AACAGGCCACCCTGCGGATCAGCCAGAGCTTCCAGAAAACCACCGAGTTTG

ACACCAACAGCACCGATATCGCCCTGAAGGTGTTCTTCTTCGACTCCTACAA

CATGAAGCACATCCACCCCCACATGAACATGGACGGCGACTACATCAACATC

TTCCCCAAGCGGAAGGCCGCCTACGACAGCAACGGAAATGTGGCCGTGGCC

TTCCTGTACTACAAGAGCATCGGCCCCCTGCTGAGCAGCTCCGACAACTTCC

TGCTGAAGCCTCAGAACTACGACAACAGCGAGGAAGAGGAACGCGTGATCA

GCAGCGTGATCTCCGTGTCCATGTCCAGCAACCCCCCCACCCTGTACGAGC

TGGAAAAGATCACCTTCACCCTGTCCCACCGGAAAGTGACCGACAGATACCG

GTCCCTGTGCGCCTTCTGGAACTACAGCCCCGACACCATGAACGGCAGCTG

GTCTAGCGAGGGCTGCGAGCTGACCTACAGCAACGAGACACACACCAGCTG

CAGATGCAACCATCTGACCCACTTCGCCATCCTGATGAGCAGCGGCCCCAG

CATCGGCATCAAGGACTACAACATCCTGACCCGGATCACACAGCTGGGCATC

ATCATCAGCCTGATCTGCCTGGCTATCTGCATCTTCACCTTTTGGTTCTTCAG

CGAGATCCAGAGCACCCGGACCACCATCCACAAGAACCTGTGCTGCAGCCT

GTTTCTGGCCGAGCTGGTGTTCCTCGTGGGCATCAACACCAATACCAACAAG

CTGTTCTGCAGCATCATTGCCGGCCTGCTGCACTACTTCTTTCTGGCTGCCT

TCGCCTGGATGTGTATCGAGGGCATCCACCTGTACCTGATCGTCGTGGGCG

TGATCTACAACAAGGGCTTCCTGCACAAGAACTTCTACATCTTCGGCTACCTG

TCCCCAGCCGTGGTCGTGGGATTTTCTGCCGCCCTGGGCTACCGGTACTAC

GGCACCACAAAAGTGTGCTGGCTGAGCACCGAGAACAATTTCATCTGGTCCT

TCATCGGCCCAGCCTGCCTGATCATCCTCGTGAACCTGCTGGCCTTCGGAGT

GATCATCTACAAGGTGTTCCGGCACACAGCCGGCCTGAAGCCTGAGGTGTC

CTGCTTCGAGAACATCAGAAGCTGCGCCAGAGGGGCCCTGGCTCTGCTGTT

TCTGCTGGGCACCACCTGGATCTTCGGCGTGCTGCATGTGGTGCACGCCAG

CGTCGTGACCGCCTACCTGTTCACCGTGTCCAACGCCTTCCAGGGGATGTTC

ATCTTTCTGTTTCTGTGCGTGCTGAGCCGGAAGATTCAGGAAGAGTACTACC

GGCTGTTCAAGAACGTGCCCTGTTGCTTCGGCTGCCTGAGAGATTACAAGGA

TGACGACGATAAGTAA

9.1.4.2 Amino acid sequence

MKRLPLLVVFSTLLNCSYTQYPYDVPDYANCTKTPCLPNAKCEIRNGIEACYCNM

GFSGNGVTICEDDNECGNLTQSCGENANCTNTEGSYYCMCVPGFRSSSNQDR

FITNDGTVCIENVNANCHLDNVCIAANINKTLTKIRSIKEPVALLQEVYRNSVTDLS

PTDIITYIEILAESSSLLGYKNNTISAKDTLSNSTLTEFVKTVNNFVQRDTFVVWDK

LSVNHRRTHLTKLMHTVEQATLRISQSFQKTTEFDTNSTDIALKVFFFDSYNMKHI

HPHMNMDGDYINIFPKRKAAYDSNGNVAVAFLYYKSIGPLLSSSDNFLLKPQNYD

NSEEEERVISSVISVSMSSNPPTLYELEKITFTLSHRKVTDRYRSLCAFWNYSPDT

MNGSWSSEGCELTYSNETHTSCRCNHLTHFAILMSSGPSIGIKDYNILTRITQLGII

ISLICLAICIFTFWFFSEIQSTRTTIHKNLCCSLFLAELVFLVGINTNTNKLFCSIIAGL

LHYFFLAAFAWMCIEGIHLYLIVVGVIYNKGFLHKNFYIFGYLSPAVVVGFSAALGY

RYYGTTKVCWLSTENNFIWSFIGPACLIILVNLLAFGVIIYKVFRHTAGLKPEVSCF

ENIRSCARGALALLFLLGTTWIFGVLHVVHASVVTAYLFTVSNAFQGMFIFLFLCV

LSRKIQEEYYRLFKNVPCCFGCLRDYKDDDDK*

9.1.5 coFL ELTD1 with HA N-terminal and FLAG C-terminal tags in pcDNA3.1 vector

9.1.5.1 Nucleotide sequence

ATGAAGAGACTGCCCCTGCTGGTGGTGTTCAGCACCCTGCTGAACTGCAGC

TACACCCAGTACCCCTACGACGTCCCCGACTACGCCAACTGCACCAAGACC

CCCTGCCTGCCCAACGCCAAGTGCGAGATCAGAAACGGCATCGAGGCCTGC

TACTGCAACATGGGCTTCAGCGGCAACGGCGTGACCATCTGCGAGGACGAC

AACGAGTGCGGCAACCTGACCCAGAGCTGCGGCGAGAACGCCAATTGCACC

AACACCGAGGGCAGCTACTACTGTATGTGCGTGCCCGGCTTCAGAAGCAGC

AGCAACCAGGACCGGTTCATCACCAACGACGGCACCGTGTGCATCGAGAAC

GTGAACGCCAACTGCCACCTGGACAACGTGTGTATCGCCGCCAACATCAACA

AGACCCTGACCAAGATCCGGTCCATCAAAGAACCCGTGGCCCTGCTGCAGG

AAGTGTACCGGAACAGCGTGACCGACCTGAGCCCCACCGACATCATCACCT

ACATCGAGATCCTGGCCGAGAGCAGCAGCCTGCTGGGCTACAAGAACAACA

CCATCAGCGCCAAGGACACCCTGAGCAACTCCACCCTGACCGAGTTCGTGA

AAACCGTGAACAACTTCGTGCAGCGGGACACCTTCGTCGTGTGGGACAAGC

TGAGCGTGAACCACAGACGGACCCACCTGACAAAGCTGATGCACACCGTGG

AACAGGCCACCCTGCGGATCAGCCAGAGCTTCCAGAAAACCACCGAGTTTG

ACACCAACAGCACCGATATCGCCCTGAAGGTGTTCTTCTTCGACTCCTACAA

CATGAAGCACATCCACCCCCACATGAACATGGACGGCGACTACATCAACATC

TTCCCCAAGCGGAAGGCCGCCTACGACAGCAACGGAAATGTGGCCGTGGCC

TTCCTGTACTACAAGAGCATCGGCCCCCTGCTGAGCAGCTCCGACAACTTCC

TGCTGAAGCCTCAGAACTACGACAACAGCGAGGAAGAGGAACGCGTGATCA

GCAGCGTGATCTCCGTGTCCATGTCCAGCAACCCCCCCACCCTGTACGAGC

TGGAAAAGATCACCTTCACCCTGTCCCACCGGAAAGTGACCGACAGATACCG

GTCCCTGTGCGCCTTCTGGAACTACAGCCCCGACACCATGAACGGCAGCTG

GTCTAGCGAGGGCTGCGAGCTGACCTACAGCAACGAGACACACACCAGCTG

CAGATGCAACCATCTGACCCACTTCGCCATCCTGATGAGCAGCGGCCCCAG

CATCGGCATCAAGGACTACAACATCCTGACCCGGATCACACAGCTGGGCATC

ATCATCAGCCTGATCTGCCTGGCTATCTGCATCTTCACCTTTTGGTTCTTCAG

CGAGATCCAGAGCACCCGGACCACCATCCACAAGAACCTGTGCTGCAGCCT

GTTTCTGGCCGAGCTGGTGTTCCTCGTGGGCATCAACACCAATACCAACAAG

CTGTTCTGCAGCATCATTGCCGGCCTGCTGCACTACTTCTTTCTGGCTGCCT

TCGCCTGGATGTGTATCGAGGGCATCCACCTGTACCTGATCGTCGTGGGCG

TGATCTACAACAAGGGCTTCCTGCACAAGAACTTCTACATCTTCGGCTACCTG

TCCCCAGCCGTGGTCGTGGGATTTTCTGCCGCCCTGGGCTACCGGTACTAC

GGCACCACAAAAGTGTGCTGGCTGAGCACCGAGAACAATTTCATCTGGTCCT

TCATCGGCCCAGCCTGCCTGATCATCCTCGTGAACCTGCTGGCCTTCGGAGT

GATCATCTACAAGGTGTTCCGGCACACAGCCGGCCTGAAGCCTGAGGTGTC

CTGCTTCGAGAACATCAGAAGCTGCGCCAGAGGGGCCCTGGCTCTGCTGTT

TCTGCTGGGCACCACCTGGATCTTCGGCGTGCTGCATGTGGTGCACGCCAG

CGTCGTGACCGCCTACCTGTTCACCGTGTCCAACGCCTTCCAGGGGATGTTC

ATCTTTCTGTTTCTGTGCGTGCTGAGCCGGAAGATTCAGGAAGAGTACTACC

GGCTGTTCAAGAACGTGCCCTGTTGCTTCGGCTGCCTGAGAGATTACAAGGA

TGACGACGATAAGTAA

9.1.5.2 Amino acid sequence

MKRLPLLVVFSTLLNCSYTQYPYDVPDYANCTKTPCLPNAKCEIRNGIEACYCNM

GFSGNGVTICEDDNECGNLTQSCGENANCTNTEGSYYCMCVPGFRSSSNQDR

FITNDGTVCIENVNANCHLDNVCIAANINKTLTKIRSIKEPVALLQEVYRNSVTDLS
PTDIITYIEILAESSSLLGYKNNTISAKDTLSNSTLTEFVKTVNNFVQRDTFVVWDK
LSVNHRRTHLTKLMHTVEQATLRISQSFQKTTEFDTNSTDIALKVFFFDSYNMKHI
HPHMNMDGDYINIFPKRKAAYDSNGNVAVAFLYYKSIGPLLSSSDNFLLKPQNYD
NSEEEERVISSVISVSMSSNPPTLYELEKITFTLSHRKVTDRYRSLCAFWNYSPDT
MNGSWSSEGCELTYSNETHTSCRCNHLTHFAILMSSGPSIGIKDYNILTRITQLGII
ISLICLAICIFTFWFFSEIQSTRTTIHKNLCCSLFLAELVFLVGINTNTNKLFCSIIAGL
LHYFFLAAFAWMCIEGIHLYLIVVGVIYNKGFLHKNFYIFGYLSPAVVVGFSAALGY
RYYGTTKVCWLSTENNFIWSFIGPACLIILVNLLAFGVIIYKVFRHTAGLKPEVSCF
ENIRSCARGALALLFLLGTTWIFGVLHVVHASVVTAYLFTVSNAFQGMFIFLFLCV
LSRKIQEEYYRLFKNVPCCFGCLRDYKDDDDK*

9.1.6 coCTF ELTD1 with N-terminal and FLAG C-terminal tags in pcDNA3.1 vector

9.1.6.1 Nucleotide sequence

ATGAAGAGACTGCCCCTGCTGGTGGTGTTCAGCACCCTGCTGAACTGCAGC
TACACCCAGTACCCCTACGACGTCCCCGACTACGCCACCCACTTCGCCATCC
TGATGAGCAGCGGCCCCAGCATCGGCATCAAGGACTACAACATCCTGACCC
GGATCACACAGCTGGGCATCATCATCAGCCTGATCTGCCTGGCTATCTGCAT
CTTCACCTTTTGGTTCTTCAGCGAGATCCAGAGCACCCGGACCACCATCCAC
AAGAACCTGTGCTGCAGCCTGTTTCTGGCCGAGCTGGTGTTCCTCGTGGGC
ATCAACACCAATACCAACAAGCTGTTCTGCAGCATCATTGCCGGCCTGCTGC
ACTACTTCTTTCTGGCTGCCTTCGCCTGGATGTGTATCGAGGGCATCCACCT
GTACCTGATCGTCGTGGGCGTGATCTACAACAAGGGCTTCCTGCACAAGAAC
TTCTACATCTTCGGCTACCTGTCCCCAGCCGTGGTCGTGGGATTTTCTGCCG
CCCTGGGCTACCGGTACTACGGCACCACAAAAGTGTGCTGGCTGAGCACCG

AGAACAATTTCATCTGGTCCTTCATCGGCCCAGCCTGCCTGATCATCCTCGT
GAACCTGCTGGCCTTCGGAGTGATCATCTACAAGGTGTTCCGGCACACAGC
CGGCCTGAAGCCTGAGGTGTCCTGCTTCGAGAACATCAGAAGCTGCGCCAG
AGGGGCCCTGGCTCTGCTGTTTCTGCTGGGCACCACCTGGATCTTCGGCGT
GCTGCATGTGGTGCACGCCAGCGTCGTGACCGCCTACCTGTTCACCGTGTC
CAACGCCTTCCAGGGGATGTTCATCTTTCTGTTTCTGTGCGTGCTGAGCCGG
AAGATTCAGGAAGAGTACTACCGGCTGTTCAAGAACGTGCCCTGTTGCTTCG
GCTGCCTGAGAGATTACAAGGATGACGACGATAAGTAA

9.1.6.2 Amino acid sequence

MKRLPLLVVFSTLLNCSYTQYPYDVPDYATHFAILMSSGPSIGIKDYNILTRITQLGI
IISLICLAICIFTFWFFSEIQSTRTTIHKNLCCSLFLAELVFLVGINTNTNKLFCSIIAGL
LHYFFLAAFAWMCIEGIHLYLIVVGVIYNKGFLHKNFYIFGYLSPAVVVGFSAALGY
RYYGTTKVCWLSTENNFIWSFIGPACLIILVNLLAFGVIIYKVFRHTAGLKPEVSCF
ENIRSCARGALALLFLLGTTWIFGVLHVVHASVVTAYLFTVSNAFQGMFIFLFLCV
LSRKIQEEYYRLFKNVPCCFGCLRDYKDDDDK*

9.1.7 co7TMΔ ELTD1 with HA N-terminal and FLAG C-terminal tags in pcDNA3.1 vector

9.1.7.1 Nucleotide sequence

ATGAAGAGACTGCCCCTGCTGGTGGTGTTCAGCACCCTGCTGAACTGCAGC
TACACCCAGTACCCCTACGACGTCCCCGACTACGCCACACAGCTGGGCATC
ATCATCAGCCTGATCTGCCTGGCTATCTGCATCTTCACCTTTTGGTTCTTCAG
CGAGATCCAGAGCACCCGGACCACCATCCACAAGAACCTGTGCTGCAGCCT
GTTTCTGGCCGAGCTGGTGTTCCTCGTGGGCATCAACACCAATACCAACAAG

CTGTTCTGCAGCATCATTGCCGGCCTGCTGCACTACTTCTTTCTGGCTGCCT
TCGCCTGGATGTGTATCGAGGGCATCCACCTGTACCTGATCGTCGTGGGCG
TGATCTACAACAAGGGCTTCCTGCACAAGAACTTCTACATCTTCGGCTACCTG
TCCCCAGCCGTGGTCGTGGGATTTTCTGCCGCCCTGGGCTACCGGTACTAC
GGCACCACAAAAGTGTGCTGGCTGAGCACCGAGAACAATTTCATCTGGTCCT
TCATCGGCCCAGCCTGCCTGATCATCCTCGTGAACCTGCTGGCCTTCGGAGT
GATCATCTACAAGGTGTTCCGGCACACAGCCGGCCTGAAGCCTGAGGTGTC
CTGCTTCGAGAACATCAGAAGCTGCGCCAGAGGGGCCCTGGCTCTGCTGTT
TCTGCTGGGCACCACCTGGATCTTCGGCGTGCTGCATGTGGTGCACGCCAG
CGTCGTGACCGCCTACCTGTTCACCGTGTCCAACGCCTTCCAGGGGATGTTC
ATCTTTCTGTTTCTGTGCGTGCTGAGCCGGAAGATTCAGGAAGAGTACTACC
GGCTGTTCAAGAACGTGCCCTGTTGCTTCGGCTGCCTGAGAGATTACAAGGA
TGACGACGATAAGTAA

9.1.7.2 Amino acid sequence

MKRLPLLVVFSTLLNCSYTQYPYDVPDYATQLGIIISLICLAICIFTFWFFSEIQSTRT
TIHKNLCCSLFLAELVFLVGINTNTNKLFCSIIAGLLHYFFLAAFAWMCIEGIHLYLIV
VGVIYNKGFLHKNFYIFGYLSPAVVVGFSAALGYRYYGTTKVCWLSTENNFIWSFI
GPACLIILVNLLAFGVIIYKVFRHTAGLKPEVSCFENIRSCARGALALLFLLGTTWIF
GVLHVVHASVVTAYLFTVSNAFQGMFIFLFLCVLSRKIQEEYYRLFKNVPCCFGC
LRDYKDDDDK*

9.1.8 coFL ELTD1 with GFP C-terminal tag in pcDNA3.1 vector

9.1.8.1 Nucleotide sequence

ATGAAGAGACTGCCCCTGCTGGTGGTGTTCAGCACCCTGCTGAACTGCAGC
TACACCCAGAACTGCACCAAGACCCCCTGCCTGCCCAACGCCAAGTGCGAG
ATCAGAAACGGCATCGAGGCCTGCTACTGCAACATGGGCTTCAGCGGCAAC

GGCGTGACCATCTGCGAGGACGACAACGAGTGCGGCAACCTGACCCAGAG

CTGCGGCGAGAACGCCAATTGCACCAACACCGAGGGCAGCTACTACTGTAT

GTGCGTGCCCGGCTTCAGAAGCAGCAGCAACCAGGACCGGTTCATCACCAA

CGACGGCACCGTGTGCATCGAGAACGTGAACGCCAACTGCCACCTGGACAA

CGTGTGTATCGCCGCCAACATCAACAAGACCCTGACCAAGATCCGGTCCATC

AAAGAACCCGTGGCCCTGCTGCAGGAAGTGTACCGGAACAGCGTGACCGAC

CTGAGCCCCACCGACATCATCACCTACATCGAGATCCTGGCCGAGAGCAGC

AGCCTGCTGGGCTACAAGAACAACACCATCAGCGCCAAGGACACCCTGAGC

AACTCCACCCTGACCGAGTTCGTGAAAACCGTGAACAACTTCGTGCAGCGG

GACACCTTCGTCGTGTGGGACAAGCTGAGCGTGAACCACAGACGGACCCAC

CTGACAAAGCTGATGCACACCGTGGAACAGGCCACCCTGCGGATCAGCCAG

AGCTTCCAGAAAACCACCGAGTTTGACACCAACAGCACCGATATCGCCCTGA

AGGTGTTCTTCTTCGACTCCTACAACATGAAGCACATCCACCCCCACATGAA

CATGGACGGCGACTACATCAACATCTTCCCCAAGCGGAAGGCCGCCTACGA

CAGCAACGGAAATGTGGCCGTGGCCTTCCTGTACTACAAGAGCATCGGCCC

CCTGCTGAGCAGCTCCGACAACTTCCTGCTGAAGCCTCAGAACTACGACAAC

AGCGAGGAAGAGGAACGCGTGATCAGCAGCGTGATCTCCGTGTCCATGTCC

AGCAACCCCCCCACCCTGTACGAGCTGGAAAAGATCACCTTCACCCTGTCCC

ACCGGAAAGTGACCGACAGATACCGGTCCCTGTGCGCCTTCTGGAACTACA

GCCCCGACACCATGAACGGCAGCTGGTCTAGCGAGGGCTGCGAGCTGACCT

ACAGCAACGAGACACACACCAGCTGCAGATGCAACCATCTGACCCACTTCGC

CATCCTGATGAGCAGCGGCCCCAGCATCGGCATCAAGGACTACAACATCCT

GACCCGGATCACACAGCTGGGCATCATCATCAGCCTGATCTGCCTGGCTATC

TGCATCTTCACCTTTTGGTTCTTCAGCGAGATCCAGAGCACCCGGACCACCA

TCCACAAGAACCTGTGCTGCAGCCTGTTTCTGGCCGAGCTGGTGTTCCTCGT

GGGCATCAACACCAATACCAACAAGCTGTTCTGCAGCATCATTGCCGGCCTG

CTGCACTACTTCTTTCTGGCTGCCTTCGCCTGGATGTGTATCGAGGGCATCC

ACCTGTACCTGATCGTCGTGGGCGTGATCTACAACAAGGGCTTCCTGCACAA

GAACTTCTACATCTTCGGCTACCTGTCCCCAGCCGTGGTCGTGGGATTTTCT

GCCGCCCTGGGCTACCGGTACTACGGCACCACAAAAGTGTGCTGGCTGAGC

ACCGAGAACAATTTCATCTGGTCCTTCATCGGCCCAGCCTGCCTGATCATCC

TCGTGAACCTGCTGGCCTTCGGAGTGATCATCTACAAGGTGTTCCGGCACAC

AGCCGGCCTGAAGCCTGAGGTGTCCTGCTTCGAGAACATCAGAAGCTGCGC

CAGAGGGGCCCTGGCTCTGCTGTTTCTGCTGGGCACCACCTGGATCTTCGG

CGTGCTGCATGTGGTGCACGCCAGCGTCGTGACCGCCTACCTGTTCACCGT

GTCCAACGCCTTCCAGGGGATGTTCATCTTTCTGTTTCTGTGCGTGCTGAGC

CGGAAGATTCAGGAAGAGTACTACCGGCTGTTCAAGAACGTGCCCTGTTGCT

TCGGCTGCCTGAGAATGGTGAGCAAGGGCGAGGAGCTGTTCACCGGGGTG

GTGCCCATCCTGGTCGAGCTGGACGGCGACGTAAACGGCCACAAGTTCAGC

GTGTCCGGCGAGGGCGAGGGCGATGCCACCTACGGCAAGCTGACCCTGAA

GTTCATCTGCACCACCGGCAAGCTGCCCGTGCCCTGGCCCACCCTCGTGAC

CACCCTGACCTACGGCGTGCAGTGCTTCAGCCGCTACCCCGACCACATGAA

GCAGCACGACTTCTTCAAGTCCGCCATGCCCGAAGGCTACGTCCAGGAGCG

CACCATCTTCTTCAAGGACGACGGCAACTACAAGACCCGCGCCGAGGTGAA

GTTCGAGGGCGACACCCTGGTGAACCGCATCGAGCTGAAGGGCATCGACTT

CAAGGAGGACGGCAACATCCTGGGGCACAAGCTGGAGTACAACTACAACAG

CCACAACGTCTATATCATGGCCGACAAGCAGAAGAACGGCATCAAGGTGAAC

TTCAAGATCCGCCACAACATCGAGGACGGCAGCGTGCAGCTCGCCGACCAC

TACCAGCAGAACACCCCCATCGGCGACGGCCCCGTGCTGCTGCCCGACAAC

CACTACCTGAGCACCCAGTCCAAGCTGAGCAAAGACCCCAACGAGAAGCGC

GATCACATGGTCCTGCTGGAGTTCGTGACCGCCGCCGGGATCACTCTCGGC

ATGGACGAGCTGTACAAGTAA

9.1.8.2 Amino acid sequence

MKRLPLLVVFSTLLNCSYTQNCTKTPCLPNAKCEIRNGIEACYCNMGFSGNGVTI

CEDDNECGNLTQSCGENANCTNTEGSYYCMCVPGFRSSSNQDRFITNDGTVCI

ENVNANCHLDNVCIAANINKTLTKIRSIKEPVALLQEVYRNSVTDLSPTDIITYIEILA

ESSSLLGYKNNTISAKDTLSNSTLTEFVKTVNNFVQRDTFVVWDKLSVNHRRTHL

TKLMHTVEQATLRISQSFQKTTEFDTNSTDIALKVFFFDSYNMKHIHPHMNMDGD

YINIFPKRKAAYDSNGNVAVAFLYYKSIGPLLSSSDNFLLKPQNYDNSEEEERVIS

SVISVSMSSNPPTLYELEKITFTLSHRKVTDRYRSLCAFWNYSPDTMNGSWSSE

GCELTYSNETHTSCRCNHLTHFAILMSSGPSIGIKDYNILTRITQLGIIISLICLAICIF

TFWFFSEIQSTRTTIHKNLCCSLFLAELVFLVGINTNTNKLFCSIIAGLLHYFFLAAF

AWMCIEGIHLYLIVVGVIYNKGFLHKNFYIFGYLSPAVVVGFSAALGYRYYGTTKV

CWLSTENNFIWSFIGPACLIILVNLLAFGVIIYKVFRHTAGLKPEVSCFENIRSCAR

GALALLFLLGTTWIFGVLHVVHASVVTAYLFTVSNAFQGMFIFLFLCVLSRKIQEE

YYRLFKNVPCCFGCLRMVSKGEELFTGVVPILVELDGDVNGHKFSVSGEGEGDA

TYGKLTLKFICTTGKLPVPWPTLVTTLTYGVQCFSRYPDHMKQHDFFKSAMPEG

YVQERTIFFKDDGNYKTRAEVKFEGDTLVNRIELKGIDFKEDGNILGHKLEYNYNS

HNVYIMADKQKNGIKVNFKIRHNIEDGSVQLADHYQQNTPIGDGPVLLPDNHYLS

TQSKLSKDPNEKRDHMVLLEFVTAAGITLGMDELYK*

9.1.9 coCTF ELTD1 with GFP C-terminal tag in pcDNA3.1 vector

9.1.9.1 Nucleotide sequence

ATGGCCTTACCAGTGACCGCCTTGCTCCTGCCGCTGGCCTTGCTGCTCCAC
GCCGCCAGGGCCACACATTTTGCAATTTTGATGTCCTCTGGTCCTTCCATTG
GTATTAAAGATTATAATATTCTTACAAGGATCACTCAACTAGGAATAATTATTT
CACTGATTTGTCTTGCCATATGCATTTTTACCTTCTGGTTCTTCAGTGAAATTC
AAAGCACCAGGACAACAATTCACAAAAATCTTTGCTGTAGCCTATTTCTTGCT
GAACTTGTTTTTCTTGTTGGGATCAATACAAATACTAATAAGCTCTTCTGTTCA
ATCATTGCTGGACTGCTACACTACTTCTTTTTAGCTGCTTTTGCATGGATGTG
CATTGAAGGCATACATCTCTATCTCATTGTTGTGGGTGTCATCTACAACAAGG
GATTTTTGCACAAGAATTTTTATATCTTTGGCTATCTAAGCCCAGCCGTGGTA
GTTGGATTTTCGGCAGCACTAGGATACAGATATTATGGCACAACCAAAGTAT
GTTGGCTTAGCACCGAAAACAACTTTATTTGGAGTTTTATAGGACCAGCATGC
CTAATCATTCTTGTTAATCTCTTGGCTTTTGGAGTCATCATATACAAAGTTTTT
CGTCACACTGCAGGGTTGAAACCAGAAGTTAGTTGCTTTGAGAACATAAGGT
CTTGTGCAAGAGGAGCCCTCGCTCTTCTGTTCCTTCTCGGCACCACCTGGAT
CTTTGGGGTTCTCCATGTTGTGCACGCATCAGTGGTTACAGCTTACCTCTTCA
CAGTCAGCAATGCTTTCCAGGGGATGTTCATTTTTTTATTCCTGTGTGTTTTAT
CTAGAAAGATTCAAGAAGAATATTACAGATTGTTCAAAAATGTCCCCTGTTGT
TTTGGATGTTTAAGG

9.1.9.2 Amino acid sequence

MALPVTALLLPLALLLHAARATHFAILMSSGPSIGIKDYNILTRITQLGIIISLICLAICI
FTFWFFSEIQSTRTTIHKNLCCSLFLAELVFLVGINTNTNKLFCSIIAGLLHYFFLAA
FAWMCIEGIHLYLIVVGVIYNKGFLHKNFYIFGYLSPAVVVGFSAALGYRYYGTTK
VCWLSTENNFIWSFIGPACLIILVNLLAFGVIIYKVFRHTAGLKPEVSCFENIRSCAR

GALALLFLLGTTWIFGVLHVVHASVVTAYLFTVSNAFQGMFIFLFLCVLSRKIQEE

YYRLFKNVPCCFGCL

9.1.10 co7TMΔ ELTD1 with GFP C-terminal tag in pcDNA3.1 vector

9.1.10.1 Nucleotide sequence

ATGGCCTTACCAGTGACCGCCTTGCTCCTGCCGCTGGCCTTGCTGCTCCAC

GCCGCCAGGGCCACTCAACTAGGAATAATTATTTCACTGATTTGTCTTGCCAT

ATGCATTTTTACCTTCTGGTTCTTCAGTGAAATTCAAAGCACCAGGACAACAA

TTCACAAAAATCTTTGCTGTAGCCTATTTCTTGCTGAACTTGTTTTTCTTGTTG

GGATCAATACAAATACTAATAAGCTCTTCTGTTCAATCATTGCTGGACTGCTA

CACTACTTCTTTTTAGCTGCTTTTGCATGGATGTGCATTGAAGGCATACATCT

CTATCTCATTGTTGTGGGTGTCATCTACAACAAGGGATTTTTGCACAAGAATT

TTTATATCTTTGGCTATCTAAGCCCAGCCGTGGTAGTTGGATTTTCGGCAGCA

CTAGGATACAGATATTATGGCACAACCAAAGTATGTTGGCTTAGCACCGAAAA

CAACTTTATTTGGAGTTTTATAGGACCAGCATGCCTAATCATTCTTGTTAATCT

CTTGGCTTTTGGAGTCATCATATACAAAGTTTTTCGTCACACTGCAGGGTTGA

AACCAGAAGTTAGTTGCTTTGAGAACATAAGGTCTTGTGCAAGAGGAGCCCT

CGCTCTTCTGTTCCTTCTCGGCACCACCTGGATCTTTGGGGTTCTCCATGTTG

TGCACGCATCAGTGGTTACAGCTTACCTCTTCACAGTCAGCAATGCTTTCCA

GGGGATGTTCATTTTTTTATTCCTGTGTGTTTTATCTAGAAAGATTCAAGAAGA

ATATTACAGATTGTTCAAAAATGTCCCCTGTTGTTTTGGATGTTTAAGG

9.1.10.2 Amino acid sequence

MALPVTALLLPLALLLHAARATQLGIIISLICLAICIFTFWFFSEIQSTRTTIHKNLCCS

LFLAELVFLVGINTNTNKLFCSIIAGLLHYFFLAAFAWMCIEGIHLYLIVVGVIYNKGF

LHKNFYIFGYLSPAVVVGFSAALGYRYYGTTKVCWLSTENNFIWSFIGPACLIILV

NLLAFGVIIYKVFRHTAGLKPEVSCFENIRSCARGALALLFLLGTTWIFGVLHVVHA

SVVTAYLFTVSNAFQGMFIFLFLCVLSRKIQEEYYRLFKNVPCCFGCLR

9.2 R script: microarray performed on ELTD1 silenced HUVECS

```
# ------------------------------------------------------
# ------------------------------------------------------
# "Silencing Analysis of ELTD1 silenced in HUVECS"
# Author: David Favara, July 2016
# Date: analysed 2015; reanalysed July 2016, May 2017
# ------------------------------------------------------
# ------------------------------------------------------
# Experiment: ELTD1 silencing microarray
# Chiptype: Illumina; Human 12v4 chip
# Samples:
# - huvec batch A (blue batch): 3x biological replicates:CT,siRNA1+2
# - silencing confirmed with WB/qPCR
# ------------------------------------------------------
# Version A of script: analysing batch A replicates (9/12 samples)
# ----------------------------
# 1) Normalisation using LIMMA
# ----------------------------

# Essentials
library("limma")

#  check you are in the right directory:
dir()

# 1.1) Ilumina normalisation and background correction using LIMMA package
x <- read.ilmn(
       files="SampleProbeProfile_David Favara.txt",
       ctrlfiles="ControlProbeProfile_David Favara.txt",
       other.columns="Detection"
       )

head(x)
dim(x)

# 1.2) Read annotation/phenodata into Illumina (designed after reviewing
targets <- readTargets("phenodata_9_samples.txt")

# 1.3) Box plot the non-normalised/corrected data
boxplot(log2(x$E), range=0, ylab="Log2 intensity", xlab="Non-normalised ELTD1
silenced HUVEC microarray samples")

# 1.4) check proportion of expressed probes for each sample/array
proportion <- propexpr(x)
proportion

# 1.5) Perform Limma normalisationPerform normexp-by-control background
correction, quantile normalization and log2 transformation
y <- neqc(x)

# 1.6) Box plot the normalised/corrected data
boxplot((y$E), range=0, ylab="Log2 intensity", xlab="Normalised ELTD1 silenced
HUVEC microarray samples")


# 1.7) remove probes whereby detection levels are insignificant
(>=detection.threshold) for ALL samples
detection.threshold <- 0.1
expressed <- apply(y$other$Detection < detection.threshold, 1, any)

# 1.8) keep expressed probes only
y <- y[expressed, ];

# 1.8.1) Review the output of the x matrix: what are it's headers:
head(y)
```

```
dim(y)

# 1.8.2) Make a new matrix y2 which only contains the required columns (remove
the non-analysed three columns)
# This will be used later on during contrast fitting
colnames(y)
y2 = y[, grep("Blue", colnames(y))]
head(y2)
dim(y2)

# 1.9) save the full table
write.table(y, file = "normalised.silenced_microarrray.txt", append = FALSE,
quote = TRUE, sep = "\t",
            eol = "\n", na = "NA", dec = ".", row.names = TRUE,
            col.names = NA, qmethod = c("escape", "double"),
            fileEncoding = "")

# ------------------------
# 2) Making contrast matrix & fitting a linear model
# ------------------------

# 2.1 Remind yourself about the target/phenodata/annotation file.
targets
targets$Group

# 2.2 Design the design matrix (must be a matrix made from factors!)
factor1 <-factor(targets$Group)
f.pairs <-factor(targets[,"SampleNo"])
design <-model.matrix(~0+factor1+f.pairs)
colnames(design)=gsub("factor1","",colnames(design))

# 2.3 check "design matrix". For 2.4 (next), remember to use y2 matrix!
Design. REMINDER: y2 = modified, normalised matrix..

# 2.4 Fit "design matrix" to data linear model to data
colnames(y2)
fit <- lmFit(y2, design)

#2.5 Define the "contrast matrix" and how it applies to "design matrix"
contrast.matrix <- makeContrasts(
             "si1-CT" = si1-CT,
             "si2-CT" = si2-CT,
             levels = design
             )
contrast.matrix

#2.6 Fit data matrix to design matrix
# make sure this was done earlier: y2 = y[, grep("Blue", colnames(y))]
fit <- lmFit(y2, design)

# 2.7 Apply the linear model and contrast matrix
fit2  <- contrasts.fit(fit, contrast.matrix)
fit3  <- eBayes(fit2)

# 2.8 Have a quick check of data from "fit3" using Limma TopTable
si1 <-topTable(fit3, coef = "si1-CT", sort.by='logFC',
adjust.method="BH",number=Inf)
head(si1)

si2 <-topTable(fit3, coef = "si2-CT", sort.by='logFC',
adjust.method="BH",number=Inf)
head(si2)

# 2.9 Save each contrast comparison to a text file
si1_minus_CT <-topTable(fit3, coef = "si1-CT", sort.by='logFC',
adjust.method="BH",number=Inf)
write.table(si1_minus_CT, file = "si1-CT.txt", append = FALSE, quote = TRUE, sep
= "\t",
            eol = "\n", na = "NA", dec = ".", row.names = TRUE,
            col.names = NA, qmethod = c("escape", "double"),
```

```
            fileEncoding = "")


si2_minus_CT <-topTable(fit3, coef = "si2-CT", sort.by='logFC',
adjust.method="BH",number=Inf)
write.table(si2_minus_CT, file = "si2-CT.txt", append = FALSE, quote = TRUE, sep
= "\t",
            eol = "\n", na = "NA", dec = ".", row.names = TRUE,
            col.names = NA, qmethod = c("escape", "double"),
            fileEncoding = "")

# 2.10 Alternative save with filtering on P Value
si1_minus_CT <-topTable(fit3, coef = "si1-CT", sort.by='P',
adjust.method="BH",number=Inf)
write.table(si1_minus_CT, file = "si1-CT.txt", append = FALSE, quote = TRUE, sep
= "\t",
            eol = "\n", na = "NA", dec = ".", row.names = TRUE,
            col.names = NA, qmethod = c("escape", "double"),
            fileEncoding = "")

si2_minus_CT <-topTable(fit3, coef = "si2-CT", sort.by='P',
adjust.method="BH",number=Inf)
write.table(si2_minus_CT, file = "si2-CT.txt", append = FALSE, quote = TRUE, sep
= "\t",
            eol = "\n", na = "NA", dec = ".", row.names = TRUE,
            col.names = NA, qmethod = c("escape", "double"),
            fileEncoding = "")

# -------------------------
# 3) Making Volcano plots
# -------------------------

# 3.1 Libraries needed: (if not prsent: install.packages('name of package')
library(dplyr)
library(ggplot2)
library(ggrepel)

# 3.2 If you want to contrasted data from the output files.
silence1 <- read.table("si1-CT.txt", header=TRUE)
head(silence1)

silence2 <- read.table("si2-CT.txt", header=TRUE)
head(silence2)

# 3.3 Use ggplot2 to make a beautifu volcano plot
#            First line sets the threshold! Theme is below
#            NB: if you want to remove the text-lines, just use geom_text
instead of geom_text_repel
#            NOTE: y axis should be 'adjusted p value' (except if you are not
filtering probe p value intensities; then make y = p value)
#            Threshold: logbase2FC = 1 (corresponds to FC of 2); adjusted p
value <0.05; (use abs command for FC: much neater!)

# 3.3.1 Plot graph (NB: must change the title (in: ggtitle) and table 'silence1'
(in: ggplot;geom_text)
g1 = ggplot(data=silence1, aes(x=logFC, y=-log10(adj.P.Val), colour=threshold)) +
    geom_point(alpha=0.5, size=4) +
    ggtitle("Microarray: si1-CT") +
    geom_hline(yintercept=1.30102999566, linetype="dashed", color = "red",
size=0.5)+geom_vline(xintercept=-1,0, linetype="dashed", color="red", size=0.5) +
    geom_vline(xintercept=1, linetype="dashed", color="red", size=0.5) +
    geom_vline(xintercept=0, linetype="dashed", color="red", size=0.5) +
    # this is where you telhel ggplot which samples to label (below); NB:
show.legend=F switches off the annoying "a" that will appear in legend box...
    geom_text_repel(data=filter(silence1, adj.P.Val<0.05, abs(logFC)>1),
aes(label=SYMBOL), show.legend=F, size=2.5,  fontface = 'bold',) +
    # Note: deleting the _repel above removes the lines and text repel feature.
    xlim(c(-4, 4)) + ylim(c(0, 2.5)) +
    xlab("log2 fold change") + ylab("-log10 adjusted p-value") +
```

```
    scale_color_manual("Threshold", values=c("#00BFC4","red"), labels = c("NS",
"Significant")) +
    theme(axis.text.x =
element_text(colour="grey20",size=16,angle=0,hjust=1,vjust=0,face="plain"),
          axis.text.y =
element_text(colour="grey20",size=16,angle=0,hjust=1,vjust=0,face="plain"),
          axis.title.x =
element_text(colour="grey20",size=20,angle=0,hjust=.5,vjust=0,face="bold"),
          axis.title.y =
element_text(colour="grey20",size=20,angle=90,hjust=.5,vjust=.5,face="bold"),
          plot.title = element_text(colour="grey20", face="bold", size=20),
          legend.title = element_text(colour="grey20", size=16, face="bold"),
          legend.background = element_rect(fill="white", size=0.5,
linetype="solid", colour ="grey20"),
          legend.text=element_text(size=12),
          panel.border = element_rect(colour = "grey20", linetype="solid",
fill=NA, size=1))

g1

# 3.4 save graph: (change the names!!)
ggsave(filename="si1-ct_repel.pdf", plot=g1)
ggsave(filename="si1-ct_repel.png", plot=g1, dpi=500)

# 3.5: perform step 3.3-3.4 again for the next graph type, changing the table and
titles.

# 3.5.1 Set Threshold    (NB: must change the table 'silence1' (in $logFC and
$adj.P.Val) x2 in line below for different graphs)
silence2$threshold = as.factor(abs(silence2$logFC) > 1 & silence2$adj.P.Val <
0.05)

# 3.5.2 Plot graph (NB: must change the title (in: ggtitle) and table 'silence1'
(in: ggplot;geom_text)
g2 = ggplot(data=silence2, aes(x=logFC, y=-log10(adj.P.Val), colour=threshold)) +
    geom_point(alpha=0.5, size=4) +
    ggtitle("Microarray: si2-CT") +
    geom_hline(yintercept=1.30102999566, linetype="dashed", color = "red",
size=0.5)+geom_vline(xintercept=-1,0, linetype="dashed", color="red", size=0.5) +
    geom_vline(xintercept=1, linetype="dashed", color="red", size=0.5) +
    geom_vline(xintercept=0, linetype="dashed", color="red", size=0.5) +
    # this is where you telhel ggplot which samples to label (below); NB:
show.legend=F switches off the annoying "a" that will appear in legend box...
    geom_text_repel(data=filter(silence2, adj.P.Val<0.05, abs(logFC)>1),
aes(label=SYMBOL), show.legend=F, size=2.5,  fontface = 'bold',) +
    xlim(c(-4, 4)) + ylim(c(0, 2.5)) +
    xlab("log2 fold change") + ylab("-log10 adjusted p-value") +
    scale_color_manual("Threshold", values=c("#00BFC4","red"), labels = c("NS",
"Significant")) +
    theme(axis.text.x =
element_text(colour="grey20",size=16,angle=0,hjust=1,vjust=0,face="plain"),
          axis.text.y =
element_text(colour="grey20",size=16,angle=0,hjust=1,vjust=0,face="plain"),
          axis.title.x =
element_text(colour="grey20",size=20,angle=0,hjust=.5,vjust=0,face="bold"),
          axis.title.y =
element_text(colour="grey20",size=20,angle=90,hjust=.5,vjust=.5,face="bold"),
          plot.title = element_text(colour="grey20", face="bold", size=20),
          legend.title = element_text(colour="grey20", size=16, face="bold"),
          legend.background = element_rect(fill="white", size=0.5,
linetype="solid", colour ="grey20"),
          legend.text=element_text(size=12),
          panel.border = element_rect(colour = "grey20", linetype="solid",
fill=NA, size=1))

g2

# 3.5.3 save graph: (change the names!!)
ggsave(filename="si2-ct_repel.pdf", plot=g2)
ggsave(filename="si2-ct_repel.png", plot=g2, dpi=500)
```

```
# ---------------
# List of up and down regulated genes
# ---------------
# si1-CT:

       # if want to split up and down regulated genes:
       # up:
       upregulated.topgenes.si1_minus_CT <- which((silence1[,"logFC"])>1 &
(silence1[,"adj.P.Val"]<0.05))
       list.upregulated.topgenes.si1_minus_CT <-
silence1[upregulated.topgenes.si1_minus_CT,]
       head(list.upregulated.topgenes.si1_minus_CT)
       dim(list.upregulated.topgenes.si1_minus_CT)

       # down:
       downregulated.topgenes.si1_minus_CT <- which((silence1[,"logFC"])<-(1) &
(silence1[,"adj.P.Val"]<0.05))
       list.downregulated.topgenes.si1_minus_CT <-
silence1[downregulated.topgenes.si1_minus_CT,]
       head(list.downregulated.topgenes.si1_minus_CT)
       dim(list.downregulated.topgenes.si1_minus_CT)


       # write output to file:
write.table(list.upregulated.topgenes.si1_minus_CT, file = "si1_minus_CT-
upregulated.txt", append = FALSE, quote = TRUE, sep = "\t",
            eol = "\n", na = "NA", dec = ".", row.names = FALSE,
            col.names = TRUE, qmethod = c("escape", "double"),
            fileEncoding = "")

write.table(list.downregulated.topgenes.si1_minus_CT, file = "si1_minus_CT-
downregulated.txt", append = FALSE, quote = TRUE, sep = "\t",
            eol = "\n", na = "NA", dec = ".", row.names = FALSE,
            col.names = TRUE, qmethod = c("escape", "double"),
            fileEncoding = "")

# si2-CT:
       # if want to split up and down regulated genes:
       # up:
       upregulated.topgenes.si2_minus_CT <- which((silence2[,"logFC"])>1 &
(silence2[,"adj.P.Val"]<0.05))
       list.upregulated.topgenes.si2_minus_CT <-
silence2[upregulated.topgenes.si2_minus_CT,]
       head(list.upregulated.topgenes.si2_minus_CT)
       dim(list.upregulated.topgenes.si2_minus_CT)

       # down:
       downregulated.topgenes.si2_minus_CT <- which((silence2[,"logFC"])<(-1) &
(silence2[,"adj.P.Val"]<0.05))
       list.downregulated.topgenes.si2_minus_CT <-
silence2[downregulated.topgenes.si2_minus_CT,]
       head(list.downregulated.topgenes.si2_minus_CT)
       dim(list.downregulated.topgenes.si2_minus_CT)


       # write output to file:
write.table(list.upregulated.topgenes.si2_minus_CT, file = "si2_minus_CT-
upregulated.txt", append = FALSE, quote = TRUE, sep = "\t",
            eol = "\n", na = "NA", dec = ".", row.names = FALSE,
            col.names = TRUE, qmethod = c("escape", "double"),
            fileEncoding = "")

write.table(list.downregulated.topgenes.si2_minus_CT, file = "si2_minus_CT-
downregulated.txt", append = FALSE, quote = TRUE, sep = "\t",
            eol = "\n", na = "NA", dec = ".", row.names = FALSE,
            col.names = TRUE, qmethod = c("escape", "double"),
            fileEncoding = "")
```

```
# -------------------------
# 4) Making Heatmap of data
# -------------------------
# Need to have      i) normalised microarray data (eg all 12 samples quantile
normalised)
#                         ii) summary output of contrast compared data
#
# Method:    1) Extract significant genes from summary output of contrast
compared data ((abs(logFC))>1 & (P.value)<0.05)
#                   2) Make a new matrix which contains data from normalised
matrix and significant genes from contrast compared data
#                   3) Make a heatmap based on this matrix.
#            4) Alternative is to select sig genes from siRNA1/2 (VENN) and then
apply this list to noramlised matrix and make heatmap from this



# load heatmap.2
library("gplots")
library("RColorBrewer"


# ---------------
# 4.1 si1-CT HEATMAP:
# ---------------
# 4.1.1 Extract sig genes from contrasted data; [Using logFC and P Value]
# -------------------------
new_si1_CT <-topTable(fit3, coef = "si1-CT", sort.by='logFC',
adjust.method="BH",number=Inf)
dim(new_si1_CT)
# filter for row names (Illumina ID's) whch fullfill the criteria of significance
(The best version). Illumina ID's are saved as row names!
genelist.si1_CT <- row.names(new_si1_CT)[which((abs(new_si1_CT[,"logFC"]))>1 &
(new_si1_CT[,"adj.P.Val"]<0.05))]
genelist.si1_CT

# -----
# 4.1.2 Apply above selected illumina ID's onto normalised matrix y2 and save
output as new dataframe si1_CT.heatmap
# -----
si1_CT.heatmap <- y2[genelist.si1_CT,]

write.table(si1_CT.heatmap, file = "si1_CT.heatmap.txt", append = FALSE, quote =
TRUE, sep = "\t",
            eol = "\n", na = "NA", dec = ".", row.names = TRUE,
            col.names = TRUE, qmethod = c("escape", "double"),
            fileEncoding = "")


# ---------------
# 4.2 si1-CT HEATMAP:
# ---------------
# 4.2.1 Extract sig genes from contrasted data; [Using logFC and P Value]
# -------------------------
new_si2_CT <-topTable(fit3, coef = "si2-CT", sort.by='logFC',
adjust.method="BH",number=Inf)
dim(new_si2_CT)
# filter for row names (Illumina ID's) whch fullfill the criteria of significance
(The best version). Illumina ID's are saved as row names!
genelist.si2_CT <- row.names(new_si2_CT)[which((abs(new_si2_CT[,"logFC"]))>1 &
(new_si2_CT[,"adj.P.Val"]<0.05))]
genelist.si2_CT

# -----
# 4.1.2 Apply above selected illumina ID's onto normalised matrix y2 and save
output as new dataframe si1_CT.heatmap
# -----
si2_CT.heatmap <- y2[genelist.si2_CT,]
```

```
write.table(si2_CT.heatmap, file = "si2_CT.heatmap.txt", append = FALSE, quote =
TRUE, sep = "\t",
            eol = "\n", na = "NA", dec = ".", row.names = TRUE,
            col.names = TRUE, qmethod = c("escape", "double"),
            fileEncoding = "")


# ---------------
# 4.3 HEATMAP consisting of shared sig. genes between si1-CT and si2-GT
# ---------------
# 4.3.1 Extract significant genes from contrast compared data; [Using logFC and P
Value]
# -------------------------
new_si1_CT <-topTable(fit3, coef = "si1-CT", sort.by='logFC',
adjust.method="BH",number=Inf)
new_si2_CT <-topTable(fit3, coef = "si2-CT", sort.by='logFC',
adjust.method="BH",number=Inf)

# filter for row names (Illumina ID's) whch fullfill the criteria of significance
(The best version). Illumina ID's are saved as row names!
genelist.si1_CT <- row.names(new_si1_CT)[which((abs(new_si1_CT[,"logFC"]))>1 &
(new_si1_CT[,"adj.P.Val"]<0.05))]
genelist.si2_CT <- row.names(new_si2_CT)[which((abs(new_si2_CT[,"logFC"]))>1 &
(new_si2_CT[,"adj.P.Val"]<0.05))]

# ---------------
# Use a Venn Diagram to extract shared genes from 2 lists
# ---------------
library(gplots)
# shows you what illumina ID's are shared between each siRNA calculation
venn(list(genelist.si1_CT, genelist.si2_CT))

# Save Venn as pdf (NB NB must end with dev.off() otherwise will not save)
pdf('si1_si2_venn_diagram).pdf')
venn(list(genelist.si1_CT, genelist.si2_CT))
dev.off()

# extract shared genes
sharedvenn <- venn(list(genelist.si1_CT, genelist.si2_CT))
genelist.shared_CT <- attr(sharedvenn,"intersections")$`A:B`

# Map list of shared genes to normalised data
shared.heatmap <- y2[genelist.shared_CT,]

write.table(shared.heatmap, file = "_shared.heatmap.txt", append = FALSE, quote =
TRUE, sep = "\t",
            eol = "\n", na = "NA", dec = ".", row.names = TRUE,
            col.names = TRUE, qmethod = c("escape", "double"),
            fileEncoding = "")

# ---------------
# Heatmap: use heatmap.2 (below) or Morpheus
# ---------------
colnames(shared.heatmap)
colnames(shared.heatmap) <-c("CT","CT","CT","siRNA 1","siRNA 1","siRNA 1","siRNA
2","siRNA 2","siRNA 2")

my_palette <- colorRampPalette(c("blue", "white", "red"))(n=50)
heatmap.2(as.matrix(shared.heatmap),
      xlab = "",
      ylab = "",
      main = "Shared silenced genes (siRNA 1 and 2)",
      labRow=test.genes$genes$SYMBOL,
      margins = c(2,10),
      Colv="NA", # turns off column clustering
      distfun = function(c) { dist(x = c, method = "euclidean") },
      scale = c("row"), #
      trace = "none",   # removes the trace in each square
      col=my_palette,
      key = TRUE,       #  key
```

```
keysize = 1.5,    #  size of key
density.info=c("none"),
)
```

9.3 R script: microarray performed on transient ELTD1 overexpressing HEK293T cells.

```
# ------------------------------------------------------
# ------------------------------------------------------
# "Silencing Analysis of ELTD1 overexpression in 293"
# Author: David Favara, July 2016
# Date: 22 July 2016       (reviewed again 24 April 2017)
# ------------------------------------------------------
# ------------------------------------------------------
# Experiment: ELTD1 overexpression microarray
# Chiptype: Illumina; Human 12v4 chip
# Samples:
# - 293T transient transfection: 3x biological replicates of: HA-FL, HA-CTF, Mock
# - 293T transient transfection: 1x biological replicate of: FL-GFP, CTF-GFP,
Mock
# - Transfection harvested at 24 hours and then passed through FACS. HA sorting
and GFP sorting performed for relevant populations.
# ------------------------------------------------------

# ------------------------------------------------------------------
# 1) Normalisation using LIMMA
# ------------------------------------------------------------------

# Essentials
library("limma")

# 1) Ilumina normalisation and background correction using LIMMA package
# NB: need the PROBE files: sample_probe.txt (your data) and control_probe.txt
(control for correction)
# Control probe:ControlProbeProfile_David Favara.txt
# Sample Probe: SampleProbeProfile_David Favara.txt
# Annotation data/phenodata: df_annotation.txt (you MUST edit this after inputing
file into
# limma as the column order of the inputted probe_profile will be changed by
limma.


# 1.1) Read the probe files into Limma and load the annotation file:
x <- read.ilmn(
       files="David_Sample_Probe_Profile.txt",
       ctrlfiles="ControlProbeProfile_David.txt",
       other.columns="Detection"
       )


# 1.2) Read annotation/phenodata into Illumina (designed after reviewing 1.1.1)
targets <- readTargets("phenodata_12_samples.txt")

# 1.3) Box plot the non-normalised/corrected data
boxplot(log2(x$E), range=0, ylab="Log2 intensity", xlab="Non-normalised ELTD1
overexpression in 293T cells samples")

# 1.4) check proportion of expressed probes for each sample/array
proportion <- propexpr(x)
proportion

# 1.5) Perform Limma normalisationPerform normexp-by-control background
correction, quantile normalization and log2 transformation
y <- neqc(x)
dim(y)

# 1.6) Box plot the normalised/corrected data (no need to log this data!)
boxplot((y$E), range=0, ylab="Log2 intensity", xlab="Normalised ELTD1
overexpression in 293T cells samples")
```

```
# 1.7) remove probes whereby detection levels are insignificant
(>=detection.threshold) for ALL samples
detection.threshold <- 0.5
expressed <- apply(y$other$Detection < detection.threshold, 1, any)


# 1.8) keep expressed probes only
y <- y[expressed, ];


# 1.8.1) Review the output of the x matrix: what are it's headers:
head(y)
dim(y)
colnames(y)



# 1.9) save the full table
write.table(y, file = "normalised.hek293overexpression_microarrray.txt", append =
FALSE, quote = TRUE, sep = "\t",
            eol = "\n", na = "NA", dec = ".", row.names = TRUE,
            col.names = NA, qmethod = c("escape", "double"),
            fileEncoding = "")

# ------------------------------------------------------------------
# 2) Making contrast matrix; fitting a linear model; applying contrast matrix to
original data
# ------------------------------------------------------------------

# 2.1 Remind yourself about the target/phenodata/anotation file.
targets
targets$Group

factor1 <-factor(c(1,2,3,4,1,2,3,4,1,2,3,4))

# Note: pairing in this case = batch / biological experiment replicate
# 2.2 Design the design matrix (must be a matrix made from factors!)
# Group = type of sample: eg CT, CTF or Mock
# F.pairs = batch number
factor1 <-factor(targets$Group)
f.pairs <-factor(targets[,"Batch"])
design <-model.matrix(~0+factor1+f.pairs)
colnames(design)=gsub("factor1","",colnames(design))

# 2.3 check "design matrix". For 2.4 (next), remember to use y2 matrix!
design

# REMINDER: y = modified, normalised matrix..

# 2.4 Fit "design matrix" to data linear model to data (help from:
https://www.bioconductor.org/help/course-
materials/2005/BioC2005/labs/lab01/estrogen/)
#        NB: in this case, choose y2 as this has the correct columns selected;
using y will give erroneous data
colnames(y)
fit <- lmFit(y, design)

# factor2 <-factor(targets[,"Group"], levels=unique(targets[,"Batch"]))
design <-model.matrix(~0+factor1+f.pairs)
colnames(design)=gsub("factor1","",colnames(design))

#factor1 <-factor(c(1,2,3,1,2,3,1,2,3,1,2,3))
#f.pairs <-factor(targets[,"SampleNo"], levels=unique(targets[,"SampleNo"]))
#design <-model.matrix(~0+factor1+f.pairs)


#2.5 Define the "contrast matrix" and how it applies to "design matrix"
contrast.matrix <- makeContrasts(
```

```
              "FL-Mock" = FL-Mock,
              "CTF-Mock" = CTF-Mock,
              "CTF-FL" = CTF-FL,
              levels = design
              )
contrast.matrix

#2.6 Fit data matrix to design matrix
fit <- lmFit(y, design)


# 2.7 Apply the linear model and contrast matrix
fit2  <- contrasts.fit(fit, contrast.matrix)
fit3  <- eBayes(fit2)

# 2.8 Have a quick check of data from "fit3" using Limma TopTable
FL <-topTable(fit3, coef = "FL-Mock", sort.by='logFC',
adjust.method="BH",number=Inf)
head(FL)

CTF <-topTable(fit3, coef = "CTF-Mock", sort.by='logFC',
adjust.method="BH",number=Inf)
head(CTF)

# 2.9 Save each contrast comparison to a text file
FL_minus_Mock<-topTable(fit3, coef = "FL-Mock", sort.by='logFC',
adjust.method="BH",number=Inf)
write.table(FL_minus_Mock, file = "_FL_minus_Mock.txt", append = FALSE, quote =
TRUE, sep = "\t",
            eol = "\n", na = "NA", dec = ".", row.names = TRUE,
            col.names = NA, qmethod = c("escape", "double"),
            fileEncoding = "")


CTF_minus_Mock <-topTable(fit3, coef = "CTF-Mock", sort.by='logFC',
adjust.method="BH",number=Inf)
write.table(CTF_minus_Mock, file = "_CTF_minus_Mock.txt", append = FALSE, quote =
TRUE, sep = "\t",
            eol = "\n", na = "NA", dec = ".", row.names = TRUE,
            col.names = NA, qmethod = c("escape", "double"),
            fileEncoding = "")


CTF_minus_FL <-topTable(fit3, coef = "CTF-FL", sort.by='logFC',
adjust.method="BH",number=Inf)
write.table(CTF_minus_FL, file = "_CTF_minus_FL.txt", append = FALSE, quote =
TRUE, sep = "\t",
            eol = "\n", na = "NA", dec = ".", row.names = TRUE,
            col.names = NA, qmethod = c("escape", "double"),
            fileEncoding = "")



# ------------------------------------------------------------------
# ------------------------------------------------------------------

# ------------------------------------------------------------------
# 3) Making Volcano plots to
# ------------------------------------------------------------------

# 3.1 Libraries needed: (if not prsent: install.packages('name of package')
library(dplyr)
library(ggplot2)
library(ggrepel)

# 3.2 If you want to contrasted data from the output files.
FL_Mock<- read.table("_FL_minus_Mock.txt", header=TRUE)
head(FL_Mock)

CTF_Mock <- read.table("_CTF_minus_Mock.txt", header=TRUE)
```

```
head(CTF_Mock)

CTF_FL <- read.table("_CTF_minus_FL.txt", header=TRUE)
head(CTF_Mock)


# 3.3 Use ggplot2 to make a beautifu volcano plot
#             First line sets the threshold! Theme is below
#             NB: if you want to remove the text-lines, just use geom_text
instead of geom_text_repel
#             NOTE: y axis should be 'adjusted p value' (except if you are not
filtering probe p value intensities; then make y = p value)
#             Threshold: logbase2FC = 1 (corresponds to FC of 2); adjusted p
value <0.05; (use abs command for FC: much neater!)

# Because detection p values are high in this sample and filtering was set to
0.5, I have been
# advised to avoid using adj.P value as filter for genes, and just use P value.

# 3.3.1 Set Threshold    (NB: must change the (in $logFC and $adj.P.Val) x2 in
line below for different graphs)
FL_Mock$threshold = as.factor(abs(FL_Mock$logFC) > 1 & FL_Mock$P.Value < 0.05)

# 3.3.1 Plot graph (NB: must change the title (in: ggtitle) and (in:
ggplot;geom_text)
g1 = ggplot(data=FL_Mock, aes(x=logFC, y=-log10(P.Value), colour=threshold)) +
    geom_point(alpha=0.5, size=4) +
    ggtitle("Microarray: FL-Mock") +
    geom_hline(yintercept=1.30102999566, linetype="dashed", color = "red",
size=0.5)+geom_vline(xintercept=-1,0, linetype="dashed", color="red", size=0.5) +
    geom_vline(xintercept=1, linetype="dashed", color="red", size=0.5) +
    geom_vline(xintercept=0, linetype="dashed", color="red", size=0.5) +
    # this is where you telhel ggplot which samples to label (below); NB:
show.legend=F switches off the annoying "a" that will appear in legend box...
    geom_text_repel(data=filter(FL_Mock, P.Value<0.05, abs(logFC)>1),
aes(label=TargetID), show.legend=F, size=2.5,  fontface = 'bold',) +
    xlim(c(-2.5, 8.5)) + ylim(c(0, 8)) +
    xlab("log2 fold change") + ylab("-log10 p-value") +
    scale_color_manual("Threshold", values=c("#00BFC4","red"), labels = c("NS",
"Significant")) +
    theme(axis.text.x =
element_text(colour="grey20",size=16,angle=0,hjust=1,vjust=0,face="plain"),
          axis.text.y =
element_text(colour="grey20",size=16,angle=0,hjust=1,vjust=0,face="plain"),
          axis.title.x =
element_text(colour="grey20",size=20,angle=0,hjust=.5,vjust=0,face="bold"),
          axis.title.y =
element_text(colour="grey20",size=20,angle=90,hjust=.5,vjust=.5,face="bold"),
          plot.title = element_text(colour="grey20", face="bold", size=20),
          legend.title = element_text(colour="grey20", size=16, face="bold"),
          legend.background = element_rect(fill="white", size=0.5,
linetype="solid", colour ="grey20"),
          legend.text=element_text(size=12),
          panel.border = element_rect(colour = "grey20", linetype="solid",
fill=NA, size=1))

g1

# 3.4 save graph: (change the names!!)
ggsave(filename="FL_Mock_notext.pdf", plot=g1)
ggsave(filename="FL_Mock_notext.png", plot=g1, dpi=500)



# 3.5: perform step 3.3-3.4 again for the next graph type, changing the table and
titles.

# 3.5.1 Set Threshold    (NB: must change the table (in $logFC and $adj.P.Val) x2
in line below for different graphs)
CTF_Mock$threshold = as.factor(abs(CTF_Mock$logFC) > 1 & CTF_Mock$P.Value < 0.05)
```

```
# 3.5.2 Plot graph (NB: must change the title (in: ggtitle) and table 'silence1'
(in: ggplot;geom_text)
g2 = ggplot(data=CTF_Mock, aes(x=logFC, y=-log10(P.Value), colour=threshold)) +
    geom_point(alpha=0.5, size=4) +
    ggtitle("Microarray: CTF-Mock") +
    geom_hline(yintercept=1.30102999566, linetype="dashed", color = "red",
size=0.5)+geom_vline(xintercept=-1,0, linetype="dashed", color="red", size=0.5) +
    geom_vline(xintercept=1, linetype="dashed", color="red", size=0.5) +
    geom_vline(xintercept=0, linetype="dashed", color="red", size=0.5) +
    # this is where you telhel ggplot which samples to label (below); NB:
show.legend=F switches off the annoying "a" that will appear in legend box...
    geom_text_repel(data=filter(CTF_Mock, P.Value<0.05, abs(logFC)>1),
aes(label=TargetID), show.legend=F, size=2.5,  fontface = 'bold',) +
    xlim(c(-2.5, 8)) + ylim(c(0, 8)) +
    xlab("log2 fold change") + ylab("-log10 p-value") +
    scale_color_manual("Threshold", values=c("#00BFC4","red"), labels = c("NS",
"Significant")) +
    theme(axis.text.x =
element_text(colour="grey20",size=16,angle=0,hjust=1,vjust=0,face="plain"),
          axis.text.y =
element_text(colour="grey20",size=16,angle=0,hjust=1,vjust=0,face="plain"),
          axis.title.x =
element_text(colour="grey20",size=20,angle=0,hjust=.5,vjust=0,face="bold"),
          axis.title.y =
element_text(colour="grey20",size=20,angle=90,hjust=.5,vjust=.5,face="bold"),
          plot.title = element_text(colour="grey20", face="bold", size=20),
          legend.title = element_text(colour="grey20", size=16, face="bold"),
          legend.background = element_rect(fill="white", size=0.5,
linetype="solid", colour ="grey20"),
          legend.text=element_text(size=12),
          panel.border = element_rect(colour = "grey20", linetype="solid",
fill=NA, size=1))

g2

# 3.5.3 save graph: (change the names!!)
ggsave(filename="CTF_Mock_notext.pdf", plot=g2)
ggsave(filename="CTF_Mock_notext.png", plot=g2, dpi=500)


# 3.6.1 Set Threshold    (NB: must change the table 'silence1' (in $logFC and
$adj.P.Val) x2 in line below for different graphs)
CTF_FL$threshold = as.factor(abs(CTF_FL$logFC) > 1 & CTF_FL$P.Value < 0.05)

# 3.6.2 Plot graph (NB: must change the title (in: ggtitle) and table (in:
ggplot;geom_text)
g3 = ggplot(data=CTF_FL, aes(x=logFC, y=-log10(P.Value), colour=threshold)) +
    geom_point(alpha=0.5, size=4) +
    ggtitle("Microarray: CTF-FL") +
    geom_hline(yintercept=1.30102999566, linetype="dashed", color = "red",
size=0.5)+geom_vline(xintercept=-1,0, linetype="dashed", color="red", size=0.5) +
    geom_vline(xintercept=1, linetype="dashed", color="red", size=0.5) +
    geom_vline(xintercept=0, linetype="dashed", color="red", size=0.5) +
    # this is where you telhel ggplot which samples to label (below); NB:
show.legend=F switches off the annoying "a" that will appear in legend box...
    geom_text_repel(data=filter(CTF_FL, P.Value<0.05, abs(logFC)>1),
aes(label=TargetID), show.legend=F, size=2.5,  fontface = 'bold',) +
    xlim(c(-5, 3)) + ylim(c(0, 8)) +
    xlab("log2 fold change") + ylab("-log10 p-value") +
    scale_color_manual("Threshold", values=c("#00BFC4","red"), labels = c("NS",
"Significant")) +
    theme(axis.text.x =
element_text(colour="grey20",size=16,angle=0,hjust=1,vjust=0,face="plain"),
          axis.text.y =
element_text(colour="grey20",size=16,angle=0,hjust=1,vjust=0,face="plain"),
          axis.title.x =
element_text(colour="grey20",size=20,angle=0,hjust=.5,vjust=0,face="bold"),
          axis.title.y =
element_text(colour="grey20",size=20,angle=90,hjust=.5,vjust=.5,face="bold"),
```

```
          plot.title = element_text(colour="grey20", face="bold", size=20),
          legend.title = element_text(colour="grey20", size=16, face="bold"),
          legend.background = element_rect(fill="white", size=0.5,
linetype="solid", colour ="grey20"),
          legend.text=element_text(size=12),
          panel.border = element_rect(colour = "grey20", linetype="solid",
fill=NA, size=1))

g3

# 3.6.3 save graph: (change the names!!)
ggsave(filename="CTF_FL_notext.pdf", plot=g3)
ggsave(filename="CTF_FL_notext.png", plot=g3, dpi=500)

topgenes.FLminusMOCK <- which((abs(FL_Mock[,"logFC"]))>1 &
(FL_Mock[,"P.Value"]<0.05))
list.topgenes.FLminusMOCK <- FL_Mock[topgenes.FLminusMOCK,]
head(list.topgenes.FLminusMOCK)
dim(list.topgenes.FLminusMOCK)

# write output to file:
write.table(list.topgenes.FLminusMOCK, file = "list.topgenes.FLminusMOCK.txt",
append = FALSE, quote = TRUE, sep = "\t",
            eol = "\n", na = "NA", dec = ".", row.names = FALSE,
            col.names = TRUE, qmethod = c("escape", "double"),
            fileEncoding = "")

      # if want to split up and down regulated genes:
      # up:
      upregulated.topgenes.FLminusMOCK <- which((FL_Mock[,"logFC"])>1 &
(FL_Mock[,"P.Value"]<0.05))
      list.upregulated.topgenes.FLminusMOCK <-
FL_Mock[upregulated.topgenes.FLminusMOCK,]
      head(list.upregulated.topgenes.FLminusMOCK)
      dim(list.upregulated.topgenes.FLminusMOCK)

      # down:
      downregulated.topgenes.FLminusMOCK <- which((FL_Mock[,"logFC"])<1 &
(FL_Mock[,"P.Value"]<0.05))
      list.downregulated.topgenes.FLminusMOCK <-
FL_Mock[downregulated.topgenes.FLminusMOCK,]
      head(list.downregulated.topgenes.FLminusMOCK)
      dim(list.downregulated.topgenes.FLminusMOCK)


      # write output to file:
write.table(list.upregulated.topgenes.FLminusMOCK, file =
"list.upregulated.topgenes.FLminusMOCK.txt", append = FALSE, quote = TRUE, sep =
"\t",
            eol = "\n", na = "NA", dec = ".", row.names = FALSE,
            col.names = TRUE, qmethod = c("escape", "double"),
            fileEncoding = "")

write.table(list.downregulated.topgenes.FLminusMOCK, file =
"list.downregulated.topgenes.FLminusMOCK.txt", append = FALSE, quote = TRUE, sep
= "\t",
            eol = "\n", na = "NA", dec = ".", row.names = FALSE,
            col.names = TRUE, qmethod = c("escape", "double"),
            fileEncoding = "")

# CTF-FL

# IF WANT TO MAKE WITH UP AND DOWN REGULATED GENES TOGETHER FOR VENN DIAGRAM
topgenes.CTFminusMOCK <- which((abs(CTF_Mock[,"logFC"]))>1 &
(CTF_Mock[,"P.Value"]<0.05))
list.topgenes.CTFminusMOCK <- CTF_Mock[topgenes.CTFminusMOCK,]
head(list.topgenes.CTFminusMOCK)
dim(list.topgenes.CTFminusMOCK)

# write output to file:
```

```
write.table(list.topgenes.CTFminusMOCK, file = "list.topgenes.CTFminusMOCK.txt",
append = FALSE, quote = TRUE, sep = "\t",
            eol = "\n", na = "NA", dec = ".", row.names = FALSE,
            col.names = TRUE, qmethod = c("escape", "double"),
            fileEncoding = "")


# if want to split up and down regulated genes:
# up:
upregulated.topgenes.CTFminusMOCK <- which((CTF_Mock[,"logFC"])>1 &
(CTF_Mock[,"P.Value"]<0.05))
list.upregulated.topgenes.CTFminusMOCK <-
CTF_Mock[upregulated.topgenes.CTFminusMOCK,]
head(list.upregulated.topgenes.CTFminusMOCK)
dim(list.upregulated.topgenes.CTFminusMOCK)

# down:
downregulated.topgenes.CTFminusMOCK <- which((CTF_Mock[,"logFC"])<1 &
(CTF_Mock[,"P.Value"]<0.05))
list.downregulated.topgenes.CTFminusMOCK <-
CTF_Mock[downregulated.topgenes.CTFminusMOCK,]
head(list.downregulated.topgenes.CTFminusMOCK)
dim(list.downregulated.topgenes.CTFminusMOCK)


# write output to file:
write.table(list.upregulated.topgenes.CTFminusMOCK, file =
"list.upregulated.topgenes.CTFminusMOCK.txt", append = FALSE, quote = TRUE, sep =
"\t",
            eol = "\n", na = "NA", dec = ".", row.names = FALSE,
            col.names = TRUE, qmethod = c("escape", "double"),
            fileEncoding = "")

write.table(list.downregulated.topgenes.CTFminusMOCK, file =
"list.downregulated.topgenes.CTFminusMOCK.txt", append = FALSE, quote = TRUE, sep
= "\t",
            eol = "\n", na = "NA", dec = ".", row.names = FALSE,
            col.names = TRUE, qmethod = c("escape", "double"),
            fileEncoding = "")


# ------------------------------------------------------------------
# 4) Making Heatmap of data
# ------------------------------------------------------------------
# Need to have      i) normalised microarray data (eg all 12 samples quantile
normalised)
#                         ii) summary output of contrast compared data
#
# Method:    1) Extract significant genes from summary output of contrast
compared data ((abs(logFC))>1 & (P.value)<0.05)
#                   2) Make a new matrix which contains data from normalised
matrix and significant genes from contrast compared data
#                   3) Make a heatmap based on this matrix.

# ---------------
# FL-MOCK HEATMAP:
# ---------------
# 4.1.2 Extract significant genes from contrast compared data; [Using logFC and P
Value]
# -------------------------
heatmaplist.FL_mock <-topTable(fit3, coef = "FL-Mock", sort.by='logFC',
adjust.method="BH",number=Inf)
dim(heatmaplist.FL_mock)
# filter for row names (Illumina ID's) whch fullfill the criteria of significance
(The best version). Illumina ID's are saved as row names!
genenames.heatmaplist.FL_mock <-
row.names(heatmaplist.FL_mock)[which((abs(heatmaplist.FL_mock[,"logFC"]))>1 &
(heatmaplist.FL_mock[,"P.Value"]<0.05))]
genenames.heatmaplist.FL_mock
```

```
# 4.1.2 Apply above selected illumina ID's onto normalised matrix y and save
output as new dataframe
FL_mock.heatmap <- y[genenames.heatmaplist.FL_mock,]

write.table(FL_mock.heatmap, file = "FL_mock.heatmap.txt", append = FALSE, quote
= TRUE, sep = "\t",
            eol = "\n", na = "NA", dec = ".", row.names = TRUE,
            col.names = TRUE, qmethod = c("escape", "double"),
            fileEncoding = "")


# ---------------
# CTF-MOCK HEATMAP:
# ---------------
# 4.2.1 Extract significant genes from contrast compared data; [Using logFC and P
Value]
# -------------------------
heatmaplist.CTF_mock <-topTable(fit3, coef = "CTF-Mock", sort.by='logFC',
adjust.method="BH",number=Inf)
dim(heatmaplist.CTF_mock)
# filter for row names (Illumina ID's) whch fullfill the criteria of significance
(The best version). Illumina ID's are saved as row names!
genenames.heatmaplist.CTF_mock <-
row.names(heatmaplist.CTF_mock)[which((abs(heatmaplist.CTF_mock[,"logFC"]))>1 &
(heatmaplist.CTF_mock[,"P.Value"]<0.05))]
genenames.heatmaplist.CTF_mock

# 4.2.2 Apply above selected illumina ID's onto normalised matrix y and save
output as new dataframe
CTF_mock.heatmap <- y[genenames.heatmaplist.CTF_mock,]

write.table(CTF_mock.heatmap, file = "CTF_mock.heatmap.txt", append = FALSE,
quote = TRUE, sep = "\t",
            eol = "\n", na = "NA", dec = ".", row.names = TRUE,
            col.names = TRUE, qmethod = c("escape", "double"),
            fileEncoding = "")

# PLOT HEATMAP USING HEATMAP.2 OR MORPHEUS
# Clustering strategy:
# one minus Pearson correlation hierarchical clustering: rows & columns
```

9.4 R script: microarray performed on stable ELTD1 overexpressing HUVECS

```
# ------------------------------------------------------
# ------------------------------------------------------
# "coELTD1 overexpression in HUVEC and HMEC cells"
# Author: David Favara, December 2016
# Date: 6.12.2016
# ------------------------------------------------------
# ------------------------------------------------------
# Experiment: ELTD1 overexpression array
# Chiptype: Illumina; Human 12v4 chip
# Samples:
# - huvec batch A (purple batch): 1x biological replicate of CT,
ELTD1_overexpression
# - huvec batch B (yellow batch): 1x biological replicate of CT,
ELTD1_overexpression
# - HMEC batch 1: 1x biological replicate of CT, ELTD1_overexpression
# - ELTD1 overexpression confirmed by RNA and WB: awaiting RAW data from Helen
Sheldon (4.12.2016)
# - NB: samples are 1-6 (A1-F1). These have been technically replicated 7-12 (A2-
F2)
# ------------------------------------------------------
# notes from a previous batch run:
# I had a lot of issues running the analysis at the contrast matrix design stage.
This was
# purely because Limma changes the order of columns once you load the original
array into
# limma. The original data is ordered as following: CT, S1, Si2, CT, Si1, Si2, (4
replicates in total)
# Limma appears to change this order to: CT, CT, CT, CT, Si1, Si1, Si1, Si1, Si2,
Si2, Si2, Si2.
# Thus, it is important to change the phenodata/annotation/"targets" file to
reflect this.
# If not, contrast comparisons will lead to bogus data.

# ------------------------------------------------------
# Version A of script: analysing HUVEC replicates (8/12 samples)
# ------------------------------------------------------
#
# 1) Normalisation using LIMMA
# ------------------------------------------------------

# Essentials
library("limma")
setwd("~/Desktop/_4.12.2016microarray/HUVEC [ in progress]/raw")

#  check you are in the right directory:
dir()

# 1) Ilumina normalisation and background correction using LIMMA package
# 1.1) Read the probe files into Limma and load the annotation file:
x <- read.ilmn(
       files="SampleProbeProfile_Helen.txt",
       ctrlfiles="ControlProbeProfile_Helen.txt",
       other.columns="Detection"
       )

# 1.2) Read annotation/phenodata into Illumina (designed after reviewing 1.1.1)
targets <- readTargets("phenodata_8_samples_huvec.txt")

# 1.3) Box plot the non-normalised/corrected data
boxplot(log2(x$E), range=0, ylab="Log2 intensity", xlab="Non-normalised ELTD1
overexrepssion HUVEC microarray samples")
```

```
# 1.4) check proportion of expressed probes for each sample/array
proportion <- propexpr(x)
proportion

# 1.5) Perform Limma normalisationPerform normexp-by-control background
correction, quantile normalization and log2 transformation
y <- neqc(x)

# 1.6) Box plot the normalised/corrected data (no need to log this data!)
boxplot((y$E), range=0, ylab="Log2 intensity", xlab="Normalised ELTD1
overexpression HUVEC microarray samples")

# 1.6.1 Plot Multi-dimensional table showing similarity between samples
plotMDS(y)

# 1.7) remove probes whereby detection levels are insignificant
(>=detection.threshold) for ALL samples
detection.threshold <- 0.1
expressed <- apply(y$other$Detection < detection.threshold, 1, any)


# 1.8) keep expressed probes only
y <- y[expressed, ];


# 1.9) Review the output of the y matrix: what are it's headers:
colnames(y)
dim(y)

# 1.9.1) Remove the excess columns which contain HMEC data: in this case it is:
E1, F1, E2, F2
   # make new matrix with E1 removed:
y1<- y[,-5]
   # check to see if column removed:
colnames(y1)
   # then remove F1
y1<- y1[,-5]
   # check to see if column removed:
colnames(y1)
   # Then remove E2
y1<- y1[,-9]
   # check to see if column removed:
colnames(y1)
   # Then remove F2
y1<- y1[,-9]
   # check to see if column removed:
colnames(y1)


# 1.10) save the full table
write.table(y1, file = "normalised.huvec_overexpression_microarrray.txt", append
= FALSE, quote = TRUE, sep = "\t",
            eol = "\n", na = "NA", dec = ".", row.names = TRUE,
            col.names = NA, qmethod = c("escape", "double"),
            fileEncoding = "")

# ------------------------------------------------------------------
# 2) Making contrast matrix; fitting a linear model; applying contrast matrix to
original data
# ------------------------------------------------------------------

# 2.1 Remind yourself about the target/phenodata/anotation file.
targets
targets$Group

# 2.2 Design the design matrix (must be a matrix made from factors!)
factor1 <-factor(targets$Group)
f.pairs <-factor(targets[,"SampleNo"])
design <-model.matrix(~0+factor1+f.pairs)
colnames(design)=gsub("factor1","",colnames(design))
```

```
# 2.3 check "design matrix". For 2.4 (next), remember to use y2 matrix!
design

# 2.4 Fit "design matrix" to data linear model to data (help from:
https://www.bioconductor.org/help/course-
materials/2005/BioC2005/labs/lab01/estrogen/)
#        NB: in this case, choose y2 as this has the correct columns selected;
using y will give erroneous data
colnames(y)
fit <- lmFit(y1, design)


#2.5 Define the "contrast matrix" and how it applies to "design matrix"
contrast.matrix <- makeContrasts(
              "coELTD1-CT" = coELTD1-CT,
              levels = design
              )
contrast.matrix

#2.6 Fit data matrix to design matrix
# make sure this was done earlier: removal of extra columns from y to make y1
fit <- lmFit(y1, design)


# 2.7 Apply the linear model and contrast matrix
fit2  <- contrasts.fit(fit, contrast.matrix)
fit3  <- eBayes(fit2)

# 2.8 Have a quick check of data from "fit3" using Limma TopTable
coELTD1_CT <-topTable(fit3, coef = "coELTD1-CT", sort.by='logFC',
adjust.method="BH",number=Inf)
head(coELTD1_CT)



# 2.9 Save each contrast comparison to a text file
coELTD1_minus_CT <-topTable(fit3, coef = "coELTD1-CT", sort.by='logFC',
adjust.method="BH",number=Inf)
write.table(coELTD1_minus_CT, file = "coELTD1_minus_CT-logfc_sorted.txt", append
= FALSE, quote = TRUE, sep = "\t",
            eol = "\n", na = "NA", dec = ".", row.names = TRUE,
            col.names = NA, qmethod = c("escape", "double"),
            fileEncoding = "")


# 2.10 Alternative save with filtering on P Value
coELTD1_minus_CT <-topTable(fit3, coef = "coELTD1-CT", sort.by='P',
adjust.method="BH",number=Inf)
write.table(coELTD1_minus_CT, file = "coELTD1_minus_CT-p_value_sorted.txt",
append = FALSE, quote = TRUE, sep = "\t",
            eol = "\n", na = "NA", dec = ".", row.names = TRUE,
            col.names = NA, qmethod = c("escape", "double"),
            fileEncoding = "")


# ---------------------------------------------------------------------
# 3) Making Volcano plots to
# ---------------------------------------------------------------------

# 3.1 Libraries needed: (if not prsent: install.packages('name of package')
library(dplyr)
library(ggplot2)
library(ggrepel)

# 3.2 If you want to contrasted data from the output files.
coELTD1_CT <- read.table("coELTD1_minus_CT.txt", header=TRUE)
head(coELTD1_CT)
```

```
# 3.3 Use ggplot2 to make a beautifu volcano plot
#            First line sets the threshold! Theme is below
#            NB: if you want to remove the text-lines, just use geom_text
instead of geom_text_repel
#            NOTE: y axis should be 'adjusted p value' (except if you are not
filtering probe p value intensities; then make y = p value)
#            Threshold: logbase2FC = 1 (corresponds to FC of 2); adjusted p
value <0.05; (use abs command for FC: much neater!)


#############
# Set y axis to adjusted p value (standard) [coELTD1_CT]
#############
# 3.3.1 Set Threshold    (NB: must change the table 'coELTD1_CT' (in $logFC and
$adj.P.Val) x2 in line below for different graphs)
coELTD1_CT$threshold = as.factor(abs(coELTD1_CT$logFC) > 1 & coELTD1_CT$adj.P.Val
< 0.05)

# 3.3.1 Plot graph (NB: must change the title (in: ggtitle) and table
'coELTD1_CT' (in: ggplot;geom_text)
g1 = ggplot(data=coELTD1_CT, aes(x=logFC, y=-log10(adj.P.Val), colour=threshold))
+
    geom_point(alpha=0.5, size=4) +
    ggtitle("Microarray: coELTD1 overexpression-CT (HUVECs)") +
    geom_hline(yintercept=1.30102999566, linetype="dashed", color = "red",
size=0.5)+geom_vline(xintercept=-1,0, linetype="dashed", color="red", size=0.5) +
    geom_vline(xintercept=1, linetype="dashed", color="red", size=0.5) +
    geom_vline(xintercept=0, linetype="dashed", color="red", size=0.5) +
    # this is where you telhel ggplot which samples to label (below); NB:
show.legend=F switches off the annoying "a" that will appear in legend box...
    geom_text_repel(data=filter(coELTD1_CT, adj.P.Val<0.05, abs(logFC)>1),
aes(label=SYMBOL), show.legend=F, size=2.5,  fontface = 'bold',) +
    xlim(c(-3, 3)) + ylim(c(0, 3.5)) +
    xlab("log2 fold change") + ylab("-log10 adjusted p-value") +
    scale_color_manual("Threshold", values=c("#00BFC4","red"), labels = c("NS",
"Significant")) +
    theme(axis.text.x =
element_text(colour="grey20",size=16,angle=0,hjust=1,vjust=0,face="plain"),
          axis.text.y =
element_text(colour="grey20",size=16,angle=0,hjust=1,vjust=0,face="plain"),
          axis.title.x =
element_text(colour="grey20",size=20,angle=0,hjust=.5,vjust=0,face="bold"),
          axis.title.y =
element_text(colour="grey20",size=20,angle=90,hjust=.5,vjust=.5,face="bold"),
          plot.title = element_text(colour="grey20", face="bold", size=20),
          legend.title = element_text(colour="grey20", size=16, face="bold"),
          legend.background = element_rect(fill="white", size=0.5,
linetype="solid", colour ="grey20"),
          legend.text=element_text(size=12),
          panel.border = element_rect(colour = "grey20", linetype="solid",
fill=NA, size=1))

g1

# 3.4 save graph: (change the names!!)
ggsave(filename="coELTD1-CT.pdf", plot=g1)
ggsave(filename="coELTD1-CT.png", plot=g1, dpi=500)

#############
# Set y axis to p value (from adjusted p value) [use this to fish for more
results) [this will be made into matrix coELTD1_CT2]
#############
# 3.5 Set Threshold    (NB: must change the table 'coELTD1_CT' (in $logFC and
$adj.P.Val) x2 in line below for different graphs)
coELTD1_CT2 <-coELTD1_CT
coELTD1_CT2$threshold = as.factor(abs(coELTD1_CT2$logFC) > 1 &
coELTD1_CT2$P.Value < 0.05)
```

```
# 3.5.2 Plot graph (NB: must change the title (in: ggtitle) and table
'coELTD1_CT' (in: ggplot;geom_text)
g2 = ggplot(data=coELTD1_CT2, aes(x=logFC, y=-log10(P.Value), colour=threshold))
+
    geom_point(alpha=0.5, size=4) +
    ggtitle("Microarray: coELTD1 overexpression-CT (HUVECs)") +
    geom_hline(yintercept=1.30102999566, linetype="dashed", color = "red",
size=0.5)+geom_vline(xintercept=-1,0, linetype="dashed", color="red", size=0.5) +
    geom_vline(xintercept=1, linetype="dashed", color="red", size=0.5) +
    geom_vline(xintercept=0, linetype="dashed", color="red", size=0.5) +
    # this is where you telhel ggplot which samples to label (below); NB:
show.legend=F switches off the annoying "a" that will appear in legend box...
    geom_text_repel(data=filter(coELTD1_CT2, P.Value<0.05, abs(logFC)>1),
aes(label=SYMBOL), show.legend=F, size=2.5,  fontface = 'bold',) +
    xlim(c(-3, 3)) + ylim(c(0, 8)) +
    xlab("log2 fold change") + ylab("-log10 P-value") +
    scale_color_manual("Threshold", values=c("#00BFC4","red"), labels = c("NS",
"Significant")) +
    theme(axis.text.x =
element_text(colour="grey20",size=16,angle=0,hjust=1,vjust=0,face="plain"),
          axis.text.y =
element_text(colour="grey20",size=16,angle=0,hjust=1,vjust=0,face="plain"),
          axis.title.x =
element_text(colour="grey20",size=20,angle=0,hjust=.5,vjust=0,face="bold"),
          axis.title.y =
element_text(colour="grey20",size=20,angle=90,hjust=.5,vjust=.5,face="bold"),
          plot.title = element_text(colour="grey20", face="bold", size=20),
          legend.title = element_text(colour="grey20", size=16, face="bold"),
          legend.background = element_rect(fill="white", size=0.5,
linetype="solid", colour ="grey20"),
          legend.text=element_text(size=12),
          panel.border = element_rect(colour = "grey20", linetype="solid",
fill=NA, size=1))

g2

# 3.5.2 save graph: (change the names!!)
ggsave(filename="coELTD1-CT_p_value.pdf", plot=g2)
ggsave(filename="coELTD1-CT_p_value.png", plot=g2, dpi=500)



# --------------------- NB ---------------------
# 3.6 save positive data from each significant list
       # Filters: adj p value <0.05 ; log2(FC) >abs(1)
       # OR:
       # Filters: p value <0.05 ; log2(FC) >abs(1)
       #
       # NOTEs:
       # This tells you which rows have Adj P Value <0.05: neat!
which(coELTD1_CT[,"adj.P.Val"]<0.05)
       # This does the same thing for fold change: which(coELTD1_CT[,"logFC"]>1 |
silence1[,"logFC"]<(-1)
       # A neater version of the above with (abs) and gives exactly the same
output: which((abs(coELTD1_CT[,"logFC"]))>1)
       # Combined: which((abs(coELTD1_CT[,"logFC"]))>1 &
(coELTD1_CT[,"adj.P.Val"]<0.05))

# --------------------- NB ---------------------
# Saving significant genes from volcano plot analysis:
       # you can increase and decrease the logFC and adjP Value parameters below

# -------------------------------------
# 3.6.1 SAVING adjusted p value values [from coELTD1_CT]
# Need to have made volcano plot and set threshold on coELTD1_CT first
# -------------------------------------

#IF WANT TO MAKE WITH UP AND DOWN REGULATED GENES TOGETHER (NB FOR HEATMAP):
topgenes.coELTD1_CT <- which((abs(coELTD1_CT[,"logFC"]))>1 &
(coELTD1_CT[,"adj.P.Val"]<0.05))
```

```
list.topgenes.coELTD1_CT <- coELTD1_CT[topgenes.coELTD1_CT,]
head(list.topgenes.coELTD1_CT)
dim(list.topgenes.coELTD1_CT)
write.table(list.topgenes.coELTD1_CT, file =
"list_of_significant_differentially_expressed_genes(logFC_and_adjusted_p_val_filt
ered).txt", append = FALSE, quote = TRUE, sep = "\t",
            eol = "\n", na = "NA", dec = ".", row.names = FALSE,
            col.names = TRUE, qmethod = c("escape", "double"),
            fileEncoding = "")

      # if want to split up and down regulated genes:
      # up:
      upregulated.topgenes.coELTD1_CT <- which((coELTD1_CT[,"logFC"])>1 &
(coELTD1_CT[,"adj.P.Val"]<0.05))
      list.upregulated.topgenes.coELTD1_CT <-
coELTD1_CT[upregulated.topgenes.coELTD1_CT,]
      head(list.upregulated.topgenes.coELTD1_CT)
      dim(list.upregulated.topgenes.coELTD1_CT)

      # down:
      downregulated.topgenes.coELTD1_CT <- which((coELTD1_CT[,"logFC"])<1 &
(coELTD1_CT[,"adj.P.Val"]<0.05))
      list.downregulated.topgenes.coELTD1_CT <-
coELTD1_CT[downregulated.topgenes.coELTD1_CT,]
      head(list.downregulated.topgenes.coELTD1_CT)
      dim(list.downregulated.topgenes.coELTD1_CT)


      # write output to file:
write.table(list.upregulated.topgenes.coELTD1_CT, file = "coELTD1_CT-
upregulated_(adjusted_p_Value).txt", append = FALSE, quote = TRUE, sep = "\t",
            eol = "\n", na = "NA", dec = ".", row.names = FALSE,
            col.names = TRUE, qmethod = c("escape", "double"),
            fileEncoding = "")

write.table(list.downregulated.topgenes.coELTD1_CT, file = "coELTD1_CT-
downregulated_(adjusted_p_value).txt", append = FALSE, quote = TRUE, sep = "\t",
            eol = "\n", na = "NA", dec = ".", row.names = FALSE,
            col.names = TRUE, qmethod = c("escape", "double"),
            fileEncoding = "")

# to save a list of genes filtered only by adj. P value:
adjpval.topgenes.coELTD1_CT <- which((coELTD1_CT[,"adj.P.Val"]<0.05))
adjpval.list.topgenes.coELTD1_CT <- coELTD1_CT[adjpval.topgenes.coELTD1_CT,]
head(adjpval.list.topgenes.coELTD1_CT)
dim(adjpval.list.topgenes.coELTD1_CT)
write.table(adjpval.list.topgenes.coELTD1_CT, file =
"extended_list_of_significant_differentially_expressed_genes(only_adjp_value_limi
ted).txt", append = FALSE, quote = TRUE, sep = "\t",
            eol = "\n", na = "NA", dec = ".", row.names = FALSE,
            col.names = TRUE, qmethod = c("escape", "double"),
            fileEncoding = "")


# -------------------------------------
# 3.6.2 SAVING p value (non-adjusted p value) values [from coELTD1_CT2]
# Need to have made volcano plot and set threshold on coELTD1_CT2 first
# -------------------------------------

#IF WANT TO MAKE WITH UP AND DOWN REGULATED GENES TOGETHER (NB FOR HEATMAP):
topgenes.coELTD1_CT2 <- which((abs(coELTD1_CT2[,"logFC"]))>1 &
(coELTD1_CT2[,"P.Value"]<0.05))
list.topgenes.coELTD1_CT2 <- coELTD1_CT2[topgenes.coELTD1_CT2,]
head(list.topgenes.coELTD1_CT2)
dim(list.topgenes.coELTD1_CT2)
write.table(list.topgenes.coELTD1_CT2, file =
"list_of_significant_differentially_expressed_genes(logFC_and_p_value_filtered).t
xt", append = FALSE, quote = TRUE, sep = "\t",
            eol = "\n", na = "NA", dec = ".", row.names = FALSE,
            col.names = TRUE, qmethod = c("escape", "double"),
```

```
            fileEncoding = "")

      # if want to split up and down regulated genes:
      # up:
      upregulated.topgenes.coELTD1_CT2 <- which((coELTD1_CT2[,"logFC"])>1 &
(coELTD1_CT2[,"P.Value"]<0.05))
      list.upregulated.topgenes.coELTD1_CT2 <-
coELTD1_CT2[upregulated.topgenes.coELTD1_CT,]
      head(list.upregulated.topgenes.coELTD1_CT2)
      dim(list.upregulated.topgenes.coELTD1_CT2)

      # down:
      downregulated.topgenes.coELTD1_CT2 <- which((coELTD1_CT2[,"logFC"])<1 &
(coELTD1_CT2[,"P.Value"]<0.05))
      list.downregulated.topgenes.coELTD1_CT2 <-
coELTD1_CT2[downregulated.topgenes.coELTD1_CT2,]
      head(list.downregulated.topgenes.coELTD1_CT2)
      dim(list.downregulated.topgenes.coELTD1_CT2)


      # write output to file:
write.table(list.upregulated.topgenes.coELTD1_CT2, file = "coELTD1_CT-
upregulated_(p_value).txt", append = FALSE, quote = TRUE, sep = "\t",
            eol = "\n", na = "NA", dec = ".", row.names = FALSE,
            col.names = TRUE, qmethod = c("escape", "double"),
            fileEncoding = "")

write.table(list.downregulated.topgenes.coELTD1_CT2, file = "coELTD1_CT-
downregulated_(p_value).txt", append = FALSE, quote = TRUE, sep = "\t",
            eol = "\n", na = "NA", dec = ".", row.names = FALSE,
            col.names = TRUE, qmethod = c("escape", "double"),
            fileEncoding = "")
----

# 3.7 next step is making a heatmap (do this to visualise whether data acts in a
similar way)

# -----------------------------------------------------------------
# 4) Making Heatmap of data
# -----------------------------------------------------------------
# Need to have      i) normalised microarray data (eg all 12 samples quantile
normalised) (eg y2 in overexpression microarray)
#                         ii) summary output of contrast compared data (eg
coELTD1-CT [each a separate matrix/table]
#
# Method:     1) Extract significant genes from summary output of contrast
compared data ((abs(logFC))>1 & (adj.P.Val)<0.05)
#                   2) Make a new matrix which contains data from normalised
matrix and significant genes from contrast compared data
#                   3) Make a heatmap based on this matrix.


# load heatmap.2 (this is within the gplots package)
library("gplots")
library("RColorBrewer")

# 4.1.1 Extract significant genes from contrast compared data; [Using logFC and
ADJUSTED P Value]
# -------------------------
heatmaplist.coELTD1_CT <-topTable(fit3, coef = "coELTD1-CT", sort.by='logFC',
adjust.method="BH",number=Inf)
dim(heatmaplist.coELTD1_CT)
# filter for row names (Illumina ID's) whch fullfill the criteria of significance
(The best version). Illumina ID's are saved as row names!
heatmaplist.coELTD1_CT <-
row.names(heatmaplist.coELTD1_CT)[which((abs(heatmaplist.coELTD1_CT[,"logFC"]))>1
& (heatmaplist.coELTD1_CT[,"adj.P.Val"]<0.05))]
heatmaplist.coELTD1_CT
```

```
# 4.1.2 Apply above selected illumina ID's onto normalised matrix y2 and save
output as new dataframe si1_CT.heatmap
coELTD1minusCT.heatmap <- y1[heatmaplist.coELTD1_CT,]

write.table(coELTD1minusCT.heatmap, file =
"heatmap_list(limited_by_adj_p_val_and_log_fc)-coELTD1-CT.txt", append = FALSE,
quote = TRUE, sep = "\t",
            eol = "\n", na = "NA", dec = ".", row.names = TRUE,
            col.names = TRUE, qmethod = c("escape", "double"),
            fileEncoding = "")


# 4.1.3 Extract significant genes from contrast compared data; [Using ADJUSTED P
Value alone]
# -------------------------
heatmaplist2.coELTD1_CT <-topTable(fit3, coef = "coELTD1-CT", sort.by='logFC',
adjust.method="BH",number=Inf)
dim(heatmaplist2.coELTD1_CT)
# filter for row names (Illumina ID's) whch fullfill the criteria of significance
(The best version). Illumina ID's are saved as row names!
heatmaplist2.coELTD1_CT <-
row.names(heatmaplist2.coELTD1_CT)[which((heatmaplist2.coELTD1_CT[,"adj.P.Val"]<0
.05))]
heatmaplist2.coELTD1_CT


# 4.1.2 Apply above selected illumina ID's onto normalised matrix y2 and save
output as new dataframe si1_CT.heatmap
coELTD1minusCT.heatmap2 <- y1[heatmaplist2.coELTD1_CT,]

write.table(coELTD1minusCT.heatmap2, file = "heatmap_list(limited_by_adj_p_val)-
coELTD1-CT.txt", append = FALSE, quote = TRUE, sep = "\t",
            eol = "\n", na = "NA", dec = ".", row.names = TRUE,
            col.names = TRUE, qmethod = c("escape", "double"),
            fileEncoding = "")

# PLOT HEATMAP USING HEATMAP.2 OR MORPHEUS
# Clustering strategy:
# one minus Pearson correlation hierarchical clustering: rows & columns
```

9.5 FIJI: script to count cells within a field of view

```
# ------------------------------------------------------
# ------------------------------------------------------
# "Script to count cells within a field of view"
# Author: David Favara, March 2017
# ------------------------------------------------------
# ------------------------------------------------------

# crop centre point of image and do this for all fields of view processed.
makeRectangle(702, 358, 820, 904);
run("Crop");

# prepares image for analysis
run("Subtract Background...", "rolling=20 light");
run("8-bit");

//run("Threshold...");
//setThreshold(0, 218);
setOption("BlackBackground", false);
run("Convert to Mask");

run("Analyze Particles...", "  show=Outlines display summarize");
```

Publications, talks, conference posters and collaborations related to thesis

Published papers relating to thesis:

1. Favara DM, Harris AL. VEGF sticky-trap: the first report of a non-systemically acting angiogenesis inhibitor. EMBO Mol Med. 2014 May;6(5):577-9
2. Favara DM, Banham AH, Harris AL. A review of ELTD1, a pro-angiogenic adhesion GPCR. Biochem Soc Trans. 2014 Dec;42(6):1658-64.

Oral presentations at conferences or other universities

1. Oral presentation: "The Role of ELTD, an angiogenic adhesion GPCR" at the **'Angiogenesis and Vascular Remodelling: New Perspectives' Conference (Biochemical Society). University of Chester, Chester, UK** (14-16/6/2014)
2. Oral presentation: "Tumour angiogenesis, VEGF and NOTCH signalling, and anti-angiogenic drug targets (1st to 3rd level anti-angiogenic targets)". **University of Cape Town Medical School. University of Cape Town, South Africa** (11/9/2014). Invited to present lecture by Professor Denver Hendricks (Deputy Dean, UCT Medical School).
3. Oral presentation: "Decoding the biology of ELTD1/ADGRL4, a novel regulator of tumour angiogenesis". **Weatherall Institute of Molecular Medicine Student Day 2016**. **Weatherall Institute of Molecular Medicine, University of Oxford** (10/2/2016).
4. Oral presentation: "Decoding the biology of ELTD1/ADGRL4, a novel regulator of tumour angiogenesis." **The 8th Adhesion GPCR Meeting, Joint workshop of the International Adhesion GPCR Consortium and Annual Symposium of the DFG Research Unit 2149**. **Kongresshalle am zoo, Leipzig, Germany** (2-4/6/2016)
5. Oral presentation: "Solving the biology of ELTD1/ADGRL4, a newly discovered regulator of tumour angiogenesis". **2016 Balliol Biomedical Conference. Holywell Manor, University of Oxford** (26/6/2016)

Posters presentations

1. Poster presentation: “ELTD1: a class 1 adhesion GPCR with angiogenic properties. **7Th International Adhesion-GPCR Workshop Meeting, Boston Children’s Hospital, Boston, Massachusetts, USA** (5-7/6/2014)
2. Poster presentation: “ELTD1: an angiogenic GPCR with angiogenic properties – preliminary experiments”. **Department of Oncology Annual Oncology Student Symposium, St. Hilda’s College, University of Oxford** (25/6/2014)
3. Poster presentation: “ELTD1: a class 1 adhesion GPCR with angiogenic properties". **Weatherall Institute of Molecular Medicine, University of Oxford** (23/2/2015)
4. Poster presentation: “ELTD1/ADGRL4, a novel adhesion GPCR regulator of tumour angiogenesis, suppresses lipid metabolism in endothelial cells, and is upregulated in breast cancer endothelium and epithelium”. **AACR 2017 Annual Meeting, Washington Convention Centre, Washington DC, USA** (1-6 April 2017)
5. Poster presentation: “ELTD1/ADGRL4, an adhesion GPCR regulator of tumour angiogenesis regulates ACLY in endothelial cells and is differentially expressed in the tumour microenvironment of primary and regional nodal breast cancer”. **The 6th Annual Cancer Research UK Oxford Centre Research Conference. Saïd Business School, University of Oxford** (23/6/2017)

Academic Outreach Talks:

1. Oral presentation: **Guest speaker and representative of Professor Harris at the annual Kennington Cancer Fund summer fete 2014.** Presented overview of work done in the Harris Laboratory to a lay audience at the Annual “Friends of Kennington Cancer Fund” Summer fete. Presented talk as representative of Professor Adrian Harris, a principal beneficiary of this fund. Kennington Village Town Hall, Oxford (29/6/2014)
2. Oral presentation: **Guest speaker and representative of Professor Harris at the annual Kennington Cancer Fund summer fete 2015**. Presented talk to the lay public detailing the Harris laboratory’s wide array of research, focussing on our work n ELTD1. Kennington Village Town Hall, Oxford (4/7/2015).
3. Oral presentation: **Welcome introduction to new graduate students to the Division of Medical Sciences, University of Oxford.** Medical Sciences Welcome Day. Spoke alongside Professor Anton van der Merwe and Dr. Sarah Norman. Medical Sciences Graduate School Welcome Event 2013-2016, Medical Sciences Teaching Centre, University of Oxford. (10/10/2013; 10/10/2014; 9/10/2014; 8/10/2015; 6/10/2016)

Organised academic symposia

2014: Member of organising team: Balliol College Biomedical Graduate **Symposium. Holywell Manor, University of Oxford, UK (17/5/2014)**

2015: Organised and chaired the first Weatherall Institute Adhesion GPCR symposium (23/01/2015, Weatherall Institute, University of Oxford). Keynote speaker: Prof Tobias Langenhan, University of Wurzburg, Germany and co-chair of the Adhesion GPCR Consortium. This was the first adhesion GPCR symposium in Oxford in 7 years.

2016: **Organised and chaired the second Weatherall Adhesion GPCR symposium (19/12/2016, Weatherall Institute, University of Oxford).** Invited guest speakers included: Dr. Ines Liebscher (who developed the tethered agonist hypothesis for orphan adhesion GPCRs) and Dr. Doreen Thor (both from the University of Leipzig, Germany)

Academic collaborations / periods as visiting researcher

2015-2016: Collaborative research student: laboratory of Dr. Ali Jazayeri and Dr. Fiona Marshall, Heptares Therapeutics, UK (total 6 months)

2016: Collaborative research student: Laboratory of Dr. Ines Liebscher, University of Leipzig (June and September, 2016)

Collaborative research student: Laboratory of Prof. Martine Smit, Dr. Saskia Nijmiejer, VU University Amsterdam (July 2016)

Bibliography

ABDUL AZIZ, N. A., MOKHTAR, N. M., HARUN, R., MOLLAH, M. M., MOHAMED ROSE, I., SAGAP, I., MOHD TAMIL, A., WAN NGAH, W. Z. & JAMAL, R. 2016. A 19-Gene expression signature as a predictor of survival in colorectal cancer. *BMC Med Genomics,* 9**,** 58.

AGRAWAL, A., PERGADIA, M. L., SACCONE, S. F., LYNSKEY, M. T., WANG, J. C., MARTIN, N. G., STATHAM, D., HENDERS, A., CAMPBELL, M., GARCIA, R., BROMS, U., TODD, R. D., GOATE, A. M., RICE, J., KAPRIO, J., HEATH, A. C., MONTGOMERY, G. W. & MADDEN, P. A. 2008. An autosomal linkage scan for cannabis use disorders in the nicotine addiction genetics project. *Arch Gen Psychiatry,* 65**,** 713-21.

AL-SHAMI, A., WILKINS, C., CRISOSTOMO, J., SESHASAYEE, D., MARTIN, F., XU, N., SUWANICHKUL, A., ANDERSON, S. J. & ORAVECZ, T. 2010. The adaptor protein Sh2d3c is critical for marginal zone B cell development and function. *J Immunol,* 185**,** 327-34.

ALTSCHUL, S. F., MADDEN, T. L., SCHAFFER, A. A., ZHANG, J., ZHANG, Z., MILLER, W. & LIPMAN, D. J. 1997. Gapped BLAST and PSI-BLAST: a new generation of protein database search programs. *Nucleic Acids Res,* 25**,** 3389-402.

ANDERSSON, E. R., SANDBERG, R. & LENDAHL, U. 2011. Notch signaling: simplicity in design, versatility in function. *Development,* 138**,** 3593-612.

ARAC, D., AUST, G., CALEBIRO, D., ENGEL, F. B., FORMSTONE, C., GOFFINET, A., HAMANN, J., KITTEL, R. J., LIEBSCHER, I., LIN, H. H., MONK, K. R., PETRENKO, A., PIAO, X., PROMEL, S., SCHIOTH, H. B., SCHWARTZ, T. W., STACEY, M., USHKARYOV, Y. A., WOBUS, M., WOLFRUM, U., XU, L. & LANGENHAN, T. 2012a. Dissecting signaling and functions of adhesion G protein-coupled receptors. *Ann N Y Acad Sci,* 1276**,** 1-25.

ARAC, D., BOUCARD, A. A., BOLLIGER, M. F., NGUYEN, J., SOLTIS, S. M., SUDHOF, T. C. & BRUNGER, A. T. 2012b. A novel evolutionarily conserved domain of cell-adhesion GPCRs mediates autoproteolysis. *EMBO J,* 31**,** 1364-78.

ASHMAN, L. K. & GRIFFITH, R. 2013. Therapeutic targeting of c-KIT in cancer. *Expert Opin Investig Drugs,* 22**,** 103-15.

BAENKE, F., PECK, B., MIESS, H. & SCHULZE, A. 2013. Hooked on fat: the role of lipid synthesis in cancer metabolism and tumour development. *Dis Model Mech,* 6**,** 1353-63.

BARRETINA, J., CAPONIGRO, G., STRANSKY, N., VENKATESAN, K., MARGOLIN, A. A., KIM, S., WILSON, C. J., LEHAR, J., KRYUKOV, G. V., SONKIN, D., REDDY, A., LIU, M., MURRAY, L., BERGER, M. F., MONAHAN, J. E., MORAIS, P., MELTZER, J., KOREJWA, A., JANE-VALBUENA, J., MAPA, F. A., THIBAULT, J., BRIC-FURLONG, E., RAMAN, P., SHIPWAY, A., ENGELS, I. H., CHENG, J., YU, G. K., YU, J., ASPESI, P., JR., DE SILVA, M., JAGTAP, K., JONES, M. D., WANG, L., HATTON,

C., PALESCANDOLO, E., GUPTA, S., MAHAN, S., SOUGNEZ, C., ONOFRIO, R. C., LIEFELD, T., MACCONAILL, L., WINCKLER, W., REICH, M., LI, N., MESIROV, J. P., GABRIEL, S. B., GETZ, G., ARDLIE, K., CHAN, V., MYER, V. E., WEBER, B. L., PORTER, J., WARMUTH, M., FINAN, P., HARRIS, J. L., MEYERSON, M., GOLUB, T. R., MORRISSEY, M. P., SELLERS, W. R., SCHLEGEL, R. & GARRAWAY, L. A. 2012. The Cancer Cell Line Encyclopedia enables predictive modelling of anticancer drug sensitivity. *Nature,* 483**,** 603-7.

BAYIN, N. S., FRENSTER, J. D., KANE, J. R., RUBENSTEIN, J., MODREK, A. S., BAITALMAL, R., DOLGALEV, I., RUDZENSKI, K., SCARABOTTOLO, L., CRESPI, D., REDAELLI, L., SNUDERL, M., GOLFINOS, J. G., DOYLE, W., PACIONE, D., PARKER, E. C., CHI, A. S., HEGUY, A., MACNEIL, D. J., SHOHDY, N., ZAGZAG, D. & PLACANTONAKIS, D. G. 2016. GPR133 (ADGRD1), an adhesion G-protein-coupled receptor, is necessary for glioblastoma growth. *Oncogenesis,* 5**,** e263.

BELLER, M., THIEL, K., THUL, P. J. & JACKLE, H. 2010. Lipid droplets: a dynamic organelle moves into focus. *FEBS Lett,* 584**,** 2176-82.

BENEDITO, R., ROCA, C., SORENSEN, I., ADAMS, S., GOSSLER, A., FRUTTIGER, M. & ADAMS, R. H. 2009. The notch ligands Dll4 and Jagged1 have opposing effects on angiogenesis. *Cell,* 137**,** 1124-35.

BENSAAD, K. & HARRIS, A. L. 2014. Hypoxia and metabolism in cancer. *Adv Exp Med Biol,* 772**,** 1-39.

BERGERS, G. & HANAHAN, D. 2008. Modes of resistance to anti-angiogenic therapy. *Nat Rev Cancer,* 8**,** 592-603.

BIASINI, M., BIENERT, S., WATERHOUSE, A., ARNOLD, K., STUDER, G., SCHMIDT, T., KIEFER, F., GALLO CASSARINO, T., BERTONI, M., BORDOLI, L. & SCHWEDE, T. 2014. SWISS-MODEL: modelling protein tertiary and quaternary structure using evolutionary information. *Nucleic Acids Res,* 42**,** W252-8.

BICKEL, P. E., TANSEY, J. T. & WELTE, M. A. 2009. PAT proteins, an ancient family of lipid droplet proteins that regulate cellular lipid stores. *Biochim Biophys Acta,* 1791**,** 419-40.

BJARNADOTTIR, T. K., FREDRIKSSON, R., HOGLUND, P. J., GLORIAM, D. E., LAGERSTROM, M. C. & SCHIOTH, H. B. 2004. The human and mouse repertoire of the adhesion family of G-protein-coupled receptors. *Genomics,* 84**,** 23-33.

BLANCO, R. & GERHARDT, H. 2013. VEGF and Notch in tip and stalk cell selection. *Cold Spring Harb Perspect Med,* 3**,** a006569.

BOHDANOWICZ, M., BALKIN, D. M., DE CAMILLI, P. & GRINSTEIN, S. 2012. Recruitment of OCRL and Inpp5B to phagosomes by Rab5 and APPL1 depletes phosphoinositides and attenuates Akt signaling. *Mol Biol Cell,* 23**,** 176-87.

BOHNEKAMP, J. & SCHONEBERG, T. 2011. Cell adhesion receptor GPR133 couples to Gs protein. *J Biol Chem,* 286**,** 41912-6.

BRAY, S. J. 2016. Notch signalling in context. *Nat Rev Mol Cell Biol,* 17**,** 722-735.

BRAZMA, A., HINGAMP, P., QUACKENBUSH, J., SHERLOCK, G., SPELLMAN, P., STOECKERT, C., AACH, J., ANSORGE, W., BALL, C. A., CAUSTON, H. C., GAASTERLAND, T., GLENISSON, P., HOLSTEGE, F. C., KIM, I. F., MARKOWITZ, V., MATESE, J. C., PARKINSON, H., ROBINSON, A., SARKANS, U., SCHULZE-KREMER, S., STEWART, J., TAYLOR, R., VILO,

J. & VINGRON, M. 2001. Minimum information about a microarray experiment (MIAME)-toward standards for microarray data. *Nat Genet,* 29**,** 365-71.

BROWN, K., FILUTA, A., LUDWIG, M. G., SEUWEN, K., JAROS, J., VIDAL, S., ARORA, K., NAREN, A. P., KANDASAMY, K., PARTHASARATHI, K., OFFERMANNS, S., MASON, R. J., MILLER, W. E., WHITSETT, J. A. & BRIDGES, J. P. 2017. Epithelial Gpr116 regulates pulmonary alveolar homeostasis via Gq/11 signaling. *JCI Insight,* 2.

CARMELIET, P. & JAIN, R. K. 2011a. Molecular mechanisms and clinical applications of angiogenesis. *Nature,* 473**,** 298-307.

CARMELIET, P. & JAIN, R. K. 2011b. Principles and mechanisms of vessel normalization for cancer and other angiogenic diseases. *Nat Rev Drug Discov,* 10**,** 417-27.

CARTY, C. L., KEENE, K. L., CHENG, Y. C., MESCHIA, J. F., CHEN, W. M., NALLS, M., BIS, J. C., KITTNER, S. J., RICH, S. S., TAJUDDIN, S., ZONDERMAN, A. B., EVANS, M. K., LANGEFELD, C. D., GOTTESMAN, R., MOSLEY, T. H., SHAHAR, E., WOO, D., YAFFE, K., LIU, Y., SALE, M. M., DICHGANS, M., MALIK, R., LONGSTRETH, W. T., JR., MITCHELL, B. D., PSATY, B. M., KOOPERBERG, C., REINER, A., WORRALL, B. B. & FORNAGE, M. 2015. Meta-Analysis of Genome-Wide Association Studies Identifies Genetic Risk Factors for Stroke in African Americans. *Stroke,* 46**,** 2063-8.

CERAMI, E., GAO, J., DOGRUSOZ, U., GROSS, B. E., SUMER, S. O., AKSOY, B. A., JACOBSEN, A., BYRNE, C. J., HEUER, M. L., LARSSON, E., ANTIPIN, Y., REVA, B., GOLDBERG, A. P., SANDER, C. & SCHULTZ, N. 2012. The cBio cancer genomics portal: an open platform for exploring multidimensional cancer genomics data. *Cancer Discov,* 2**,** 401-4.

CHAUDHARY, A., HILTON, M. B., SEAMAN, S., HAINES, D. C., STEVENSON, S., LEMOTTE, P. K., TSCHANTZ, W. R., ZHANG, X. M., SAHA, S., FLEMING, T. & ST CROIX, B. 2012. TEM8/ANTXR1 blockade inhibits pathological angiogenesis and potentiates tumoricidal responses against multiple cancer types. *Cancer Cell,* 21**,** 212-26.

CHEN, D., BHAT-NAKSHATRI, P., GOSWAMI, C., BADVE, S. & NAKSHATRI, H. 2013. ANTXR1, a stem cell-enriched functional biomarker, connects collagen signaling to cancer stem-like cells and metastasis in breast cancer. *Cancer Res,* 73**,** 5821-33.

CHENG, Z., GARVIN, D., PAGUIO, A., STECHA, P., WOOD, K. & FAN, F. 2010. Luciferase Reporter Assay System for Deciphering GPCR Pathways. *Curr Chem Genomics,* 4**,** 84-91.

CHYPRE, M., ZAIDI, N. & SMANS, K. 2012. ATP-citrate lyase: a mini-review. *Biochem Biophys Res Commun,* 422**,** 1-4.

COOKE, J. P. & GHEBREMARIAM, Y. T. 2008. Endothelial nicotinic acetylcholine receptors and angiogenesis. *Trends Cardiovasc Med,* 18**,** 247-53.

CROFT, D., MUNDO, A. F., HAW, R., MILACIC, M., WEISER, J., WU, G., CAUDY, M., GARAPATI, P., GILLESPIE, M., KAMDAR, M. R., JASSAL, B., JUPE, S., MATTHEWS, L., MAY, B., PALATNIK, S., ROTHFELS, K., SHAMOVSKY, V., SONG, H., WILLIAMS, M., BIRNEY, E., HERMJAKOB, H., STEIN, L. & D'EUSTACHIO, P. 2014. The Reactome pathway knowledgebase. *Nucleic Acids Res,* 42**,** D472-7.

CUI, X. B., SHEN, Y. Y., JIN, T. T., LI, S., LI, T. T., ZHANG, S. M., PENG, H., LIU, C. X., LI, S. G., YANG, L., LI, N., HU, J. M., JIANG, J. F., LI, M., LIANG, W. H., LI, Y., WEI, Y. T., SUN, Z. Z., WU, C. Y., CHEN, Y. Z. & LI, F. 2015. SLC39A6: a potential target for diagnosis and therapy of esophageal carcinoma. *J Transl Med,* 13**,** 321.

CURRIE, E., SCHULZE, A., ZECHNER, R., WALTHER, T. C. & FARESE, R. V., JR. 2013. Cellular fatty acid metabolism and cancer. *Cell Metab,* 18**,** 153-61.

DAI, S., WANG, X., LI, X. & CAO, Y. 2015a. MicroRNA-139-5p acts as a tumor suppressor by targeting ELTD1 and regulating cell cycle in glioblastoma multiforme. *Biochem Biophys Res Commun,* 467**,** 204-10.

DAI, X., LI, T., BAI, Z., YANG, Y., LIU, X., ZHAN, J. & SHI, B. 2015b. Breast cancer intrinsic subtype classification, clinical use and future trends. *Am J Cancer Res,* 5**,** 2929-43.

DAIL, M., KALO, M. S., SEDDON, J. A., COTE, J. F., VUORI, K. & PASQUALE, E. B. 2004. SHEP1 function in cell migration is impaired by a single amino acid mutation that disrupts association with the scaffolding protein cas but not with Ras GTPases. *J Biol Chem,* 279**,** 41892-902.

DALY, M. E., MAKRIS, A., REED, M. & LEWIS, C. E. 2003. Hemostatic regulators of tumor angiogenesis: a source of antiangiogenic agents for cancer treatment? *J Natl Cancer Inst,* 95**,** 1660-73.

DE BOCK, K., GEORGIADOU, M., SCHOORS, S., KUCHNIO, A., WONG, B. W., CANTELMO, A. R., QUAEGEBEUR, A., GHESQUIERE, B., CAUWENBERGHS, S., EELEN, G., PHNG, L. K., BETZ, I., TEMBUYSER, B., BREPOELS, K., WELTI, J., GEUDENS, I., SEGURA, I., CRUYS, B., BIFARI, F., DECIMO, I., BLANCO, R., WYNS, S., VANGINDERTAEL, J., ROCHA, S., COLLINS, R. T., MUNCK, S., DAELEMANS, D., IMAMURA, H., DEVLIEGER, R., RIDER, M., VAN VELDHOVEN, P. P., SCHUIT, F., BARTRONS, R., HOFKENS, J., FRAISL, P., TELANG, S., DEBERARDINIS, R. J., SCHOONJANS, L., VINCKIER, S., CHESNEY, J., GERHARDT, H., DEWERCHIN, M. & CARMELIET, P. 2013. Role of PFKFB3-driven glycolysis in vessel sprouting. *Cell,* 154**,** 651-63.

DEANE, C. A. S. & BROWN, I. R. 2017. Differential Targeting of Hsp70 Heat Shock Proteins HSPA6 and HSPA1A with Components of a Protein Disaggregation/Refolding Machine in Differentiated Human Neuronal Cells following Thermal Stress. *Front Neurosci,* 11**,** 227.

DEL ALAMO, D., ROUAULT, H. & SCHWEISGUTH, F. 2011. Mechanism and significance of cis-inhibition in Notch signalling. *Curr Biol,* 21**,** R40-7.

DEMBERG, L. M., ROTHEMUND, S., SCHONEBERG, T. & LIEBSCHER, I. 2015. Identification of the tethered peptide agonist of the adhesion G protein-coupled receptor GPR64/ADGRG2. *Biochem Biophys Res Commun,* 464**,** 743-7.

DEMBERG, L. M., WINKLER, J., WILDE, C., SIMON, K. U., SCHON, J., ROTHEMUND, S., SCHONEBERG, T., PROMEL, S. & LIEBSCHER, I. 2017. Activation of Adhesion G Protein-coupled Receptors: AGONIST SPECIFICITY OF STACHEL SEQUENCE-DERIVED PEPTIDES. *J Biol Chem,* 292**,** 4383-4394.

DEWIRE, S. M., AHN, S., LEFKOWITZ, R. J. & SHENOY, S. K. 2007. Beta-arrestins and cell signaling. *Annu Rev Physiol,* 69**,** 483-510.

DIETERICH, L. C., MELLBERG, S., LANGENKAMP, E., ZHANG, L., ZIEBA, A., SALOMAKI, H., TEICHERT, M., HUANG, H., EDQVIST, P. H., KRAUS, T.,

AUGUSTIN, H. G., OLOFSSON, T., LARSSON, E., SODERBERG, O., MOLEMA, G., PONTEN, F., GEORGII-HEMMING, P., ALAFUZOFF, I. & DIMBERG, A. 2012. Transcriptional profiling of human glioblastoma vessels indicates a key role of VEGF-A and TGFbeta2 in vascular abnormalization. *J Pathol,* 228**,** 378-90.

EICHSTAEDT, C. A., ANTAO, T., PAGANI, L., CARDONA, A., KIVISILD, T. & MORMINA, M. 2014. The Andean adaptive toolkit to counteract high altitude maladaptation: genome-wide and phenotypic analysis of the Collas. *PLoS One,* 9**,** e93314.

FINN, R. D., ATTWOOD, T. K., BABBITT, P. C., BATEMAN, A., BORK, P., BRIDGE, A. J., CHANG, H. Y., DOSZTANYI, Z., EL-GEBALI, S., FRASER, M., GOUGH, J., HAFT, D., HOLLIDAY, G. L., HUANG, H., HUANG, X., LETUNIC, I., LOPEZ, R., LU, S., MARCHLER-BAUER, A., MI, H., MISTRY, J., NATALE, D. A., NECCI, M., NUKA, G., ORENGO, C. A., PARK, Y., PESSEAT, S., PIOVESAN, D., POTTER, S. C., RAWLINGS, N. D., REDASCHI, N., RICHARDSON, L., RIVOIRE, C., SANGRADOR-VEGAS, A., SIGRIST, C., SILLITOE, I., SMITHERS, B., SQUIZZATO, S., SUTTON, G., THANKI, N., THOMAS, P. D., TOSATTO, S. C., WU, C. H., XENARIOS, I., YEH, L. S., YOUNG, S. Y. & MITCHELL, A. L. 2017. InterPro in 2017-beyond protein family and domain annotations. *Nucleic Acids Res,* 45**,** D190-d199.

FISCHER, A., SCHUMACHER, N., MAIER, M., SENDTNER, M. & GESSLER, M. 2004. The Notch target genes Hey1 and Hey2 are required for embryonic vascular development. *Genes Dev,* 18**,** 901-11.

FLICEK, P., AMODE, M. R., BARRELL, D., BEAL, K., BILLIS, K., BRENT, S., CARVALHO-SILVA, D., CLAPHAM, P., COATES, G., FITZGERALD, S., GIL, L., GIRON, C. G., GORDON, L., HOURLIER, T., HUNT, S., JOHNSON, N., JUETTEMANN, T., KAHARI, A. K., KEENAN, S., KULESHA, E., MARTIN, F. J., MAUREL, T., MCLAREN, W. M., MURPHY, D. N., NAG, R., OVERDUIN, B., PIGNATELLI, M., PRITCHARD, B., PRITCHARD, E., RIAT, H. S., RUFFIER, M., SHEPPARD, D., TAYLOR, K., THORMANN, A., TREVANION, S. J., VULLO, A., WILDER, S. P., WILSON, M., ZADISSA, A., AKEN, B. L., BIRNEY, E., CUNNINGHAM, F., HARROW, J., HERRERO, J., HUBBARD, T. J., KINSELLA, R., MUFFATO, M., PARKER, A., SPUDICH, G., YATES, A., ZERBINO, D. R. & SEARLE, S. M. 2014. Ensembl 2014. *Nucleic Acids Res,* 42**,** D749-55.

FOLKMAN, J. 1971. Tumor angiogenesis: therapeutic implications. *N Engl J Med,* 285**,** 1182-6.

FRENKEL-MORGENSTERN, M., DANON, T., CHRISTIAN, T., IGARASHI, T., COHEN, L., HOU, Y. M. & JENSEN, L. J. 2012. Genes adopt non-optimal codon usage to generate cell cycle-dependent oscillations in protein levels. *Mol Syst Biol,* 8**,** 572.

GARCHON, H. J., DJABIRI, F., VIARD, J. P., GAJDOS, P. & BACH, J. F. 1994. Involvement of human muscle acetylcholine receptor alpha-subunit gene (CHRNA) in susceptibility to myasthenia gravis. *Proc Natl Acad Sci U S A,* 91**,** 4668-72.

GEER, L. Y., MARCHLER-BAUER, A., GEER, R. C., HAN, L., HE, J., HE, S., LIU, C., SHI, W. & BRYANT, S. H. 2010. The NCBI BioSystems database. *Nucleic Acids Res,* 38**,** D492-6.

GERHARDT, H., GOLDING, M., FRUTTIGER, M., RUHRBERG, C., LUNDKVIST, A., ABRAMSSON, A., JELTSCH, M., MITCHELL, C., ALITALO, K., SHIMA, D. & BETSHOLTZ, C. 2003. VEGF guides angiogenic sprouting utilizing endothelial tip cell filopodia. *J Cell Biol,* 161**,** 1163-77.

GHAJAR, C. M., PEINADO, H., MORI, H., MATEI, I. R., EVASON, K. J., BRAZIER, H., ALMEIDA, D., KOLLER, A., HAJJAR, K. A., STAINIER, D. Y., CHEN, E. I., LYDEN, D. & BISSELL, M. J. 2013. The perivascular niche regulates breast tumour dormancy. *Nat Cell Biol,* 15**,** 807-17.

GHOSH, E., KUMARI, P., JAIMAN, D. & SHUKLA, A. K. 2015. Methodological advances: the unsung heroes of the GPCR structural revolution. *Nat Rev Mol Cell Biol,* 16**,** 69-81.

GOEL, S., DUDA, D. G., XU, L., MUNN, L. L., BOUCHER, Y., FUKUMURA, D. & JAIN, R. K. 2011. Normalization of the vasculature for treatment of cancer and other diseases. *Physiol Rev,* 91**,** 1071-121.

GOODMAN, O. B., JR., KRUPNICK, J. G., SANTINI, F., GUREVICH, V. V., PENN, R. B., GAGNON, A. W., KEEN, J. H. & BENOVIC, J. L. 1996. Beta-arrestin acts as a clathrin adaptor in endocytosis of the beta2-adrenergic receptor. *Nature,* 383**,** 447-50.

GOODWIN, A. M. 2007. In vitro assays of angiogenesis for assessment of angiogenic and anti-angiogenic agents. *Microvasc Res,* 74**,** 172-83.

GOPALKRISHNAN, R. V., CHRISTIANSEN, K. A., GOLDSTEIN, N. I., DEPINHO, R. A. & FISHER, P. B. 1999. Use of the human EF-1alpha promoter for expression can significantly increase success in establishing stable cell lines with consistent expression: a study using the tetracycline-inducible system in human cancer cells. *Nucleic Acids Res,* 27**,** 4775-82.

GROTE, A., HILLER, K., SCHEER, M., MUNCH, R., NORTEMANN, B., HEMPEL, D. C. & JAHN, D. 2005. JCat: a novel tool to adapt codon usage of a target gene to its potential expression host. *Nucleic Acids Res,* 33**,** W526-31.

GUBERMAN, J. M., AI, J., ARNAIZ, O., BARAN, J., BLAKE, A., BALDOCK, R., CHELALA, C., CROFT, D., CROS, A., CUTTS, R. J., DI GENOVA, A., FORBES, S., FUJISAWA, T., GADALETA, E., GOODSTEIN, D. M., GUNDEM, G., HAGGARTY, B., HAIDER, S., HALL, M., HARRIS, T., HAW, R., HU, S., HUBBARD, S., HSU, J., IYER, V., JONES, P., KATAYAMA, T., KINSELLA, R., KONG, L., LAWSON, D., LIANG, Y., LOPEZ-BIGAS, N., LUO, J., LUSH, M., MASON, J., MOREEWS, F., NDEGWA, N., OAKLEY, D., PEREZ-LLAMAS, C., PRIMIG, M., RIVKIN, E., ROSANOFF, S., SHEPHERD, R., SIMON, R., SKARNES, B., SMEDLEY, D., SPERLING, L., SPOONER, W., STEVENSON, P., STONE, K., TEAGUE, J., WANG, J., WANG, J., WHITTY, B., WONG, D. T., WONG-ERASMUS, M., YAO, L., YOUENS-CLARK, K., YUNG, C., ZHANG, J. & KASPRZYK, A. 2011. BioMart Central Portal: an open database network for the biological community. *Database (Oxford),* 2011**,** bar041.

HAMANN, J., AUST, G., ARAC, D., ENGEL, F. B., FORMSTONE, C., FREDRIKSSON, R., HALL, R. A., HARTY, B. L., KIRCHHOFF, C., KNAPP, B., KRISHNAN, A., LIEBSCHER, I., LIN, H. H., MARTINELLI, D. C., MONK, K. R., PEETERS, M. C., PIAO, X., PROMEL, S., SCHONEBERG, T., SCHWARTZ, T. W., SINGER, K., STACEY, M., USHKARYOV, Y. A., VALLON, M., WOLFRUM, U., WRIGHT, M. W., XU, L., LANGENHAN, T. & SCHIOTH, H. B. 2015. International Union of Basic and Clinical

Pharmacology. XCIV. Adhesion G Protein-Coupled Receptors. *Pharmacol Rev,* 67**,** 338-67.
HAMANN, J., VOGEL, B., VAN SCHIJNDEL, G. M. & VAN LIER, R. A. 1996. The seven-span transmembrane receptor CD97 has a cellular ligand (CD55, DAF). *J Exp Med,* 184**,** 1185-9.
HANAHAN, D. & WEINBERG, ROBERT A. 2011. Hallmarks of Cancer: The Next Generation. *Cell,* 144**,** 646-674.
HANLON, C. D. & ANDREW, D. J. 2015. Outside-in signaling--a brief review of GPCR signaling with a focus on the Drosophila GPCR family. *J Cell Sci,* 128**,** 3533-42.
HARJES, U., BRIDGES, E., MCINTYRE, A., FIELDING, B. A. & HARRIS, A. L. 2014. Fatty acid-binding protein 4, a point of convergence for angiogenic and metabolic signaling pathways in endothelial cells. *J Biol Chem,* 289**,** 23168-76.
HARJES, U., KALUCKA, J. & CARMELIET, P. 2016. Targeting fatty acid metabolism in cancer and endothelial cells. *Crit Rev Oncol Hematol,* 97**,** 15-21.
HARKENSEE, C., OKA, A., ONIZUKA, M., MIDDLETON, P. G., INOKO, H., NAKAOKA, H., GENNERY, A. R., ANDO, K., MORISHIMA, Y. & JAPAN MARROW DONOR, P. 2013. Microsatellite scanning of the immunogenome associates MAPK14 and ELTD1 with graft-versus-host disease in hematopoietic stem cell transplantation. *Immunogenetics,* 65**,** 417-27.
HATZIVASSILIOU, G., ZHAO, F., BAUER, D. E., ANDREADIS, C., SHAW, A. N., DHANAK, D., HINGORANI, S. R., TUVESON, D. A. & THOMPSON, C. B. 2005. ATP citrate lyase inhibition can suppress tumor cell growth. *Cancer Cell,* 8**,** 311-21.
HECKMANN, J. M., MORRISON, K. E., EMERYK-SZAJEWSKA, B., STRUGALSKA, H., BERGOFFEN, J., WILLCOX, N. & NEWSOM-DAVIS, J. 1996. Human muscle acetylcholine receptor alpha-subunit gene (CHRNA1) association with autoimmune myasthenia gravis in black, mixed-ancestry and Caucasian subjects. *J Autoimmun,* 9**,** 175-80.
HEDGES, S. B., MARIN, J., SULESKI, M., PAYMER, M. & KUMAR, S. 2015. Tree of life reveals clock-like speciation and diversification. *Mol Biol Evol,* 32**,** 835-45.
HEESCHEN, C., JANG, J. J., WEIS, M., PATHAK, A., KAJI, S., HU, R. S., TSAO, P. S., JOHNSON, F. L. & COOKE, J. P. 2001. Nicotine stimulates angiogenesis and promotes tumor growth and atherosclerosis. *Nat Med,* 7**,** 833-9.
HEESCHEN, C., WEIS, M., AICHER, A., DIMMELER, S. & COOKE, J. P. 2002. A novel angiogenic pathway mediated by non-neuronal nicotinic acetylcholine receptors. *J Clin Invest,* 110**,** 527-36.
HEISSIG, B., HATTORI, K., DIAS, S., FRIEDRICH, M., FERRIS, B., HACKETT, N. R., CRYSTAL, R. G., BESMER, P., LYDEN, D., MOORE, M. A., WERB, Z. & RAFII, S. 2002. Recruitment of stem and progenitor cells from the bone marrow niche requires MMP-9 mediated release of kit-ligand. *Cell,* 109**,** 625-37.
HELLSTROM, M., PHNG, L. K., HOFMANN, J. J., WALLGARD, E., COULTAS, L., LINDBLOM, P., ALVA, J., NILSSON, A. K., KARLSSON, L., GAIANO, N., YOON, K., ROSSANT, J., IRUELA-ARISPE, M. L., KALEN, M., GERHARDT,

H. & BETSHOLTZ, C. 2007. Dll4 signalling through Notch1 regulates formation of tip cells during angiogenesis. *Nature,* 445**,** 776-80.
HERBERT, J. M., STEKEL, D., SANDERSON, S., HEATH, V. L. & BICKNELL, R. 2008. A novel method of differential gene expression analysis using multiple cDNA libraries applied to the identification of tumour endothelial genes. *BMC Genomics,* 9**,** 153.
HOLLIDAY, D. L. & SPEIRS, V. 2011. Choosing the right cell line for breast cancer research. *Breast Cancer Res,* 13**,** 215.
HORI, K., SEN, A. & ARTAVANIS-TSAKONAS, S. 2013. Notch signaling at a glance. *J Cell Sci,* 126**,** 2135-40.
HU, L., CHEN, H. Y., HAN, T., YANG, G. Z., FENG, D., QI, C. Y., GONG, H., ZHAI, Y. X., CAI, Q. P. & GAO, C. F. 2016. Downregulation of DHRS9 expression in colorectal cancer tissues and its prognostic significance. *Tumour Biol,* 37**,** 837-45.
HUANG, Y. S., CHIANG, N. Y., HU, C. H., HSIAO, C. C., CHENG, K. F., TSAI, W. P., YONA, S., STACEY, M., GORDON, S., CHANG, G. W. & LIN, H. H. 2012. Activation of myeloid cell-specific adhesion class G protein-coupled receptor EMR2 via ligation-induced translocation and interaction of receptor subunits in lipid raft microdomains. *Mol Cell Biol,* 32**,** 1408-20.
HUANG, Z., RUAN, H. B., XIAN, L., CHEN, W., JIANG, S., SONG, A., WANG, Q., SHI, P., GU, X. & GAO, X. 2014. The stem cell factor/Kit signalling pathway regulates mitochondrial function and energy expenditure. *Nat Commun,* 5**,** 4282.
HUSON, D. H. & SCORNAVACCA, C. 2012. Dendroscope 3: an interactive tool for rooted phylogenetic trees and networks. *Syst Biol,* 61**,** 1061-7.
HWANG, J., KIM, C. W., SON, K. N., HAN, K. Y., LEE, K. H., KLEINMAN, H. K., KO, J., NA, D. S., KWON, B. S., GHO, Y. S. & KIM, J. 2004. Angiogenic activity of human CC chemokine CCL15 in vitro and in vivo. *FEBS Lett,* 570**,** 47-51.
JACKSON, D. G. 2004. Biology of the lymphatic marker LYVE-1 and applications in research into lymphatic trafficking and lymphangiogenesis. *Apmis,* 112**,** 526-38.
JACKSON, V. A., DEL TORO, D., CARRASQUERO, M., ROVERSI, P., HARLOS, K., KLEIN, R. & SEIRADAKE, E. 2015. Structural basis of latrophilin-FLRT interaction. *Structure,* 23**,** 774-81.
JAIN, R. K. 2005. Normalization of tumor vasculature: an emerging concept in antiangiogenic therapy. *Science,* 307**,** 58-62.
JAKOBSSON, L., FRANCO, C. A., BENTLEY, K., COLLINS, R. T., PONSIOEN, B., ASPALTER, I. M., ROSEWELL, I., BUSSE, M., THURSTON, G., MEDVINSKY, A., SCHULTE-MERKER, S. & GERHARDT, H. 2010. Endothelial cells dynamically compete for the tip cell position during angiogenic sprouting. *Nat Cell Biol,* 12**,** 943-53.
JAYSON, G. C., KERBEL, R., ELLIS, L. M. & HARRIS, A. L. 2016. Antiangiogenic therapy in oncology: current status and future directions. *Lancet*.
JIANG, L., BOUFERSAOUI, A., YANG, C., KO, B., RAKHEJA, D., GUEVARA, G., HU, Z. & DEBERARDINIS, R. J. 2016. Quantitative metabolic flux analysis reveals an unconventional pathway of fatty acid synthesis in cancer cells deficient for the mitochondrial citrate transport protein. *Metab Eng*.
KAKIZAWA, S. 2013. Nitric Oxide-Induced Calcium Release: Activation of Type 1 Ryanodine Receptor, a Calcium Release Channel, through Non-Enzymatic

Post-Translational Modification by Nitric Oxide. *Front Endocrinol (Lausanne),* 4**,** 142.
KAMENS, J. 2015. The Addgene repository: an international nonprofit plasmid and data resource. *Nucleic Acids Res,* 43**,** D1152-7.
KANEHISA, M., FURUMICHI, M., TANABE, M., SATO, Y. & MORISHIMA, K. 2017. KEGG: new perspectives on genomes, pathways, diseases and drugs. *Nucleic Acids Res,* 45**,** D353-d361.
KANGSAMAKSIN, T., TATTERSALL, I. W. & KITAJEWSKI, J. 2014. Notch functions in developmental and tumour angiogenesis by diverse mechanisms. *Biochem Soc Trans,* 42**,** 1563-8.
KAPLAN, E. L. & MEIER, P. 1958. Nonparametric Estimation from Incomplete Observations. *Journal of the American Statistical Association,* 53**,** 457-481.
KELM, J. M., TIMMINS, N. E., BROWN, C. J., FUSSENEGGER, M. & NIELSEN, L. K. 2003. Method for generation of homogeneous multicellular tumor spheroids applicable to a wide variety of cell types. *Biotechnol Bioeng,* 83**,** 173-80.
KISHORE, A. & HALL, R. A. 2016. Versatile Signaling Activity of Adhesion GPCRs. *Handb Exp Pharmacol,* 234**,** 127-146.
KISHORE, A., PURCELL, R. H., NASSIRI-TOOSI, Z. & HALL, R. A. 2016. Stalk-dependent and Stalk-independent Signaling by the Adhesion G Protein-coupled Receptors GPR56 (ADGRG1) and BAI1 (ADGRB1). *J Biol Chem,* 291**,** 3385-94.
KITAGAWA, M. 2016. Notch signalling in the nucleus: roles of Mastermind-like (MAML) transcriptional coactivators. *J Biochem,* 159**,** 287-94.
KOLUKULA, V. K., SAHU, G., WELLSTEIN, A., RODRIGUEZ, O. C., PREET, A., IACOBAZZI, V., D'ORAZI, G., ALBANESE, C., PALMIERI, F. & AVANTAGGIATI, M. L. 2014. SLC25A1, or CIC, is a novel transcriptional target of mutant p53 and a negative tumor prognostic marker. *Oncotarget,* 5**,** 1212-25.
KRISHNAN, A., ALMEN, M. S., FREDRIKSSON, R. & SCHIOTH, H. B. 2012. The origin of GPCRs: identification of mammalian like Rhodopsin, Adhesion, Glutamate and Frizzled GPCRs in fungi. *PLoS One,* 7**,** e29817.
KUHNERT, F., KIRSHNER, J. R. & THURSTON, G. 2011. Dll4-Notch signaling as a therapeutic target in tumor angiogenesis. *Vasc Cell,* 3**,** 20.
KULESHOV, M. V., JONES, M. R., ROUILLARD, A. D., FERNANDEZ, N. F., DUAN, Q., WANG, Z., KOPLEV, S., JENKINS, S. L., JAGODNIK, K. M., LACHMANN, A., MCDERMOTT, M. G., MONTEIRO, C. D., GUNDERSEN, G. W. & MA'AYAN, A. 2016. Enrichr: a comprehensive gene set enrichment analysis web server 2016 update. *Nucleic Acids Res,* 44**,** W90-7.
KUSMINSKI, C. M., SHETTY, S., ORCI, L., UNGER, R. H. & SCHERER, P. E. 2009. Diabetes and apoptosis: lipotoxicity. *Apoptosis,* 14**,** 1484-95.
KUTMON, M., RIUTTA, A., NUNES, N., HANSPERS, K., WILLIGHAGEN, E. L., BOHLER, A., MELIUS, J., WAAGMEESTER, A., SINHA, S. R., MILLER, R., COORT, S. L., CIRILLO, E., SMEETS, B., EVELO, C. T. & PICO, A. R. 2016. WikiPathways: capturing the full diversity of pathway knowledge. *Nucleic Acids Res,* 44**,** D488-94.
LADI, E., NICHOLS, J. T., GE, W., MIYAMOTO, A., YAO, C., YANG, L. T., BOULTER, J., SUN, Y. E., KINTNER, C. & WEINMASTER, G. 2005. The divergent DSL ligand Dll3 does not activate Notch signaling but cell

autonomously attenuates signaling induced by other DSL ligands. *J Cell Biol,* 170**,** 983-92.
LANGENHAN, T., AUST, G. & HAMANN, J. 2013. Sticky signaling--adhesion class G protein-coupled receptors take the stage. *Sci Signal,* 6**,** re3.
LANGENHAN, T., BARR, M. M., BRUCHAS, M. R., EWER, J., GRIFFITH, L. C., MAIELLARO, I., TAGHERT, P. H., WHITE, B. H. & MONK, K. R. 2015. Model Organisms in G Protein-Coupled Receptor Research. *Mol Pharmacol,* 88**,** 596-603.
LANNER, J. T., GEORGIOU, D. K., JOSHI, A. D. & HAMILTON, S. L. 2010. Ryanodine receptors: structure, expression, molecular details, and function in calcium release. *Cold Spring Harb Perspect Biol,* 2**,** a003996.
LAWRENCE, M. S., STOJANOV, P., MERMEL, C. H., ROBINSON, J. T., GARRAWAY, L. A., GOLUB, T. R., MEYERSON, M., GABRIEL, S. B., LANDER, E. S. & GETZ, G. 2014. Discovery and saturation analysis of cancer genes across 21 tumour types. *Nature,* 505**,** 495-501.
LEE, K. T., BYUN, M. J., KANG, K. S., PARK, E. W., LEE, S. H., CHO, S., KIM, H., KIM, K. W., LEE, T., PARK, J. E., PARK, W., SHIN, D., PARK, H. S., JEON, J. T., CHOI, B. H., JANG, G. W., CHOI, S. H., KIM, D. W., LIM, D., PARK, H. S., PARK, M. R., OTT, J., SCHOOK, L. B., KIM, T. H. & KIM, H. 2011. Neuronal genes for subcutaneous fat thickness in human and pig are identified by local genomic sequencing and combined SNP association study. *PLoS One,* 6**,** e16356.
LEFKOWITZ, R. J. 2007. Seven transmembrane receptors: something old, something new. *Acta Physiol (Oxf),* 190**,** 9-19.
LENNARTSSON, J. & RONNSTRAND, L. 2012. Stem cell factor receptor/c-Kit: from basic science to clinical implications. *Physiol Rev,* 92**,** 1619-49.
LETUNIC, I., DOERKS, T. & BORK, P. 2015. SMART: recent updates, new developments and status in 2015. *Nucleic Acids Res,* 43**,** D257-60.
LI, D., MASIERO, M., BANHAM, A. H. & HARRIS, A. L. 2014. The notch ligand JAGGED1 as a target for anti-tumor therapy. *Front Oncol,* 4**,** 254.
LI, J. L., SAINSON, R. C., OON, C. E., TURLEY, H., LEEK, R., SHELDON, H., BRIDGES, E., SHI, W., SNELL, C., BOWDEN, E. T., WU, H., CHOWDHURY, P. S., RUSSELL, A. J., MONTGOMERY, C. P., POULSOM, R. & HARRIS, A. L. 2011. DLL4-Notch signaling mediates tumor resistance to anti-VEGF therapy in vivo. *Cancer Res,* 71**,** 6073-83.
LIEBSCHER, I., SCHON, J., PETERSEN, S. C., FISCHER, L., AUERBACH, N., DEMBERG, L. M., MOGHA, A., COSTER, M., SIMON, K. U., ROTHEMUND, S., MONK, K. R. & SCHONEBERG, T. 2014. A Tethered Agonist within the Ectodomain Activates the Adhesion G Protein-Coupled Receptors GPR126 and GPR133. *Cell Rep,* 9**,** 2018-26.
LIEBSCHER, I., SCHONEBERG, T. & PROMEL, S. 2013. Progress in demystification of adhesion G protein-coupled receptors. *Biol Chem,* 394**,** 937-50.
LIN, H.-H., CHANG, G.-W., DAVIES, J. Q., STACEY, M., HARRIS, J. & GORDON, S. 2004. Autocatalytic Cleavage of the EMR2 Receptor Occurs at a Conserved G Protein-coupled Receptor Proteolytic Site Motif. *Journal of Biological Chemistry,* 279**,** 31823-31832.
LIS, R., KARRASCH, C. C., POULOS, M. G., KUNAR, B., REDMOND, D., DURAN, J. G. B., BADWE, C. R., SCHACHTERLE, W., GINSBERG, M., XIANG, J., TABRIZI, A. R., SHIDO, K., ROSENWAKS, Z., ELEMENTO, O., SPECK, N.

A., BUTLER, J. M., SCANDURA, J. M. & RAFII, S. 2017. Conversion of adult endothelium to immunocompetent haematopoietic stem cells. *Nature,* 545**,** 439-445.

LIU, T., QIAN, W. J., GRITSENKO, M. A., CAMP, D. G., 2ND, MONROE, M. E., MOORE, R. J. & SMITH, R. D. 2005. Human plasma N-glycoproteome analysis by immunoaffinity subtraction, hydrazide chemistry, and mass spectrometry. *J Proteome Res,* 4**,** 2070-80.

LIVINGSTONE, C. D. & BARTON, G. J. 1993. Protein sequence alignments: a strategy for the hierarchical analysis of residue conservation. *Comput Appl Biosci,* 9**,** 745-56.

LOBOV, I. B., RENARD, R. A., PAPADOPOULOS, N., GALE, N. W., THURSTON, G., YANCOPOULOS, G. D. & WIEGAND, S. J. 2007. Delta-like ligand 4 (Dll4) is induced by VEGF as a negative regulator of angiogenic sprouting. *Proc Natl Acad Sci U S A,* 104**,** 3219-24.

LUO, Z. X., YUAN, C. X., MENG, Q. J. & JI, Q. 2011. A Jurassic eutherian mammal and divergence of marsupials and placentals. *Nature,* 476**,** 442-5.

LUTTRELL, L. M. & LEFKOWITZ, R. J. 2002. The role of beta-arrestins in the termination and transduction of G-protein-coupled receptor signals. *J Cell Sci,* 115**,** 455-65.

MAGRANE, M. & CONSORTIUM, U. 2011. UniProt Knowledgebase: a hub of integrated protein data. *Database,* 2011**,** bar009-bar009.

MANNING, D. L., ROBERTSON, J. F., ELLIS, I. O., ELSTON, C. W., MCCLELLAND, R. A., GEE, J. M., JONES, R. J., GREEN, C. D., CANNON, P., BLAMEY, R. W. & ET AL. 1994. Oestrogen-regulated genes in breast cancer: association of pLIV1 with lymph node involvement. *Eur J Cancer,* 30a**,** 675-8.

MARCHLER-BAUER, A., DERBYSHIRE, M. K., GONZALES, N. R., LU, S., CHITSAZ, F., GEER, L. Y., GEER, R. C., HE, J., GWADZ, M., HURWITZ, D. I., LANCZYCKI, C. J., LU, F., MARCHLER, G. H., SONG, J. S., THANKI, N., WANG, Z., YAMASHITA, R. A., ZHANG, D., ZHENG, C. & BRYANT, S. H. 2015. CDD: NCBI's conserved domain database. *Nucleic Acids Res,* 43**,** D222-6.

MARTIN, S. & PARTON, R. G. 2006. Lipid droplets: a unified view of a dynamic organelle. *Nat Rev Mol Cell Biol,* 7**,** 373-8.

MARTINEZ-POVEDA, B., GARCIA-VILAS, J. A., CARDENAS, C., MELGAREJO, E., QUESADA, A. R. & MEDINA, M. A. 2013. The brominated compound aeroplysinin-1 inhibits proliferation and the expression of key pro-inflammatory molecules in human endothelial and monocyte cells. *PLoS One,* 8**,** e55203.

MASIERO, M., SIMOES, F. C., HAN, H. D., SNELL, C., PETERKIN, T., BRIDGES, E., MANGALA, L. S., WU, S. Y., PRADEEP, S., LI, D., HAN, C., DALTON, H., LOPEZ-BERESTEIN, G., TUYNMAN, J. B., MORTENSEN, N., LI, J. L., PATIENT, R., SOOD, A. K., BANHAM, A. H., HARRIS, A. L. & BUFFA, F. M. 2013. A core human primary tumor angiogenesis signature identifies the endothelial orphan receptor ELTD1 as a key regulator of angiogenesis. *Cancer Cell,* 24**,** 229-41.

MATSUI, J., WAKABAYASHI, T., ASADA, M., YOSHIMATSU, K. & OKADA, M. 2004. Stem cell factor/c-kit signaling promotes the survival, migration, and capillary tube formation of human umbilical vein endothelial cells. *J Biol Chem,* 279**,** 18600-7.

MATSUSHITA, H., LELIANOVA, V. G. & USHKARYOV, Y. A. 1999. The latrophilin family: multiply spliced G protein-coupled receptors with differential tissue distribution. *FEBS Letters,* 443**,** 348-352.

MCCUDDEN, C. R., HAINS, M. D., KIMPLE, R. J., SIDEROVSKI, D. P. & WILLARD, F. S. 2005. G-protein signaling: back to the future. *Cell Mol Life Sci,* 62**,** 551-77.

MCWILLIAM, H., LI, W., ULUDAG, M., SQUIZZATO, S., PARK, Y. M., BUSO, N., COWLEY, A. P. & LOPEZ, R. 2013. Analysis Tool Web Services from the EMBL-EBI. *Nucleic Acids Res,* 41**,** W597-600.

MELNYCHUK, R. M., STREBLOW, D. N., SMITH, P. P., HIRSCH, A. J., PANCHEVA, D. & NELSON, J. A. 2004. Human cytomegalovirus-encoded G protein-coupled receptor US28 mediates smooth muscle cell migration through Galpha12. *J Virol,* 78**,** 8382-91.

MELO, R. C., D'AVILA, H., WAN, H. C., BOZZA, P. T., DVORAK, A. M. & WELLER, P. F. 2011. Lipid bodies in inflammatory cells: structure, function, and current imaging techniques. *J Histochem Cytochem,* 59**,** 540-56.

MENDIOLA, M., MARTINEZ-MARIN, V., HERRANZ, J., HEREDIA, V., YEBENES, L., ZAMORA, P., CASTELO, B., PINTO, A., MIGUEL, M., DIAZ, E., GAMEZ, A., FRESNO, J. A., RAMIREZ DE MOLINA, A., HARDISSON, D., ESPINOSA, E. & REDONDO, A. 2016. Predictive value of angiogenesis-related gene profiling in patients with HER2-negative metastatic breast cancer treated with bevacizumab and weekly paclitaxel. *Oncotarget,* 7**,** 24217-27.

MESSNER, B., KERN, J., WIEDEMANN, D., SCHWAIGER, S., TURKCAN, A., PLONER, C., TROCKENBACHER, A., AUMAYR, K., BONAROS, N., LAUFER, G., STUPPNER, H., UNTERGASSER, G. & BERNHARD, D. 2013. 5-Methoxyleoligin, a lignan from Edelweiss, stimulates CYP26B1-dependent angiogenesis in vitro and induces arteriogenesis in infarcted rat hearts in vivo. *PLoS One,* 8**,** e58342.

MIGITA, T., OKABE, S., IKEDA, K., IGARASHI, S., SUGAWARA, S., TOMIDA, A., TAGUCHI, R., SOGA, T. & SEIMIYA, H. 2013. Inhibition of ATP citrate lyase induces an anticancer effect via reactive oxygen species: AMPK as a predictive biomarker for therapeutic impact. *Am J Pathol,* 182**,** 1800-10.

MILO, R., JORGENSEN, P., MORAN, U., WEBER, G. & SPRINGER, M. 2010. BioNumbers--the database of key numbers in molecular and cell biology. *Nucleic Acids Res,* 38**,** D750-3.

MONAHAN-EARLEY, R., DVORAK, A. M. & AIRD, W. C. 2013. Evolutionary origins of the blood vascular system and endothelium. *J Thromb Haemost,* 11 Suppl 1**,** 46-66.

MULLER, A., WINKLER, J., FIEDLER, F., SASTRADIHARDJA, T., BINDER, C., SCHNABEL, R., KUNGEL, J., ROTHEMUND, S., HENNIG, C., SCHONEBERG, T. & PROMEL, S. 2015. Oriented Cell Division in the C. elegans Embryo Is Coordinated by G-Protein Signaling Dependent on the Adhesion GPCR LAT-1. *PLoS Genet,* 11**,** e1005624.

MUTHUSAMY, N., CHEN, Y. J., YIN, D. M., MEI, L. & BERGSON, C. 2015. Complementary roles of the neuron-enriched endosomal proteins NEEP21 and calcyon in neuronal vesicle trafficking. *J Neurochem,* 132**,** 20-31.

NAKATSU, M. N., DAVIS, J. & HUGHES, C. C. 2007. Optimized fibrin gel bead assay for the study of angiogenesis. *J Vis Exp***,** 186.

NAKATSU, M. N. & HUGHES, C. C. 2008. An optimized three-dimensional in vitro model for the analysis of angiogenesis. *Methods Enzymol,* 443**,** 65-82.
NECHIPORUK, T., URNESS, L. D. & KEATING, M. T. 2001. ETL, a novel seven-transmembrane receptor that is developmentally regulated in the heart. ETL is a member of the secretin family and belongs to the epidermal growth factor-seven-transmembrane subfamily. *J Biol Chem,* 276**,** 4150-7.
NIJMEIJER, S. 2016. Signaling and modulation of adhesion GPCRs GPR56 (ADGRG1) and ELTD1 (ADGRL4). *8th International Adhesion GPCR Workshop (Joint workshop of the International Adhesion GPCR Consortium and Annual Symposium of the DFG Research Unit 2149).* Leipzig.
NIJMEIJER, S., KOENEN, J., SMIT, M. J., LEURS, R. & VISCHER, H. F. 2015. Signalling and pharmacological modulation of adhesion GPCRs GPR56 (ADGRG1) and ELTD1 (ADGRL4). *GPCRs: Beyond Structure Towards Therapy.* Monash University Prato Centre, Italy: Biochemical Society.
NISHIMURA, D. 2001. BioCarta. *Biotech Software & Internet Report,* 2**,** 117-120.
NOONAN, E., GIARDINA, C. & HIGHTOWER, L. 2008. Hsp70B' and Hsp72 form a complex in stressed human colon cells and each contributes to cytoprotection. *Exp Cell Res,* 314**,** 2468-76.
NORDSTROM, K. J., LAGERSTROM, M. C., WALLER, L. M., FREDRIKSSON, R. & SCHIOTH, H. B. 2009. The Secretin GPCRs descended from the family of Adhesion GPCRs. *Mol Biol Evol,* 26**,** 71-84.
NOWELL, C. S. & RADTKE, F. 2017. Notch as a tumour suppressor. *Nat Rev Cancer,* 17**,** 145-159.
OKAJIMA, D., KUDO, G. & YOKOTA, H. 2010. Brain-specific angiogenesis inhibitor 2 (BAI2) may be activated by proteolytic processing. *J Recept Signal Transduct Res,* 30**,** 143-53.
OLDHAM, W. M. & HAMM, H. E. 2008. Heterotrimeric G protein activation by G-protein-coupled receptors. *Nat Rev Mol Cell Biol,* 9**,** 60-71.
PAAVOLA, K. J., SIDIK, H., ZUCHERO, J. B., ECKART, M. & TALBOT, W. S. 2014. Type IV collagen is an activating ligand for the adhesion G protein-coupled receptor GPR126. *Sci Signal,* 7**,** ra76.
PAAVOLA, K. J., STEPHENSON, J. R., RITTER, S. L., ALTER, S. P. & HALL, R. A. 2011. The N terminus of the adhesion G protein-coupled receptor GPR56 controls receptor signaling activity. *J Biol Chem,* 286**,** 28914-21.
PATEL, N. S., LI, J. L., GENERALI, D., POULSOM, R., CRANSTON, D. W. & HARRIS, A. L. 2005. Up-regulation of delta-like 4 ligand in human tumor vasculature and the role of basal expression in endothelial cell function. *Cancer Res,* 65**,** 8690-7.
PAULSEN, S. J., ROSENKILDE, M. M., EUGEN-OLSEN, J. & KLEDAL, T. N. 2005. Epstein-Barr virus-encoded BILF1 is a constitutively active G protein-coupled receptor. *J Virol,* 79**,** 536-46.
PEKOW, J., DOUGHERTY, U., HUANG, Y., GOMETZ, E., NATHANSON, J., COHEN, G., LEVY, S., KOCHERGINSKY, M., VENU, N., WESTERHOFF, M., HART, J., NOFFSINGER, A. E., HANAUER, S. B., HURST, R. D., FICHERA, A., JOSEPH, L. J., LIU, Q. & BISSONNETTE, M. 2013. Gene signature distinguishes patients with chronic ulcerative colitis harboring remote neoplastic lesions. *Inflamm Bowel Dis,* 19**,** 461-70.
PEROU, C. M., SORLIE, T., EISEN, M. B., VAN DE RIJN, M., JEFFREY, S. S., REES, C. A., POLLACK, J. R., ROSS, D. T., JOHNSEN, H., AKSLEN, L. A., FLUGE, O., PERGAMENSCHIKOV, A., WILLIAMS, C., ZHU, S. X.,

LONNING, P. E., BORRESEN-DALE, A. L., BROWN, P. O. & BOTSTEIN, D. 2000. Molecular portraits of human breast tumours. *Nature,* 406**,** 747-52.
PETERSEN, T. N., BRUNAK, S., VON HEIJNE, G. & NIELSEN, H. 2011. SignalP 4.0: discriminating signal peptides from transmembrane regions. *Nat Methods,* 8**,** 785-6.
PFAFFL, M. W. 2001. A new mathematical model for relative quantification in real-time RT-PCR. *Nucleic Acids Res,* 29**,** e45.
PHNG, L. K. & GERHARDT, H. 2009. Angiogenesis: a team effort coordinated by notch. *Dev Cell,* 16**,** 196-208.
PONCE, M. L. 2009. Tube formation: an in vitro matrigel angiogenesis assay. *Methods Mol Biol,* 467**,** 183-8.
PORTO NETO, L. R., BUNCH, R. J., HARRISON, B. E. & BARENDSE, W. 2011. DNA variation in the gene ELTD1 is associated with tick burden in cattle. *Anim Genet,* 42**,** 50-5.
POTAPOVA, I. A., EL-MAGHRABI, M. R., DORONIN, S. V. & BENJAMIN, W. B. 2000. Phosphorylation of recombinant human ATP:citrate lyase by cAMP-dependent protein kinase abolishes homotropic allosteric regulation of the enzyme by citrate and increases the enzyme activity. Allosteric activation of ATP:citrate lyase by phosphorylated sugars. *Biochemistry,* 39**,** 1169-79.
PROMEL, S., FRICKENHAUS, M., HUGHES, S., MESTEK, L., STAUNTON, D., WOOLLARD, A., VAKONAKIS, I., SCHONEBERG, T., SCHNABEL, R., RUSS, A. P. & LANGENHAN, T. 2012. The GPS motif is a molecular switch for bimodal activities of adhesion class G protein-coupled receptors. *Cell Rep,* 2**,** 321-31.
PROMEL, S., LANGENHAN, T. & ARAC, D. 2013. Matching structure with function: the GAIN domain of Adhesion-GPCR and PKD1-like proteins. *Trends Pharmacol Sci,* 34**,** 470-8.
QUAX, T. E., CLAASSENS, N. J., SOLL, D. & VAN DER OOST, J. 2015. Codon Bias as a Means to Fine-Tune Gene Expression. *Mol Cell,* 59**,** 149-61.
RAHMAN, M. & MOHAMMED, S. 2015. Breast cancer metastasis and the lymphatic system. *Oncol Lett,* 10**,** 1233-1239.
REEVES, C. V., DUFRAINE, J., YOUNG, J. A. & KITAJEWSKI, J. 2010. Anthrax toxin receptor 2 is expressed in murine and tumor vasculature and functions in endothelial proliferation and morphogenesis. *Oncogene,* 29**,** 789-801.
ROSS, A. C. & ZOLFAGHARI, R. 2011. Cytochrome P450s in the regulation of cellular retinoic acid metabolism. *Annu Rev Nutr,* 31**,** 65-87.
SALAZAR, N. C., CHEN, J. & ROCKMAN, H. A. 2007. Cardiac GPCRs: GPCR signaling in healthy and failing hearts. *Biochim Biophys Acta,* 1768**,** 1006-18.
SCHILLING, J., NEPOMUCENO, A. I., PLANCHART, A., YODER, J. A., KELLY, R. M., MUDDIMAN, D. C., DANIELS, H. V., HIRAMATSU, N. & READING, B. J. 2015. Machine learning reveals sex-specific 17beta-estradiol-responsive expression patterns in white perch (Morone americana) plasma proteins. *Proteomics,* 15**,** 2678-90.
SCHINDELIN, J., ARGANDA-CARRERAS, I., FRISE, E., KAYNIG, V., LONGAIR, M., PIETZSCH, T., PREIBISCH, S., RUEDEN, C., SAALFELD, S., SCHMID, B., TINEVEZ, J. Y., WHITE, D. J., HARTENSTEIN, V., ELICEIRI, K., TOMANCAK, P. & CARDONA, A. 2012. Fiji: an open-source platform for biological-image analysis. *Nat Methods,* 9**,** 676-82.

SCHIOTH, H. B. & FREDRIKSSON, R. 2005. The GRAFS classification system of G-protein coupled receptors in comparative perspective. *Gen Comp Endocrinol,* 142**,** 94-101.
SCHIOTH, H. B., NORDSTROM, K. J. & FREDRIKSSON, R. 2010. The adhesion GPCRs; gene repertoire, phylogeny and evolution. *Adv Exp Med Biol,* 706**,** 1-13.
SCHOLZ, N., GEHRING, J., GUAN, C., LJASCHENKO, D., FISCHER, R., LAKSHMANAN, V., KITTEL, R. J. & LANGENHAN, T. 2015. The adhesion GPCR latrophilin/CIRL shapes mechanosensation. *Cell Rep,* 11**,** 866-74.
SCHONEBERG, T., LIEBSCHER, I., LUO, R., MONK, K. R. & PIAO, X. 2015. Tethered agonists: a new mechanism underlying adhesion G protein-coupled receptor activation. *J Recept Signal Transduct Res***,** 1-4.
SCHOORS, S., BRUNING, U., MISSIAEN, R., QUEIROZ, K. C., BORGERS, G., ELIA, I., ZECCHIN, A., CANTELMO, A. R., CHRISTEN, S., GOVEIA, J., HEGGERMONT, W., GODDE, L., VINCKIER, S., VAN VELDHOVEN, P. P., EELEN, G., SCHOONJANS, L., GERHARDT, H., DEWERCHIN, M., BAES, M., DE BOCK, K., GHESQUIERE, B., LUNT, S. Y., FENDT, S. M. & CARMELIET, P. 2015. Fatty acid carbon is essential for dNTP synthesis in endothelial cells. *Nature,* 520**,** 192-7.
SCHOORS, S., DE BOCK, K., CANTELMO, A. R., GEORGIADOU, M., GHESQUIERE, B., CAUWENBERGHS, S., KUCHNIO, A., WONG, B. W., QUAEGEBEUR, A., GOVEIA, J., BIFARI, F., WANG, X., BLANCO, R., TEMBUYSER, B., CORNELISSEN, I., BOUCHE, A., VINCKIER, S., DIAZ-MORALLI, S., GERHARDT, H., TELANG, S., CASCANTE, M., CHESNEY, J., DEWERCHIN, M. & CARMELIET, P. 2014. Partial and transient reduction of glycolysis by PFKFB3 blockade reduces pathological angiogenesis. *Cell Metab,* 19**,** 37-48.
SEGARRA, M., WILLIAMS, C. K., SIERRA MDE, L., BERNARDO, M., MCCORMICK, P. J., MARIC, D., REGINO, C., CHOYKE, P. & TOSATO, G. 2008. Dll4 activation of Notch signaling reduces tumor vascularity and inhibits tumor growth. *Blood,* 112**,** 1904-11.
SERBAN, F., DAIANU, O., TATARANU, L. G., ARTENE, S. A., EMAMI, G., GEORGESCU, A. M., ALEXANDRU, O., PURCARU, S. O., TACHE, D. E., DANCIULESCU, M. M., SFREDEL, V. & DRICU, A. 2017. Silencing of epidermal growth factor, latrophilin and seven transmembrane domain-containing protein 1 (ELTD1) via siRNA-induced cell death in glioblastoma. *J Immunoassay Immunochem,* 38**,** 21-33.
SHIN, H. W., HAYASHI, M., CHRISTOFORIDIS, S., LACAS-GERVAIS, S., HOEPFNER, S., WENK, M. R., MODREGGER, J., UTTENWEILER-JOSEPH, S., WILM, M., NYSTUEN, A., FRANKEL, W. N., SOLIMENA, M., DE CAMILLI, P. & ZERIAL, M. 2005. An enzymatic cascade of Rab5 effectors regulates phosphoinositide turnover in the endocytic pathway. *J Cell Biol,* 170**,** 607-18.
SILVA, J. P., LELIANOVA, V., HOPKINS, C., VOLYNSKI, K. E. & USHKARYOV, Y. 2009. Functional cross-interaction of the fragments produced by the cleavage of distinct adhesion G-protein-coupled receptors. *J Biol Chem,* 284**,** 6495-506.
SMITH, J. J., KURAKU, S., HOLT, C., SAUKA-SPENGLER, T., JIANG, N., CAMPBELL, M. S., YANDELL, M. D., MANOUSAKI, T., MEYER, A., BLOOM, O. E., MORGAN, J. R., BUXBAUM, J. D., SACHIDANANDAM, R.,

SIMS, C., GARRUSS, A. S., COOK, M., KRUMLAUF, R., WIEDEMANN, L. M., SOWER, S. A., DECATUR, W. A., HALL, J. A., AMEMIYA, C. T., SAHA, N. R., BUCKLEY, K. M., RAST, J. P., DAS, S., HIRANO, M., MCCURLEY, N., GUO, P., ROHNER, N., TABIN, C. J., PICCINELLI, P., ELGAR, G., RUFFIER, M., AKEN, B. L., SEARLE, S. M., MUFFATO, M., PIGNATELLI, M., HERRERO, J., JONES, M., BROWN, C. T., CHUNG-DAVIDSON, Y. W., NANLOHY, K. G., LIBANTS, S. V., YEH, C. Y., MCCAULEY, D. W., LANGELAND, J. A., PANCER, Z., FRITZSCH, B., DE JONG, P. J., ZHU, B., FULTON, L. L., THEISING, B., FLICEK, P., BRONNER, M. E., WARREN, W. C., CLIFTON, S. W., WILSON, R. K. & LI, W. 2013. Sequencing of the sea lamprey (Petromyzon marinus) genome provides insights into vertebrate evolution. *Nat Genet,* 45**,** 415-21, 421e1-2.

SMYTH, G. K. 2004. Linear models and empirical bayes methods for assessing differential expression in microarray experiments. *Stat Appl Genet Mol Biol,* 3**,** Article3.

ST CROIX, B., RAGO, C., VELCULESCU, V., TRAVERSO, G., ROMANS, K. E., MONTGOMERY, E., LAL, A., RIGGINS, G. J., LENGAUER, C., VOGELSTEIN, B. & KINZLER, K. W. 2000. Genes expressed in human tumor endothelium. *Science,* 289**,** 1197-202.

STACEY, M., CHANG, G. W., DAVIES, J. Q., KWAKKENBOS, M. J., SANDERSON, R. D., HAMANN, J., GORDON, S. & LIN, H. H. 2003. The epidermal growth factor-like domains of the human EMR2 receptor mediate cell attachment through chondroitin sulfate glycosaminoglycans. *Blood,* 102**,** 2916-24.

STATON, C. A., REED, M. W. & BROWN, N. J. 2009. A critical analysis of current in vitro and in vivo angiogenesis assays. *Int J Exp Pathol,* 90**,** 195-221.

STEPHENSON, J. R., PAAVOLA, K. J., SCHAEFER, S. A., KAUR, B., VAN MEIR, E. G. & HALL, R. A. 2013. Brain-specific angiogenesis inhibitor-1 signaling, regulation, and enrichment in the postsynaptic density. *J Biol Chem,* 288**,** 22248-56.

STOVEKEN, H. M., HAJDUCZOK, A. G., XU, L. & TALL, G. G. 2015. Adhesion G protein-coupled receptors are activated by exposure of a cryptic tethered agonist. *Proc Natl Acad Sci U S A,* 112**,** 6194-9.

STUNNENBERG, H. G. & HIRST, M. 2016. The International Human Epigenome Consortium: A Blueprint for Scientific Collaboration and Discovery. *Cell,* 167**,** 1145-1149.

SUN, J., ALUVILA, S., KOTARIA, R., MAYOR, J. A., WALTERS, D. E. & KAPLAN, R. S. 2010. Mitochondrial and Plasma Membrane Citrate Transporters: Discovery of Selective Inhibitors and Application to Structure/Function Analysis. *Mol Cell Pharmacol,* 2**,** 101-110.

SUZUKI, N., HAJICEK, N. & KOZASA, T. 2009. Regulation and physiological functions of G12/13-mediated signaling pathways. *Neurosignals,* 17**,** 55-70.

SWIERS, G., RODE, C., AZZONI, E. & DE BRUIJN, M. F. 2013. A short history of hemogenic endothelium. *Blood Cells Mol Dis,* 51**,** 206-12.

SWIFT, M. R. & WEINSTEIN, B. M. 2009. Arterial-venous specification during development. *Circ Res,* 104**,** 576-88.

THURSTON, G., NOGUERA-TROISE, I. & YANCOPOULOS, G. D. 2007. The Delta paradox: DLL4 blockade leads to more tumour vessels but less tumour growth. *Nat Rev Cancer,* 7**,** 327-31.

TOWNER, R. A., JENSEN, R. L., COLMAN, H., VAILLANT, B., SMITH, N., CASTEEL, R., SAUNDERS, D., GILLESPIE, D. L., SILASI-MANSAT, R., LUPU, F., GILES, C. B. & WREN, J. D. 2013. ELTD1, a potential new biomarker for gliomas. *Neurosurgery,* 72**,** 77-90; discussion 91.

TURYN, J., SCHLICHTHOLZ, B., DETTLAFF-POKORA, A., PRESLER, M., GOYKE, E., MATUSZEWSKI, M., KMIEC, Z., KRAJKA, K. & SWIERCZYNSKI, J. 2003. Increased activity of glycerol 3-phosphate dehydrogenase and other lipogenic enzymes in human bladder cancer. *Horm Metab Res,* 35**,** 565-9.

VAN OORT, R. J., RESPRESS, J. L., LI, N., REYNOLDS, C., DE ALMEIDA, A. C., SKAPURA, D. G., DE WINDT, L. J. & WEHRENS, X. H. 2010. Accelerated development of pressure overload-induced cardiac hypertrophy and dysfunction in an RyR2-R176Q knockin mouse model. *Hypertension,* 55**,** 932-8.

VARIS, A., WOLF, M., MONNI, O., VAKKARI, M. L., KOKKOLA, A., MOSKALUK, C., FRIERSON, H., JR., POWELL, S. M., KNUUTILA, S., KALLIONIEMI, A. & EL-RIFAI, W. 2002. Targets of gene amplification and overexpression at 17q in gastric cancer. *Cancer Res,* 62**,** 2625-9.

VERVOORT, V. S., ROSELLI, S., OSHIMA, R. G. & PASQUALE, E. B. 2007. Splice variants and expression patterns of SHEP1, BCAR3 and NSP1, a gene family involved in integrin and receptor tyrosine kinase signaling. *Gene,* 391**,** 161-70.

VOGELSTEIN, B. & KINZLER, K. W. 2015. The Path to Cancer --Three Strikes and You're Out. *N Engl J Med,* 373**,** 1895-8.

VOGELSTEIN, B., PAPADOPOULOS, N., VELCULESCU, V. E., ZHOU, S., DIAZ, L. A., JR. & KINZLER, K. W. 2013. Cancer genome landscapes. *Science,* 339**,** 1546-58.

VOLYNSKI, K. E., SILVA, J. P., LELIANOVA, V. G., ATIQUR RAHMAN, M., HOPKINS, C. & USHKARYOV, Y. A. 2004. Latrophilin fragments behave as independent proteins that associate and signal on binding of LTX(N4C). *Embo j,* 23**,** 4423-33.

WALLGARD, E., LARSSON, E., HE, L., HELLSTROM, M., ARMULIK, A., NISANCIOGLU, M. H., GENOVE, G., LINDAHL, P. & BETSHOLTZ, C. 2008. Identification of a core set of 58 gene transcripts with broad and specific expression in the microvasculature. *Arterioscler Thromb Vasc Biol,* 28**,** 1469-76.

WALTER, S., ATZMON, G., DEMERATH, E. W., GARCIA, M. E., KAPLAN, R. C., KUMARI, M., LUNETTA, K. L., MILANESCHI, Y., TANAKA, T., TRANAH, G. J., VOLKER, U., YU, L., ARNOLD, A., BENJAMIN, E. J., BIFFAR, R., BUCHMAN, A. S., BOERWINKLE, E., COUPER, D., DE JAGER, P. L., EVANS, D. A., HARRIS, T. B., HOFFMANN, W., HOFMAN, A., KARASIK, D., KIEL, D. P., KOCHER, T., KUNINGAS, M., LAUNER, L. J., LOHMAN, K. K., LUTSEY, P. L., MACKENBACH, J., MARCIANTE, K., PSATY, B. M., REIMAN, E. M., ROTTER, J. I., SESHADRI, S., SHARDELL, M. D., SMITH, A. V., VAN DUIJN, C., WALSTON, J., ZILLIKENS, M. C., BANDINELLI, S., BAUMEISTER, S. E., BENNETT, D. A., FERRUCCI, L., GUDNASON, V., KIVIMAKI, M., LIU, Y., MURABITO, J. M., NEWMAN, A. B., TIEMEIER, H. & FRANCESCHINI, N. 2011. A genome-wide association study of aging. *Neurobiol Aging,* 32**,** 2109.e15-28.

WANDEL, E., SAALBACH, A., SITTIG, D., GEBHARDT, C. & AUST, G. 2012. Thy-1 (CD90) is an interacting partner for CD97 on activated endothelial cells. *J Immunol,* 188**,** 1442-50.

WANG, D., YIN, L., WEI, J., YANG, Z. & JIANG, G. 2017. ATP citrate lyase is increased in human breast cancer, depletion of which promotes apoptosis. *Tumour Biol,* 39**,** 1010428317698338.

WANG, H. Y., FU, J. C., LEE, Y. C. & LU, P. J. 2013. Hyperthermia stress activates heat shock protein expression via propyl isomerase 1 regulation with heat shock factor 1. *Mol Cell Biol,* 33**,** 4889-99.

WANG, S. C., YE, L., SANDERS, A. J., RUGE, F., HARDING, K. G. & JIANG, W. G. 2016a. Tumour endothelial marker-8 in wound healing and its impact on the proliferation and migration of keratinocytes. *Int J Mol Med,* 37**,** 293-8.

WANG, T., WARD, Y., TIAN, L., LAKE, R., GUEDEZ, L., STETLER-STEVENSON, W. G. & KELLY, K. 2005. CD97, an adhesion receptor on inflammatory cells, stimulates angiogenesis through binding integrin counterreceptors on endothelial cells. *Blood,* 105**,** 2836-44.

WANG, Y., XU, X., PAN, M. & JIN, T. 2016b. ELMO1 Directly Interacts with Gbetagamma Subunit to Transduce GPCR Signaling to Rac1 Activation in Chemotaxis. *J Cancer,* 7**,** 973-83.

WATERHOUSE, A. M., PROCTER, J. B., MARTIN, D. M., CLAMP, M. & BARTON, G. J. 2009. Jalview Version 2--a multiple sequence alignment editor and analysis workbench. *Bioinformatics,* 25**,** 1189-91.

WEI, X., SCHNEIDER, J. G., SHENOUDA, S. M., LEE, A., TOWLER, D. A., CHAKRAVARTHY, M. V., VITA, J. A. & SEMENKOVICH, C. F. 2011. De novo lipogenesis maintains vascular homeostasis through endothelial nitric-oxide synthase (eNOS) palmitoylation. *J Biol Chem,* 286**,** 2933-45.

WEIDNER, N., SEMPLE, J. P., WELCH, W. R. & FOLKMAN, J. 1991. Tumor angiogenesis and metastasis--correlation in invasive breast carcinoma. *N Engl J Med,* 324**,** 1-8.

WELLEN, K. E., HATZIVASSILIOU, G., SACHDEVA, U. M., BUI, T. V., CROSS, J. R. & THOMPSON, C. B. 2009. ATP-citrate lyase links cellular metabolism to histone acetylation. *Science,* 324**,** 1076-80.

WETTSCHURECK, N. & OFFERMANNS, S. 2005. Mammalian G proteins and their cell type specific functions. *Physiol Rev,* 85**,** 1159-204.

WHO. *Cancer Fact Sheet (January 2017)* [Online]. WHO Media Centre: World Health Organization. Available: http://www.who.int/mediacentre/factsheets/fs297/en/ [Accessed 18 July 2017].

WICKHAM, H. 2009. *ggplot2: Elegant Graphics for Data Analysis*, Springer Publishing Company, Incorporated.

WILDE, C., FISCHER, L., LEDE, V., KIRCHBERGER, J., ROTHEMUND, S., SCHONEBERG, T. & LIEBSCHER, I. 2016. The constitutive activity of the adhesion GPCR GPR114/ADGRG5 is mediated by its tethered agonist. *Faseb j,* 30**,** 666-73.

WILLIAMS, C., CHOUDHURY, R., MCKENZIE, E. & LOWE, M. 2007. Targeting of the type II inositol polyphosphate 5-phosphatase INPP5B to the early secretory pathway. *J Cell Sci,* 120**,** 3941-51.

XIAO, J., JIANG, H., ZHANG, R., FAN, G., ZHANG, Y., JIANG, D. & LI, H. 2012. Augmented cardiac hypertrophy in response to pressure overload in mice lacking ELTD1. *PLoS One,* 7**,** e35779.

XU, X. & JIN, T. 2017. ELMO Proteins Transduce G Protein-Coupled Receptor Signal to Control Reorganization of Actin Cytoskeleton in Chemotaxis of Eukaryotic Cells. *Small GTPases*, 0.

YAHAGI, N., SHIMANO, H., HASEGAWA, K., OHASHI, K., MATSUZAKA, T., NAJIMA, Y., SEKIYA, M., TOMITA, S., OKAZAKI, H., TAMURA, Y., IIZUKA, Y., OHASHI, K., NAGAI, R., ISHIBASHI, S., KADOWAKI, T., MAKUUCHI, M., OHNISHI, S., OSUGA, J. & YAMADA, N. 2005. Co-ordinate activation of lipogenic enzymes in hepatocellular carcinoma. *Eur J Cancer,* 41**,** 1316-22.

YAMAGUCHI, H., ISHII, E., SAITO, S., TASHIRO, K., FUJITA, I., YOSHIDOMI, S., OHTUBO, M., AKAZAWA, K. & MIYAZAKI, S. 1996. Umbilical vein endothelial cells are an important source of c-kit and stem cell factor which regulate the proliferation of haemopoietic progenitor cells. *Br J Haematol,* 94**,** 606-11.

YE, J., COULOURIS, G., ZARETSKAYA, I., CUTCUTACHE, I., ROZEN, S. & MADDEN, T. L. 2012. Primer-BLAST: a tool to design target-specific primers for polymerase chain reaction. *BMC Bioinformatics,* 13**,** 134.

YORDY, J. S., MOUSSA, O., PEI, H., CHAUSSABEL, D., LI, R. & WATSON, D. K. 2005. SP100 inhibits ETS1 activity in primary endothelial cells. *Oncogene,* 24**,** 916-31.

ZAIDI, N., SWINNEN, J. V. & SMANS, K. 2012. ATP-citrate lyase: a key player in cancer metabolism. *Cancer Res,* 72**,** 3709-14.

ZIEGLER, J., PODY, R., COUTINHO DE SOUZA, P., EVANS, B., SAUNDERS, D., SMITH, N., MALLORY, S., NJOKU, C., DONG, Y., CHEN, H., DONG, J., LERNER, M., MIAN, O., TUMMALA, S., BATTISTE, J., FUNG, K. M., WREN, J. D. & TOWNER, R. A. 2017. ELTD1, an effective anti-angiogenic target for gliomas: preclinical assessment in mouse GL261 and human G55 xenograft glioma models. *Neuro Oncol,* 19**,** 175-185.